Geospatial Analyses of Natural Disasters: Economic Impacts, Societal Responses, and Political Bias

Dissertation

zur Erlangung des wirtschafts- und sozialwissenschaftlichen Doktorgrades
„Doctor rerum politicarum“
der Ruprecht-Karls-Universität Heidelberg

vorgelegt von

Sven Philip Kunze

November 2020

Geospatial Analyses of Natural Disasters: Economic Impacts, Societal Responses, and Political Bias

Sven Philip Kunze

FIRST SUPERVISOR AND EXAMINER OF THE DISSERTATION
Prof. Dr. Axel Dreher
Professor of Economics
Chair of International and Development Politics
Alfred-Weber-Institute for Economics
Ruprecht-Karls-Universität Heidelberg

SECOND SUPERVISOR AND EXAMINER OF THE DISSERTATION
Prof. Dr. Eric Strobl
Professor of Economics
Climate and Environmental Economics
Department of Economics
Universität Bern

THIRD EXAMINER OF THE DISSERTATION
Prof. Dr. Jale Tosun
Professor of Political Science
Chair of Political Science
Institute of Political Science
Ruprecht-Karls-Universität Heidelberg

Für Elfriede, Giesela und Peter

Contents

List of Figures

List of Tables

Introduction

Natural disasters have always had a major influence on human civilizations. From the great Lisbon earthquake in 1755, to Hurricane Katrina in 2005, to the recent COVID-19 pandemic, natural disasters have had the power to shape the process of society's development. Over the 1950–2019 period natural disasters have affected 113 million people every year, which translates into an average yearly economic loss of USD 12 billion (Guha-Sapir & CRED, 2020). While richer economies are more resilient to damage from natural hazards, poorer countries and especially poorer people are overexposed to them, are more vulnerable, and have a reduced capacity to deal with the short- and long-term consequences of disasters (Hallegatte et al., 2016). A current study estimates that if there were no disasters next year, 26 million people would be able to get out of extreme poverty (Rozenberg & Hallegatte, 2016).[1] The recently declared "climate emergency" (Ripple et al., 2019), which refers to the increasing number and intensity of climate-related hazards, such as droughts, floods, or tropical cyclones (IPCC, 2014; Knutson et al., 2020), puts even more pressure on finding adequate policy responses to the threat of natural disasters. Driven by the increasing integration of the local and global economy, local disasters could additionally evolve into cascading risks for a whole country and the international economy (Wenz & Levermann, 2016).

The international community has realized the increasing risk of and damage from natural disasters and aims to reduce their negative consequences. One example for their efforts is the Paris Agreement 2015 adopted by the participating countries of the United Nations Framework Convention on Climate Change (UNFCCC) to limit the rise in the global average temperature to below 2°C to prevent dangerous climate change. This agreement calls the participating countries to an "[...] assessment of climate change impacts and vulnerability, with a view to formulate nationally determined prioritized actions [...]" and urges them to "[...] recognize the importance of averting, minimizing and addressing loss and damage

[1] Extreme poverty refers to people living on less than USD 1.9 per day.

associated with the adverse effects of climate change, including extreme weather events [...]" (UNFCCC, 2015, 10–12). In the same year, the United Nations member states have also agreed on a broader agreement to prevent risks and damage from all types of disasters. The Sendai Framework for Disaster Risk Reduction 2015–2030 formulates specific goals for 2030, such as a substantial reduction of disaster mortality, affectedness, and economic damage, and demands a better understanding of disaster risk and impacts (UNISDR, 2015).

These impacts can be manifold and include, for example, effects on birth weight (Deschenes et al., 2009), conflict (Hsiang et al., 2013; Nel & Righarts, 2008), economic growth (Felbermayr & Gröschl, 2014; Strobl, 2012), energy supply (Auffhammer et al., 2017), migration (Boustan et al., 2012; Strobl, 2011), and trade (Felbermayr & Gröschl, 2013; Hamano & Vermeulen, 2019). For many effects, the exact extent and the underlying mechanism are not completely understood. For example, for the effects on economic growth, some studies find positive growth effects from natural disasters (e.g., Albala-Bertrand, 1993; Cuaresma et al., 2008), whereas other studies find negative consequences (e.g., Felbermayr & Gröschl, 2014; Strobl, 2012). The duration of disaster impacts is also empirically unclear. While some evidence shows that the impacts last only a few months (Heinen et al., 2018), other studies find medium-term impacts of several years (Elliott et al., 2015; Strobl, 2012) or even long-term impacts of up to 20 years (Hsiang & Jina, 2014). However, before effective efforts to reduce disaster risk and damage can take place, the exact extent of the damage and the underlying mechanisms of the impacts must be better understood. Geospatial methods paired with satellite data can help to better target policies when local damage data are incomplete or scarce (UNDRR, 2019). Moreover, to reduce potential negative disaster consequences, one needs fast and objective disaster aid, which can have positive economic recovery effects (Bjørnskov, 2019; Davlasheridze et al., 2017; de Mel et al., 2012). Targeting international disaster aid to people in need is especially important, given its small size compared to the damage caused by natural disasters (Becerra et al., 2014, 2015; UNDRR, 2019). However, previous research has shown that national and international relief is prone to political influences rendering it less effective (Bommer et al., 2019; Cohen & Werker, 2008; Fink & Redaelli, 2011).

In light of these findings, this thesis has two goals. The first is to better understand how natural disasters influence the economy and society. The second is to analyze how national and international disaster relief respond to natural disasters. In all chapters, I use geospatial analyses to combine geophysical, hydrological, or meteorological data with socioeconomic

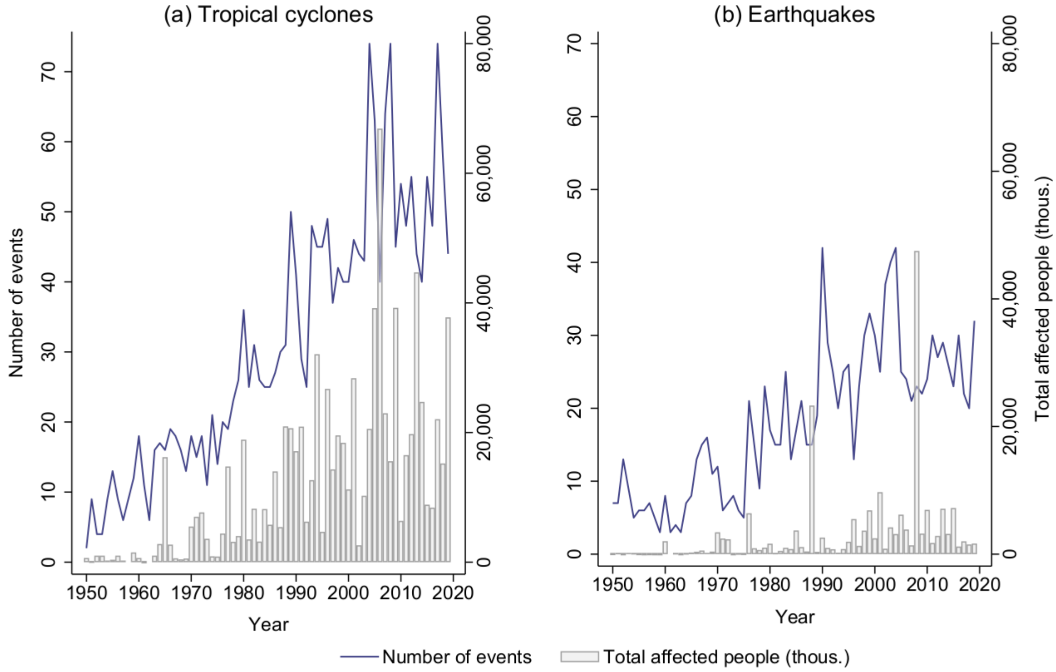

Figure A: Reported number of events and affected people – Tropical cyclones and earthquakes, 1950–2019

Notes: This figure shows the reported number of natural disasters and reported number of affected people for for tropical cyclones and earthquakes for the period 1950–2019. The data source for this figure is the EM-DAT database (Guha-Sapir & CRED, 2020).

data to analyze the respective research questions of the chapters and overcome potential data measurement problems. I focus on two different disaster types: tropical cyclones and earthquakes. For both types of disasters, one observes an increase in the reported number of events and affected people since 1950 (see Figure A). Tropical cyclones are one of the most frequent and most damaging climate hazards. Their damage amounts to USD 2,111 billion, and there are approximately 44 yearly damage events for the 1980–2018 period (Guha-Sapir & CRED, 2020; Munich Re, 2018). Earthquakes occur less frequently than tropical cyclones but can also have devastating consequences when they occur. In the past decades, they have been responsible for 20,000 deaths per year on average (UNDRR, 2019).

My thesis is structured as follows. The first two chapters focus on the impacts of tropical cyclones on economic sectors (Chapter 1) and coastal settlements (Chapter 2). In the remaining two chapters, I analyze the policy responses to natural disasters. Chapter 3 comprises an analysis of the political bias in national disaster aid after hurricanes in the United States, and Chapter 4 examines the allocation of international disaster relief after the 2015 Nepal earthquake. Figure B displays how the individual chapters interact.

In the next paragraphs, I highlight the contributions and connections of the individual chapters in more detail. The thesis starts by analyzing the impacts of tropical cyclones, which are large rotating wind systems in the subtropics and one of the most damaging climatic disasters. Because of their randomness in timing and their intensity, they pose a considerable threat to local economies. In view of the continuously growing interconnection between economic sectors, it is important to understand direct sectoral and spillover effects between the sectors when developing a holistic damage analysis (Shughrue et al., 2020; Wenz & Levermann, 2016). In Chapter 1, I analyze direct and indirect sectoral GDP responses to tropical cyclones in a global sample of 205 countries for the 1970–2015 period. I use a meteorological wind model to derive a new local damage function that takes account of the different exposure of sectors. Together with global data on sectoral GDP growth per country, I disentangle the sectoral impact of tropical cyclones. Furthermore, I identify spillover effects between the individual sectors. My findings help to better understand important economic trickle-down effects of natural disasters. With this chapter, I can identify sectors that show no direct GDP effects but affect other sectors through a change in their input-output structure.

In the second chapter of this thesis, I turn to the impacts of tropical cyclone-generated storm surges. This chapter focuses on the areas with the highest risk of tropical cyclone damage, the so-called low elevation coastal zones (LECZ). For these areas, the greatest threats are tropical cyclone-driven storm surges. Due to data scarcity, this damage component of tropical cyclones has been mostly ignored in the empirical literature. In Chapter 2, in joint

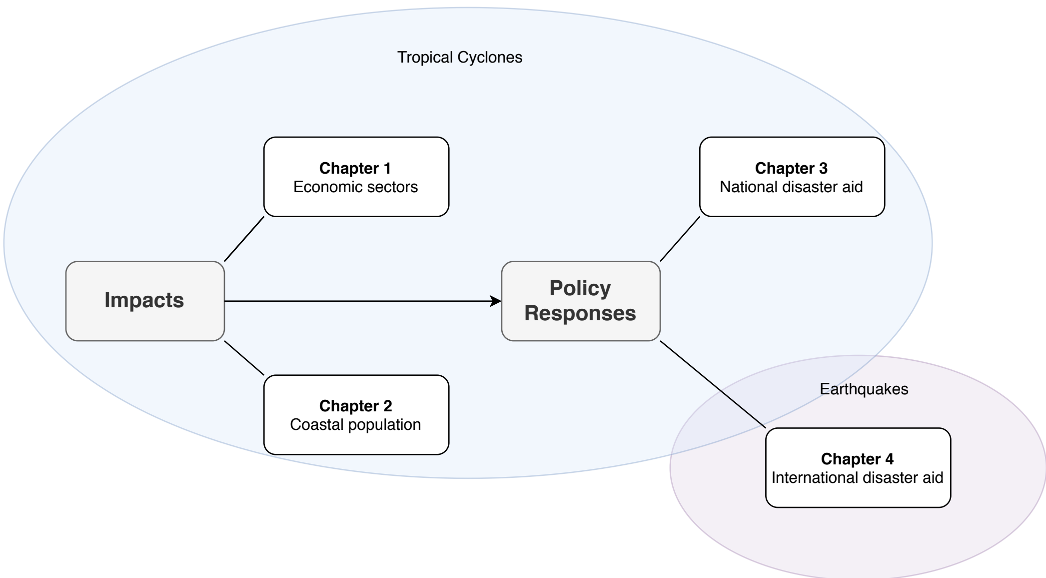

Figure B: Overview of chapters

work with my co-author Eric A. Strobl, I close this gap by generating a tropical cyclone-generated storm surge data set for every tropical cyclone ever recorded. We then use these data to analyze how many people are still living in high-risk areas and how the total, urban, and rural coastal populations have changed in response to storm surge damage in the past 70 years. Even though we find that some adaptation of coastal settlements in the most recent decades has taken place, still more than 32 million people live in storm surge-exposed areas.

Overall, Chapters 1 and 2 provide evidence of long-term consequences of natural disasters. In Chapter 1, I show that, even 17 years after the occurrence of a tropical cyclone, negative sectoral growth effects remain. The results of Chapter 2 demonstrate that changes in coastal settlements can still be detected up to 10 years after a storm surge event. Both chapters highlight that still much has to be done to reduce long-term impacts of natural disasters. One possibility to achieve this goal is to allocate disaster aid after natural disasters in a fast and needs-based manner. However, as part of distributive politics (Fink & Redaelli, 2011), disaster aid is prone to political bias (Bommer et al., 2019) that might distort effective help. Chapters 3 and 4 thus analyze the potential political bias in national and international disaster aid responses.

In Chapter 3, together with Stephan A. Schneider, I use the objective tropical cyclone damage measures developed in Chapters 1 and 2 to answer the question, to what extent the allocation of federal disaster aid in the United States is influenced by the party interests of the ruling president. By analyzing all hurricane strikes in the 1965–2018 period, we indeed find a political bias, which only exists for medium-intensity hurricanes where the decision for granting aid is unclear. In total, 13% (USD 500 million) of the U.S. annual federal aid budget is spent out of political motives, where presidents help politically aligned governors. With our results, we are the first to find a nonlinear political alignment effect in distributive politics, which highlights that many previous empirical results in the distributive politics literature tend to be oversimplified by assuming a linear relationship of the functional form assumptions in their analyses.

Given these comparably large political distortions in national disaster relief, the final chapter of this thesis analyzes whether there are also distortions in international disaster aid. In the case where a disaster is so disastrous that a whole country is overwhelmed by it, the UN can call for internationally coordinated help using a so-called flash appeal. This occurred in response to the 2015 Nepal earthquake which killed 8,800 people and affected nearly a fifth of Nepal's population (Guha-Sapir & CRED, 2020). In Chapter 4, together with Vera Z. Eichenauer, Andreas Fuchs, and Eric A. Strobl, I analyze the allocation of international disaster aid. By using a new data set on geo-coded international aid of the UN flash appeal in Nepal, we study whether its allocation follows physical and socioeconomic vulnerabilities. While the first distribution of international disaster aid corresponds to geophysical damage, the later funding decisions are biased by caste, geographical, and political considerations.

Chapters 3 and 4 show that the distribution of urgently needed aid after disasters is foremostly prone to political and religious influences. To be more effective, domestic and international disaster aid should become more need-oriented in the future, and institutional mechanisms should be designed to reduce political and other biases. Only with these changes at hand we will potentially achieve a situation where we have a "build-back-better in recovery, rehabilitation, and reconstruction" of the economy, as stated in priority area 4 of the Sendai Framework for Disaster Risk Reduction (UNISDR, 2015). Beside of the identification of political biases in international and national disaster relief, this thesis contributes to a better understanding of the timing and mechanism of the economic effects of natural disasters by identifying directly and indirectly affected sectors. What is more, this thesis is the first to systematically analyze the influence of storm surge damage on coastal settlements. Finally, this thesis helps to better identify damage of natural disasters by developing new data sets, which I explain in more detail in the next section.

Data Contribution and Methodological Approach

With my dissertation, I contribute several data sets to the research community. In Chapter 1, I generate a new tropical cyclone damage data set that distinguishes between different sectoral exposures in generating a weighted damage function. The damage data set incorporates a meteorological wind field model that calculates spatial and time-varying wind speeds for all tropical cyclones recorded. I then spatially join it with different exposure data sets. While, for the majority of sectors, the population is a suitable exposure weight (Elliott et al., 2019; Heinen et al., 2018), this is not true for the agricultural sectors. For these sectors, I use agricultural land as an exposure weight. The resulting damage data are at a resolution of $0.1° \times 0.1°$, which I then aggregate to a country-year panel data set for 205 countries for the 1950–2015 period.[2] In Chapter 2, I generate a new global data set for tropical cyclone-driven

[2] $0.1°$ corresponds to approximately 10 km at the equator.

storm surges. Besides tropical cyclone wind speed and pressure input, our model combines data on the coastal and ocean geography, the current tide, and the angle at which storms make landfall. With these inputs we can generate, in a hydrodynamic model, one-hourly inundation maps for coastal areas at risk at a spatial resolution of $0.1° \times 0.1°$ for all tropical cyclones of the 1850–2015 period. In Chapter 3, besides using wind and storm surge damage, we process hurricane-related rainfall data from Roth (2018) and join it on a $0.01° \times 0.01°$ grid to the individual U.S. counties.[3] We thus create a panel data set for hurricane-related excessive rainfall damage for all counties for the 1965–2018 period.

In all chapters, I use geospatial analyses to combine physical disaster intensity data with socioeconomic data to answer the respective research questions. By generating new measures of disaster damage, I thereby advance the damage impact literature. The majority of empirical studies uses report-based data to measure potential damage (Lazzaroni & van Bergeijk, 2014). However, using report-based data in empirical analyses of disaster impacts has several disadvantages: they are prone to measurement errors, such as under- or over-reporting (Kousky, 2014), they include only disasters above a certain damage threshold (Davlasheridze et al., 2017), and they are mostly based on insurance data leading to further selection and endogeneity problems (Felbermayr & Gröschl, 2014). By modeling damage directly from physical-intensity data, I circumvent these problems. In all chapters, I use geophysical intensity measures to model the impacts of the natural disasters researched. In Chapters 1–3, I use these modeled geophysical intensity variables in multivariate panel ordinary least squares fixed-effects regression models to analyze the respective research questions. Certain regions may have a higher probability of being hit by a natural disaster. However, in all panel data regression models, I account for this possibility by including location fixed effects. Therefore, the researched natural disasters are random draws from the underlying probability distribution and are thus plausibly exogenous to the dependent variables analyzed. These circumstances then allow me to causally identify the main effects analyzed. I further control for time fixed effects and area-specific trends over time, to further account for potential unobservable factors. In Chapter 4, I use negative binomial and ordinary least squares regression models to analyze the allocation decisions of the UN flash appeal at the municipality level. As I only have cross-sectional data for this chapter's analysis, a causal identification of the effects is not always possible. However, I construct an earthquake damage

[3] $0.01°$ corresponds to approximately 1 km at the equator.

function from geophysical indicators and a pre-event building type distribution, which are both exogenous to the post-event disaster aid. Additionally, reverse causality is also not a concern, as most variables are collected prior to the earthquake. Furthermore, I try to minimize omitted variable concerns by including a large set of control variables and regional fixed effects.

Summary of the Chapters

Chapter 1

Tropical cyclones are responsible for nearly half of natural disaster damage worldwide and have an enormous impact on economic development. However, their potentially negative influences on economic outcomes is not well understood. In order to design efficient adaptation and mitigation policies in the future, it is important to identify sectors at high risk and sectoral spillover effects. Therefore, I analyze direct and indirect responses of seven economic sector aggregates to tropical cyclone damage in a global sample of 205 countries for the 1970–2015 period. I generate a new tropical cyclone damage measure that considers different exposure weights of the sectors. In a multivariate panel data fixed-effects analysis, I find an immediately negative sectoral GDP growth effect for two sectoral aggregates – agriculture, hunting, forestry, and fishing, as well as wholesale, retail trade, restaurants, and hotels. While the agricultural sectors recover after four years, in the wholesale retail trade, restaurants, and hotels sector aggregate, the negative influence of tropical cyclone damage persists up to 17 years. By analyzing sectoral Input-Output data, I can only identify minor sectoral spillover effects. However, the analysis reveals the crucial role of the manufacturing sector aggregate. This chapter adds to the literature on the macroeconomic effects of disasters and the Input-Output analysis of disasters. The findings can be used to inform international and national policymakers in specifying their adaptation and mitigation strategies to climate change.

Chapter 2

People in low elevation coastal zones are at a high risk of tropical cyclone-generated storm surge damage. However, no global data set on this damage exists. In this chapter, we close this gap by generating the first global data set on storm surges resulting from tropical cyclones. In a hydrodynamic model, we include data on the topography of the ocean and coast, the respective tidal cycle, and the motion and intensity of tropical cyclones to estimate global storm surge damage on a 10 x 10 km resolution for the 1850–2015 period. To identify the exposure of coastal populations and their responses over time, we combine these data with historical spatial population data, which are available at a 10 x 10 km resolution and decadal frequency. We find that, on average globally, the regions with the highest storm surge hazard lie in Eastern Asia, North America, and South-Eastern Africa and that three quarters of exposed coastal populations live in Eastern, South-Eastern, and Southern Asia. In our fixed-effects panel data analysis with data for the 1950–2010 period, we identify a negative response of coastal population counts to storm surges. However, when we decompose this effect over time, we observe that the negative response only begins in the two most recent decades, while for the first decade (1960), we see a net increase in populations in storm surge risk zones. Our findings oppose many existing studies that are based on older data or population projections, which show that people migrate to disaster-prone areas. With this chapter, we add to two strands of the literature, on the disaster impacts of tropical cyclones literature and on the settlement responses to natural disasters literature. Our findings and the generated data set can help policymakers to better understand the current exposure and past responses of coastal populations to the risk of storm surges.

Chapter 3

Natural disasters can have severe negative effects on local populations, and fast disaster aid is needed to reduce the potential damage. However, natural disasters also create possibilities for politicians to increase their prestige. The U.S. federal disaster declaration process is especially prone to this threat because, in this system, the decision to grant federal disaster aid funds relies solely on the president. Our theoretical model predicts that the president's discretionary power is greatest for medium-intensity disasters, when the public opinion on whether to grant aid is ambiguous. We test the model predictions in a multivariate panel fixed-effects model by using damage data of all hurricane strikes between the 1965–2018 period. We model the spatial destructiveness of hurricanes by using data on wind speed, rainfall, and storm surge damage. By interacting hurricane intensity with political alignment in a flexible regression, we show a nonlinear political alignment effect, which is most pronounced for medium-intensity hurricanes and about eight times higher than the average effect. Additionally, the effect is higher in election years and for hurricanes closer to the elections in November. In contrast to the alignment bias for medium-intensity hurricanes, we identify no political influence for low- and high-intensity hurricanes. Overall, we find that every year about USD 500 million are spent out of political motives for federal disaster relief. This corresponds to 13% of the overall hurricane-related aid. With this chapter, we add to several strands of the literature including the strand on alignment bias in intergovernmental transfers, the strand on accountability of politicians by the electorate, the strand on executive decision-making in the United States, and the strand on disaster impacts. Our analysis points out weaknesses in the U.S. federal disaster system which could be reduced, for example, by installing an expert commission for decisions regarding political disaster funds for low- and medium-intensity disasters, with the president remaining in charge of extreme events.

Chapter 4

The 2015 Nepal earthquake was one of the most destructive natural disasters in the history of Nepal. The damage was so great that, four days after the earthquake, a so-called UN flash appeal was issued, which calls for a coordinated disaster aid effort by the international community. The flash appeal identified 184 projects, and requested USD 422 million to help Nepal. By using a georeferenced data set of these aid projects, we first analyze the allocation decision of the design stage of the flash appeal. Our analysis combines data on physical damage, based on earthquake ground shaking intensities and house characteristics, socioeconomic data, electoral statistics, and geographical characteristics. We find that at the design stage aid projects are located in areas with the greatest amount of damage. However, other socioeconomic vulnerability variables do not play into the allocation decision. Out of the 184 proposed aid projects, only 64 actually received funding, and our analysis shows that these funding decisions were distorted by ethnic, political, and religious considerations. With this chapter, we contribute to the literature on humanitarian aid and disaster impacts. Our analyses show that need orientation on both stages – design and funding – for international flash appeals should be improved.

1 Unraveling the Effects of Tropical Cyclones on Economic Sectors Worldwide: Direct and Indirect Impacts

It has been published as:

Kunze, S. (2021). Unraveling the Effects of Tropical Cyclones on Economic Sectors Worldwide: Direct and Indirect Impacts. *Environmental and Resource Economics* 78, 545–569.

Abstract: This paper examines the current, lagged, and indirect effects of tropical cyclones on annual sectoral growth worldwide. The main explanatory variable is a new damage measure for local tropical cyclone intensity based on meteorological data weighted for individual sectoral exposure, which is included in a panel analysis for a maximum of 205 countries over the 1970–2015 period. I find a significantly negative influence of tropical cyclones on two sector aggregates including agriculture, as well as trade and tourism. In subsequent years, tropical cyclones negatively affect the majority of all sectors. However, the Input-Output analysis shows that production processes are sticky and indirect economic effects are limited.

1.1 Introduction

Tropical cyclones can have devastating economic consequences. Globally they are among the most destructive natural hazards. From 1980–2018 tropical cyclones were responsible for nearly half of all natural disaster losses worldwide, with damage amounting to an aggregate of USD 2,111 billion (Munich Re, 2018). Driven by climate change, at least in some ocean basins (Elsner et al., 2008; Mendelsohn et al., 2012), and the higher exposure of people in large urban agglomerations near oceans (World Bank, 2010), the overall damage and the number of people affected by tropical cyclones have been increasing since the 1970s (Guha-Sapir & CRED, 2020). Thus, tropical cyclones are and will continue to be a serious threat to the life and assets of a large number of people worldwide.

In order to design effective mitigation and adaptation disaster policies to this threat, it is important to understand the economic impact of natural disasters. Economic sectors most vulnerable to direct capital destruction of tropical cyclones must be identified. However, time-delayed effects must also be taken into account since some damage, such as supply-chain interruptions or demand-sided impacts, will only be visible after a certain time lag (Botzen et al., 2019; Kousky, 2014). Perhaps the most challenging task is to identify critical sectors that may be responsible for widespread spillover effects leading to substantial modifications in other sectors' production input schemes. This study aims to better understand the sectoral impacts of tropical cyclones by looking at the direct and indirect effects in a large data set covering 205 countries from 1970–2015. Additionally, a new damage measure is developed that considers the varying levels of exposure of different sectors.

From a theoretical perspective, a natural disaster can have both positive and negative effects. Direct negative impacts can result from the destruction of productive capital, infrastructure, or buildings, and thereby can generate a negative income shock for the whole economy (Kousky, 2014). Positive effects include, for instance, as a consequence of the destruction of capital, that the marginal productivity of capital increases, making it more attractive to invest in capital in the affected area (Klomp & Valckx, 2014). Furthermore, a shortage in the labor force can lead to a wage increase, which can serve as an incentive for workers from other regions to migrate to the affected region, also leading to a positive effect (Hallegatte & Przyluski, 2010). Given the different theoretical possibilities, it is not surprising that the empirically identified effects are rather ambiguous. They can best be summarized by three possible hypotheses: *recovery to trend*, *build-back-better*, and *no recovery* (Chhibber & Laajaj, 2008).

The *recovery to trend* hypothesis characterizes a pattern where after a negative effect in the short run, the economy recovers to the previous growth path after some time. Possible mechanisms for this situation are, for example, additional capital flows – such as remittances from relatives living abroad (Yang, 2008) – international aid (de Mel et al., 2012), insurance payments (Nguyen & Noy, 2019), or government spending (Ouattara & Strobl, 2013), which help the economy reach its pre-disaster income level. Other studies identify negative effects that are only significant in the short run but are insignificant in the long run (Bertinelli & Strobl, 2013; Elliott et al., 2015; Strobl, 2012). The *build-back-better* hypothesis describes a situation where natural disasters first trigger a downturn of the economy, which is then followed by a positive stimulus, leading to a higher growth path than in the pre-disaster period. This hypothesis is supported by empirical findings for a positive GDP growth effect for Latin American countries (Albala-Bertrand, 1993), for high-income countries (Cuaresma et al., 2008), and for a cross-section of 153 countries (Toya & Skidmore, 2007). In contrast to this, the *no recovery* hypothesis states that natural disasters can lead to a permanent decrease of the income level without the prospect of reaching the pre-disaster growth path again. This could result from a situation where recovery measures are not effectively implemented or where various negative income effects accumulate over time (Hsiang & Jina, 2014). Additionally, low- and middle-income countries suffer the greatest losses from natural disasters (Felbermayr & Gröschl, 2014).

This paper contributes to two strands of the literature. First, I add to the research area on the macroeconomic effects of disasters. Older empirical studies suffer to a large extent from endogeneity problems in their econometric analysis because their damage data are based on reports and insurance data, such as the Emergency Events Database (EM-DAT) database. Such data are positively correlated with GDP (Felbermayr & Gröschl, 2014) and prone to measurement errors (Kousky, 2014). More recent studies have started to use physical data, such as observed wind speeds, to generate a more objective damage function for the impacts of tropical cyclones (e.g., Bakkensen et al., 2018; Elliott et al., 2019; Felbermayr & Gröschl, 2014; Hsiang, 2010; Strobl, 2011). To address the varying economic exposure of affected areas, studies have used population (Strobl, 2012), nightlight intensity (Heinen et al., 2018) or exposed area (Hsiang & Jina, 2014) to weight the respective physical intensities of tropical cyclones. However, an area weight has the disadvantage of including largely unpopulated areas, such as deserts, which are economically meaningless. In contrast, for the agricultural sector, it would be misleading to take a nighttime light or a population weight, since these areas have a rather low population density. Therefore, I propose a new damage measure that explicitly considers these different exposures. For the agricultural sector, I use the fraction of exposed agricultural land, while for the remaining sectors, I use gridded population data.

Furthermore, only a minority of studies explicitly investigate the disasters' influences on sectoral economic development. For example, Loayza et al. (2012) investigate the effect of natural disasters on three sectors (agriculture, manufacturing, service) in a global sample for the period 1961–2005. Based on damage estimates from EM-DAT, the authors find a negative effect for the agricultural and a positive effect for the industrial sector. Based on physical intensity data, Hsiang (2010) analyzes the effect of Hurricanes on seven sectoral aggregates in a regional study for 26 Caribbean countries. He finds a negative effect for the ISIC sectors agriculture, hunting, forestry, and fishing (A&B), mining, and utilities (C&E), wholesale, retail trade, restaurants, and hotels (G–H), but a positive effect for the construction sector (F). Other studies analyze the disasters' impact on single sectors, such as the agricultural (Blanc & Strobl, 2016; Mohan, 2017) or the manufacturing sector (Bulte et al., 2018).

In total, I extend this research area in three ways: First, I introduce a new objective damage measure that allows for sector-specific exposure of tropical cyclones. It is based on a physical wind model and thereby overcomes criticism of report-based damage data. Second, I use this new damage data to analyze all (exposed) countries (84) to tropical cyclones worldwide, which allows me to obtain more generalizable results.[4] Third, I conduct a thorough assessment of the long-term sectoral influences of tropical cyclones, as there is evidence, that long-term effects on total GDP exist (Felbermayr & Gröschl, 2014; Hsiang & Jina, 2014; Onuma et al., 2020). For sectoral GDP effects, however, no such evidence exists so far.

Second and most importantly, I contribute to the literature on Input-Output analysis of natural disasters. While there exists a lot of theoretical work on the importance of cross-sectional linkages in consequence of a shock (see, e.g., Acemoglu et al., 2012; Dupor, 1999; Horvath, 2000), recent empirical studies focus on the shock propagation in production

[4]This is an improvement in comparison to Hsiang (2010) who only focuses on 26 Caribbean countries, which are highly exposed but only account for 11% of global GDP in 2015 (United Nations Statistical Division, 2015c).

networks within the United States of America (Barrot & Sauvagnat, 2016) or after single natural disasters, such as the 2011 earthquake in Japan (Boehm et al., 2019; Cole et al., 2019). These empirical studies all share that they use firm-level data to draw conclusions on upstream and downstream production disruptions. However, little is known about the empirical Input-Output effects across broader sectors after a natural disaster shock. In a single country study on floods in Germany, Sieg et al. (2019) show that indirect impacts are nearly as high as direct impacts. For tropical cyclones, no empirical cross-country study on indirect effects exists so far. With this paper, I close this research gap by using an Input-Output panel data set to analyze potential sectoral interactions after the occurrence of a tropical cyclone. This allows me to analyze whether any key sectors exist that, if damaged, result in direct damage of other sectors.

The main causal identification stems from the exogenous nature of tropical cyclones, whose intensity and position are difficult to predict even 24 hours before they strike (NHC, 2016). Based on a fine-gridded wind field model, I generate a new sector-specific damage measure weighted by either agricultural land use or population data. This exogenous measure allows me to identify an immediate negative growth effect of tropical cyclones for two out of seven sectoral aggregates including *agriculture, hunting, forestry, and fishing* and *wholesale, retail trade, restaurants, and hotels*. The largest negative impacts can be attributed to the annual growth in the *agriculture, hunting, forestry, and fishing* sector aggregate, where a standard deviation increase in tropical cyclone damage is associated with a decrease of 262 percentage points of the annual sectoral growth rate. This corresponds to a mean annual global loss of USD 16.7 billion (measured in constant 2005 USD) for the sample average. In the years following a tropical cyclone, the majority of sectors experience negative growth effects. Within the *agriculture, hunting, forestry, and fishing* sectors, the negative effects become less pronounced with a zero effect being present after four years, while the *wholesale, retail trade, restaurants, and hotels* sectoral aggregate experiences a persistent negative growth even after 20 years.

Based on the Input-Output analysis, there are only a small number of significant sectoral shifts. This suggests that the production chains of the economy are only slightly disrupted by tropical storms, and indirect impacts are thus negligible. Nevertheless, we can learn from this analysis the important role of those *manufacturing* sectors that are not directly affected. They are responsible for a demand shock in the *mining and quarrying* sectoral aggregate, leading to delayed negative growth effects being persistent over 10 years. At the same time, other sectors demand more from the *manufacturing* sectors, resulting in a zero aggregate negative effect for them. Additionally, within the *agriculture, hunting, forestry, and fishing* sectors, only the fishing sector experiences indirect negative effects. Moreover, for the vast majority of sectors, the indirect effects do not last longer than one year.

The remainder of this chapter is structured as follows: section 1.2 contains a description of the data source, introduces the construction of the tropical cyclone damage measure, and presents descriptive statistics. In section 1.3, the empirical approach is described. Section 1.4 presents the main results as well as robustness checks. Section 1.5 concludes with a discussion of the results and highlights policy implications.

1.2 Data

1.2.1 Tropical Cyclone Data

Tropical cyclones are large, cyclonically rotating wind systems that form over tropical or sub-tropical oceans and are mostly concentrated on months in summer or early autumn in both hemispheres (Korty, 2013b). Their destructiveness has three sources: damaging winds, storm surges, and heavy rainfalls. The damaging winds are responsible for serious destruction of buildings and vegetation. In coastal areas, storm surges can lead to flooding, the destruction of infrastructures and buildings, the erosion of shorelines, and the salinization of the vegetation (Le Cozannet et al., 2013; Terry, 2007). Torrential rainfall can cause serious in-land flooding, thereby augmenting the risk coming from storm surges (Terry, 2007).

Since the commonly used report-based EM-DAT data set (Lazzaroni & van Bergeijk, 2014) has been criticized for measurement errors (Kousky, 2014), endogeneity, and reverse causality problems (Felbermayr & Gröschl, 2014), I use meteorological data on wind speeds to generate a proxy for the destructive power of tropical cyclones.[5] This approach is in line with previous empirical studies (e.g., Hsiang, 2010; Strobl, 2011, 2012), but I advance this literature by generating a sector-specific damage function. I take advantage of the International Best Track Archive for Climate Stewardship (IBTrACS) provided by the National Oceanic and

[5]For example, Loayza et al. (2012) use data from EM-DAT as main input for their explanatory variables. They are, however, aware of data problems, such as incomplete reports, fluctuating quality of the reports, and correlation with GDP. Therefore, they take five-year averages of the number of affected people normalized by the total population as main explanatory variable. In comparison, in my analysis, I take meteorological data as input which is exogenous to the political and economic situation, contains all existing tropical cyclones, and has no quality fluctuations.

Atmospheric Administration (Knapp et al., 2010). It is a unification of all best track data on tropical cyclones collected by weather agencies worldwide. Best track data are a postseason reanalysis from different available data sources, including satellites, ships, aviation, and surface measurements, that are used to describe the position and intensity of tropical cyclones (Kruk et al., 2010).[6]

To calculate a new aggregate and meaningful measure of tropical cyclone damage separated by economic sectors on a country-year level, I make use of the CLIMADA model developed by Aznar-Siguan & Bresch (2019) at a resolution of 0.1°.[7] The model employs the well-established Holland (1980) analytical wind field model to calculate spatially varying wind speed intensities around each raw data observation track.[8] The model is restricted to raw data wind speed intensities above 54 km/h and it interpolates the 6-hourly raw data observations from the IBTrACS data to hourly observations.[9]

Consequently, for each grid point g, a wind speed S is calculated depending on the maximum sustained wind speed (M), the forward speed (T), the distance (D) from the storm center, and the radius of the maximum wind (R) [10]:

$$S_g = \begin{cases} \max(0, ((M - abs(T)) * \frac{R}{D}^{\frac{3}{2}} * e^{1-\frac{R}{D}^{\frac{3}{2}}}) + T), & \text{if } D < 10 * R \text{ from center to outer core} \\ 0, & \text{if } D > 10 * R \text{ out of radius.} \end{cases} \tag{1.1}$$

As a result, I generate hourly wind fields for each of the 7,814 tropical cyclones in my sample period (1970–2015).[11] Figure 1.1 illustrates the resulting modeled wind fields for Hurricane Ike in 2008 on its way to the U.S. coast. The individual colors represent different wind speed intensities. The wind speed drops with distance to the center of the hurricane and as soon as it makes landfall.

[6] Further details on the data on tropical cyclones can be found in Appendix 1.6.1.

[7] 0.1° corresponds to approximately 10 kilometers at the equator.

[8] See the CLIMADA manual for further details on the methods used https://github.com/davidnbresch/climada/blob/master/docs/climada_manual.pdf.

[9] For the latitude and longitude the model takes a spline interpolation, whereas for intensity and time observations it uses a linear interpolation.

[10] The radius of maximum wind (R, in km) is related to the latitude (L) of the respective raw data tropical cyclone position in the following way:

$$R = \begin{cases} 30, & \text{if } L \leqq 24° \\ 30 + 2.5 * abs(L) - 24, & \text{if } L > 24° \\ 75, & \text{if } L > 42°. \end{cases}$$

[11] Since the tropical cyclone data are available at global coverage since 1950, I will extend my database later for further specifications.

One major effort of this paper is to generate a new meaningful sectoral damage variable on a country-year level. In total, I use two different aggregation methods. First, I account for the economic exposure by weighting the maximum occurred wind speed per grid cell and year by the number of exposed people living in that grid cell relative to the total population of the country. This is a well-established method (Elliott et al., 2019; Heinen et al., 2018; Strobl, 2012). However, since agricultural areas are seldom highly populated using a population-weighted damage function for the agricultural sectors would be biased. Therefore, I propose a new spatial exposure weight for the agricultural sector, namely agricultural land, which consists of the sum of land used for grazing and crops in km^2 per grid cell. All weights are available in the HYDE 3.2 data set (Klein Goldewijk et al., 2017) at a spatial resolution of around 10x10 kilometers.[12] To avoid potential endogeneity concerns, I lag the respective weights by one period.

Figure 1.2 demonstrates why it is important to differentiate between exposed agriculture and population. Panel a displays the percentage of agricultural land, whereas b shows the distribution of population in Australia in 2008. A damage function that takes into account only the exposed population would underestimate the damage caused to the agricultural sector, given the large unpopulated but agriculturally used areas in the north and west of Australia.

It has been shown that the damage of tropical cyclones increases non-linearly with wind speed and occurs only above a certain threshold. I follow Emanuel (2011) by including the

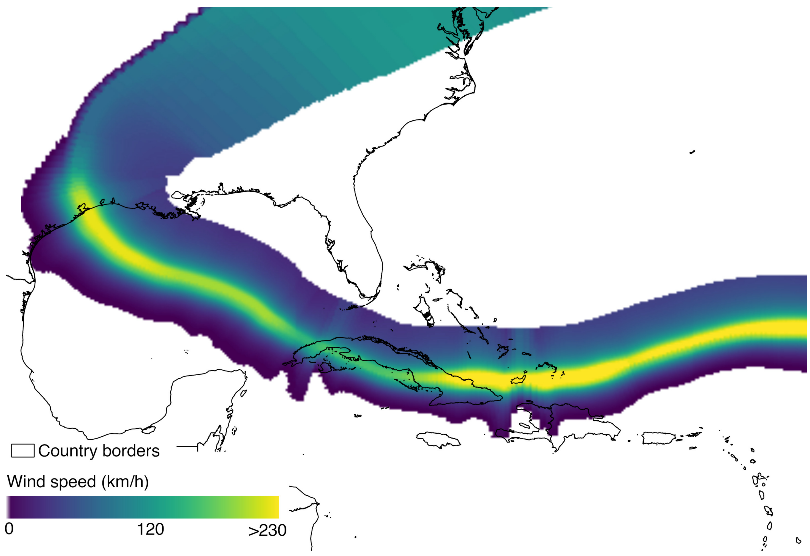

Figure 1.1: Wind field model for Hurricane Ike, 2008

[12] Before 2000, only decadal data are available. Hence, I interpolate the data to generate yearly observations.

cube of wind speed above a cut-off wind speed of 92 km/h. Taking all considerations together, I calculate the following tropical cyclone damage for each country i and year t:

$$Damage_{i,t} = \frac{\sum_{g \in i} w_{g,t-1}}{W_{i,t-1}} * \sum_{g \in i} S(max)^3_{g,t} \mathbb{1}_{S(max)>92}, \tag{1.2}$$

where $w_{g,t-1}$ are the exposure weights, agricultural land, or population, in grid g in period $t-1$. The sum of these exposure weights $w_{g,t-1}$ is divided by the total sum of the weights $W_{i,t-1}$ in country i in period $t-1$. This index is then multiplied by the cubed maximum wind speed $S(max)^3_{g,t}$ in grid g and year t as calculated by Equation 1.1 but only for values above 92 km/h.

There are two important points to note about this tropical cyclone damage variable. First, I only use the damage fraction due to maximum wind speed of tropical cyclones. Even though, I thereby omit potential rainfall and storm surge damage, it is a common simplification in the literature (Elliott et al., 2019; Hsiang, 2010; Strobl, 2011, 2012). However, to control for possible rainfall damage, I conduct a robustness test which includes a variable for precipitation (see Appendix Table 1.24 and and Figures 1.26–1.32) For storm surge damage this is not possible, since there exists no global data set so far.

Second, only the maximum wind speed per grid cell and year is used for the calculation of the tropical cyclone damage. This means that if a grid cell of a country was exposed to two storms in one year, only the physically more intense storm is considered. In the sample used, 70% of all grid-points are hit once by a tropical cyclone per year, whereas 20% are hit twice

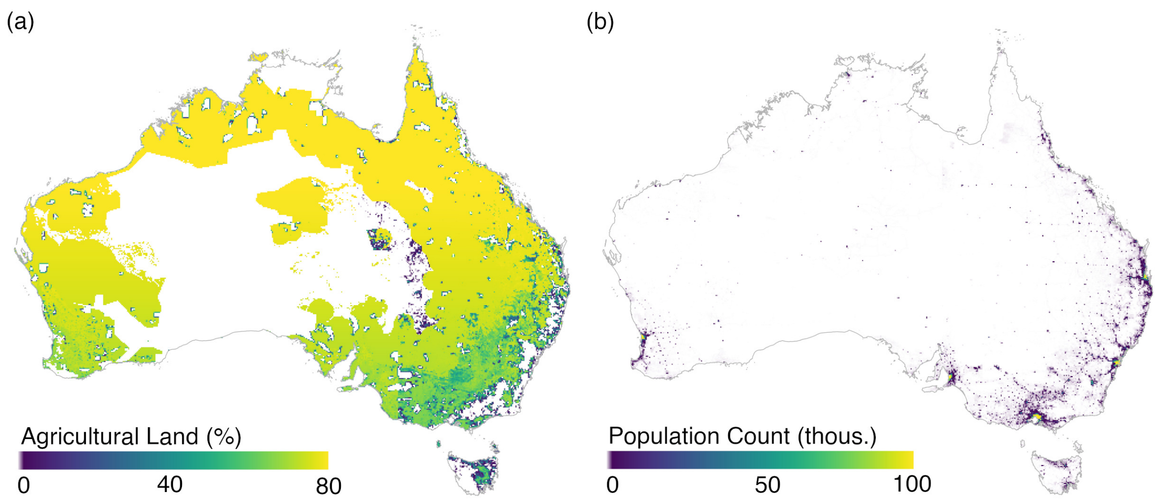

Figure 1.2: Agricultural land and population count in Australia, 2008

and 10% more than twice. To allow for the possibility of multiple tropical cyclones per year and country, I conduct two robustness tests. In the first test, I introduce a variable which counts the yearly frequency of tropical cyclones above 92 km/h per country (see Appendix Table 1.40 and Figures 1.26–1.32). In the second test, I take the mean wind speed cubed ($(S(mean)^3_{g,t})$) above 92 km/h per grid and year to calculate the $damage_{i,t}$ (see Appendix Table 1.41 and Figures 1.26–1.32).

1.2.2 Sectoral GDP Data

The sectoral GDP data originate from the United Nations Statistical Division (UNSD) (United Nations Statistical Division, 2015b). Sectoral GDP is defined as gross value added per sector aggregate and is collected for different economic activities following the International Standard Industrial Classification (ISIC) revision number 3.1. Gross value added is defined by the UNSD as "the value of output less the value of intermediate consumption" (United Nations Statistical Division, 2015a). The variables are measured in constant 2005 USD. The different economic activities are classified as follows with the respective ISIC codes given in parentheses: *agriculture, hunting, forestry, and fishing (A&B); mining, and utilities (C&E); manufacturing (D); construction (F); wholesale, retail trade, restaurants, and hotels (G–H); transport, storage, and communication (I); other activities (J–P)*, which include, inter alia, the financial and government sector. Appendix 1.6.2 provides a more detailed description of the composition of the individual ISIC categories. The data are collected every year for as many countries and regions as possible.[13] The sample used in my analysis covers the 1970–2015 period and includes a maximum of 205 countries.[14]

1.2.3 Input-Output Data

To analyze potential sectoral shifts within the economy after a tropical cyclone, I take advantage of the Input-Output data of EORA26 (Lenzen et al., 2012, 2013). It contains data on 26 homogeneous sectors for 189 countries from 1990 until 2015 and is the only Input-Output panel data set with (nearly) global coverage available. However, one disadvantage of the

[13]If the official data of the countries or regions are not available, the UNSD consults additional data sources. The procedure is hierarchical and reaches from other official governmental publications over publications from other international organizations to the usage of data from commercial providers (United Nations Statistical Division, 2015b).

[14]The sample is larger than the maximum size of recognized sovereign states as it also includes quasi-autonomous countries such as the Marshall Islands, if data are provided for them by the UNSD. Furthermore, one can argue that only countries exposed to tropical cyclones are relevant for this analysis; therefore, Table 1.36 provides a regression of the main result for exposed countries only.

EORA26 data set is that parts of the data are estimated and not measured. On the other hand, EORA26 works continuously on quality check reports and compares its result to other Input-Output databases such as GTAP or WIOD.[15]

To be consistent with the remaining analysis, I aggregate the given 26 sectors to the previously used seven sectoral aggregates.[16] For my analysis, I calculate the Input-Output coefficients by dividing the specific input of each sector by the total input of each sector given in the transaction matrix of the data:

$$IO_t^{j,k} = \frac{Input_t^{j,k}}{TotalInput_t^{j}} \tag{1.3}$$

The resulting Input-Output coefficients $IO^{j,k}$ range between 0 and 1 in year t. They indicate how much input from sector k is needed to produce one unit of output of sector j. Consequently, the Input-Output coefficients give an idea of the structural interactions of sectors within an economy and hence help to disentangle the indirect effects of tropical cyclone damage.[17]

1.2.4 Further Control Data

As tropical cyclones are highly correlated with higher temperature and precipitation (Auffhammer et al., 2013), I control for the mean temperature and precipitation of a country in further specifications. For both variables, I use the year-by-year variation calculated from the Climatic Research Unit (CRU) version 4.01, which is available at a resolution of approximately 5 kilometers since 1901 (University of East Anglia Climatic Research Unit et al., 2017). Together with further control variables, Table 1.2 in Appendix 1.6.3 lists the exact definition of all variables used.

1.2.5 Descriptive Statistics

Figure 1.3 shows the country-year observations of the tropical cyclone damage variable for (a) exposed agricultural land and (b) exposed population. Country-year observations above two standard deviations are labeled with the respective ISO3 code. While the distribution reveals

[15]I decide not to use the WIOD database because its country sample is not very exposed to tropical cyclones. Additionally, the GTAP database is not available to me and only covers a few years.

[16]I also explore the effects on the 26 individual sectors later in this paper.

[17]I decide to only examine changes in the Input-Output coefficients and not indirect costs because this approach almost needs no assumptions. Input-Output models that analyze indirect costs, such as the Inoperability Input-Ouptut model (Haimes & Jiang, 2001) or the Ghosh model (Ghosh, 1958), require many problematic assumptions (Oosterhaven, 2017).

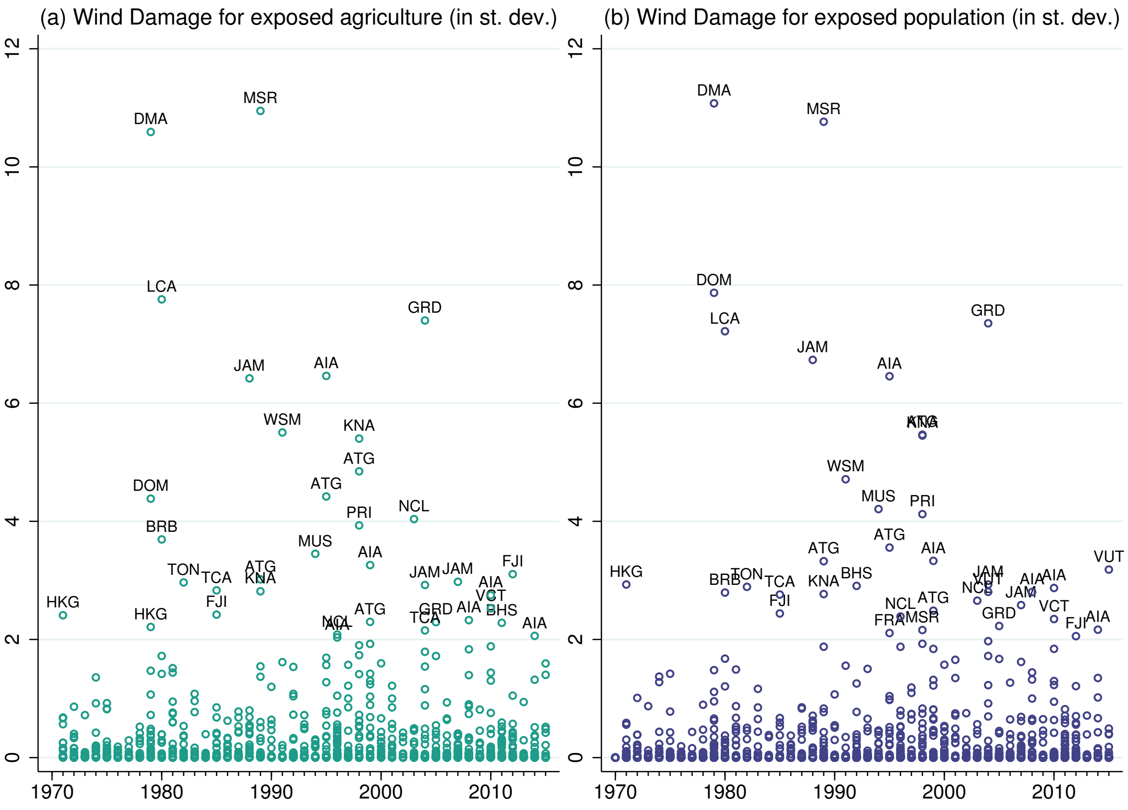

Figure 1.3: Distribution of tropical cyclone damage, 1970–2015

Notes: This figure demonstrates the distribution of the tropical cyclone damage variable (in standard deviations) for exposed agricultural areas (a) and exposed population (b) from 1970–2015.

that on average, geographically smaller countries, such as Hong Kong, Dominica or Jamaica, have a higher damage, there exists a difference between both damage measures, even for the highly exposed countries. Moreover, extreme damaging tropical cyclones are relatively rare. A one standard deviation strong event has a probability of 8.9% among events above zero for agricultural damage and 8% for population damage.[18]

To demonstrate the average intersectoral connections within my sample, Figure 1.4 displays the average Input-Output coefficients for all countries for all available years (1990–2015). The different colors represent different average coefficients, ranging from 0 (light purple) to 0.24 (dark purple). On average, the sector aggregates *agriculture, hunting, forestry, and fishing (A&B)* and *mining and utilities (C&E)* are only slightly dependent on other sectors, while there is a stronger dependence for the remaining sectoral aggregates. The cross-sectoral dependence is most pronounced for *manufacturing (D)* and *other activities (J–P)*. This is not surprising since the *manufacturing (D)* sector needs a lot of input materials from other

[18]The underlying calculations for these numbers are as follows: agricultural damage: $91/1027 = 0.0886$, population damage: $82/1035 = 0.0801$.

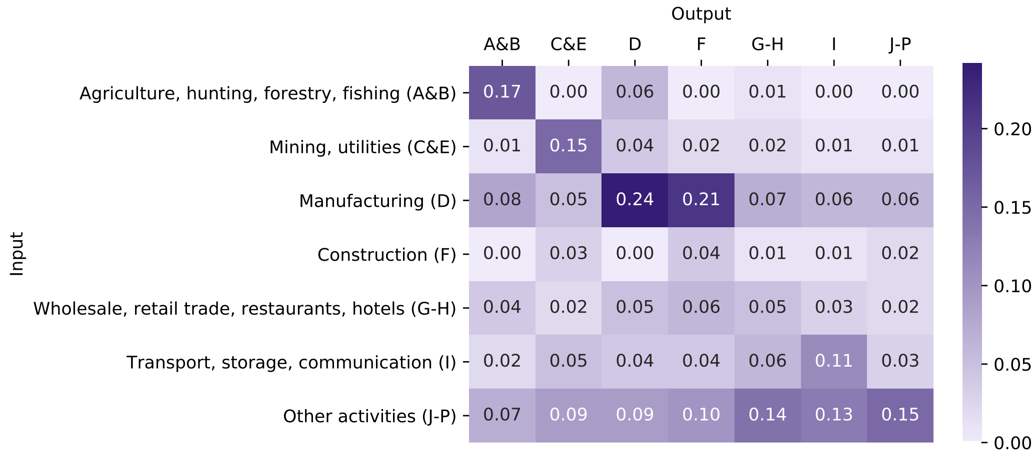

Figure 1.4: Heatmap of Input-Output coefficient averages, 1990–2015

Notes: Input-Output coefficients show how much input one sector needs to produce one unit of output. The coefficients range between zero and one.

sectors (Sieg et al., 2019), and the sector *other activities (J–P)* comprises, among others, the financial sector. Tables 1.3 and 1.4 in Appendix 1.6.4 show the main descriptive statistics for all variables used in this study.

1.3 Empirical Approach

1.3.1 Direct Effects

In order to examine tropical cyclones as exogenous weather shocks, I pursue a panel data approach with year and country fixed effects in a simple growth equation framework (Dell et al., 2014; Strobl, 2012). The analysis is conducted on a country-year level. To identify the causal effects of tropical cyclone intensity on sectoral per capita growth, I use the following set of regression equations, which constitutes my main specifications:

$$Growth^{j}_{i,t-1->t} = \alpha^{j} + \beta^{j} * Damage_{i,t} + \gamma^{j} * \mathbf{Z}_{i,t-1} + \delta^{j}_{t} + \theta^{j}_{i} + \mu^{j}_{i} * t + \epsilon^{j}_{i,t}, \tag{1.4}$$

where the dependent variable $Growth^{j}_{i,t-1->t}$ is the annual value added per capita growth rate of sector j in country i. The main specification is estimated for each of the $j(=1,\ldots,7)$ sector aggregates separately. $Damage_{i,t}$ is the derived damage function for country i at year t from Equation 1.2. Consequently, β^{j} is the coefficient of main interest in this specification. By calculating the annual sectoral GDP per capita growth rate, I lose the first year of observation of the panel. The sample period hence reduces to 1971–2015. In further specifications, I include additional control variables $\mathbf{Z}_{i,t-1}$ to account for potential socioeconomic or climatic influences. Moreover, I include time fixed effects δ_t to account for time trends and other events common to all countries in the sample. The country fixed effects θ_i control for unobservable time-invariant country-specific effects, such as culture, institutional background, and geographic location. Additionally, I allow for country-specific linear trends $\mu_i * t$. This assumption is relaxed in further specifications by allowing more flexible country-specific trends (e.g., squared). The error term $\epsilon_{i,t}$ is clustered at the country level.

The growth literature predicts that some potential positive or negative impacts of natural disasters emerge only after a few years. It is therefore important to examine their effects over time (Felbermayr & Gröschl, 2014). To analyze the effect of tropical cyclones in the longer run, I introduced lags of the tropical cyclone damage variable to the main specification 1.4. Since the tropical cyclone data has global coverage since 1950, I am able to introduce lags of up to 20 years without losing observations of my dependent variable, which ranges from 1971–2015. This allows me to identify which of the competing hypotheses – *build-back-better*, *recovery to trend*, or *no recovery* – is appropriate for which sector. In detail, this model can be described by the following set of regression equations:

$$Growth^{j}_{i,t-1->t} = \alpha^{j} + \sum_{L=0}^{20}(\beta^{j}_{t-L} * Damage_{i,t-L}) + \gamma^{j} * \mathbf{Z}_{i,t-1} + \delta^{j}_{t} + \theta^{j}_{i} + \mu^{j}_{i} * t + \epsilon^{j}_{i,t}, \quad (1.5)$$

where all variables are defined as in Equation 1.4. I show point coefficient estimates as well as accumulated effects and error statistics calculated via a linear combination of the lagged β_{t-L} coefficients.[19]

1.3.2 Indirect Effects

To analyze potential indirect effects which could emerge because of changes in the Input-Output composition of the individual sectors, I test the following set of equations for the different Input(j)-Output(k) combinations:

$$IO^{j,k}_{i,t} = \alpha^{j,k} + \beta^{j,k} * Damage_{i,t} + \lambda^{j,k} * IO^{j,k}_{i,t-1} + \gamma^{j,k} * \mathbf{Z}_{i,t-1} + \delta^{j,k}_{t} + \theta^{j,k}_{i} + \mu^{j,k}_{i} * t + \epsilon^{j,k}_{i,t}, \quad (1.6)$$

[19] This approach follows Hsiang & Jina (2014) which analyze the accumulated long-term GDP growth effects of tropical cyclones worldwide. I expand their approach by not looking at overall GDP but at disaggregated GDP responses for seven sectoral aggregates. Furthermore, I use a more specific damage function than Hsiang & Jina (2014) which takes account of different sectoral exposure.

where $IO_{i,t}^{j,k}$ indicates the Input-Output coefficient of sectors j and k in year t and country i. Depending on the level of aggregation, I run 49 (7*7) or 676 (26*26) different regressions. In contrast to Equation 1.4 I introduce a lagged dependent variable, since I suspect a strong path dependence of the Input-Output coefficient, i.e., most sectors plan their inputs at least one period ahead. Additionally, the lagged dependent variable controls for a sluggish adjustment to shocks of the individual sector input composition. The remaining variables are defined as in Equation 1.4. In general, this analysis reveals production scheme transformations that can result from both supply and demand changes of the sectors due to tropical cyclones.

1.3.3 Identification Strategy

The main causal identification stems from the occurrence of tropical cyclones, which are unpredictable in time and location (NHC, 2016) and vary randomly within geographic regions (Dell et al., 2014). As demonstrated in Figure 1.3, their intensity and frequency are spread considerably between years and countries. Additionally, tropical cyclone intensity is measured by remote sensing methods and other meteorological measurements. After controlling for country and time specific effects, my estimation approaches allow for a causal identification of the direct and indirect responses to tropical cyclones' damages with only little assumption needed (Dell et al., 2014). To underpin the causal identification, I conduct a falsification test, where I introduce leads instead of lags of the $Damage$ variable, as well as a Fisher randomization test. Furthermore, one could also argue that the estimation results are biased by the fact that certain regions have a higher exposure to tropical cyclones than others. However, the country fixed effects partly control for this concern. Additionally, I cluster the standard errors at broader regional levels as a further robustness test.

As tropical cyclones are exogenous to sectoral economic growth, the greatest threat to causal identification could arise by omitting important time-varying climatic variables that are correlated with tropical cyclones (Auffhammer et al., 2013). Therefore, I include the mean level of temperature and precipitation as additional climate controls in a further specification. Both variables are associated with the occurrence of tropical cyclones since they only form when water temperatures exceed 26 °C and torrential rainfalls usually constitute part of them.

To be in line with the related growth literature, I estimate a further specification where I add a set of socioeconomic control variables (Felbermayr & Gröschl, 2014; Islam, 1995; Strobl, 2012). It comprises the logged per capita value added of the respective sector j to simulate a dynamic panel model, the population growth rate, a variable for openness (i.e., imports plus exports divided by GDP), and the growth rate of gross capital formation.[20] Including these socioeconomic control variables introduce some threats to causal inference. First, as shown by Nickell (1981), there is a systematic bias of panel regressions with a lagged dependent variable and fixed effects. However, it has been demonstrated that this bias can be neglected if the panel is longer than 15 time periods (Dell et al., 2014). As my panel has a length of 25–45 years, depending on the chosen model, I assume this bias will not influence my analysis.[21] Second, all control variables are measured in *t-1* to reduce potential endogeneity problems stemming from the fact that control variables in t can also be influenced by tropical cyclone intensities in t (Dell et al., 2014). Admittedly, this will not fully solve potential endogeneity problems, and concerns about bad controls (Angrist & Pischke, 2009) and “over-controlling” (Dell et al., 2014) remain.

Finally, the standard errors $\epsilon_{i,t}$ could be biased by the autocorrelation of unobservable omitted variables (Hsiang, 2016). To deal with this problem, I will re-estimate my regression models with Newey-West (Newey & West, 1987) as well as spatial HAC standard errors (Fetzer, 2020; Hsiang, 2010), which allow for a temporal correlation of 10 years and a spatial correlation of 1000 kilometer radius.[22]

Generally speaking, the proposed models offer a simple but strong way for causal interpretation of the impact of tropical cyclones on sectoral growth. The weighted tropical cyclone damage variables are orthogonal to economic growth as well as the Input-Output coefficients, and the panel approach allows me to identify the causal effect.

[20] The logged per capita value added is not included for the robustness tests of the indirect effects of model 1.6, because it already compromises a lagged dependent variable.

[21] For the dynamic analysis, the panel length is 65 years, and for the Input-Output regression, it comprises 20 years.

[22] I tested my data extensively for outliers having a high influence on my results. In particular, I calculated the leverage and dfbeta of the *damage* coefficient. Observations were excluded if they were above the $(2k + 2)/n$ threshold for leverage and above the $2/sqrt(n)$ threshold for dfbeta. In total, I exclude five country-year observations from my analysis: Dominican Republic 1979, Grenada 2004, Montserrat 1989, Myanmar 1977, and Saint Lucia 1980. However, as an additional robustness test, I also show a regression where I include these outliers and the results remain unchanged.

1.4 Results

1.4.1 Direct Effects

Table 1.1 presents the results of the main specification for each of the seven annual sectoral GDP per capita growth rates. The coefficients show the increase of the respective damage variable by a standard deviation. Previous empirical studies on the relationship between economic development and tropical cyclone damage found a negative influence on GDP growth (e.g., Bertinelli & Strobl, 2013; Gröger & Zylberberg, 2016; Strobl, 2011). My results indicate that this negative aggregate effect can be attributed to two sectoral aggregates, including *agriculture, hunting, forestry, and fishing; manufacturing* and *wholesale, retail trade, restaurants, and hotels.* Tropical cyclones have the largest negative effect on the *agriculture, hunting, forestry, and fishing* aggregate compared to other sectoral aggregates. The absolute size of this effect is approximately more than 2.5 times the size of the coefficient in the *wholesale, retail trade, restaurants, and hotels* sector aggregate. In general, a one standard deviation increase in tropical cyclone damage is associated with a decrease in the annual growth rate in the sector aggregate *agriculture, hunting, forestry, and fishing* of 2.62 percentage points. For the sample average (0.88) of the regression of Column (1), this effect

Table 1.1: The effect of tropical cyclone damage on sectoral GDP growth

Dependent Variables: *Per capita growth rate (%) in sector aggregate*

	Agriculture, hunting, forestry, fishing	Mining, utilities	Manu-facturing	Construc-tion	Wholesale, retail trade, restau-rants, hotels	Transport, storage, communi-cation	Other activities
	(1)	(2)	(3)	(4)	(5)	(6)	(7)
Damage_t	-2.6219***	-0.7682	-0.7242	0.7306	-1.1552**	-0.4861	-0.1886
	(0.4582)	(0.8424)	(0.5211)	(0.6645)	(0.5129)	(0.3649)	(0.2642)
	[0.0000]	[0.3629]	[0.1661]	[0.2729]	[0.0254]	[0.1843]	[0.4762]
N	8,500	8,500	8,500	8,500	8,500	8,500	8,500
Clusters	205	205	205	205	205	205	205
P-value	0.0000	0.3629	0.1661	0.2729	0.0254	0.1843	0.4762
Mean DV	0.8800	3.7458	2.6095	3.2388	2.5256	3.7030	2.5519

Notes: $*p < 0.1, **p < 0.05, ***p < 0.01$. Panel OLS regression results with clustered standard errors by countries in parentheses (), and p-values in brackets []. The coefficients show the effect of a one standard deviation increase in tropical cyclone damage on the per capita growth rate in a given sectoral aggregate. The standard deviations are 2,236,738 for the agricultural and 2,269,395 for the remaining sectors, calculated for the whole sample of positive wind speed observations. The sample covers the period 1971 through 2015. Damage_t is the weighted damage measure for tropical cyclone intensity in year t. For the sector aggregate agriculture, hunting, forestry and fishing it is weighted by exposed agricultural land in t-1, whereas for the remaining sector aggregates it is weighted by exposed population in t-1. All regressions include country and year fixed effects as well as country-specific linear trends.

can be translated into a decrease of 298 percent, as displayed in Figure 1.5. In terms of total losses, this decrease results in a mean yearly loss of USD 16.7 billion (measured in constant 2005 USD) for the sample average (USD 5.63 billion). This large negative effect is not surprising. The agricultural sector relies heavily on environmental conditions as most of its production facilities lie outside of buildings and are hence more vulnerable to the destructiveness of tropical cyclones. In addition to damaging wind speed, salty sea spread and storm surge can cause salinization of the soil, leaving it useless for cultivation.

These results are line with previous empirical studies. Hsiang (2010) also finds the largest negative effects of tropical cyclones for the agricultural sector aggregate, while Loayza et al. (2012) demonstrate that only the agricultural sector is negatively affected. Mohan (2017) provides further evidence that in Caribbean countries agricultural crops are more severely affected by hurricanes compared to livestock.

For the sector aggregate *wholesale, retail trade, restaurants, and hotels*, a one standard deviation increase in tropical cyclone damage cause a decrease of -1.16 percentage points of the annual per capita growth rate. Put in relation to the sample average per capita growth rate (2.53%), the effect translates to a decrease of -46%. Hsiang (2010) also finds a negative effect of hurricanes for this sectoral aggregate for the Caribbean countries, whereas Loayza

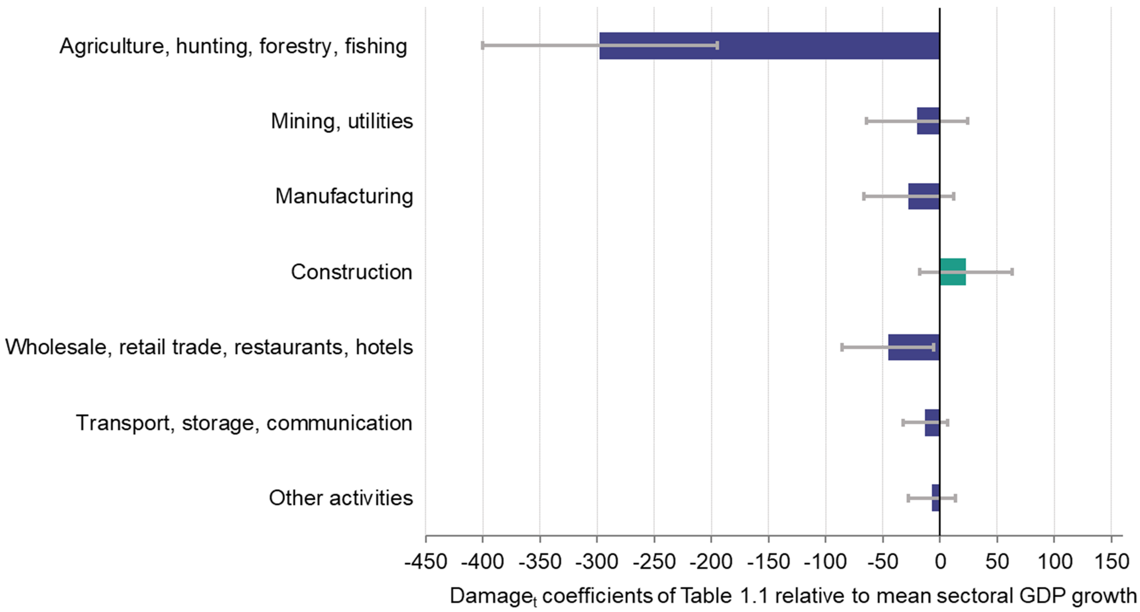

Figure 1.5: Effects of tropical cyclone damage on sectoral GDP growth

Notes: This figure shows the effect of a one standard deviation increase in tropical cyclone damage on the per capita sectoral GDP growth rate compared to the sample average (in %). The error bars depict the 95% confidence intervals.

et al. (2012) find no significant for the service sector.[23] Likely reason for this downturn could be less (domestic and international) touristic income for the restaurant and hotel sectors (Hsiang, 2010; Lenzen et al., 2019). In consequence to tropical cyclone damage, less tourists visit affected countries (Hsiang, 2010), since they perceive these destinations as too risky to travel to (Forster et al., 2012).

It is not empirically clear how long past tropical cyclones influence present economic growth rates. While some studies provide evidence of only a short-term economic impact of tropical cyclones (Bertinelli & Strobl, 2013; Elliott et al., 2019), Felbermayr & Gröschl (2014) show that storms from the previous five years can also have a negative growth effect. In addition, in a recent working paper, Hsiang & Jina (2014) even demonstrate a long-term negative impact of tropical cyclones of up to 20 years.

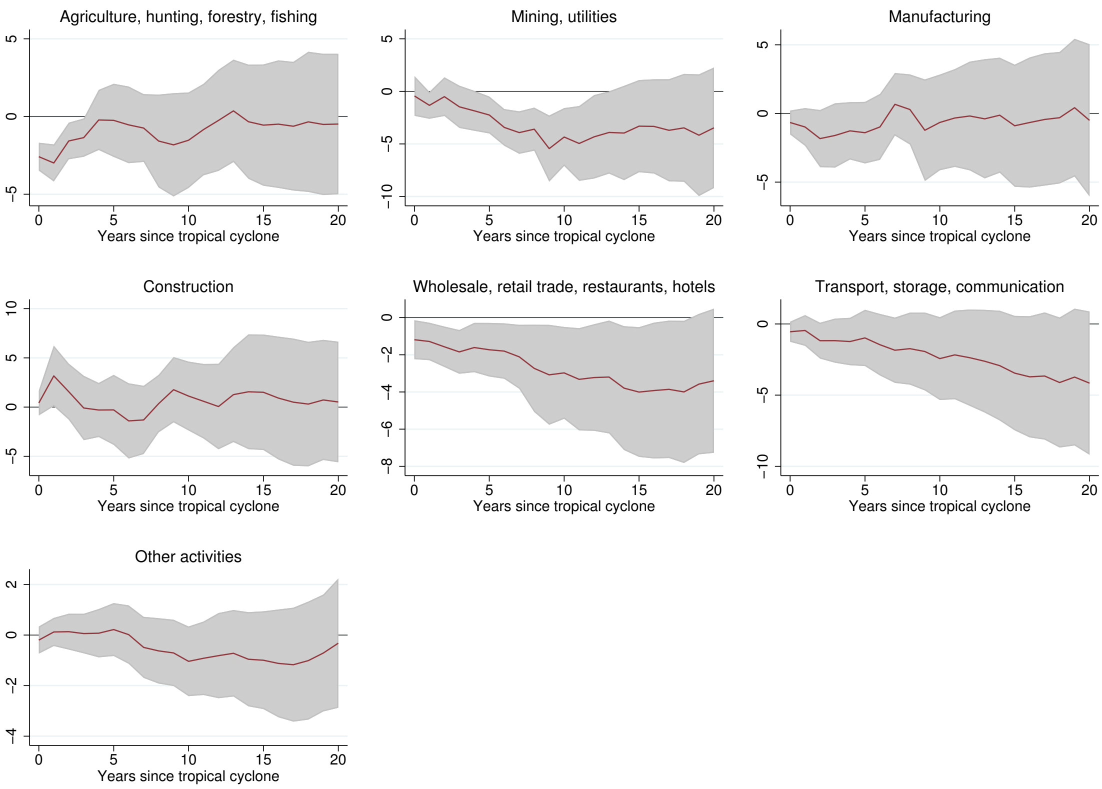

Figure 1.6: Cumulative lagged influence of tropical cyclone damage on sectoral GDP growth (20 years)

Notes: The y-axis displays the cumulative coefficient of tropical cyclone damage on the respective per capita growth rates, and the x-axis shows the years since the tropical cyclone passed. The gray areas represent the respective 95% confidence intervals and the red line indicates the respective (connected) cumulative point estimates. The underlying estimations can be found in Tables 1.12–1.13 in Appendix 1.6.4.

[23] Loayza et al. (2012) only differentiates between three sectors: agriculture, manufacturing, and service.

Figure 1.6 illustrates the cumulative point estimates of the past influence of tropical cyclone damage on the different sectoral growth variables.[24] The x-axis represents the lags of the damage variable, while the y-axis indicates the size of the cumulative coefficient β (in standard deviations). The gray shaded area specifies the respective 95% confidence bands, and the red line depicts the connected estimates. Appendix 1.6.4 presents further statistics: Figures 1.13–1.15 show the cumulative results for different lag lengths (5, 10, 15), and Tables 1.12–1.13 exhibit the underlying estimations. The individual point estimates are shown in Figures 1.9–1.12, while Tables 1.5–1.11 show the regression results.

Figure 1.6 demonstrates that three out of seven sectoral aggregates suffer from delayed negative impacts of tropical cyclones. The *agriculture, hunting, forestry, and fishing* sector aggregate first depicts negative growth rates but then quickly recovers after four years. Despite having the largest negative shock, destroyed capital is relatively quickly replaced. The situation is completely different in the *wholesale, retail trade, restaurants, and hotels* sector aggregate, where a negative influence can be observed over almost the entire 20-year period. This finding undermines the evidence presented in the main specification: Even several years after the occurrence of a tropical cyclone, tourists avoid restaurants and hotels in devastated areas. This behavior most likely speaks for an enduring risk adjustment of tourists.

Surprisingly, the sector aggregate *mining and utilities* turns negative three years after the tropical cyclone has hit the country. As section 1.4.2 demonstrates, this effect may be driven by less demand from the *manufacturing* sectors. Upon examining the underlying estimates in Tables 1.12-1.13 in Appendix 1.6.4, it is evident that the *transport, storage, communication* sectoral aggregate also turns negative, at least at the 90% confidence interval.[25]

In total, the majority of all sectoral aggregates experience lagged negative growth effects due to tropical cyclones. This finding clearly opposes the *build-back-better* hypothesis as well as the *recovery to trend* hypothesis. It rather points to the presence of (delayed) negative effects of tropical cyclones from which the sectors cannot recover. The result offers a better understanding of the finding of Hsiang & Jina (2014), who show that tropical cyclones have long-lasting negative impacts on GDP growth by demonstrating which sectors are responsible

[24] The cumulative effects are calculated by F-tests of the respective lag lengths; for example, the coefficient and confidence intervals after two years are calculated by the F-test: Damage+L1.Damage+L2.Damage. The tests are conducted with the STATA command `parmest` (Newson, 1998).

[25] After one year, we can also detect a positive effect in the construction sector, which is not surprising given the higher number of orders due to reconstruction efforts.

for the long-lasting GDP downturn that they identify. Additionally, this finding undermines the urgency to analyze past influences beyond one or two years when examining the economic impacts of natural disasters.

1.4.2 Indirect Effects

The analysis of the past influences of tropical cyclone damage demonstrates that the sectoral growth response following a tropical cyclone is a complex undertaking. It remains unclear if there exists some key sector, which, if damaged, results in a negative shock for the other sectors. Additionally, it is unexplained how the sectors are interconnected and if their structural dependence changes. Therefore, in this section, I investigate, by means of the Input-Output analysis, how the sectors change their interaction after a tropical cyclone has hit a country. This will provide further insights into whether production processes are seriously distorted by tropical cyclones. To the best of my knowledge, this is the first paper that analyzes global sectoral interactions after the occurrence of a tropical cyclone.

Since the sample period is reduced to 1990–2015 due to data availability, I re-estimated the regression model of the main specification 1.2 for the reduced sample of model 1.6. Table 1.21 in Appendix 1.6.4 reveals that even with the smaller sample, all previously found effects can be identified again. Therefore, we can be sure that the reduced sample size does not drive the new results.

Figure 1.7 illustrates the connections of significant changes of the Input-Output coefficient together with the effect size relative to the sample average of the respective Input-Output coefficients in parentheses (in %) resulting from model 1.6. The coefficients are interpreted by a one standard deviation increase in tropical cyclone damage (above zero).[26] For example, due to a standard deviation increase of tropical cyclone damage, the *manufacturing* sectors use 0.66% less input from the construction sector aggregate relative to the average Input-Output coefficient (0.0045) to produce one unit of output. The red and green arrow colors represent significant negative and positive effects, whereas the color intensities denote different p-values. Circle diameters represent the average proportional share on total GDP ranging from 32% (*other activities*), over 12% (*manufacturing*) to 6% (*construction*).[27]

[26] The underlying estimations can be found in Tables 1.14–1.20 in Appendix 1.6.4.

[27] The other proportional shares on total GDP are: *Wholesale, retail trade, restaurants, hotels* (15%); *agriculture, hunting, forestry, fishing* (14%); *mining and utilities* (10%); *transport, storage, communication* (8%).

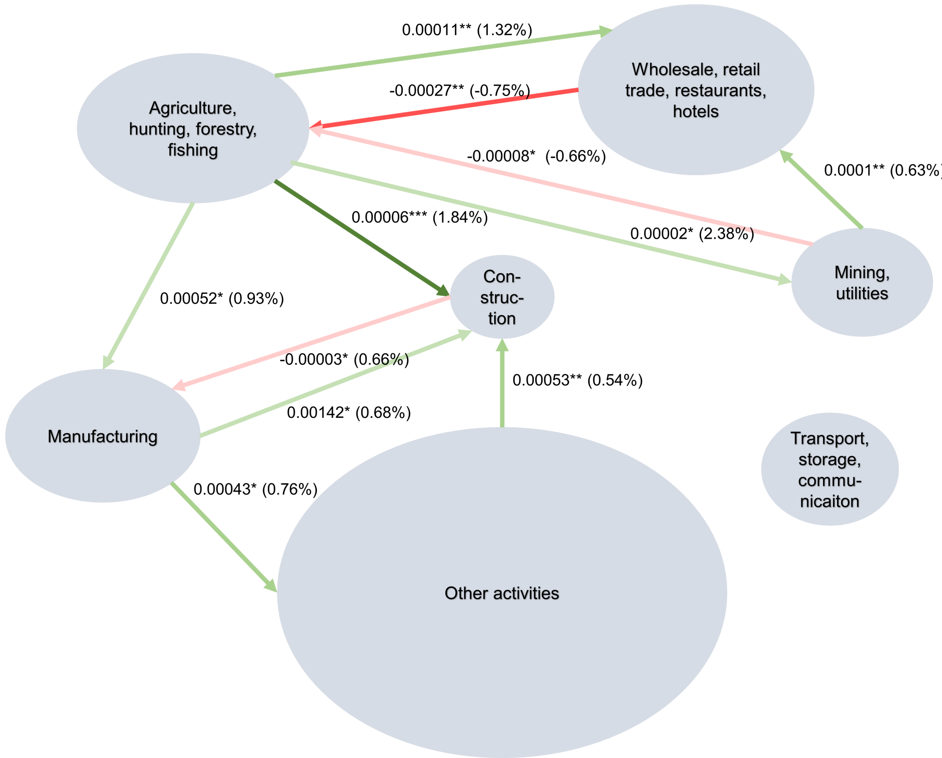

Figure 1.7: Significant effects of tropical cyclone damage on Input-Output coefficients

Notes: This figure shows the significant effects of a one standard deviation increase in tropical cyclone damage on the respective Input-Output coefficient. The number in parentheses compares the coefficients to the sample average of the respective Input-Output coefficient (in %). Note that Input-Output coefficients can only range between 0–1. Circle diameter is proportional to the average sectoral share on total GDP. The arrows depict all significant coefficients between the sectoral aggregates, with negative coefficients in red and positive in green. The start of the arrow shows the input, and the end denotes the respective output. Asterisks and color intensities indicate p-values according to: *** p<0.01, ** p<0.05, * p<0.1.

Tropical cyclones only lead to a small number of production process changes with coefficients being relatively small. Out of 49 parameter estimates, only 12 are significantly different from zero.[28] As expected, the heavily damaged *agriculture, hunting, forestry, and fishing* sector aggregate experiences the most changes. It asks for less input from the *wholesale, retail trade, restaurants, hotels* and *mining and utilities* sector aggregates, which results from a supply shock in the agricultural sector. Concurrently, the *construction* sector demands significantly more input (1.84%) from the *agriculture, hunting, forestry, and fishing* sector. This change can be regarded as reconstruction efforts, which is also reflected in the relatively rapid recovery of the agricultural sector aggregate in Figure 1.6. The second most indirectly affected sector is the *construction* sector. It demands more input from three other sector aggregates, while the *manufacturing* sectors use less input from it. Given these positive

[28]The manufacturing sectors use significantly less input from itself, which is not shown in Figure 1.7.

demand effects, one may ask why a significant contemporaneous positive direct effect for the *construction* sector cannot be seen. One reason could be that the destruction of productive capital outweighs the higher number of orders. However, one year later, as shown in Figure 1.6, these positive demand shocks lead to a positive growth impulse in the *construction* sector.

Compared to the existing literature, the non-existing of a direct positive contemporaneous response of the construction sector is a new finding. For example, Hsiang (2010) finds an immediate positive response of the construction sector. In a similar manner, Mohan & Strobl (2017) find evidence that a positive growth effect of the construction sector, financed by international aid or government programs, lead to a fast recovery of South-Pacific Islands after tropical cyclones.[29]

Since the EORA26 database also offers the data decomposed for 26 sectors, this section demonstrates the results of model 1.6 in more detail. It would be tedious to show 26x26 regression models; Figure 1.8 thus reduces the complexity of the analysis by showing only the sign of the significant coefficients together with color intensities representing different p-values.

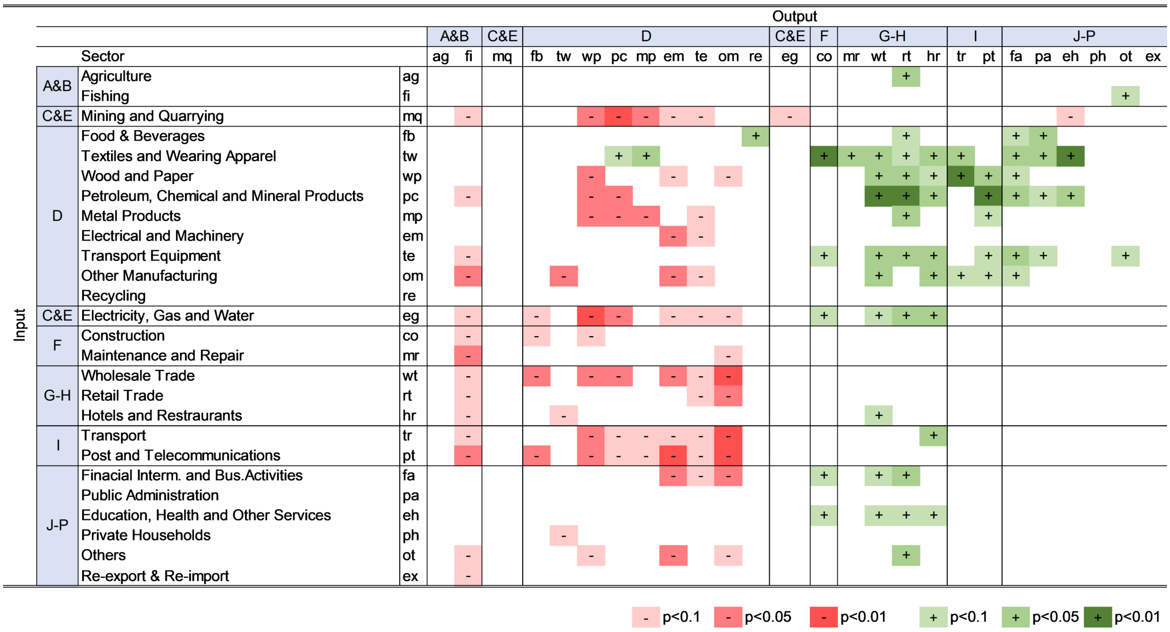

Figure 1.8: Significant effects of tropical cyclone damage on disaggregated Input-Output coefficients

Notes: The colored areas depict all significant coefficients between the sectors, with negative coefficients in red and positive in green. Color intensities indicate p-values according to: p<0.01, p<0.05, p<0.1.

[29] I also tested for lagged cumulative effects. The results can be found in Figure 1.16 in Appendix 1.6.4. They show that there are nearly no lagged responses present. I also checked for different lag lengths, but could hardly find any effect above a lag length of five years.

Figure 1.8 reveals some patterns that are not visible on the aggregate level. The most interesting changes can be observed within the single sectors of the *manufacturing (D)* aggregate. They ask significantly less input from other sector aggregates, while, at the same time, sectors from other aggregates ask more input from the *manufacturing* sectors. These opposing production changes may be one of the reasons why we can see no aggregate direct cost effects. Nevertheless, it unveils the importance of the *manufacturing* sectors, as already demonstrated by their strong intersectoral connection in Figure 1.4. This importance for the sectoral composition was already demonstrated by Bulte et al. (2018). The authors find that after the 2008 Wenchuan Earthquake neighboring counties suffer from indirect negative growth effects due to changes within the manufacturing sectors.

The sectors least affected by indirect changes are the *agriculture (ag), recycling (re), private households (ph)*, and *export (ex)* sectors. Figure 1.8 also offers an explanation for the downturn of the *mining and utilities (C&E)* sector aggregate after some years, as shown in Figure 1.6: The *manufacturing* sectors ask significantly less input from it. Additionally, it becomes clear that the *fishing* sector is responsible for the negative supply shock in the *agriculture, hunting, forestry, and fishing* sector aggregate. Possible reasons for these indirect effects, could be changes in fishing patterns in response to tropical cyclones (Bacheler et al., 2019) or the destruction of vessels. While the importance of the fishing sector for indirect tropical cyclones' effects is a novel finding, it does not mean that other agricultural sectors do not exhibit negative direct effects.[30]

It is evident from this analysis that many potential production changes are canceled out because of counteracting indirect effects. This may be the reason why, on the aggregate level for indirect influences (see Figure 1.7), we can only see significant changes in one quarter of all Input-Output connections, while in Model 1.4 for the direct costs, only two sector aggregates are negatively affected. Furthermore, although the *manufacturing* sector shows no direct monetary damage, it is responsible for several changes in the production schemes of other sectors, leading to a monetary downturn in the *mining and utilities (C&E)* sectoral aggregate.

[30] In light of this finding, one could question the reliability of the agricultural weighting scheme for the damage variable. Therefore, I re-estimate the results of Equation 1.4 and 1.6 with the population weighted damage for the agricultural sectoral aggregate. Appendix Table 1.43 and 1.54 show that the results remain qualitatively unchanged.

1.4.3 Sensitivity Analysis

To underline the credibility of my regression analyses, I test the sensitivity of my results in various ways. First, I run two randomization tests: a Placebo test by using leads instead of the contemporaneous measure of the *damage* variable and a Fisher randomization test, where I randomly permute the years.[31] Second, to rule out potential omitted variable biases, I include additional climatological variables (precipitation and temperature) and a set of socioeconomic variables (population growth rate, economic openness, the growth rate of the gross capital formation, and logged per capita value added of the respective sector).[32] Third, I test different trend specifications: region-specific, nonlinear, and no trends at all. Fourth, to alleviate concerns of biased uncertainty measures (Hsiang, 2016), I calculate different standard errors: Newey-West standard errors with a lag length of 10 years and Conley-HAC standard errors, allowing for a spatial and temporal dependence within a radius of 1000 kilometers and within a time span of 10 years. Furthermore, I cluster the standard errors at broader regional levels to account for the event that tropical cyclones can also affect neighboring countries within one region.[33] Finally, I test two sub-samples, one with all potential outliers and one where I include only the countries exposed to tropical cyclones.[34]

Appendix 1.6.5 exhibits the resulting robustness tests for the direct and indirect sectoral effects.[35] For the direct sectoral effects, the significant results remain robust in all different specifications underlining their credibility for the empirical model used. While the placebo test yields no significant coefficients, the coefficients and p-value remain relatively stable in all remaining robustness tests, as summarized in Figure 1.18. Furthermore, the results of the randomization test show that the H_0 of no effect of tropical cyclone damage can be rejected at the 1% and 5% level of confidence for the *agriculture, hunting, forestry, and fishing* and *wholesale, retail trade, restaurants, and hotels* sectors, respectively. The results of the Input-Output analysis, summarized in Appendix 1.6.5.2, are a little less robust. However, on

[31] For the Placebo test I have to forward the *damage* variable by two periods, since the *damage* in t index consists of the affected agricultural land/exposed population in *t-1*. To implement the Fisher randomization test, I use the code generated by Heß (2017) and randomly permute the years of the tropical cyclone damage variable for 2000 repetitions. By doing so, I test the null-hypothesis of no effect of the damage variable.

[32] Since climatological impacts are most likely nonlinear, I also include squared precipitation and temperature in a further robustness test.

[33] These regions include East Asia and Pacific, Europe and Central Asia, Latin America and Caribbean, Middle East and North Africa, North America, South Asia, and Sub-Saharan Africa.

[34] Exposed countries are defined as having at least one positive *damage* observation over the sample period.

[35] Appendix 1.6.5 first shows the results of the randomization tests, followed by coefficient plots that summarize the remaining specifications. The underlying tables are only included for the direct sectoral effects, while the robustness tables for the Input-Output analysis are available upon request.

average, the previously found effects can be replicated for 10 out of the 12 robustness tests.[36] Given the reduced quality of the data and a shorter time span (20 years), the Input-Output analysis still offers solid results.

1.5 Conclusion

This study provides an explanation about which sectors contribute to an overall negative GDP-effect identified by previous studies (Elliott et al., 2015; Noy, 2009; Strobl, 2012). To quantify the destructiveness of tropical cyclones, I construct a new damage measure based on meteorological data weighted by different exposure of the sectors. I show that tropical cyclones have a significantly negative impact on the annual growth rate of two sectoral aggregates: *agriculture, hunting, forestry, and fishing* and *wholesale, retail trade, restaurants, and hotels.* The dynamic analysis reveals that past tropical cyclones have a negative influence on the majority of sectors providing evidence for the *no recovery* hypothesis discussed in the literature. The Input-Output analysis demonstrates that production processes are only slightly disturbed by tropical cyclones. However, we still can learn from this analysis of how certain direct effects evolve.

The outcomes of this study can serve as a guide for local governments and international organizations to revise and refine their adaptation and mitigation strategies. The findings can help them to identify the sectors for which they must reduce disaster risk. The results indicate that the policies should focus on the direct costs of tropical cyclones. Immediately after the disaster, the policy should concentrate on the *agriculture, hunting, forestry, and fishing*, and the *wholesale, retail trade, restaurants, and hotels* sector aggregates, as they are most vulnerable, and/or recovery measures have not been conducted efficiently in these sectors. Likewise, the contemporaneous, non-significant effect for the remaining sectors can be explained as a result of lower vulnerability and/or efficient recovery measures, which attenuate the potentially negative effect of tropical cyclones. In the years following the tropical cyclone, the efforts should be broadened to support the *mining, and utilities*, and the *transport, storage, and communication* sectors. Most worryingly, the majority of all sectors experience delayed negative effects underpinning how far away the international community remains from a *build-back better* or *recovery to trend* situation for tropical cyclone-affected economies. As the *manufacturing* sectors are responsible for much of the counterbalancing of

[36] The robustness tests that frequently fail are those with Conley-HAC and Newey-West standard errors.

indirect effects, they should not be forgotten by policymakers, even though they show no direct negative effects.

Better post-disaster assistance is not the only required improvement; policymakers should also find ways to better prepare the affected sectors of their economy for possible effects of tropical cyclones before they strike. However, the presented results are generalized for 205 countries at most, and every specific country should make an analysis of their specific vulnerability and individual exposure. Nonetheless, the results can provide general guidance for international disaster relief organizations that are active in various countries on how to direct their long-run disaster relief programs. The results are particularly pressing, as tropical cyclones will continue to intensify due to global warming (Knutson et al., 2020), and, simultaneously, more people will be exposed to tropical cyclones. In this respect, the results of this research can also be used to calculate the future costs of climate change.

1.6 Appendices

1.6.1 Tropical Cyclone Data

The unified data of the IBTrACS data set identifies each storm uniquely by assigning an identification number, its geospatial position and its intensity given by maximum sustained wind speed and minimum sea level pressure. The data are reported at six-hour intervals. Data from IBTrACS are available from 1842 until today, but global coverage of the measurement has only been guaranteed since the start of satellite remote sensing in the late 1970s (Schreck et al., 2014). However, this restriction is for the most part only a concern for non-land-falling tropical cyclones as land-falling tropical cyclones were already covered by the other measurement methods (Knapp, 2016). For my analysis, I use the latest published version, the "IBTrACS-All data" version v03r09, for the 1950–2015 period.

One pitfall of the IBTrACS data is that the data of the maximum sustained wind speed of the different weather agencies are aggregated according to different rules. Weather agencies in the North Atlantic basin use the maximum sustained wind speed average over a one-minute period, agencies from China and Hong Kong use two-minute periods, agencies from India use three-minute periods, and the remaining agencies use ten-minute periods, which is the norm of the World Meteorological Organization (Kruk et al., 2010). As the conversion factor to consistent ten-minute averages is contested, the IBTrACS data set stopped converging it since version 03 (Kruk et al., 2010). This inconsistent measurement introduces a measurement error in the data, where maximum sustained wind speed over a one-minute period is approximately 13% higher than over a ten-minute period (National Weather Service, 2015). However, this bias can partly be attenuated by country fixed effects.[37]

[37] To further control for this potential bias, I calculate a specification with tropical cyclone basin fixed effects, instead of country fixed effects. Appendix Table 1.42 and Figures 1.26–1.32 show the respective robustness tests.

1.6.2 Detailed Description ISIC Sector Classification

A) Agriculture, hunting and forestry

1) Agriculture, hunting and related service activities
2) Forestry, logging and related service activities

B) Fishing

3) Fishing, aquaculture and service activities incidental to fishing

C) Mining and quarrying

4) Mining of coal and lignite; extraction of peat
5) Extraction of crude petroleum and natural gas; service activities incidental to oil and gas extraction, excluding surveying
6) Mining of uranium and thorium ores
7) Mining of metal ores
8) Other mining and quarrying

D) Manufacturing

9) Manufacture of food products and beverages
10) Manufacture of tobacco products
11) Manufacture of textiles
12) Manufacture of wearing apparel; dressing and dyeing of fur
13) Tanning and dressing of leather; manufacture of luggage, handbags, saddlery, harness and footwear
14) Manufacture of wood and of products of wood and cork, except furniture; manufacture of articles of straw and plaiting materials
15) Manufacture of paper and paper products
16) Publishing, printing and reproduction of recorded media
17) Manufacture of coke, refined petroleum products and nuclear fuel
18) Manufacture of chemicals and chemical products
19) Manufacture of rubber and plastics products
20) Manufacture of other non-metallic mineral products
21) Manufacture of basic metals
22) Manufacture of fabricated metal products, except machinery and equipment
23) Manufacture of machinery and equipment n.e.c.
24) Manufacture of office, accounting and computing machinery
25) Manufacture of electrical machinery and apparatus n.e.c.
26) Manufacture of radio, television and communication equipment and apparatus
27) Manufacture of medical, precision and optical instruments, watches and clocks
28) Manufacture of motor vehicles, trailers and semi-trailers
29) Manufacture of other transport equipment
30) Manufacture of furniture; manufacturing n.e.c.
31) Recycling

E) Electricity, gas and water supply

32) Electricity, gas, steam and hot water supply

33) Collection, purification and distribution of water

F) Construction

34) Construction

G) Wholesale and retail trade; repair of motor vehicles, motorcycles and personal and household goods

35) Sale, maintenance and repair of motor vehicles and motorcycles; re-tail sale of automotive fuel
36) Wholesale trade and commission trade, except of motor vehicles and motorcycles
37) Retail trade, except of motor vehicles and motorcycles; repair of personal and household goods

H) Hotels and restaurants

38) Hotels and restaurants

I) Transport, storage and communication

39) Land transport; transport via pipelines
40) Water transport
41) Air transport
42) Supporting and auxiliary transport activities; activities of travel agencies
43) Post and telecommunications

J) Financial intermediation

44) Financial intermediation, except insurance and pension funding
45) Insurance and pension funding, except compulsory social security
46) Activities auxiliary to financial intermediation

K) Real estate, renting and business activities

47) Real estate activities
48) Renting of machinery and equipment without operator and of personal and household goods
49) Computer and related activities
50) Research and development
51) Other business activities

L) Public administration and defense; compulsory social security

52) Public administration and defense; compulsory social security

M) Education

53) Education

N) Health and social work

54) Health and social work

O) Other community, social and personal service activities

55) Sewage and refuse disposal, sanitation and similar activities
56) Activities of membership organizations n.e.c.
57) Recreational, cultural and sporting activities
58) Other service activities

P) Activities of private households as employers and undifferentiated production activities of private households

59) Activities of private households as employers of domestic staff

60) Undifferentiated goods-producing activities of private households for own use

61) Undifferentiated service-producing activities of private households for own use

Q) Extraterritorial organizations and bodies

62) Extraterritorial organizations and bodies

1.6.3 Definitions and Sources of Variables

Table 1.2: Definitions and sources of variables

Variable	Definition	Units	Source
Growth rate pc sector A&B	Annual per capita growth rate of the ISIC sector A&B: agriculture, hunting, forestry, and fishing	2005 const. USD, %	United Nations Statistical Division (2015c)
Growth rate pc sector C&E	Annual per capita growth rate of the ISIC sector C&E: mining, manufacturing, and utilities	2005 const. USD, %	United Nations Statistical Division (2015c)
Growth rate pc sector D	Annual per capita growth rate of the ISIC sector D: manufacturing	2005 const. USD, %	United Nations Statistical Division (2015c)
Growth rate pc sector F	Annual per capita growth rate of the ISIC sector F: construction	2005 const. USD, %	United Nations Statistical Division (2015c)
Growth rate pc sector G–H	Annual per capita growth rate of the ISIC sector G–H: wholesale, retail trade, restaurants, hotels	2005 const. USD, %	United Nations Statistical Division (2015c)
Growth rate pc sector I	Annual per capita growth rate of the ISIC sector I: transport, storage, communication	2005 const. USD, %	United Nations Statistical Division (2015c)
Growth rate pc sector J–P	Annual per capita growth rate of the ISIC sector J–P: other activities	2005 const. USD, %	United Nations Statistical Division (2015c)
Input-Output coefficients	Input-Output coefficients: Specific input divided by total input		Lenzen et al. (2012, 2013)
Damage	Weighted cubic wind speed by exposed population or agricultural land	km^3/h^3	Own modeling after Knapp et al. (2010)
Population Count	Population counts	Inhabitants/gridcell	Klein Goldewijk et al. (2011)
Cropland	Total cropland area	km^2/gridcell	Klein Goldewijk et al. (2011)
Grazing Land	Total land used for grazing	km^2/gridcell	Klein Goldewijk et al. (2011)
Temperature	Yearly mean air temperature	Degree Celsius	University of East Anglia Climatic Research Unit et al. (2017)
Precipitation	Yearly precipitation	mm	University of East Anglia Climatic Research Unit et al. (2017)
Log pc value added	Logarithm of the per capita value added of the respective ISIC sector	2005 const. USD	United Nations Statistical Division (2015c)
Trade openness	Imports plus exports divided by GDP	2005 const. USD, %	United Nations Statistical Division (2015c)
Population growth	Annual population growth rate	%	United Nations Statistical Division (2015c)
Capital growth	Annual growth rate of the gross capital formation	2005 const. USD, %	United Nations Statistical Division (2015c)

1.6.4 Additional Statistics and Results

Table 1.3: Summary statistics

Variable	Obs.	Mean	St. dev.	Min	Max	Mean if storm	St. dev. if storm
Damage (agriculture)	8,750	74,433.30	600,971.10	0.00	23700000.00	174,749.50	911,327.40
Damage (population)	8,750	74,753.80	613,559.80	0.00	25100000.00	175,501.90	930,734.80
Growth rate pc sector A&B	8,500	0.88	10.63	-80.28	167.28	1.04	9.08
Growth rate pc sector C&E	8,500	3.75	30.44	-99.75	995.48	4.07	23.27
Growth rate pc sector D	8,500	2.61	26.63	-95.24	1,745.50	2.29	9.88
Growth rate pc sector F	8,500	3.24	25.78	-96.31	1,453.02	2.67	14.62
Growth rate pc sector G–H	8,500	2.53	12.74	-80.57	459.62	2.33	7.26
Growth rate pc sector I	8,500	3.70	15.50	-91.94	659.28	3.51	7.36
Growth rate pc sector J–P	8,500	2.55	10.45	-77.67	375.99	2.55	5.34
Temperature	8,229	19.77	8.25	-17.30	29.60	20.14	8.66
Precipitation	8,229	1,247.85	867.93	9.80	6,699.00	1,543.78	888.15
Log pc value added A&B	8,683	5.40	0.79	2.34	8.23	5.47	0.76
Log pc value added C&E	8,676	4.97	2.23	-4.13	11.26	5.09	2.04
Log pc value added D	8,683	5.66	1.82	-3.06	10.52	5.97	1.77
Log pc value added F	8,685	5.06	1.85	-1.97	9.31	5.42	1.79
Log pc value added G–H	8,684	6.04	1.67	0.49	10.30	6.41	1.59
Log pc value added I	8,683	5.36	1.76	-0.84	9.23	5.68	1.66
Log pc value added J–P	8,685	6.78	1.92	0.43	11.03	7.14	1.87
Trade openness	8,428	195.47	834.45	0.07	18,015.42	1,116.75	0.10
Population growth	8,500	1.73	1.94	-54.70	19.27	1.39	-16.55
Capital growth	8,293	6.27	30.73	-376.22	1,263.33	4.89	19.50

Table 1.4: Summary statistics Input-Output coefficients

	Obs.	Mean	St. dev.	Min	Max
$IO^{A\&B,A\&B}$	4647	.1662722	.1709245	1.00e-06	.974811
$IO^{A\&B,C\&E}$	4647	.0121479	.0124637	4.56e-06	.1369842
$IO^{A\&B,D}$	4647	.0846725	.0552218	.000056	.299829
$IO^{A\&B,F}$	4647	.0037546	.0043553	0	.131224
$IO^{A\&B,G\text{-}H}$	4647	.0356446	.0355103	4.56e-08	.4175104
$IO^{A\&B,I}$	4647	.0219238	.0179971	9.25e-06	.1859521
$IO^{A\&B,J\text{-}P}$	4647	.070706	.0536481	.000173	.4691
$IO^{C\&E,A\&B}$	4647	.0008422	.0016779	3.97e-08	.0258813
$IO^{C\&E,C\&E}$	4647	.1514745	.1176578	.0000802	.9996359
$IO^{C\&E,D}$	4647	.0537984	.0564091	.000087	.884369
$IO^{C\&E,F}$	4647	.0277999	.0226761	2.06e-08	.1834678
$IO^{C\&E,G\text{-}H}$	4647	.0192595	.0145801	1.29e-06	.1063142
$IO^{C\&E,I}$	4647	.0486505	.0301493	.000016	.398454
$IO^{C\&E,J\text{-}P}$	4647	.0881599	.0518342	.0000348	.4748183
$IO^{D,A\&B}$	4647	.0563642	.0542414	1.42e-07	.5359839
$IO^{D,C\&E}$	4647	.0393183	.0466088	.000141	.60063
$IO^{D,D}$	4647	.2399205	.1103603	.000605	.998675
$IO^{D,F}$	4647	.0045227	.002871	7.39e-08	.0316864
$IO^{D,G\text{-}H}$	4647	.0536236	.0230651	4.00e-06	.214414
$IO^{D,I}$	4647	.0359096	.0153304	.0000742	.1480716
$IO^{D,J\text{-}P}$	4647	.0855877	.040535	.0000556	.3476429
$IO^{F,A\&B}$	4647	.0033265	.0053454	0	.080139
$IO^{F,C\&E}$	4647	.0161254	.0139202	2.74e-07	.1273087
$IO^{F,D}$	4647	.2098782	.0715656	8.39e-07	.4854064
$IO^{F,F}$	4647	.0395914	.0822892	0	.996022
$IO^{F,G\text{-}H}$	4647	.0645109	.0290355	1.10e-06	.2101925
$IO^{F,I}$	4647	.0395516	.0194235	4.22e-06	.1451188
$IO^{F,J\text{-}P}$	4647	.098781	.0484502	.000022	.376105
$IO^{G\text{-}H,A\&B}$	4647	.0084109	.010755	1.65e-06	.1156533
$IO^{G\text{-}H,C\&E}$	4647	.0158055	.0088905	9.37e-06	.0968774
$IO^{G\text{-}H,D}$	4647	.0711979	.0433933	4.00e-06	.624181
$IO^{G\text{-}H,F}$	4647	.0061702	.0042947	5.93e-09	.0553494
$IO^{G\text{-}H,G\text{-}H}$	4647	.053871	.0695904	.0000693	.9245332
$IO^{G\text{-}H,I}$	4647	.061231	.0328779	.000019	.473436
$IO^{G\text{-}H,J\text{-}P}$	4647	.1391351	.0555886	.0003702	.5434914
$IO^{I,A\&B}$	4647	.0004068	.0012979	2.22e-08	.015707
$IO^{I,C\&E}$	4647	.0099685	.0087259	.00002	.099051
$IO^{I,D}$	4647	.0620294	.0393132	.0000266	.3060028
$IO^{I,F}$	4647	.0087888	.0061438	2.04e-08	.0458489
$IO^{I,G\text{-}H}$	4647	.0276095	.0295263	3.00e-06	.252107
$IO^{I,I}$	4647	.1094513	.0749535	.0000306	.9978023
$IO^{I,J\text{-}P}$	4647	.1300935	.0564797	.0001369	.313433
$IO^{J\text{-}P,A\&B}$	4647	.0026576	.0092353	6.00e-06	.257432
$IO^{J\text{-}P,C\&E}$	4647	.0122318	.0075814	.000102	.0716968
$IO^{J\text{-}P,D}$	4647	.0565184	.029694	.0000751	.2703193
$IO^{J\text{-}P,F}$	4647	.0173059	.0090651	0	.076051
$IO^{J\text{-}P,G\text{-}H}$	4647	.0231643	.0119405	.0000253	.1070365
$IO^{J\text{-}P,I}$	4647	.0318075	.0144938	.0000448	.1364643
$IO^{J\text{-}P,J\text{-}P}$	4647	.1450746	.0787744	.000394	.740301

Table 1.5: Lagged influence of tropical cyclone damage on GDP growth of sector aggregate agriculture, hunting, forestry, fishing

Dependent Variables: *Per capita growth rate (%) in sector aggregate*

	Agriculture, hunting, forestry, fishing	Agriculture, hunting, forestry, fishing	Agriculture, hunting, forestry, fishing	Agriculture, hunting, forestry, fishing
	(1)	(2)	(3)	(4)
Damage_{t}	-2.6275***	-2.6406***	-2.5945***	-2.5847***
	(0.4531)	(0.4556)	(0.4503)	(0.4556)
	[0.0000]	[0.0000]	[0.0000]	[0.0000]
$\text{Damage}_{\text{t-1}}$	-0.4314	-0.4681	-0.4076	-0.4047
	(0.4467)	(0.4532)	(0.4500)	(0.4497)
	[0.3353]	[0.3029]	[0.3662]	[0.3691]
$\text{Damage}_{\text{t-2}}$	1.4378***	1.4368***	1.4179***	1.4161***
	(0.3995)	(0.4028)	(0.4083)	(0.4022)
	[0.0004]	[0.0005]	[0.0006]	[0.0005]
$\text{Damage}_{\text{t-3}}$	0.2373	0.2169	0.2185	0.2152
	(0.3331)	(0.3256)	(0.3279)	(0.3305)
	[0.4771]	[0.5060]	[0.5059]	[0.5156]
$\text{Damage}_{\text{t-4}}$	1.1155*	1.1231*	1.1233*	1.1374*
	(0.5863)	(0.5828)	(0.5793)	(0.5818)
	[0.0585]	[0.0553]	[0.0539]	[0.0519]
$\text{Damage}_{\text{t-5}}$	-0.0860	-0.0638	-0.0172	-0.0268
	(0.3097)	(0.3083)	(0.3104)	(0.3077)
	[0.7815]	[0.8363]	[0.9559]	[0.9306]
$\text{Damage}_{\text{t-6}}$		-0.3046	-0.3012	-0.2889
		(0.4460)	(0.4259)	(0.4235)
		[0.4953]	[0.4802]	[0.4958]
$\text{Damage}_{\text{t-7}}$		-0.1822	-0.1972	-0.2056
		(0.5307)	(0.5404)	(0.5513)
		[0.7317]	[0.7156]	[0.7095]
$\text{Damage}_{\text{t-8}}$		-0.8401	-0.8437	-0.8357
		(1.2063)	(1.1881)	(1.1967)
		[0.4870]	[0.4784]	[0.4858]
$\text{Damage}_{\text{t-9}}$		-0.2056	-0.2377	-0.2458
		(0.4608)	(0.4477)	(0.4542)
		[0.6559]	[0.5960]	[0.5890]
$\text{Damage}_{\text{t-10}}$		0.2774	0.2851	0.2979
		(0.4825)	(0.4631)	(0.4773)
		[0.5659]	[0.5387]	[0.5332]
$\text{Damage}_{\text{t-11}}$			0.6831	0.6864
			(0.7825)	(0.7740)
			[0.3837]	[0.3762]
$\text{Damage}_{\text{t-12}}$			0.5987	0.5896
			(0.4491)	(0.4456)
			[0.1841]	[0.1873]
$\text{Damage}_{\text{t-13}}$			0.5975**	0.6132**
			(0.3017)	(0.3059)
			[0.0490]	[0.0463]
$\text{Damage}_{\text{t-14}}$			-0.6914*	-0.6979*
			(0.4100)	(0.4051)
			[0.0932]	[0.0865]
$\text{Damage}_{\text{t-15}}$			-0.2214	-0.2189
			(0.4041)	(0.4006)
			[0.5844]	[0.5854]
$\text{Damage}_{\text{t-16}}$				0.0631
				(0.2907)
				[0.8283]
$\text{Damage}_{\text{t-17}}$				-0.1343
				(0.3827)
				[0.7261]
$\text{Damage}_{\text{t-18}}$				0.2813
				(0.3274)
				[0.3912]
$\text{Damage}_{\text{t-19}}$				-0.1659
				(0.5556)
				[0.7655]
$\text{Damage}_{\text{t-20}}$				0.0244
				(0.1876)
				[0.8966]
N	8,500	8,500	8,500	8,500
Clusters	205	205	205	205
P-value	0.0000	0.0000	0.0000	0.0000
Mean DV	0.8800	0.8800	0.8800	0.8800

Notes: $*p < 0.1, **p < 0.05, ***p < 0.01$. Panel OLS regression results with clustered standard errors by countries in parentheses (), and p-values in brackets []. The coefficients show the effect of a one standard deviation increase in tropical cyclone damage on the per capita growth rate in a given sectoral aggregate. The standard deviations are 2,236,738 for the agricultural and 2,269,395 for the remaining sectors, calculated for the whole sample of positive wind speed observations. Damage_{t} is the weighted damage measure for tropical cyclone intensity in year t. For the sector aggregate agriculture, hunting, forestry and fishing it is weighted by exposed agricultural land in t-1, whereas for the remaining sector aggregates it is weighted by exposed population in t-1. All regressions include country and year fixed effects as well as country-specific linear trends.

Table 1.6: Lagged influence of tropical cyclone damage on GDP growth of sector aggregate mining, utilities

Dependent Variables: *Per capita growth rate (%) in sector aggregate*

	Mining, utilities	Mining, utilities	Mining, utilities	Mining, utilities
	(1)	(2)	(3)	(4)
Damage_{t}	-0.6876	-0.5101	-0.4927	-0.4347
	(0.8734)	(0.9150)	(0.8834)	(0.9616)
	[0.4321]	[0.5778]	[0.5776]	[0.6517]
Damage_{t-1}	-0.7455	-0.8769	-0.8343	-0.8934
	(0.7873)	(0.8026)	(0.7857)	(0.8479)
	[0.3448]	[0.2759]	[0.2896]	[0.2933]
Damage_{t-2}	0.7484	0.7583	0.8130	0.8259
	(0.6098)	(0.6138)	(0.6176)	(0.6286)
	[0.2212]	[0.2181]	[0.1895]	[0.1904]
Damage_{t-3}	-0.9537**	-0.9694**	-0.9714**	-0.9672**
	(0.4539)	(0.4599)	(0.4579)	(0.4729)
	[0.0368]	[0.0363]	[0.0351]	[0.0421]
Damage_{t-4}	-0.3247	-0.3908	-0.3862	-0.3796
	(0.3517)	(0.3638)	(0.3695)	(0.3960)
	[0.3569]	[0.2840]	[0.2972]	[0.3389]
Damage_{t-5}	-0.4838*	-0.4029*	-0.3679	-0.3992
	(0.2583)	(0.2437)	(0.2536)	(0.2476)
	[0.0625]	[0.0998]	[0.1484]	[0.1085]
Damage_{t-6}		-1.1859**	-1.2196**	-1.1819**
		(0.4730)	(0.5131)	(0.4967)
		[0.0129]	[0.0184]	[0.0183]
Damage_{t-7}		-0.5146	-0.4506	-0.4911
		(0.3822)	(0.3920)	(0.4168)
		[0.1797]	[0.2517]	[0.2400]
Damage_{t-8}		0.2670	0.2856	0.3268
		(0.3256)	(0.3305)	(0.3144)
		[0.4131]	[0.3885]	[0.2998]
Damage_{t-9}		-1.8192*	-1.8233*	-1.8472*
		(1.0021)	(1.0098)	(1.0186)
		[0.0709]	[0.0725]	[0.0712]
Damage_{t-10}		0.9977	1.0499	1.1008
		(0.6531)	(0.6605)	(0.6855)
		[0.1281]	[0.1135]	[0.1098]
Damage_{t-11}			-0.5780	-0.6148
			(0.5170)	(0.5562)
			[0.2648]	[0.2703]
Damage_{t-12}			0.6477	0.6350
			(0.4428)	(0.4434)
			[0.1451]	[0.1536]
Damage_{t-13}			0.3826	0.4128
			(0.5633)	(0.5500)
			[0.4977]	[0.4537]
Damage_{t-14}			-0.0418	-0.0526
			(0.6378)	(0.6398)
			[0.9478]	[0.9345]
Damage_{t-15}			0.6175	0.6515
			(0.7947)	(0.8284)
			[0.4381]	[0.4325]
Damage_{t-16}				-0.0241
				(0.8067)
				[0.9762]
Damage_{t-17}				-0.3680
				(0.5713)
				[0.5202]
Damage_{t-18}				0.2299
				(0.5707)
				[0.6874]
Damage_{t-19}				-0.6999
				(0.5209)
				[0.1805]
Damage_{t-20}				0.7053
				(0.8842)
				[0.4260]
N	8,500	8,500	8,500	8,500
Clusters	205	205	205	205
P-value	0.0000	0.0000	0.0000	0.0000
Mean DV	3.7458	3.7458	3.7458	3.7458

Notes: $*p < 0.1, **p < 0.05, ***p < 0.01$. Panel OLS regression results with clustered standard errors by countries in parentheses (), and p-values in brackets []. The coefficients show the effect of a one standard deviation increase in tropical cyclone damage on the per capita growth rate in a given sectoral aggregate. The standard deviations are 2,236,738 for the agricultural and 2,269,395 for the remaining sectors, calculated for the whole sample of positive wind speed observations. Damage_{t} is the weighted damage measure for tropical cyclone intensity in year t. For the sector aggregate agriculture, hunting, forestry and fishing it is weighted by exposed agricultural land in t-1, whereas for the remaining sector aggregates it is weighted by exposed population in t-1. All regressions include country and year fixed effects as well as country-specific linear trends.

Table 1.7: Lagged influence of tropical cyclone damage on GDP growth of sector aggregate manufacturing

Dependent Variables: *Per capita growth rate (%) in sector aggregate*

	Manufacturing	Manufacturing	Manufacturing	Manufacturing
	(1)	(2)	(3)	(4)
$Damage_t$	-0.7744	-0.6328	-0.5932	-0.6580
	(0.5118)	(0.4759)	(0.4708)	(0.4413)
	[0.1318]	[0.1852]	[0.2091]	[0.1375]
$Damage_{t-1}$	-0.3449	-0.3864	-0.4121	-0.3278
	(0.5540)	(0.5974)	(0.5993)	(0.6004)
	[0.5343]	[0.5184]	[0.4925]	[0.5857]
$Damage_{t-2}$	-0.8700	-0.8277	-0.8301	-0.8441
	(0.5939)	(0.5821)	(0.5779)	(0.5906)
	[0.1445]	[0.1566]	[0.1524]	[0.1545]
$Damage_{t-3}$	0.3528	0.2814	0.2392	0.2274
	(0.4764)	(0.4708)	(0.4590)	(0.4481)
	[0.4598]	[0.5508]	[0.6028]	[0.6123]
$Damage_{t-4}$	0.3191	0.3004	0.3181	0.3357
	(0.4506)	(0.4650)	(0.4647)	(0.4519)
	[0.4797]	[0.5190]	[0.4944]	[0.4585]
$Damage_{t-5}$	-0.2016	-0.1280	-0.1582	-0.1330
	(0.4904)	(0.4855)	(0.5077)	(0.5085)
	[0.6814]	[0.7923]	[0.7556]	[0.7939]
$Damage_{t-6}$		0.4072	0.4422	0.4179
		(0.4026)	(0.4073)	(0.4064)
		[0.3131]	[0.2788]	[0.3049]
$Damage_{t-7}$		1.6369**	1.6176**	1.6485**
		(0.7152)	(0.7124)	(0.7055)
		[0.0231]	[0.0242]	[0.0204]
$Damage_{t-8}$		-0.3192	-0.3443	-0.3760
		(0.5348)	(0.5369)	(0.5329)
		[0.5512]	[0.5221]	[0.4813]
$Damage_{t-9}$		-1.5212	-1.5311	-1.5149
		(0.9531)	(0.9427)	(0.9532)
		[0.1120]	[0.1059]	[0.1135]
$Damage_{t-10}$		0.6595	0.6194	0.5703
		(0.4769)	(0.4789)	(0.4961)
		[0.1682]	[0.1973]	[0.2517]
$Damage_{t-11}$			0.2667	0.3225
			(0.2858)	(0.3103)
			[0.3518]	[0.2999]
$Damage_{t-12}$			0.1428	0.1468
			(0.4045)	(0.4030)
			[0.7244]	[0.7161]
$Damage_{t-13}$			-0.1894	-0.2056
			(0.3984)	(0.4187)
			[0.6350]	[0.6238]
$Damage_{t-14}$			0.2558	0.2630
			(0.3295)	(0.3233)
			[0.4385]	[0.4168]
$Damage_{t-15}$			-0.7252*	-0.7666*
			(0.3965)	(0.4048)
			[0.0689]	[0.0597]
$Damage_{t-16}$				0.2342
				(0.3046)
				[0.4428]
$Damage_{t-17}$				0.2235
				(0.2860)
				[0.4354]
$Damage_{t-18}$				0.1259
				(0.2085)
				[0.5464]
$Damage_{t-19}$				0.7305*
				(0.3708)
				[0.0502]
$Damage_{t-20}$				-0.9221
				(0.6077)
				[0.1307]
N	8,500	8,500	8,500	8,500
Clusters	205	205	205	205
P-value	0.2321	0.1081	0.0087	0.0000
Mean DV	2.6095	2.6095	2.6095	2.6095

Notes: $*p < 0.1, **p < 0.05, ***p < 0.01$. Panel OLS regression results with clustered standard errors by countries in parentheses (), and p-values in brackets []. The coefficients show the effect of a one standard deviation increase in tropical cyclone damage on the per capita growth rate in a given sectoral aggregate. The standard deviations are 2,236,738 for the agricultural and 2,269,395 for the remaining sectors, calculated for the whole sample of positive wind speed observations. $Damage_t$ is the weighted damage measure for tropical cyclone intensity in year t. For the sector aggregate agriculture, hunting, forestry and fishing it is weighted by exposed agricultural land in t-1, whereas for the remaining sector aggregates it is weighted by exposed population in t-1. All regressions include country and year fixed effects as well as country-specific linear trends.

Table 1.8: Lagged influence of tropical cyclone damage on GDP growth of sector aggregate construction

Dependent Variables: *Per capita growth rate (%) in sector aggregate*

	Construction	Construction	Construction	Construction
	(1)	(2)	(3)	(4)
Damage_{t}	0.6080	0.5245	0.4851	0.4199
	(0.6260)	(0.6393)	(0.6323)	(0.6430)
	[0.3325]	[0.4129]	[0.4439]	[0.5144]
Damage_{t-1}	2.6311**	2.6978**	2.7381**	2.7534**
	(1.1531)	(1.1470)	(1.1793)	(1.1488)
	[0.0235]	[0.0196]	[0.0212]	[0.0174]
Damage_{t-2}	-1.6493*	-1.6037*	-1.5749*	-1.6063*
	(0.8377)	(0.8226)	(0.8130)	(0.8257)
	[0.0503]	[0.0526]	[0.0541]	[0.0531]
Damage_{t-3}	-1.7602***	-1.6796***	-1.6273***	-1.6556***
	(0.4487)	(0.4626)	(0.4648)	(0.4489)
	[0.0001]	[0.0004]	[0.0006]	[0.0003]
Damage_{t-4}	-0.0905	-0.1140	-0.1654	-0.2049
	(0.6021)	(0.5750)	(0.5996)	(0.6076)
	[0.8806]	[0.8430]	[0.7829]	[0.7363]
Damage_{t-5}	0.0690	0.0223	0.0271	0.0113
	(0.7443)	(0.7373)	(0.7371)	(0.7475)
	[0.9262]	[0.9759]	[0.9707]	[0.9879]
Damage_{t-6}		-1.0995**	-1.0783**	-1.1177**
		(0.4633)	(0.4671)	(0.4647)
		[0.0186]	[0.0220]	[0.0171]
Damage_{t-7}		0.0687	0.0857	0.0964
		(0.4763)	(0.4669)	(0.4873)
		[0.8855]	[0.8545]	[0.8433]
Damage_{t-8}		1.6210*	1.6803*	1.6541*
		(0.9750)	(0.9757)	(0.9884)
		[0.0980]	[0.0866]	[0.0958]
Damage_{t-9}		1.4358**	1.4250**	1.4181**
		(0.6005)	(0.5921)	(0.5756)
		[0.0177]	[0.0170]	[0.0146]
Damage_{t-10}		-0.6059**	-0.5987**	-0.6467**
		(0.2685)	(0.2791)	(0.2885)
		[0.0251]	[0.0331]	[0.0261]
Damage_{t-11}			-0.5109	-0.5271
			(0.5518)	(0.5639)
			[0.3555]	[0.3510]
Damage_{t-12}			-0.5298	-0.5381
			(0.6212)	(0.6260)
			[0.3947]	[0.3910]
Damage_{t-13}			1.2311	1.2136
			(1.1028)	(1.0968)
			[0.2656]	[0.2698]
Damage_{t-14}			0.2925	0.2873
			(0.9485)	(0.9502)
			[0.7581]	[0.7627]
Damage_{t-15}			-0.0251	-0.0529
			(0.3925)	(0.3886)
			[0.9491]	[0.8919]
Damage_{t-16}				-0.5861*
				(0.3420)
				[0.0880]
Damage_{t-17}				-0.4172
				(0.6622)
				[0.5294]
Damage_{t-18}				-0.1922
				(0.3900)
				[0.6226]
Damage_{t-19}				0.4175
				(0.4051)
				[0.3039]
Damage_{t-20}				-0.2049
				(0.2578)
				[0.4276]
N	8,500	8,500	8,500	8,500
Clusters	205	205	205	205
P-value	0.0000	0.0000	0.0000	0.0000
Mean DV	3.2388	3.2388	3.2388	3.2388

Notes: $*p < 0.1, **p < 0.05, ***p < 0.01$. Panel OLS regression results with clustered standard errors by countries in parentheses (), and p-values in brackets []. The coefficients show the effect of a one standard deviation increase in tropical cyclone damage on the per capita growth rate in a given sectoral aggregate. The standard deviations are 2,236,738 for the agricultural and 2,269,395 for the remaining sectors, calculated for the whole sample of positive wind speed observations. Damage_t is the weighted damage measure for tropical cyclone intensity in year t. For the sector aggregate agriculture, hunting, forestry and fishing it is weighted by exposed agricultural land in t-1, whereas for the remaining sector aggregates it is weighted by exposed population in t-1. All regressions include country and year fixed effects as well as country-specific linear trends.

Table 1.9: Lagged influence of tropical cyclone damage on GDP growth of sector aggregate wholesale, retail trade, restaurants, hotels

Dependent Variables: *Per capita growth rate (%) in sector aggregate*

	Wholesale, retail trade, restaurants, hotels	Wholesale, retail trade, restaurants, hotels	Wholesale, retail trade, restaurants, hotels	Wholesale, retail trade, restaurants, hotels
	(1)	(2)	(3)	(4)
$Damage_t$	-1.1769**	-1.1636**	-1.1665**	-1.1895**
	(0.5216)	(0.5343)	(0.5317)	(0.5317)
	[0.0251]	[0.0306]	[0.0294]	[0.0263]
$Damage_{t-1}$	-0.0479	-0.0801	-0.1049	-0.0936
	(0.5161)	(0.5332)	(0.5395)	(0.5403)
	[0.9261]	[0.8807]	[0.8461]	[0.8626]
$Damage_{t-2}$	-0.2738	-0.2956	-0.3109	-0.2848
	(0.2400)	(0.2435)	(0.2374)	(0.2390)
	[0.2554]	[0.2262]	[0.1917]	[0.2347]
$Damage_{t-3}$	-0.2410	-0.2624	-0.2908	-0.2768
	(0.2378)	(0.2306)	(0.2278)	(0.2258)
	[0.3120]	[0.2564]	[0.2032]	[0.2216]
$Damage_{t-4}$	0.2640	0.2649	0.2323	0.2346
	(0.2349)	(0.2428)	(0.2496)	(0.2561)
	[0.2625]	[0.2765]	[0.3531]	[0.3607]
$Damage_{t-5}$	-0.1599	-0.1490	-0.1426	-0.1183
	(0.2364)	(0.2377)	(0.2484)	(0.2544)
	[0.4996]	[0.5315]	[0.5665]	[0.6424]
$Damage_{t-6}$		-0.0454	-0.0794	-0.0722
		(0.2788)	(0.2764)	(0.2760)
		[0.8708]	[0.7741]	[0.7940]
$Damage_{t-7}$		-0.3164	-0.3272	-0.3076
		(0.3797)	(0.3849)	(0.3855)
		[0.4056]	[0.3963]	[0.4258]
$Damage_{t-8}$		-0.6149	-0.6285	-0.6202
		(0.5242)	(0.5272)	(0.5252)
		[0.2422]	[0.2345]	[0.2390]
$Damage_{t-9}$		-0.3311	-0.3650	-0.3482
		(0.2344)	(0.2388)	(0.2340)
		[0.1594]	[0.1278]	[0.1383]
$Damage_{t-10}$		0.1107	0.1148	0.1026
		(0.3226)	(0.3186)	(0.3101)
		[0.7319]	[0.7190]	[0.7411]
$Damage_{t-11}$			-0.3550	-0.3461
			(0.2501)	(0.2556)
			[0.1574]	[0.1772]
$Damage_{t-12}$			0.0860	0.0966
			(0.1860)	(0.1853)
			[0.6444]	[0.6027]
$Damage_{t-13}$			0.0246	0.0273
			(0.2290)	(0.2291)
			[0.9146]	[0.9053]
$Damage_{t-14}$			-0.6195	-0.5974
			(0.4335)	(0.4253)
			[0.1545]	[0.1617]
$Damage_{t-15}$			-0.2120	-0.2104
			(0.1901)	(0.1802)
			[0.2662]	[0.2443]
$Damage_{t-16}$				0.0808
				(0.1772)
				[0.6490]
$Damage_{t-17}$				0.0653
				(0.1978)
				[0.7418]
$Damage_{t-18}$				-0.1388
				(0.2015)
				[0.4918]
$Damage_{t-19}$				0.4196**
				(0.1768)
				[0.0185]
$Damage_{t-20}$				0.1802
				(0.3450)
				[0.6019]
N	8,500	8,500	8,500	8,500
Clusters	205	205	205	205
P-value	0.0000	0.0003	0.0000	0.0000
Mean DV	2.5256	2.5256	2.5256	2.5256

Notes: $*p < 0.1, **p < 0.05, ***p < 0.01$. Panel OLS regression results with clustered standard errors by countries in parentheses (), and p-values in brackets []. The coefficients show the effect of a one standard deviation increase in tropical cyclone damage on the per capita growth rate in a given sectoral aggregate. The standard deviations are 2,236,738 for the agricultural and 2,269,395 for the remaining sectors, calculated for the whole sample of positive wind speed observations. $Damage_t$ is the weighted damage measure for tropical cyclone intensity in year t. For the sector aggregate agriculture, hunting, forestry and fishing it is weighted by exposed agricultural land in t-1, whereas for the remaining sector aggregates it is weighted by exposed population in t-1. All regressions include country and year fixed effects as well as country-specific linear trends.

Table 1.10: Lagged influence of tropical cyclone damage on GDP growth of sector aggregate transport, storage, communication

Dependent Variables: *Per capita growth rate (%) in sector aggregate*

	Transport, storage, communication	Transport, storage, communication	Transport, storage, communication	Transport, storage, communication
	(1)	(2)	(3)	(4)
$Damage_t$	-0.5071	-0.4901	-0.4922	-0.5464
	(0.3708)	(0.3755)	(0.3607)	(0.3582)
	[0.1729]	[0.1933]	[0.1738]	[0.1287]
$Damage_{t-1}$	0.1078	0.1025	0.0706	0.0890
	(0.3787)	(0.3723)	(0.3672)	(0.3592)
	[0.7761]	[0.7834]	[0.8477]	[0.8046]
$Damage_{t-2}$	-0.6321**	-0.6508**	-0.6910**	-0.7171***
	(0.2768)	(0.2757)	(0.2697)	(0.2694)
	[0.0234]	[0.0192]	[0.0111]	[0.0084]
$Damage_{t-3}$	0.0341	0.0355	0.0165	0.0016
	(0.2741)	(0.2647)	(0.2700)	(0.2691)
	[0.9010]	[0.8935]	[0.9513]	[0.9952]
$Damage_{t-4}$	0.0163	-0.0151	-0.0287	-0.0614
	(0.3971)	(0.3990)	(0.3957)	(0.3952)
	[0.9673]	[0.9698]	[0.9422]	[0.8768]
$Damage_{t-5}$	0.2730	0.2602	0.2475	0.2535
	(0.2892)	(0.2842)	(0.2921)	(0.2955)
	[0.3462]	[0.3609]	[0.3978]	[0.3920]
$Damage_{t-6}$		-0.4360	-0.4293	-0.4769*
		(0.2875)	(0.2779)	(0.2798)
		[0.1309]	[0.1240]	[0.0899]
$Damage_{t-7}$		-0.3668	-0.4075	-0.3878
		(0.3245)	(0.3420)	(0.3499)
		[0.2596]	[0.2348]	[0.2690]
$Damage_{t-8}$		0.1728	0.1510	0.1112
		(0.5338)	(0.5449)	(0.5508)
		[0.7465]	[0.7819]	[0.8402]
$Damage_{t-9}$		-0.1954	-0.2129	-0.1991
		(0.2675)	(0.2621)	(0.2635)
		[0.4661]	[0.4176]	[0.4508]
$Damage_{t-10}$		-0.4255**	-0.4540**	-0.4994**
		(0.1894)	(0.1972)	(0.1996)
		[0.0257]	[0.0223]	[0.0131]
$Damage_{t-11}$			0.2563	0.2603
			(0.4631)	(0.4645)
			[0.5805]	[0.5758]
$Damage_{t-12}$			-0.1970	-0.1973
			(0.2412)	(0.2407)
			[0.4150]	[0.4134]
$Damage_{t-13}$			-0.2124	-0.2478
			(0.2475)	(0.2563)
			[0.3917]	[0.3348]
$Damage_{t-14}$			-0.3103	-0.3094
			(0.3806)	(0.3797)
			[0.4159]	[0.4161]
$Damage_{t-15}$			-0.4994***	-0.5263***
			(0.1736)	(0.1711)
			[0.0044]	[0.0024]
$Damage_{t-16}$				-0.2597
				(0.2497)
				[0.2994]
$Damage_{t-17}$				0.0558
				(0.2539)
				[0.8264]
$Damage_{t-18}$				-0.4558**
				(0.1959)
				[0.0209]
$Damage_{t-19}$				0.3820
				(0.2513)
				[0.1300]
$Damage_{t-20}$				-0.4261*
				(0.2430)
				[0.0811]
N	8,500	8,500	8,500	8,500
Clusters	205	205	205	205
P-value	0.0024	0.0002	0.0007	0.0000
Mean DV	3.7030	3.7030	3.7030	3.7030

Notes: $*p < 0.1, **p < 0.05, ***p < 0.01$. Panel OLS regression results with clustered standard errors by countries in parentheses (), and p-values in brackets []. The coefficients show the effect of a one standard deviation increase in tropical cyclone damage on the per capita growth rate in a given sectoral aggregate. The standard deviations are 2,236,738 for the agricultural and 2,269,395 for the remaining sectors, calculated for the whole sample of positive wind speed observations. $Damage_t$ is the weighted damage measure for tropical cyclone intensity in year t. For the sector aggregate agriculture, hunting, forestry and fishing it is weighted by exposed agricultural land in t-1, whereas for the remaining sector aggregates it is weighted by exposed population in t-1. All regressions include country and year fixed effects as well as country-specific linear trends.

Table 1.11: Lagged influence of tropical cyclone damage on GDP growth of sector aggregate other activities

Dependent Variables: *Per capita growth rate (%) in sector aggregate*

	Other activities	Other activities	Other activities	Other activities
	(1)	(2)	(3)	(4)
Damage_{t}	-0.1957	-0.1992	-0.1983	-0.1986
	(0.2653)	(0.2701)	(0.2741)	(0.2726)
	[0.4616]	[0.4616]	[0.4701]	[0.4672]
Damage_{t-1}	0.3164*	0.3095*	0.3163*	0.3207*
	(0.1764)	(0.1782)	(0.1716)	(0.1743)
	[0.0743]	[0.0840]	[0.0667]	[0.0672]
Damage_{t-2}	0.0273	-0.0005	-0.0147	0.0115
	(0.2312)	(0.2195)	(0.2134)	(0.2190)
	[0.9060]	[0.9983]	[0.9451]	[0.9582]
Damage_{t-3}	-0.0826	-0.0844	-0.0872	-0.0737
	(0.1412)	(0.1356)	(0.1354)	(0.1317)
	[0.5593]	[0.5342]	[0.5203]	[0.5762]
Damage_{t-4}	0.0314	0.0175	0.0105	0.0145
	(0.2182)	(0.2183)	(0.2235)	(0.2171)
	[0.8856]	[0.9364]	[0.9625]	[0.9470]
Damage_{t-5}	0.1313	0.1167	0.1297	0.1435
	(0.1549)	(0.1588)	(0.1625)	(0.1602)
	[0.3976]	[0.4630]	[0.4256]	[0.3714]
Damage_{t-6}		-0.2200	-0.2209	-0.1996
		(0.1667)	(0.1638)	(0.1623)
		[0.1884]	[0.1788]	[0.2200]
Damage_{t-7}		-0.5182	-0.5235	-0.5060
		(0.3682)	(0.3664)	(0.3610)
		[0.1609]	[0.1546]	[0.1625]
Damage_{t-8}		-0.1524	-0.1565	-0.1374
		(0.1293)	(0.1302)	(0.1258)
		[0.2396]	[0.2305]	[0.2761]
Damage_{t-9}		-0.0685	-0.0803	-0.0805
		(0.1915)	(0.1868)	(0.1871)
		[0.7207]	[0.6677]	[0.6673]
Damage_{t-10}		-0.3355**	-0.3338**	-0.3326**
		(0.1636)	(0.1630)	(0.1598)
		[0.0416]	[0.0419]	[0.0387]
Damage_{t-11}			0.1267	0.1200
			(0.2717)	(0.2727)
			[0.6414]	[0.6605]
Damage_{t-12}			0.0901	0.1043
			(0.2600)	(0.2621)
			[0.7294]	[0.6911]
Damage_{t-13}			0.0736	0.0931
			(0.1716)	(0.1895)
			[0.6685]	[0.6239]
Damage_{t-14}			-0.2511	-0.2361
			(0.2044)	(0.1998)
			[0.2206]	[0.2388]
Damage_{t-15}			-0.0480	-0.0384
			(0.1275)	(0.1208)
			[0.7066]	[0.7510]
Damage_{t-16}				-0.1259
				(0.1884)
				[0.5050]
Damage_{t-17}				-0.0509
				(0.1613)
				[0.7526]
Damage_{t-18}				0.1624
				(0.1738)
				[0.3512]
Damage_{t-19}				0.2999***
				(0.1126)
				[0.0084]
Damage_{t-20}				0.3898
				(0.4822)
				[0.4199]
N	8,500	8,500	8,500	8,500
Clusters	205	205	205	205
P-value	0.3635	0.0001	0.0000	0.0000
Mean DV	2.5519	2.5519	2.5519	2.5519

Notes: $*p < 0.1, **p < 0.05, ***p < 0.01$. Panel OLS regression results with clustered standard errors by countries in parentheses (), and p-values in brackets []. The coefficients show the effect of a one standard deviation increase in tropical cyclone damage on the per capita growth rate in a given sectoral aggregate. The standard deviations are 2,236,738 for the agricultural and 2,269,395 for the remaining sectors, calculated for the whole sample of positive wind speed observations. Damage_{t} is the weighted damage measure for tropical cyclone intensity in year t. For the sector aggregate agriculture, hunting, forestry and fishing it is weighted by exposed agricultural land in t-1, whereas for the remaining sector aggregates it is weighted by exposed population in t-1. All regressions include country and year fixed effects as well as country-specific linear trends.

Table 1.12: Lagged cumulative influence of tropical cyclone damage on sectoral GDP growth (0–9 years)

	Dependent Variables: *Per capita growth rate (%) in sector aggregates*									
Accumulated damage effects after:	0 years	1 year	2 years	3 years	4 years	5 years	6 years	7 years	8 years	9 years
Agriculture, hunting,	-2.5847***	-2.9894***	-1.5733***	-1.3581**	-0.2207	-0.2475	-0.5364	-0.7421	-1.5777	-1.8236
forestry, fishing	(0.4556)	(0.6064)	(0.5989)	(0.6257)	(0.9810)	(1.1938)	(1.2518)	(1.1060)	(1.5156)	(1.6854)
	[0.0000]	[0.0000]	[0.0093]	[0.0311]	[0.8222]	[0.8360]	[0.6687]	[0.5030]	[0.2991]	[0.2805]
Mining, utilities	-0.4347	-1.3281**	-0.5021	-1.4693	-1.8489*	-2.2481**	-3.4300***	-3.9211***	-3.5943***	-5.4415***
	(0.9616)	(0.6495)	(0.9336)	(1.0208)	(0.9635)	(0.8910)	(0.8866)	(1.0249)	(1.0404)	(1.5957)
	[0.6517]	[0.0422]	[0.5913]	[0.1516]	[0.0564]	[0.0124]	[0.0001]	[0.0002]	[0.0007]	[0.0008]
Manufacturing	-0.6580	-0.9857	-1.8298*	-1.6024	-1.2667	-1.3997	-0.9818	0.6667	0.2908	-1.2242
	(0.4413)	(0.6982)	(1.0553)	(1.1886)	(1.0598)	(1.1366)	(1.2176)	(1.1558)	(1.2954)	(1.8766)
	[0.1375]	[0.1595]	[0.0844]	[0.1791]	[0.2334]	[0.2196]	[0.4210]	[0.5647]	[0.8226]	[0.5149]
Construction	0.4199	3.1734**	1.5671	-0.0886	-0.2935	-0.2822	-1.3998	-1.3034	0.3507	1.7688
	(0.6430)	(1.5599)	(1.4459)	(1.6583)	(1.3940)	(1.8048)	(1.9385)	(1.7578)	(1.4824)	(1.6819)
	[0.5144]	[0.0432]	[0.2797]	[0.9575]	[0.8334]	[0.8759]	[0.4710]	[0.4592]	[0.8132]	[0.2942]
Wholesale, retail	-1.1895**	-1.2831**	-1.5680***	-1.8448***	-1.6101**	-1.7285**	-1.8006**	-2.1082**	-2.7285**	-3.0767**
trade, restaurants,	(0.5317)	(0.5111)	(0.5520)	(0.5966)	(0.6731)	(0.7312)	(0.7562)	(0.8723)	(1.1894)	(1.3632)
hotels	[0.0263]	[0.0128]	[0.0050]	[0.0023]	[0.0177]	[0.0190]	[0.0182]	[0.0165]	[0.0228]	[0.0251]
Transport, storage,	-0.5464	-0.4574	-1.1745*	-1.1729	-1.2342	-0.9808	-1.4577	-1.8455	-1.7342	-1.9333
communication	(0.3582)	(0.5481)	(0.6388)	(0.7866)	(0.8444)	(1.0020)	(1.0969)	(1.1639)	(1.2830)	(1.3875)
	[0.1287]	[0.4049]	[0.0674]	[0.1375]	[0.1454]	[0.3288]	[0.1854]	[0.1144]	[0.1780]	[0.1650]
Other activities	-0.1986	0.1221	0.1337	0.0599	0.0744	0.2179	0.0183	-0.4877	-0.6251	-0.7056
	(0.2726)	(0.2826)	(0.3602)	(0.3968)	(0.4851)	(0.5311)	(0.5864)	(0.6128)	(0.6558)	(0.6657)
	[0.4672]	[0.6661]	[0.7110]	[0.8801]	[0.8783]	[0.6820]	[0.9751]	[0.4270]	[0.3416]	[0.2904]
N	8,500	8,500	8,500	8,500	8,500	8,500	8,500	8,500	8,500	8,500

Notes: $*p < 0.1, **p < 0.05, ***p < 0.01$. F-tests of panel OLS regression results with clustered standard errors by countries in parentheses (), and p-values in brackets []. The coefficients show the effect of a one standard deviation increase in tropical cyclone damage accumulated over different years on the per capita growth rate in a given sectoral aggregate. The standard deviations are 2,236,738 for the agricultural and 2,269,395 for the remaining sectors, calculated for the whole sample of positive wind speed observations. The independent variable is Damage_{t}, which is the weighted damage measure for tropical cyclone intensity in year t. For the sector aggregate agriculture, hunting, forestry and fishing it is weighted by exposed agricultural land in t-1, whereas for the remaining sector aggregates it is weighted by exposed population in t-1. All regressions include country and year fixed effects as well as country-specific linear trends.

Table 1.13: Lagged cumulative influence of tropical cyclone damage on sectoral GDP growth (10–20 years)

	Dependent Variables: *Per capita growth rate (%) in sector aggregates*										
Accumulated damage effects after:	10 years	11 years	12 years	13 years	14 years	15 years	16 years	17 years	18 years	19 years	20 years
Agriculture, hunting,	-1.5257	-0.8392	-0.2497	0.3636	-0.3343	-0.5532	-0.4901	-0.6243	-0.3430	-0.5089	-0.4845
forestry, fishing	(1.5593)	(1.4932)	(1.6496)	(1.6716)	(1.8635)	(1.9798)	(2.0824)	(2.0996)	(2.2881)	(2.3054)	(2.2923)
	[0.3290]	[0.5747]	[0.8799]	[0.8280]	[0.8578]	[0.7802]	[0.8142]	[0.7665]	[0.8810]	[0.8255]	[0.8328]
Mining, utilities	-4.3407***	-4.9555***	-4.3205**	-3.9076*	-3.9602*	-3.3087	-3.3328	-3.7008	-3.4709	-4.1708	-3.4655
	(1.3957)	(1.8049)	(2.0143)	(1.9848)	(2.2766)	(2.2232)	(2.2751)	(2.4650)	(2.6024)	(2.9363)	(2.9092)
	[0.0021]	[0.0066]	[0.0331]	[0.0503]	[0.0834]	[0.1382]	[0.1445]	[0.1348]	[0.1838]	[0.1570]	[0.2350]
Manufacturing	-0.6539	-0.3314	-0.1846	-0.3903	-0.1272	-0.8938	-0.6595	-0.4360	-0.3100	0.4204	-0.5016
	(1.7681)	(1.8058)	(2.0077)	(2.2014)	(2.1249)	(2.2555)	(2.4040)	(2.4435)	(2.4294)	(2.5437)	(2.8126)
	[0.7119]	[0.8546]	[0.9268]	[0.8595]	[0.9523]	[0.6923]	[0.7841]	[0.8586]	[0.8986]	[0.8689]	[0.8586]
Construction	1.1221	0.5950	0.0569	1.2705	1.5579	1.5050	0.9188	0.5016	0.3094	0.7269	0.5220
	(1.7752)	(1.9211)	(2.2023)	(2.4460)	(2.9568)	(2.9755)	(3.1644)	(3.2770)	(3.2086)	(3.0947)	(3.1083)
	[0.5280]	[0.7571]	[0.9794]	[0.6040]	[0.5988]	[0.6136]	[0.7718]	[0.8785]	[0.9233]	[0.8145]	[0.8668]
Wholesale, retail	-2.9741**	-3.3202**	-3.2236**	-3.1963**	-3.7937**	-4.0041**	-3.9233**	-3.8580**	-3.9968**	-3.5772*	-3.3970*
trade, restaurants,	(1.2533)	(1.3953)	(1.4542)	(1.5393)	(1.6894)	(1.7692)	(1.8532)	(1.8745)	(1.9393)	(1.9157)	(1.9666)
hotels	[0.0186]	[0.0183]	[0.0277]	[0.0391]	[0.0258]	[0.0247]	[0.0355]	[0.0408]	[0.0406]	[0.0633]	[0.0856]
Transport, storage,	-2.4327	-2.1724	-2.3697	-2.6174	-2.9269	-3.4532*	-3.7129*	-3.6571	-4.1130*	-3.7310	-4.1570
communication	(1.4760)	(1.5800)	(1.7156)	(1.8306)	(1.9560)	(2.0391)	(2.1587)	(2.2660)	(2.3168)	(2.4371)	(2.5539)
	[0.1009]	[0.1707]	[0.1687]	[0.1543]	[0.1361]	[0.0919]	[0.0870]	[0.1081]	[0.0773]	[0.1273]	[0.1051]
Other activities	-1.0382	-0.9182	-0.8139	-0.7209	-0.9570	-0.9954	-1.1212	-1.1721	-1.0097	-0.7098	-0.3201
	(0.6989)	(0.7375)	(0.8542)	(0.8682)	(0.9444)	(0.9810)	(1.0815)	(1.1432)	(1.1841)	(1.1733)	(1.2970)
	[0.1389]	[0.2145]	[0.3418]	[0.4074]	[0.3121]	[0.3115]	[0.3011]	[0.3064]	[0.3948]	[0.5459]	[0.8053]
N	8,500	8,500	8,500	8,500	8,500	8,500	8,500	8,500	8,500	8,500	8,500

Notes: $*p < 0.1, **p < 0.05, ***p < 0.01$. F-tests of panel OLS regression results with clustered standard errors by countries in parentheses (), and p-values in brackets []. The coefficients show the effect of a one standard deviation increase in tropical cyclone damage accumulated over different years on the per capita growth rate in a given sectoral aggregate. The standard deviations are 2,236,738 for the agricultural and 2,269,395 for the remaining sectors, calculated for the whole sample of positive wind speed observations. The independent variable is Damage_t, which is the weighted damage measure for tropical cyclone intensity in year t. For the sector aggregate agriculture, hunting, forestry and fishing it is weighted by exposed agricultural land in t-1, whereas for the remaining sector aggregates it is weighted by exposed population in t-1. All regressions include country and year fixed effects as well as country-specific linear trends.

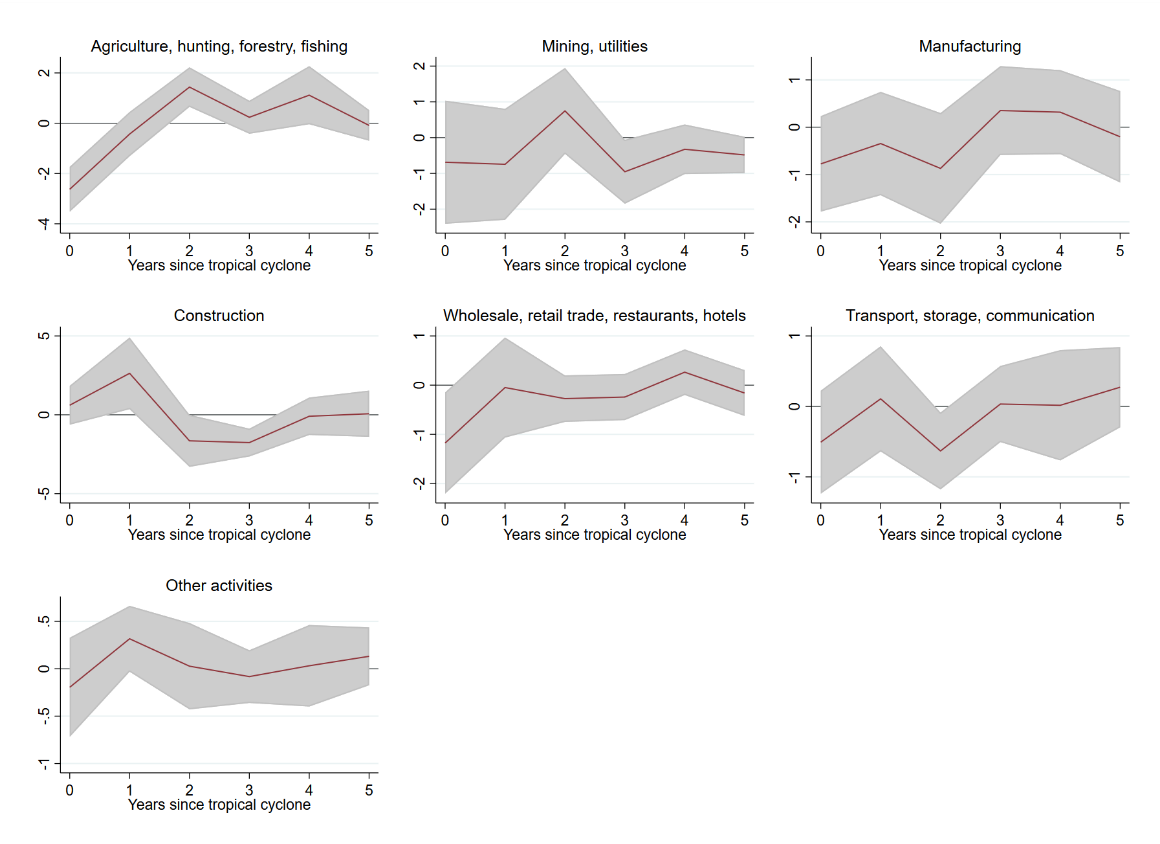

Figure 1.9: Lagged influence of tropical cyclone damage on sectoral GDP growth (5 years)

Notes: The y-axis displays the coefficient of tropical cyclone damage on the respective per capita growth rates and the x-axis shows the years since the tropical cyclone passed. The gray areas represent the respective 95% confidence interval and the red line the respective (connected) point estimates. The underlying estimations can be found in Tables 1.5–1.11 in Appendix 1.6.4.

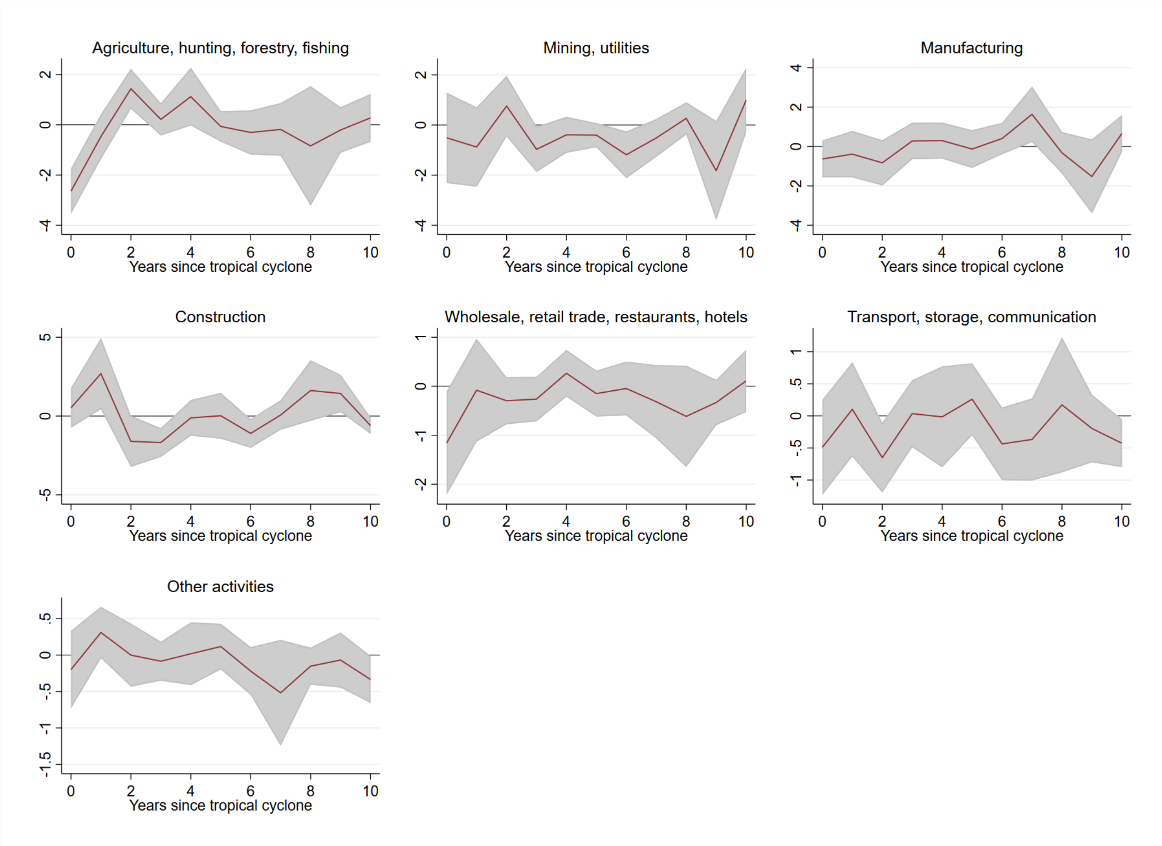

Figure 1.10: Lagged influence of tropical cyclone damage on sectoral GDP growth (10 years)

Notes: The y-axis displays the coefficient of tropical cyclone damage on the respective per capita growth rates and the x-axis shows the years since the tropical cyclone passed. The gray areas represent the respective 95% confidence interval and the red line the respective (connected) point estimates. The underlying estimations can be found in Tables 1.5–1.11 in Appendix 1.6.4.

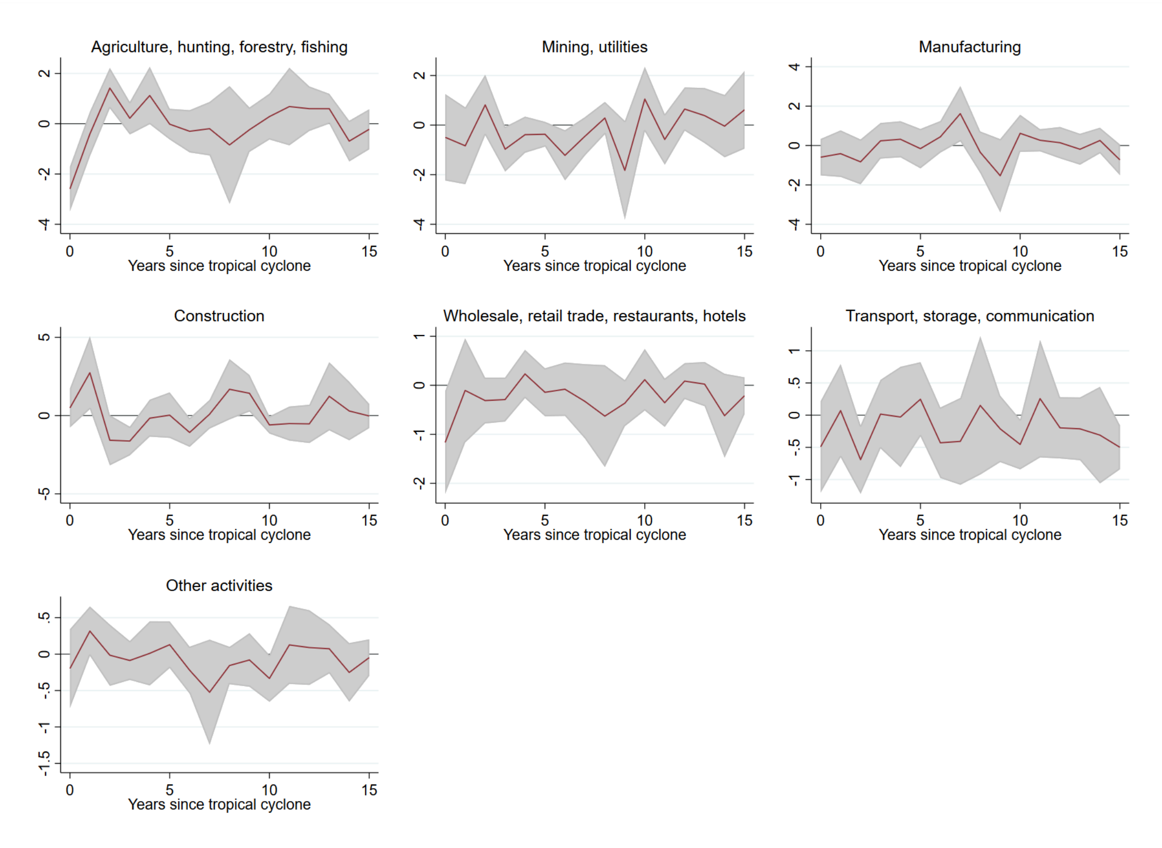

Figure 1.11: Lagged influence of tropical cyclone damage on sectoral GDP growth (15 years)

Notes: The y-axis displays the coefficient of tropical cyclone damage on the respective per capita growth rates and the x-axis shows the years since the tropical cyclone passed. The gray areas represent the respective 95% confidence interval and the red line the respective (connected) point estimates. The underlying estimations can be found in Tables 1.5–1.11 in Appendix 1.6.4.

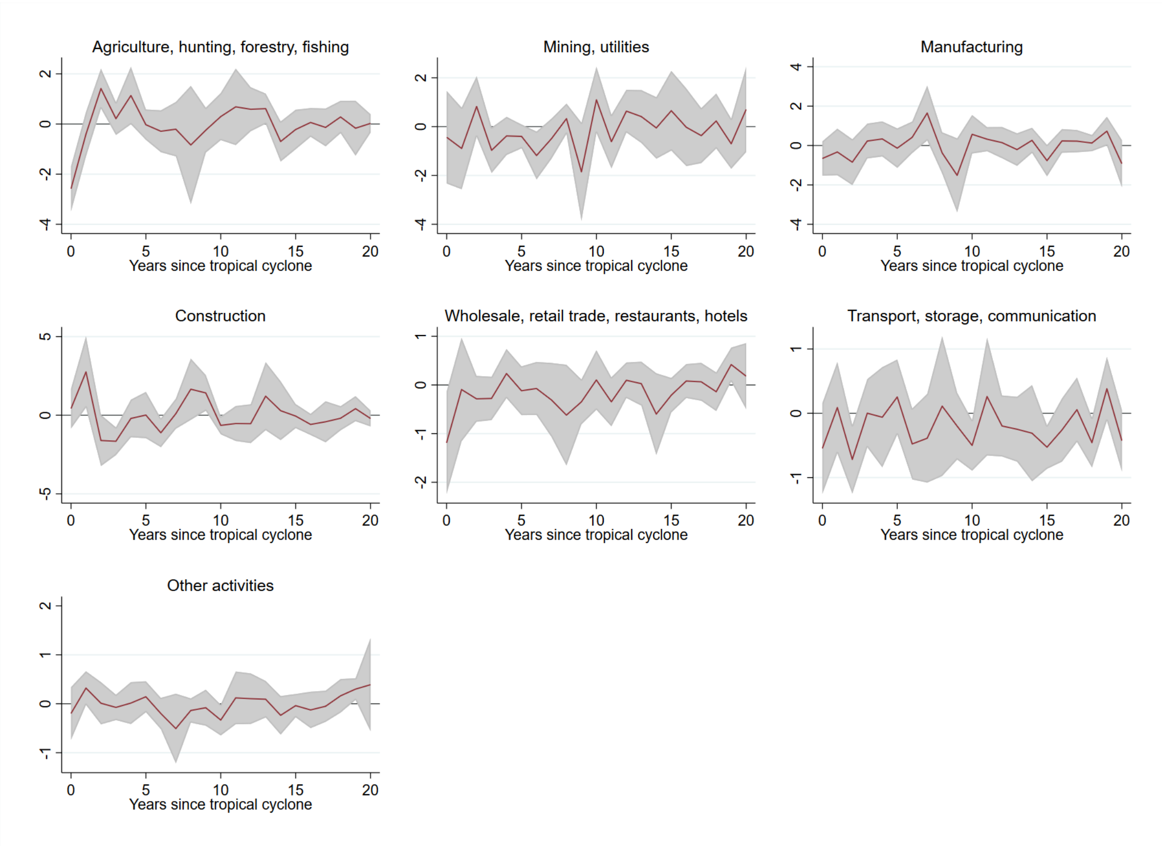

Figure 1.12: Lagged influence of tropical cyclone damage on sectoral GDP growth (20 years)

Notes: The y-axis displays the coefficient of tropical cyclone damage on the respective per capita growth rates and the x-axis shows the years since the tropical cyclone passed. The gray areas represent the respective 95% confidence interval and the red line the respective (connected) point estimates. The underlying estimations can be found in Tables 1.5–1.11 in Appendix 1.6.4.

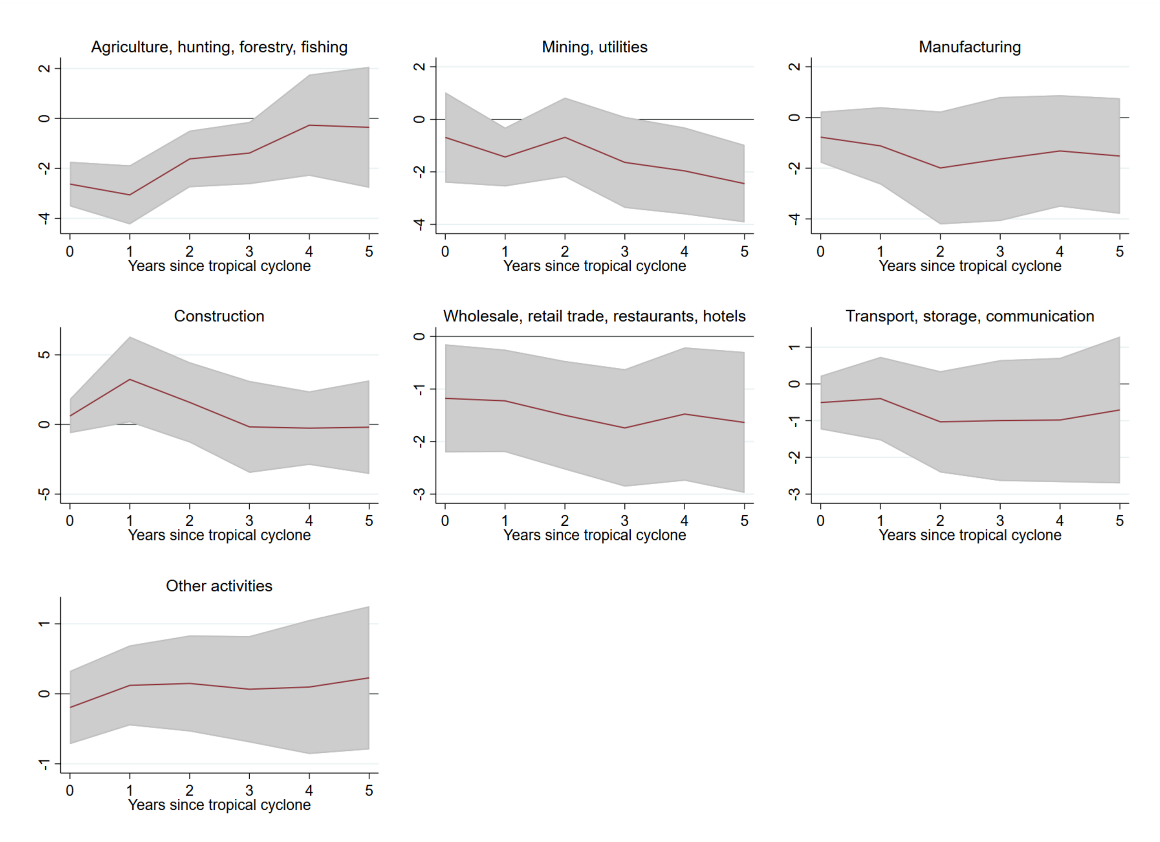

Figure 1.13: Cumulative lagged influence of tropical cyclone damage on sectoral GDP growth (5 years)

Notes: The y-axis displays the cumulative coefficient of tropical cyclone damage on the respective per capita growth rates and the x-axis shows the years since the tropical cyclone passed. The gray areas represent the respective 95% confidence interval and the red line the respective cumulative (connected) point estimates. The underlying estimations can be found in Tables 1.12–1.13 in Appendix 1.6.4.

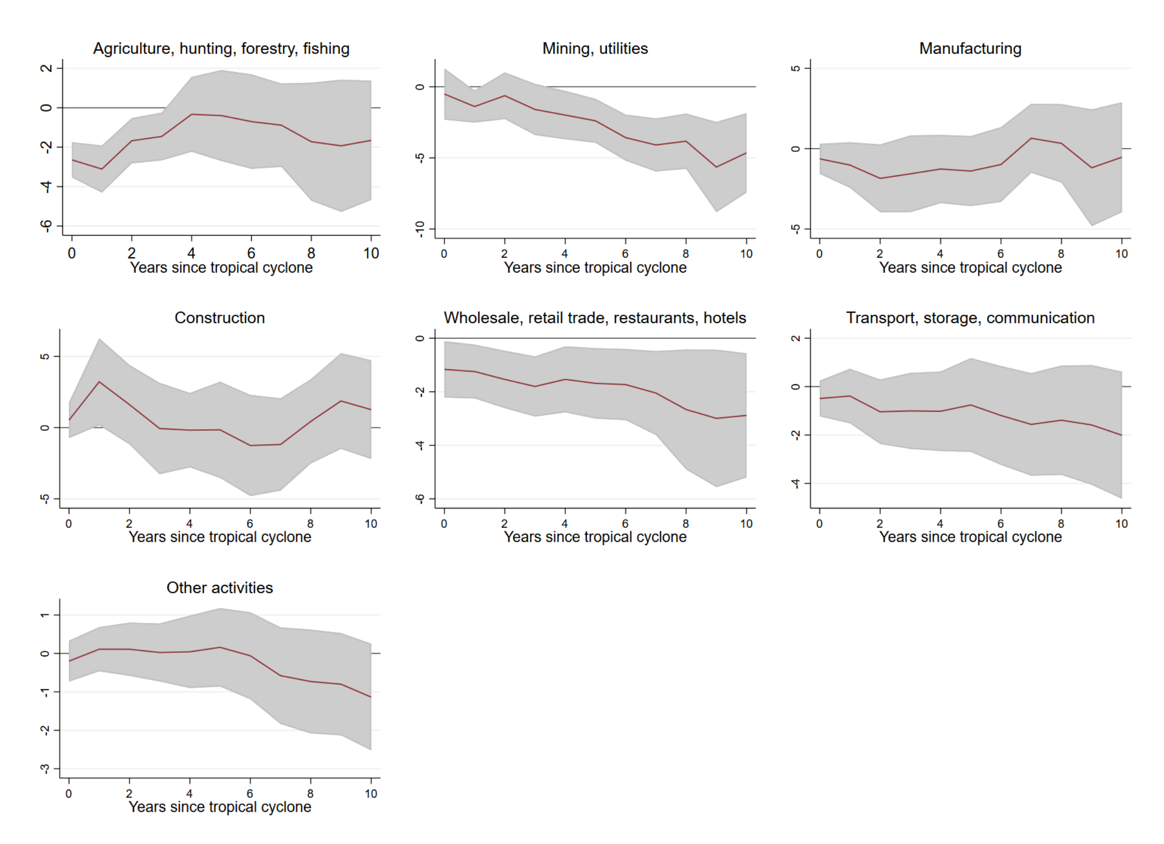

Figure 1.14: Cumulative lagged influence of tropical cyclone damage on sectoral GDP growth (10 years)

Notes: The y-axis displays the cumulative coefficient of tropical cyclone damage on the respective per capita growth rates and the x-axis shows the years since the tropical cyclone passed. The gray areas represent the respective 95% confidence interval and the red line the respective cumulative (connected) point estimates. The underlying estimations can be found in Tables 1.12–1.13 in Appendix 1.6.4.

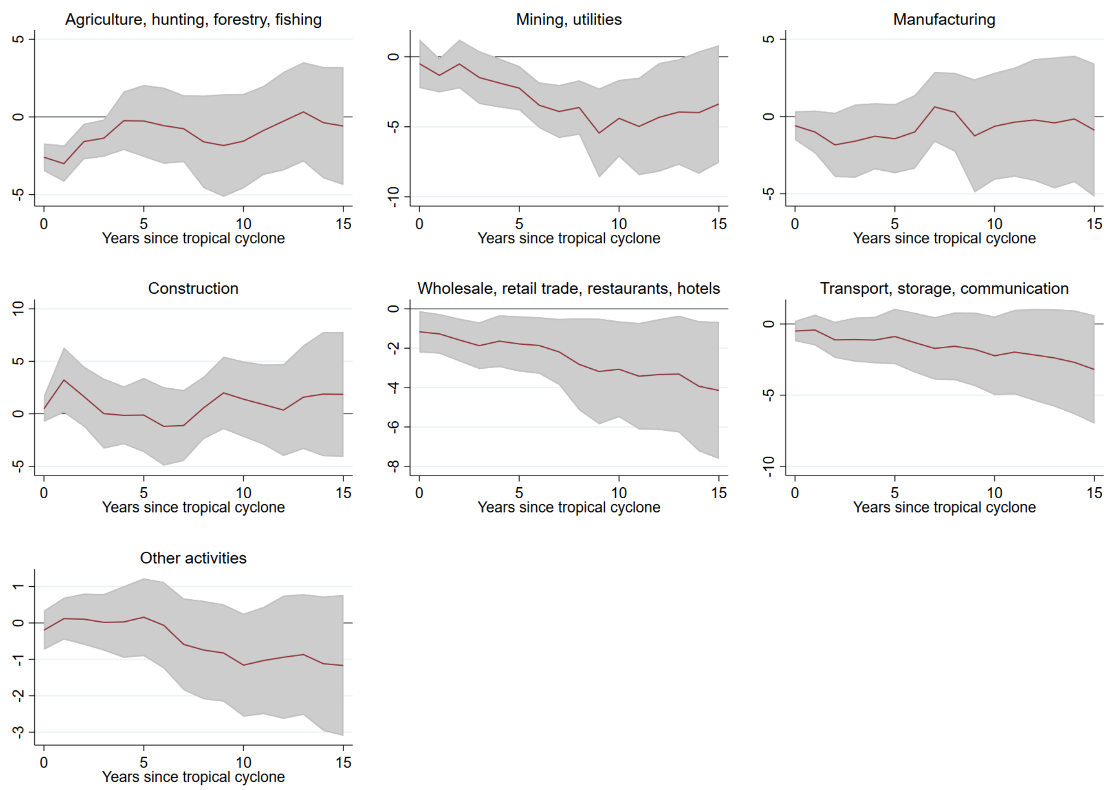

Figure 1.15: Cumulative lagged influence of tropical cyclone damage on sectoral GDP growth (15 years)

Notes: The y-axis displays the cumulative coefficient of tropical cyclone damage on the respective per capita growth rates and the x-axis shows the years since the tropical cyclone passed. The gray areas represent the respective 95% confidence interval and the red line the respective cumulative (connected) point estimates. The underlying estimations can be found in Tables 1.12–1.13 in Appendix 1.6.4.

Table 1.14: Effects of tropical cyclone damage on Input-Output coefficients of sector aggregate agriculture, hunting, forestry and fishing (A&B)

Dependent Variables: *Input-Output coefficient (IO)*

	$IO^{A\&B,A\&B}$	$IO^{A\&B,C\&E}$	$IO^{A\&B,D}$	$IO^{A\&B,F}$	$IO^{A\&B,G\text{-}H}$	$IO^{A\&B,I}$	$IO^{A\&B,J\text{-}P}$
	(1)	(2)	(3)	(4)	(5)	(6)	(7)
$Damage_t$	-0.00004	-0.00008*	-0.00034	-0.00004	-0.00027**	-0.00016	-0.00038
	(0.00075)	(0.00005)	(0.00041)	(0.00003)	(0.00012)	(0.00014)	(0.00027)
	[0.95825]	[0.08510]	[0.40568]	[0.19239]	[0.01954]	[0.24485]	[0.15445]
$IO^{A\&B,A\&B}_{t-1}$	0.81383***						
	(0.04690)						
	[0.00000]						
$IO^{A\&B,C\&E}_{t-1}$		0.93027***					
		(0.05625)					
		[0.00000]					
$IO^{A\&B,D}_{t-1}$			0.85587***				
			(0.01276)				
			[0.00000]				
$IO^{A\&B,F}_{t-1}$				1.24487***			
				(0.15348)			
				[0.00000]			
$IO^{A\&B,G\text{-}H}_{t-1}$					0.84204***		
					(0.02799)		
					[0.00000]		
$IO^{A\&B,I}_{t-1}$						0.85337***	
						(0.02055)	
						[0.00000]	
$IO^{A\&B,J\text{-}P}_{t-1}$							0.90448***
							(0.01996)
							[0.00000]
N	4,490	4,490	4,490	4,490	4,490	4,490	4,490
Clusters	182	182	182	182	182	182	182
P-value	0.00000	0.00000	0.00000	0.00000	0.00000	0.00000	0.00000
Mean DV	0.16618	0.01220	0.08494	0.00377	0.03579	0.02204	0.07102

Notes: $*p < 0.1, **p < 0.05, ***p < 0.01$. Panel OLS regression results with clustered standard errors by countries in parentheses (), and p-values in brackets []. The coefficients show the effect of a one standard deviation increase in tropical cyclone damage on the respective Input-Output coefficients. The standard deviations are 2,236,738 for the agricultural and 2,269,395 for the remaining sectors, calculated for the whole sample of positive wind speed observations. $Damage_t$ is the weighted damage measure for tropical cyclone intensity in year t. For the sector aggregate agriculture, hunting, forestry and fishing it is weighted by exposed agricultural land in t-1, whereas for the remaining sector aggregates it is weighted by exposed population in t-1. The dependent variables are Input-Output coefficients (IO) and can range between 0-1. For example the coefficient $IO^{A\&B,D}_t$ displays how much input the sector aggregate A&B needs from sector aggregate D to produce one unit of output. The sector abbreviations represent the following sector aggregates: agriculture, hunting, forestry, and fishing (A&B), mining, and utilities (C&E), manufacturing (D), construction (F), wholesale, retail trade, restaurants, and hotels (G-H), transport, storage, and communication (I), other activities (J-P). All regressions include country and year fixed effects as well as country-specific linear trends.

Table 1.15: Effects of tropical cyclone damage on Input-Output coefficients of sector aggregate mining and utilities (C&E)

Dependent Variables: *Input-Output coefficient (IO)*

	$IO^{C\&E,A\&B}$	$IO^{C\&E,C\&E}$	$IO^{C\&E,D}$	$IO^{C\&E,F}$	$IO^{C\&E,G\text{-}H}$	$IO^{C\&E,I}$	$IO^{C\&E,J\text{-}P}$
	(1)	(2)	(3)	(4)	(5)	(6)	(7)
$Damage_t$	0.00002*	0.00106	-0.00025	-0.00014	-0.00015	-0.00020	-0.00010
	(0.00001)	(0.00154)	(0.00025)	(0.00012)	(0.00017)	(0.00021)	(0.00045)
	[0.09364]	[0.49122]	[0.31567]	[0.25528]	[0.36630]	[0.34866]	[0.82336]
$IO^{C\&E,A\&B}_{t\text{-}1}$	0.74893***						
	(0.06455)						
	[0.00000]						
$IO^{C\&E,C\&E}_{t\text{-}1}$		0.84491***					
		(0.05335)					
		[0.00000]					
$IO^{C\&E,D}_{t\text{-}1}$			0.89889***				
			(0.01903)				
			[0.00000]				
$IO^{C\&E,F}_{t\text{-}1}$				0.89490***			
				(0.02000)			
				[0.00000]			
$IO^{C\&E,G\text{-}H}_{t\text{-}1}$					0.81616***		
					(0.05525)		
					[0.00000]		
$IO^{C\&E,I}_{t\text{-}1}$						0.81922***	
						(0.05698)	
						[0.00000]	
$IO^{C\&E,J\text{-}P}_{t\text{-}1}$							0.89500***
							(0.02070)
							[0.00000]
N	4,490	4,490	4,490	4,490	4,490	4,490	4,490
Clusters	182	182	182	182	182	182	182
P-value	0.00000	0.00000	0.00000	0.00000	0.00000	0.00000	0.00000
Mean DV	0.00084	0.15156	0.05376	0.02778	0.01925	0.04862	0.08812

Notes: $*p < 0.1, **p < 0.05, ***p < 0.01$. Panel OLS regression results with clustered standard errors by countries in parentheses (), and p-values in brackets []. The coefficients show the effect of a one standard deviation increase in tropical cyclone damage on the respective Input-Output coefficients. The standard deviations are 2,236,738 for the agricultural and 2,269,395 for the remaining sectors, calculated for the whole sample of positive wind speed observations. $Damage_t$ is the weighted damage measure for tropical cyclone intensity in year t. For the sector aggregate agriculture, hunting, forestry and fishing it is weighted by exposed agricultural land in t-1, whereas for the remaining sector aggregates it is weighted by exposed population in t-1. The dependent variables are Input-Output coefficients (IO) and can range between 0-1. For example the coefficient $IO^{C\&E,D}_t$ displays how much input the sector aggregate C&E needs from sector aggregate D to produce one unit of output. The sector abbreviations represent the following sector aggregates: agriculture, hunting, forestry, and fishing (A&B), mining, and utilities (C&E), manufacturing (D), construction (F), wholesale, retail trade, restaurants, and hotels (G-H), transport, storage, and communication (I), other activities (J-P). All regressions include country and year fixed effects as well as country-specific linear trends.

Table 1.16: Effects of tropical cyclone damage on Input-Output coefficients of sector aggregate manufacturing (D)

Dependent Variables: *Input-Output coefficient (IO)*

	$IO^{D,A\&B}$	$IO^{D,C\&E}$	$IO^{D,D}$	$IO^{D,F}$	$IO^{D,G\text{-}H}$	$IO^{D,I}$	$IO^{D,J\text{-}P}$
	(1)	(2)	(3)	(4)	(5)	(6)	(7)
$Damage_t$	0.00052*	-0.00031	-0.00152*	-0.00003*	-0.00033	-0.00029	-0.00036
	(0.00029)	(0.00028)	(0.00085)	(0.00002)	(0.00022)	(0.00022)	(0.00022)
	[0.0770]	[0.2632]	[0.0768]	[0.0811]	[0.1348]	[0.1899]	[0.1064]
$IO^{D,A\&B}_{t-1}$	0.85952***						
	(0.03335)						
	[0.0000]						
$IO^{D,C\&E}_{t-1}$		0.77462***					
		(0.04997)					
		[0.0000]					
$IO^{D,D}_{t-1}$			0.80588***				
			(0.04449)				
			[0.0000]				
$IO^{D,F}_{t-1}$				0.96723***			
				(0.06204)			
				[0.0000]			
$IO^{D,G\text{-}H}_{t-1}$					0.84009***		
					(0.03605)		
					[0.0000]		
$IO^{D,I}_{t-1}$						0.90409***	
						(0.06205)	
						[0.0000]	
$IO^{D,J\text{-}P}_{t-1}$							0.87878***
							(0.01853)
							[0.0000]
N	4,490	4,490	4,490	4,490	4,490	4,490	4,490
Clusters	182	182	182	182	182	182	182
P-value	0.00000	0.00000	0.00000	0.00000	0.00000	0.00000	0.00000
Mean DV	0.05578	0.03927	0.23938	0.00452	0.05355	0.03589	0.08555

Notes: $*p < 0.1, **p < 0.05, ***p < 0.01$. Panel OLS regression results with clustered standard errors by countries in parentheses (), and p-values in brackets []. The coefficients show the effect of a one standard deviation increase in tropical cyclone damage on the respective Input-Output coefficients. The standard deviations are 2,236,738 for the agricultural and 2,269,395 for the remaining sectors, calculated for the whole sample of positive wind speed observations. $Damage_t$ is the weighted damage measure for tropical cyclone intensity in year t. For the sector aggregate agriculture, hunting, forestry and fishing it is weighted by exposed agricultural land in t-1, whereas for the remaining sector aggregates it is weighted by exposed population in t-1. The dependent variables are Input-Output coefficients (IO) and can range between 0-1. For example the coefficient $IO^{D,F}_t$ displays how much input the sector aggregate D needs from sector aggregate F to produce one unit of output. The sector abbreviations represent the following sector aggregates: agriculture, hunting, forestry, and fishing (A&B), mining, and utilities (C&E), manufacturing (D), construction (F), wholesale, retail trade, restaurants, and hotels (G-H), transport, storage, and communication (I), other activities (J-P). All regressions include country and year fixed effects as well as country-specific linear trends.

Table 1.17: Effects of tropical cyclone damage on Input-Output coefficients of sector aggregate construction (F)

Dependent Variables: *Input-Output coefficient (IO)*

	$IO^{F,A\&B}$	$IO^{F,C\&E}$	$IO^{F,D}$	$IO^{F,F}$	$IO^{F,G\text{-}H}$	$IO^{F,I}$	$IO^{F,J\text{-}P}$
	(1)	(2)	(3)	(4)	(5)	(6)	(7)
$Damage_t$	0.00006***	-0.00006	0.00142*	-0.00073	0.00019	-0.00009	0.00053**
	(0.00002)	(0.00011)	(0.00078)	(0.00082)	(0.00023)	(0.00021)	(0.00023)
	[0.00111]	[0.57363]	[0.07080]	[0.37456]	[0.40417]	[0.67856]	[0.02526]
$IO^{F,A\&B}_{t\text{-}1}$	0.85276***						
	(0.02954)						
	[0.00000]						
$IO^{F,C\&E}_{t\text{-}1}$		0.81229***					
		(0.03102)					
		[0.00000]					
$IO^{F,D}_{t\text{-}1}$			0.77678***				
			(0.08966)				
			[0.00000]				
$IO^{F,F}_{t\text{-}1}$				0.85699***			
				(0.07010)			
				[0.00000]			
$IO^{F,G\text{-}H}_{t\text{-}1}$					0.83059***		
					(0.01923)		
					[0.00000]		
$IO^{F,I}_{t\text{-}1}$						0.79211***	
						(0.05507)	
						[0.00000]	
$IO^{F,J\text{-}P}_{t\text{-}1}$							0.86569***
							(0.01474)
							[0.00000]
N	4,490	4,490	4,490	4,490	4,490	4,490	4,490
Clusters	182	182	182	182	182	182	182
P-value	0.00000	0.00000	0.00000	0.00000	0.00000	0.00000	0.00000
Mean DV	0.00326	0.01606	0.20939	0.03962	0.06433	0.03951	0.09867

Notes: $*p < 0.1, **p < 0.05, ***p < 0.01$. Panel OLS regression results with clustered standard errors by countries in parentheses (), and p-values in brackets []. The coefficients show the effect of a one standard deviation increase in tropical cyclone damage on the respective Input-Output coefficients. The standard deviations are 2,236,738 for the agricultural and 2,269,395 for the remaining sectors, calculated for the whole sample of positive wind speed observations. $Damage_t$ is the weighted damage measure for tropical cyclone intensity in year t. For the sector aggregate agriculture, hunting, forestry and fishing it is weighted by exposed agricultural land in t-1, whereas for the remaining sector aggregates it is weighted by exposed population in t-1. The dependent variables are Input-Output coefficients (IO) and can range between 0-1. For example the coefficient $IO^{F,G\text{-}H}_t$ displays how much input the sector aggregate F needs from sector aggregate G-H to produce one unit of output. The sector abbreviations represent the following sector aggregates: agriculture, hunting, forestry, and fishing (A&B), mining, and utilities (C&E), manufacturing (D), construction (F), wholesale, retail trade, restaurants, and hotels (G-H), transport, storage, and communication (I), other activities (J-P). All regressions include country and year fixed effects as well as country-specific linear trends.

Table 1.18: Effects of tropical cyclone damage on Input-Output coefficients of sector aggregate wholesale, retail trade, restaurants and hotels (G-H)

Dependent Variables: *Input-Output coefficient (IO)*

	$IO^{G\text{-}H,A\&B}$	$IO^{G\text{-}H,C\&E}$	$IO^{G\text{-}H,D}$	$IO^{G\text{-}H,F}$	$IO^{G\text{-}H,G\text{-}H}$	$IO^{G\text{-}H,I}$	$IO^{G\text{-}H,J\text{-}P}$
	(1)	(2)	(3)	(4)	(5)	(6)	(7)
$Damage_t$	0.00011**	0.00010**	0.00058	0.00002	0.00158	-0.00001	0.00049
	(0.00005)	(0.00004)	(0.00045)	(0.00002)	(0.00119)	(0.00019)	(0.00063)
	[0.04378]	[0.01794]	[0.20337]	[0.32710]	[0.18587]	[0.96554]	[0.44368]
$IO^{G\&H,A\&B}_{t\text{-}1}$	0.86464***						
	(0.03825)						
	[0.00000]						
$IO^{G\&H,C\&E}_{t\text{-}1}$		0.82509***					
		(0.02879)					
		[0.00000]					
$IO^{G\&H,D}_{t\text{-}1}$			0.86836***				
			(0.03732)				
			[0.00000]				
$IO^{G\&H,F}_{t\text{-}1}$				0.79217***			
				(0.02664)			
				[0.00000]			
$IO^{G\&H,G\text{-}H}_{t\text{-}1}$					0.84379***		
					(0.07443)		
					[0.00000]		
$IO^{G\&H,I}_{t\text{-}1}$						0.87736***	
						(0.02081)	
						[0.00000]	
$IO^{G\&H,J\text{-}P}_{t\text{-}1}$							0.91386***
							(0.02899)
							[0.00000]
N	4,490	4,490	4,490	4,490	4,490	4,490	4,490
Clusters	182	182	182	182	182	182	182
P-value	0.0000	0.0000	0.0000	0.0000	0.0000	0.0000	0.0000
Mean DV	0.00831	0.01580	0.07093	0.00617	0.05380	0.06116	0.13920

Notes: $*p < 0.1, **p < 0.05, ***p < 0.01$. Panel OLS regression results with clustered standard errors by countries in parentheses (), and p-values in brackets []. The coefficients show the effect of a one standard deviation increase in tropical cyclone damage on the respective Input-Output coefficients. The standard deviations are 2,236,738 for the agricultural and 2,269,395 for the remaining sectors, calculated for the whole sample of positive wind speed observations. $Damage_t$ is the weighted damage measure for tropical cyclone intensity in year t. For the sector aggregate agriculture, hunting, forestry and fishing it is weighted by exposed agricultural land in t-1, whereas for the remaining sector aggregates it is weighted by exposed population in t-1. The dependent variables are Input-Output coefficients (IO) and can range between 0-1. For example the coefficient $IO^{GH,F}_t$ displays how much input the sector aggregate G-H needs from sector aggregate F to produce one unit of output. The sector abbreviations represent the following sector aggregates: agriculture, hunting, forestry, and fishing (A&B), mining, and utilities (C&E), manufacturing (D), construction (F), wholesale, retail trade, restaurants, and hotels (G-H), transport, storage, and communication (I), other activities (J-P). All regressions include country and year fixed effects as well as country-specific linear trends.

Table 1.19: Effects of tropical cyclone damage on Input-Output coefficients of sector aggregate transport, communication and infrastructure (I)

Dependent Variables: *Input-Output coefficient (IO)*

	$IO^{I,A\&B}$	$IO^{I,C\&E}$	$IO^{I,D}$	$IO^{I,F}$	$IO^{I,G\text{-}H}$	$IO^{I,I}$	$IO^{I,J\text{-}P}$
	(1)	(2)	(3)	(4)	(5)	(6)	(7)
$Damage_t$	0.00001	-0.00002	0.00039	0.00002	0.00001	0.00061	0.00014
	(0.00001)	(0.00004)	(0.00042)	(0.00003)	(0.00016)	(0.00055)	(0.00072)
	[0.37763]	[0.59378]	[0.35267]	[0.48078]	[0.96794]	[0.27302]	[0.84708]
$IO^{I,A\&B}_{t\text{-}1}$	0.75844***						
	(0.06742)						
	[0.00000]						
$IO^{I,C\&E}_{t\text{-}1}$		0.83975***					
		(0.03543)					
		[0.00000]					
$IO^{I,D}_{t\text{-}1}$			0.79606***				
			(0.03055)				
			[0.00000]				
$IO^{I,F}_{t\text{-}1}$				0.84223***			
				(0.02507)			
				[0.00000]			
$IO^{I,G\text{-}H}_{t\text{-}1}$					0.81081***		
					(0.07214)		
					[0.00000]		
$IO^{I,I}_{t\text{-}1}$						0.75830***	
						(0.09322)	
						[0.00000]	
$IO^{I,J\text{-}P}_{t\text{-}1}$							0.85232***
							(0.02148)
							[0.00000]
N	4,490	4,490	4,490	4,490	4,490	4,490	4,490
Clusters	182	182	182	182	182	182	182
P-value	0.00000	0.00000	0.00000	0.00000	0.00000	0.00000	0.00000
Mean DV	0.00041	0.00996	0.06178	0.00877	0.02755	0.10965	0.12995

Notes: $*p < 0.1, **p < 0.05, ***p < 0.01$. Panel OLS regression results with clustered standard errors by countries in parentheses (), and p-values in brackets []. The coefficients show the effect of a one standard deviation increase in tropical cyclone damage on the respective Input-Output coefficients. The standard deviations are 2,236,738 for the agricultural and 2,269,395 for the remaining sectors, calculated for the whole sample of positive wind speed observations. $Damage_t$ is the weighted damage measure for tropical cyclone intensity in year t. For the sector aggregate agriculture, hunting, forestry and fishing it is weighted by exposed agricultural land in t-1, whereas for the remaining sector aggregates it is weighted by exposed population in t-1. The dependent variables are Input-Output coefficients (IO) and can range between 0-1. For example the coefficient $IO^{I,F}_t$ displays how much input the sector aggregate I needs from sector aggregate F to produce one unit of output. The sector abbreviations represent the following sector aggregates: agriculture, hunting, forestry, and fishing (A&B), mining, and utilities (C&E), manufacturing (D), construction (F), wholesale, retail trade, restaurants, and hotels (G-H), transport, storage, and communication (I), other activities (J-P). All regressions include country and year fixed effects as well as country-specific linear trends.

Table 1.20: Effects of tropical cyclone damage on Input-Output coefficients of sector aggregate other activities (J-P)

	Dependent Variables: *Input-Output coefficient (IO)*						
	$IO^{J\text{-}P,A\&B}$	$IO^{J\text{-}P,C\&E}$	$IO^{J\text{-}P,D}$	$IO^{J\text{-}P,F}$	$IO^{J\text{-}P,G\text{-}H}$	$IO^{J\text{-}P,I}$	$IO^{J\text{-}P,J\text{-}P}$
	(1)	(2)	(3)	(4)	(5)	(6)	(7)
$Damage_t$	0.00004	0.00000	0.00043*	0.00003	0.00004	-0.00003	-0.00012
	(0.00003)	(0.00005)	(0.00023)	(0.00008)	(0.00009)	(0.00016)	(0.00039)
	[0.24367]	[0.93791]	[0.05994]	[0.73487]	[0.70197]	[0.85695]	[0.75992]
$IO^{J\text{-}P,A\&B}_{t\text{-}1}$	0.71852***						
	(0.27363)						
	[0.00938]						
$IO^{J\text{-}P,C\&E}_{t\text{-}1}$		0.87298***					
		(0.03855)					
		[0.00000]					
$IO^{J\text{-}P,D}_{t\text{-}1}$			0.77269***				
			(0.08736)				
			[0.00000]				
$IO^{J\text{-}P,F}_{t\text{-}1}$				0.80920***			
				(0.03406)			
				[0.00000]			
$IO^{J\text{-}P,G\text{-}H}_{t\text{-}1}$					0.79393***		
					(0.05463)		
					[0.00000]		
$IO^{J\text{-}P,I}_{t\text{-}1}$						0.88210***	
						(0.04426)	
						[0.00000]	
$IO^{J\text{-}P,J\text{-}P}_{t\text{-}1}$							0.76232***
							(0.07446)
							[0.00000]
N	4,490	4,490	4,490	4,490	4,490	4,490	4,490
Clusters	182	182	182	182	182	182	182
P-value	0.00001	0.00000	0.00000	0.00000	0.00000	0.00000	0.00000
Mean DV	0.00266	0.01221	0.05630	0.01723	0.02307	0.03172	0.14495

Notes: $*p < 0.1, **p < 0.05, ***p < 0.01$. Panel OLS regression results with clustered standard errors by countries in parentheses (), and p-values in brackets []. The coefficients show the effect of a one standard deviation increase in tropical cyclone damage on the respective Input-Output coefficients. The standard deviations are 2,236,738 for the agricultural and 2,269,395 for the remaining sectors, calculated for the whole sample of positive wind speed observations. $Damage_t$ is the weighted damage measure for tropical cyclone intensity in year t. For the sector aggregate agriculture, hunting, forestry and fishing it is weighted by exposed agricultural land in t-1, whereas for the remaining sector aggregates it is weighted by exposed population in t-1. The dependent variables are Input-Output coefficients (IO) and can range between 0-1. For example the coefficient $IO^{J\text{-}P,F}_{t}$ displays how much input the sector aggregate JP needs from sector aggregate F to produce one unit of output. The sector abbreviations represent the following sector aggregates: agriculture, hunting, forestry, and fishing (A&B), mining, and utilities (C&E), manufacturing (D), construction (F), wholesale, retail trade, restaurants, and hotels (G-H), transport, storage, and communication (I), other activities (J-P). All regressions include country and year fixed effects as well as country-specific linear trends.

Table 1.21: Robustness – Input-Output sample

Dependent Variables: *Per capita growth rate (%) in sector aggregate*

	Agriculture, hunting, forestry, fishing	Mining, utilities	Manu-facturing	Construc-tion	Wholesale, retail trade, restau-rants, hotels	Transport, storage, communi-cation	Other activities
	(1)	(2)	(3)	(4)	(5)	(6)	(7)
Damage_t	-2.6738***	-0.7476	0.0793	-1.2425	-1.1227***	-0.0780	-0.0272
	(0.6167)	(0.5568)	(0.6927)	(1.2898)	(0.3678)	(0.4348)	(0.3057)
	[0.0000]	[0.1810]	[0.9090]	[0.3367]	[0.0026]	[0.8578]	[0.9293]
N	4,490	4,490	4,490	4,490	4,490	4,490	4,490
Clusters	182	182	182	182	182	182	182
P-value	0.0000	0.1810	0.9090	0.3367	0.0026	0.8578	0.9293
Mean DV	0.8402	3.3496	2.5646	3.8989	2.7094	4.1525	2.4175

Notes: $*p < 0.1, **p < 0.05, ***p < 0.01$. Panel OLS regression results with clustered standard errors by countries in parentheses (), and p-values in brackets []. The coefficients show the effect of a one standard deviation increase in tropical cyclone damage on the per capita growth rate in a given sectoral aggregate. The standard deviations are 2,236,738 for the agricultural and 2,269,395 for the remaining sectors, calculated for the whole sample of positive wind speed observations. The sample covers the period 1990 through 2015. Damage_t is the weighted damage measure for tropical cyclone intensity in year t. For the sector aggregate agriculture, hunting, forestry and fishing it is weighted by exposed agricultural land in t-1, whereas for the remaining sector aggregates it is weighted by exposed population in t-1. All regressions include country and year fixed effects as well as country-specific linear trends.

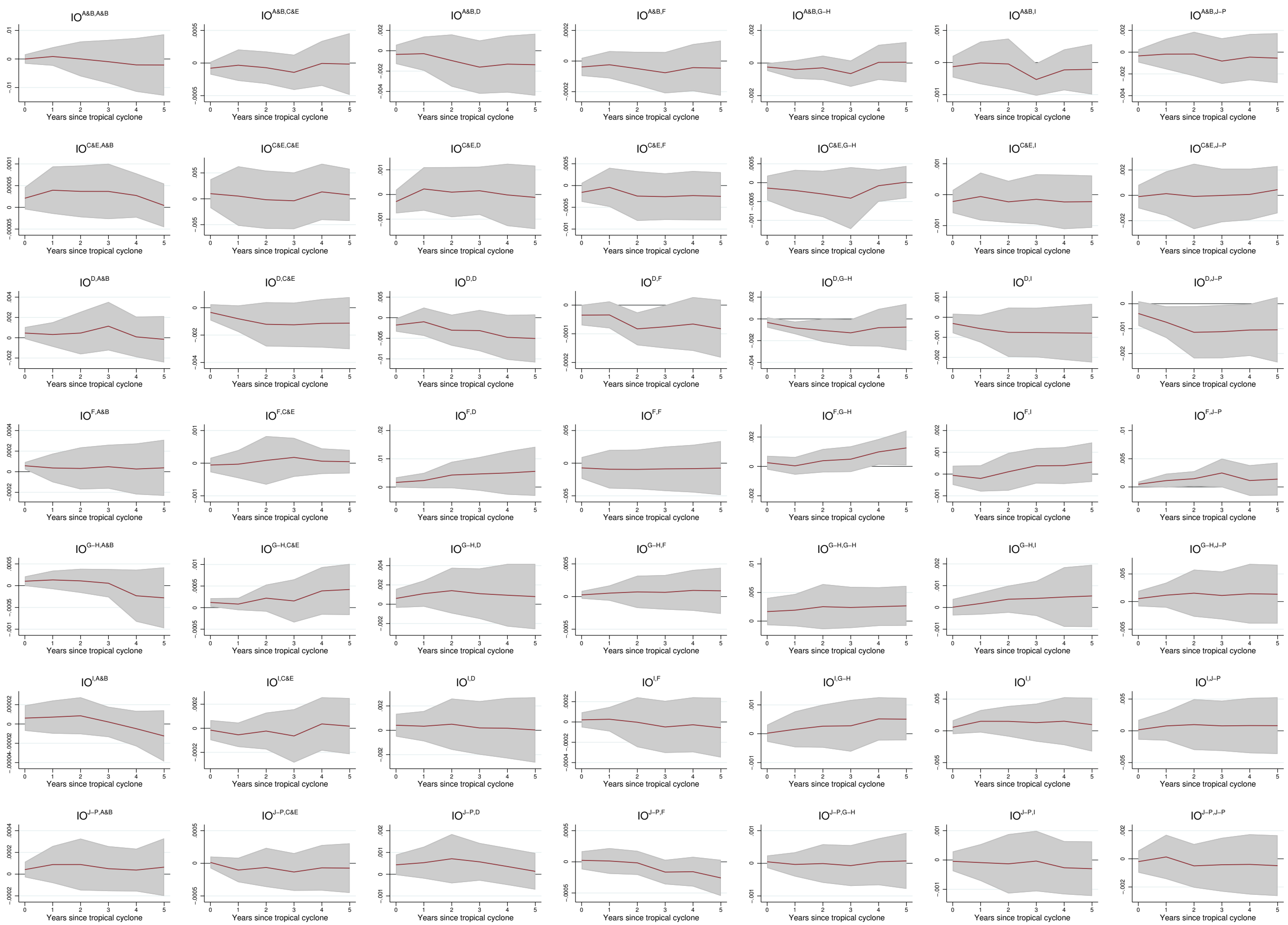

Figure 1.16: Cumulative lagged influence of tropical cyclone damage on Input-Output coefficients (5 years)

Notes: The y-axis displays the cumulative coefficient of tropical cyclone damage on the respective Input-Output coefficient and the x-axis shows the years since the tropical cyclone passed. The gray areas represent the respective 95% confidence interval and the red line the respective cumulative (connected) point estimates.

1.6.5 Robustness Statistics

1.6.5.1 Direct Effects

Table 1.22: Robustness – Placebo test

Dependent Variables: *Per capita growth rate (%) in sector aggregate*

	Agriculture, hunting, forestry, fishing	Mining, utilities	Manu-facturing	Construc-tion	Wholesale, retail trade, restau-rants, hotels	Transport, storage, communi-cation	Other activities
	(1)	(2)	(3)	(4)	(5)	(6)	(7)
Damage_{t+2}	0.2800	0.1413	-0.1306	0.3074	-0.0170	0.2501	-0.0656
	(0.2114)	(0.3928)	(0.3284)	(0.5417)	(0.2709)	(0.2010)	(0.1130)
	[0.1868]	[0.7195]	[0.6912]	[0.5710]	[0.9499]	[0.2147]	[0.5623]
N	8,092	8,092	8,092	8,092	8,092	8,092	8,092
Clusters	205	205	205	205	205	205	205
P-value	0.1868	0.7195	0.6912	0.5710	0.9499	0.2147	0.5623
Mean DV	0.8735	3.9027	2.6874	3.2847	2.5517	3.7559	2.5872

Notes: $*p < 0.1, **p < 0.05, ***p < 0.01$. Panel OLS regression results with clustered standard errors by countries in parentheses (), and p-values in brackets []. The coefficients show the effect of a one standard deviation increase in tropical cyclone damage on the per capita growth rate in a given sectoral aggregate. The standard deviations are 2,236,738 for the agricultural and 2,269,395 for the remaining sectors, calculated for the whole sample of positive wind speed observations. The sample covers the period 1971 through 2015. Damage_{t+2} is the weighted damage measure for tropical cyclone intensity in year t+2. For the sector aggregate agriculture, hunting, forestry and fishing it is weighted by exposed agricultural land in t+1, whereas for the remaining sector aggregates it is weighted by exposed population in t+1. All regressions include country and year fixed effects as well as country-specific linear trends.

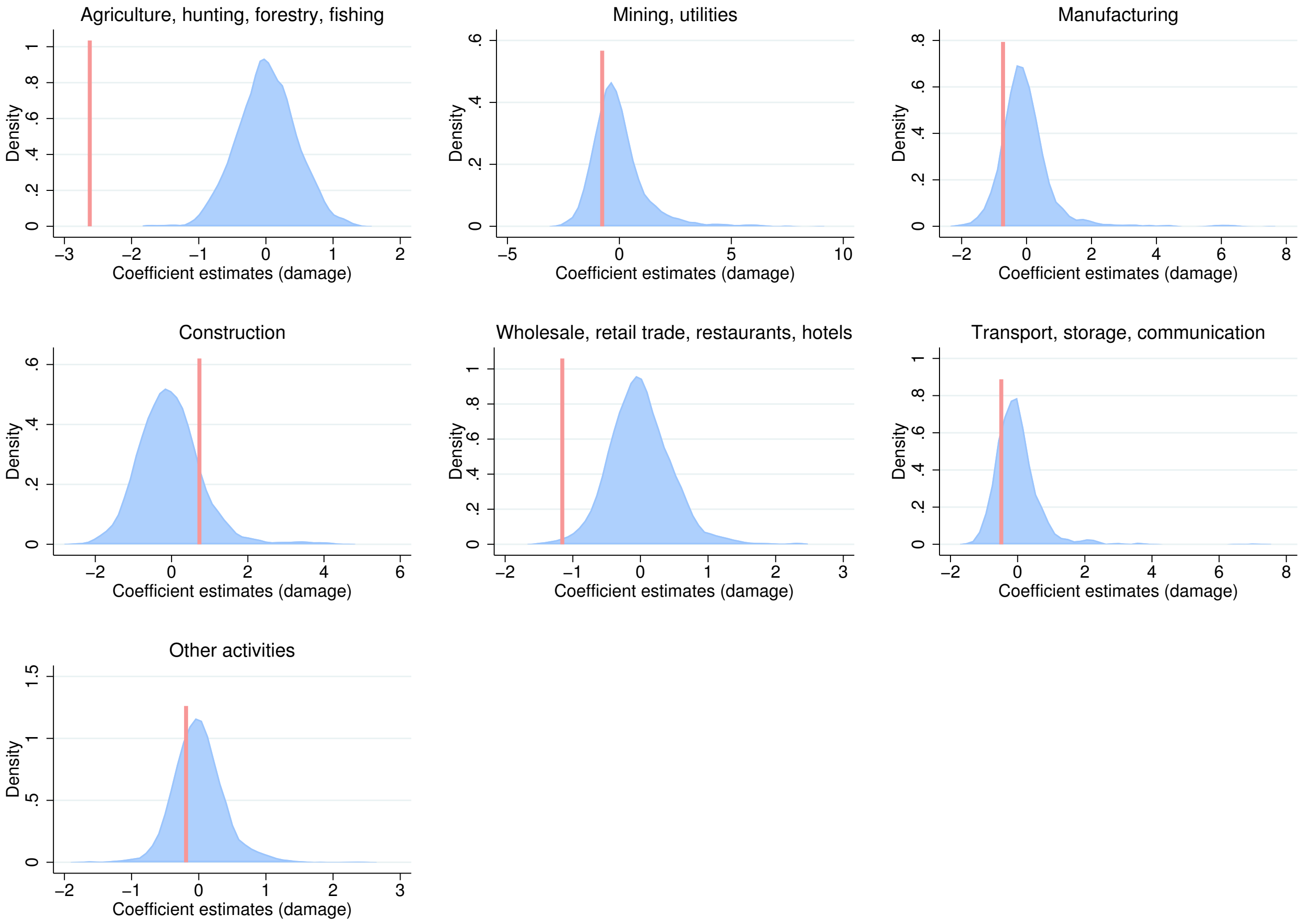

Figure 1.17: Randomization tests – Sectoral GDP growth

Notes: This figure shows the Fisher randomization test results for the $damage_t$ variable where the years are permuted for 2,000 repetitions. It displays the kernel density plots (blue) of the randomization coefficient estimates together the results of model 1.4 (red bar).

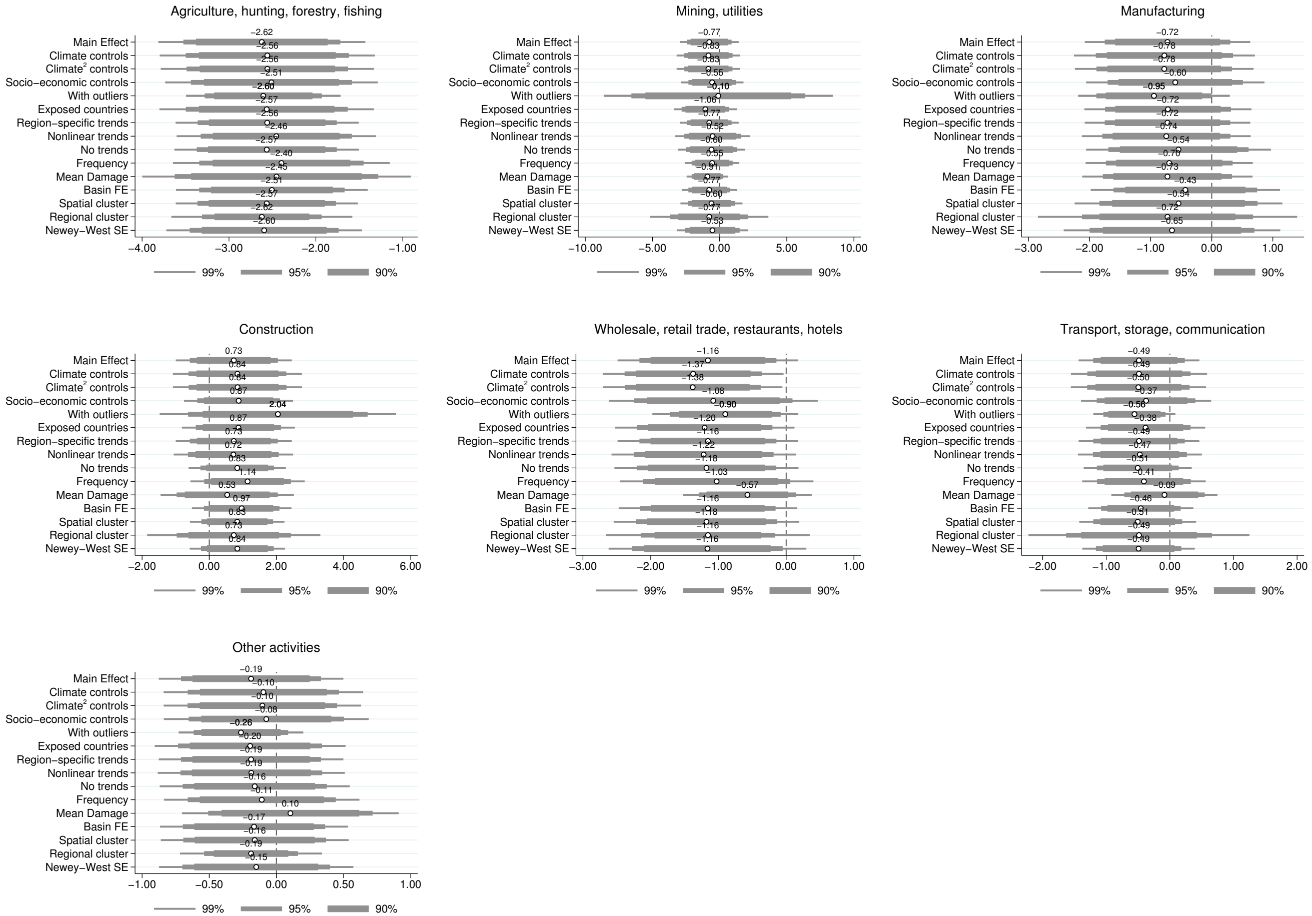

Figure 1.18: Overview robustness tests – Sectoral GDP growth

Notes: Coefficient plots for different robustness tests for direct effects of tropical cyclone damage of model 1.4. The underlying regressions are shown in Tables 1.23–1.46.

Table 1.23: Robustness – Temperature control variables

Dependent Variables: *Per capita growth rate (%) in sector aggregate*

	Agriculture, hunting, forestry, fishing	Mining, utilities	Manu-facturing	Construc-tion	Wholesale, retail trade, restau-rants, hotels	Transport, storage, communi-cation	Other activities
	(1)	(2)	(3)	(4)	(5)	(6)	(7)
Damage_t	-2.5247***	-0.8171	-0.6918	0.8478	-1.3570***	-0.4830	-0.1038
	(0.4758)	(0.9290)	(0.5825)	(0.7365)	(0.5137)	(0.4061)	(0.2855)
	[0.0000]	[0.3802]	[0.2364]	[0.2511]	[0.0089]	[0.2358]	[0.7167]
Temperature_t	-0.4693	-0.2674	-0.0911	-0.2456	-0.2755	0.5192	0.2818
	(0.3236)	(0.9645)	(0.6324)	(0.5503)	(0.3549)	(0.4588)	(0.3586)
	[0.1486]	[0.7819]	[0.8856]	[0.6559]	[0.4385]	[0.2592]	[0.4330]
N	7,992	7,992	7,992	7,992	7,992	7,992	7,992
Clusters	193	193	193	193	193	193	193
P-value	0.0000	0.6779	0.4863	0.4668	0.0201	0.3020	0.6974
Mean DV	0.8441	3.7568	2.6349	3.2407	2.4850	3.7287	2.5230

Notes: $*p < 0.1, **p < 0.05, ***p < 0.01$. Panel OLS regression results with clustered standard errors by countries in parentheses (), and p-values in brackets []. The coefficients show the effect of a one standard deviation increase in tropical cyclone damage on the per capita growth rate in a given sectoral aggregate. The standard deviations are 2,236,738 for the agricultural and 2,269,395 for the remaining sectors, calculated for the whole sample of positive wind speed observations. The sample covers the period 1971 through 2015. Damage_t is the weighted damage measure for tropical cyclone intensity in year t. For the sector aggregate agriculture, hunting, forestry and fishing it is weighted by exposed agricultural land in t-1, whereas for the remaining sector aggregates it is weighted by exposed population in t-1. Temperature is measured in degree Celsius. All regressions include country and year fixed effects as well as country-specific linear trends.

Table 1.24: Robustness – Precipitation control variables

Dependent Variables: *Per capita growth rate (%) in sector aggregate*

	Agriculture, hunting, forestry, fishing	Mining, utilities	Manu-facturing	Construc-tion	Wholesale, retail trade, restau-rants, hotels	Transport, storage, communi-cation	Other activities
	(1)	(2)	(3)	(4)	(5)	(6)	(7)
Damage_t	-2.5641***	-0.8320	-0.7753	0.8379	-1.3739***	-0.4842	-0.0960
	(0.4760)	(0.9105)	(0.5694)	(0.7375)	(0.5127)	(0.4124)	(0.2849)
	[0.0000]	[0.3619]	[0.1749]	[0.2573]	[0.0080]	[0.2418]	[0.7366]
Precipitation_t	0.0008	0.0003	0.0019	0.0002	0.0004	0.0000	-0.0002
	(0.0005)	(0.0013)	(0.0016)	(0.0015)	(0.0004)	(0.0007)	(0.0003)
	[0.1204]	[0.7892]	[0.2435]	[0.8765]	[0.3310]	[0.9829]	[0.5946]
N	7,992	7,992	7,992	7,992	7,992	7,992	7,992
Clusters	193	193	193	193	193	193	193
P-value	0.0000	0.5776	0.2191	0.5078	0.0221	0.4908	0.8182
Mean DV	0.8441	3.7568	2.6349	3.2407	2.4850	3.7287	2.5230

Notes: $*p < 0.1, **p < 0.05, ***p < 0.01$. Panel OLS regression results with clustered standard errors by countries in parentheses (), and p-values in brackets []. The coefficients show the effect of a one standard deviation increase in tropical cyclone damage on the per capita growth rate in a given sectoral aggregate. The standard deviations are 2,236,738 for the agricultural and 2,269,395 for the remaining sectors, calculated for the whole sample of positive wind speed observations. The sample covers the period 1971 through 2015. Damage_t is the weighted damage measure for tropical cyclone intensity in year t. For the sector aggregate agriculture, hunting, forestry and fishing it is weighted by exposed agricultural land in t-1, whereas for the remaining sector aggregates it is weighted by exposed population in t-1. Precipitation is measured in milimeters. All regressions include country and year fixed effects as well as country-specific linear trends.

Table 1.25: Robustness – Precipitation and temperature control variables

Dependent Variables: *Per capita growth rate (%) in sector aggregate*

	Agriculture, hunting, forestry, fishing	Mining, utilities	Manu-facturing	Construc-tion	Wholesale, retail trade, restau-rants, hotels	Transport, storage, communi-cation	Other activities
	(1)	(2)	(3)	(4)	(5)	(6)	(7)
Damage_t	-2.5590***	-0.8312	-0.7752	0.8387	-1.3730***	-0.4860	-0.0969
	(0.4760)	(0.9102)	(0.5694)	(0.7388)	(0.5129)	(0.4113)	(0.2856)
	[0.0000]	[0.3623]	[0.1750]	[0.2577]	[0.0081]	[0.2388]	[0.7348]
Precipitation_t	0.0007	0.0003	0.0019	0.0002	0.0004	0.0001	-0.0002
	(0.0005)	(0.0013)	(0.0016)	(0.0015)	(0.0004)	(0.0007)	(0.0003)
	[0.1390]	[0.8013]	[0.2334]	[0.8887]	[0.3650]	[0.9198]	[0.6437]
Temperature_t	-0.4423	-0.2554	-0.0202	-0.2378	-0.2619	0.5217	0.2760
	(0.3204)	(0.9533)	(0.5958)	(0.5401)	(0.3556)	(0.4599)	(0.3556)
	[0.1690]	[0.7891]	[0.9730]	[0.6602]	[0.4623]	[0.2580]	[0.4386]
N	7,992	7,992	7,992	7,992	7,992	7,992	7,992
Clusters	193	193	193	193	193	193	193
P-value	0.0000	0.7682	0.2853	0.6748	0.0369	0.4925	0.8517
Mean DV	0.8441	3.7568	2.6349	3.2407	2.4850	3.7287	2.5230

Notes: $*p < 0.1, **p < 0.05, ***p < 0.01$. Panel OLS regression results with clustered standard errors by countries in parentheses (), and p-values in brackets []. The coefficients show the effect of a one standard deviation increase in tropical cyclone damage on the per capita growth rate in a given sectoral aggregate. The standard deviations are 2,236,738 for the agricultural and 2,269,395 for the remaining sectors, calculated for the whole sample of positive wind speed observations. The sample covers the period 1971 through 2015. Damage_t is the weighted damage measure for tropical cyclone intensity in year t. For the sector aggregate agriculture, hunting, forestry and fishing it is weighted by exposed agricultural land in t-1, whereas for the remaining sector aggregates it is weighted by exposed population in t-1. Precipitation is measured in milimeters and temperature in degree Celsius. All regressions include country and year fixed effects as well as country-specific linear trends.

Table 1.26: Robustness – Precipitation and temperature squared control variables

	Dependent Variables: *Per capita growth rate (%) in sector aggregate*						
	Agriculture, hunting, forestry, fishing	Mining, utilities	Manu-facturing	Construc-tion	Wholesale, retail trade, restau-rants, hotels	Transport, storage, communi-cation	Other activities
	(1)	(2)	(3)	(4)	(5)	(6)	(7)
Damage_t	-2.5586***	-0.8335	-0.7780	0.8432	-1.3795***	-0.4952	-0.1046
	(0.4716)	(0.9085)	(0.5621)	(0.7390)	(0.5088)	(0.4082)	(0.2825)
	[0.0000]	[0.3601]	[0.1679]	[0.2553]	[0.0073]	[0.2265]	[0.7117]
Precipitation_t	0.0074***	0.0000	0.0058***	-0.0008	0.0033***	0.0043***	0.0028***
	(0.0018)	(0.0045)	(0.0021)	(0.0026)	(0.0011)	(0.0015)	(0.0010)
	[0.0000]	[0.9949]	[0.0055]	[0.7661]	[0.0024]	[0.0040]	[0.0034]
Precipitation_t^2	-0.0000***	0.0000	-0.0000**	0.0000	-0.0000***	-0.0000***	-0.0000***
	(0.0000)	(0.0000)	(0.0000)	(0.0000)	(0.0000)	(0.0000)	(0.0000)
	[0.0001]	[0.9333]	[0.0320]	[0.6513]	[0.0012]	[0.0003]	[0.0009]
Temperature_t	0.5378	-0.6870	0.8767	0.0846	-0.2075	0.6124	0.1631
	(0.3452)	(0.7100)	(0.7258)	(0.6794)	(0.5370)	(0.5837)	(0.5643)
	[0.1209]	[0.3345]	[0.2286]	[0.9010]	[0.6996]	[0.2955]	[0.7729]
Precipitation_t^2	-0.0343***	0.0168	-0.0328*	-0.0133	-0.0003	-0.0009	0.0063
	(0.0117)	(0.0409)	(0.0196)	(0.0210)	(0.0137)	(0.0165)	(0.0130)
	[0.0037]	[0.6821]	[0.0961]	[0.5284]	[0.9829]	[0.9554]	[0.6292]
N	7,992	7,992	7,992	7,992	7,992	7,992	7,992
Clusters	193	193	193	193	193	193	193
P-value	0.0000	0.8272	0.0047	0.8527	0.0062	0.0046	0.0175
Mean DV	0.8441	3.7568	2.6349	3.2407	2.4850	3.7287	2.5230

Notes: $*p < 0.1, **p < 0.05, ***p < 0.01$. Panel OLS regression results with clustered standard errors by countries in parentheses (), and p-values in brackets []. The coefficients show the effect of a one standard deviation increase in tropical cyclone damage on the per capita growth rate in a given sectoral aggregate. The standard deviations are 2,236,738 for the agricultural and 2,269,395 for the remaining sectors, calculated for the whole sample of positive wind speed observations. The sample covers the period 1971 through 2015. Damage_t is the weighted damage measure for tropical cyclone intensity in year t. For the sector aggregate agriculture, hunting, forestry and fishing it is weighted by exposed agricultural land in t-1, whereas for the remaining sector aggregates it is weighted by exposed population in t-1. Precipitation is measured in milimeters and temperature in degree Celsius. All regressions include country and year fixed effects as well as country-specific linear trends.

Table 1.27: Robustness – Socioeconomic control variables

Dependent Variables: *Per capita growth rate (%) in sector aggregate*

	Agriculture, hunting, forestry, fishing	Mining, utilities	Manu-facturing	Construc-tion	Wholesale, retail trade, restau-rants, hotels	Transport, storage, communi-cation	Other activities
	(1)	(2)	(3)	(4)	(5)	(6)	(7)
$Damage_t$	-2.5111***	-0.5517	-0.5968	0.8748	-1.0761*	-0.3748	-0.0754
	(0.4702)	(0.8971)	(0.5615)	(0.6245)	(0.5929)	(0.3934)	(0.2932)
	[0.0000]	[0.5392]	[0.2891]	[0.1628]	[0.0710]	[0.3419]	[0.7973]
Log pc value added$_{t\text{-}1}$	-8.6382***	-10.3300***	-14.7435*	-12.7315***	-7.6492***	-8.5118***	-7.2226***
	(1.0997)	(3.6141)	(7.9749)	(3.6421)	(1.1502)	(1.9726)	(1.2506)
	[0.0000]	[0.0047]	[0.0660]	[0.0006]	[0.0000]	[0.0000]	[0.0000]
Population growth$_{t\text{-}1}$	-0.2484	0.5531	0.7243	0.5887	0.0752	-0.1808	-0.0675
	(0.1671)	(0.6103)	(0.8187)	(0.5371)	(0.1833)	(0.4064)	(0.1861)
	[0.1388]	[0.3659]	[0.3774]	[0.2743]	[0.6822]	[0.6568]	[0.7173]
Capital growth$_{t\text{-}1}$	0.0009	0.0272	0.0040	0.0412*	0.0535**	0.0358*	0.0060
	(0.0058)	(0.0165)	(0.0270)	(0.0240)	(0.0254)	(0.0187)	(0.0088)
	[0.8712]	[0.1018]	[0.8828]	[0.0873]	[0.0365]	[0.0561]	[0.4967]
Trade openness$_{t\text{-}1}$	0.0008***	0.0026**	0.0027*	0.0019**	0.0008**	0.0006	0.0009**
	(0.0002)	(0.0013)	(0.0014)	(0.0008)	(0.0004)	(0.0003)	(0.0004)
	[0.0014]	[0.0434]	[0.0648]	[0.0216]	[0.0442]	[0.1119]	[0.0156]
N	8,249	8,249	8,249	8,249	8,249	8,249	8,249
Clusters	203	203	203	203	203	203	203
P-value	0.0000	0.0275	0.0000	0.0000	0.0000	0.0004	0.0000
Mean DV	0.8576	3.7800	2.6098	3.2809	2.5274	3.7516	2.5350

Notes: $*p < 0.1, **p < 0.05, ***p < 0.01$. Panel OLS regression results with clustered standard errors by countries in parentheses (), and p-values in brackets []. The coefficients show the effect of a one standard deviation increase in tropical cyclone damage on the per capita growth rate in a given sectoral aggregate. The standard deviations are 2,236,738 for the agricultural and 2,269,395 for the remaining sectors, calculated for the whole sample of positive wind speed observations. The sample covers the period 1971 through 2015. $Damage_t$ is the weighted damage measure for tropical cyclone intensity in year t. For the sector aggregate agriculture, hunting, forestry and fishing it is weighted by exposed agricultural land in t-1, whereas for the remaining sector aggregates it is weighted by exposed population in t-1. All regressions include country and year fixed effects, country-specific linear trends, and the respective socioeconomic control variables, which are all measured in t-1: log per capita value added of the re-spective sector, population growth rate, openness, investment rate.

Table 1.28: Robustness – Socioeconomic control variables for sector aggregate A&B

Dependent Variables: *Per capita growth rate (%) in sector aggregate*

	Agriculture, hunting, forestry, fishing	Agriculture, hunting, forestry, fishing	Agriculture, hunting, forestry, fishing	Agriculture, hunting, forestry, fishing
	(1)	(2)	(3)	(4)
Damage_{t}	-2.5365***	-2.6476***	-2.6670***	-2.6664***
	(0.4652)	(0.4647)	(0.4607)	(0.4607)
	[0.0000]	[0.0000]	[0.0000]	[0.0000]
Log pc value $\text{added}_{\text{t-1}}$	-8.5243***			
	(1.0985)			
	[0.0000]			
Population $\text{growth}_{\text{t-1}}$		-0.2480		
		(0.1627)		
		[0.1291]		
Capital $\text{growth}_{\text{t-1}}$			-0.0005	
			(0.0059)	
			[0.9267]	
Trade $\text{openness}_{\text{t-1}}$				0.0002
				(0.0002)
				[0.3385]
N	8,249	8,249	8,249	8,249
Clusters	203	203	203	203
P-value	0.0000	0.0000	0.0000	0.0000
Mean DV	0.8576	0.8576	0.8576	0.8576

Notes: $*p < 0.1, **p < 0.05, ***p < 0.01$. Panel OLS regression results with clustered standard errors by countries in parentheses (), and p-values in brackets []. The coefficients show the effect of a one standard deviation increase in tropical cyclone damage on the per capita growth rate in a given sectoral aggregate. The standard deviations are 2,236,738 for the agricultural and 2,269,395 for the remaining sectors, calculated for the whole sample of positive wind speed observations. The sample covers the period 1971 through 2015. Damage_{t} is the weighted damage measure for tropical cyclone intensity in year t. For the sector aggregate agriculture, hunting, forestry and fishing it is weighted by exposed agricultural land in t-1, whereas for the remaining sector aggregates it is weighted by exposed population in t-1. All regressions include country and year fixed effects, country-specific linear trends, and the respective socioeconomic control variables, which are all measured in t-1: log per capita value added of the re-spective sector, population growth rate, openness, investment rate.

Table 1.29: Robustness – Socioeconomic control variables for sector aggregate C&E

Dependent Variables: *Per capita growth rate (%) in sector aggregate*

	Mining, utilities	Mining, utilities	Mining, utilities	Mining, utilities
	(1)	(2)	(3)	(4)
Damage_{t}	-0.5328	-0.8364	-0.8396	-0.8080
	(0.8298)	(0.7722)	(0.7741)	(0.7727)
	[0.5215]	[0.2800]	[0.2794]	[0.2969]
Log pc value $\text{added}_{\text{t-1}}$	-10.1346***			
	(3.5445)			
	[0.0047]			
Population $\text{growth}_{\text{t-1}}$		0.2839		
		(0.6254)		
		[0.6503]		
Capital $\text{growth}_{\text{t-1}}$			0.0327*	
			(0.0169)	
			[0.0550]	
Trade $\text{openness}_{\text{t-1}}$				0.0010
				(0.0010)
				[0.3256]
N	8,249	8,249	8,249	8,249
Clusters	203	203	203	203
P-value	0.0093	0.5181	0.1043	0.3530
Mean DV	3.7800	3.7800	3.7800	3.7800

Notes: $*p < 0.1, **p < 0.05, ***p < 0.01$. Panel OLS regression results with clustered standard errors by countries in parentheses (), and p-values in brackets []. The coefficients show the effect of a one standard deviation increase in tropical cyclone damage on the per capita growth rate in a given sectoral aggregate. The standard deviations are 2,236,738 for the agricultural and 2,269,395 for the remaining sectors, calculated for the whole sample of positive wind speed observations. The sample covers the period 1971 through 2015. Damage_{t} is the weighted damage measure for tropical cyclone intensity in year t. For the sector aggregate agriculture, hunting, forestry and fishing it is weighted by exposed agricultural land in t-1, whereas for the remaining sector aggregates it is weighted by exposed population in t-1. All regressions include country and year fixed effects, country-specific linear trends, and the respective socioeconomic control variables, which are all measured in t-1: log per capita value added of the re-spective sector, population growth rate, openness, investment rate.

Table 1.30: Robustness – Socioeconomic control variables for sector aggregate D

Dependent Variables: *Per capita growth rate (%) in sector aggregate*

	Manu-facturing	Manu-facturing	Manu-facturing	Manu-facturing
	(1)	(2)	(3)	(4)
Damage_{t}	-0.5286	-0.7829*	-0.7348	-0.7210
	(0.5327)	(0.4602)	(0.4668)	(0.4655)
	[0.3222]	[0.0904]	[0.1170]	[0.1230]
Log pc value $\text{added}_{\text{t-1}}$	-14.4572*			
	(7.8463)			
	[0.0669]			
Population $\text{growth}_{\text{t-1}}$		0.7290		
		(0.8938)		
		[0.4157]		
Capital $\text{growth}_{\text{t-1}}$			0.0128	
			(0.0213)	
			[0.5470]	
Trade $\text{openness}_{\text{t-1}}$				0.0006**
				(0.0003)
				[0.0436]
N	8,249	8,249	8,249	8,249
Clusters	203	203	203	203
P-value	0.0447	0.1760	0.2657	0.0469
Mean DV	2.6098	2.6098	2.6098	2.6098

Notes: $*p < 0.1, **p < 0.05, ***p < 0.01$. Panel OLS regression results with clustered standard errors by countries in parentheses (), and p-values in brackets []. The coefficients show the effect of a one standard deviation increase in tropical cyclone damage on the per capita growth rate in a given sectoral aggregate. The standard deviations are 2,236,738 for the agricultural and 2,269,395 for the remaining sectors, calculated for the whole sample of positive wind speed observations. The sample covers the period 1971 through 2015. Damage_{t} is the weighted damage measure for tropical cyclone intensity in year t. For the sector aggregate agriculture, hunting, forestry and fishing it is weighted by exposed agricultural land in t-1, whereas for the remaining sector aggregates it is weighted by exposed population in t-1. All regressions include country and year fixed effects, country-specific linear trends, and the respective socioeconomic control variables, which are all measured in t-1: log per capita value added of the re-spective sector, population growth rate, openness, investment rate.

Table 1.31: Robustness – Socioeconomic control variables for sector aggregate F

Dependent Variables: *Per capita growth rate (%) in sector aggregate*

	Construction	Construction	Construction	Construction
	(1)	(2)	(3)	(4)
$Damage_t$	0.8510	0.6745	0.6548	0.6910
	(0.5943)	(0.6648)	(0.6539)	(0.6606)
	[0.1537]	[0.3116]	[0.3179]	[0.2968]
Log pc value $added_{t-1}$	-12.4440***			
	(3.5391)			
	[0.0005]			
Population $growth_{t-1}$		0.1896		
		(0.4891)		
		[0.6987]		
Capital $growth_{t-1}$			0.0440**	
			(0.0216)	
			[0.0430]	
Trade $openness_{t-1}$				0.0002
				(0.0003)
				[0.4814]
N	8,249	8,249	8,249	8,249
Clusters	203	203	203	203
P-value	0.0012	0.5386	0.0705	0.4603
Mean DV	3.2809	3.2809	3.2809	3.2809

Notes: $*p < 0.1, **p < 0.05, ***p < 0.01$. Panel OLS regression results with clustered standard errors by countries in parentheses (), and p-values in brackets []. The coefficients show the effect of a one standard deviation increase in tropical cyclone damage on the per capita growth rate in a given sectoral aggregate. The standard deviations are 2,236,738 for the agricultural and 2,269,395 for the remaining sectors, calculated for the whole sample of positive wind speed observations. The sample covers the period 1971 through 2015. $Damage_t$ is the weighted damage measure for tropical cyclone intensity in year t. For the sector aggregate agriculture, hunting, forestry and fishing it is weighted by exposed agricultural land in t-1, whereas for the remaining sector aggregates it is weighted by exposed population in t-1. All regressions include country and year fixed effects, country-specific linear trends, and the respective socioeconomic control variables, which are all measured in t-1: log per capita value added of the re-spective sector, population growth rate, openness, investment rate.

Table 1.32: Robustness – Socioeconomic control variables for sector aggregate G–H

Dependent Variables: *Per capita growth rate (%) in sector aggregate*				
	Wholesale, retail trade, restaurants, hotels	Wholesale, retail trade, restaurants, hotels	Wholesale, retail trade, restaurants, hotels	Wholesale, retail trade, restaurants, hotels
	(1)	(2)	(3)	(4)
Damage_{t}	-0.9141	-1.0459*	-1.0937**	-1.0486*
	(0.6028)	(0.5453)	(0.5456)	(0.5460)
	[0.1310]	[0.0565]	[0.0464]	[0.0562]
Log pc value $\text{added}_{\text{t-1}}$	-7.6211***			
	(1.1515)			
	[0.0000]			
Population $\text{growth}_{\text{t-1}}$		-0.0566		
		(0.2039)		
		[0.7815]		
Capital $\text{growth}_{\text{t-1}}$			0.0548**	
			(0.0263)	
			[0.0385]	
Trade $\text{openness}_{\text{t-1}}$				0.0003
				(0.0002)
				[0.1595]
N	8,249	8,249	8,249	8,249
Clusters	203	203	203	203
P-value	0.0000	0.1531	0.0202	0.0610
Mean DV	2.5274	2.5274	2.5274	2.5274

Notes: $*p < 0.1, **p < 0.05, ***p < 0.01$. Panel OLS regression results with clustered standard errors by countries in parentheses (), and p-values in brackets []. The coefficients show the effect of a one standard deviation increase in tropical cyclone damage on the per capita growth rate in a given sectoral aggregate. The standard deviations are 2,236,738 for the agricultural and 2,269,395 for the remaining sectors, calculated for the whole sample of positive wind speed observations. The sample covers the period 1971 through 2015. Damage_{t} is the weighted damage measure for tropical cyclone intensity in year t. For the sector aggregate agriculture, hunting, forestry and fishing it is weighted by exposed agricultural land in t-1, whereas for the remaining sector aggregates it is weighted by exposed population in t-1. All regressions include country and year fixed effects, country-specific linear trends, and the respective socioeconomic control variables, which are all measured in t-1: log per capita value added of the re-spective sector, population growth rate, openness, investment rate.

Table 1.33: Robustness – Socioeconomic control variables for sector aggregate I

Dependent Variables: *Per capita growth rate (%) in sector aggregate*

	Transport, storage, communication	Transport, storage, communication	Transport, storage, communication	Transport, storage, communication
	(1)	(2)	(3)	(4)
Damage_{t}	-0.3690	-0.4633	-0.5150	-0.4829
	(0.4063)	(0.3740)	(0.3775)	(0.3823)
	[0.3648]	[0.2169]	[0.1740]	[0.2080]
Log pc value $\text{added}_{\text{t-1}}$	-8.5883***			
	(1.9869)			
	[0.0000]			
Population $\text{growth}_{\text{t-1}}$		-0.2716		
		(0.4565)		
		[0.5525]		
Capital $\text{growth}_{\text{t-1}}$			0.0380*	
			(0.0206)	
			[0.0663]	
Trade $\text{openness}_{\text{t-1}}$				0.0004
				(0.0002)
				[0.1348]
N	8,249	8,249	8,249	8,249
Clusters	203	203	203	203
P-value	0.0001	0.4088	0.0604	0.1841
Mean DV	3.7516	3.7516	3.7516	3.7516

Notes: $*p < 0.1, **p < 0.05, ***p < 0.01$. Panel OLS regression results with clustered standard errors by countries in parentheses (), and p-values in brackets []. The coefficients show the effect of a one standard deviation increase in tropical cyclone damage on the per capita growth rate in a given sectoral aggregate. The standard deviations are 2,236,738 for the agricultural and 2,269,395 for the remaining sectors, calculated for the whole sample of positive wind speed observations. The sample covers the period 1971 through 2015. Damage_{t} is the weighted damage measure for tropical cyclone intensity in year t. For the sector aggregate agriculture, hunting, forestry and fishing it is weighted by exposed agricultural land in t-1, whereas for the remaining sector aggregates it is weighted by exposed population in t-1. All regressions include country and year fixed effects, country-specific linear trends, and the respective socioeconomic control variables, which are all measured in t-1: log per capita value added of the re-spective sector, population growth rate, openness, investment rate.

Table 1.34: Robustness – Socioeconomic control variables for sector aggregate J–P

Dependent Variables: *Per capita growth rate (%) in sector aggregate*				
	Other activities	Other activities	Other activities	Other activities
	(1)	(2)	(3)	(4)
Damage_{t}	-0.1455	-0.2366	-0.2530	-0.2431
	(0.2663)	(0.2463)	(0.2478)	(0.2477)
	[0.5855]	[0.3380]	[0.3085]	[0.3276]
Log pc value $\text{added}_{\text{t-1}}$	-7.1717***			
	(1.2283)			
	[0.0000]			
Population $\text{growth}_{\text{t-1}}$		-0.1124		
		(0.2103)		
		[0.5935]		
Capital $\text{growth}_{\text{t-1}}$			0.0094	
			(0.0086)	
			[0.2775]	
Trade $\text{openness}_{\text{t-1}}$				0.0004
				(0.0003)
				[0.1080]
N	8,249	8,249	8,249	8,249
Clusters	203	203	203	203
P-value	0.0000	0.5462	0.3059	0.1739
Mean DV	2.5350	2.5350	2.5350	2.5350

Notes: $*p < 0.1, **p < 0.05, ***p < 0.01$. Panel OLS regression results with clustered standard errors by countries in parentheses (), and p-values in brackets []. The coefficients show the effect of a one standard deviation increase in tropical cyclone damage on the per capita growth rate in a given sectoral aggregate. The standard deviations are 2,236,738 for the agricultural and 2,269,395 for the remaining sectors, calculated for the whole sample of positive wind speed observations. The sample covers the period 1971 through 2015. Damage_{t} is the weighted damage measure for tropical cyclone intensity in year t. For the sector aggregate agriculture, hunting, forestry and fishing it is weighted by exposed agricultural land in t-1, whereas for the remaining sector aggregates it is weighted by exposed population in t-1. All regressions include country and year fixed effects, country-specific linear trends, and the respective socioeconomic control variables, which are all measured in t-1: log per capita value added of the re-spective sector, population growth rate, openness, investment rate.

Table 1.35: Robustness – With outliers

	Dependent Variables: *Per capita growth rate (%) in sector aggregate*						
	Agriculture, hunting, forestry, fishing	Mining, utilities	Manu-facturing	Construc-tion	Wholesale, retail trade, restau-rants, hotels	Transport, storage, communi-cation	Other activities
	(1)	(2)	(3)	(4)	(5)	(6)	(7)
Damage_t	-2.6049***	-0.0986	-0.9457**	2.0446	-0.8982**	-0.5571**	-0.2636
	(0.3414)	(3.2776)	(0.4771)	(1.3543)	(0.4137)	(0.2477)	(0.1782)
	[0.0000]	[0.9760]	[0.0488]	[0.1326]	[0.0311]	[0.0256]	[0.1406]
N	8,611	8,611	8,611	8,611	8,611	8,611	8,611
Clusters	210	210	210	210	210	210	210
P-value	0.0000	0.9760	0.0488	0.1326	0.0311	0.0256	0.1406
Mean DV	0.8767	24.2969	2.6107	3.2691	2.5209	3.6908	2.5528

Notes: $*p < 0.1, **p < 0.05, ***p < 0.01$. Panel OLS regression results with clustered standard errors by countries in parentheses (), and p-values in brackets []. The coefficients show the effect of a one standard deviation increase in tropical cyclone damage on the per capita growth rate in a given sectoral aggregate. The standard deviations are 2,236,738 for the agricultural and 2,269,395 for the remaining sectors, calculated for the whole sample of positive wind speed observations. The sample covers the period 1971 through 2015. Damage_t is the weighted damage measure for tropical cyclone intensity in year t. For the sector aggregate agriculture, hunting, forestry and fishing it is weighted by exposed agricultural land in t-1, whereas for the remaining sector aggregates it is weighted by exposed population in t-1. All regressions include country and year fixed effects as well as country-specific linear trends. These regressions explictly include the following identified outliers: Dominican Republic 1979, Grenada 2004, Montserrat 1989, Myanmar 1977, Saint Lucia 1980.

Table 1.36: Robustness – Only exposed countries

	Dependent Variables: *Per capita growth rate (%) in sector aggregate*						
	Agriculture, hunting, forestry, fishing	Mining, utilities	Manu-facturing	Construc-tion	Wholesale, retail trade, restau-rants, hotels	Transport, storage, communi-cation	Other activities
	(1)	(2)	(3)	(4)	(5)	(6)	(7)
Damage_t	-2.5656***	-1.0617	-0.7166	0.8698	-1.2040**	-0.3823	-0.1959
	(0.4683)	(0.8886)	(0.5185)	(0.6384)	(0.5029)	(0.3552)	(0.2694)
	[0.0000]	[0.2356]	[0.1706]	[0.1767]	[0.0189]	[0.2850]	[0.4693]
N	3,622	3,622	3,622	3,622	3,622	3,622	3,622
Clusters	84	84	84	84	84	84	84
P-value	0.0000	0.2356	0.1706	0.1767	0.0189	0.2850	0.4693
Mean DV	1.0412	4.0654	2.2929	2.6719	2.3282	3.5110	2.5494

Notes: $*p < 0.1, **p < 0.05, ***p < 0.01$. Panel OLS regression results with clustered standard errors by countries in parentheses (), and p-values in brackets []. The coefficients show the effect of a one standard deviation increase in tropical cyclone damage on the per capita growth rate in a given sectoral aggregate. The standard deviations are 2,236,738 for the agricultural and 2,269,395 for the remaining sectors, calculated for the whole sample of positive wind speed observations. The sample covers the period 1971 through 2015. Damage_t is the weighted damage measure for tropical cyclone intensity in year t. For the sector aggregate agriculture, hunting, forestry and fishing it is weighted by exposed agricultural land in t-1, whereas for the remaining sector aggregates it is weighted by exposed population in t-1. All regressions include country and year fixed effects as well as country-specific linear trends.

Table 1.37: Robustness – Region-specific linear trends

Dependent Variables: *Per capita growth rate (%) in sector aggregate*

	Agriculture, hunting, forestry, fishing	Mining, utilities	Manu-facturing	Construc-tion	Wholesale, retail trade, restau-rants, hotels	Transport, storage, communi-cation	Other activities
	(1)	(2)	(3)	(4)	(5)	(6)	(7)
$Damage_t$	-2.5604***	-0.5822	-0.5362	0.8452	-1.1757**	-0.5040	-0.1541
	(0.4057)	(0.9474)	(0.5813)	(0.5620)	(0.5189)	(0.3246)	(0.2740)
	[0.0000]	[0.5396]	[0.3574]	[0.1342]	[0.0245]	[0.1220]	[0.5744]
N	8,500	8,500	8,500	8,500	8,500	8,500	8,500
Clusters	205	205	205	205	205	205	205
P-value	0.0000	0.5396	0.3574	0.1342	0.0245	0.1220	0.5744
Mean DV	0.8800	3.7458	2.6095	3.2388	2.5256	3.7030	2.5519

Notes: $*p < 0.1, **p < 0.05, ***p < 0.01$. Panel OLS regression results with clustered standard errors by countries in parentheses (), and p-values in brackets []. The coefficients show the effect of a one standard deviation increase in tropical cyclone damage on the per capita growth rate in a given sectoral aggregate. The standard deviations are 2,236,738 for the agricultural and 2,269,395 for the remaining sectors, calculated for the whole sample of positive wind speed observations. The sample covers the period 1971 through 2015. $Damage_t$ is the weighted damage measure for tropical cyclone intensity in year t. For the sector aggregate agriculture, hunting, forestry and fishing it is weighted by exposed agricultural land in t-1, whereas for the remaining sector aggregates it is weighted by exposed population in t-1. All regressions include country and year fixed effects as well as regional-specific linear trends. The regions are East Asian and Pacific, Europe and Central Asia, Latin America and the Caribbean, Middle East and North Africa, North America, South Asia, Sub-Saharan Africa.

Table 1.38: Robustness – Country-specific nonlinear trends

Dependent Variables: *Per capita growth rate (%) in sector aggregate*

	Agriculture, hunting, forestry, fishing	Mining, utilities	Manu-facturing	Construc-tion	Wholesale, retail trade, restau-rants, hotels	Transport, storage, communi-cation	Other activities
	(1)	(2)	(3)	(4)	(5)	(6)	(7)
$Damage_t$	-2.4560***	-0.5203	-0.7438	0.7197	-1.2175**	-0.4722	-0.1869
	(0.4411)	(1.0678)	(0.5316)	(0.6839)	(0.5234)	(0.3745)	(0.2677)
	[0.0000]	[0.6266]	[0.1633]	[0.2939]	[0.0210]	[0.2088]	[0.4859]
N	8,500	8,500	8,500	8,500	8,500	8,500	8,500
Clusters	205	205	205	205	205	205	205
P-value	0.0000	0.6266	0.1633	0.2939	0.0210	0.2088	0.4859
Mean DV	0.8800	3.7458	2.6095	3.2388	2.5256	3.7030	2.5519

Notes: $*p < 0.1, **p < 0.05, ***p < 0.01$. Panel OLS regression results with clustered standard errors by countries in parentheses (), and p-values in brackets []. The coefficients show the effect of a one standard deviation increase in tropical cyclone damage on the per capita growth rate in a given sectoral aggregate. The standard deviations are 2,236,738 for the agricultural and 2,269,395 for the remaining sectors, calculated for the whole sample of positive wind speed observations. The sample covers the period 1971 through 2015. $Damage_t$ is the weighted damage measure for tropical cyclone intensity in year t. For the sector aggregate agriculture, hunting, forestry and fishing it is weighted by exposed agricultural land in t-1, whereas for the remaining sector aggregates it is weighted by exposed population in t-1. All regressions include country and year fixed effects as well as country-specific nonlinear trends.

Table 1.39: Robustness – Without country-specific linear trends

Dependent Variables: *Per capita growth rate (%) in sector aggregate*

	Agriculture, hunting, forestry, fishing	Mining, utilities	Manu-facturing	Construc-tion	Wholesale, retail trade, restau-rants, hotels	Transport, storage, communi-cation	Other activities
	(1)	(2)	(3)	(4)	(5)	(6)	(7)
Damage_t	-2.5655***	-0.6040	-0.5440	0.8345	-1.1767**	-0.5056	-0.1614
	(0.4086)	(0.9613)	(0.5817)	(0.5570)	(0.5225)	(0.3264)	(0.2721)
	[0.0000]	[0.5305]	[0.3507]	[0.1356]	[0.0254]	[0.1229]	[0.5537]
N	8,500	8,500	8,500	8,500	8,500	8,500	8,500
Clusters	205	205	205	205	205	205	205
P-value	0.0000	0.5305	0.3507	0.1356	0.0254	0.1229	0.5537
Mean DV	0.8800	3.7458	2.6095	3.2388	2.5256	3.7030	2.5519

Notes: $*p < 0.1, **p < 0.05, ***p < 0.01$. Panel OLS regression results with clustered standard errors by countries in parentheses (), and p-values in brackets []. The coefficients show the effect of a one standard deviation increase in tropical cyclone damage on the per capita growth rate in a given sectoral aggregate. The standard deviations are 2,236,738 for the agricultural and 2,269,395 for the remaining sectors, calculated for the whole sample of positive wind speed observations. The sample covers the period 1971 through 2015. Damage_t is the weighted damage measure for tropical cyclone intensity in year t. For the sector aggregate agriculture, hunting, forestry and fishing it is weighted by exposed agricultural land in t-1, whereas for the remaining sector aggregates it is weighted by exposed population in t-1. All regressions include country and year fixed effects.

Table 1.40: Robustness – Frequency (country)

Dependent Variables: *Per capita growth rate (%) in sector aggregate*

	Agriculture, hunting, forestry, fishing	Mining, utilities	Manu-facturing	Construc-tion	Wholesale, retail trade, restau-rants, hotels	Transport, storage, communi-cation	Other activities
	(1)	(2)	(3)	(4)	(5)	(6)	(7)
Damage_t	-2.3963***	-0.5540	-0.6960	1.1408*	-1.0266*	-0.4081	-0.1089
	(0.4796)	(0.7744)	(0.5261)	(0.6542)	(0.5495)	(0.3736)	(0.2796)
	[0.0000]	[0.4752]	[0.1874]	[0.0827]	[0.0631]	[0.2759]	[0.6973]
$\text{Frequency}_{\text{country}}$	-0.4371***	-0.4442	-0.0586	-0.8507***	-0.2667*	-0.1617	-0.1652**
	(0.1425)	(0.4659)	(0.1941)	(0.2871)	(0.1367)	(0.1122)	(0.0678)
	[0.0025]	[0.3415]	[0.7632]	[0.0034]	[0.0524]	[0.1512]	[0.0156]
N	8,500	8,500	8,500	8,500	8,500	8,500	8,500
Clusters	205	205	205	205	205	205	205
P-value	0.0000	0.5650	0.3772	0.0061	0.0053	0.1669	0.0278
Mean DV	0.8800	3.7458	2.6095	3.2388	2.5256	3.7030	2.5519

Notes: $*p < 0.1, **p < 0.05, ***p < 0.01$. Panel OLS regression results with clustered standard errors by countries in parentheses (), and p-values in brackets []. The coefficients show the effect of a one standard deviation increase in tropical cyclone damage on the per capita growth rate in a given sectoral aggregate. The standard deviations are 2,236,738 for the agricultural and 2,269,395 for the remaining sectors, calculated for the whole sample of positive wind speed observations. The sample covers the period 1971 through 2015. Damage_t is the weighted damage measure for tropical cyclone intensity in year t. For the sector aggregate agriculture, hunting, forestry and fishing it is weighted by exposed agricultural land in t-1, whereas for the remaining sector aggregates it is weighted by exposed population in t-1. $Frequency_{country}$ counts the number of tropical cyclones above 92 km/h per year and country. All regressions include country and year fixed effects as well as country-specific linear trends.

Table 1.41: Robustness – Mean wind speed

Dependent Variables: *Per capita growth rate (%) in sector aggregate*

	Agriculture, hunting, forestry, fishing	Mining, utilities	Manu-facturing	Construc-tion	Wholesale, retail trade, restau-rants, hotels	Transport, storage, communi-cation	Other activities
	(1)	(2)	(3)	(4)	(5)	(6)	(7)
Mean Damage_{t}	-2.4532***	-0.9061	-0.7252	0.5341	-0.5721	-0.0855	0.1042
	(0.5941)	(0.5948)	(0.5363)	(0.7637)	(0.3649)	(0.3207)	(0.3102)
	[0.0001]	[0.1292]	[0.1778]	[0.4851]	[0.1185]	[0.7901]	[0.7374]
N	8,500	8,500	8,500	8,500	8,500	8,500	8,500
Clusters	205	205	205	205	205	205	205
P-value	0.0001	0.1292	0.1778	0.4851	0.1185	0.7901	0.7374
Mean DV	0.8800	3.7458	2.6095	3.2388	2.5256	3.7030	2.5519

Notes: $*p < 0.1, **p < 0.05, ***p < 0.01$. Panel OLS regression results with clustered standard errors by countries in parentheses (), and p-values in brackets []. The coefficients show the effect of a one standard deviation increase in tropical cyclone damage on the per capita growth rate in a given sectoral aggregate. The standard deviations are 1,930,581 for the agricultural and 1,910,947 for the remaining sectors, calculated for the whole sample of positive wind speed observations. The sample covers the period 1971 through 2015. Mean Damage_{t} is the weighted damage measure for tropical cyclone intensity in year t. For the sector aggregate agriculture, hunting, forestry and fishing it is weighted by exposed agricultural land in t-1, whereas for the remaining sector aggregates it is weighted by exposed population in t-1. Mean Damage_{t} is based on the mean wind speed per country and year above 92 km/h. All regressions include country and year fixed effects as well as country-specific linear trends.

Table 1.42: Robustness – Basin fixed effects

Dependent Variables: *Per capita growth rate (%) in sector aggregate*

	Agriculture, hunting, forestry, fishing	Mining, utilities	Manu-facturing	Construc-tion	Wholesale, retail trade, restau-rants, hotels	Transport, storage, communi-cation	Other activities
	(1)	(2)	(3)	(4)	(5)	(6)	(7)
Damage_{t}	-2.5060***	-0.7693	-0.4317	0.9662*	-1.1553**	-0.4572	-0.1666
	(0.4241)	(0.7883)	(0.5961)	(0.5703)	(0.5066)	(0.3176)	(0.2688)
	[0.0000]	[0.3303]	[0.4698]	[0.0918]	[0.0236]	[0.1515]	[0.5362]
N	8,500	8,500	8,500	8,500	8,500	8,500	8,500
Clusters	205	205	205	205	205	205	205
P-value	0.0000	0.3303	0.4698	0.0918	0.0236	0.1515	0.5362
Mean DV	0.8800	3.7458	2.6095	3.2388	2.5256	3.7030	2.5519

Notes: $*p < 0.1, **p < 0.05, ***p < 0.01$. Panel OLS regression results with clustered standard errors by countries in parentheses (), and p-values in brackets []. The coefficients show the effect of a one standard deviation increase in tropical cyclone damage on the per capita growth rate in a given sectoral aggregate. The standard deviations are 2,236,738 for the agricultural and 2,269,395 for the remaining sectors, calculated for the whole sample of positive wind speed observations. The sample covers the period 1971 through 2015. Damage_{t} is the weighted damage measure for tropical cyclone intensity in year t. For the sector aggregate agriculture, hunting, forestry and fishing it is weighted by exposed agricultural land in t-1, whereas for the remaining sector aggregates it is weighted by exposed population in t-1. All regressions include tropical cyclones' basin and year fixed effects as well as country-specific linear trends.

Table 1.43: Robustness – Population Weight for sector aggregate A&B

Dependent Variables: *Per capita growth rate (%) in sector aggregate*

	Agriculture, hunting, forestry, fishing
	(1)
Damage_t	-2.5242***
	(0.4423)
	[0.0000]
N	8,500
Clusters	205
P-value	0.0000
Mean DV	0.8800

Notes: $*p < 0.1, **p < 0.05, ***p < 0.01$. Panel OLS regression results with clustered standard errors by countries in parentheses (), and p-values in brackets []. The coefficients show the effect of a one standard deviation increase in tropical cyclone damage on the per capita growth rate in a given sectoral aggregate. The standard deviation is 2,269,395, calculated for the whole sample of positive wind speed observations. The sample covers the period 1971 through 2015. Damage_t is the weighted damage measure for tropical cyclone intensity in year t. It is weighted by exposed population in t-1. All regressions include country and year fixed effects as well as country-specific linear trends.

Table 1.44: Robustness – Conley HAC standard errors

Dependent Variables: *Per capita growth rate (%) in sector aggregate*

	Agriculture, hunting, forestry, fishing	Mining, utilities	Manu-facturing	Construc-tion	Wholesale, retail trade, restau-rants, hotels	Transport, storage, communi-cation	Other activities
	(1)	(2)	(3)	(4)	(5)	(6)	(7)
Damage_t	-2.5655***	-0.6040	-0.5440	0.8345	-1.1767**	-0.5056	-0.1614
	(0.4068)	(0.8961)	(0.6600)	(0.5451)	(0.5318)	(0.3565)	(0.2712)
	[0.0000]	[0.5003]	[0.4098]	[0.1258]	[0.0269]	[0.1561]	[0.5519]
N	8,500	8,500	8,500	8,500	8,500	8,500	8,500

Notes: $*p < 0.1, **p < 0.05, ***p < 0.01$. Panel OLS regression results with clustered standard errors by countries in parentheses (), and p-values in brackets []. The coefficients show the effect of a one standard deviation increase in tropical cyclone damage on the per capita growth rate in a given sectoral aggregate. The standard deviations are 2,236,738 for the agricultural and 2,269,395 for the remaining sectors, calculated for the whole sample of positive wind speed observations. The sample covers the period 1971 through 2015. Damage_t is the weighted damage measure for tropical cyclone intensity in year t. For the sector aggregate agriculture, hunting, forestry and fishing it is weighted by exposed agricultural land in t-1, whereas for the remaining sector aggregates it is weighted by exposed population in t-1. All regressions include country and year fixed effects as well as country-specific linear trends. For all regressions, Conley HAC standards with a maximum lag length of 10 and a spatial cutoff of 1000 km are calculated.

Table 1.45: Robustness – Regional clusters

Dependent Variables: *Per capita growth rate (%) in sector aggregate*

	Agriculture, hunting, forestry, fishing	Mining, utilities	Manu-facturing	Construc-tion	Wholesale, retail trade, restau-rants, hotels	Transport, storage, communi-cation	Other activities
	(1)	(2)	(3)	(4)	(5)	(6)	(7)
Damage_{t}	-2.6219***	-0.7682	-0.7242	0.7306	-1.1552**	-0.4861	-0.1886
	(0.2809)	(1.1861)	(0.5725)	(0.6953)	(0.4053)	(0.4685)	(0.1426)
	[0.0001]	[0.5412]	[0.2527]	[0.3339]	[0.0292]	[0.3395]	[0.2341]
N	8,500	8,500	8,500	8,500	8,500	8,500	8,500
Clusters	7	7	7	7	7	7	7
P-value	0.0001	0.5412	0.2527	0.3339	0.0292	0.3395	0.2341
Mean DV	0.8800	3.7458	2.6095	3.2388	2.5256	3.7030	2.5519

Notes: $*p < 0.1, **p < 0.05, ***p < 0.01$. Panel OLS regression results with clustered standard errors by regions in parentheses (), and p-values in brackets []. The coefficients show the effect of a one standard deviation increase in tropical cyclone damage on the per capita growth rate in a given sectoral aggregate. The standard deviations are 2,236,738 for the agricultural and 2,269,395 for the remaining sectors, calculated for the whole sample of positive wind speed observations. The sample covers the period 1971 through 2015. Damage_{t} is the weighted damage measure for tropical cyclone intensity in year t. For the sector aggregate agriculture, hunting, forestry and fishing it is weighted by exposed agricultural land in t-1, whereas for the remaining sector aggregates it is weighted by exposed population in t-1. The regions are East Asian and Pacific, Europe and Central Asia, Latin America and the Caribbean, Middle East and North Africa, North America, South Asia, Sub-Saharan Africa. All regressions include country and year fixed effects as well as country-specific linear trends.

Table 1.46: Robustness – Newey-West standard errors

Dependent Variables: *Per capita growth rate (%) in sector aggregate*

	Agriculture, hunting, forestry, fishing	Mining, utilities	Manu-facturing	Construc-tion	Wholesale, retail trade, restau-rants, hotels	Transport, storage, communi-cation	Other activities
	(1)	(2)	(3)	(4)	(5)	(6)	(7)
Damage_{t}	-2.5950***	-0.5325	-0.6506	0.8369	-1.1619**	-0.4921	-0.1500
	(0.4370)	(1.0325)	(0.6882)	(0.5510)	(0.5665)	(0.3429)	(0.2806)
	[0.0000]	[0.6060]	[0.3445]	[0.1288]	[0.0403]	[0.1513]	[0.5929]
N	8,500	8,500	8,500	8,500	8,500	8,500	8,500
P-value	0.0000	0.0000	0.0000	0.0000	0.0000	0.0000	0.0000
Mean DV	0.8800	3.7458	2.6095	3.2388	2.5256	3.7030	2.5519

Notes: $*p < 0.1, **p < 0.05, ***p < 0.01$. Panel OLS regression results with clustered standard errors by countries in parentheses (), and p-values in brackets []. The coefficients show the effect of a one standard deviation increase in tropical cyclone damage on the per capita growth rate in a given sectoral aggregate. The standard deviations are 2,236,738 for the agricultural and 2,269,395 for the remaining sectors, calculated for the whole sample of positive wind speed observations. The sample covers the period 1971 through 2015. Damage_{t} is the weighted damage measure for tropical cyclone intensity in year t. For the sector aggregate agriculture, hunting, forestry and fishing it is weighted by exposed agricultural land in t-1, whereas for the remaining sector aggregates it is weighted by exposed population in t-1. All regressions include country and year fixed effects as well as country-specific linear trends. For all regressions Newey-West standard errors with a maximum lag length of 10 years are calculated.

1.6.5.2 Indirect Effects

Table 1.47: Robustness – Placebo test Input-Output coefficients of sector aggregate (A&B)

Dependent Variables: : *Input-Output coefficients (IO)*

	$IO_t^{A\&B,A\&B}$	$IO_t^{A\&B,C\&E}$	$IO_t^{A\&B,D}$	$IO_t^{A\&B,F}$	$IO_t^{A\&B,G\text{-}H}$	$IO_t^{A\&B,I}$	$IO_t^{A\&B,J\text{-}P}$
	(1)	(2)	(3)	(4)	(5)	(6)	(7)
$Damage_{t+2}$	-0.00134	-0.00002	-0.00001	-0.00001	-0.00015	0.00003	-0.00011
	(0.00133)	(0.00005)	(0.00037)	(0.00002)	(0.00014)	(0.00010)	(0.00041)
	[0.31705]	[0.70470]	[0.97559]	[0.66644]	[0.30366]	[0.79136]	[0.79816]
$IO_{t-1}^{A\&B,A\&B}$	0.80645***						
	(0.05008)						
	[0.00000]						
$IO_{t-1}^{A\&B,C\&E}$		0.85656***					
		(0.00966)					
		[0.00000]					
$IO_{t-1}^{A\&B,D}$			0.84284***				
			(0.01386)				
			[0.00000]				
$IO_{t-1}^{A\&B,F}$				0.78281***			
				(0.05125)			
				[0.00000]			
$IO_{t-1}^{A\&B,G\text{-}H}$					0.82225***		
					(0.03118)		
					[0.00000]		
$IO_{t-1}^{A\&B,I}$						0.84184***	
						(0.02293)	
						[0.00000]	
$IO_{t-1}^{A\&B,J\text{-}P}$							0.87825***
							(0.01491)
							[0.00000]
N	4,128	4,128	4,128	4,128	4,128	4,128	4,128
Clusters	182	182	182	182	182	182	182
P-value	0.00000	0.00000	0.00000	0.00000	0.00000	0.00000	0.00000
Mean DV	0.16742	0.01225	0.08573	0.00379	0.03616	0.02231	0.07167

Notes: $*p < 0.1, **p < 0.05, ***p < 0.01$. Panel OLS regression results with clustered standard errors by countries in parentheses (), and p-values in brackets []. The coefficients show the effect of a one standard deviation increase in tropical cyclone damage on the respective Input-Output coefficients. The standard deviations are 2,236,738 for the agricultural and 2,269,395 for the remaining sectors, calculated for the whole sample of positive wind speed observations. $Damage_{t+2}$ is the weighted damage measure for tropical cyclone intensity in year t+2. For the sector aggregate agriculture, hunting, forestry and fishing it is weighted by exposed agricultural land in t+1, whereas for the remaining sector aggregates it is weighted by exposed population in t+1. The dependent variables are Input-Output coefficients (IO) and can range between 0-1. For example the coefficient $IO_t^{A\&B,D}$ displays how much input the sector aggregate A&B needs from sector aggregate D to produce one unit of output. The sector abbreviations represent the following sector aggregates: agriculture, hunting, forestry, and fishing (A&B), mining, and utilities (C&E), manufacturing (D), construction (F), wholesale, retail trade, restaurants, and hotels (G-H), transport, storage, and communication (I), other activities (J-P). All regressions include country and year fixed effects as well as country-specific linear trends.

Table 1.48: Robustness – Placebo test Input-Output coefficients of sector aggregate (C&E)

Dependent Variables: *Input-Output coefficients (IO)*

	$IO_t^{C\&E,A\&B}$	$IO_t^{C\&E,C\&E}$	$IO_t^{C\&E,D}$	$IO_t^{C\&E,F}$	$IO_t^{C\&E,G\text{-}H}$	$IO_t^{C\&E,I}$	$IO_t^{C\&E,J\text{-}P}$
	(1)	(2)	(3)	(4)	(5)	(6)	(7)
$Damage_{t+2}$	0.00001	0.00313	-0.00058	-0.00006	-0.00021	-0.00017	-0.00026
	(0.00001)	(0.00258)	(0.00039)	(0.00020)	(0.00018)	(0.00031)	(0.00063)
	[0.36703]	[0.22702]	[0.13804]	[0.74574]	[0.24310]	[0.58776]	[0.67726]
$IO_{t-1}^{C\&E,A\&B}$	0.73657***						
	(0.06345)						
	[0.00000]						
$IO_{t-1}^{C\&E,C\&E}$		0.83415***					
		(0.05844)					
		[0.00000]					
$IO_{t-1}^{C\&E,D}$			0.89133***				
			(0.02168)				
			[0.00000]				
$IO_{t-1}^{C\&E,F}$				0.88360***			
				(0.02112)			
				[0.00000]			
$IO_{t-1}^{C\&E,G\text{-}H}$					0.79680***		
					(0.06043)		
					[0.00000]		
$IO_{t-1}^{C\&E,I}$						0.79961***	
						(0.05834)	
						[0.00000]	
$IO_{t-1}^{C\&E,J\text{-}P}$							0.87720***
							(0.02265)
							[0.00000]
N	4,128	4,128	4,128	4,128	4,128	4,128	4,128
Clusters	182	182	182	182	182	182	182
P-value	0.00000	0.00000	0.00000	0.00000	0.00000	0.00000	0.00000
Mean DV	0.00084	0.15083	0.05438	0.02809	0.01938	0.04883	0.08881

Notes: $*p < 0.1, **p < 0.05, ***p < 0.01$. Panel OLS regression results with clustered standard errors by countries in parentheses (), and p-values in brackets []. The coefficients show the effect of a one standard deviation increase in tropical cyclone damage on the respective Input-Output coefficients. The standard deviations are 2,236,738 for the agricultural and 2,269,395 for the remaining sectors, calculated for the whole sample of positive wind speed observations. $Damage_{t+2}$ is the weighted damage measure for tropical cyclone intensity in year t+2. For the sector aggregate agriculture, hunting, forestry and fishing it is weighted by exposed agricultural land in t+1, whereas for the remaining sector aggregates it is weighted by exposed population in t+1. The dependent variables are Input-Output coefficients (IO) and can range between 0-1. For example the coefficient $IO_t^{C\&E,D}$ displays how much input the sector aggregate C&E needs from sector aggregate D to produce one unit of output. The sector abbreviations represent the following sector aggregates: agriculture, hunting, forestry, and fishing (A&B), mining, and utilities (C&E), manufacturing (D), construction (F), wholesale, retail trade, restaurants, and hotels (G-H), transport, storage, and communication (I), other activities (J-P). All regressions include country and year fixed effects as well as country-specific linear trends.

Table 1.49: Robustness – Placebo test Input-Output coefficients of sector aggregate (D)

Dependent Variables: *Input-Output coefficients (IO)*

	$IO_t^{D,A\&B}$	$IO_t^{D,C\&E}$	$IO_t^{D,D}$	$IO_t^{D,F}$	$IO_t^{D,G\text{-}H}$	$IO_t^{D,I}$	$IO_t^{D,J\text{-}P}$
	(1)	(2)	(3)	(4)	(5)	(6)	(7)
$Damage_{t+2}$	0.00020	-0.00020	0.00012	-0.00000	-0.00001	-0.00002	0.00017
	(0.00019)	(0.00016)	(0.00140)	(0.00002)	(0.00012)	(0.00009)	(0.00027)
	[0.2990]	[0.1977]	[0.9332]	[0.7865]	[0.9369]	[0.8179]	[0.5261]
$IO_{t-1}^{D,A\&B}$	0.83958***						
	(0.03525)						
	[0.0000]						
$IO_{t-1}^{D,C\&E}$		0.75357***					
		(0.05013)					
		[0.0000]					
$IO_{t-1}^{D,D}$			0.79306***				
			(0.04695)				
			[0.0000]				
$IO_{t-1}^{D,F}$				0.83620***			
				(0.01902)			
				[0.0000]			
$IO_{t-1}^{D,G\text{-}H}$					0.78251***		
					(0.03204)		
					[0.0000]		
$IO_{t-1}^{D,I}$						0.82467***	
						(0.02131)	
						[0.0000]	
$IO_{t-1}^{D,J\text{-}P}$							0.84057***
							(0.01983)
							[0.0000]
N	4,128	4,128	4,128	4,128	4,128	4,128	4,128
Clusters	182	182	182	182	182	182	182
P-value	0.00000	0.00000	0.00000	0.00000	0.00000	0.00000	0.00000
Mean DV	0.05549	0.03909	0.24042	0.00452	0.05353	0.03586	0.08546

Notes: $*p < 0.1, **p < 0.05, ***p < 0.01$. Panel OLS regression results with clustered standard errors by countries in parentheses (), and p-values in brackets []. The coefficients show the effect of a one standard deviation increase in tropical cyclone damage on the respective Input-Output coefficients. The standard deviations are 2,236,738 for the agricultural and 2,269,395 for the remaining sectors, calculated for the whole sample of positive wind speed observations. $Damage_{t+2}$ is the weighted damage measure for tropical cyclone intensity in year t+2. For the sector aggregate agriculture, hunting, forestry and fishing it is weighted by exposed agricultural land in t+1, whereas for the remaining sector aggregates it is weighted by exposed population in t+1. The dependent variables are Input-Output coefficients (IO) and can range between 0-1. For example the coefficient $IO_t^{D,F}$ displays how much input the sector aggregate D needs from sector aggregate F to produce one unit of output. The sector abbreviations represent the following sector aggregates: agriculture, hunting, forestry, and fishing (A&B), mining, and utilities (C&E), manufacturing (D), construction (F), wholesale, retail trade, restaurants, and hotels (G-H), transport, storage, and communication (I), other activities (J-P). All regressions include country and year fixed effects as well as country-specific linear trends.

Table 1.50: Robustness – Placebo test Input-Output coefficients of sector aggregate (F)

Dependent Variables: *Input-Output coefficients (IO)*

	$IO_t^{F,A\&B}$	$IO_t^{F,C\&E}$	$IO_t^{F,D}$	$IO_t^{F,F}$	$IO_t^{F,G\text{-}H}$	$IO_t^{F,I}$	$IO_t^{F,J\text{-}P}$
	(1)	(2)	(3)	(4)	(5)	(6)	(7)
$Damage_{t+2}$	0.00004**	-0.00008	0.00058	0.00016	0.00021	0.00009	0.00079*
	(0.00002)	(0.00008)	(0.00049)	(0.00116)	(0.00020)	(0.00015)	(0.00041)
	[0.02802]	[0.35420]	[0.23891]	[0.88889]	[0.28878]	[0.55218]	[0.05359]
$IO_{t-1}^{F,A\&B}$	0.82738***						
	(0.02152)						
	[0.00000]						
$IO_{t-1}^{F,C\&E}$		0.80762***					
		(0.03261)					
		[0.00000]					
$IO_{t-1}^{F,D}$			0.75346***				
			(0.09827)				
			[0.00000]				
$IO_{t-1}^{F,F}$				0.85201***			
				(0.07531)			
				[0.00000]			
$IO_{t-1}^{F,G\text{-}H}$					0.80791***		
					(0.02005)		
					[0.00000]		
$IO_{t-1}^{F,I}$						0.77454***	
						(0.05936)	
						[0.00000]	
$IO_{t-1}^{F,J\text{-}P}$							0.85000***
							(0.01407)
							[0.00000]
N	4,128	4,128	4,128	4,128	4,128	4,128	4,128
Clusters	182	182	182	182	182	182	182
P-value	0.00000	0.00000	0.00000	0.00000	0.00000	0.00000	0.00000
Mean DV	0.00319	0.01603	0.21046	0.03908	0.06434	0.03950	0.09892

Notes: $*p < 0.1, **p < 0.05, ***p < 0.01$. Panel OLS regression results with clustered standard errors by countries in parentheses (), and p-values in brackets []. The coefficients show the effect of a one standard deviation increase in tropical cyclone damage on the respective Input-Output coefficients. The standard deviations are 2,236,738 for the agricultural and 2,269,395 for the remaining sectors, calculated for the whole sample of positive wind speed observations. $Damage_{t+2}$ is the weighted damage measure for tropical cyclone intensity in year t+2. For the sector aggregate agriculture, hunting, forestry and fishing it is weighted by exposed agricultural land in t+1, whereas for the remaining sector aggregates it is weighted by exposed population in t+1. The dependent variables are Input-Output coefficients (IO) and can range between 0-1. For example the coefficient $IO_t^{F,G\text{-}H}$ displays how much input the sector aggregate F needs from sector aggregate G-H to produce one unit of output. The sector abbreviations represent the following sector aggregates: agriculture, hunting, forestry, and fishing (A&B), mining, and utilities (C&E), manufacturing (D), construction (F), wholesale, retail trade, restaurants, and hotels (G-H), transport, storage, and communication (I), other activities (J-P). All regressions include country and year fixed effects as well as country-specific linear trends.

Table 1.51: Robustness – Placebo test Input-Output coefficients of sector aggregate (G-H)

Dependent Variables: *Input-Output coefficients (IO)*

	$IO_t^{G\text{-}H,A\&B}$	$IO_t^{G\text{-}H,C\&E}$	$IO_t^{G\text{-}H,D}$	$IO_t^{G\text{-}H,F}$	$IO_t^{G\text{-}H,G\text{-}H}$	$IO_t^{G\text{-}H,I}$	$IO_t^{G\text{-}H,J\text{-}P}$
	(1)	(2)	(3)	(4)	(5)	(6)	(7)
$Damage_{t+2}$	0.00006	0.00001	0.00025	0.00001	0.00282	0.00017	0.00047
	(0.00006)	(0.00004)	(0.00031)	(0.00003)	(0.00192)	(0.00024)	(0.00093)
	[0.25606]	[0.84014]	[0.41821]	[0.83753]	[0.14446]	[0.45985]	[0.60896]
$IO_{t-1}^{G\text{-}H,A\&B}$	0.85308***						
	(0.03951)						
	[0.00000]						
$IO_{t-1}^{G\text{-}H,C\&E}$		0.82517***					
		(0.03417)					
		[0.00000]					
$IO_{t-1}^{G\text{-}H,D}$			0.86195***				
			(0.04354)				
			[0.00000]				
$IO_{t-1}^{G\text{-}H,F}$				0.78960***			
				(0.02916)			
				[0.00000]			
$IO_{t-1}^{G\text{-}H,G\text{-}H}$					0.83892***		
					(0.07918)		
					[0.00000]		
$IO_{t-1}^{G\text{-}H,I}$						0.85301***	
						(0.02086)	
						[0.00000]	
$IO_{t-1}^{G\text{-}H,J\text{-}P}$							0.90666***
							(0.03344)
							[0.00000]
N	4,128	4,128	4,128	4,128	4,128	4,128	4,128
Clusters	182	182	182	182	182	182	182
P-value	0.0000	0.0000	0.0000	0.0000	0.0000	0.0000	0.0000
Mean DV	0.00826	0.01583	0.07150	0.00622	0.05366	0.06138	0.13970

Notes: $*p < 0.1, **p < 0.05, ***p < 0.01$. Panel OLS regression results with clustered standard errors by countries in parentheses (), and p-values in brackets []. The coefficients show the effect of a one standard deviation increase in tropical cyclone damage on the respective Input-Output coefficients. The standard deviations are 2,236,738 for the agricultural and 2,269,395 for the remaining sectors, calculated for the whole sample of positive wind speed observations. $Damage_{t+2}$ is the weighted damage measure for tropical cyclone intensity in year t+2. For the sector aggregate agriculture, hunting, forestry and fishing it is weighted by exposed agricultural land in t+1, whereas for the remaining sector aggregates it is weighted by exposed population in t+1. The dependent variables are Input-Output coefficients (IO) and can range between 0-1. For example the coefficient $IO_t^{G\text{-}H,F}$ displays how much input the sector aggregate G-H needs from sector aggregate F to produce one unit of output. The sector abbreviations represent the following sector aggregates: agriculture, hunting, forestry, and fishing (A&B), mining, and utilities (C&E), manufacturing (D), construction (F), wholesale, retail trade, restaurants, and hotels (G-H), transport, storage, and communication (I), other activities (J-P). All regressions include country and year fixed effects as well as country-specific linear trends.

Table 1.52: Robustness – Placebo test Input-Output coefficients of sector aggregate (I)

	Dependent Variables: *Input-Output coefficients (IO)*						
	$IO_t^{I,A\&B}$	$IO_t^{I,C\&E}$	$IO_t^{I,D}$	$IO_t^{I,F}$	$IO_t^{I,G\text{-}H}$	$IO_t^{I,I}$	$IO_t^{I,J\text{-}P}$
	(1)	(2)	(3)	(4)	(5)	(6)	(7)
$Damage_{t+2}$	0.00000	0.00000	-0.00008	0.00000	0.00003	0.00111	-0.00001
	(0.00000)	(0.00003)	(0.00020)	(0.00003)	(0.00007)	(0.00082)	(0.00056)
	[0.45717]	[0.88410]	[0.69209]	[0.99657]	[0.61316]	[0.17533]	[0.98117]
$IO_{t-1}^{I,A\&B}$	0.73506***						
	(0.06792)						
	[0.00000]						
$IO_{t-1}^{I,C\&E}$		0.81433***					
		(0.03431)					
		[0.00000]					
$IO_{t-1}^{I,D}$			0.78372***				
			(0.03216)				
			[0.00000]				
$IO_{t-1}^{I,F}$				0.84054***			
				(0.03044)			
				[0.00000]			
$IO_{t-1}^{I,G\text{-}H}$					0.78946***		
					(0.07373)		
					[0.00000]		
$IO_{t-1}^{I,I}$						0.74516***	
						(0.09716)	
						[0.00000]	
$IO_{t-1}^{I,J\text{-}P}$							0.83369***
							(0.01953)
							[0.00000]
N	4,128	4,128	4,128	4,128	4,128	4,128	4,128
Clusters	182	182	182	182	182	182	182
P-value	0.00000	0.00000	0.00000	0.00000	0.00000	0.00000	0.00000
Mean DV	0.00041	0.00998	0.06225	0.00886	0.02776	0.10992	0.13054

Notes: $*p < 0.1, **p < 0.05, ***p < 0.01$. Panel OLS regression results with clustered standard errors by countries in parentheses (), and p-values in brackets []. The coefficients show the effect of a one standard deviation increase in tropical cyclone damage on the respective Input-Output coefficients. The standard deviations are 2,236,738 for the agricultural and 2,269,395 for the remaining sectors, calculated for the whole sample of positive wind speed observations. $Damage_{t+2}$ is the weighted damage measure for tropical cyclone intensity in year t+2. For the sector aggregate agriculture, hunting, forestry and fishing it is weighted by exposed agricultural land in t+1, whereas for the remaining sector aggregates it is weighted by exposed population in t+1. The dependent variables are Input-Output coefficients (IO) and can range between 0-1. For example the coefficient $IO_t^{I,F}$ displays how much input the sector aggregate I needs from sector aggregate F to produce one unit of output. The sector abbreviations represent the following sector aggregates: agriculture, hunting, forestry, and fishing (A&B), mining, and utilities (C&E), manufacturing (D), construction (F), wholesale, retail trade, restaurants, and hotels (G-H), transport, storage, and communication (I), other activities (J-P). All regressions include country and year fixed effects as well as country-specific linear trends.

Table 1.53: Robustness – Placebo test Input-Output coefficients of sector aggregate (J-P)

Dependent Variables: *Input-Output coefficients (IO)*

	$IO_t^{J\text{-}P,A\&B}$	$IO_t^{J\text{-}P,C\&E}$	$IO_t^{J\text{-}P,D}$	$IO_t^{J\text{-}P,F}$	$IO_t^{J\text{-}P,G\text{-}H}$	$IO_t^{J\text{-}P,I}$	$IO_t^{J\text{-}P,J\text{-}P}$
	(1)	(2)	(3)	(4)	(5)	(6)	(7)
$Damage_{t+2}$	0.00005	-0.00001	0.00027	0.00010	0.00007	0.00010	0.00077
	(0.00004)	(0.00006)	(0.00020)	(0.00007)	(0.00007)	(0.00015)	(0.00052)
	[0.19941]	[0.82050]	[0.17815]	[0.16892]	[0.34915]	[0.47840]	[0.13686]
$IO_{t-1}^{J\text{-}P,A\&B}$	0.47027***						
	(0.04664)						
	[0.00000]						
$IO_{t-1}^{J\text{-}P,C\&E}$		0.85946***					
		(0.03964)					
		[0.00000]					
$IO_{t-1}^{J\text{-}P,D}$			0.72580***				
			(0.08154)				
			[0.00000]				
$IO_{t-1}^{J\text{-}P,F}$				0.79041***			
				(0.03416)			
				[0.00000]			
$IO_{t-1}^{J\text{-}P,G\text{-}H}$					0.76205***		
					(0.05821)		
					[0.00000]		
$IO_{t-1}^{J\text{-}P,I}$						0.83273***	
						(0.01998)	
						[0.00000]	
$IO_{t-1}^{J\text{-}P,J\text{-}P}$							0.74783***
							(0.07843)
							[0.00000]
N	4,128	4,128	4,128	4,128	4,128	4,128	4,128
Clusters	182	182	182	182	182	182	182
P-value	0.00000	0.00000	0.00000	0.00000	0.00000	0.00000	0.00000
Mean DV	0.00256	0.01218	0.05638	0.01734	0.02314	0.03174	0.14534

Notes: $*p < 0.1, **p < 0.05, ***p < 0.01$. Panel OLS regression results with clustered standard errors by countries in parentheses (), and p-values in brackets []. The coefficients show the effect of a one standard deviation increase in tropical cyclone damage on the respective Input-Output coefficients. The standard deviations are 2,236,738 for the agricultural and 2,269,395 for the remaining sectors, calculated for the whole sample of positive wind speed observations. $Damage_{t+2}$ is the weighted damage measure for tropical cyclone intensity in year t+2. For the sector aggregate agriculture, hunting, forestry and fishing it is weighted by exposed agricultural land in t+1, whereas for the remaining sector aggregates it is weighted by exposed population in t+1. The dependent variables are Input-Output coefficients (IO) and can range between 0-1. For example the coefficient $IO_t^{J\text{-}P,F}$ displays how much input the sector aggregate J-P needs from sector aggregate F to produce one unit of output. The sector abbreviations represent the following sector aggregates: agriculture, hunting, forestry, and fishing (A&B), mining, and utilities (C&E), manufacturing (D), construction (F), wholesale, retail trade, restaurants, and hotels (G-H), transport, storage, and communication (I), other activities (J-P). All regressions include country and year fixed effects as well as country-specific linear trends.

Table 1.54: Robustness – Population weight for Input-Output coefficients of sector aggregate A&B

Dependent Variables: *Input-Output coefficient (IO)*

	$IO^{A\&B,A\&B}$	$IO^{A\&B,C\&E}$	$IO^{A\&B,D}$	$IO^{A\&B,F}$	$IO^{A\&B,G\text{-}H}$	$IO^{A\&B,I}$	$IO^{A\&B,J\text{-}P}$
	(1)	(2)	(3)	(4)	(5)	(6)	(7)
$Damage_t$	-0.00025	-0.00013**	-0.00056	-0.00005*	-0.00033**	-0.00022	-0.00047
	(0.00081)	(0.00006)	(0.00051)	(0.00003)	(0.00013)	(0.00017)	(0.00035)
	[0.75815]	[0.02745]	[0.26628]	[0.09233]	[0.01341]	[0.21042]	[0.17662]
$IO^{A\&B,A\&B}_{t-1}$	0.81383***						
	(0.04689)						
	[0.00000]						
$IO^{A\&B,C\&E}_{t-1}$		0.93030***					
		(0.05625)					
		[0.00000]					
$IO^{A\&B,D}_{t-1}$			0.85592***				
			(0.01274)				
			[0.00000]				
$IO^{A\&B,F}_{t-1}$				1.24489***			
				(0.15347)			
				[0.00000]			
$IO^{A\&B,G\text{-}H}_{t-1}$					0.84205***		
					(0.02798)		
					[0.00000]		
$IO^{A\&B,I}_{t-1}$						0.85344***	
						(0.02055)	
						[0.00000]	
$IO^{A\&B,J\text{-}P}_{t-1}$							0.90449***
							(0.01996)
							[0.00000]
N	4,490	4,490	4,490	4,490	4,490	4,490	4,490
Clusters	182	182	182	182	182	182	182
P-value	0.00000	0.00000	0.00000	0.00000	0.00000	0.00000	0.00000
Mean DV	0.16618	0.01220	0.08494	0.00377	0.03579	0.02204	0.07102

Notes: $*p < 0.1, **p < 0.05, ***p < 0.01$. Panel OLS regression results with clustered standard errors by countries in parentheses (), and p-values in brackets []. The coefficients show the effect of a one standard deviation increase in tropical cyclone damage on the per capita growth rate in a given sectoral aggregate. The standard deviation is 2,269,395, calculated for the whole sample of positive wind speed observations. $Damage_t$ is the weighted damage measure for tropical cyclone intensity in year t. It is weighted by exposed population in t-1. The dependent variables are Input-Output coefficients (IO) and can range between 0-1. For example the coefficient $IO^{A\&B,D}_t$ displays how much input the sector aggregate A&B needs from sector aggregate D to produce one unit of output. The sector abbreviations represent the following sector aggregates: agriculture, hunting, forestry, and fishing (A&B), mining, and utilities (C&E), manufacturing (D), construction (F), wholesale, retail trade, restaurants, and hotels (G-H), transport, storage, and communication (I), other activities (J-P). All regressions include country and year fixed effects as well as country-specific linear trends.

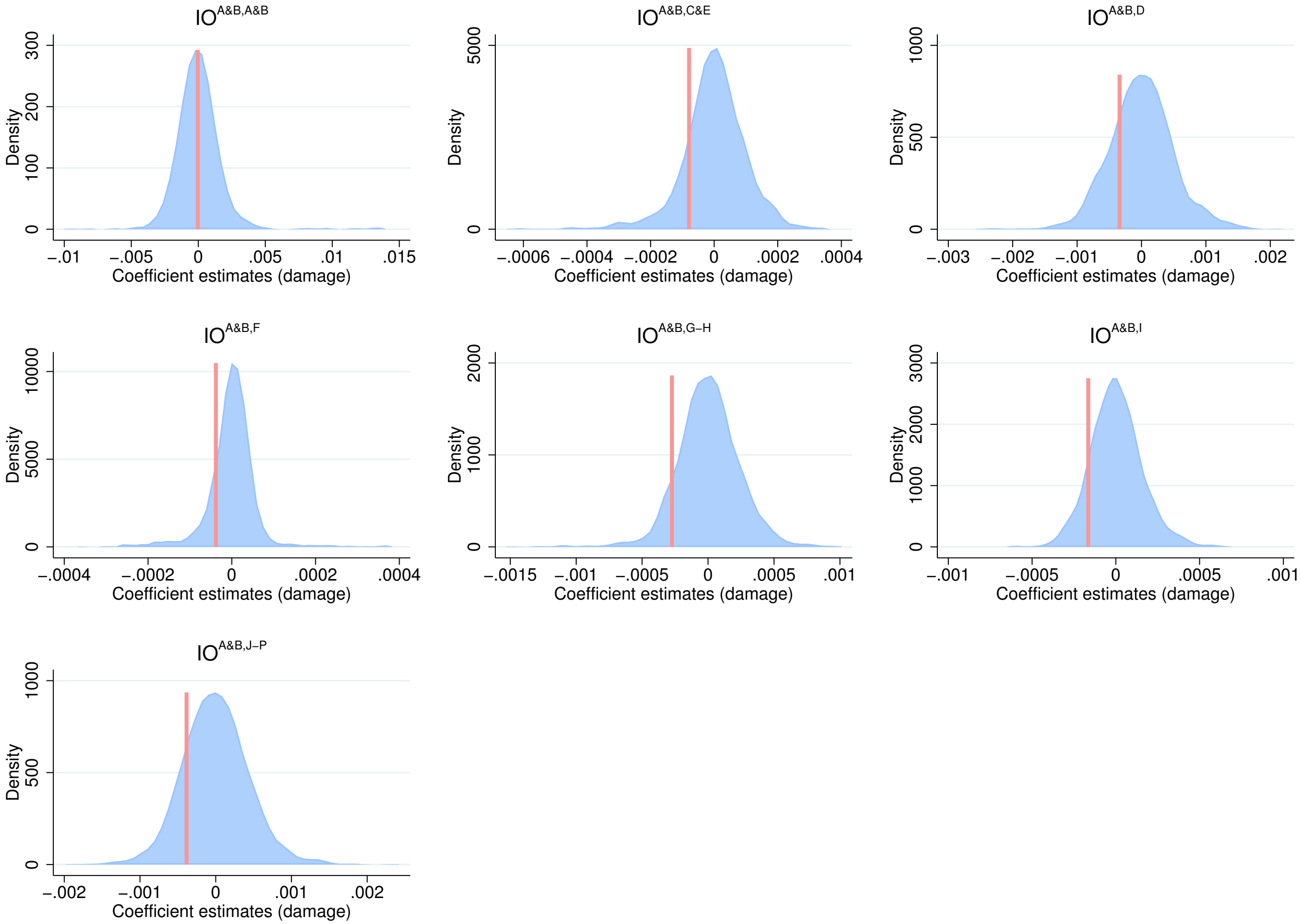

Figure 1.19: Randomization tests – Input-Output coefficients of sector aggregate A&B

Notes: This figure shows the Fisher randomization test results for the $damage_t$ variable where the years are permuted for 2000 repetitions. It displays the kernel density plots (blue) of the randomization coefficient estimates together the results of model 1.6 (red bar). The sector abbreviations represent the following sector aggregates: agriculture, hunting, forestry, and fishing (A&B), mining, and utilities (C&E), manufacturing (D), construction (F), wholesale, retail trade, restaurants, and hotels (G–H), transport, storage, and communication (I), other activities (J–P).

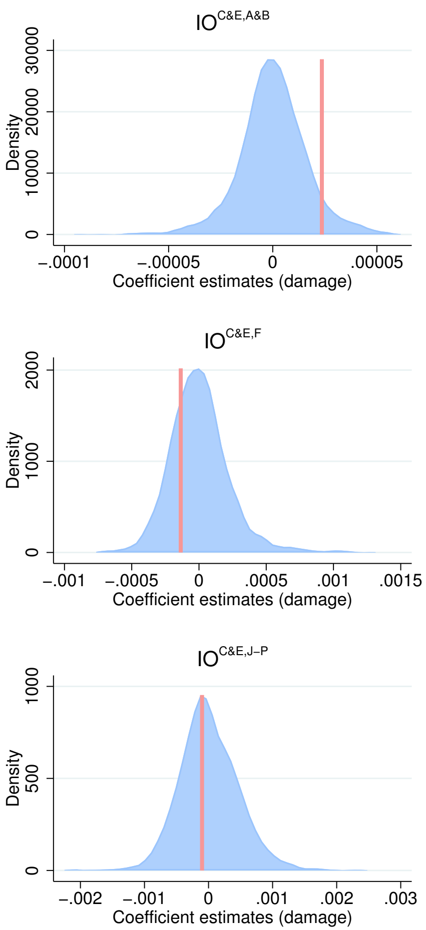

Figure 1.20: Randomization tests – Input-Output coefficients of sector aggregate C&E

Notes: This figure shows the Fisher randomization test results for the $damage_t$ variable where the years are permuted for 2000 repetitions. It displays the kernel density plots (blue) of the randomization coefficient estimates together the results of model 1.6 (red bar). The sector abbreviations represent the following sector aggregates: agriculture, hunting, forestry, and fishing (A&B), mining, and utilities (C&E), manufacturing (D), construction (F), wholesale, retail trade, restaurants, and hotels (G–H), transport, storage, and communication (I), other activities (J–P).

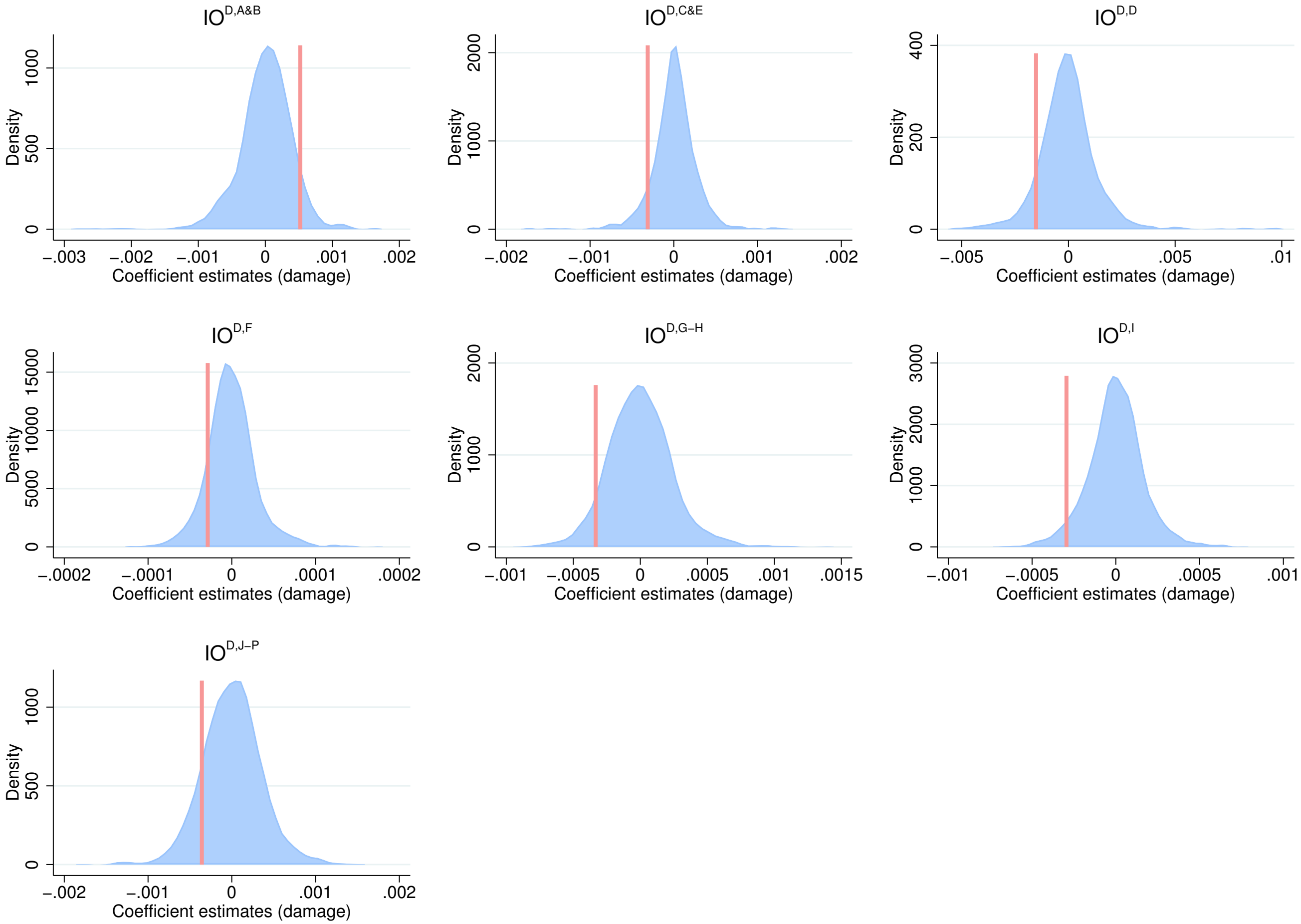

Figure 1.21: Randomization tests – Input-Output coefficients of sector aggregate D

Notes: This figure shows the Fisher randomization test results for the $damage_t$ variable where the years are permuted for 2000 repetitions. It displays the kernel density plots (blue) of the randomization coefficient estimates together the results of model 1.6 (red bar). The sector abbreviations represent the following sector aggregates: agriculture, hunting, forestry, and fishing (A&B), mining, and utilities (C&E), manufacturing (D), construction (F), wholesale, retail trade, restaurants, and hotels (G–H), transport, storage, and communication (I), other activities (J–P).

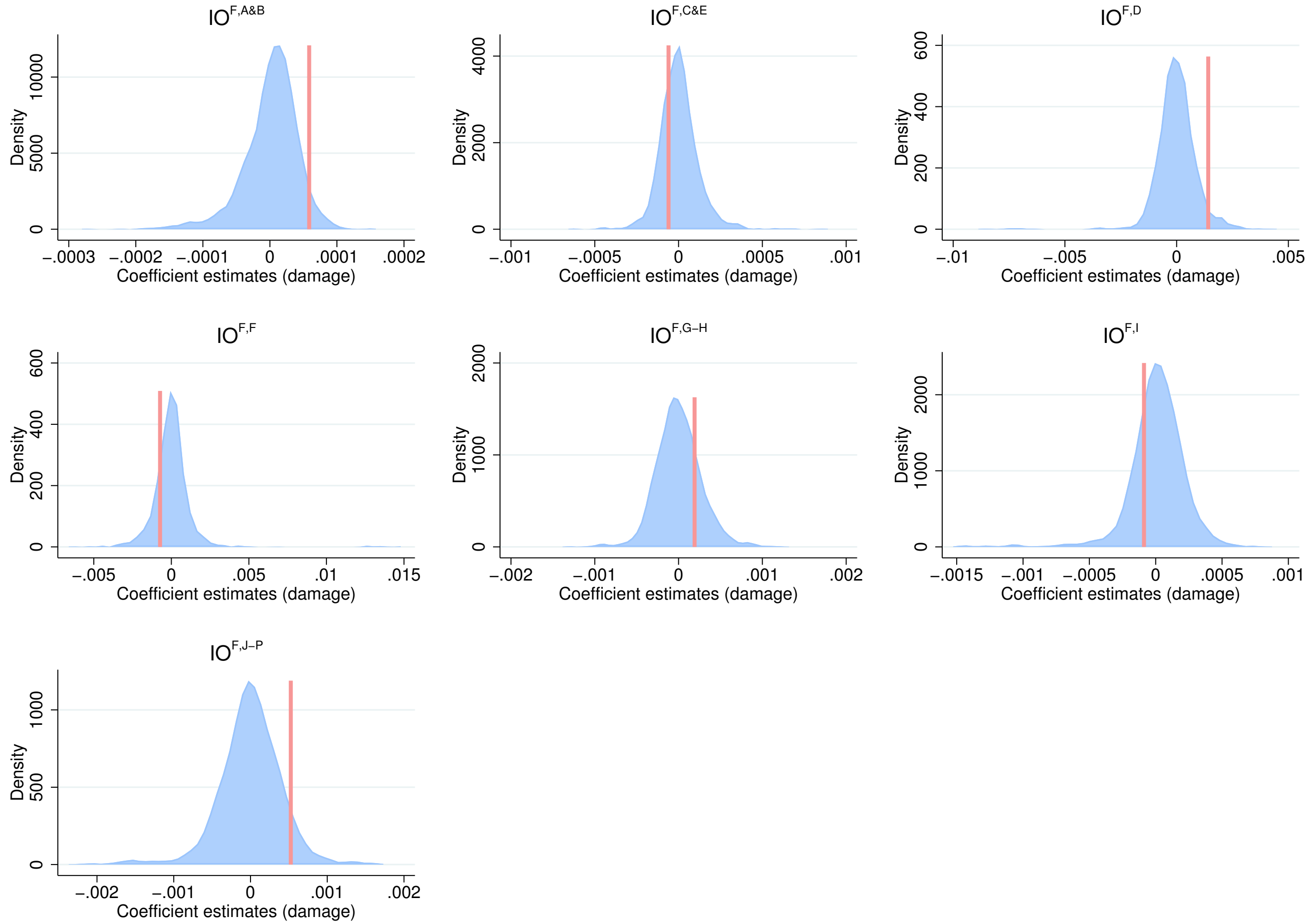

Figure 1.22: Randomization tests – Input-Output coefficients of sector aggregate F

Notes: This figure shows the Fisher randomization test results for the $damage_t$ variable where the years are permuted for 2000 repetitions. It displays the kernel density plots (blue) of the randomization coefficient estimates together the results of model 1.6 (red bar). The sector abbreviations represent the following sector aggregates: agriculture, hunting, forestry, and fishing (A&B), mining, and utilities (C&E), manufacturing (D), construction (F), wholesale, retail trade, restaurants, and hotels (G–H), transport, storage, and communication (I), other activities (J–P).

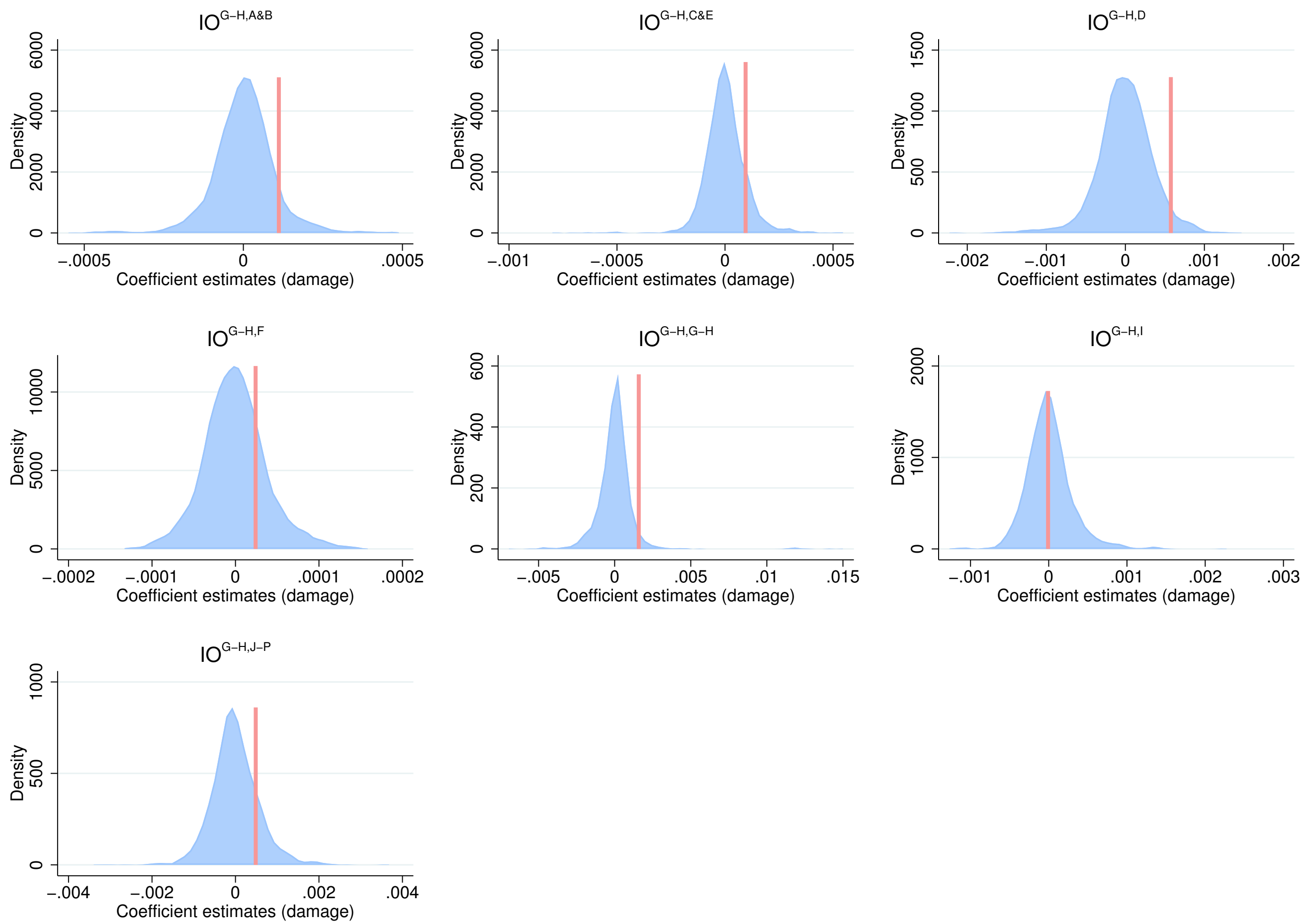

Figure 1.23: Randomization tests – Input-Output coefficients of sector aggregate G–H

Notes: This figure shows the Fisher randomization test results for the $damage_t$ variable where the years are permuted for 2000 repetitions. It displays the kernel density plots (blue) of the randomization coefficient estimates together the results of model 1.6 (red bar). The sector abbreviations represent the following sector aggregates: agriculture, hunting, forestry, and fishing (A&B), mining, and utilities (C&E), manufacturing (D), construction (F), wholesale, retail trade, restaurants, and hotels (G–H), transport, storage, and communication (I), other activities (J–P).

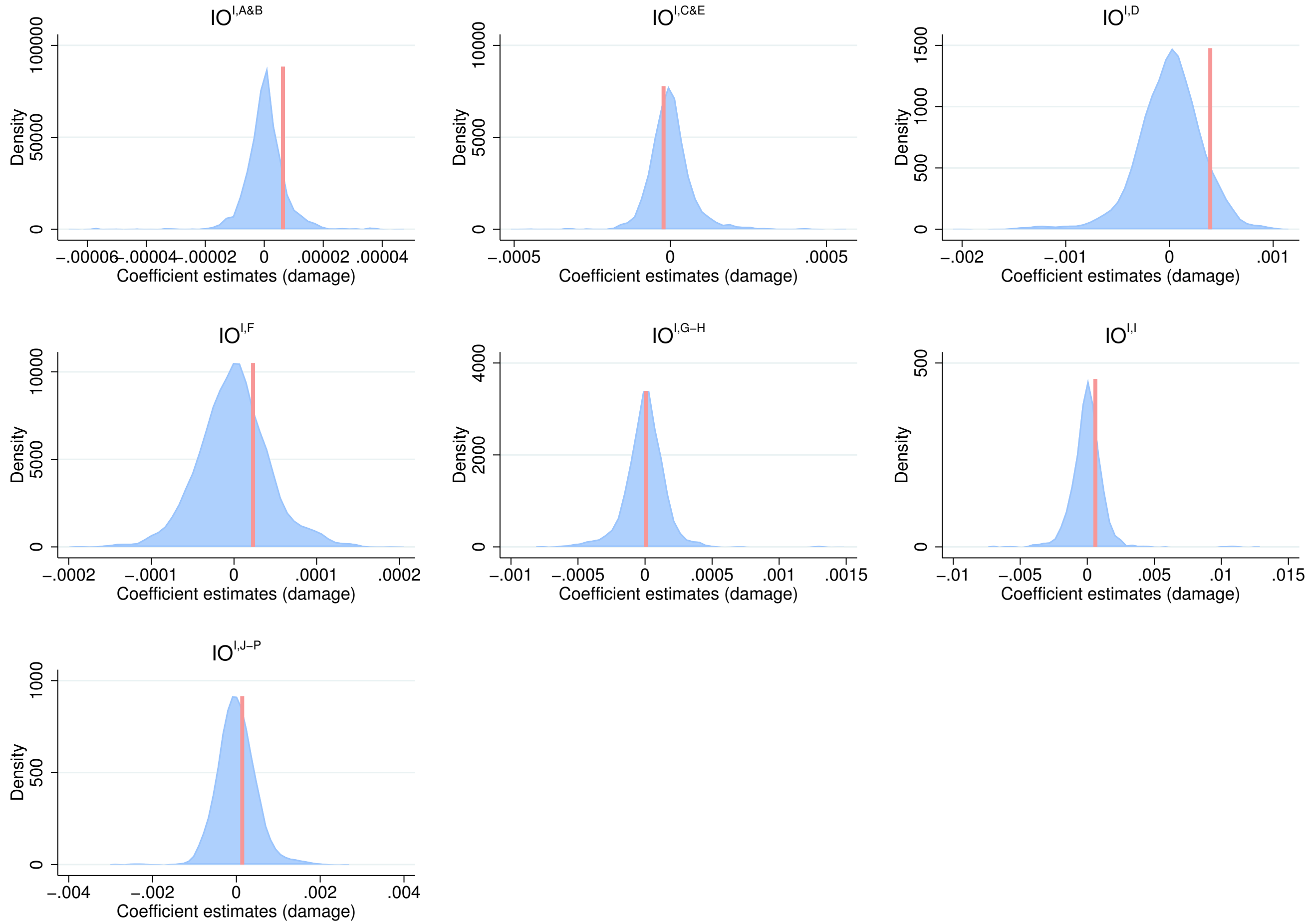

Figure 1.24: Randomization tests – Input-Output coefficients of sector aggregate I

Notes: This figure shows the Fisher randomization test results for the $damage_t$ variable where the years are permuted for 2000 repetitions. It displays the kernel density plots (blue) of the randomization coefficient estimates together the results of model 1.6 (red bar). The sector abbreviations represent the following sector aggregates: agriculture, hunting, forestry, and fishing (A&B), mining, and utilities (C&E), manufacturing (D), construction (F), wholesale, retail trade, restaurants, and hotels (G–H), transport, storage, and communication (I), other activities (J–P).

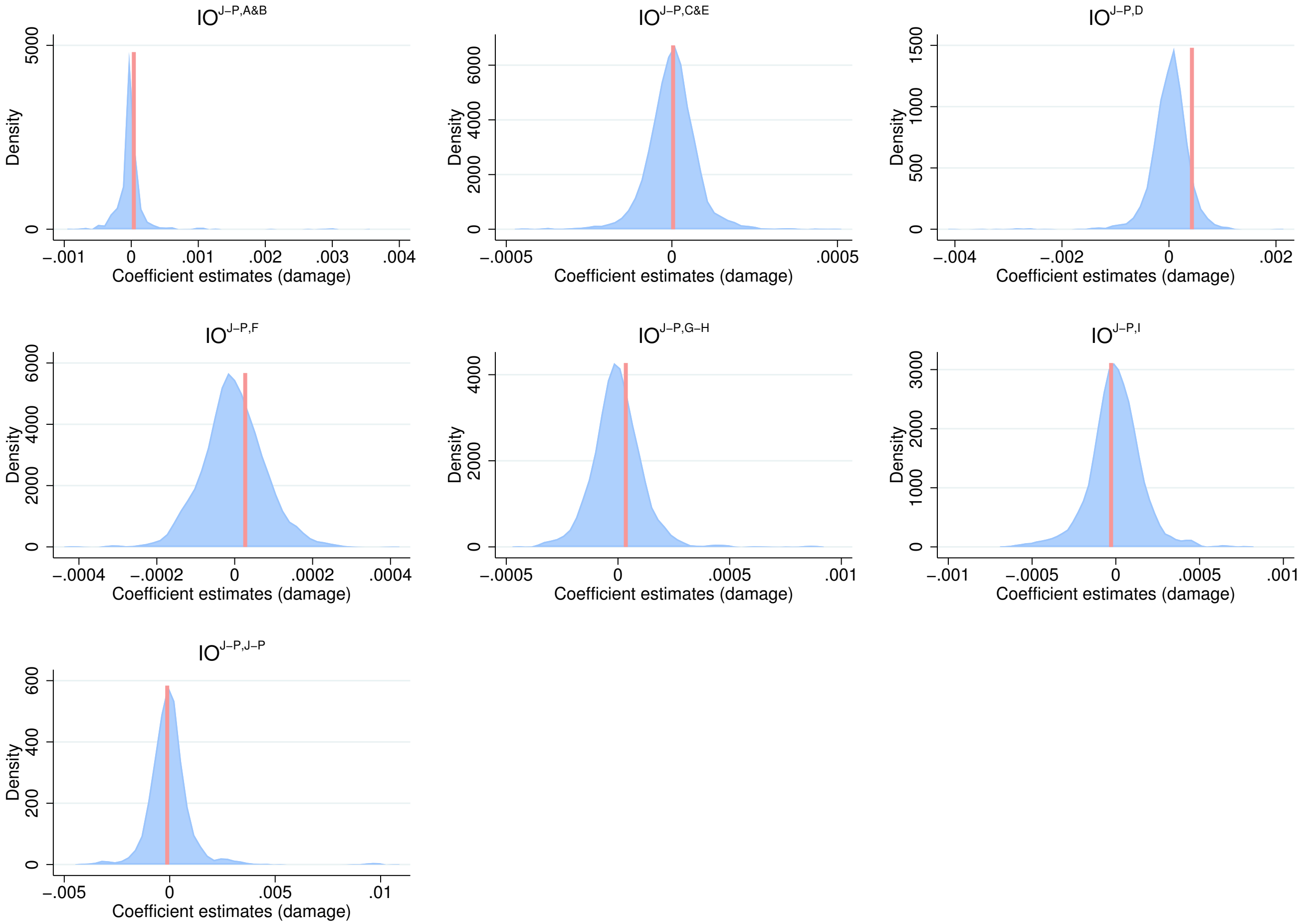

Figure 1.25: Randomization tests – Input-Output coefficients of sector aggregate J–P

Notes: This figure shows the Fisher randomization test results for the $damage_t$ variable where the years are permuted for 2000 repetitions. It displays the kernel density plots (blue) of the randomization coefficient estimates together the results of model 1.6 (red bar). The sector abbreviations represent the following sector aggregates: agriculture, hunting, forestry, and fishing (A&B), mining, and utilities (C&E), manufacturing (D), construction (F), wholesale, retail trade, restaurants, and hotels (G–H), transport, storage, and communication (I), other activities (J–P).

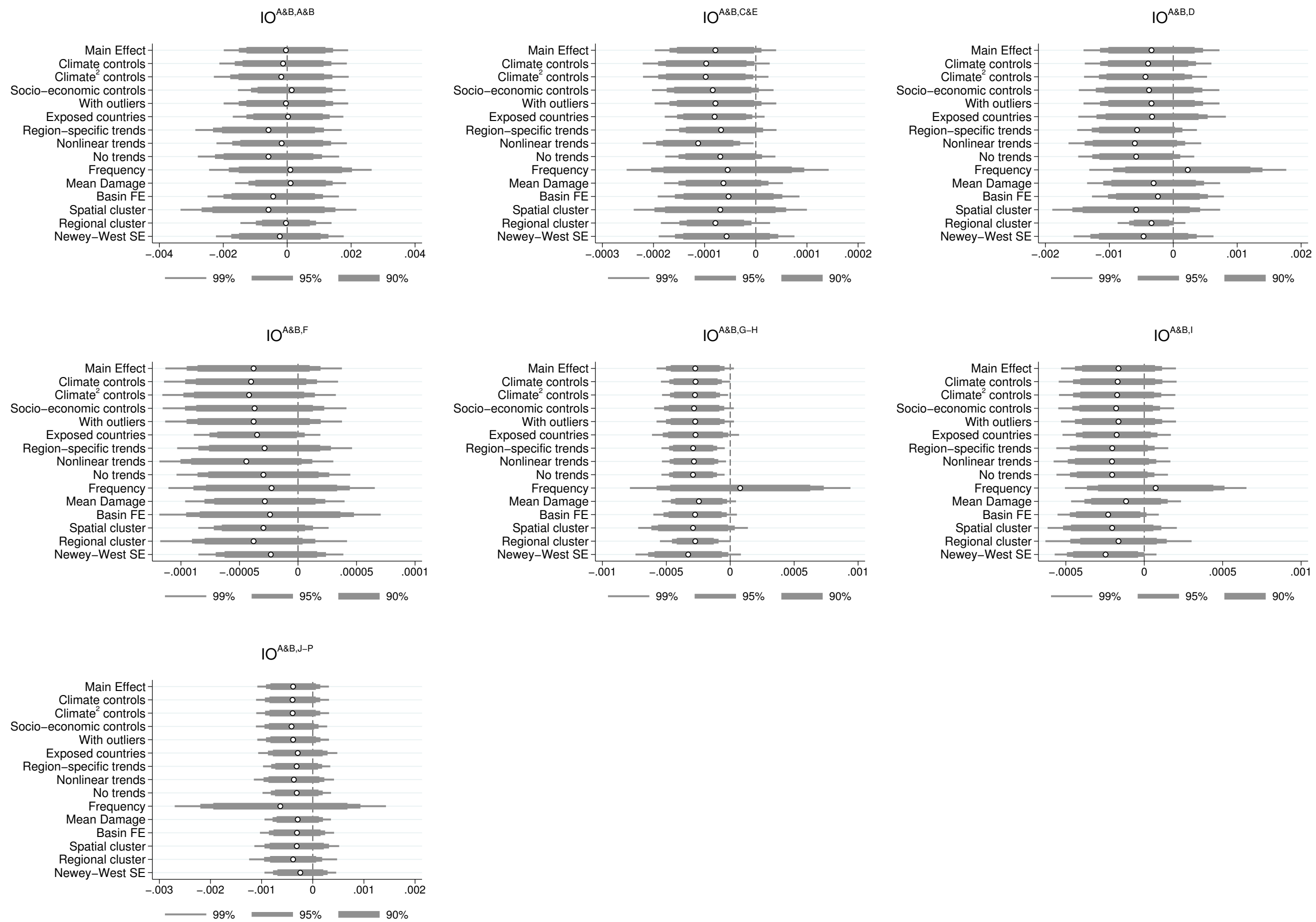

Figure 1.26: Overview robustness tests – Input-Output coefficients of sector aggregate A&B

Notes: This figure shows coefficient plots for different robustness tests for indirect effects of tropical cyclone damage on Input-Output coefficients of sector aggregate A&B. The sector abbreviations represent the following sector aggregates: agriculture, hunting, forestry, and fishing (A&B), mining, and utilities (C&E), manufacturing (D), construction (F), wholesale, retail trade, restaurants, and hotels (G–H), transport, storage, and communication (I), other activities (J–P).

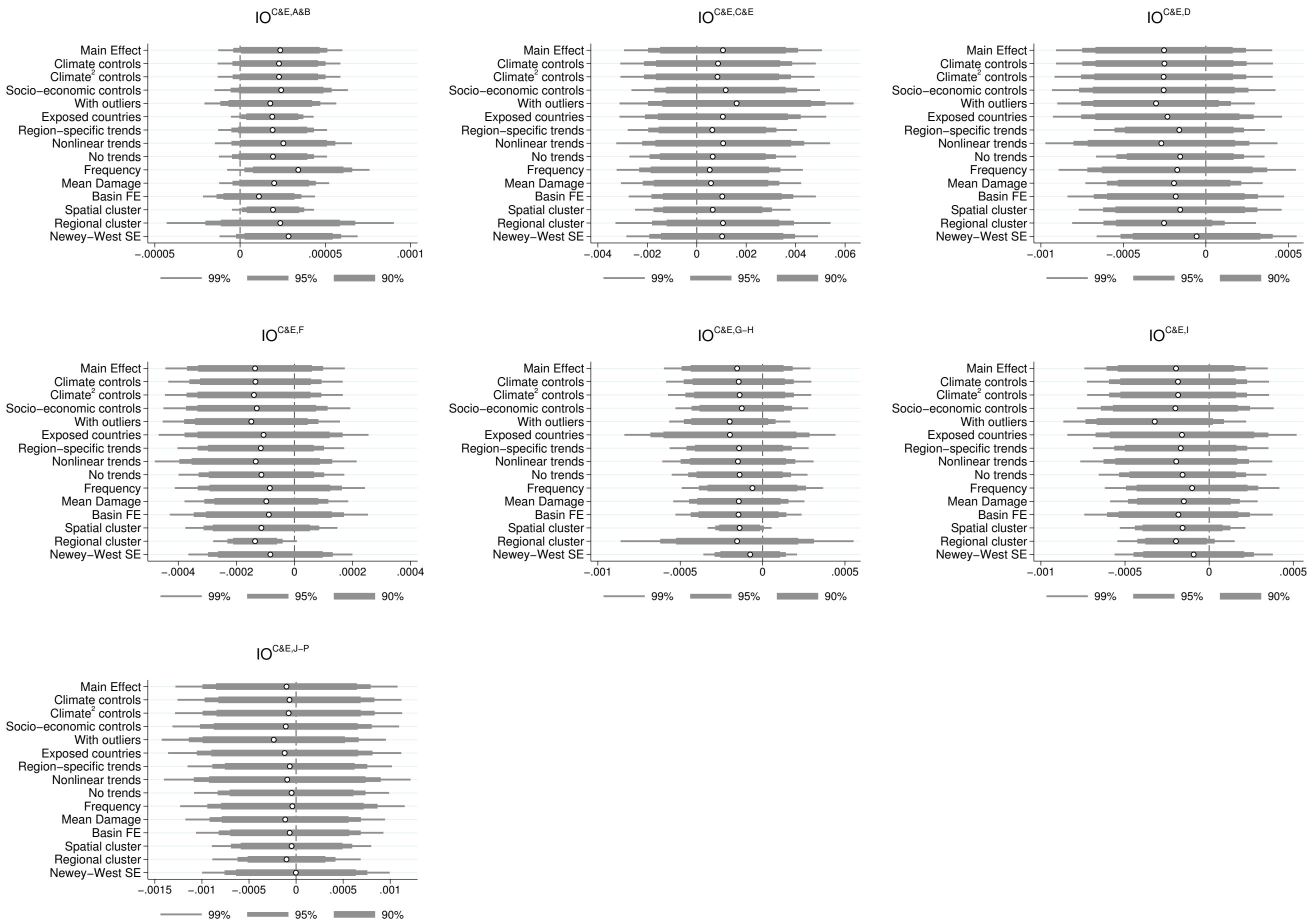

Figure 1.27: Overview robustness tests – Input-Output coefficients of sector aggregate C&E.

Notes: This figure shows coefficient plots for different robustness tests for indirect effects of tropical cyclone damage on Input-Output coefficients of sector aggregate C&E. The sector abbreviations represent the following sector aggregates: agriculture, hunting, forestry, and fishing (A&B), mining, and utilities (C&E), manufacturing (D), construction (F), wholesale, retail trade, restaurants, and hotels (G–H), transport, storage, and communication (I), other activities (J–P).

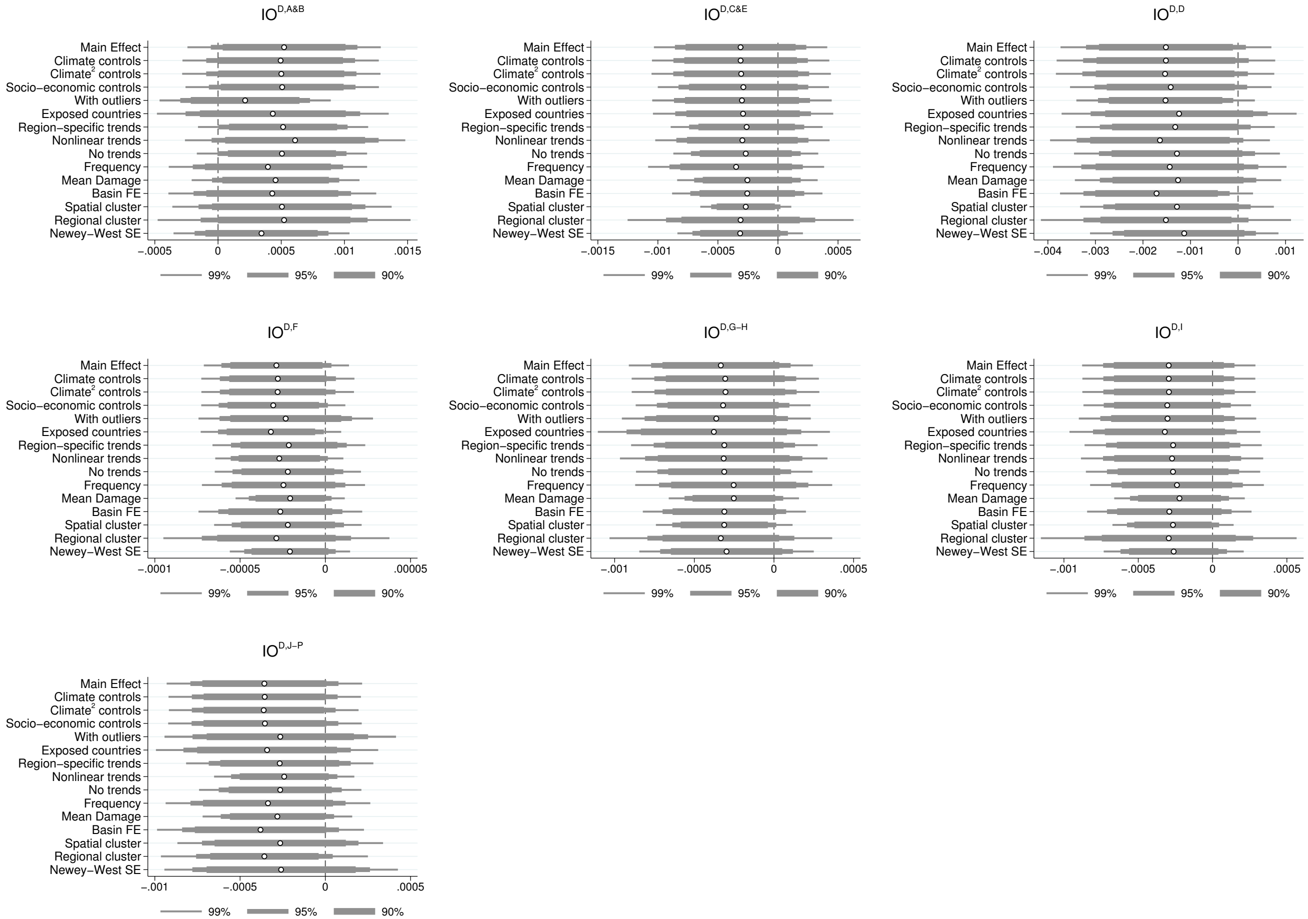

Figure 1.28: Overview robustness tests – Input-Output coefficients of sector aggregate D

Notes: This figure shows coefficient plots for different robustness tests for indirect effects of tropical cyclone damage on Input-Output coefficients of sector aggregate D. The sector abbreviations represent the following sector aggregates: agriculture, hunting, forestry, and fishing (A&B), mining, and utilities (C&E), manufacturing (D), construction (F), wholesale, retail trade, restaurants, and hotels (G–H), transport, storage, and communication (I), other activities (J–P).

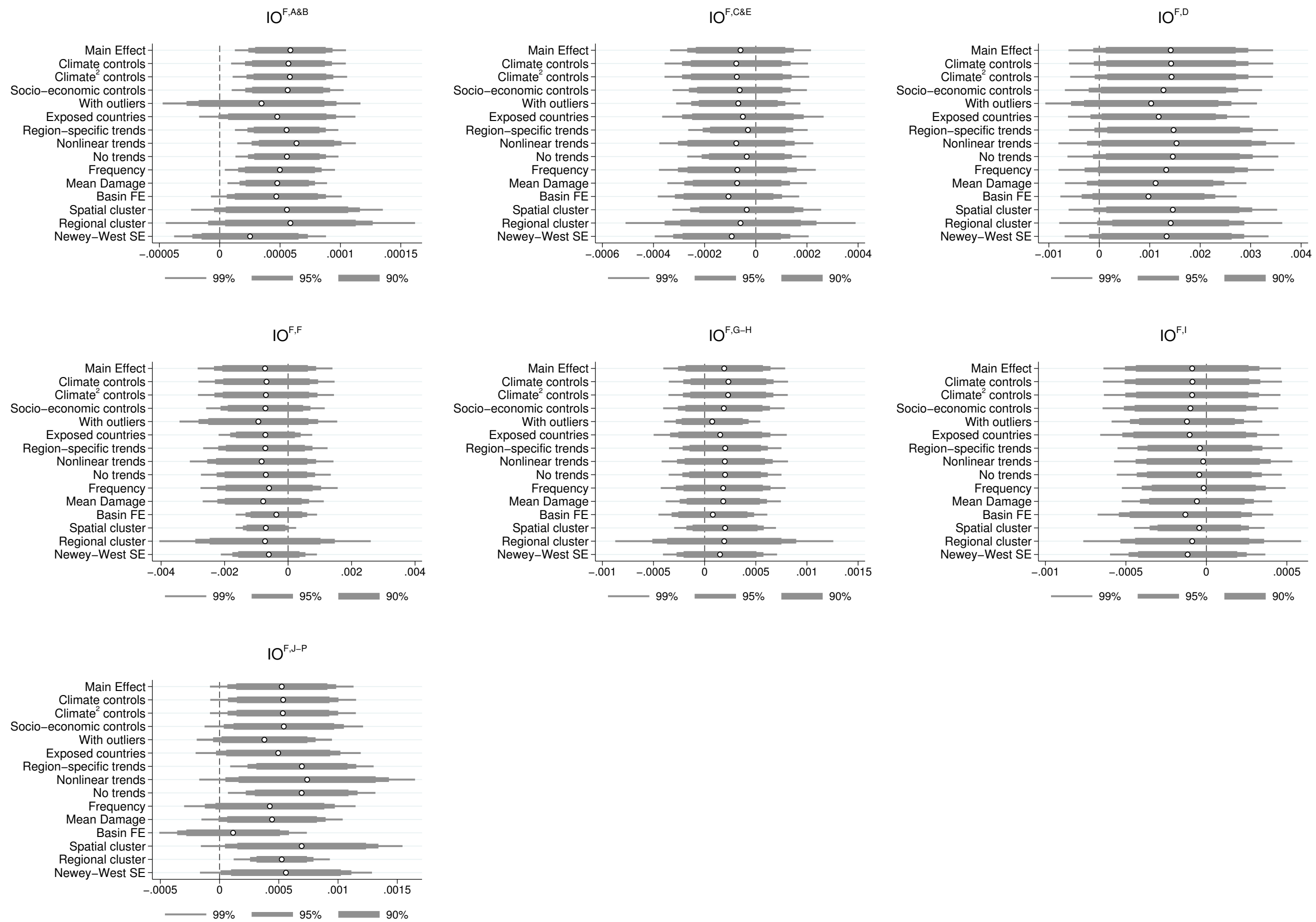

Figure 1.29: Overview robustness tests – Input-Output coefficients of sector aggregate F

Notes: This figure shows coefficient plots for different robustness tests for indirect effects of tropical cyclone damage on Input-Output coefficients of sector aggregate F. The sector abbreviations represent the following sector aggregates: agriculture, hunting, forestry, and fishing (A&B), mining, and utilities (C&E), manufacturing (D), construction (F), wholesale, retail trade, restaurants, and hotels (G–H), transport, storage, and communication (I), other activities (J–P).

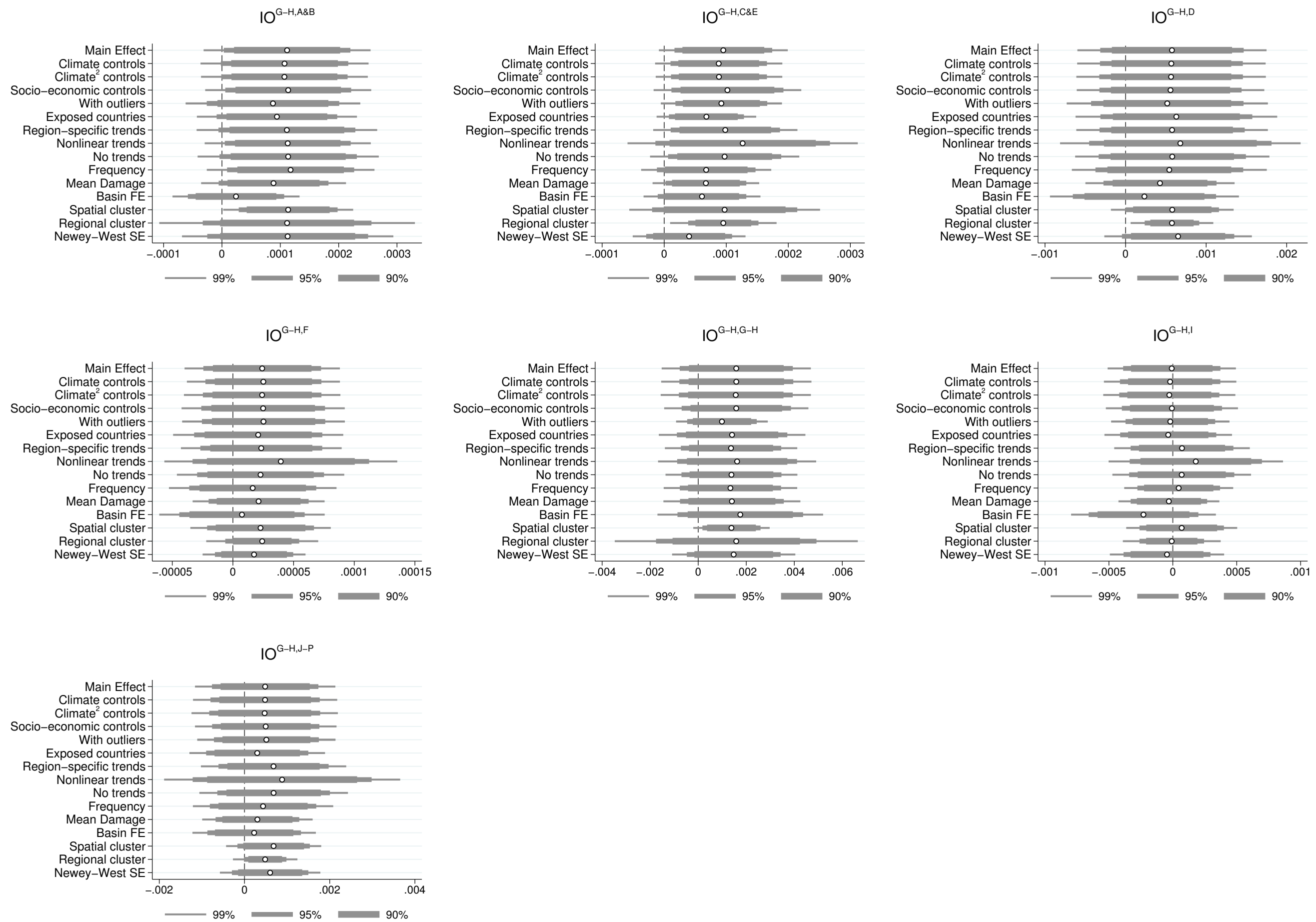

Figure 1.30: Overview robustness tests – Input-Output coefficients of sector aggregate G–H

Notes: This figure shows coefficient plots for different robustness tests for indirect effects of tropical cyclone damage on Input-Output coefficients of sector aggregate G–H. The sector abbreviations represent the following sector aggregates: agriculture, hunting, forestry, and fishing (A&B), mining, and utilities (C&E), manufacturing (D), construction (F), wholesale, retail trade, restaurants, and hotels (G–H), transport, storage, and communication (I), other activities (J–P).

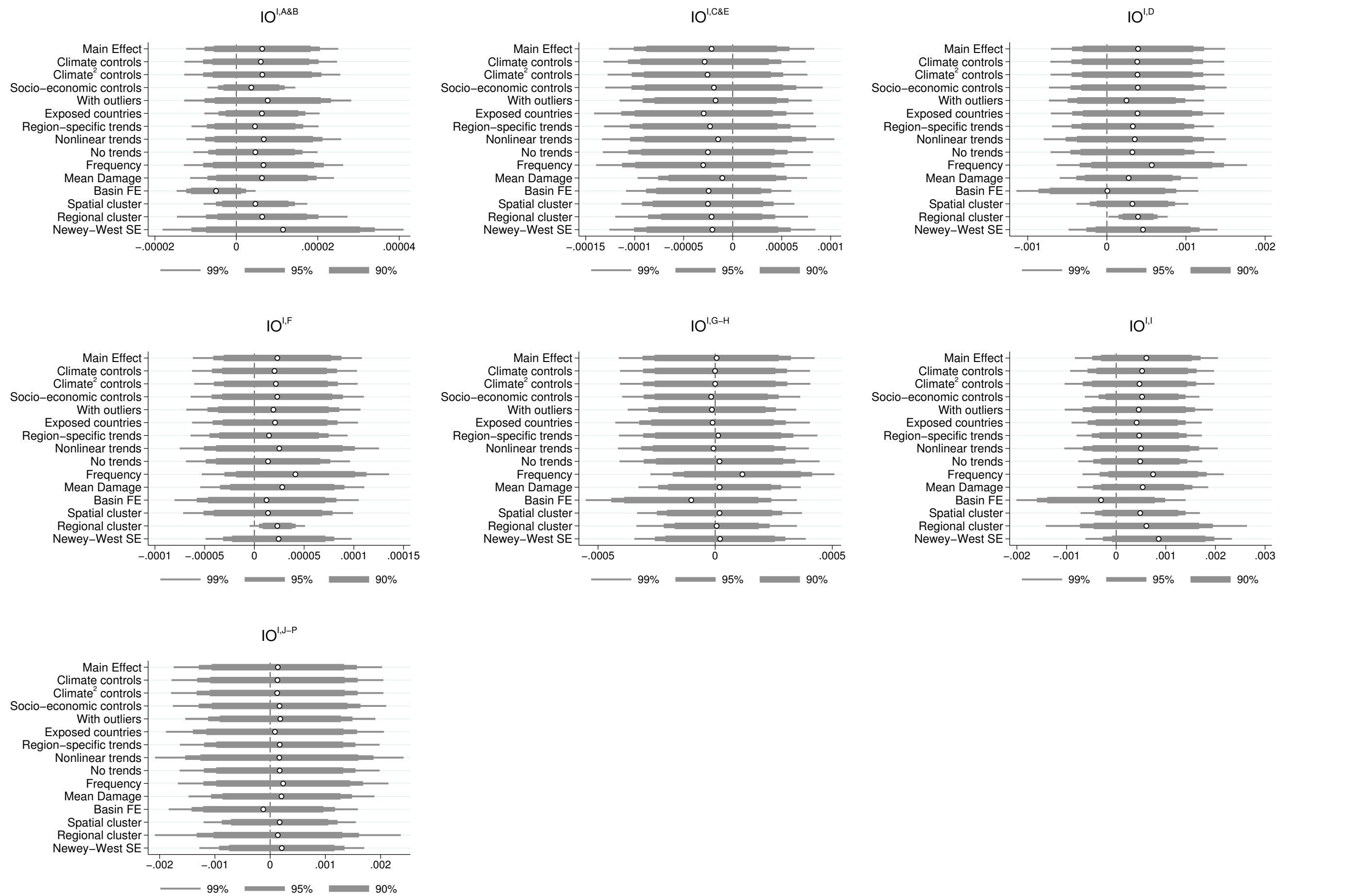

Figure 1.31: Overview robustness tests – Input-Output coefficients of sector aggregate I

Notes: This figure shows coefficient plots for different robustness tests for indirect effects of tropical cyclone damage on Input-Output coefficients of sector aggregate I. The sector abbreviations represent the following sector aggregates: agriculture, hunting, forestry, and fishing (A&B), mining, and utilities (C&E), manufacturing (D), construction (F), wholesale, retail trade, restaurants, and hotels (G–H), transport, storage, and communication (I), other activities (J–P).

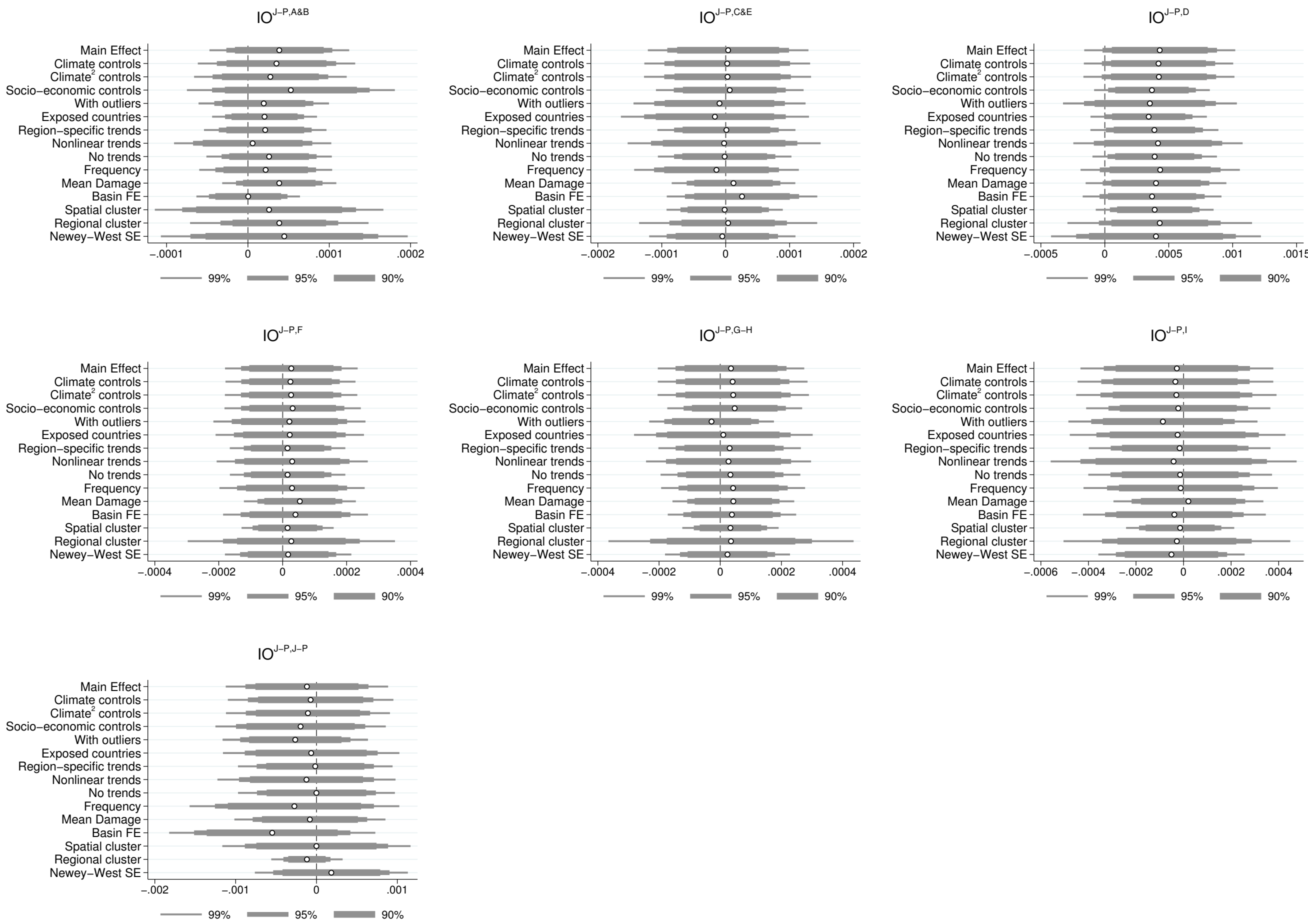

Figure 1.32: Overview robustness tests – Input-Output coefficients of sector aggregate J–P

Notes: This figure shows coefficient plots for different robustness tests for indirect effects of tropical cyclone damage on Input-Output coefficients of sector aggregate J–P. The sector abbreviations represent the following sector aggregates: agriculture, hunting, forestry, and fishing (A&B), mining, and utilities (C&E), manufacturing (D), construction (F), wholesale, retail trade, restaurants, and hotels (G–H), transport, storage, and communication (I), other activities (J–P).

2 The Global Long-Term Effects of Storm Surge Damage on Human Settlements in Coastal Areas

This chapter is joint work with Eric A. Strobl. It has not yet been published.

Abstract: People in low-lying coastal areas live under the potentially great threat of damage due to coastal flooding from tropical cyclones. Understanding how coastal population settlements react to such events is of high importance for society in order to consider future potential adaptation strategies and policies. In this study, we generate a new global hydrological data set on storm surge damage for the period 1850–2010. By combining this new data set with spatial data on human populations at a resolution of 10 km, we analyze the influence of storm surge damage on the rural, urban, and total population in low elevation coastal zones. We find that 8% of the global coastal population moved away per decade over the 1950–2010 period as a consequence of storm surges, on average. It is the urban population where we find the largest reductions (-15%). We show that the exposed coastal population has adapted over time and started to reduce its exposure in recent decades. This finding applies to most regions, with the exceptions of North America, Oceania, and Western Asia.

2.1 Introduction

The influence of nature on human settlements is immense. While a friendly and calm environment can lead to prosperity and growth, a hostile environment with frequent natural disasters can result in stagnation, collapse, and even death. In this regard, tropical cyclones are arguably one of the most significant climatic events to pose a threat to the prosperous development of human societies. For instance, during the 1970–2019 period, Guha-Sapir & CRED (2020) estimate that tropical cyclones have caused deaths of up to 962,000 people and costs of nearly USD 1,600 billion. A number of factors contribute to damage induced by tropical cyclones, but mainly these are storm surges, high wind speeds, and extreme precipitation. The greatest threat resulting from a tropical cyclone to coastal populations is generally the accompanying storm surge (Needham et al., 2015), and around 250 million people are vulnerable to storm surge events every year (Intergovernmental Panel on Climate Change, 1994). Particularly people in low elevation coastal zones (LECZ), which are defined as areas contiguous to the coastal shoreline that are below 10 m above sea level, have the highest flooding risk. In the (near) future, sea level rise and the intensification of tropical cyclones through climate change, as well as rapid human-induced land subsidence are likely to further increase local exposure (Bhatia et al., 2019; Mendelsohn et al., 2012; Rahmstorf, 2017; Woodruff et al., 2013). Current cost estimates of this increased exposure amount to 1 trillion USD per year by 2050 (Hallegatte et al., 2013). Reducing exposure can thus be economically meaningful. This is also reflected in a current study by Hallegatte et al. (2016). The authors estimate that reducing the exposure to floods of poor people by 5% in Malawi, would result in a reduction of asset losses by yearly USD 2.2 million. According to the authors this reduction would lead to a well-being gain of USD 19 million per year. Therefore, understanding how coastal exposure to storm surge damage has developed is of great importance in designing economically appropriate risk reduction policies.

The economic possibilities, transportation access, geopolitical considerations, and recreational opportunities have generally made living near the coast attractive to humans (de Sherbinin et al., 2012; Fang & Jawitz, 2019; Hauer et al., 2020). Unsurprisingly, settlements near the coast then have tended to urbanize earlier (Motamed et al., 2014). This attraction may be so strong to induce positive population growth even in multi-hazard coastal areas (de Sherbinin et al., 2012; Kocornik-Mina et al., 2020). In fact, currently around 634 million (McGranahan et al., 2007) to 1.4 billion (Neumann et al., 2015) people are living in coastal flooding zones, and different studies estimate that this population will continue to grow in the future (Hallegatte et al., 2013; Jongman et al., 2012; Neumann et al., 2015). The decision to live in a high risk area should depend on net expected gains and this calculation is likely to be updated as new events occur (Cameron & Shah, 2015). However, there exists evidence that people seem to systematically underestimate the losses of tail risk climatic events (Botzen et al., 2015). Moreover, damaging events such as floods have been shown to actually cause inward migration to affected areas (Boustan et al., 2012), in particular by poorer people (McCaughey et al., 2018; Strobl, 2011). Nevertheless, the current evidence is much too limited in scope and context to draw any conclusions with regard to the likely adjustment behavior of the growing coastal population across the globe to the possibility of more and/or more intense tropical storm surges. However, without knowing the exact exposure and how it has changed over time, possible disaster risk policies lack the foundation for an evidence-based decision.

In this study, we explicitly analyze how local population sizes in potentially hazardous areas respond to storm surges caused from tropical cyclones. Because storm surge levels from tropical cyclones at the global level are hard to model, no global tropical cyclone-driven storm surge data set exists. Most studies instead focus on wind effects (see, e.g., Felbermayr & Gröschl, 2014; Hsiang, 2010; Strobl, 2011), while a minority of studies also includes precipitation damage (Bakkensen et al., 2018). Previous studies analyzing the exposure of coastal populations to coastal flooding have used extreme sea level data to derive the exposure to storm surge threats and combined it with climate change or socioeconomic scenarios (Bouwer, 2018; Hallegatte et al., 2013; Hauer, 2017). Such static statistical analysis is suited for risk assessment rather than for the causal identification of the relationship between storm surges and human settlement outcomes. Unfortunately, while there are historical observations of actual storm surges available, these are extremely limited in time, space, and quality. For example, the widely used SURGEDAT data set comprises only 172 validated empirical observations since 1897 (Needham & Keim, 2012). One step forward in modeling storm surge damage was the recently established Global Tide and Surge Reanalysis (GTSR) model for a global time series of general storm surge threats from 1979–2014. It combines inputs from the ERA-interim reanalysis data[38] for wind speed and pressure with tidal inputs in a

[38]The ERA-interim reanalysis data are produced by the European Centre for Medium-Range Weather Forecasts (ECMWF). Reanalysis data are usually long-term weather and climate observations that are collected by

hydrodynamic model (Muis et al., 2016). However, because of the coarse spatial and temporal resolution of the ERA-interim reanalysis input, approximately 75 km and 6h respectively, the derived model outputs tend to underestimate the observed storm surge levels (Bloemendaal et al., 2019; Muis et al., 2016). Additionally within the GTSR data, it is not possible to attribute coastal storm surge heights specifically to tropical cyclones, since they do not constitute an individual input of the model.

The main contribution of this study is the development of the first tropical cyclone-generated storm surge data set of all historical tropical cyclones. This new data set not only covers a very long time period (1860–2010). It also allows one to estimate storm surge water levels attributable to specific historical events. Storm surges usually form for two reasons – pressure differences between the eye of the storm and the surrounding environment and strong winds. Moreover, the magnitude of the storm surge depends on the coastal and ocean geography (bathymetry), the current tide, the forward speed of the tropical cyclone, and the angle at which the storm makes landfall. Our data set is based on a hydrodynamic model that combines all of these input factors and allows us to calculate one-hourly coastal inundation maps at a resolution of 10 × 10 km for all tropical cyclones ever recorded in the International Best Track Archive for Climate Stewardship (IBTrACS) (Knapp et al., 2010).

We combine our storm surge damage data with local time-varying (decadal) population data from the HYDE data set (Klein Goldewijk et al., 2017), which is available at a resolution of 10 km after 1700. For our analysis, we include all grids in LECZ that lie in countries that had at least one positive storm surge observation in our data set. Using a multivariate grid-cell-level-fixed-effects panel regression model at a resolution of 10 x 10 km, we analyze the causal responses of the local total, rural, and urban populations in LECZ to storm surge damage globally and in terms of nine world regions. If data coverage of the tropical cyclones allows it, our sample ranges from 1860–2010. This range is only possible for regions within the North Atlantic basin, which compromises North America and Central America and the Caribbean. For the global sample and the other regions, the period reduces to 1950–2010.[39] To see if there may have been any adaptation in the population's response to storm surge damage, we also identify decadal differences in our estimates. Additionally, we investigate whether factors such as the agricultural suitability of the land or income levels may have

different methods during different time periods. Within the reanalysis data set these different methods are harmonized by one common method to make the data comparable across time periods.

[39] Since we are looking at decadal data, and the last data entry for population data is 2015, the last fully observed decade is 2010.

played a role in preventing people from moving away from hazardous areas. Our analysis contributes to the debate on whether (long-term) adaptation to disasters is taking place, an issue especially urgent in the light of climate change and increasing coastal population numbers. Hence, politicians and international organizations can learn from our analysis in terms of where and to what extent people are exposed to coastal storm surges, and how coastal populations have responded to such events over the last 70 years. Policymakers can use our damage and exposure estimates to improve and update coastal flood plain maps. What is more, our results can also serve as an input for cost-benefit analyses and to better assess coastal populations' vulnerabilities considering different socioeconomic and institutional backgrounds in the future.

We find that Eastern Asia, North America, and South-Eastern Africa are the regions most exposed to past storm surges. While in all regions, fewer people live in exposed compared to non-exposed LECZ, one can observe a simultaneous population increase in both zones in some world regions, such as Western Asia. In 2010, three quarters of all people exposed to storm surge threats lived in Eastern Asia, South-Eastern Asia, and Southern Asia. In general, the urban population is more exposed than the rural population. We show, that in response to storm surges, fewer people live in exposed areas on average. However, this was not true over the entire time period of our analysis; rather, we can identify a shift from positive to negative local population numbers in more recent decades for most regions. What is more, it is the urban population which drives our effect, while the rural population tends to be bound to agricultural resources.

The remainder of this paper is structured as follows. Section 2.2 describes the data sources, provides an estimation of the storm surge damage, and presents summary statistics. Section 2.3 describes our method and empirical identification strategy, and Section 2.4 presents the main results. Section 2.5 concludes with a discussion of the results and policy implications.

2.2 Data

2.2.1 Storm Surge Damage

Storm surges can cause different kinds of damage in LECZ. They can lead to coastal flooding, the destruction of infrastructure, the erosion of the shoreline, and the salinization of vegetation, leaving it useless for agricultural cultivation (Le Cozannet et al., 2013). Furthermore, compared to wind speed and rainfall, they are the most frequent cause of tropical cyclone-related deaths. Storm surges typically arise due to two characteristics. First, the strong cyclone winds generate giant waves that move toward the coastlines. Second, there is a fast, transitory rise in the local sea level due to a decline in the atmospheric pressure in the eye of the tropical cyclone (Terry, 2007). The magnitude of storm surges additionally depends on the tidal circle, i.e., high tides amplify the wave height, whereas low tides reduces it. What is more, the bathymetry, which refers to the geography of the ocean's surface, is another important influence on the storm surge height. Other relevant factors are the forward speed of the storm and the impact angle of the tropical cyclone on the coast.

The storm surge model we employ is based on the DELFT3D model, which is an open-source hydrodynamic software, offered by the University of Delft.[40] With this software one can globally model different hydrological processes. We used the code offered and rewrote it for our global tropical cyclone-based storm surge model.[41] The main input of our model, tropical cyclone raw data, comes from the International Best Track Archive for Climate Stewardship (IBTrACS), which is a combination of all available best track tropical cyclone data worldwide (Knapp et al., 2010). We use the v03r10 version, which provides six-hourly tropical cyclone raw data observations (location, minimum sea level pressure, wind speed) for all storms over the 1842–2017 period. As indicated by the decadal distribution of the tropical cyclone raw data in Appendix Figure 2.15, only storms within the North Atlantic basin were consistently tracked from the 1850s onward (see also Appendix Figures 2.17 and 2.20). Global coverage of landfalling tropical cyclones is approximately reached by 1940, and we thus restrict the global sample of tropical cyclones to the 1940–2017 period (Kossin et al., 2013). For the extended period from the 1850s onward, we limit our sample to only those storms that fully or partially transpassed the North Atlantic basin and to countries that lie at least partially within this basin (Central America and the Caribbean and North America). This applies to the analyses shown in Figures 2.7 and 2.8. For the bathymetry input, we use data from GEBCO 8.2 (British Oceanographic Data Centre, 2010). It contains a continuous terrain model for the ocean and the coast at a spatial resolution of approximately 1 km (30 arc-seconds) at the equator and is generated by ship and satellite data. For the tidal

[40] Appendix Figure 2.12 summarizes our modelling steps.

[41] The model is written in MATLAB and the computation time for the global model is 72h, parallelized on a 10-core computer.

conditions we take the TPXO 7.2 Global Inverse Tidal Model (Egbert & Erofeeva, 2002) which contains time series of all ocean tides globally.

Since we are only interested in coastal population at risk of storm surges, we restrict our model to areas around potentially exposed LECZ. To reduce computation time, we split the exposed LECZ into different model areas. Figure 2.1 plots the 48 identified model areas for our storm surge model. We only consider tropical cyclones with a maximum raw track distance of 100 km to the coasts in our model areas, which leaves us with 6504 tropical cyclones.[42] For each of these raw tracks, we calculate pressure drop and wind fields for every hour of their observation time since both are important factors for storm surges.[43]

The basis of the calculation of the storm surge model builds a three-dimensional grid that allows us to combine the bathymetry and tidal information with tropical cyclone inputs (pressure drop and wind fields, velocity, and angle of landfall). The resolution is 0.1° x 0.1°, which corresponds to approximately 10 km at the equator. For the third dimension, we only include areas below 10 m in altitude since storm surges are normally not higher than 10 m.[44] With these inputs, we then calculate each tropical cyclone's storm surge-related water level (above sea level) for every hour of their observation time. From these hourly maps we subsequently take the maximum water level per grid and per tropical cyclone further into

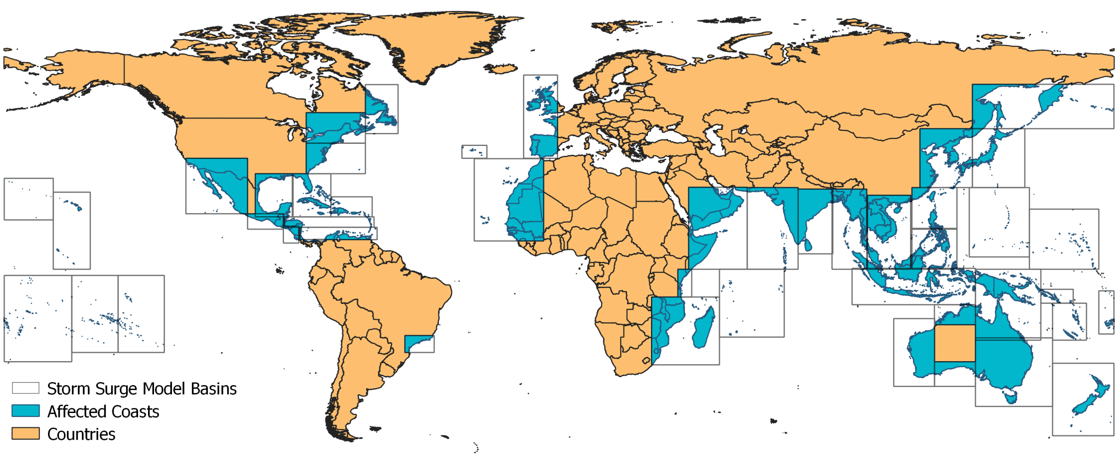

Figure 2.1: Covered areas of storm surge model

[42]The reasons for not including more tropical cyclones with a higher distance are the following: First, tropical cyclones with a distance higher than 100 km seldom cause any significant damage. Second, to guarantee a feasible computation time of the model, we must restrict the model only to potentially damaging tropical cyclones.

[43]Compared to previous models, we are not using a simple rectangular grid, but a more precise curve-linear spiderweb grid as a basis for the field calculations. The pressure drop and wind fields are based on the well-established Holland (1980) model. For further information on the Holland model see Chapter 1.2.1.

[44]See Appendix Figure 2.10 for an illustration of the 3D grid in the Gulf of Mexico.

account. To not falsely overestimate the tidal component of the model, we only select coastal grids within a radius of 500 km around each tropical cyclone.

To test the sensitivity of our modeled storm surge data, we compare it to the few validated observations available from the Global Peak Surge Map database (Needham & Keim, 2012).[45] Figure 2.2 plots four tropical cyclones with the resulting storm surge levels (color scale) and compares them with storm surge observations at the coast. In all cases our model is very close to actual coastal storm surge observations. In Appendix Figure 2.9 we plot 101 storm surge observations with a high level of confidence of a correct observation against our modeled storm surge levels. The root-mean-square error is 0.95, and the R^2 corresponds to 64.3%, a relatively high value given that our storm surge model runs at a spatial resolution of 10 km.

Figure 2.3 shows the average modeled storm surge inundation levels along the coast for the years 1940–2010.[46] The average water levels range between 0 m and 5.4 m. The

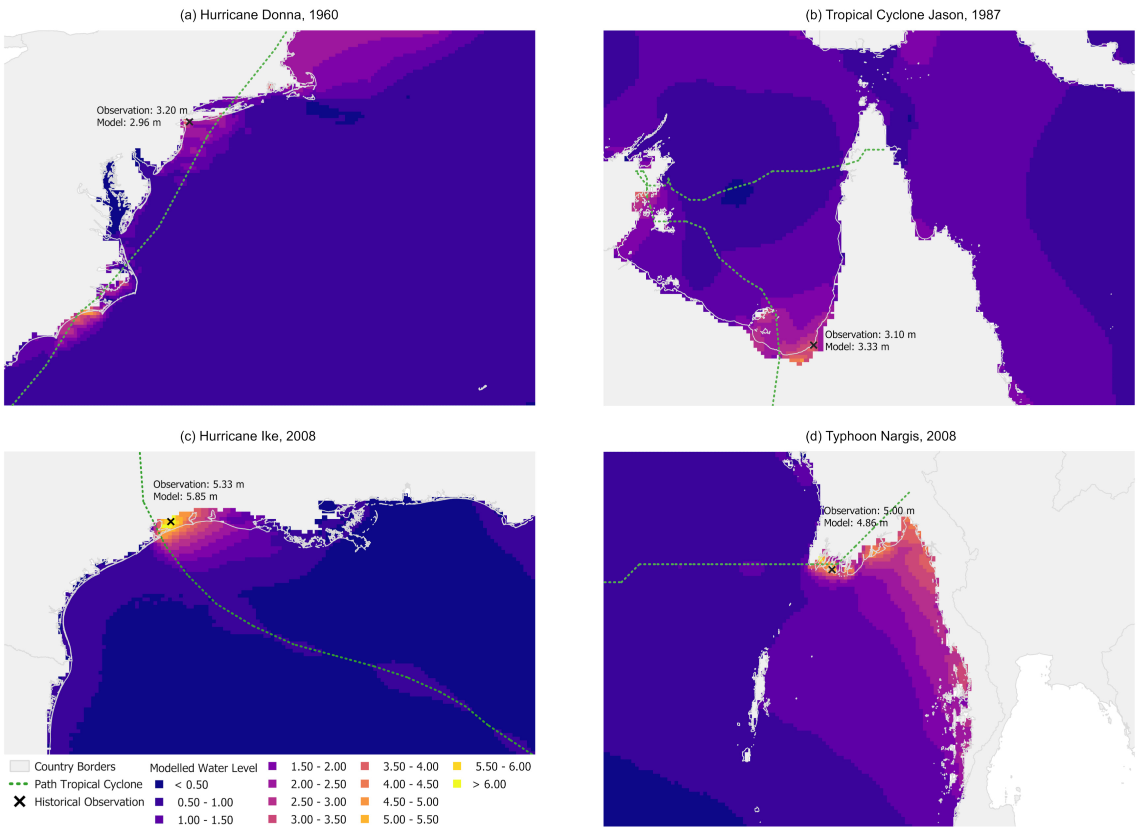

Figure 2.2: Validation examples for storm surge model

Notes: This figure compares the modeled storm surge heights against historic observations of the SURGEDAT data set for four different tropical cyclones.

[45] The data are freely available at http://surge.srcc.lsu.edu/data.html (accessed 25 October 2020).

[46] We start in decade 1940, because global coverage of tropical cyclones starts here. Since the population data are decadal until 2000 and the last yearly data entry is in 2015, we take the decade 2010 as our last data entry. Consequently, our storm surge model covers the 1940–2010 period.

exposure of storm surge damage is globally unequally distributed. The regions Eastern Asia, North America, and South-Eastern Africa experience the highest levels of storm surge-related flooding on average, with mean water levels in exposed LECZ of 0.24 m, 0.14 m, and 0.1 m, respectively. The least exposed regions are Europe (0.05 m), Central America and the Caribbean (0.04 m), and Western Asia (0.02 m). At the country level, as plotted in Appendix Figure 2.16, the most exposed countries on average are South Korea (0.38 m), Comoros (0.27 m), Taiwan (0.27 m), North Korea (0.26 m), Mozambique (0.24 m), Madagascar (0.24 m), Japan (0.2 m), the Philippines (0.2 m), Hong Kong (0.19 m), and China (0.17 m).[47]

To translate the modeled water levels into damage, we use a previously employed damage index for the destruction of residual infrastructures (Genovese & Green, 2015), which is capped at 70% destruction. Consequently, we calculate the *Storm surge damage* in grid i and year t as follows:

$$Storm\ surge\ damage_{it} = MIN[0.168341 * Water\ level_{it}, 0.7] \tag{2.1}$$

To combine the yearly $Storm\ surge\ damage_{it}$ with the decadal population data, we take the mean per decade d.

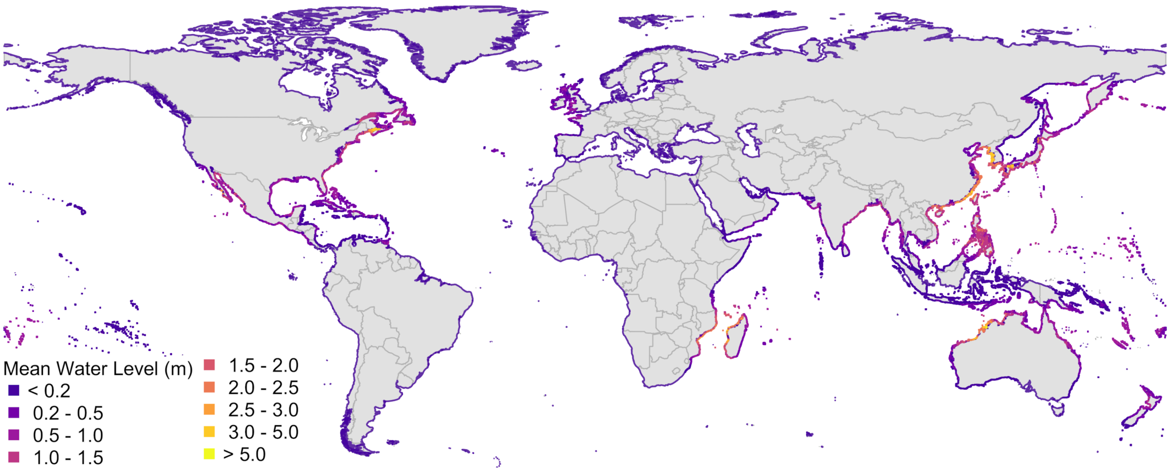

Figure 2.3: Average storm surge levels induced by tropical cyclones, 1940–2010

Notes: This figure shows the average storm surge water levels in meters (color scale) along the coast resulting from our model, averaged over 1940-2010.

[47] Appendix Figures 2.17–2.23 show the individual annual exposure for each country categorized by region, and Appendix Figure 2.16 lists all countries ordered by mean exposure.

2.2.2 Wind Speed and Rainfall Damage

To control for other potential damage of tropical cyclones to coastal populations, we need data on the two remaining damage sources, wind speed and rainfall. To obtain an accurate estimate of spatial wind speed from the IBTrACS raw data (Knapp et al., 2010), we use the model generated by Kunze (2021).[48] This model calculates wind fields with spatially varying wind speeds for each tropical cyclone at a resolution of 10 x 10 km because the tropical cyclone raw data give no indication of the spatial destructiveness of the wind speeds. Due to the physical nature of energy dissipation during a storm, the relationship between wind speed and damage is best proxied in a cubic manner (Emanuel, 2006). To account for this, we use the following damage index ($Wind\ damage_{is}$), describing the fraction of property damaged at grid i by wind exposure to tropical cyclones (Emanuel, 2011):

$$Wind\ damage_{is} = \frac{v_{is}^3}{1 + v_{is}^3}, \tag{2.2}$$

where

$$v_{is} = \frac{MAX[(V_{is} - V_{thresh}), 0]}{v_{half} - v_{thresh}}. \tag{2.3}$$

V_{is} is the maximum wind speed of storm s at grid i where, in our context, each point i corresponds to a population grid i's centroid. V_{thresh} is the threshold below which no damage occurs, and V_{half} is the threshold at which half of the property is damaged. We assume V_{thresh} and V_{half} to be 93 km/h (i.e., 50 kts) and 203 km/h (i.e., 150 kts), respectively (Emanuel, 2011). Within each year, we take the maximum $Wind\ damage_i$ per grid i, from which we calculate the mean $Wind\ damage_{id}$ per decade d.

For tropical cyclone-related rain damage, we use the parametric R-CLIPER model (Lonfat et al., 2007). Based on the estimated wind fields, this model calculates the respective rain fields in mm/h for each tropical cyclone in our sample. We do not calculate a damage function for rainfall since we would need more information on the surface geography to calculate a meaningful function. Within each year, we take the maximum $Rainfall_i$ per grid i, from which we calculate the mean $Rainfall_{id}$ per decade d.

[48]This model is an application of the CLIMADA model (Aznar-Siguan & Bresch, 2019). For further details see Chapter 1.2.1. Figure 1.1 shows an example of the modeled wind fields for Hurricane Ike.

2.2.3 Population Data

For population data, we use the historic gridded population data of the History Database of the Global Environment (HYDE) data set version 3.2.1, which provides global population maps for every 10 years from 1700 until 2000 and yearly data for the 2000–2015 period (Klein Goldewijk et al., 2017). This data set is a combination of different historic databases to generate an internally consistent spatial population data set over a long time series. It is based among others on historical data from Livi Bacci (2007), Maddison (2001), McEvedy & Jones (1978), Populstat (Lahmeyer, 2004), and country-specific local sources (Klein Goldewijk et al., 2017).[49] In a spatial weighting procedure based on population density from the Landscan (2006) satellite, historic maps of total, urban, and population counts are then generated (Klein Goldewijk et al., 2011). It is the only globally available data source for long-term population maps (Leyk et al., 2019). For our statistical analysis, we utilize the decadal data from 1860–2010. The decade d corresponds to the mean for the years d to $d-9$. For example, the decade 1860 is the mean of the years 1851–1860.[50] We restrict our data to years where we have data for the whole decade. Since the first storm observation is in 1842 and the last population observation in 2015, our sample period is at most 1860–2010. Given the missing data in the global tropical cyclone data set before 1940, our sample period for the global analysis is restricted to 1950–2010. The HYDE data set offers data on total, rural, and urban population counts measured in inhabitants/grid cell at a spatial resolution of around 10 km, from which we form our dependent variable *Population* for the different types measured.[51] Since we are only interested in people living in LECZ, we use data from the Shuttle Radar Topography Mission (SRTM) elevation data set (Brecht et al., 2007; McGranahan et al., 2007) to identify land areas contiguous with the coastline up to 10 m above sea level.[52]

Figure 2.4 depicts the development of population counts for LECZ exposed (orange solid line) and not exposed (purple dash-dotted line) to storm surge damage over the 1860–2010 period for each region. In all regions, fewer people live in exposed than in non-exposed LECZ. Moreover, in most exposed localities the population growth rate is lower compared

[49] A complete list of country-specific local sources is presented in the Supplementary files of Klein Goldewijk et al. (2017). Other major inputs can be found at https://themasites.pbl.nl/tridion/en/themasites/hyde/basicdrivingfactors/population/references.html, last accessed November 2021.

[50] See the method section for a more precise description of the time dimension.

[51] The exact spatial resolution of the data set is 0.5 arc minutes.

[52] The underlying map layer for country borders originates from DIVA GIS. See Appendix Figure 2.11 for an example of identified LECZ in Asia. We test our main specification for a non-LECZ sample in Appendix Table 2.39 as a placebo test.

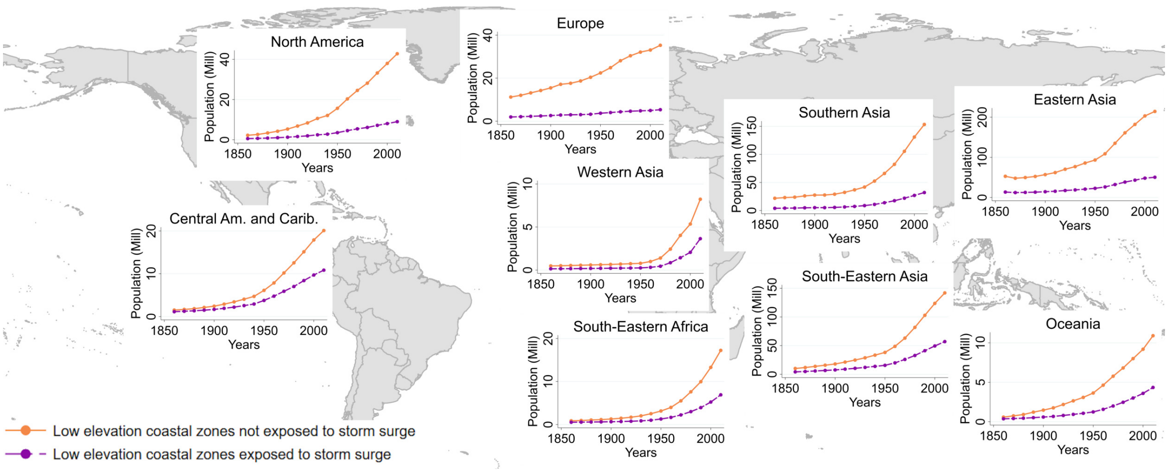

Figure 2.4: Population count for low elevation coastal zones exposed and not exposed to storm surge damage, 1860–2010

Notes: The different world regions include countries that experienced at least one positive storm surge observation over the sample period. Orange lines represent population trends for low elevation coastal zones in exposed regions that never experienced a storm surge event. Purple lines are population trends for low elevation coastal zones that experienced at least one storm surge event.

to non-exposed LECZ, particularly in more recent decades. If one compares the population development in LECZ to those living in other areas (Appendix Figure 2.14), one discovers that, since 1970 in Oceania, relatively more individuals live in LECZ, but as demonstrated in Figure 2.4, an increasing number of these have chosen to live in unexposed LECZ. Population trends in South-Eastern Asia depict a similar behavior. The general spatial population change between 1950 and 2010 reveals (Appendix Figure 2.13) that there has been a rural net population exodus in most industrialized countries. Conversely, most regions in Asia, Africa, and South America have seen widespread population growth in all parts of the country.

Our new storm surge data set allows us to better describe current exposure than previous studies because our data set is based on past storm surge events. It is arguably more precise than the data previously used in the literature. Previous empirical studies (Bakkensen & Mendelsohn, 2016; Bouwer & Jonkman, 2018) have mainly based their analysis on incomplete observational data such as SURGEDAT which contains only 172 validated observations since 1897 (Needham & Keim, 2012). In contrast our data set consists of 6,504 storm surge events for the 1842–2015 period. Figure 2.5 illustrates how many people are still living in exposed areas in 2010, classified by region and population type (rural and urban). Panels a–c display the distribution of total population by nine world regions for different levels of past exposure. Column 1 of Panel a shows that most people with more than one past storm surge event of any height live in South-Eastern Asia (57.66 million). If one compares Panels a–c, one can observe that the higher the past exposure, the fewer people live in these areas. Additionally, Figure 2.5 reveals that the majority of threatened population lives in Eastern, South-Eastern and Southern Asia. For all exposure levels displayed, these regions comprise at least 76% of the globally exposed population. Although there appears to be a negative correlation between level of exposure and population, in 2010 6.43 million people were still living in a highly exposed area with more than 100 2 m storm surge events having occurred in the 1950–2010 period. Of these 6.43 million people, 6 million are living in Eastern Asia, followed by 0.39 million in South-Eastern Asia, and 0.04 million in South-Eastern Africa.

Relative to the total population exposure shown in Panels a–c, Panels d–f illustrate which part of the population (rural or urban) was most exposed in 2010. These panels show the quantile distribution of the rural and urban country populations at risk, where the plotted

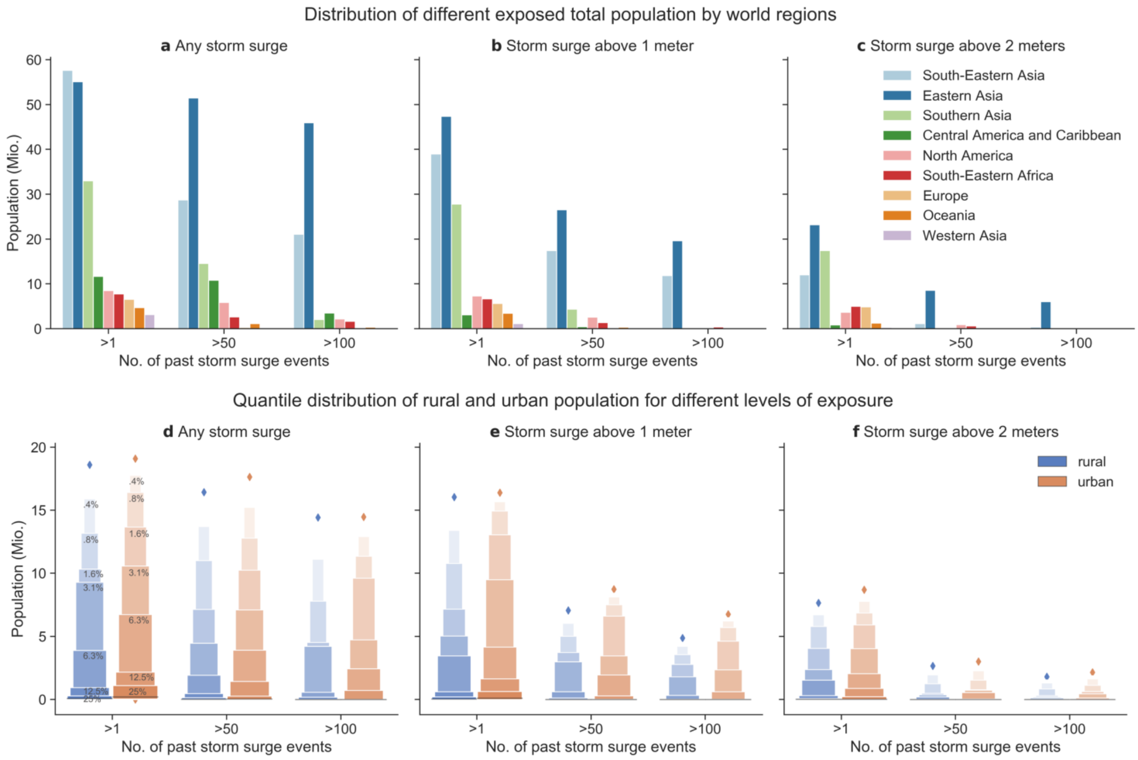

Figure 2.5: Storm surge exposed population, 2010

Notes: Panels a–c show the exposed total population in nine world regions. Panel a displays the number of people living in areas that experienced more than 1, 50, or 100 storm surge events above zero between 1950 and 2010. Panel b displays the number of people living in areas that experienced more than 1, 50, or 100 storm surge events above 1 m between 1950 and 2010. Panel c displays the number of people living in areas that experienced more than 1, 50, or 100 storm surge events above 2 m between 1950 and 2010. Panels d–f show the quantile distribution (letter values) of exposed rural and urban populations per country in 2010 for different levels of exposure. The plotted boxes are the successive letter values, which range from the fourths (25%) (bottom box) up to the 256th (0.4%) (highest box). In total, there are seven letter values plotted. As an example, in the left column of Panel d the respective letter values are labeled. The diamonds represent the corresponding most extreme country observations.

boxes refer to different quantiles (letter values) of the distribution.[53] These are the fourth (25%), the eights (12.5%), the 16th (6.25%), the 32nd (3.13%), the 64th (1.6%), the 128th (0.8%), and the 256th (0.4%) quantiles. The bottom box of each distribution refers to the fourth quantile, i.e., 25% of all country observations fall in that box, and the top most box refers to the 256th quantile, i.e., 0.4% of all country observations fall in the box range. The diamond illustrates the most extreme country observation. Accordingly, while comparing rural and urban population country distributions at risk, the figure demonstrates that urban populations live at higher risk, but at the same time, with higher exposure there are fewer differences. The most extreme observation (diamond) refers in all cases to rural or urban population at risk living in China.

With our new storm surge data, we were able to show how many people are still living in exposed areas in 2010. In Figures 2.4 and 2.5, we have seen that there exists a negative correlation between the level of exposure and number of people. In the next section, we introduce our method for systematically identifying this result.

2.3 Method and Empirical Identification

To analyze the influence of past storm surge damage on coastal population, we pursue a multivariate grid-cell-level-fixed-effects panel data regression approach. We restrict our sample to LECZ that lie within countries that have been exposed to at least one tropical cyclone.[54] The level of analysis are the 49,115 exposed coastal zones' grid cells at a resolution of 10 x 10 km, which we observe globally over seven decades. This leaves us with 343,805 panel observations over the 1950–2010 period. As our main specification we estimate the following model:

$$\begin{aligned} Population_{id} = \alpha + \beta Storm\ surge\ damage_{id} + \gamma Wind\ damage_{id} + \delta Rainfall_{id} \\ + \theta_i + \mu_d + \nu_j * d + \varepsilon_{id}, \end{aligned} \tag{2.4}$$

where $Storm\ surge\ damage_{id}$, $Wind\ damage_{id}$, and $Rainfall_{id}$ are the means of decade d averaged over the yearly data from $d - 9$ to d in grid i. $Population_{id}$ is the total, rural, or urban population count of decade d in grid i. The grid-specific fixed effects θ_i capture effects

[53] Letter values are order statistics that help to better illustrate and understand the tails of a distribution (Hofmann et al., 2017). We use the `boxenplot`-command in Python Seaborn to generate the plot.

[54] Appendix Tables 2.40 and 2.41 relax this restriction by including all exposed coastal zones within a radius of 50 and 100 km, respectively.

that do not change over time, such as culture, geography, or institutional background. To control for events common to all grids within a specific decade, we include decade fixed effects μ_d. We also include country j-specific linear time trends ($\nu_j * d$) that account for changing patterns over time for the individual countries, such as changes in the population growth rate, improvements in coastal protection, resulting in less vulnerability, or changes in climate patterns.[55] Standard errors are clustered by affected grid × decade × country.[56] Affected grid is defined as either having a positive value for $\textit{Storm surge damage}_{id}$, $\textit{Wind damage}_{id}$, or $Rainfall_{id}$.

The occurrence and intensity of tropical cyclones are arguably random by nature, as complex processes, such as storm surges, are hard to predict. In fact, even 24 hours before a potential land fall, the error margin of the intensity and location of the respective storm is still high (NHC, 2016). Consequently, one can argue that the estimated coefficient β on storm surge captures the causal impact of storm surge on population count after accounting for grid-cell-level fixed effects. More precisely, it is likely that individuals will make location decisions in part with respect to their expectations of factors, such as storm surge, i.e., with regard to their expected local distribution of such events. Assuming a stable distribution over the sample period, the location-specific fixed effects θ_i will control for these expectation-based decisions. Thus, the remaining variation in $\textit{Storm surge damage}_{id}$, after controlling for $\textit{Wind damage}_{id}$ and $Rainfall_{id}$, consists of only random realizations from the local distribution. One remaining confounding factor that might render estimates on $\textit{Storm surge damage}_{id}$ non-causal could be that other climatic factors, such as temperature, might be correlated with storm surge and affect local population (Auffhammer et al., 2013; Hsiang, 2016). We account for this potential influence by including data on temperature in a robustness test (see Appendix Table 2.31). Another remaining possible violation of the identifying assumption could be that the distribution of local storm surge is time varying rather than time invariant, and that local populations are aware of this and adjust their expectation regarding the local distribution of storm surge accordingly. However, arguably this is unlikely to be a realistic concern, as any sort of tropical storm signal is only likely to emerge with climate change over the very long run (Emanuel, 2011). To further argue for a causal identification of our

[55] In Appendix Table 2.33 we also include nonlinear time trends.

[56] We also test for other cluster choices: country, ADM1, region, and affected grid × decade. Appendix Tables 2.35–2.38 show the results.

model, we conduct a Fisher randomization test, where we randomly reshuffle storm surge observations between decades (see Appendix Figure 2.30).

To analyze possible heterogeneities by decade, we introduce an interaction term to Equation 2.4, where we interact each tropical cyclone damage variable with a decadal indicator variable ($\sum_{k=1960,1970,...}^{2010} \rho_k * Decade_k$). The model then transforms to:

$$\begin{aligned} Population_{id} = \alpha + \beta Storm\ surge\ damage_{id} + \left(\sum_{k=1960,1970,...}^{2010} \rho_k Decade_k \times Storm\ surge\ damage_{id} \right) \\ + \gamma Wind\ damage_{id} + \left(\sum_{k=1960,1970,...}^{2010} \lambda_k Decade_k \times Wind\ damage_{id} \right) \\ + \delta Rainfall_{id} + \left(\sum_{k=1960,1970,...}^{2010} \xi_k Decade_k \times Rainfall_{id} \right) + \theta_i + \mu_d + \nu_j * d + \varepsilon_{id}, \quad (2.5) \end{aligned}$$

where all variables are defined as in Equation 2.4. From this estimation, we calculate the average effects of *Storm surge damage* per decade, i.e., the results of the F-tests $\beta + \rho_{1960}$, $\beta + \rho_{1970}$, $\beta + \rho_{1980}$, $\beta + \rho_{1990}$, $\beta + \rho_{2000}$, and $\beta + \rho_{2010}$. The base decade for all regressions is 1950.

To further explore heterogeneous treatment effects, we run modifications of Model 2.4, where we include interactions with agricultural crop suitability and income. For data on crop suitability, we take the Overall Crop Suitability (1961-1990) data assembled in the GLUES project at a resolution of 1 km (Zabel et al., 2014). We spatially join the satellite data with our data set and form four different bins according to the data's 0.25, 0.5, and 0.75 percentile cutoffs. The bins refer to low (0–3), middle (3–22), high (22–48), and highest agricultural suitability (>48). The base category is zero suitability. Data on income classes correspond to World Bank country income classifications, available from 1987–2019.[57] For the period 1990–2010 we employ the mode of the four different income classes (low, lower middle, upper middle, high income) per country and decade. For the decades 1950–1980 or other missing entries, we use the last available income class entry for each country. The base category refers to high income countries. Appendix Tables 2.42–2.51 show summary statistics for all variables used, both globally and differentiated by nine world regions.

[57]The data are available at http://databank.worldbank.org/data/download/site-content/OGHIST.xls (accessed 25 October 2020).

2.4 Results

By using decadal panel data from 1950–2010 at a resolution of 10 km x 10 km for LECZ in 77 storm surge-exposed countries, we analyze the effect of storm surge damage on local total, rural, and urban population counts by means of a multivariate fixed-effects panel regression model. Table 2.1 shows the results for the global sample from 1950–2010. As already indicated

Table 2.1: The average effect of storm surge damage – All exposed countries

	Total population count	Rural population count	Urban population count
	(1)	(2)	(3)
Storm surge damage	-7,765	-2,155	-9,590
	(3,254.40)	(1,328.91)	(3,838.30)
	[0.02]	[0.11]	[0.01]
Wind damage	-10,324	-484	-10,122
	(7,432.14)	(2,406.80)	(6,649.50)
	[0.17]	[0.84]	[0.13]
Rainfall	-19	-.69	-15
	(16.38)	(8.07)	(11.85)
	[0.25]	[0.93]	[0.21]
Observations	343,805	343,805	343,805
Clusters	785	785	785
Mean dependent variable	10,973	5,641	7,206
SD storm surge damage	0.1128	0.1128	0.1128

Notes: Panel ordinary least squares regression results with clustered standard errors by affected grid × decade × country in parentheses (), and p-values in brackets []. The coefficients show the marginal effect of the different tropical cyclone damage types on the total, urban and rural population counts. The sample covers the decades from 1950 through 2010 for all low elevation coastal zones in exposed countries. *Storm surge damage* is the mean storm surge damage function of decade d averaged over the yearly data from d-9 to d in grid cell i, *Wind damage* is the mean decadal wind damage function of decade d averaged over the yearly data from d-9 to d in grid cell i, and *Rainfall* is the mean decadal tropical cyclones' rainfall (in mm) of decade d averaged over the yearly data from d-9 to d in grid cell i. All regressions include decade and grid fixed effects as well as country-specific linear trends.

by the descriptive Figures 2.4 and 2.5, we find a negative effect of storm surge damage on the total population count (Column 1). While storm surge damage also has a negative influence on the urban population count (Column 3), wind damage and rainfall never have a significant influence on any population type. This result underlines the importance to account for storm surges, when analyzing the damage of tropical cyclones. Panel a of Figure 2.6 displays the storm surge damage coefficients of Columns 1–3, interpreted by a one standard deviation increase. If storm surge damage increases by a standard deviation (0.1128), there is a decrease of 876±721 people living in an exposed grid. Compared to the average population living in an exposed grid (10,973), this constitutes a reduction of 8% per decade. This average effect on the total population count seems to be driven by people who inhabit exposed urban areas (-1,081±850), while for rural populations the effect amounts to a reduction of -243±294.

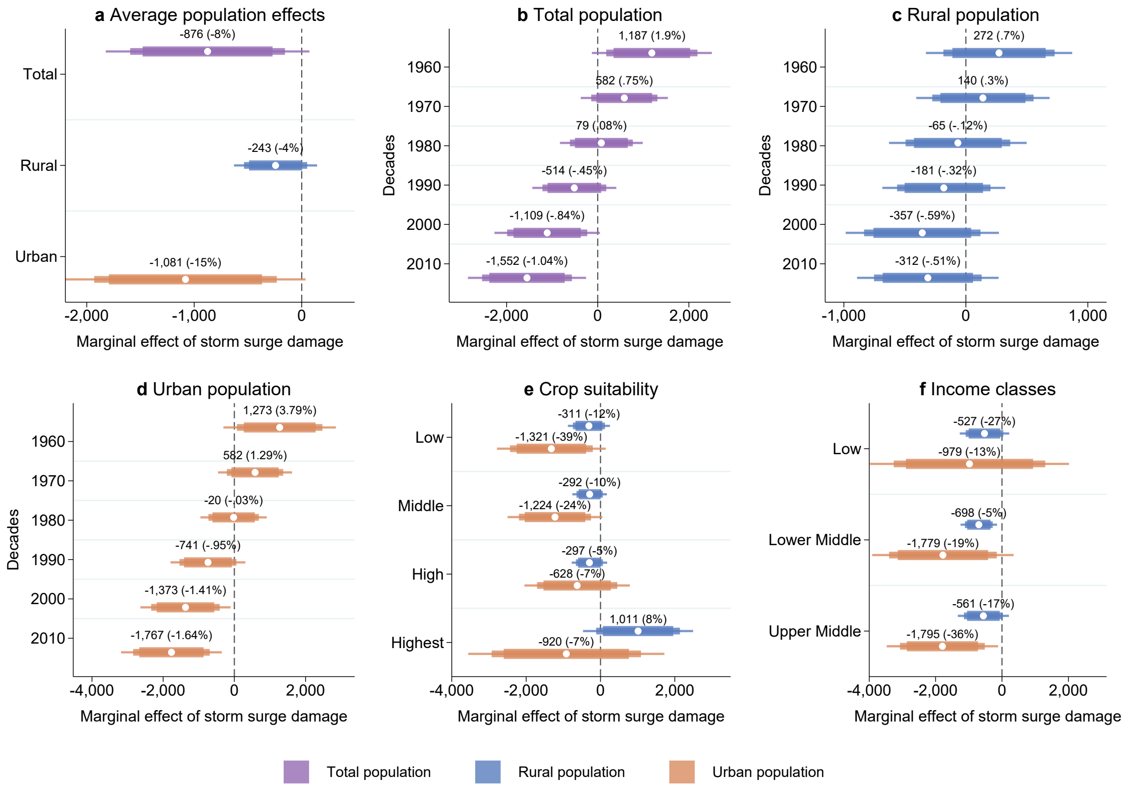

Figure 2.6: Effects of storm surge damage on the global total, rural, or urban population count, 1950–2010

Notes: Panel a displays the average effect for all exposed countries. The numbers represent the mean estimator with the relative effect in comparison to the sample average in parentheses. Panels b–d show the average effects of a standard deviation increase in storm surge damage per decade for the total (b), rural (c), and urban (d) population counts compared to 1950. The numbers represent the mean estimator with the relative effect in comparison to the sample average per decade in parentheses. Panel e displays the marginal effect of storm surge damage on the rural (blue) and urban (orange) population counts for different classes of crop suitability. The classes refer to the 0.25, 0.5, and 0.75 percentile cutoff points of the crop suitability data. They are 0–3 for low suitability, 3–22 for middle suitability, 22–48 for high suitability, and larger than 48 for highest suitability. The base category is zero crop suitability. The numbers represent the mean estimator with the relative effect in comparison to the sample average in parentheses. Panel f shows the marginal effects of storm surge damage on rural (blue) and urban (orange) population count for different World Bank income classes. The base category is the high income class. The numbers represent the mean estimator with the relative effect in comparison to the sample average in parentheses. In all panels the line widths characterize the 90%, 95%, and 99% confidence intervals. The standard deviation of a storm surge above zero is 0.1128.

Panels b–d depict the average effects per decade compared to 1950 for the total, rural, and urban population counts with the implied percentage impact relative to the decadal population mean given in parentheses.[58] While for the total population in 1960, more of the population (+1,187±1,001) lived in exposed areas after storm surge damage as a consequence of coastal flooding, for every subsequent decade, the coefficients become increasingly negative, and significantly so in 2000 (-1,109±879) and 2010 (-1,552±985). One could argue that the lower coefficients in recent decades are due to more people moving to the coast. However,

[58] The underlying estimations are in Appendix Tables 2.2–2.4.

when we compare these absolute coefficients with their respective decadal means (given in parentheses), we also observe a decrease in recent decades. One should note in this regard that this effect is net of the country-specific linear trends included in all specifications, which account for country-specific factors such as population growth.

A similar behavior can be observed for people living in urban areas (Panel d). For rural areas (Panel c) the qualitative pattern is analogous but with no decadal coefficient being statistically different from zero at the 95% confidence interval. This analysis implies that, while there was on average an overall net negative impact over time, adaptation has taken place in recent years. This adaptation effect is largely driven by urban populations, perhaps unsurprisingly since these tend to be more mobile and have access to more financial resources to move away from hazardous areas (McCaughey et al., 2018; Plane et al., 2005). In contrast, rural populations tend to be bound to local resources to a greater degree because of, for example, agricultural possibilities (Hauer et al., 2020). This behavior is underlined by Panel e, which plots the average effect of storm surge damage for different levels of local crop suitability.[59] For the highest levels of crop suitability (75th percentile), one discovers a positive effect only for rural populations, although strictly speaking we cannot make any causal inference from this result as crop suitability may be correlated with other factors that drive parameter heterogeneity.

Panel f displays the heterogeneous treatment effects for World Bank income classes.[60] It shows that rural and urban people in low income areas do not move away from areas hit by storm surges compared to people in high income countries, as indicated by their insignificant coefficients. For lower and upper middle income countries, we find significant negative coefficients. As before, the effect is more negative for urban compared to rural populations.

When looking at the effect of past storm surges on the total, rural, and urban populations for different world regions (Figure 2.7), one notices different responses by region.[61] For the majority of regions, the reaction of the population is negative as a result of a damaging storm surge, with the strongest negative effects seen in Central America and the Caribbean (-901±391) and South-Eastern Asia (-2,128±1,429). In relation to the average population living in LECZ, the effects in the two aforementioned world regions are also relatively high, with

[59]The underlying estimations can be found in Appendix Tables 2.5 and 2.6.
[60]Appendix Tables 2.7 and 2.8 display the respective estimations.
[61]The underlying estimations are shown in Appendix Tables 2.9–2.17.

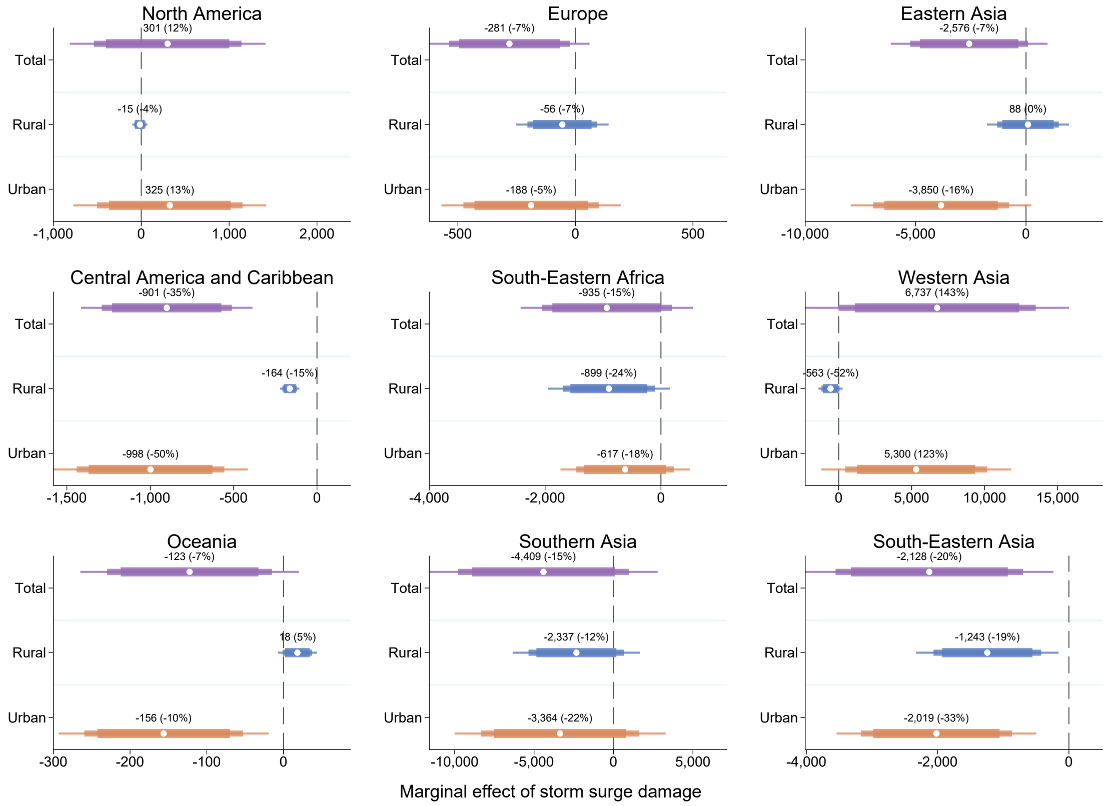

Figure 2.7: Effects of storm surge damage on the global total, rural, or urban population count for different world regions

Notes: The numbers and the white dot show the effect of a standard deviation increase (0.1128) in storm surge damage on total, rural, or urban population count. The number in parentheses displays the effect size relative to the respective population count sample average. The line widths characterize the 90%, 95%, and 99% confidence intervals.

reductions of 35% and 20%, respectively. For Eastern Asia, the effect for the total population is not significant, as already indicated by the high number of people living in exposure in Figure 2.5. There is no significant effect in North America, whereas one can identify a relatively strong, positive response on the total population in Western Asia (+6,737±6,737), and a moderate positive effect on the rural population in Oceania (+18±19). Again, for most regions, urban populations seem to be the driving force behind the reduction effect on the total population, with notable exceptions in South-Eastern Africa and South-Eastern Asia.

Figure 2.8 depicts the regional responses of the total population to storm surge damage per decade compared to 1950.[62] For most exposed world regions, we see a trend moving from positive to increasing negative coefficients in recent decades. However, this behavior cannot be detected for North America, Oceania, and Western Asia. In Eastern Asia, we can observe a decreasing pattern, although only the most recent decade is statistically significant at the

[62] Appendix Tables 2.18–2.26 show the corresponding estimation results.

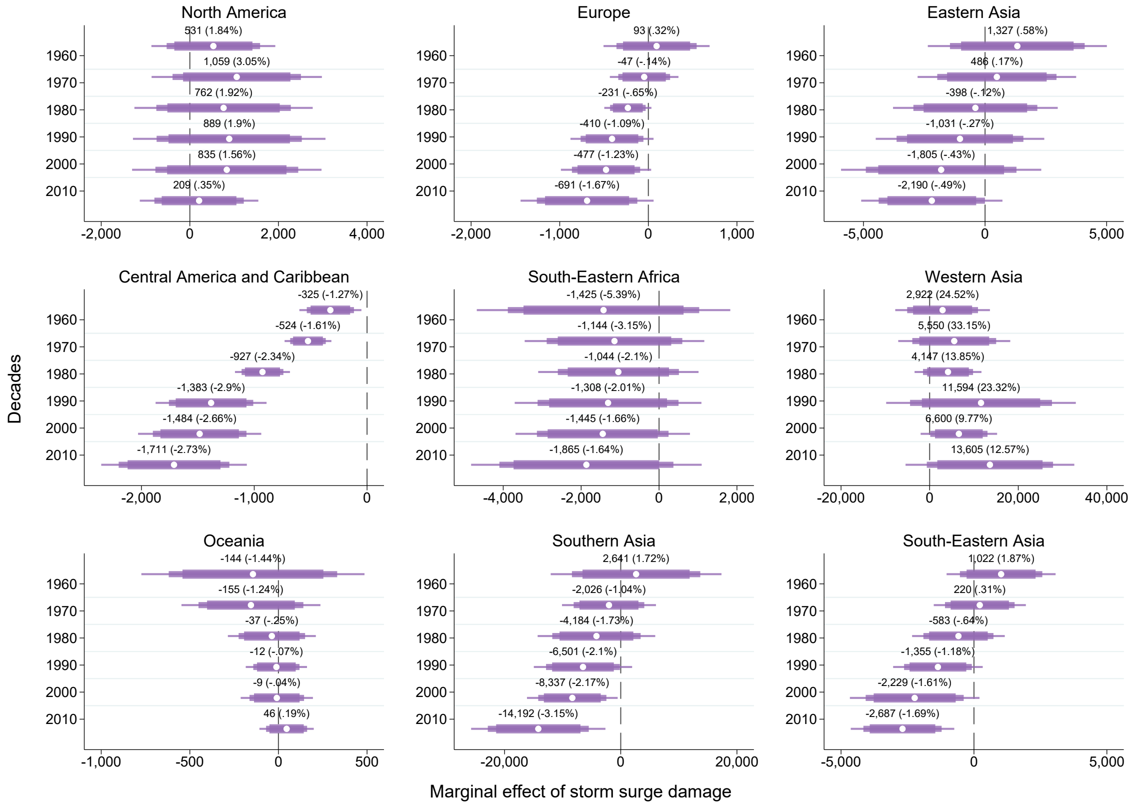

Figure 2.8: Effects of storm surge damage per decade on the total population count for different world regions

Notes: The figure shows the effect of a standard deviation increase in storm surge damage (0.1128) on the total population count per decade for nine different world regions. The plotted coefficients are the average effects per decade compared to 1950. The line widths characterize the 90%, 95%, and 99% confidence intervals.

95% confidence level. For Oceania, there is a small but increasing pattern over time, and the same is true for Western Asia. Again, the urban population effect per decade mimics the effect of storm surge damage on the total population (see Appendix Figure 2.27). However, this is not true for rural populations (see Appendix Figure 2.26), where a decreasing pattern with negative responses can only be found for South-Eastern Africa, Southern, South-Eastern, and Western Asia. When one examines the decadal effect over the period 1860–2010 for Central America and the Caribbean and North America (see Appendix Figures 2.28 and 2.29), one detects that, for Central American and the Caribbean, the decreasing pattern had already started in the 1870s. By contrast, for North America, the longer series looks rather like a positive trend.

To test the sensitivity of the main statistical analysis (Panel a of Figure 2.6), we check for different sub-samples, clustering, and model specifications in Appendix 2.6.3. We experiment with excluding potential outliers larger than Cook's distance of $4/n$ (Appendix Table 2.27).

Since the population data might be inflated by smaller numbers, we calculate sub-samples, where we exclude unpopulated areas, areas below 10 inhabitants, and areas below 100 inhabitants (Appendix Tables 2.28–2.30). As warmer temperatures are associated with tropical cyclones, we include temperature as an additional control variable in a further test (Appendix Table 2.31). Since there is evidence that climate might have a nonlinear impact (Burke et al., 2015), we also experiment with squared climate controls in another robustness test (Appendix Table 2.32). In a similar vein, we also include squared country-specific time trends (Appendix Table 2.33). As there was an improvement in the measurement of tropical cyclones with the start of satellite measurement in 1979, we also run a sub-sample with a restricted time period of 1980–2010 (Appendix Table 2.34). Additionally, we conduct different clustering choices of the standard errors: country, ADM1, region, and affected grid × decade (Appendix Table 2.35–2.38). In all conducted robustness tests, the p-value of the storm surge damage coefficient for total population count remains below 0.05. Notable exceptions are the robustness tests with regional clustering (Appendix Table 2.37) and with the reduced sample period (Appendix Table 2.34), where the p-values are larger than 0.05 but still below the 0.1 threshold.[63]

Furthermore, we run a Fisher randomization test, where we randomly redistribute storm surge events between decades for 1,000 repetitions (Appendix Figure 2.30). The test yields that 98.1% of the t-statistics of the randomly allocated storm surge events are larger than the t-statistic of our model (-2.39). Hence, we can be relatively confident that our results are not random, but due to a systematic pattern. What is more, we conduct a Placebo test in Appendix Table 2.39 where we restrict the sample to non-LECZ areas. As expected, we find no significant effect for the storm surge damage variable. In a similar manner, we run two analyses where we include all coastal areas irrespective of the altitude in a radius of 50 km (Appendix Table 2.40) and 100 km (Appendix Table 2.41). With the exception of a significant negative effect on urban populations for the 50 km sample, we find no significant effect of storm surge damage on total, rural, and urban populations in both samples.

[63]The coefficient estimates for the urban population count are a little bit less robust with only 8 out of 12 conducted robustness tests yielding a p-value below 0.1. As the coefficient for the rural population count in Table 2.1 is only slightly insignificant, it is not surprising that only 5 out of 12 robustness tests show a p-value less than 0.1.

2.5 Conclusion

This is the first study to have employed historical tropical storm data, population exposure, and a global storm surge model to investigate what role exposure to storm surge has played in the distribution of populations along the world's coasts. There have been considerable differences in exposure to storm surge damage across the globe, with regions like Eastern Asia, North America, and South-Eastern Africa being most affected. When it comes to population exposure, we find that three quarters of all people at risk live in Eastern, South-Eastern and Southern Asia. This finding is in line with previous extreme value statistical studies (Hallegatte et al., 2013; Jongman et al., 2012; Neumann et al., 2015). Simultaneously, we observe that the share of people on the coast living in the potentially most dangerous areas, the LECZ, is decreasing in most regions. Nevertheless, compared to non-coastal areas, there are some regions, such as Oceania and South-Eastern Asia, where LECZ have witnessed a relative increase in population. Perhaps unsurprisingly, it is the urban rather than the rural population that has been most exposed to storm surge events (Neumann et al., 2015).

Our regression analysis allowed us to systematically link the trends observed in terms of storm surge events and coastal population counts. Overall, we find that greater storm surge exposure has globally led to a reduction of the population in the LECZ, where a one standard deviation storm surge event leads to an 8% reduction in the total population per exposed 10 x 10 km grid and decade. This finding contrasts many previous studies, which found evidence of no migration (Fischer & Malmberg, 2001; Kocornik-Mina et al., 2020), no permanent migration (Bohra-Mishra et al., 2014; Lu et al., 2016), or even net-positive migration (Boustan et al., 2012; de Sherbinin et al., 2012) in response to flooding. Our results appear to be primarily driven by people living in urban areas and may be due to the likelihood that they have more means than rural residents whose income depends on local natural resources (Hauer et al., 2020). In fact, we show that the impact of storm surges on population counts in rural areas depends on the crop suitability of the area. We also find that, in (currently) richer countries, the net reduction in population after storm surges is larger than in their poorer counterparts. This result may be because richer individuals are more mobile than poorer ones, a feature that has been, for instance, observed in the United States after hurricanes (Strobl, 2011). Poor populations are sometimes trapped by natural disasters, as they are more vulnerable and have fewer financial resources to move away (Black et al., 2013). This finding could also be explained by the cheaper housing costs inducing these people to move to more dangerous areas (McCaughey et al., 2018).

Our panel structure allows us to decompose the estimated effect over time. This decomposition suggests that overall there has been a slowly evolving structural change in the response of populations to storm surge events. More precisely, while in earlier decades these led to a net increase in population numbers, over time this response has reversed into a net fall. Possible reasons for the previous rise may be that the damage due to storm surges induced creative destruction (Cavallo & Noy, 2011), in that it induced new opportunities for growing industries such as manufacturing, tourism, and transportation (Barragán & de Andrés, 2015) and hence net population growth. The fall of exposed populations in recent decades after damaging storm surge events is encouraging, as it suggests that on average coastal populations adapt to this recurring threat and relocate. This finding is most likely not driven by increases in mortality due to storm surges since other studies find a fall in storm surge-related deaths in recent years (Bakkensen et al., 2018; Bouwer & Jonkman, 2018).

We notably find considerable differences across regions in terms of how storm surges affect population counts in LECZ. In particular, while most regions on average saw their populations in these areas reduced because of storm surges, Oceania's rural populations and Western Asia's urban populations responded positively, while there was no effect on North America's rural and urban populations. For the latter region, this may not be surprising, as it has been shown that much of the coastal population growth has been driven by productivity and quality of life gains (Rappaport & Sachs, 2003). Furthermore, for urban residents in Western Asia, it could be that they prefer living near the coast even though that often means living in an exposed area, given the milder coastal climate compared to dry hinterland (Mansour, 2019). As most areas in Oceania consist of small islands and people heavily depend on coastal and oceanic fishing, (rural) people hardly seem to have any other choice than living in LECZ (Hanich et al., 2018). However, as we have shown, people try to move to unexposed LECZ.

Overall, our findings suggest individuals show adaptive behavior, at least for some regions in modern times, in response to damaging storm surge events. If, as has been predicted, climate change is likely to lead to at least greater, if not more frequent, storm surge events after tropical cyclones (Knutson et al., 2020), then we should expect the share of population in exposed LECZ to decline. However, projected sea level rise (Kulp & Strauss, 2019) and future population growth, especially in Asia (Hallegatte et al., 2013), could very well offset or even outweigh our effect. Furthermore, it must be pointed out that, as of 2010, 32 million people were still living in median-exposed LECZ (more than 100 1-m historic events) and 6.4 million in highly-exposed (more than 100 2-m historic events) LECZ. Our results are a first step to better understand the responses of coastal populations to storm surge damage. Policy makers can use our results to further analyze them in cost-benefit analyses. In this regard, better disaggregated data on global insurance coverage, reconstruction aid, protection measures, or other flood adaptation policies, would be helpful to assess costs and benefits of staying in or resettle from a storm surge area.

Our analysis is limited by the fact that we do not incorporate the role of protection measures, which could be artificial, such as dykes, or natural, such as mangroves and coral reefs, in our storm surge modeling. Hence, we are likely to overestimate storm surge heights in high income countries (Ward et al., 2017), leading to potential attenuation bias. However, since we do not take sea level rise or human-induced land subsidence into account, we tend to underestimate the experienced storm surge threat (Wrathall et al., 2019). Additionally, a finer and more flexible grid (Bloemendaal et al., 2019; Muis et al., 2016), the consideration of river flows and deltas (Eilander et al., 2020), and more precise elevation data such as CostalDEM (Kulp & Strauss, 2019) could improve the precision of our storm surge model output.

Another limitation of our analysis is that we can only derive conclusions regarding the impacts of storm surge events in terms of local population counts. These changes may be due to inward migration, outward migration, births, and/or deaths. In terms of migration patterns, one should note that a number of studies have shown that there is likely to be net outward migration (Berlemann & Steinhardt, 2017; Boustan et al., 2020), although the actual underlying dynamics may be more complex. For instance, in the United States hurricanes have been shown to induce people to both move out of affected coastal areas and others to move into them, with the latter likely due to new employment opportunities caused by the destruction (Strobl, 2011). While there are likely to be some deaths as a response to natural disasters such as storm surges (Frankenberger et al., 2020), it appears their overall death rate has substantially declined over time (Bakkensen et al., 2018; Bouwer, 2018). Finally, with regard to births, the evidence is rather mixed: there are likely some short-term declines (Lin, 2010) but also possibly some increases in fertility, depending on the strength of the storm or the time horizon (Evans et al., 2010). More disaggregated data in terms of the drivers of the components of population counts would allow one to explore these facets further.

2.6 Appendices

2.6.1 Supplemental Figures

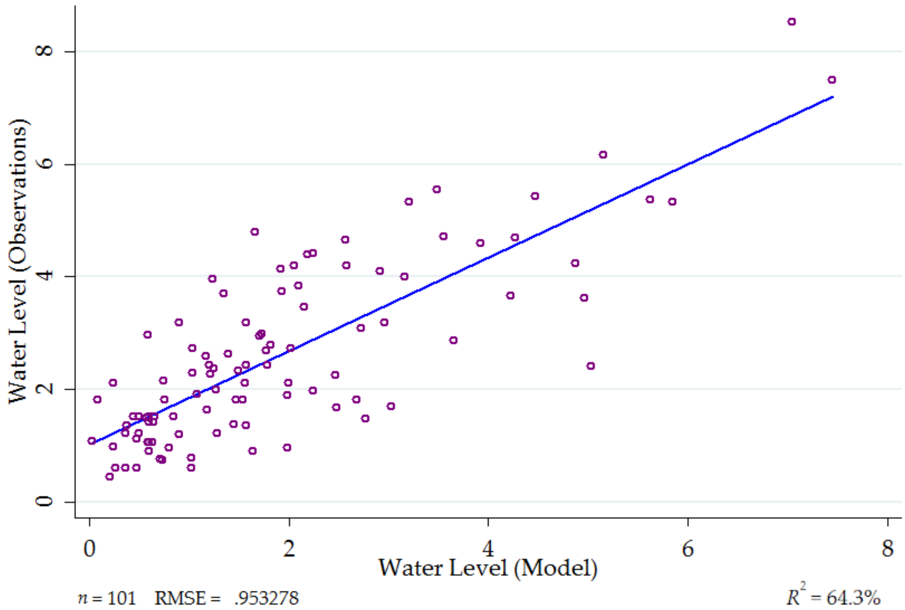

Figure 2.9: Observational data vs. storm surge model results

Notes: This figure compares the modeled storm surge heights against 101 historic observations of the SURGEDAT data set with a high level of confidence.

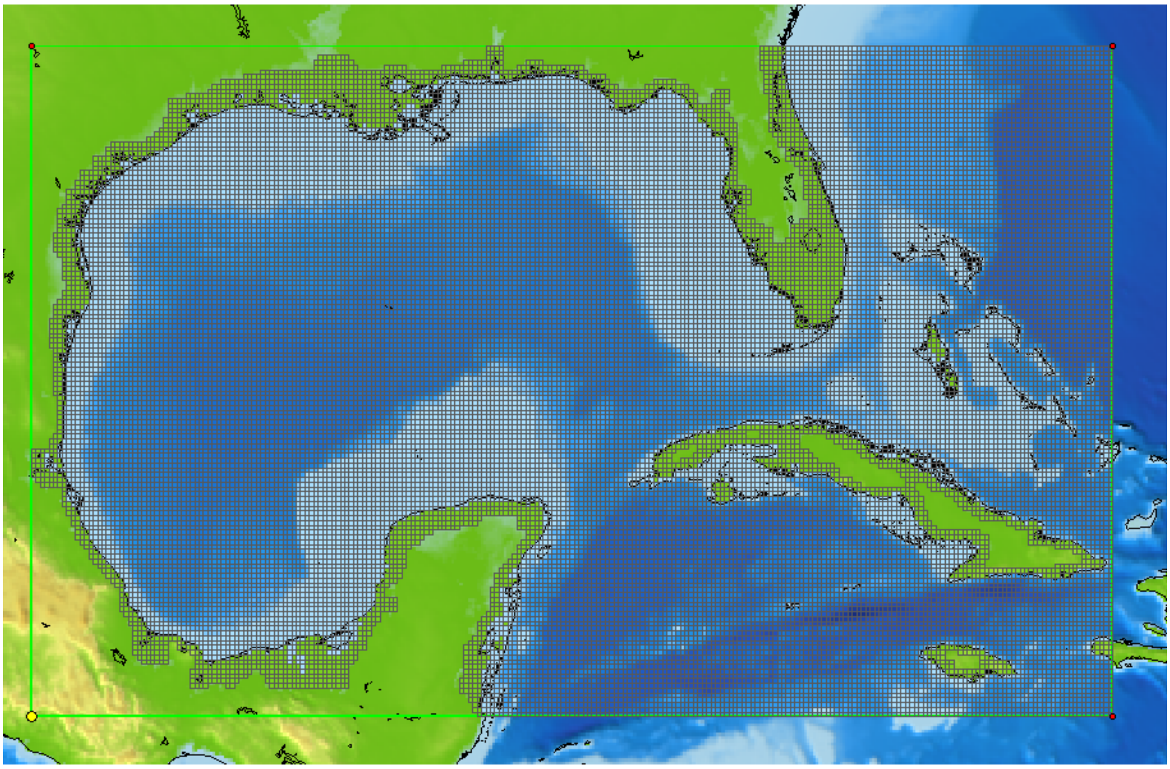

Figure 2.10: Grid example for the Gulf of Mexico

Notes: This figure shows an example of the 3D-grid used for the storm surge model in the Gulf of Mexico and surrounding LECZ.

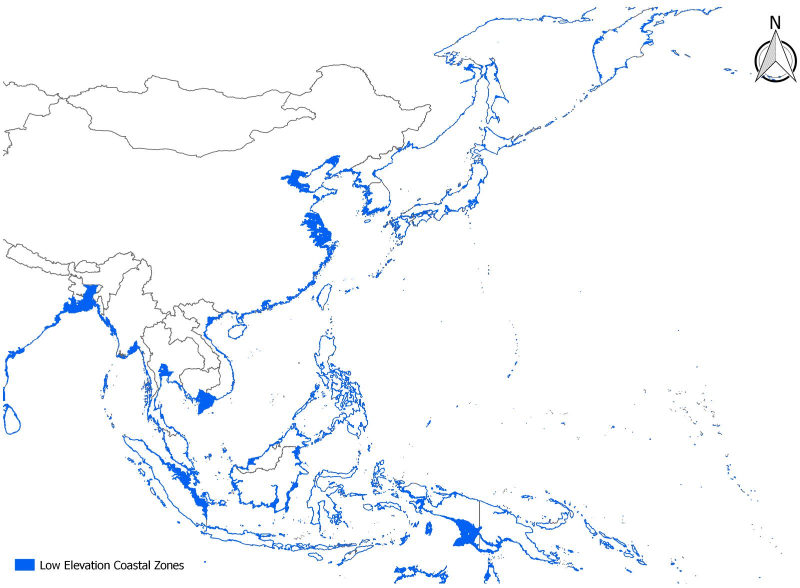

Figure 2.11: Identified low elevation coastal zones in Asia

Notes: This figure shows an example of the identified low elevation coastal zones (LECZ) in Asia.

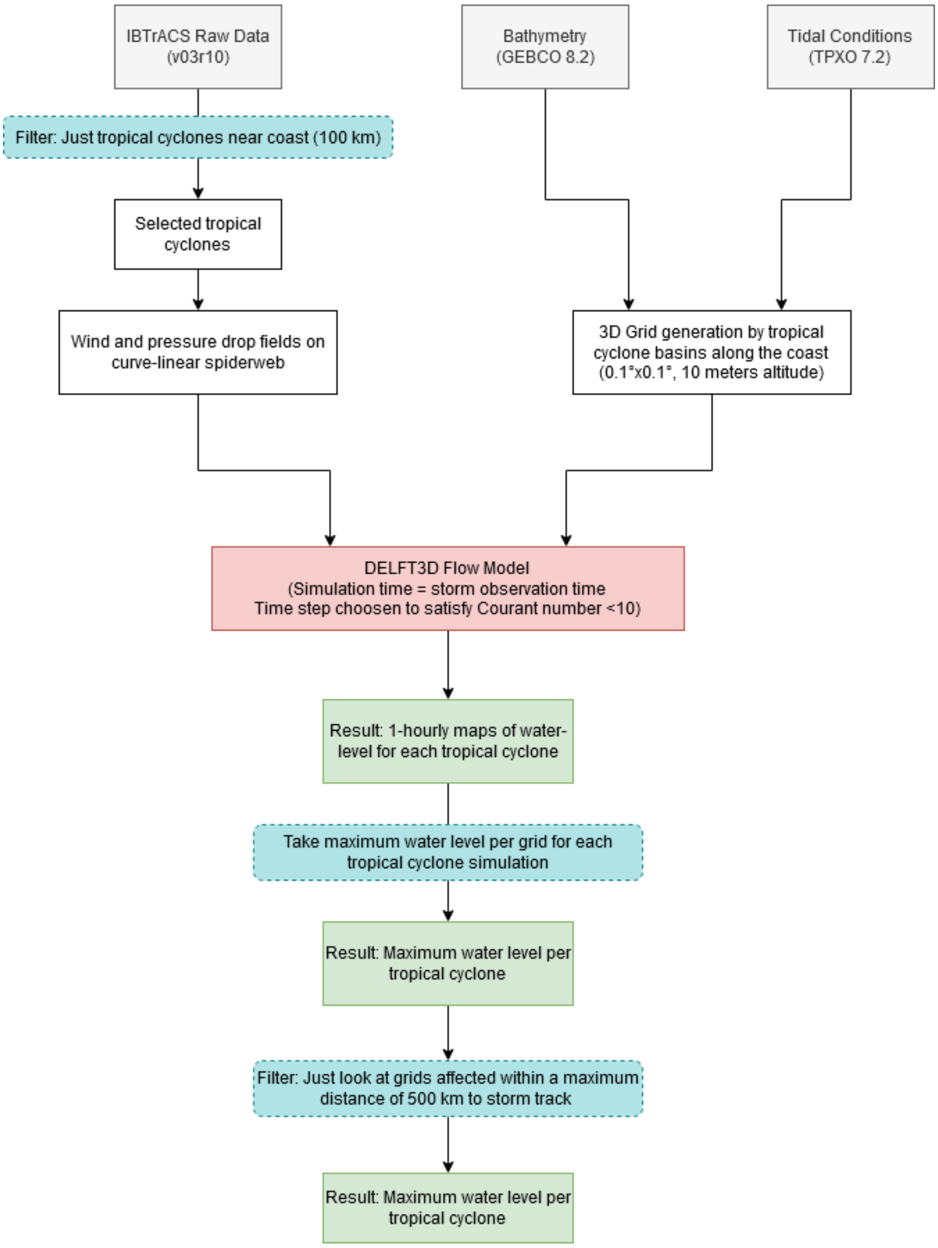

Figure 2.12: Schematic figure of the storm surge model steps with input data

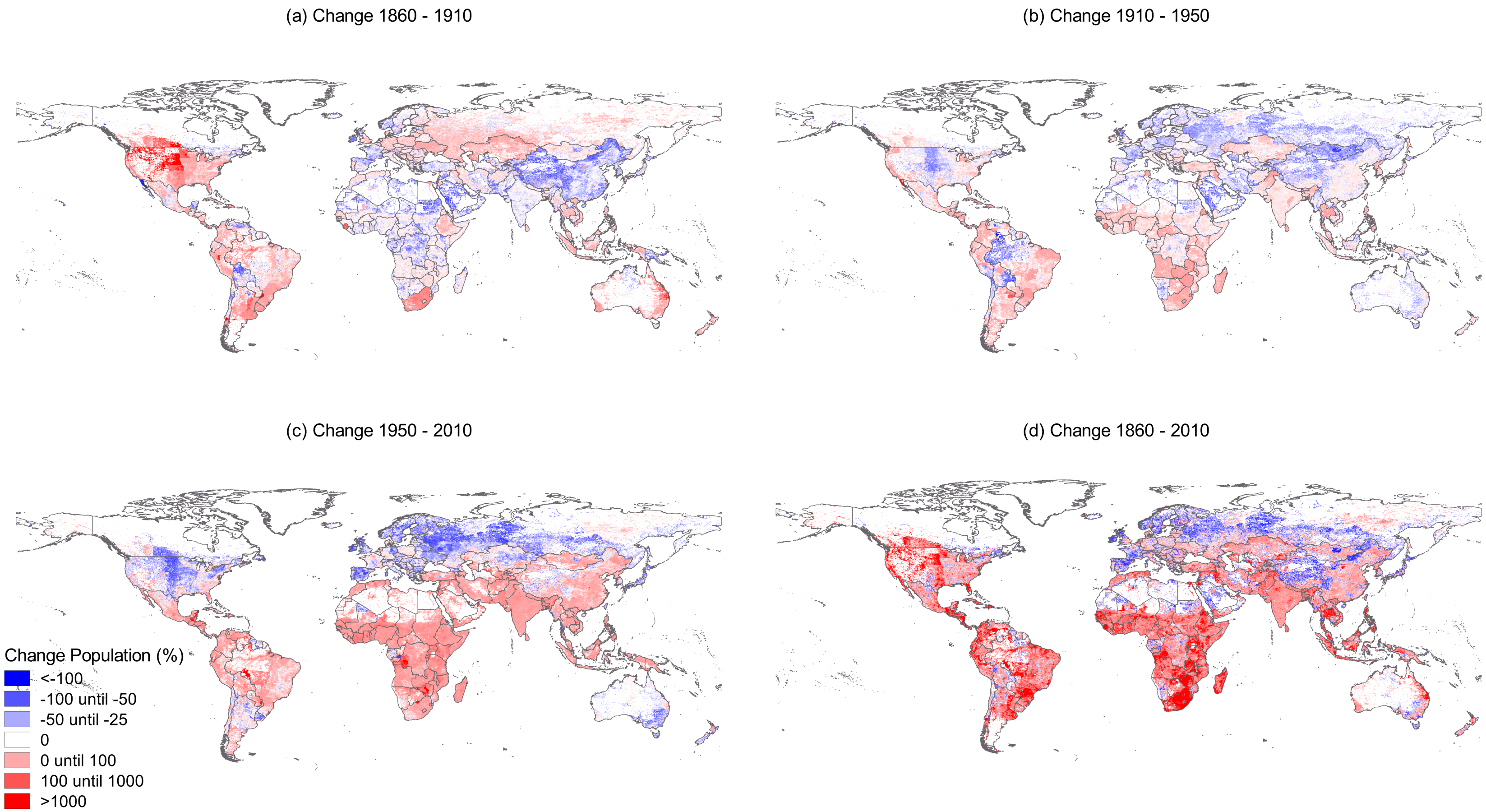

Figure 2.13: Percentage changes in total population count over different time periods

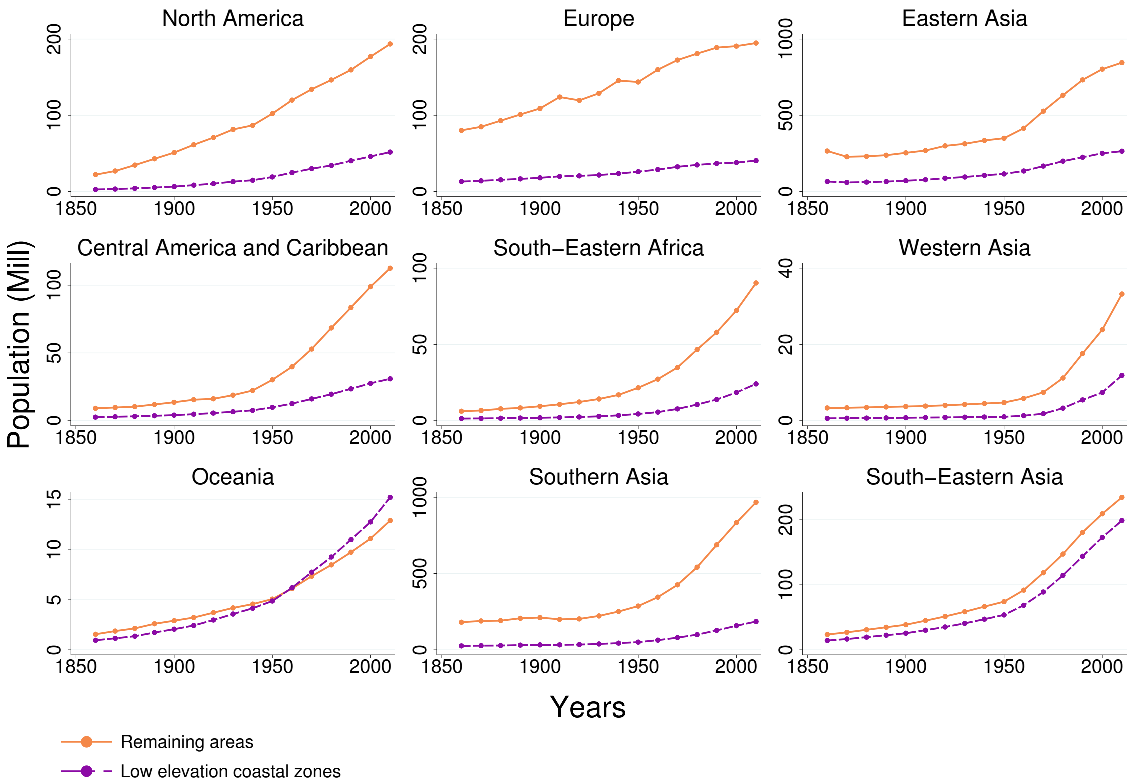

Figure 2.14: Population count for low elevation coastal zones and remaining areas, 1860–2010

Notes: The different world regions include countries that experienced at least one positive storm surge observation. Purple lines constitute population trends for low elevation coastal zones, whereas orange lines are population trends in remaining areas (non-low elevation coastal zones).

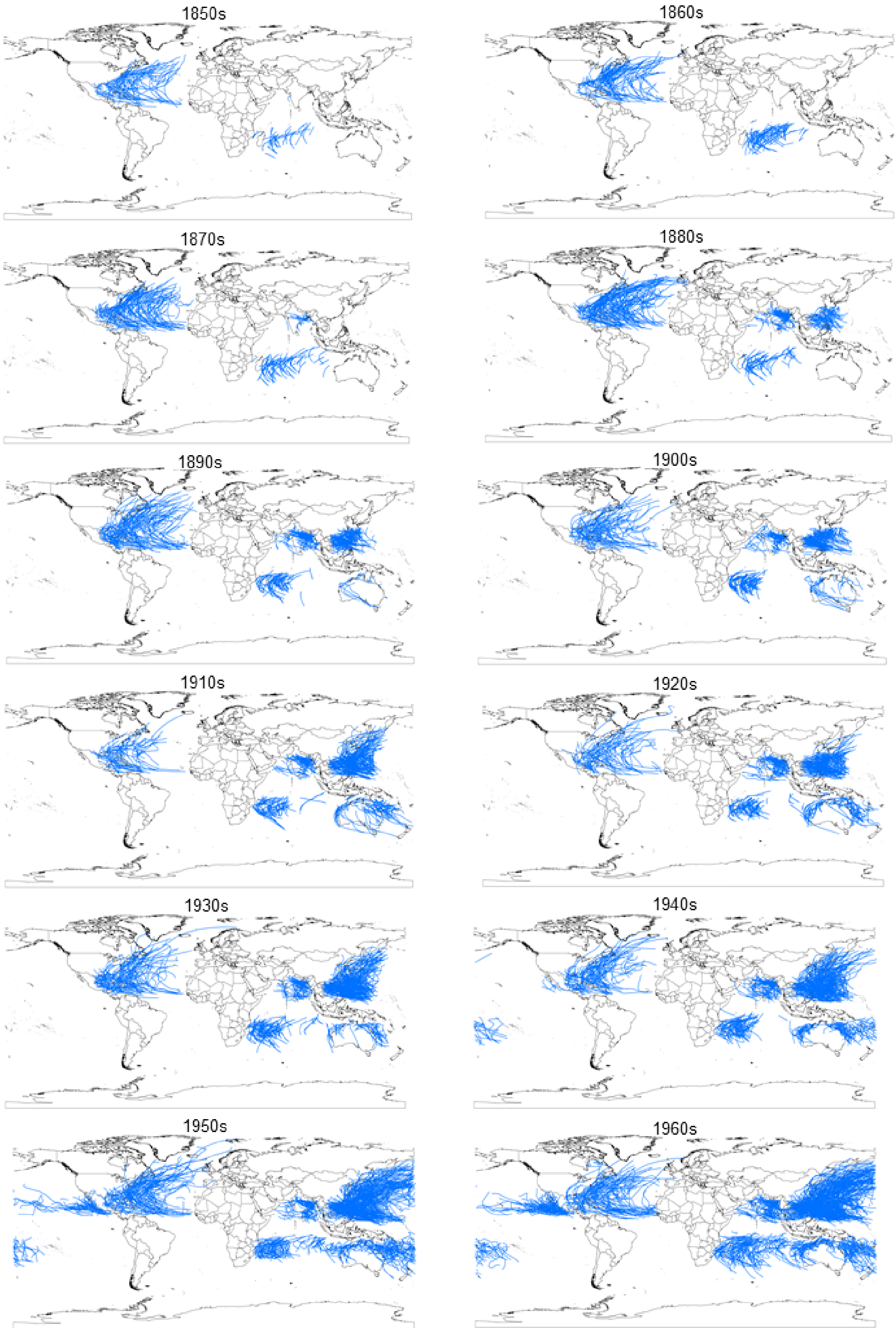

Figure 2.15: Worldwide occurrence of tropical cyclones per decade, 1850–1960

Notes: The blue lines are tropical cyclone raw data tracks.

Figure 2.16: Yearly mean storm surge damage, 1940–2010

Notes: The 77 exposed countries or areas are ordered by their mean exposure. Storm surge damage is a damage index ranging from 0 to 0.7.

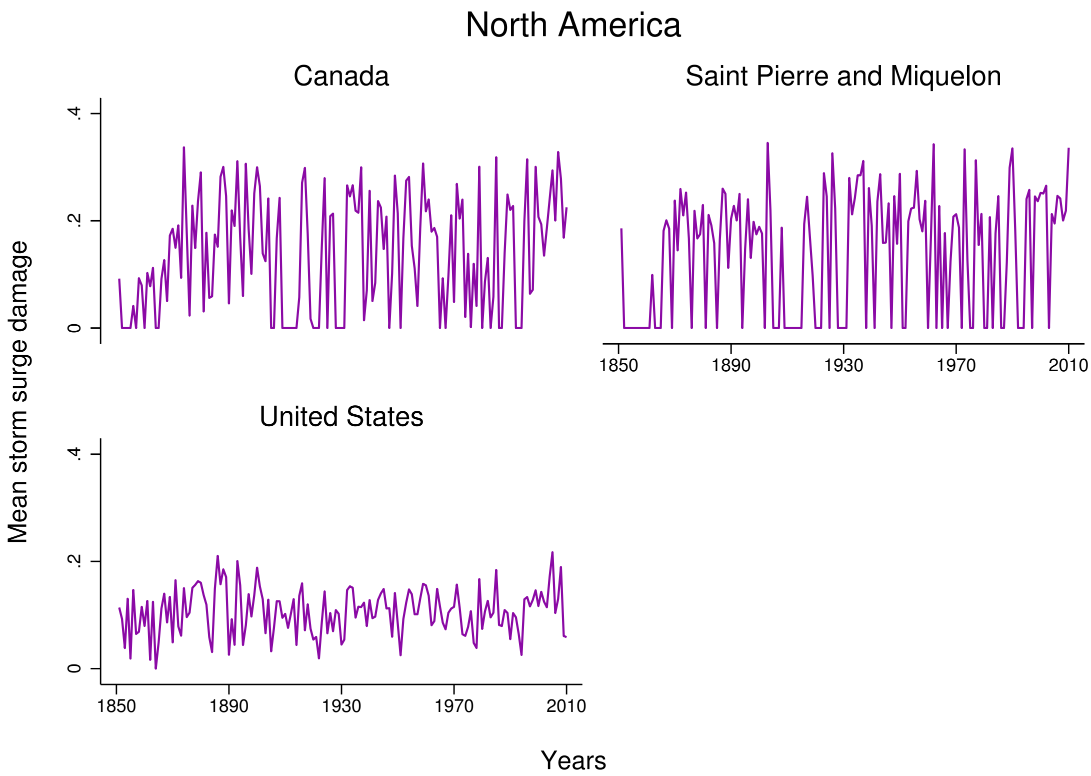

Figure 2.17: Yearly mean storm surge damage in North America, 1850–2010

Notes: This figure shows the yearly mean storm surge damage by country or area in North America. Storm surge damage is a damage index ranging from 0 to 0.7.

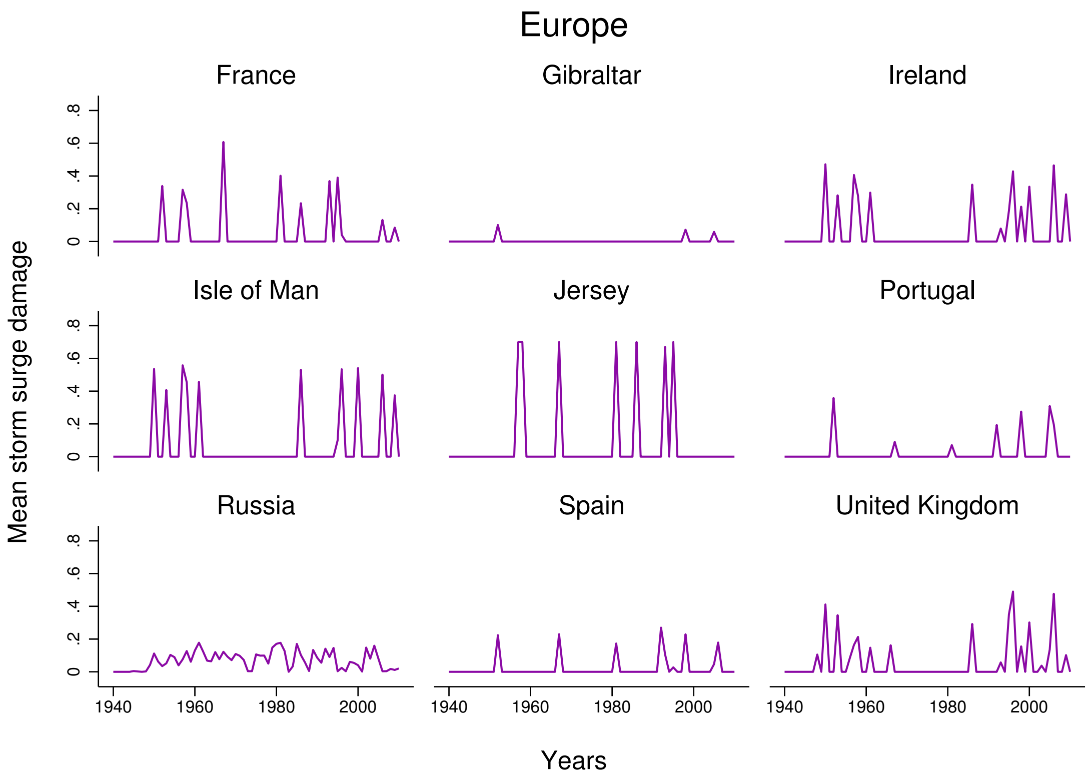

Figure 2.18: Yearly mean storm surge damage in Europe, 1940–2010

Notes: This figure shows the yearly mean storm surge damage by country or area in Europe. Storm surge damage is a damage index ranging from 0 to 0.7.

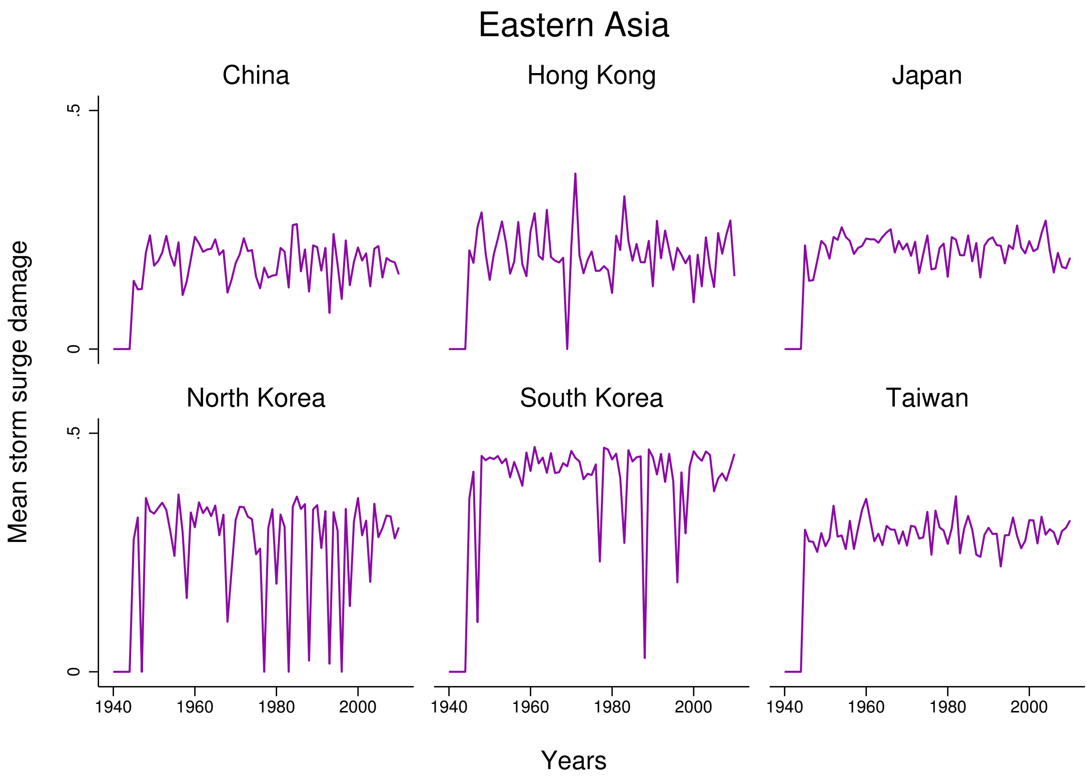

Figure 2.19: Yearly mean storm surge damage in Eastern Asia, 1940–2010

Notes: This figure shows the yearly mean storm surge damage by country or area in Eastern Asia. Storm surge damage is a damage index ranging from 0 to 0.7.

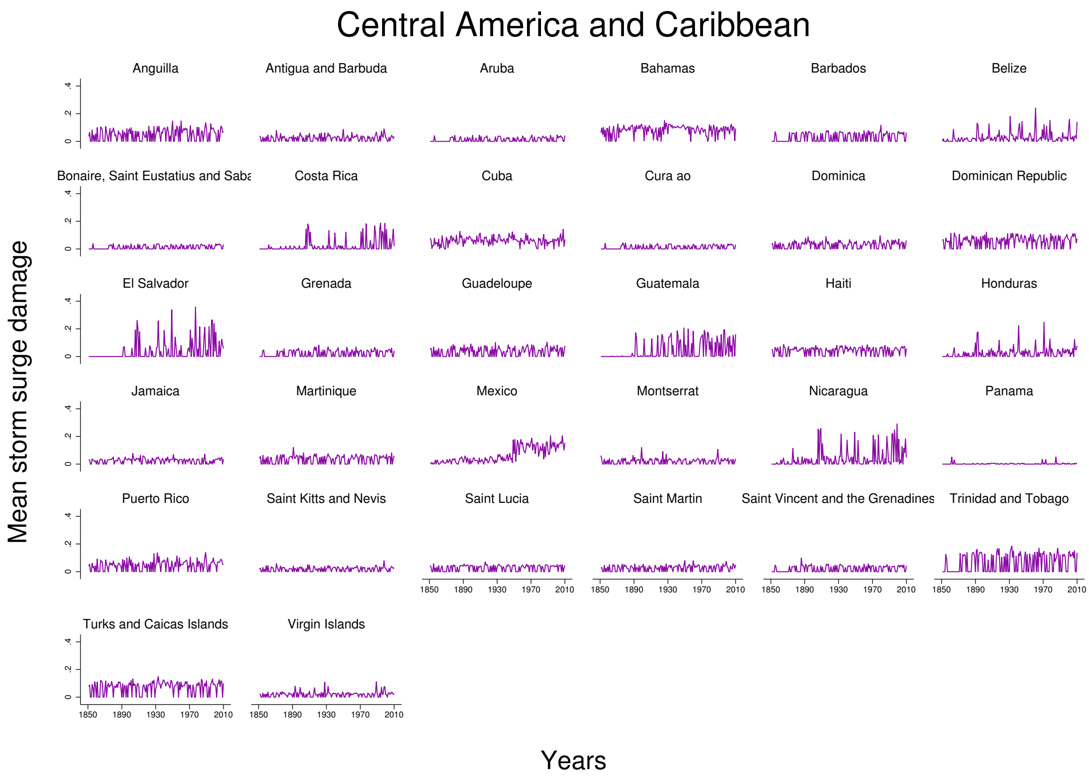

Figure 2.20: Yearly mean storm surge damage in Central America and Caribbean, 1850–2010

Notes: This figure shows the yearly mean storm surge damage by country or area in Central America and Caribbean. Storm surge damage is a damage index ranging from 0 to 0.7.

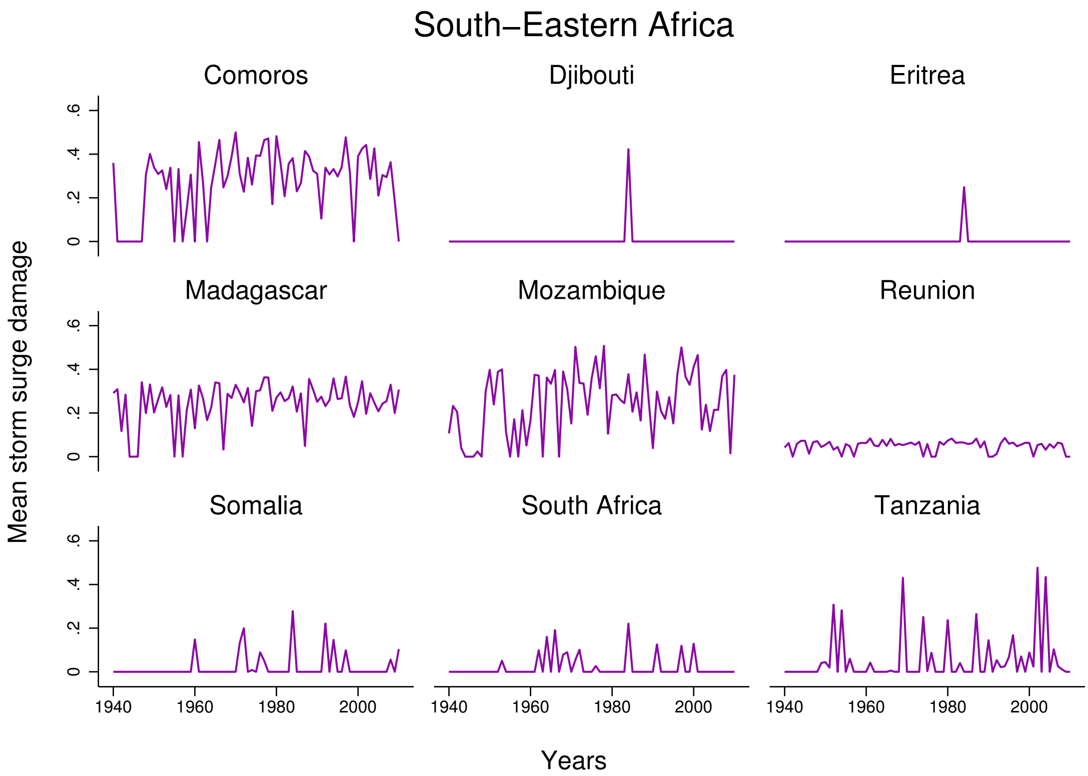

Figure 2.21: Yearly mean storm surge damage in South-Eastern Africa, 1940–2010

Notes: This figure shows the yearly mean storm surge damage by country or area in South-Eastern Africa. Storm surge damage is a damage index ranging from 0 to 0.7.

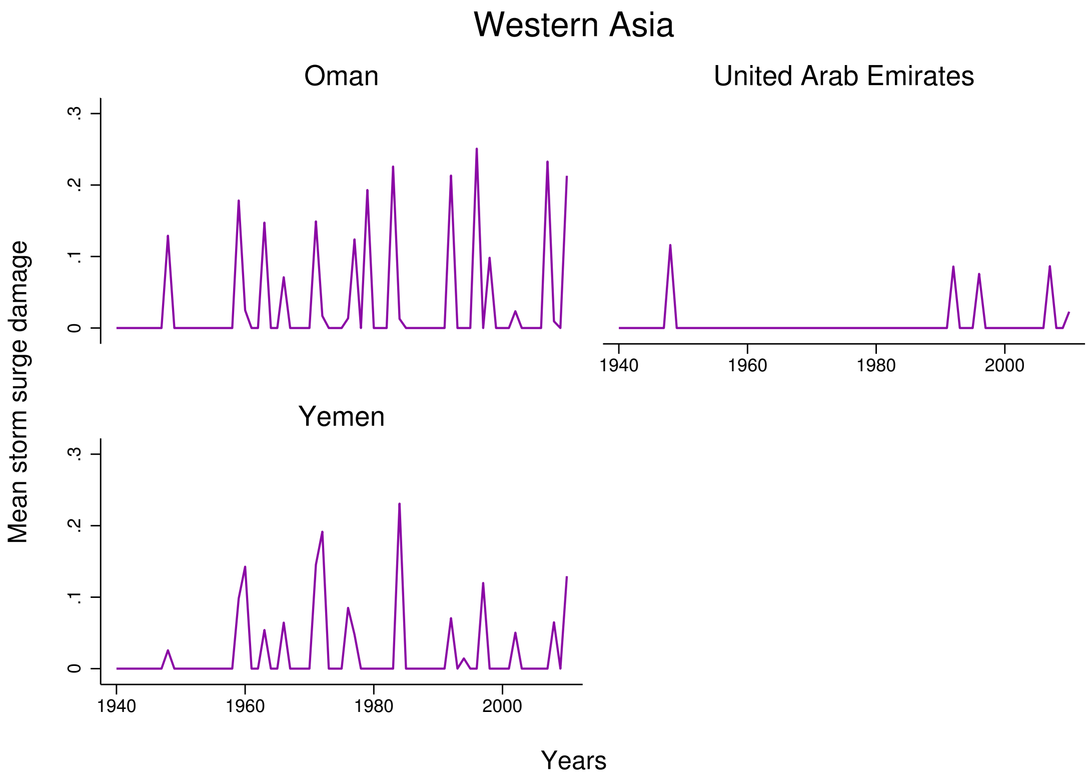

Figure 2.22: Yearly mean storm surge damage in Western Asia, 1940–2010

Notes: This figure shows the yearly mean storm surge damage by country or area in Western Asia. Storm surge damage is a damage index ranging from 0 to 0.7.

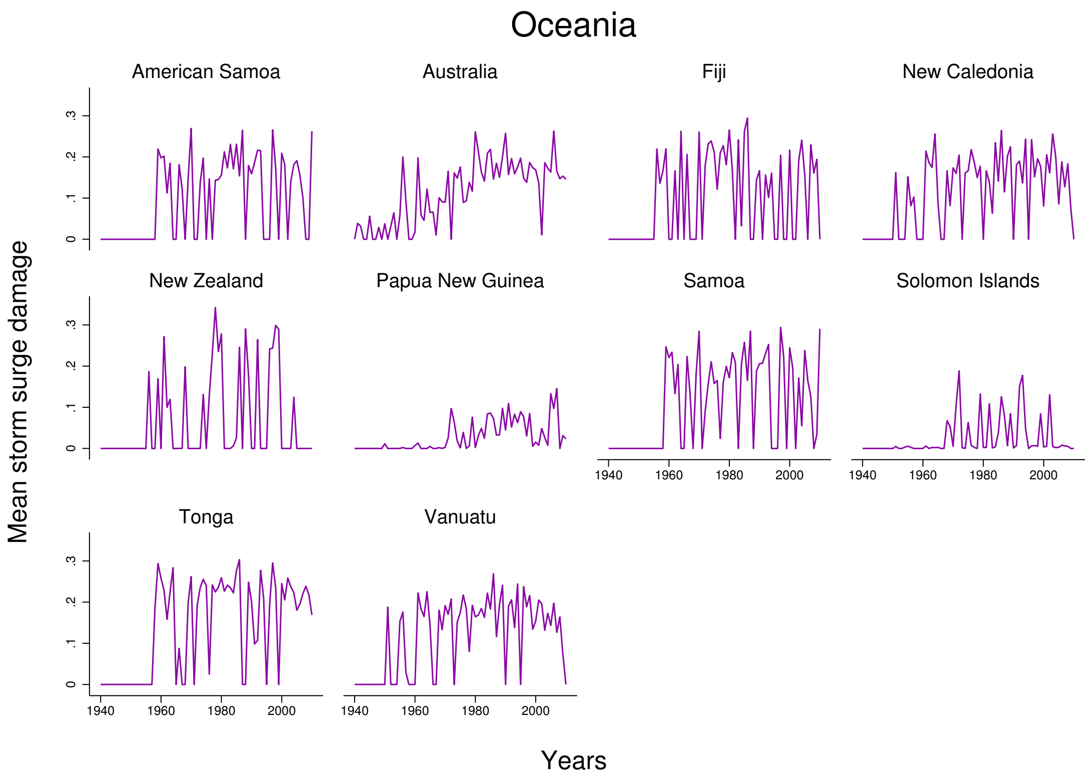

Figure 2.23: Yearly mean storm surge damage in Oceania, 1940–2010

Notes: This figure shows the yearly mean storm surge damage by country or area in Oceania. Storm surge damage is a damage index ranging from 0 to 0.7.

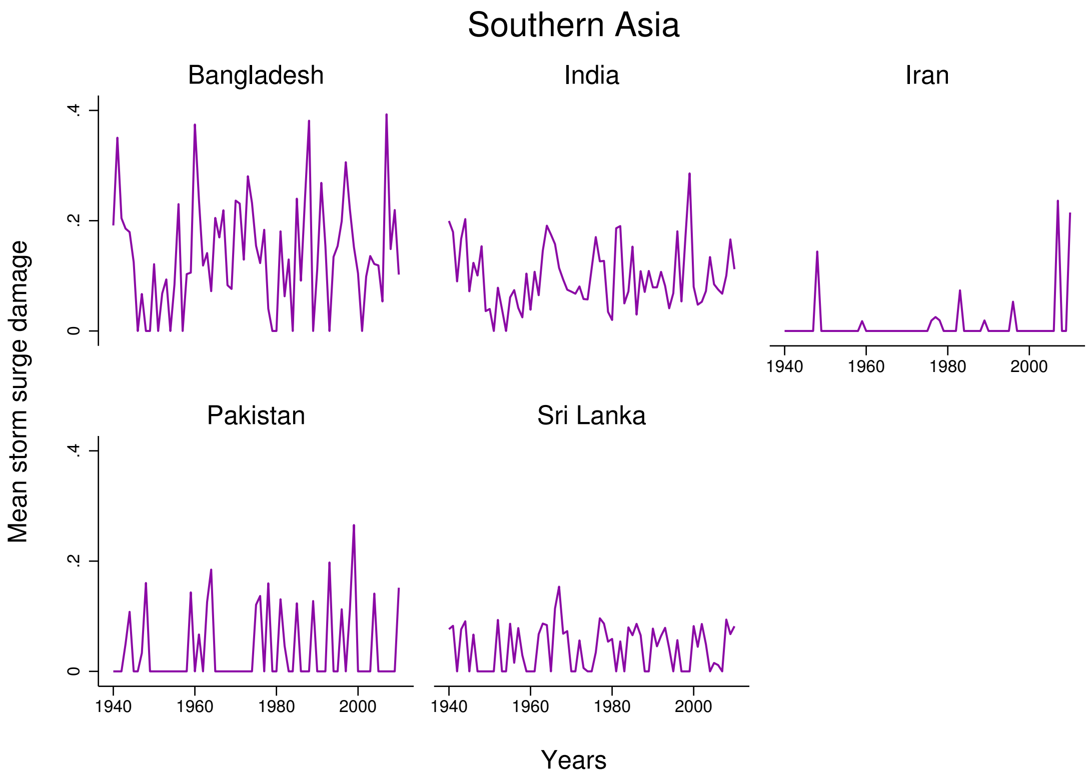

Figure 2.24: Yearly mean storm surge damage in Southern Asia, 1940–2010

Notes: This figure shows the yearly mean storm surge damage by country or area in Southern Asia. Storm surge damage is a damage index ranging from 0 to 0.7.

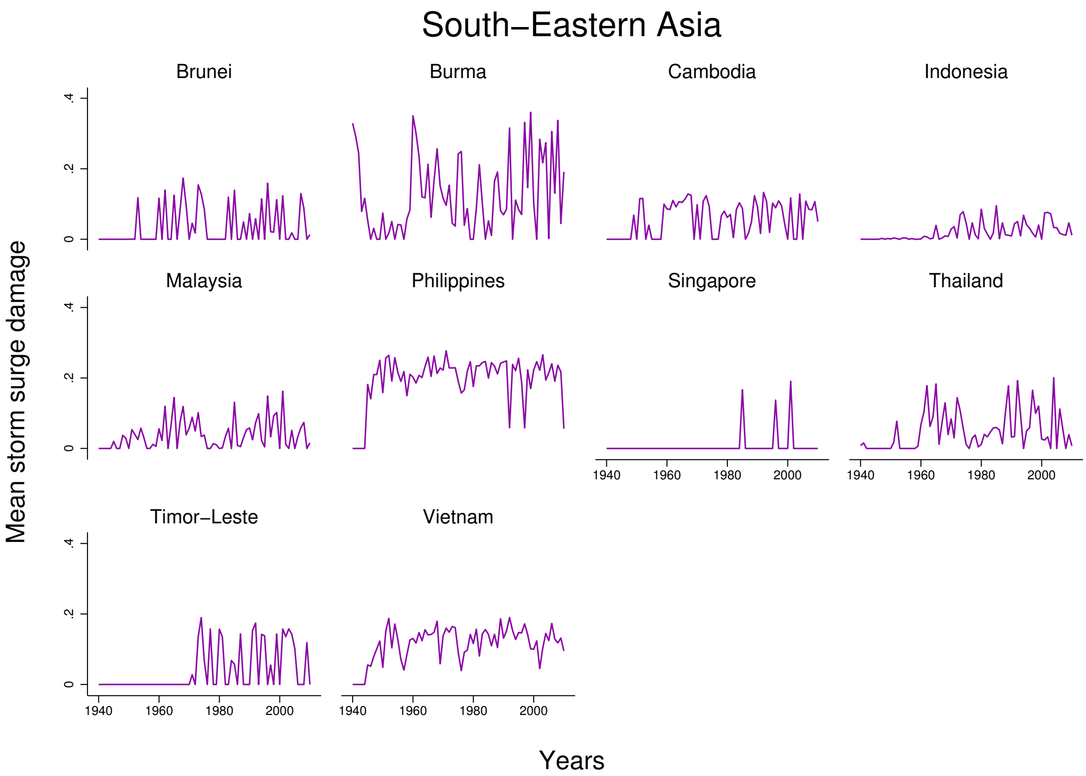

Figure 2.25: Yearly mean storm surge damage in South-Eastern Asia, 1940–2010

Notes: This figure shows the yearly mean storm surge damage by country or area in South-Eastern Asia. Storm surge damage is a damage index ranging from 0 to 0.7.

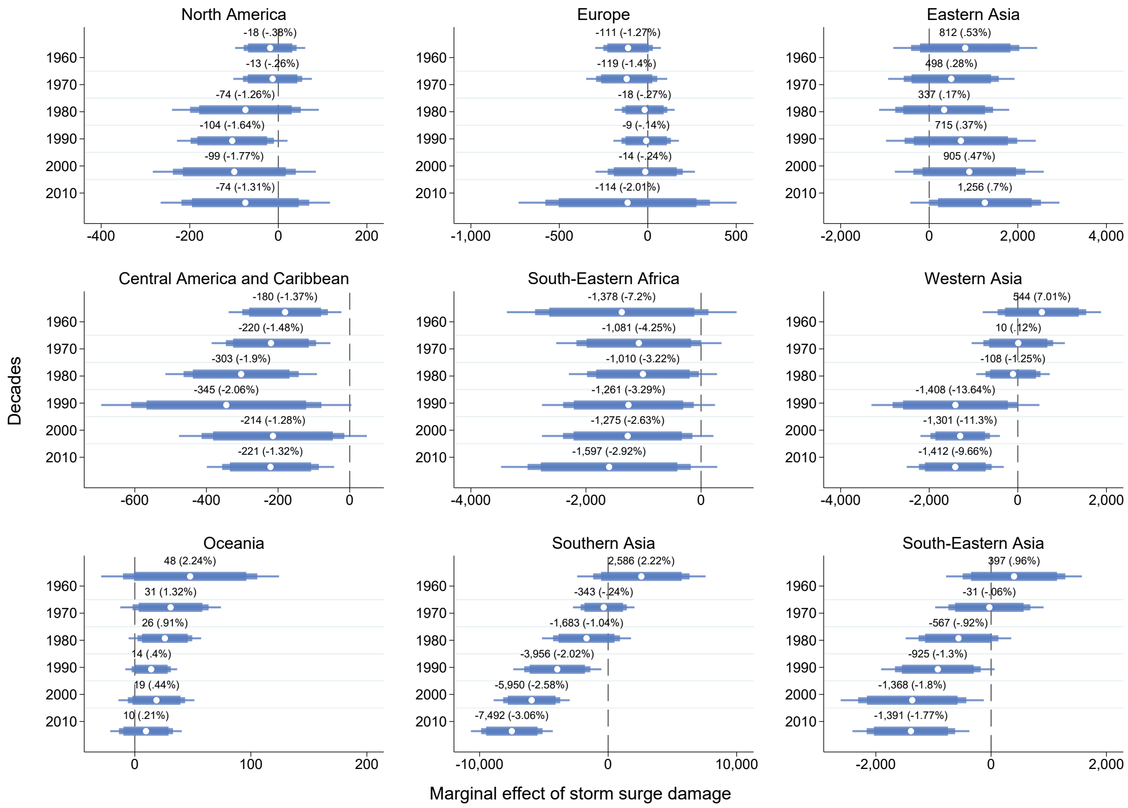

Figure 2.26: Effects of storm surge damage per decade on the rural population count for different world regions

Notes: The figure shows the effect of a standard deviation increase in storm surge damage (0.1128) on the rural population count per decade for nine different world regions. The plotted coefficients are the average effects per decade compared to 1950. The line widths characterize the 90%, 95%, and 99% confidence intervals. The numbers represent the mean estimator with the relative effect in comparison to the sample average per decade in parentheses.

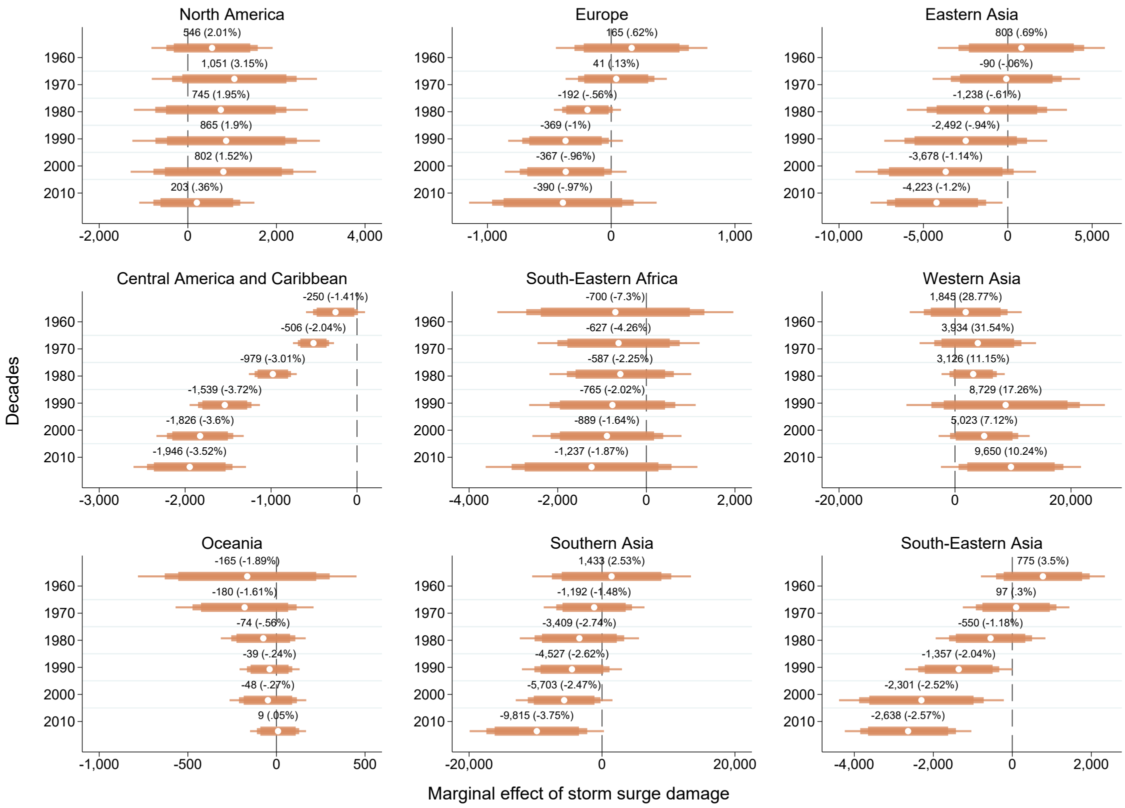

Figure 2.27: Effects of storm surge damage per decade on the urban population count for different world regions

Notes: The figure shows the effect of a standard deviation increase in storm surge damage (0.1128) on the urban population count per decades for nine different world regions. The plotted coefficients are the average effects per decade compared to 1950. The line widths characterize the 90%, 95%, and 99% confidence intervals. The numbers represent the mean estimator with the relative effect in comparison to the sample average per decade in parentheses.

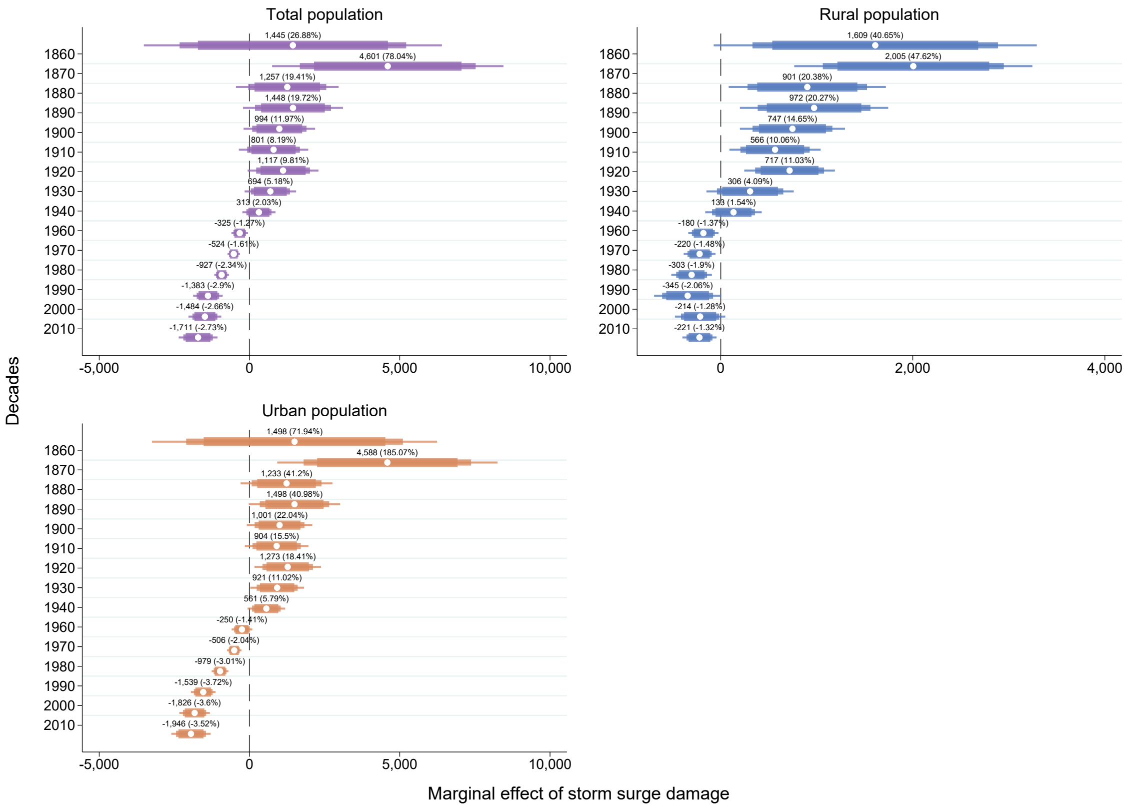

Figure 2.28: Effects of storm surge damage per decade on the total, rural, and population count in Central America and the Caribbean, 1860–2010

Notes: The figure shows the effect of a standard deviation increase in storm surge damage (0.1128) on the total, rural, and urban population count per decade for Central America and the Caribbean. The plotted coefficients are the average effects per decade compared to 1950. The line widths characterize the 90%, 95%, and 99% confidence intervals. The numbers represent the mean estimator with the relative effect in comparison to the sample average per decade in parentheses.

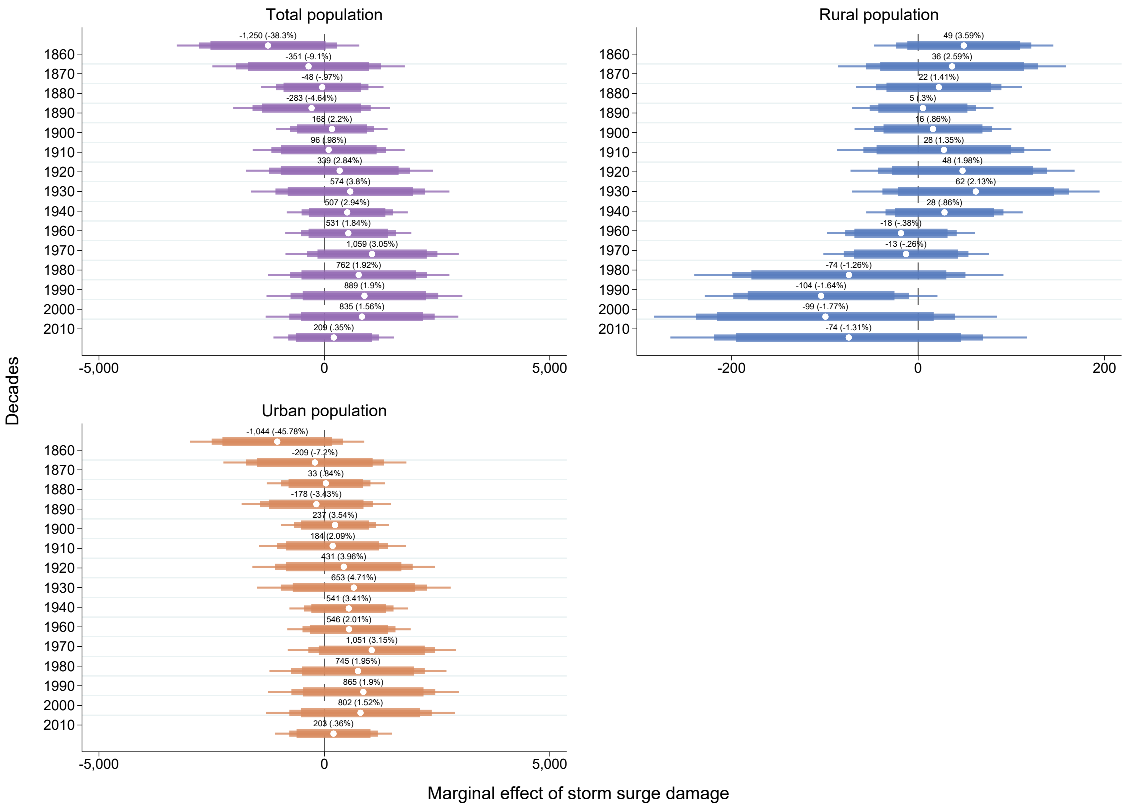

Figure 2.29: Effects of storm surge damage per decade on the total, rural, and population count in North America, 1860–2010

Notes: The figure shows the effect of a standard deviation increase in storm surge damage (0.1128) on the total, rural, and urban population count per decade for North America. The plotted coefficients are the average effects per decade compared to 1950. The line widths characterize the 90%, 95%, and 99% confidence intervals. The numbers represent the mean estimator with the relative effect in comparison to the sample average per decade in parentheses.

2.6.2 Underlying Tables for Figures

Table 2.2: The average decadal effect of storm surge damage – Total population count

	Rural population count					
	1960	1970	1980	1990	2000	2010
Storm surge damage	1,187	582	79	-514	-1,109	-1,552
	(509.73)	(370.18)	(351.57)	(356.83)	(447.91)	(501.75)
	[0.02]	[0.12]	[0.82]	[0.15]	[0.01]	[0.00]
Observations	343,805	343,805	343,805	343,805	343,805	343,805

Notes: Panel ordinary least squares regression results with clustered standard errors by affected grid × decade × country in parentheses (), and p-values in brackets []. The coefficients show the marginal effect of the different tropical cyclone damage types on Rural population count. The sample covers the decades from 1950 through 2010 for all low elevation coastal zones in exposed countries. *Storm surge damage* is the mean storm surge damage function of decade d averaged over the yearly data from d-9 to d in grid cell i. All regressions control for *Wind damage* and *Rainfall* and include decade and grid fixed effects as well as country-specific linear trends.

Table 2.3: The average decadal effect of storm surge damage – Rural population count

	Rural population count					
	1960	1970	1980	1990	2000	2010
Storm surge damage	272	140	-65	-181	-357	-312
	(232.31)	(211.76)	(218.60)	(195.14)	(243.21)	(224.77)
	[0.24]	[0.51]	[0.77]	[0.35]	[0.14]	[0.17]
Observations	343,805	343,805	343,805	343,805	343,805	343,805

Notes: Panel ordinary least squares regression results with clustered standard errors by affected grid × decade × country in parentheses (), and p-values in brackets []. The coefficients show the marginal effect of the different tropical cyclone damage types on Rural population count. The sample covers the decades from 1950 through 2010 for all low elevation coastal zones in exposed countries. *Storm surge damage* is the mean storm surge damage function of decade d averaged over the yearly data from d-9 to d in grid cell i. All regressions control for *Wind damage* and *Rainfall* and include decade and grid fixed effects as well as country-specific linear trends.

Table 2.4: The average decadal effect of storm surge damage – Urban population count

	Urban population count					
	1960	1970	1980	1990	2000	2010
Storm surge damage	1,273	582	-20	-741	-1,373	-1,767
	(611.90)	(403.04)	(360.97)	(407.12)	(490.84)	(548.25)
	[0.04]	[0.15]	[0.95]	[0.07]	[0.01]	[0.00]
Observations	343,805	343,805	343,805	343,805	343,805	343,805

Notes: Panel ordinary least squares regression results with clustered standard errors by affected grid × decade × country in parentheses (), and p-values in brackets []. The coefficients show the marginal effect of the different tropical cyclone damage types on Urban population count. The sample covers the decades from 1950 through 2010 for all low elevation coastal zones in exposed countries. *Storm surge damage* is the mean storm surge damage function of decade *d* averaged over the yearly data from *d-9* to *d* in grid cell *i*. All regressions control for *Wind damage* and *Rainfall* and include decade and grid fixed effects as well as country-specific linear trends.

Table 2.5: The average effect of storm surge damage for different levels of crop suitabilities – Rural population count

	Rural population count			
	Low suitability	Middle suitability	High suitability	Highest suitability
Storm surge damage	-2,760	-2,588	-2,638	8,965
	(1,946.52)	(1,600.25)	(1,642.59)	(5,098.28)
	[0.16]	[0.11]	[0.11]	[0.08]
Observations	343,805	343,805	343,805	343,805

Notes: Panel ordinary least squares regression results with clustered standard errors by affected grid × decade × country in parentheses (), and p-values in brackets []. The coefficients show the marginal effects of Storm surge damage on the rural population count for different classes of crop suitability. The classes refer to the 0.25, 0.5, 0.75 percentile cutoff points of the crop suitability data. They are: 0–3 for low suitability, 3–22 fir middle suitability, 22–48 for high suitability, and greater than 48 for highest suitability. The base category is 0 crop suitability. The sample covers the decades from 1950 through 2010 for all low elevation coastal zones in exposed countries. *Storm surge damage* is the mean of decade *d* averaged over the yearly data from *d-9* to *d* in grid cell *i*. All regressions control for *Wind damage* and *Rainfall* and include decade and grid fixed effects as well as country-specific linear trends.

Table 2.6: The average effect of storm surge damage for different levels of crop suitabilities – Urban population count

	Urban population count			
	Low suitability	Middle suitability	High suitability	Highest suitability
Storm surge damage	-11,712	-10,855	-5,567	-8,155
	(5,038.74)	(4,386.42)	(4,884.41)	(9,085.49)
	[0.02]	[0.01]	[0.25]	[0.37]
Observations	343,805	343,805	343,805	343,805

Notes: Panel ordinary least squares regression results with clustered standard errors by affected grid × decade × country in parentheses (), and p-values in brackets []. The coefficients show the marginal effects of Storm surge damage on the urban population count for different classes of crop suitability. The classes refer to the 0.25, 0.5, 0.75 percentile cutoff points of the crop suitability data. They are: 0–3 for low suitability, 3–22 for middle suitability, 22–48 for high suitability, and larger than 48 for highest suitability. The base category is 0 crop suitability. The sample covers the decades from 1950 through 2010 for all low elevation coastal zones in exposed countries. *Storm surge damage* is the mean of decade *d* averaged over the yearly data from *d-9* to *d* in grid cell *i*. All regressions control for *Wind damage* and *Rainfall* and include decade and grid fixed effects as well as country-specific linear trends.

Table 2.7: The average effect of storm surge damage for different income classes – Rural popuation count

	Rural population count		
	Low income	Lower middle income	Upper middle income
Storm surge damage	-4,676	-6,188	-4,973
	(2,564.38)	(1,891.85)	(2,650.02)
	[0.07]	[0.00]	[0.06]
Observations	343,805	343,805	343,805

Notes: Panel ordinary least squares regression results with clustered standard errors by affected grid × decade × country in parentheses (), and p-values in brackets []. The coefficients show the marginal effects of Storm surge damage on rural popuation count for different World Bank income classes. The base category is high income class. The sample covers the decades from 1950 through 2010 for all low elevation coastal zones in exposed countries. *Storm surge damage* is the mean of decade *d* averaged over the yearly data from *d-9* to *d* in grid cell *i*. All regressions control for *Wind damage* and *Rainfall* and include decade and grid fixed effects as well as country-specific linear trends.

Table 2.8: The average effect of storm surge damage for different income classes – Urban popuation count

	Urban population count		
	Low income	Lower middle income	Upper middle income
Storm surge damage	-8,685	-15,777	-15,917
	(10,327.95)	(7,337.45)	(5,776.56)
	[0.40]	[0.03]	[0.01]
Observations	343,805	343,805	343,805

Notes: Panel ordinary least squares regression results with clustered standard errors by affected grid × decade × country in parentheses (), and p-values in brackets []. The coefficients show the marginal effects of storm surge damage on the urban popuation count for different World Bank income classes. The base category is high income class. The sample covers the decades from 1950 through 2010 for all low elevation coastal zones in exposed countries. *Storm surge damage* is the mean of decade *d* averaged over the yearly data from *d-9* to *d* in grid cell *i*. All regressions control for *Wind damage* and *Rainfall* and include decade and grid fixed effects as well as country-specific linear trends.

Table 2.9: The average effect of storm surge damage – Central America and Caribbean

	Total population count	Rural population count	Urban population count
	(1)	(2)	(3)
Storm surge damage	-7,991	-1,452	-8,854
	(1,763.69)	(198.02)	(1,999.92)
	[0.00]	[0.00]	[0.00]
Wind damage	-5,919	-544	-4,517
	(3,154.90)	(982.20)	(2,984.01)
	[0.06]	[0.58]	[0.13]
Rainfall	2.8	-1	2.5
	(3.89)	(1.07)	(3.89)
	[0.47]	[0.34]	[0.51]
Observations	70,128	70,128	70,128
Clusters	584	584	584
Mean dependent variable	2,587	1,098	1,988
SD storm surge damage	0.1128	0.1128	0.1128

Notes: Panel ordinary least squares regression results with clustered standard errors by affected grid × decade × country in parentheses (), and p-values in brackets []. The coefficients show the marginal effect of the different tropical cyclone damage types on the total, urban and rural population counts. The sample covers the decades from 1860 through 2010 for all low elevation coastal zones in exposed countries in Central America and Caribbean. *Storm surge damage* is the mean storm surge damage function of decade *d* averaged over the yearly data from *d-9* to *d* in grid cell *i*, *Wind damage* is the mean decadal wind damage function of decade *d* averaged over the yearly data from *d-9* to *d* in grid cell *i*, and *Rainfall* is the mean decadal tropical cyclones' rainfall (in mm) of decade *d* averaged over the yearly data from *d-9* to *d* in grid cell *i*. All regressions include decade and grid fixed effects as well as country-specific linear trends.

Table 2.10: The average effect of storm surge damage – Eastern Asia

	Total population count	Rural population count	Urban population count
	(1)	(2)	(3)
Storm surge damage	-22,843	779	-34,145
	(11,846.38)	(6,192.59)	(13,647.22)
	[0.06]	[0.90]	[0.02]
Wind damage	-44,672	-724	-46,159
	(23,143.04)	(8,137.68)	(22,523.02)
	[0.06]	[0.93]	[0.04]
Rainfall	30	21	23
	(54.25)	(13.99)	(61.12)
	[0.58]	[0.13]	[0.71]
Observations	36,771	36,771	36,771
Clusters	63	63	63
Mean dependent variable	36,944	19,884	24,297
SD storm surge damage	0.1128	0.1128	0.1128

Notes: Panel ordinary least squares regression results with clustered standard errors by affected grid × decade × country in parentheses (), and p-values in brackets []. The coefficients show the marginal effect of the different tropical cyclone damage types on the total, urban and rural population counts. The sample covers the decades from 1950 through 2010 for all low elevation coastal zones in exposed countries in Eastern Asia. *Storm surge damage* is the mean storm surge damage function of decade d averaged over the yearly data from d-9 to d in grid cell i, *Wind damage* is the mean decadal wind damage function of decade d averaged over the yearly data from d-9 to d in grid cell i, and *Rainfall* is the mean decadal tropical cyclones' rainfall (in mm) of decade d averaged over the yearly data from d-9 to d in grid cell i. All regressions include decade and grid fixed effects as well as country-specific linear trends.

Table 2.11: The average effect of storm surge damage – Europe

	Total population count	Rural population count	Urban population count
	(1)	(2)	(3)
Storm surge damage	-2,489	-493	-1,671
	(1,150.24)	(663.88)	(1,287.14)
	[0.03]	[0.46]	[0.20]
Wind damage	17,565	8,162	16,411
	(8,094.24)	(4,882.50)	(10,420.82)
	[0.03]	[0.10]	[0.12]
Rainfall	6.7	-19	9.6
	(33.38)	(12.75)	(35.71)
	[0.84]	[0.14]	[0.79]
Observations	60,956	60,956	60,956
Clusters	96	96	96
Mean dependent variable	3,904	810	3,708
SD storm surge damage	0.1128	0.1128	0.1128

Notes: Panel ordinary least squares regression results with clustered standard errors by affected grid × decade × country in parentheses (), and p-values in brackets []. The coefficients show the marginal effect of the different tropical cyclone damage types on the total, urban and rural population counts. The sample covers the decades from 1950 through 2010 for all low elevation coastal zones in exposed countries in Europe. *Storm surge damage* is the mean storm surge damage function of decade d averaged over the yearly data from d-9 to d in grid cell i, *Wind damage* is the mean decadal wind damage function of decade d averaged over the yearly data from d-9 to d in grid cell i, and *Rainfall* is the mean decadal tropical cyclones' rainfall (in mm) of decade d averaged over the yearly data from d-9 to d in grid cell i. All regressions include decade and grid fixed effects as well as country-specific linear trends.

Table 2.12: The average effect of storm surge damage – North America

	Total population count	Rural population count	Urban population count
	(1)	(2)	(3)
Storm surge damage	2,665	-130	2,885
	(3,740.38)	(288.53)	(3,688.13)
	[0.48]	[0.65]	[0.44]
Wind damage	2,464	-142	2,612
	(4,800.22)	(405.41)	(4,875.78)
	[0.61]	[0.73]	[0.59]
Rainfall	-21	-1.1	-21
	(11.95)	(1.35)	(11.87)
	[0.08]	[0.40]	[0.08]
Observations	122,480	122,480	122,480
Clusters	80	80	80
Mean dependent variable	2,576	394	2,428
SD storm surge damage	0.1128	0.1128	0.1128

Notes: Panel ordinary least squares regression results with clustered standard errors by affected grid × decade × country in parentheses (), and p-values in brackets []. The coefficients show the marginal effect of the different tropical cyclone damage types on the total, urban and rural population counts. The sample covers the decades from 1860 through 2010 for all low elevation coastal zones in exposed countries in North America. *Storm surge damage* is the mean storm surge damage function of decade d averaged over the yearly data from d-9 to d in grid cell i, *Wind damage* is the mean decadal wind damage function of decade d averaged over the yearly data from d-9 to d in grid cell i, and *Rainfall* is the mean decadal tropical cyclones' rainfall (in mm) of decade d averaged over the yearly data from d-9 to d in grid cell i. All regressions include decade and grid fixed effects as well as country-specific linear trends.

Table 2.13: The average effect of storm surge damage – Oceania

	Total population count	Rural population count	Urban population count
	(1)	(2)	(3)
Storm surge damage	-1,086	160	-1,386
	(479.12)	(86.09)	(460.99)
	[0.03]	[0.07]	[0.00]
Wind damage	-6,851	-221	-6,422
	(6,964.77)	(343.83)	(6,774.67)
	[0.33]	[0.52]	[0.35]
Rainfall	-16	.99	-16
	(5.29)	(1.02)	(4.67)
	[0.00]	[0.33]	[0.00]
Observations	38,591	38,591	38,591
Clusters	89	89	89
Mean dependent variable	1,741	348	1,510
SD storm surge damage	0.1128	0.1128	0.1128

Notes: Panel ordinary least squares regression results with clustered standard errors by affected grid × decade × country in parentheses (), and p-values in brackets []. The coefficients show the marginal effect of the different tropical cyclone damage types on the total, urban and rural population counts. The sample covers the decades from 1950 through 2010 for all low elevation coastal zones in exposed countries in Oceania. *Storm surge damage* is the mean storm surge damage function of decade d averaged over the yearly data from d-9 to d in grid cell i, *Wind damage* is the mean decadal wind damage function of decade d averaged over the yearly data from d-9 to d in grid cell i, and *Rainfall* is the mean decadal tropical cyclones' rainfall (in mm) of decade d averaged over the yearly data from d-9 to d in grid cell i. All regressions include decade and grid fixed effects as well as country-specific linear trends.

Table 2.14: The average effect of storm surge damage – South-Eastern Africa

	Total population count	Rural population count	Urban population count
	(1)	(2)	(3)
Storm surge damage	-8,292	-7,976	-5,475
	(5,013.38)	(3,544.74)	(3,767.37)
	[0.10]	[0.03]	[0.15]
Wind damage	-17,413	-5,733	-4,477
	(18,785.94)	(5,490.82)	(20,934.90)
	[0.36]	[0.30]	[0.83]
Rainfall	8.6	.94	3.4
	(10.45)	(6.65)	(7.67)
	[0.41]	[0.89]	[0.66]
Observations	13,216	13,216	13,216
Clusters	90	90	90
Mean dependent variable	6,425	3,757	3,468
SD storm surge damage	0.1128	0.1128	0.1128

Notes: Panel ordinary least squares regression results with clustered standard errors by affected grid × decade × country in parentheses (), and p-values in brackets []. The coefficients show the marginal effect of the different tropical cyclone damage types on the total, urban and rural population counts. The sample covers the decades from 1950 through 2010 for all low elevation coastal zones in exposed countries in South-Eastern Africa. *Storm surge damage* is the mean storm surge damage function of decade d averaged over the yearly data from d-9 to d in grid cell i, *Wind damage* is the mean decadal wind damage function of decade d averaged over the yearly data from d-9 to d in grid cell i, and *Rainfall* is the mean decadal tropical cyclones' rainfall (in mm) of decade d averaged over the yearly data from d-9 to d in grid cell i. All regressions include decade and grid fixed effects as well as country-specific linear trends.

Table 2.15: The average effect of storm surge damage – South-Eastern Asia

	Total population count	Rural population count	Urban population count
	(1)	(2)	(3)
Storm surge damage	-18,868	-11,027	-17,906
	(6,393.74)	(3,671.29)	(5,146.95)
	[0.00]	[0.00]	[0.00]
Wind damage	12,255	1,608	10,686
	(17,371.72)	(6,906.30)	(12,945.36)
	[0.48]	[0.82]	[0.41]
Rainfall	-7	8.7	-3.2
	(20.22)	(9.73)	(16.23)
	[0.73]	[0.37]	[0.85]
Observations	77,658	77,658	77,658
Clusters	108	108	108
Mean dependent variable	10,835	6,650	6,086
SD storm surge damage	0.1128	0.1128	0.1128

Notes: Panel ordinary least squares regression results with clustered standard errors by affected grid × decade × country in parentheses (), and p-values in brackets []. The coefficients show the marginal effect of the different tropical cyclone damage types on the total, urban and rural population counts. The sample covers the decades from 1950 through 2010 for all low elevation coastal zones in exposed countries in South-Eastern Asia. *Storm surge damage* is the mean storm surge damage function of decade d averaged over the yearly data from d-9 to d in grid cell i, *Wind damage* is the mean decadal wind damage function of decade d averaged over the yearly data from d-9 to d in grid cell i, and *Rainfall* is the mean decadal tropical cyclones' rainfall (in mm) of decade d averaged over the yearly data from d-9 to d in grid cell i. All regressions include decade and grid fixed effects as well as country-specific linear trends.

Table 2.16: The average effect of storm surge damage – Southern Asia

	Total population count	Rural population count	Urban population count
	(1)	(2)	(3)
Storm surge damage	-39,097	-20,726	-29,834
	(23,917.97)	(13,347.76)	(22,122.03)
	[0.11]	[0.13]	[0.18]
Wind damage	-43,746	-23,101	-44,207
	(59,312.62)	(20,243.39)	(47,181.69)
	[0.46]	[0.26]	[0.35]
Rainfall	-171	-85	-89
	(93.65)	(42.63)	(62.83)
	[0.07]	[0.05]	[0.16]
Observations	25,536	25,536	25,536
Clusters	58	58	58
Mean dependent variable	29,907	19,099	15,627
SD storm surge damage	0.1128	0.1128	0.1128

Notes: Panel ordinary least squares regression results with clustered standard errors by affected grid × decade × country in parentheses (), and p-values in brackets []. The coefficients show the marginal effect of the different tropical cyclone damage types on the total, urban and rural population counts. The sample covers the decades from 1950 through 2010 for all low elevation coastal zones in exposed countries in Southern Asia. *Storm surge damage* is the mean storm surge damage function of decade d averaged over the yearly data from d-9 to d in grid cell i, *Wind damage* is the mean decadal wind damage function of decade d averaged over the yearly data from d-9 to d in grid cell i, and *Rainfall* is the mean decadal tropical cyclones' rainfall (in mm) of decade d averaged over the yearly data from d-9 to d in grid cell i. All regressions include decade and grid fixed effects as well as country-specific linear trends.

Table 2.17: The average effect of storm surge damage – Western Asia

	Total population count	Rural population count	Urban population count
	(1)	(2)	(3)
Storm surge damage	59,746	-4,994	47,001
	(29,723.88)	(2,737.74)	(21,361.23)
	[0.05]	[0.08]	[0.03]
Wind damage	-177,520	8,068	-145,965
	(76,106.89)	(8,193.00)	(85,857.62)
	[0.02]	[0.33]	[0.10]
Rainfall	-23	-4.9	-35
	(69.58)	(6.79)	(78.55)
	[0.74]	[0.48]	[0.66]
Observations	6,811	6,811	6,811
Clusters	44	44	44
Mean dependent variable	4,728	1,093	4,299
SD storm surge damage	0.1128	0.1128	0.1128

Notes: Panel ordinary least squares regression results with clustered standard errors by affected grid × decade × country in parentheses (), and p-values in brackets []. The coefficients show the marginal effect of the different tropical cyclone damage types on the total, urban and rural population counts. The sample covers the decades from 1950 through 2010 for all low elevation coastal zones in exposed countries in Western Asia. *Storm surge damage* is the mean storm surge damage function of decade d averaged over the yearly data from d-9 to d in grid cell i, *Wind damage* is the mean decadal wind damage function of decade d averaged over the yearly data from d-9 to d in grid cell i, and *Rainfall* is the mean decadal tropical cyclones' rainfall (in mm) of decade d averaged over the yearly data from d-9 to d in grid cell i. All regressions include decade and grid fixed effects as well as country-specific linear trends.

Table 2.18: The average decadal effect of storm surge damage - Central America and Caribbean

	Total population count					
	1960	1970	1980	1990	2000	2010
Storm surge damage	-325	-524	-927	-1,383	-1,484	-1,711
	(106.42)	(80.29)	(94.29)	(190.32)	(211.24)	(249.75)
	[0.00]	[0.00]	[0.00]	[0.00]	[0.00]	[0.00]
Observations	70,128	70,128	70,128	70,128	70,128	70,128

Notes: Panel ordinary least squares regression results with clustered standard errors by affected grid × decade × country in parentheses (), and p-values in brackets []. The coefficients show the average effect of storm surge damage on Total population count for different decades compared to 1950. The sample covers the decades from 1860 through 2010 for all low elevation coastal zones in exposed countries in Central America and Caribbean. *Storm surge damage* is the mean storm surge damage function of decade d averaged over the yearly data from d-9 to d in grid cell i. All regressions control for *Wind damage* and *Rainfall* and include decade and grid fixed effects as well as country-specific linear trends.

Table 2.19: The average decadal effect of storm surge damage - Eastern Asia

	Total population count					
	1960	1970	1980	1990	2000	2010
Storm surge damage	1,327	486	-398	-1,031	-1,805	-2,190
	(1,385.33)	(1,226.84)	(1,274.51)	(1,304.01)	(1,549.20)	(1,093.13)
	[0.34]	[0.69]	[0.76]	[0.43]	[0.25]	[0.05]
Observations	36,771	36,771	36,771	36,771	36,771	36,771

Notes: Panel ordinary least squares regression results with clustered standard errors by affected grid × decade × country in parentheses (), and p-values in brackets []. The coefficients show the average effect of storm surge damage on Total population count for different decades compared to 1950. The sample covers the decades from 1950 through 2010 for all low elevation coastal zones in exposed countries in Eastern Asia. *Storm surge damage* is the mean storm surge damage function of decade d averaged over the yearly data from d-9 to d in grid cell i. All regressions control for *Wind damage* and *Rainfall* and include decade and grid fixed effects as well as country-specific linear trends. All regressions include decade and grid fixed effects as well as country-specific linear trends.

Table 2.20: The average decadal effect of storm surge damage - Europe

	Total population count					
	1960	1970	1980	1990	2000	2010
Storm surge damage	93	-47	-231	-410	-477	-691
	(227.80)	(147.28)	(101.21)	(178.37)	(193.77)	(285.63)
	[0.68]	[0.75]	[0.02]	[0.02]	[0.02]	[0.02]
Observations	60,956	60,956	60,956	60,956	60,956	60,956

Notes: Panel ordinary least squares regression results with clustered standard errors by affected grid × decade × country in parentheses (), and p-values in brackets []. The coefficients show the average effect of storm surge damage on Total population count for different decades compared to 1950. The sample covers the decades from 1950 through 2010 for all low elevation coastal zones in exposed countries in Europe. *Storm surge damage* is the mean storm surge damage function of decade d averaged over the yearly data from d-9 to d in grid cell i. All regressions control for *Wind damage* and *Rainfall* and include decade and grid fixed effects as well as country-specific linear trends. All regressions include decade and grid fixed effects as well as country-specific linear trends.

Table 2.21: The average decadal effect of storm surge damage - North America

	Total population count					
	1960	1970	1980	1990	2000	2010
Storm surge damage	531	1,059	762	889	835	209
	(529.70)	(727.94)	(762.42)	(823.16)	(809.82)	(506.80)
	[0.32]	[0.15]	[0.32]	[0.28]	[0.31]	[0.68]
Observations	122,480	122,480	122,480	122,480	122,480	122,480

Notes: Panel ordinary least squares regression results with clustered standard errors by affected grid × decade × country in parentheses (), and p-values in brackets []. The coefficients show the average effect of storm surge damage on Total population count for different decades compared to 1950. The sample covers the decades from 1860 through 2010 for all low elevation coastal zones in exposed countries in North America. *Storm surge damage* is the mean storm surge damage function of decade *d* averaged over the yearly data from *d-9* to *d* in grid cell *i*. All regressions control for *Wind damage* and *Rainfall* and include decade and grid fixed effects as well as country-specific linear trends.

Table 2.22: The average decadal effect of storm surge damage - Oceania

	Total population count					
	1960	1970	1980	1990	2000	2010
Storm surge damage	-144	-155	-37	-12	-9.2	46
	(239.10)	(148.90)	(94.26)	(65.64)	(77.41)	(58.24)
	[0.55]	[0.30]	[0.69]	[0.86]	[0.91]	[0.43]
Observations	38,591	38,591	38,591	38,591	38,591	38,591

Notes: Panel ordinary least squares regression results with clustered standard errors by affected grid × decade × country in parentheses (), and p-values in brackets []. The coefficients show the average effect of storm surge damage on Total population count for different decades compared to 1950. The sample covers the decades from 1950 through 2010 for all low elevation coastal zones in exposed countries in Oceania. *Storm surge damage* is the mean storm surge damage function of decade *d* averaged over the yearly data from *d-9* to *d* in grid cell *i*. All regressions control for *Wind damage* and *Rainfall* and include decade and grid fixed effects as well as country-specific linear trends. All regressions include decade and grid fixed effects as well as country-specific linear trends.

Table 2.23: The average decadal effect of storm surge damage - South-Eastern Africa

	Total population count					
	1960	1970	1980	1990	2000	2010
Storm surge damage	-1,425	-1,144	-1,044	-1,308	-1,445	-1,865
	(1,236.07)	(875.85)	(781.73)	(910.30)	(850.47)	(1,124.14)
	[0.25]	[0.19]	[0.19]	[0.15]	[0.09]	[0.10]
Observations	13,216	13,216	13,216	13,216	13,216	13,216

Notes: Panel ordinary least squares regression results with clustered standard errors by affected grid × decade × country in parentheses (), and p-values in brackets []. The coefficients show the average effect of storm surge damage on Total population count for different decades compared to 1950. The sample covers the decades from 1950 through 2010 for all low elevation coastal zones in exposed countries in South-Eastern Africa. *Storm surge damage* is the mean storm surge damage function of decade *d* averaged over the yearly data from *d-9* to *d* in grid cell *i*. All regressions control for *Wind damage* and *Rainfall* and include decade and grid fixed effects as well as country-specific linear trends. All regressions include decade and grid fixed effects as well as country-specific linear trends.

Table 2.24: The average decadal effect of storm surge damage - South-Eastern Asia

	Total population count					
	1960	1970	1980	1990	2000	2010
Storm surge damage	1,022	220	-583	-1,355	-2,229	-2,687
	(781.78)	(660.81)	(664.92)	(642.64)	(929.66)	(742.34)
	[0.19]	[0.74]	[0.38]	[0.04]	[0.02]	[0.00]
Observations	77,658	77,658	77,658	77,658	77,658	77,658

Notes: Panel ordinary least squares regression results with clustered standard errors by affected grid × decade × country in parentheses (), and p-values in brackets []. The coefficients show the average effect of storm surge damage on Total population count for different decades compared to 1950. The sample covers the decades from 1950 through 2010 for all low elevation coastal zones in exposed countries in South-Eastern Asia. *Storm surge damage* is the mean storm surge damage function of decade *d* averaged over the yearly data from *d-9* to *d* in grid cell *i*. All regressions control for *Wind damage* and *Rainfall* and include decade and grid fixed effects as well as country-specific linear trends. All regressions include decade and grid fixed effects as well as country-specific linear trends.

Table 2.25: The average decadal effect of storm surge damage - Southern Asia

	Total population count					
	1960	1970	1980	1990	2000	2010
Storm surge damage	2,641	-2,026	-4,184	-6,501	-8,337	-14,192
	(5,513.90)	(3,034.08)	(3,797.24)	(3,174.71)	(2,928.71)	(4,338.25)
	[0.63]	[0.51]	[0.28]	[0.05]	[0.01]	[0.00]
Observations	25,536	25,536	25,536	25,536	25,536	25,536

Notes: Panel ordinary least squares regression results with clustered standard errors by affected grid × decade × country in parentheses (), and p-values in brackets []. The coefficients show the average effect of storm surge damage on Total population count for different decades compared to 1950. The sample covers the decades from 1950 through 2010 for all low elevation coastal zones in exposed countries in Southern Asia. *Storm surge damage* is the mean storm surge damage function of decade *d* averaged over the yearly data from *d-9* to *d* in grid cell *i*. All regressions control for *Wind damage* and *Rainfall* and include decade and grid fixed effects as well as country-specific linear trends. All regressions include decade and grid fixed effects as well as country-specific linear trends.

Table 2.26: The average decadal effect of storm surge damage - Western Asia

	Total population count					
	1960	1970	1980	1990	2000	2010
Storm surge damage	2,922	5,550	4,147	11,594	6,600	13,605
	(3,964.39)	(4,691.12)	(2,800.31)	(7,940.80)	(3,202.12)	(7,066.21)
	[0.47]	[0.24]	[0.15]	[0.15]	[0.05]	[0.06]
Observations	6,811	6,811	6,811	6,811	6,811	6,811

Notes: Panel ordinary least squares regression results with clustered standard errors by affected grid × decade × country in parentheses (), and p-values in brackets []. The coefficients show the average effect of storm surge damage on Total population count for different decades compared to 1950. The sample covers the decades from 1950 through 2010 for all low elevation coastal zones in exposed countries in Western Asia. *Storm surge damage* is the mean storm surge damage function of decade *d* averaged over the yearly data from *d-9* to *d* in grid cell *i*. All regressions control for *Wind damage* and *Rainfall* and include decade and grid fixed effects as well as country-specific linear trends. All regressions include decade and grid fixed effects as well as country-specific linear trends.

2.6.3 Robustness Tests

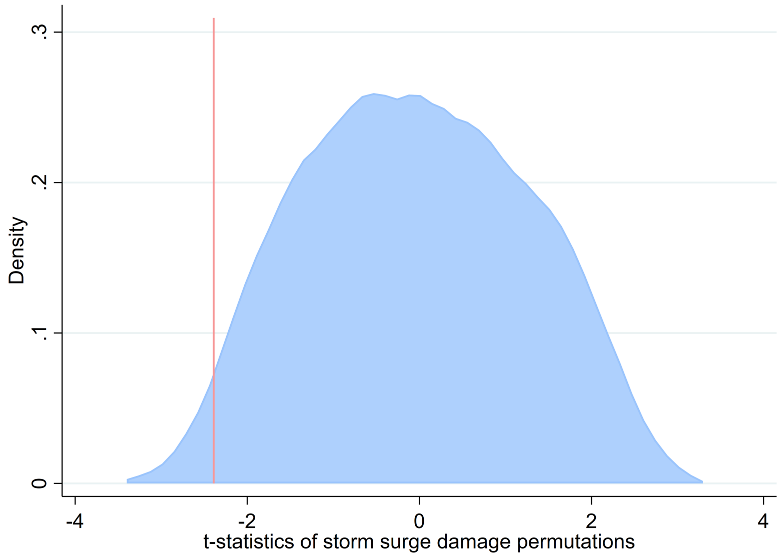

Figure 2.30: Randomization test for storm surge damage

Notes: This figure shows the t-statistics of the Fisher randomization test results for the storm surge damage variable where the decades are permuted for 1000 repetitions. It displays the kernel density plots (blue) of the randomized t-statistics together with the results of the main model (Figure 3, Panel a) (red bar).

Table 2.27: Robustness – Excluding outliers

	Total population count	Rural population count	Urban population count
	(1)	(2)	(3)
Storm surge damage	-1,099	-810	-1,465
	(385.08)	(430.48)	(448.52)
	[0.00]	[0.06]	[0.00]
Wind damage	-2,021	-2,239	247
	(737.70)	(1,159.75)	(1,306.32)
	[0.01]	[0.05]	[0.85]
Rainfall	-3.8	3.1	-8
	(1.74)	(2.32)	(2.99)
	[0.03]	[0.18]	[0.01]
Observations	171,652	171,652	171,652
Clusters	350	350	350
Mean dependent variable	2,529	1,748	1,328
SD storm surge damage	0.1128	0.1128	0.1128

Notes: Panel ordinary least squares regression results with clustered standard errors by affected grid × decade × country in parentheses (), and p-values in brackets []. The coefficients show the marginal effect of the different tropical cyclone damage types on the total, urban and rural population counts. The sample covers the decades from 1950 through 2010 for all low elevation coastal zones in exposed countries. *Storm surge damage* is the mean storm surge damage function of decade d averaged over the yearly data from *d-9* to d in grid cell i, *Wind damage* is the mean decadal wind damage function of decade d averaged over the yearly data from *d-9* to d in grid cell i, and *Rainfall* is the mean decadal tropical cyclones' rainfall (in mm) of decade d averaged over the yearly data from *d-9* to d in grid cell i. All regressions include decade and grid fixed effects as well as country-specific linear trends. In this regression all outliers larger than Cook's Distance of $4/N$ are excluded.

Table 2.28: Robustness – Excluding unpopulated areas

	Total population count	Rural population count	Urban population count
	(1)	(2)	(3)
Storm surge damage	-7,901	-2,199	-12,577
	(3,281.58)	(1,366.42)	(8,178.42)
	[0.02]	[0.11]	[0.12]
Wind damage	-10,312	-1,320	-8,334
	(7,480.87)	(2,597.37)	(19,432.26)
	[0.17]	[0.61]	[0.67]
Rainfall	-19	-.87	-53
	(16.47)	(8.60)	(33.54)
	[0.25]	[0.92]	[0.11]
Observations	340,426	324,210	85,443
Clusters	785	783	756
Mean dependent variable	11,082	5,980	28,847
SD storm surge damage	0.1128	0.1128	0.1128

Notes: Panel ordinary least squares regression results with clustered standard errors by affected grid × decade × country in parentheses (), and p-values in brackets []. The coefficients show the marginal effect of the different tropical cyclone damage types on the total, urban and rural population counts. The sample covers the decades from 1950 through 2010 for all low elevation coastal zones in exposed countries. *Storm surge damage* is the mean storm surge damage function of decade *d* averaged over the yearly data from *d-9* to *d* in grid cell *i*, *Wind damage* is the mean decadal wind damage function of decade *d* averaged over the yearly data from *d-9* to *d* in grid cell *i*, and *Rainfall* is the mean decadal tropical cyclones' rainfall (in mm) of decade *d* averaged over the yearly data from *d-9* to *d* in grid cell *i*. All regressions include decade and grid fixed effects as well as country-specific linear trends. In this regression all oberservations with zero population are excluded.

Table 2.29: Robustness – Excluding areas with less than 10 people

	Total population count	Rural population count	Urban population count
	(1)	(2)	(3)
Storm surge damage	-9,131	-2,631	-12,621
	(3,805.82)	(1,674.95)	(8,232.38)
	[0.02]	[0.12]	[0.13]
Wind damage	-10,730	-1,321	-8,247
	(8,180.27)	(2,783.97)	(19,470.38)
	[0.19]	[0.64]	[0.67]
Rainfall	-18	-.93	-53
	(17.66)	(9.19)	(33.64)
	[0.31]	[0.92]	[0.11]
Observations	300,591	281,939	84,986
Clusters	785	783	756
Mean dependent variable	12,550	6,876	29,002
SD storm surge damage	0.1128	0.1128	0.1128

Notes: Panel ordinary least squares regression results with clustered standard errors by affected grid × decade × country in parentheses (), and p-values in brackets []. The coefficients show the marginal effect of the different tropical cyclone damage types on the total, urban and rural population counts. The sample covers the decades from 1950 through 2010 for all low elevation coastal zones in exposed countries. *Storm surge damage* is the mean storm surge damage function of decade *d* averaged over the yearly data from *d-9* to *d* in grid cell *i*, *Wind damage* is the mean decadal wind damage function of decade *d* averaged over the yearly data from *d-9* to *d* in grid cell *i*, and *Rainfall* is the mean decadal tropical cyclones' rainfall (in mm) of decade *d* averaged over the yearly data from *d-9* to *d* in grid cell *i*. All regressions include decade and grid fixed effects as well as country-specific linear trends. In this regression all oberservations with less than 10 people are excluded.

Table 2.30: Robustness – Excluding areas with less than 100 people

	Total population count	Rural population count	Urban population count
	(1)	(2)	(3)
Storm surge damage	-10,330	-2,928	-13,241
	(4,637.70)	(2,151.72)	(8,767.58)
	[0.03]	[0.17]	[0.13]
Wind damage	-11,304	-857	-8,255
	(9,126.16)	(3,005.22)	(19,881.63)
	[0.22]	[0.78]	[0.68]
Rainfall	-19	-2.6	-53
	(18.64)	(9.66)	(34.54)
	[0.31]	[0.79]	[0.12]
Observations	247,723	227,254	80,278
Clusters	784	782	756
Mean dependent variable	15,219	8,521	30,700
SD storm surge damage	0.1128	0.1128	0.1128

Notes: Panel ordinary least squares regression results with clustered standard errors by affected grid × decade × country in parentheses (), and p-values in brackets []. The coefficients show the marginal effect of the different tropical cyclone damage types on the total, urban and rural population counts. The sample covers the decades from 1950 through 2010 for all low elevation coastal zones in exposed countries. *Storm surge damage* is the mean storm surge damage function of decade d averaged over the yearly data from d-9 to d in grid cell i, *Wind damage* is the mean decadal wind damage function of decade d averaged over the yearly data from d-9 to d in grid cell i, and *Rainfall* is the mean decadal tropical cyclones' rainfall (in mm) of decade d averaged over the yearly data from d-9 to d in grid cell i. All regressions include decade and grid fixed effects as well as country-specific linear trends. In this regression all oberservations with less than 100 people are excluded.

Table 2.31: Robustness – Including temperature controls

	Total population count	Rural population count	Urban population count
	(1)	(2)	(3)
Storm surge damage	-7,735	-2,215	-9,533
	(3,254.44)	(1,336.63)	(3,823.69)
	[0.02]	[0.10]	[0.01]
Wind damage	-9,832	-369	-9,665
	(7,410.11)	(2,398.03)	(6,626.68)
	[0.18]	[0.88]	[0.15]
Rainfall	-19	-.75	-15
	(16.43)	(8.06)	(11.92)
	[0.25]	[0.93]	[0.22]
Temperature	-217	-171	-183
	(260.26)	(109.12)	(266.62)
	[0.41]	[0.12]	[0.49]
Observations	308,665	308,665	308,665
Clusters	785	785	785
Mean dependent variable	12,198	6,279	7,999
SD storm surge damage	0.1128	0.1128	0.1128

Notes: Panel ordinary least squares regression results with clustered standard errors by affected grid × decade × country in parentheses (), and p-values in brackets []. The coefficients show the marginal effect of the different tropical cyclone damage types on the total, urban and rural population counts. The sample covers the decades from 1950 through 2010 for all low elevation coastal zones in exposed countries. *Storm surge damage* is the mean storm surge damage function of decade d averaged over the yearly data from d-9 to d in grid cell i, *Wind damage* is the mean decadal wind damage function of decade d averaged over the yearly data from d-9 to d in grid cell i, and *Rainfall* is the mean decadal tropical cyclones' rainfall (in mm) of decade d averaged over the yearly data from d-9 to d in grid cell i. *Temperature* is the mean decadal tropical cyclones' temperature (in degree Celsius) of decade d averaged over the yearly data from d-9 to d in grid cell i. All regressions include decade and grid fixed effects as well as country-specific linear trends.

Table 2.32: Robustness – Including squared climate controls

	Total population count	Rural population count	Urban population count
	(1)	(2)	(3)
Storm surge damage	-7,436	-2,370	-9,137
	(3,398.42)	(1,405.34)	(3,933.96)
	[0.03]	[0.09]	[0.02]
Wind damage	-9,777	-410	-9,579
	(7,486.21)	(2,392.90)	(6,702.92)
	[0.19]	[0.86]	[0.15]
Rainfall	-23	2	-21
	(20.07)	(9.18)	(15.80)
	[0.25]	[0.83]	[0.18]
Rainfall^2	.0047	-.0027	.0065
	(0.01)	(0.00)	(0.01)
	[0.52]	[0.46]	[0.26]
Temperature	-378	-107	-377
	(254.15)	(91.38)	(269.78)
	[0.14]	[0.24]	[0.16]
Temperature^2	12	-4.9	15
	(7.41)	(2.76)	(6.76)
	[0.10]	[0.07]	[0.03]
Observations	308,665	308,665	308,665
Clusters	785	785	785
Mean dependent variable	12,198	6,279	7,999
SD storm surge damage	0.1128	0.1128	0.1128

Notes: Panel ordinary least squares regression results with clustered standard errors by affected grid × decade × country in parentheses (), and p-values in brackets []. The coefficients show the marginal effect of the different tropical cyclone damage types on the total, urban and rural population counts. The sample covers the decades from 1950 through 2010 for all low elevation coastal zones in exposed countries. *Storm surge damage* is the mean storm surge damage function of decade d averaged over the yearly data from d-9 to d in grid cell i, *Wind damage* is the mean decadal wind damage function of decade d averaged over the yearly data from d-9 to d in grid cell i, and *Rainfall* is the mean decadal tropical cyclones' rainfall (in mm) of decade d averaged over the yearly data from d-9 to d in grid cell i. *Temperature* is the mean decadal tropical cyclones' temperature (in degree Celsius) of decade d averaged over the yearly data from d-9 to d in grid cell i. All regressions include decade and grid fixed effects as well as country-specific linear trends.

Table 2.33: Robustness – Squared country specific time trend

	Total population count	Rural population count	Urban population count
	(1)	(2)	(3)
Storm surge damage	-7,554	-2,199	-9,277
	(3,139.31)	(1,280.10)	(3,742.80)
	[0.02]	[0.09]	[0.01]
Wind damage	-10,857	-1,029	-10,330
	(7,476.87)	(2,535.68)	(6,637.10)
	[0.15]	[0.68]	[0.12]
Rainfall	-14	1.8	-11
	(16.95)	(8.51)	(12.09)
	[0.42]	[0.83]	[0.36]
Observations	343,805	343,805	343,805
Clusters	785	785	785
Mean dependent variable	10,973	5,641	7,206
SD storm surge damage	0.1128	0.1128	0.1128

Notes: Panel ordinary least squares regression results with clustered standard errors by affected grid × decade × country in parentheses (), and p-values in brackets []. The coefficients show the marginal effect of the different tropical cyclone damage types on the total, urban and rural population counts. The sample covers the decades from 1950 through 2010 for all low elevation coastal zones in exposed countries. *Storm surge damage* is the mean storm surge damage function of decade d averaged over the yearly data from d-9 to d in grid cell i, *Wind damage* is the mean decadal wind damage function of decade d averaged over the yearly data from d-9 to d in grid cell i, and *Rainfall* is the mean decadal tropical cyclones' rainfall (in mm) of decade d averaged over the yearly data from d-9 to d in grid cell i. All regressions include decade and grid fixed effects as well as country-specific squared trends.

Table 2.34: Robustness – Sample period 1980-2010

	Total population count	Rural population count	Urban population count
	(1)	(2)	(3)
Storm surge damage	-6,409	-692	-6,503
	(3,190.14)	(979.93)	(3,242.25)
	[0.05]	[0.48]	[0.05]
Wind damage	1,777	1,231	2,539
	(5,343.77)	(1,567.28)	(5,077.76)
	[0.74]	[0.43]	[0.62]
Rainfall	-.93	2.6	-.43
	(8.22)	(3.39)	(7.87)
	[0.91]	[0.44]	[0.96]
Observations	196,460	196,460	196,460
Clusters	443	443	443
Mean dependent variable	13,789	6,524	9,653
SD storm surge damage	0.1157	0.1157	0.1157

Notes: Panel ordinary least squares regression results with clustered standard errors by affected grid × decade × country in parentheses (), and p-values in brackets []. The coefficients show the marginal effect of the different tropical cyclone damage types on the total, urban and rural population counts. The sample covers the decades 1980 through 2010 for all low elevation coastal zones in exposed countries. *Storm surge damage* is the mean storm surge damage function of decade d averaged over the yearly data from d-9 to d in grid cell i, *Wind damage* is the mean decadal wind damage function of decade d averaged over the yearly data from d-9 to d in grid cell i, and *Rainfall* is the mean decadal tropical cyclones' rainfall (in mm) of decade d averaged over the yearly data from d-9 to d in grid cell i. All regressions include decade and grid fixed effects as well as country-specific linear trends.

Table 2.35: Robustness – country clustering

	Total population count	Rural population count	Urban population count
	(1)	(2)	(3)
Storm surge damage	-7,765	-2,155	-9,590
	(2,447.24)	(1,434.44)	(3,223.06)
	[0.00]	[0.14]	[0.00]
Wind damage	-10,324	-484	-10,122
	(7,256.51)	(3,248.08)	(5,885.59)
	[0.16]	[0.88]	[0.09]
Rainfall	-19	-.69	-15
	(19.84)	(12.28)	(10.28)
	[0.34]	[0.96]	[0.15]
Observations	343,805	343,805	343,805
Clusters	91	91	91
Mean dependent variable	10,973	5,641	7,206
SD storm surge damage	0.1128	0.1128	0.1128

Notes: Panel ordinary least squares regression results with clustered standard errors by country in parentheses (), and p-values in brackets []. The coefficients show the marginal effect of the different tropical cyclone damage types on the total, urban and rural population counts. The sample covers the decades from 1950 through 2010 for all low elevation coastal zones in exposed countries. *Storm surge damage* is the mean storm surge damage function of decade d averaged over the yearly data from d-9 to d in grid cell i, *Wind damage* is the mean decadal wind damage function of decade d averaged over the yearly data from d-9 to d in grid cell i, and *Rainfall* is the mean decadal tropical cyclones' rainfall (in mm) of decade d averaged over the yearly data from d-9 to d in grid cell i. All regressions include decade and grid fixed effects as well as country-specific linear trends.

Table 2.36: Robustness – Admin level 1 clustering

	Total population count	Rural population count	Urban population count
	(1)	(2)	(3)
Storm surge damage	-7,765	-2,155	-9,590
	(2,368.45)	(1,167.23)	(2,446.47)
	[0.00]	[0.07]	[0.00]
Wind damage	-10,324	-484	-10,122
	(6,014.90)	(2,795.89)	(5,766.01)
	[0.09]	[0.86]	[0.08]
Rainfall	-19	-.69	-15
	(18.16)	(11.39)	(12.27)
	[0.30]	[0.95]	[0.23]
Observations	343,805	343,805	343,805
Clusters	80	80	80
Mean dependent variable	10,973	5,641	7,206
SD storm surge damage	0.1128	0.1128	0.1128

Notes: Panel ordinary least squares regression results with clustered standard errors by administrative level 1 in parentheses (), and p-values in brackets []. The coefficients show the marginal effect of the different tropical cyclone damage types on the total, urban and rural population counts. The sample covers the decades from 1950 through 2010 for all low elevation coastal zones in exposed countries. *Storm surge damage* is the mean storm surge damage function of decade d averaged over the yearly data from d-9 to d in grid cell i, *Wind damage* is the mean decadal wind damage function of decade d averaged over the yearly data from d-9 to d in grid cell i, and *Rainfall* is the mean decadal tropical cyclones' rainfall (in mm) of decade d averaged over the yearly data from d-9 to d in grid cell i. All regressions include decade and grid fixed effects as well as country-specific linear trends.

Table 2.37: Robustness – Region clustering

	Total population count	Rural population count	Urban population count
	(1)	(2)	(3)
Storm surge damage	-7,765	-2,155	-9,590
	(3,709.30)	(1,942.56)	(5,116.83)
	[0.07]	[0.30]	[0.10]
Wind damage	-10,324	-484	-10,122
	(9,110.97)	(1,637.79)	(8,253.29)
	[0.29]	[0.78]	[0.25]
Rainfall	-19	-.69	-15
	(19.69)	(10.92)	(10.48)
	[0.36]	[0.95]	[0.19]
Observations	343,805	343,805	343,805
Clusters	9	9	9
Mean dependent variable	10,973	5,641	7,206
SD storm surge damage	0.1128	0.1128	0.1128

Notes: Panel ordinary least squares regression results with clustered standard errors by region in parentheses (), and p-values in brackets []. The regions are Central America and Caribbean, Eastern Asia, North America, Oceania, South-Eastern Africa, South-Eastern Asia, Southern Asia, and Western Asia. The coefficients show the marginal effect of the different tropical cyclone damage types on the total, urban and rural population counts. The sample covers the decades from 1950 through 2010 for all low elevation coastal zones in exposed countries. *Storm surge damage* is the mean storm surge damage function of decade d averaged over the yearly data from d-9 to d in grid cell i, *Wind damage* is the mean decadal wind damage function of decade d averaged over the yearly data from d-9 to d in grid cell i, and *Rainfall* is the mean decadal tropical cyclones' rainfall (in mm) of decade d averaged over the yearly data from d-9 to d in grid cell i. All regressions include decade and grid fixed effects as well as country-specific linear trends.

Table 2.38: Robustness – Affected area × decade clustering

	Total population count	Rural population count	Urban population count
	(1)	(2)	(3)
Storm surge damage	-7,765	-2,155	-9,590
	(2,995.80)	(996.37)	(4,448.75)
	[0.02]	[0.05]	[0.05]
Wind damage	-10,324	-484	-10,122
	(9,204.63)	(1,673.26)	(7,915.73)
	[0.28]	[0.78]	[0.22]
Rainfall	-19	-.69	-15
	(12.67)	(5.23)	(10.14)
	[0.16]	[0.90]	[0.17]
Observations	343,805	343,805	343,805
Clusters	14	14	14
Mean dependent variable	10,973	5,641	7,206
SD storm surge damage	0.1128	0.1128	0.1128

Notes: Panel ordinary least squares regression results with clustered standard errors by affected grid × decade in parentheses (), and p-values in brackets []. The coefficients show the marginal effect of the different tropical cyclone damage types on the total, urban and rural population counts. The sample covers the decades from 1950 through 2010 for all low elevation coastal zones in exposed countries. *Storm surge damage* is the mean storm surge damage function of decade d averaged over the yearly data from d-9 to d in grid cell i, *Wind damage* is the mean decadal wind damage function of decade d averaged over the yearly data from d-9 to d in grid cell i, and *Rainfall* is the mean decadal tropical cyclones' rainfall (in mm) of decade d averaged over the yearly data from d-9 to d in grid cell i. All regressions include decade and grid fixed effects as well as country-specific linear trends.

Table 2.39: Robustness – Non LECZ

	Total population count	Rural population count	Urban population count
	(1)	(2)	(3)
Storm surge damage	-987	312	-3,607
	(4,442.99)	(1,307.28)	(4,022.91)
	[0.82]	[0.81]	[0.37]
Wind damage	-5,163	-261	-5,279
	(3,767.70)	(1,961.78)	(3,414.24)
	[0.17]	[0.89]	[0.12]
Rainfall	1.6	.75	.13
	(14.73)	(10.14)	(9.33)
	[0.91]	[0.94]	[0.99]
Observations	3,838,212	3,838,212	3,838,212
Clusters	926	926	926
Mean dependent variable	3,313	2,152	1,826
SD storm surge damage	0.1128	0.1128	0.1128

Notes: Panel ordinary least squares regression results with clustered standard errors by affected grid × decade × country in parentheses (), and p-values in brackets []. The coefficients show the marginal effect of the different tropical cyclone damage types on the total, urban and rural population counts. The sample covers the decades from 1950 through 2010 for all non low elevation coastal zones in exposed countries. *Storm surge damage* is the mean storm surge damage function of decade d averaged over the yearly data from d-9 to d in grid cell i, *Wind damage* is the mean decadal wind damage function of decade d averaged over the yearly data from d-9 to d in grid cell i, and *Rainfall* is the mean decadal tropical cyclones' rainfall (in mm) of decade d averaged over the yearly data from d-9 to d in grid cell i. All regressions include decade and grid fixed effects as well as country-specific linear trends.

Table 2.40: Robustness – Coastal area of 50 km

	Total population count	Rural population count	Urban population count
	(1)	(2)	(3)
Storm surge damage	-2,350	-1,022	-4,534
	(1,659.25)	(972.30)	(2,189.66)
	[0.16]	[0.29]	[0.04]
Wind damage	-4,858	756	-4,918
	(5,428.84)	(1,648.54)	(5,108.02)
	[0.37]	[0.65]	[0.34]
Rainfall	-21	-1.5	-20
	(9.15)	(4.56)	(7.74)
	[0.03]	[0.75]	[0.01]
Area	Coastal 50 km	Coastal 50 km	Coastal 50 km
Observations	734,426	734,426	734,426
Clusters	845	845	845
Mean dependent variable	7,747	4,130	5,054
SD storm surge damage	0.1128	0.1128	0.1128

Notes: Panel ordinary least squares regression results with clustered standard errors by affected grid × decade × country in parentheses (), and p-values in brackets []. The coefficients show the marginal effect of the different tropical cyclone damage types on the total, urban and rural population counts. The sample covers the decades from 1950 through 2010 for coastal areas of 50 km in exposed countries. *Storm surge damage* is the mean storm surge damage function of decade d averaged over the yearly data from d-9 to d in grid cell i, *Wind damage* is the mean decadal wind damage function of decade d averaged over the yearly data from d-9 to d in grid cell i, and *Rainfall* is the mean decadal tropical cyclones' rainfall (in mm) of decade d averaged over the yearly data from d-9 to d in grid cell i. All regressions include decade and grid fixed effects as well as country-specific linear trends.

Table 2.41: Robustness – Coastal area of 100 km

	Total population count	Rural population count	Urban population count
	(1)	(2)	(3)
Storm surge damage	138	-104	-2,409
	(1,592.68)	(946.67)	(1,861.07)
	[0.93]	[0.91]	[0.20]
Wind damage	-3,895	1,062	-4,218
	(4,989.27)	(1,555.81)	(4,616.65)
	[0.44]	[0.49]	[0.36]
Rainfall	-22	-4	-21
	(9.39)	(4.82)	(7.22)
	[0.02]	[0.41]	[0.00]
Area	Coastal 100 km	Coastal 100 km	Coastal 100 km
Observations	1,041,852	1,041,852	1,041,852
Clusters	847	847	847
Mean dependent variable	6,811	3,779	4,312
SD storm surge damage	0.1128	0.1128	0.1128

Notes: Panel ordinary least squares regression results with clustered standard errors by affected grid × decade × country in parentheses (), and p-values in brackets []. The coefficients show the marginal effect of the different tropical cyclone damage types on the total, urban and rural population counts. The sample covers the decades from 1950 through 2010 for coastal areas of 100 km in exposed countries. *Storm surge damage* is the mean storm surge damage function of decade d averaged over the yearly data from d-9 to d in grid cell i, *Wind damage* is the mean decadal wind damage function of decade d averaged over the yearly data from d-9 to d in grid cell i, and *Rainfall* is the mean decadal tropical cyclones' rainfall (in mm) of decade d averaged over the yearly data from d-9 to d in grid cell i. All regressions include decade and grid fixed effects as well as country-specific linear trends.

2.6.4 Additional Tables

Table 2.42: Summary Statistics – LECZ global sample

	Observations	Mean	St.dev.	Min	Max
Total population count	343,805	10,973.10	41,039.03	0.00	2.22e+06
Rural population count	343,805	5,640.89	18,278.40	0.00	1.66e+06
Urban population count	343,805	7,206.26	37,787.83	0.00	1.76e+06
Storm surge damage	343,805	0.02	0.07	0.00	0.70
Wind damage	343,805	0.01	0.02	0.00	0.48
Rainfall (mm)	343,805	15.85	24.10	0.00	195.02
Storm surge water level (m)	343,805	0.15	0.43	0.00	7.34
Temperature (Degr. Celsius)	308,665	10.78	13.43	-27.61	30.95
Crop suitability	343,805	27.36	24.89	0.00	92.19

Table 2.43: Summary Statistics – LECZ in Central America and Caribbean

	Observations	Mean	St.dev.	Min	Max
Total population count	30,681	4,569.67	18,380.20	0.00	587916.00
Rural population count	30,681	1,692.46	5,870.93	0.00	242874.00
Urban population count	30,681	3,793.86	17,485.16	0.00	501164.00
Storm surge damage	30,681	0.03	0.06	0.00	0.58
Wind damage	30,681	0.01	0.03	0.00	0.19
Rainfall (mm)	30,681	30.44	21.75	0.00	128.71
Storm surge water level (m)	30,681	0.20	0.36	0.00	4.65
Temperature (Degr. Celsius)	30,681	10.73	9.61	-11.51	27.93
Crop suitability	30,681	32.91	25.89	0.00	92.19

Table 2.44: Summary Statistics – LECZ in Eastern Asia

	Observations	Mean	St.dev.	Min	Max
Total population count	36,771	36,944.01	71,789.49	2.00	1.69e+06
Rural population count	36,771	19,884.06	25,281.32	0.00	580450.00
Urban population count	36,771	24,296.98	73,694.44	0.00	1.63e+06
Storm surge damage	36,771	0.05	0.12	0.00	0.70
Wind damage	36,771	0.02	0.03	0.00	0.40
Rainfall (mm)	36,771	32.79	30.75	0.13	195.02
Storm surge water level (m)	36,771	0.32	0.72	0.00	5.27
Temperature (Degr. Celsius)	36,771	2.06	5.76	-11.99	22.45
Crop suitability	36,771	39.39	23.88	0.00	86.00

Table 2.45: Summary Statistics – LECZ in Europe

	Observations	Mean	St.dev.	Min	Max
Total population count	60,956	3,903.60	14,934.74	0.00	476189.00
Rural population count	60,956	810.19	3,462.80	0.00	161356.00
Urban population count	60,956	3,708.26	15,159.07	0.00	476189.00
Storm surge damage	60,956	0.01	0.03	0.00	0.37
Wind damage	60,956	0.00	0.00	0.00	0.05
Rainfall (mm)	60,956	0.71	2.08	0.00	26.61
Storm surge water level (m)	60,956	0.04	0.18	0.00	2.99
Temperature (Degr. Celsius)	33,236	-8.59	6.89	-26.88	10.13
Crop suitability	60,956	10.16	16.61	0.00	79.93

Table 2.46: Summary Statistics – LECZ in North America

	Observations	Mean	St.dev.	Min	Max
Total population count	53,585	4,601.67	23,271.81	0.00	1.13e+06
Rural population count	53,585	602.30	1,356.09	0.00	16,870.00
Urban population count	53,585	4,415.76	22,987.61	0.00	1.05e+06
Storm surge damage	53,585	0.02	0.06	0.00	0.63
Wind damage	53,585	0.01	0.03	0.00	0.31
Rainfall (mm)	53,585	17.83	22.64	0.00	116.54
Storm surge water level (m)	53,585	0.12	0.40	0.00	7.34
Temperature (Degr. Celsius)	46,165	-2.06	8.63	-27.61	21.57
Crop suitability	53,585	17.96	20.71	0.00	88.83

Table 2.47: Summary Statistics – LECZ in Oceania

	Observations	Mean	St.dev.	Min	Max
Total population count	38,591	1,740.56	8,662.71	0.00	258929.00
Rural population count	38,591	347.65	1,494.23	0.00	83,546.50
Urban population count	38,591	1,509.62	8,444.29	0.00	234084.60
Storm surge damage	38,591	0.02	0.07	0.00	0.70
Wind damage	38,591	0.00	0.01	0.00	0.20
Rainfall (mm)	38,591	13.78	20.97	0.00	136.80
Storm surge water level (m)	38,591	0.14	0.42	0.00	6.18
Temperature (Degr. Celsius)	38,591	21.42	5.65	-1.89	30.30
Crop suitability	38,591	28.67	21.91	0.00	84.00

Table 2.48: Summary Statistics – LECZ in South-Eastern Africa

	Observations	Mean	St.dev.	Min	Max
Total population count	13,216	6,425.05	29,569.39	0.00	742390.00
Rural population count	13,216	3,757.05	19,084.41	0.00	476915.60
Urban population count	13,216	3,468.45	19,981.27	0.00	364403.20
Storm surge damage	13,216	0.05	0.12	0.00	0.69
Wind damage	13,216	0.00	0.01	0.00	0.13
Rainfall (mm)	13,216	19.21	23.59	0.00	120.12
Storm surge water level (m)	13,216	0.32	0.75	0.00	5.14
Temperature (Degr. Celsius)	13,216	22.87	4.53	-5.38	29.95
Crop suitability	13,216	24.55	21.35	0.00	89.00

Table 2.49: Summary Statistics – LECZ in South-Eastern Asia

	Observations	Mean	St.dev.	Min	Max
Total population count	77,658	10,834.79	43,900.83	0.00	2.22e+06
Rural population count	77,658	6,649.52	24,418.37	0.00	1.66e+06
Urban population count	77,658	6,086.03	34,795.95	0.00	1.73e+06
Storm surge damage	77,658	0.02	0.06	0.00	0.67
Wind damage	77,658	0.00	0.02	0.00	0.48
Rainfall (mm)	77,658	11.94	25.46	0.00	188.12
Storm surge water level (m)	77,658	0.14	0.39	0.00	5.11
Temperature (Degr. Celsius)	77,658	22.82	6.07	-8.72	30.95
Crop suitability	77,658	39.00	23.56	0.00	87.99

Table 2.50: Summary Statistics – LECZ in Southern Asia

	Observations	Mean	St.dev.	Min	Max
Total population count	25,536	29,907.36	69,553.50	0.00	1.92e+06
Rural population count	25,536	19,099.36	29,023.98	0.00	750183.20
Urban population count	25,536	15,627.33	67,768.59	0.00	1.76e+06
Storm surge damage	25,536	0.02	0.05	0.00	0.44
Wind damage	25,536	0.00	0.01	0.00	0.16
Rainfall (mm)	25,536	22.96	22.01	0.00	137.18
Storm surge water level (m)	25,536	0.12	0.31	0.00	2.64
Temperature (Degr. Celsius)	25,536	12.59	7.31	-10.83	28.65
Crop suitability	25,536	35.47	26.31	0.00	83.00

Table 2.51: Summary Statistics – LECZ in Western Asia

	Observations	Mean	St.dev.	Min	Max
Total population count	6,811	4,727.67	26,097.54	0.00	724493.00
Rural population count	6,811	1,092.83	3,187.95	0.00	61,983.00
Urban population count	6,811	4,299.10	25,825.23	0.00	634361.10
Storm surge damage	6,811	0.01	0.02	0.00	0.12
Wind damage	6,811	0.00	0.00	0.00	0.05
Rainfall (mm)	6,811	1.63	4.85	0.00	41.26
Storm surge water level (m)	6,811	0.03	0.09	0.00	0.72
Temperature (Degr. Celsius)	6,811	11.63	7.41	-8.73	26.35
Crop suitability	6,811	0.40	1.89	0.00	41.79

3 Disastrous Discretion – The Nonlinear Political Bias in U.S. Hurricane Relief

This chapter is joint work with Stephan A. Schneider.

Another version of this chapter has appeared as:

Schneider, S. A., & Kunze, S. (2021). Disastrous Discretion: Ambiguous Decision Situations Forster Political Favoritism. *KOF Working Papers No. 491.*

Abstract: Allocation decisions are vulnerable to political influence, but little is known about when politicians can use their discretion to pursue their strategic goals. We show the nonlinearity of political favoritism in an exogenous framework of U.S. disaster relief. Based on a simple theoretical model, we demonstrate that political biases are most pronounced when the need for a disaster declaration is ambiguous. Exploiting the spatiotemporal randomness of all hurricane strikes in the United States from 1965–2018, we find that presidents favor areas governed by their fellow party members when allocating disaster declarations. Our nonlinear estimations reveal that political influence varies immensely with respect to storm intensity. The alignment bias for medium-strength hurricanes exceeds standard linear estimates eightfold.

3.1 Introduction

Natural disasters constitute severe negative shocks for people in affected regions. But disasters also create opportunities for politicians. They can show their leadership skills in the light of a catastrophic event that attracts substantial public attention and may be able to use disaster relief as an instrument for strategic fund distribution. This raises concerns of political factors undermining an efficient allocation of disaster assistance.

In this paper, we use random spatiotemporal variation in physical hurricane intensities to identify a nonlinear political bias in U.S. federal disaster declarations. Previous analyses of various political-economic settings provide evidence for different forms of home-region favoritism (e.g., Burgess et al., 2015; Carozzi & Repetto, 2016; Gehring & Schneider, 2018; Hodler & Raschky, 2014) and increased government spending to politically aligned areas (e.g., Berry et al., 2010; Brollo & Nannicini, 2012; Curto-Grau et al., 2018; Fiva & Halse, 2016).[64] However, little is known about whether politicians generally act in a self-interested manner or whether only specific situations foster such behavior that results in the biased allocations that the literature observes. We argue that political-economic relationships are in fact nonlinear, being over-proportionally strong in ambiguous situations that allow politicians to make targeted use of their discretion (cf. Durante & Zhuravskaya, 2018; Hodler et al., 2010). Studying the political reaction to hurricanes, we show that the strength of the political bias in executive decision-making on whether to provide disaster relief depends on the degree to which a specific event presents a favorable opportunity for strategic behavior. To the best of our knowledge, this is the first empirical analysis that reveals how the strength of political favoritism in a distributive policy, such as public disaster relief, varies systematically with the severity of the respective situation.

Based on a simple theoretical model, we derive that political effects are only moderate when examining the average of all disaster events. However, in the case of medium-strength disasters, when public opinion on whether to provide aid is divided, political influence is substantially larger. These are the situations in which political actors are in a relatively

[64] In addition, evidence exists that governments favor areas with electorally more important constituents in their funding allocations (e.g., Kauder et al., 2016; Kriner & Reeves, 2015). Similarly, manifold evidence documents political biases and the existence of political budget cycles in the domain of foreign aid (e.g., Bommer et al., 2019; Dreher et al., 2019; Faye & Niehaus, 2012) and the Bretton-Woods-institutions (e.g., Eichenauer et al., 2020; Lang & Presbitero, 2018). Kuziemko & Werker (2006) and Dreher et al. (2009) show, for instance, that states with a temporary seat on the U.N. Security Council receive more U.S. aid and a higher number of World Bank projects respectively. Gassebner & Gnutzmann-Mkrtchyan (2018) find that countries voting in line with the United States are more likely to be given trade preferences.

better position to (mis)use their discretionary power. In contrast, biased behavior should not be politically affordable and thus not be prevalent if a disaster is either very weak or very strong: the allocation of disaster relief is unambiguously required in the latter case and clearly unwarranted in the former. Acting against the public opinion in such situations could be politically costly.

To test these propositions, we present an empirical assessment of all hurricane-related federal disaster declarations issued by U.S. presidents between 1965–2018. We analyze random shocks from hurricanes, whose physical damage we model by using fine-grid meteorological data. For every hurricane that hit the United States in our 54-year sample period, we apply a meteorological model to estimate the individual spatial destructiveness on a 1×1 kilometer scale. Focusing the analysis on U.S. hurricanes has both high socioeconomic relevance and several empirical advantages.

First, hurricanes are the most destructive natural disasters in the United States, with high economic relevance and substantial public attention. Within the last decade, hurricanes have been responsible for more than 50% of all disaster-related damage. The 2017 hurricane season has been the costliest in the United States to date: the three major hurricanes, Harvey, Irma, and Maria, alone caused 3,167 fatalities and USD 278 billion in damage.[65]

Second, the random trajectories and varying physical strengths of hurricanes at different locations make them an ideal object of research in our county-level analysis. Given different baseline risks between counties, for which we control by including county fixed effects and time trends, the timing, location, and severity of hurricane strikes are random and unpredictable (e.g., Aguado & Burt, 2015; Hsiang, 2010; Strobl, 2011).

Third, by combining new data on all causes of hurricane damage (wind speed, rainfall, and storm surge) with our political-economic framework, we are able to present new causal evidence on whether the U.S. disaster relief system provides relief to the regions most strongly affected or whether efficient allocation is actually undermined by political factors. We study the issuance of federal disaster declarations – a unilateral decision of the U.S. president in response to an exogenous shock (Gasper & Reeves, 2011). We focus on the president's binary choice to declare an event a disaster or not. A federal disaster declaration is the requirement for the provision of relief by the Federal Emergency Management Agency (FEMA). The

[65] The source for all numbers cited in this paragraph is as follows: https://www.ncdc.noaa.gov/billions/, last accessed August 6, 2020.

president does not decide the actual relief payment amounts, which FEMA bureaucrats determine during the recovery phase in the years to follow.[66]

To that end, we observe a quasi-experiment in which politicians are randomly selected by a stochastic natural process to react to a shock unpredictable in timing and location. Hurricanes trigger the political decision-making process. Since the hurricane season usually ends before major elections take place in November, all political factors are predetermined when the disaster strikes; for example, the governor of an affected state, who requests federal relief from the president, is either politically aligned or unaligned with the president. Based on the observed disaster intensity, the president must make a decision as to whether a federal disaster declaration is necessary. To capture the causal political alignment effect, our identifying assumption is that, conditional on location, year, time trends, and random hurricane strength, there exists no other explanatory factor that systematically explains both the changing political alignment status and the probability of a county receiving a disaster declaration.[67] Our data allow us to flexibly estimate heterogeneous political effects for different levels of disaster intensity. By interacting our political variable of interest with high-dimensional polynomial and semi-parametric hurricane intensity measures, we can test our hypothesis of a nonlinear political bias without making any strict functional form assumptions for hurricane damage or the unknown pattern of political influence.

Our results show that the probability of receiving a disaster declaration is significantly higher on average when the requesting governor and the president are co-partisans. However, the 2.7-percentage point increase we find on average for all storm intensities conceals the actual heterogeneity of the effect and underestimates its economic significance. Our flexible nonlinear estimations show that political factors are up to eight times more important for medium-strength disasters. The probability of observing a disaster declaration in an area with medium damage increases by up to 21 percentage points if the governor and the

[66] For details about the relief system, see Section 3.2.1 and Appendix 3.7.1. Data on the actual relief amounts paid out by FEMA for hurricane disasters are only available for a limited period starting in 1998. Similarly, we collected data on governors' declaration requests via a Freedom of Information Act inquiry from FEMA. However, the available time period is only 1992–2015. We show estimations using these data in the appendix. Both analyses yield insignificant results, but we do not see the results as conclusive due to the stark data limitations. We thus focus the analysis on actual declarations as the observable outcomes of the declaration process to assess the degree of political bias in disaster relief allocations. Regions affected by disasters also experience an influx of transfers other than disaster declaration funds. However, the influence of politics cannot be isolated when examining general social welfare payments, disaster loans, private donations or efforts by other non-profit organizations. These all play an important role in disaster response.

[67] To rule out remaining endogeneity concerns about the alignment status, we show that our results hold in subsamples of close election outcomes, where it is essentially random whether the incumbent governor is aligned or unaligned with the president.

president are from the same party. For low and extremely high wind speeds, the influence of political alignment is close to zero and insignificant. Taking the heterogeneous relationship into account, we calculate that the political alignment effect for hurricane-related disasters amounts to at least USD 500 million on average per year. In comparison, conventional average estimates from the related literature underestimate the economic magnitude by a factor of 3 to 5.

We document that other political factors are also highly influential for intermediate storm intensities and show further heterogeneities of the analyzed relationship. For instance, our results indicate that areas with low electoral support for the president's party receive fewer declarations and that the alignment effect is more pronounced for governors who have been elected with smaller margins. Using triple interactions, we analyze within- and between-year political relief cycles. We find that presidents are more likely to declare a disaster for storms occurring closer to elections in November.

The results hold in various alternative specifications, e.g., when including 10 lags of hurricanes or declarations, and when allowing a separate disaster intensity function for each state. We also restrict the analysis to various subsamples (excluding, for instance, individual decades or states, dropping observations with high leverage and outliers, and focusing on swing states and coastal counties). In addition to showing various robust alternative choices regarding conventional levels of one- or two-way clustering, we employ a randomization approach based on simulations with placebo-treatment allocations. Not relying on any parametric clustering assumptions, we can infer a positive relationship between declarations and political alignment for a broad range of intermediate wind intensities.

Our findings add to several strands of the literature. First, we contribute to the literature on the alignment bias in intergovernmental transfers. Various studies document this effect for different countries (e.g., Brollo & Nannicini 2012, for Brazil; Quinckhardt 2019, for Germany; Arulampalam et al. 2009, for India; Bracco et al. 2015, for Italy; Fiva & Halse 2016, for Norway; Curto-Grau et al. 2018, for Spain; and Larcinese et al. 2006, for the United States). While this literature establishes that alignment with the central government is an important political factor to understand biases in distributive politics 'on average', it remains unclear how this relationship varies in different situations and whether the described linear relationships in the literature are conclusive (see Lang & Presbitero, 2018). Our analysis provides the first systematic test for a nonlinear political bias. We show that specific constellations shape politicians' incentives so that some allocation decisions are prone to an alignment bias, while others are not.

Second, we thereby relate to the debate on whether and when politicians are effectively held accountable for their actions by the electorate (e.g., Balles et al., 2020; Besley & Burgess, 2002; Besley & Case, 1995; Christenson & Kriner, 2019; Snyder & Strömberg, 2010). Focusing on the importance of media attention, Durante & Zhuravskaya (2018) and Djourelova & Durante (2019) demonstrate how politicians time unpopular executive and military actions to days when public attention in the United States is diverted by other events. The novel approach of our analysis is that we do not refer to unrelated third events that divert public attention but that the treatment heterogeneity of the disaster itself creates a variety of situations that are more or less suitable for strategic political behavior. Our results correspond to the notion that politicians rather find it feasible to act in a politically biased fashion when they are not confronted with a situation in which the electorate clearly expects a particular action. Our theoretical model also establishes the role of public opinion as an important factor to control politicians' unilateral actions.

Third, in studying executive decision-making in the United States, we add to the literature on U.S. distributive politics. Existing studies find, for instance, that states with a higher vote share for the president in previous elections (e.g., Dynes & Huber, 2015; Larcinese et al., 2006), areas electing president's co-partisan House members (Berry et al., 2010; Kriner & Reeves, 2015), and those with Congress members who belong to the majority party (Albouy, 2013) receive more spending. Recent evidence from Bostashvili & Ujhelyi (2019) documents the existence of political budget cycles in U.S. highway spending.[68]

Previous studies on U.S. disaster declarations suggest that election-year cycles exist and that electorally more important or competitive states are favored in the allocation of disaster relief; however evidence on the existence of an alignment bias is mixed (see Garrett & Sobel, 2003; Gasper, 2015; Reeves, 2011). While these analyses cover 8 to 25 years, our county-level panel spans 54 years (1965–2018). Importantly, our approach differs from these analyses by modeling disaster intensity directly from fine-grid physical data instead of relying on

[68]Further evidence on political budget cycles mostly exists for developing countries and young democracies (Aidt et al., 2020; Brender & Drazen, 2008; Gonschorek et al., 2018; Shi & Svensson, 2006). Cole et al. (2012) and Besley & Burgess (2002) find, for instance, that Indian governments increase calamity relief and public food distribution in election years. However, Potrafke (2020) and Schneider (2010) find election-year shifts in budget composition toward more visible government expenditures in established democracies, Bjørnskov & Voigt (2020) show electoral cycles in state of emergency declarations after terrorist attacks, and Bohn & Sturm (2020) present evidence for dampening effects of expected economic downturns.

potentially endogenous reported damage estimates like, e.g., the frequently used SHELDUS or EM-DAT data. These data sets have several shortcomings. The damage data are self-reported or stem from insurance claims and governmental reports, which results in measurement bias. Furthermore, they include only disasters above a certain monetary threshold, which leads to incomplete coverage. Appendix 3.7.3 summarizes the criticism regarding the usage of reported damage data (see also Dell et al., 2014; Felbermayr & Gröschl, 2014; Gallagher, 2019). We overcome these issues by applying physical and meteorological data to proxy for hurricane damage directly, which allows for an exogenous identification of impacts on a fine-grid level.

Fourth, by applying the physical hurricane damage model, our contribution applies recent insights from the disaster impact literature in a political-economic framework. We thereby relate to studies on the effects of extreme weather events (e.g., Auffhammer, 2018; Bakkensen et al., 2018; Elliott et al., 2019; Kalkuhl & Wenz, 2020; Noy, 2009). This literature establishes the analysis of exogenous random weather shocks such as hurricanes in economics and studies their manifold socioeconomic consequences (Dell et al., 2012; Deryugina, 2017; Deryugina et al., 2018; Elliott et al., 2015; Felbermayr & Gröschl, 2014; Hsiang & Jina, 2014; Klomp, 2016; Kunze, 2021; Strobl, 2011, 2012). We advance the damage literature by using not only a selection of possible physical sources of hurricane damage but the entirety of them: wind speed, rainfall, and storm surge. Overall, spatial wind speed intensities remain the most important physical explanatory variable in our model since storm surge is only present at the coast and precipitation is highly localized. However, controlling for damage in a comprehensive way is useful to isolate political influence from objective factors of need for the issuance of a disaster declaration.

The disaster impact literature demonstrates that relief, prevention, and insurance are important to mitigate damage from natural disasters (e.g., Cohen & Werker, 2008; Davlasheridze et al., 2017; Healy & Malhotra, 2009). Hence, it is essential that these mechanisms function efficiently (e.g., Eichenauer et al., 2020; Klomp, 2016; Strobl, 2011). Our findings add to the understanding of the biased behavior of politicians in disaster relief allocation decisions. Learning more about these political-economic processes is crucial for designing better functioning mechanisms in the future.

The paper is structured as follows: after motivating our study by presenting a brief theoretical framework for the political economy of disaster relief allocation and deriving our main hypothesis, Section 3.3 describes our data. We explain the storm intensity measures and how we use them to model disaster severity. Subsequently, we outline our empirical strategy in Section 3.4. Section 3.5 contains the results from the empirical estimations and provides various sensitivity tests. The paper concludes with a discussion of the implications of our findings regarding the functioning of democratic control of politicians in general and the specific potential changes to the relief system that we propose.

3.2 Disaster Relief Allocation: A Political-Economic Framework

In this section, we describe the disaster declaration process and introduce a simple model for the president's rationale in allocating disaster relief. We use these to derive our main hypothesis of a heterogeneous political alignment bias. It relates to theoretical models on the political economy of fiscal federalism that account for interactions of different levels of government (e.g., Bracco et al., 2015; Curto-Grau et al., 2018; Dixit & Londregan, 1998; Geys & Vermeir, 2014). Our model is mainly based on Arulampalam et al. (2009) and Solé-Ollé & Sorribas-Navarro (2008), who assert that the central government can behave opportunistically by using its discretion in grant allocation to make politically motivated transfers to local governments. We adapt the structure of these models to the U.S. disaster declaration framework. Our model introduces the impact of natural disasters and the allocation of disaster relief.[69] Before presenting the model set-up, the following section briefly explains the system of federal disaster declarations in the United States (see also Appendix 3.7.1 for an in-depth discussion).

3.2.1 Disaster Declarations in the United States of America

The U.S. president has the executive power to declare a federal disaster, which results in the allocation of federal funds. The declaration process has been in place since 1950 and has "changed very little over time" (Lindsay & McCarthy, 2015, 20). It works as follows: if a natural disaster appears to overwhelm local and state capacities in an affected area, the

[69] The purpose of our model is to generate insights for the empirical framework of U.S. disaster declarations. However, the model could be developed further to be applicable to other types of aid or salient distributive policies that concentrate benefits in certain regions while being financed through general taxes. This applies, for instance, to international development aid, redistribution schemes intended to support economically weaker regions, or funds being allocated according to eligibility criteria, e.g., in the EU (see, e.g., Asatryan & Havlik, 2020; Budjan & Fuchs, forthcoming; Gehring & Schneider, 2018, 2020; Michaelowa et al., 2018).

state's governor can initiate a preliminary damage assessment and send an official disaster declaration request to the president.[70] Based on the information collected from the state, FEMA makes a recommendation to the White House, but it is solely at the president's discretion whether or not to declare the event a federal disaster (see, e.g., FEMA, 2017b). Presidents have wide discretionary power regarding under which circumstances and in which areas they declare a disaster and which requests they deny. Their decision does not require any explanation or justification (Reeves, 2011). The president issues a declaration to a specific state and explicitly lists the counties eligible for federal help.[71] Only contingent upon a presidential disaster declaration can FEMA initiate its work on site.

There exist two types of disaster declarations: emergency declarations, which are financially capped and intended to ensure a quick response, and major disaster declarations, which are more comprehensive and essentially release a potentially unlimited amount of money once they are issued. Disaster declarations can cover both public and individual assistance, under which individuals may, for instance, receive financial grants, temporary housing, unemployment benefits, or crisis counseling (see also Appendix 3.7.1). Crucially, FEMA determines the amount of financial assistance needed and decides which individuals or public entities in the declared area are eligible for relief.

The model that we present in the following section takes the interactions of the different levels of government into account and formalizes the unilateral decision-making of the president as well as the reaction of the electorate.

3.2.2 Theoretical Model

3.2.2.1 Model Set-Up and Theoretical Embedding

We study presidential disaster declarations in a two-party system where local governments can be aligned (A) or unaligned (U) with the federal government. Our model incorporates voters' electoral reactions to declarations accounting for their own utility and fairness concerns. As disaster relief is non-programmatic and connected to individual past events, we focus on

[70] To facilitate reading, we use the term "governor". However, tribal chief executives, the mayor of Washington D.C., and the heads of U.S. trust or commonwealth territories, have the same rights to request declarations.

[71] While the governor can propose counties for the disaster declaration, "the president [...] may choose to include some but not all of the counties recommended by the governor" (Sylves, 2008, 83–84). Notably, the president can even declare an emergency without a gubernatorial request when "he determines that an emergency exists for which the primary responsibility for response rests with the United States [...]" (McCarthy, 2014, 9).

retrospective voting.[72] We show that the declaration behavior of vote-maximizing presidents differs with the alignment status of the affected counties.

In our model, hurricanes with intensities $s_i \in [0, +\infty)$ randomly hit counties $i = \{1, ..., N\}$, with populations normalized to 1. The corresponding damage $h(s_i)$ is strictly increasing in s_i. U.S. presidents have the power to issue federal disaster declarations $D_i \in \{0, 1\}$ at the county level. Relief amounts $\psi h(s_i)$ for each declaration are determined by FEMA, where $\psi \in (0, 1)$ is the fixed share of damage mitigated due to disaster relief.

Disaster declarations are highly visible. They are usually accompanied by substantive public attention and media coverage, providing information to voters and thereby bringing the issue of disaster relief to the fore.[73] The fact that decisions regarding the issuance of disaster declarations are straightforward to understand and directly observable by voters distinguishes our study from related models in the literature where voters can only rate the indirect consequences of allocations or politicians' efforts (e.g., Arulampalam et al., 2009; Bracco et al., 2015; Geys & Vermeir, 2014; Hodler et al., 2010).

For simplicity, we assume that voters' electoral decisions are defined by only two criteria. First is a fixed ideological position X, which represents the ensemble of all other political preferences as a point on a one-dimensional spectrum (cf. Dixit & Londregan, 1998; Solé-Ollé & Sorribas-Navarro, 2008). The ideology spectrum in county i follows a single-peaked county-specific distribution with $X_i \in (-\infty; \infty)$. The respective cumulative distribution function $\Phi(X_i)$ is common knowledge. More negative values of X denote a stronger ideological bias of voters toward the party of the president.

Second, the voters' electoral decisions depend on the effect of federal disaster relief on their utility u_i. Various studies find that voters blame the government and punish incumbents if a natural disaster occurs (e.g., Cole et al., 2012). However, Gasper & Reeves (2011) show empirically that the electorate behaves 'attentively' and rewards politicians in elections for a vigorous disaster response, including federal disaster relief spending.[74] We incorporate these

[72] Regarding social transfers in general, voters react to both past spending (e.g., de La O, 2013; Levitt & Snyder, 1997; Manacorda et al., 2011) and future promises (Elinder et al., 2015).

[73] The media plays an important role as an intermediary in disaster assistance by communicating information to the electorate. Eisensee & Strömberg (2007) show that the amount of U.S. aid in response to a foreign disaster was higher over the 1968–2002 period if the disaster received more media attention. Strömberg (2004) demonstrates that U.S. counties with many radio listeners received more relief funds in new deal spending, and Besley & Burgess (2002) show that Indian governments spend more on relief in the case of food shortages in regions in which newspaper circulation is higher. While we do not explicitly model the media, our theory accounts for different levels of national public attention (cf. Durante & Zhuravskaya, 2018).

[74] See, for example, the evidence presented by Bechtel & Hainmueller (2011) for Germany, Cole et al. (2012) for India, Lazarev et al. (2014) for Russia, and Gasper & Reeves (2011) as well as Healy & Malhotra (2009) for

reactions by integrating disaster damage and relief in the voters' private utility function u_i with $u_i' > 0$ and $u_i'' < 0$:

$$u_i\Big(-h(s_i) \cdot \big(1 - D_i \cdot \psi\big) - \tau\Big). \tag{3.1}$$

Hurricane damage $h(s_i)$ decreases voters' utility. However, receiving a disaster declaration D_i mitigates hurricane damage by the factor ψ. Therefore, voters' private utility gain from a declaration in their county is strictly positive and increases with disaster intensity s_i. Relief is funded by lump-sum taxes $\tau = N^{-1} \sum_{k=1}^{N} \big(D_k \cdot \psi h(s_k)\big)$.

As shown by Alesina & Angeletos (2005), societies value redistribution more if they perceive that wealth outcomes are, to a larger extent, determined by luck. Furthermore, experimental and empirical evidence demonstrates that voters consider social and fairness concerns in their preferences for redistributive policies, such as disaster relief (Bechtel & Mannino, 2017; Durante et al., 2014; Meya et al., 2020). To account for this, we introduce a fairness component $f_i = \alpha \sum_{j=1, j \neq i}^{N} \big(D_j \cdot (s_j - \underline{s})\big)$, by which voters assess declarations to all other counties. The threshold $\underline{s} > 0$ is the disaster strength above which voters start to support relief provision to another county. The smaller the difference $s_j - \underline{s}$, the smaller is the potential electoral reward or punishment from voters outside county i. Finally, α>0 denotes the relative importance of fairness considerations or the strength of the national public opinion.

Based on this and taking the voters' ideological positions X_i into account, voter i decides to vote for the party of the president if

$$u_i + f_i \geq X_i. \tag{3.2}$$

In general, however, presidential disaster declarations are preceded by a governor's request. We assume that voters also account for the local governor's efforts and attribute some share of the utility gain from disaster relief to the governor's party. That is, if the governor is politically unaligned with the president, the president's party might capture less of the voters' reward for a declaration, even in a federal election (cf. Curto-Grau et al., 2018; Geys & Vermeir, 2014). Therefore, we define θ as the amount of 'vote leakage' (Arulampalam et al., 2009; Solé-Ollé & Sorribas-Navarro, 2008), i.e., the share of voter goodwill that the party

the U.S. A recent reanalysis of Gasper & Reeves (2011) by Gallagher (2019) finds no evidence for attentive behavior of the electorate after applying corrections to the data used (see also our discussion about the shortcomings of reported damage data in Appendix 3.7.3).

of the president does not receive.[75] In unaligned counties, the electorate's support for the president's party is then defined as

$$(1-\theta)u_i + f_i \geq X_i + \theta u_i. \tag{3.3}$$

If the state government and the president happen to be aligned, there is no 'vote leakage' to the opposition party ($\theta = 0$). The expression simplifies to Equation 3.2, and the president's party captures the entire electoral benefit from a declaration.

In practice, $\theta > 0$ represents the conflicting incentives that presidents face when declaring a disaster in an unaligned county. Neither governors nor presidents can be assumed to willingly offer a stage for the opposing party to claim the benefits of disaster relief, but they would also want to benefit from the electoral reward of a declaration themselves. In the aligned case ($\theta = 0$), incentives to support co-partisans are manifold as politicians need them to follow through with their political agenda or to defend their political legacy (Alesina & Tabellini, 2007). Particularly for upcoming election campaigns, where key aligned politicians act as major endorsers and campaigners for their parties' candidates, it is important to strengthen their own political team and alliances (cf. Ansolabehere & Snyder, 2006; Carozzi et al., forthcoming; Zudenkova, 2011).

In summary, the president faces two different voter reaction functions when deciding on disaster declarations for aligned (A) and unaligned counties (U):

$$\hat{X_i^A} = u_i + f_i \geq X_i \tag{3.4}$$

$$\hat{X_i^U} = (1-2\theta)u_i + f_i \geq X_i. \tag{3.5}$$

$\hat{X_i^A}$ and $\hat{X_i^U}$ are the thresholds below which all voters vote for the party of the president. By issuing a disaster declaration, the president can shift $\hat{X}_i$. Thus, presidents' decisions can alter the number of votes for their parties by making some voters with ideological positions close to the threshold change their vote decision. The degree to which a disaster declaration shifts

[75]We focus the analysis on presidents, who have the declaration decisions in all counties at their disposal. As we assume that local governors only care about the utility of their own constituents, they always have an incentive to request disaster relief (cf. Carozzi & Repetto, 2016; Weingast et al., 1981) We restrict the analysis to the case where $\theta \in [0, 0.5]$. Values > 0.5 (i.e., the governor's party capturing more benefits from a presidential declaration than the presidents themselves) would imply reversed incentives for the president as the marginal utility of declarations becomes negative in unaligned counties (Solé-Ollé & Sorribas-Navarro, 2008).

$\hat{X}_i$ depends on various factors. It will for instance take a larger shift to the right if hurricane intensity s is higher and if the respective governor is politically aligned.

3.2.2.2 Model Solution and Implications

We assume that presidents maximize the electoral support for their party across all counties using the following objective function:

$$\max_{D_m^A, D_n^U} \sum_{m=1}^{N^A} \Phi(\hat{X}_m^A) + \sum_{n=1}^{N^U} \Phi(\hat{X}_n^U), \tag{3.6}$$

where $D_1^A, ...D_{N^A}^A$ and $D_1^U, ..., D_{N^U}^U$ are the $N = N^U + N^A$ declaration decisions in all aligned (A) and unaligned counties (U). The first-order conditions (FOCs) of this optimization are the *ceteris paribus* differences in electoral support for the president from issuing a declaration in county i. To simplify the notation in this discrete optimization, we write the FOCs as $\Delta\Phi_i^A = 0$ and $\Delta\Phi_i^U = 0$, respectively.[76] To isolate the alignment effect, we assume that the distribution function Φ and voter preferences u_i are equal in aligned and unaligned counties.

Based on the FOCs, presidents decide to declare a disaster in all counties where they receive a positive electoral response. Due to the fairness component, presidents only receive positive support from declarations for hurricanes with damage $h(s_i) > h(s^*)$. *Ceteris paribus*, this critical hurricane intensity threshold s^* however differs between aligned (A) and unaligned counties (U). The utility increase from a declaration for voters is higher the more severe the destruction $h(s_i)$ is. Due to vote leakage, the president receives a higher reward for issuing a declaration for the same hurricane intensity in aligned counties compared to unaligned counties. Therefore $s^{*U} > s^{*A}$ is required so that $\Delta\Phi^A = \Delta\Phi^U = 0$ holds with any $0 < \theta < 0.5$. The critical hurricane strength above which it is beneficial for the president to issue a disaster declaration is higher for unaligned counties than for aligned counties.

To evaluate when the alignment bias – the difference between s^{*U} and s^{*A} – is higher, we discuss the other relevant parameters in the model. First, the alignment bias is stronger when the amount of vote leakage θ is higher. Second, if fairness considerations α are stronger, voters weight the effects on inhabitants of other counties relatively higher. A stronger public opinion undermines the strength of the alignment bias (cf. Besley & Burgess, 2002; Durante

[76] $\Delta\Phi^A$ and $\Delta\Phi^U$ are short notations for $\Delta\Phi_i^A = \Phi\big(u_i(D_i = 1, s_i) + f_i\big) + (N-1)\cdot\Phi\big(u_{-i} + \alpha(s_i - \underline{s}) + \alpha\sum_{j=1,j\neq -i}^{N} D_j(s_j - \underline{s})\big) - \Phi\big(u_i(D_i = 0, s_i) + f_i\big) + (N-1)\cdot\Phi\big(u_{-i} + \alpha\sum_{j=1,j\neq -i}^{N} D_j(s_j - \underline{s})\big)$ and $\Delta\Phi_i^U = \Phi\big((1-2\theta)u_i(D_i = 1, s_i) + f_i\big) + (N-1)\cdot\Phi\big(u_{-i} + \alpha(s_i - \underline{s}) + \alpha\sum_{j=1,j\neq -i}^{N} D_j(s_j - \underline{s})\big) - \Phi\big((1-2\theta)u_i(D_i = 0, s_i) + f_i\big) + (N-1)\cdot\Phi\big(u_{-i} + \alpha\sum_{j=1,j\neq -i}^{N} D_j(s_j - \underline{s})\big)$.

& Zhuravskaya, 2018; Snyder & Strömberg, 2010). Likewise, the alignment bias is weaker if the president is office-motivated to a lesser degree (cf. Hodler et al., 2010). Third, if there are fewer voters with strong ideologies, i.e., the distribution of Φ is narrower around zero, the potential electoral benefits from a declaration increase. There are more voters that switch their electoral decision due to a declaration.

Apart from the emergence of an average alignment bias, we derive the crucial refinement that certain constellations influence the incentives of election-motivated politicians such that some allocation decisions are susceptible to an alignment bias while others are not. For hurricanes with very high [very low] intensities, all affected counties unanimously receive [do not receive] a declaration. An alignment bias occurs only in counties that fall within an intermediate interval of disaster severity. In these cases, the president only declares a disaster if a county is aligned. This theoretical result corresponds to our hypothesis that political considerations in relief allocation only come into play for medium-strength disasters, i.e., when public opinion is not entirely for or against issuing a declaration. These are the situations in which politicians can make use of their discretion to pursue their strategic political goals. We test our theoretical result of a heterogeneous political bias in our empirical analysis.

3.3 Data

3.3.1 Hurricane Data

Hurricanes are chaotic weather shocks that hit the United States in a season usually ranging from June to November each year.[77] Even 48 hours before landfall, the exact hurricane location is impossible to predict (Aguado & Burt, 2015; Rappaport et al., 2009), which is reflected in the chaotic behavior of hurricane raw tracks displayed in Panel a of Figure 3.1. In general, hurricanes have three major damage sources: wind, excessive rainfall, and storm surge along the coast. As wind intensity is highly correlated with the other two damage sources, it is common in the literature to use wind speed as the sole damage proxy (Hsiang, 2010; Kunze, 2021; Strobl, 2011). We additionally model damage using new rainfall and coastal flooding data to account for all possible hurricane damage. However, as rainfall is

[77]See Appendix 3.7.2 for details about hurricane genesis and impacts.

highly localized and storm surge occurs only in coastal counties, we utilize wind intensity as our primary damage variable while always controlling for the other two factors.

To model hurricane damage, we use meteorological data on wind speed from the International Best Track Archive for Climate Stewardship (IBTrACS) data set provided by the National Oceanic and Atmospheric Administration (Knapp et al., 2010) for the years 1965–2018. It contains data on all hurricanes, tropical storms, and tropical depressions collected from various weather agencies via satellites, ships, airplanes, or weather stations. The raw tracks data include six-hourly observations of the exact position, wind speed, and minimum sea pressure of each storm. However, the raw data tracks, as displayed in Panel a of Figure 3.1, have no information on the spatial size and destructiveness of hurricanes. To calculate spatial destructiveness, we apply Kunze's (Kunze, 2021) implementation of the meteorological CLIMADA model (Aznar-Siguan & Bresch, 2019), which generates spatially varying wind fields for each individual storm track in the sample at a resolution of 1×1 km.

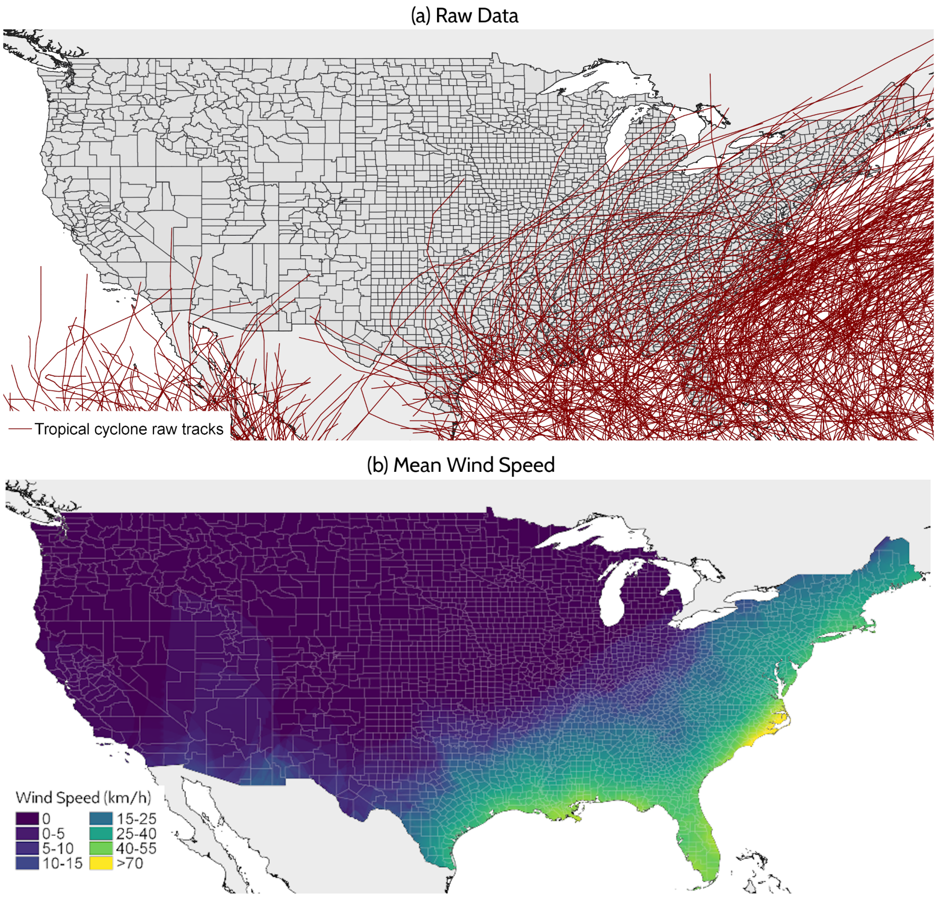

Figure 3.1: Hurricane raw tracks and modeled *Wind Speed* average, 1965–2018

Notes: Panel a displays the tropical cyclone raw tracks (red lines). Panel b shows the average annual *Wind Speed* exposure for the period 1965–2018 computed from our meteorological wind field model. The colors represent different average *Wind Speed* intensities, ranging from purple (0 km/h) to yellow (>70 km/h).

Appendix 3.7.4 describes the wind field model in more detail. In total, we have data on 275 tropical cyclones in our sample. Panel b of Figure 3.1 displays the average wind speed exposure over the 1965–2018 period, as derived from our wind field model.

The variable *Wind Speed* represents the maximum annual hurricane-related wind speed in each county. We thereby account for the most damaging hurricanes per county and year, which are responsible for the majority of catastrophic consequences and are established as a valid predictor of destruction and disaster declarations (Hsiang, 2010; Murnane & Elsner, 2012; Nordhaus, 2010; Strobl, 2011). Appendix Figure 3.29 shows the strong relationship between *Wind Speed* and the likelihood of observing a disaster declaration. The majority of counties has one hurricane event per year (66%). Around 22% have two events per year. To account for the possibility of multiple shocks, we include the yearly frequency of hurricanes in a robustness test for our estimation. Since the hurricane data are available at a higher time frequency than years, we also generate a variable that indicates the exact month for the strongest hurricane per county-year observation. In comparison to other political-economic studies, the usage of the physical intensity data is a clear advantage. Older studies (e.g., Davlasheridze et al., 2017; Eisensee & Strömberg, 2007; Gasper, 2015; Healy & Malhotra, 2009; Reeves, 2011) rely primarily on reported damage data, such as SHELDUS or EM-DAT, which are prone to measurement errors, missing data, and endogeneity (Felbermayr & Gröschl, 2014; Gallagher, 2019; Kousky, 2014). We discuss their shortcomings in Appendix 3.7.3. We circumvent these problems by applying objective and exogenous physical intensity measures to model damage from hurricanes.

Figure 3.2 displays the annual variation of the *Wind Speed* variable at the county level. One can see that the exposure to hurricanes varies significantly over time. Given the nature of the wind field model, observations well below the common hurricane threshold of 119 km/h are present in our data for two reasons. First, the raw data include all tropical cyclones. In addition to hurricanes, the IBTrACS data set also covers less intense tropical storms and tropical depressions. Second, the wind field model computes wind intensities for the whole extent of the hurricane. Typically, the most intense wind speeds occur around the eyewall, at the center of the hurricane, while wind speeds decrease when moving further away from the center. To show the robustness of our approach, we also calculate specifications without less intense tropical cyclones and with a specific hurricane damage function proposed by Emanuel

(2011), which uses a specific functional form with a lower bound cut-off value (see Appendix 3.7.4).

To also account for the two remaining damage sources of hurricanes, namely, storm surge and rainfall, we control for their influence in all our specifications. We use the newly developed storm surge data set by Kunze & Strobl (2020) to generate the maximum inundation level (in meters) per county and year (*Storm Surge*). The data set is based on a hydrodynamic model that generates one-hourly water level maps at the coast for all tropical cyclones recorded in the IBTrACS data set (Knapp et al., 2010). In addition, we also control for hurricane-related *Rainfall*, which is another cause of hurricane damage (Bakkensen et al., 2018). Unlike wind speed, precipitation does not decrease steadily when moving away from the storm's center. Our variable captures the maximum total rainfall (in mm) collected from weather stations during individual hurricanes in affected counties. We construct the *Rainfall* variable from the raw data of Roth (2018). The special feature of our rainfall data is that they solely capture daily precipitation from hurricanes at exact coordinates. *Rainfall* thus accounts for the maximum hurricane-related precipitation value per county and year.

3.3.2 Disaster Declarations

The raw data for our dependent variable *Declaration* originate from the openFEMA database (FEMA, 2019), which contains a county listing of all disaster declarations since 1965. Conse-

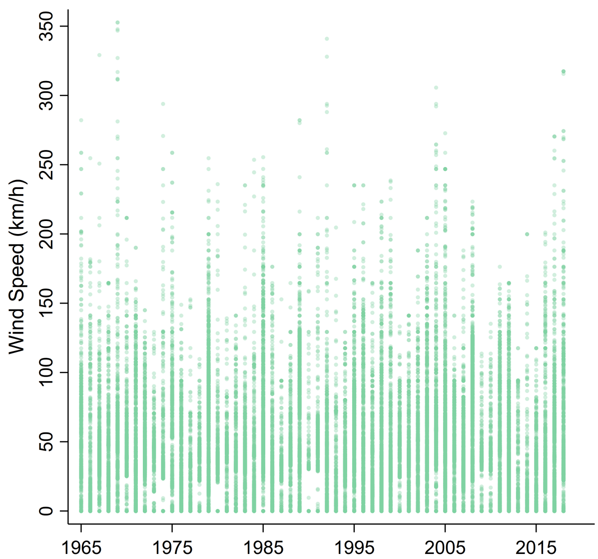

Figure 3.2: Yearly variation of maximum *Wind Speed* per county, 1965–2018

Notes: Each point in the figure represents one county-level *Wind Speed* observation over the period 1965–2018.

quently, our level of analysis is the county-year level. We construct *Declaration* as an indicator of 1, if a county received at least one hurricane-related disaster declaration in a given year and 0 if otherwise. Following Reeves (2011), we include both major disaster declarations and emergency declarations for our indicator.[78] We also present results with a separate indicator for emergency and major disaster declarations. In our data, 8,094 county-year observations received at least one *Declaration.* Furthermore, we collected information on disaster declaration denials by the president via a Freedom of Information request (2019-FEFO-00419) to FEMA. Unfortunately, data on rejected requests for hurricane disasters only cover the 1992–2015 period, with only 188 county-year declaration denials reported to us by FEMA in connection with tropical cyclones.[79] The variation is too small to infer any robust relationships, but for completeness we show results where we include data on FEMA requests in the Appendix (Table 3.11).

3.3.3 Political Variables of Interest

To assess the effect of governors and presidents being fellow party members, we construct the variable *Aligned Governor* based on data from Klarner (2013) and the National Governors Association. It takes a value of 1 if the president and the governor belong to the same political party and 0 if otherwise.[80] On average, the *Aligned Governor* status changes 10.7 times for an individual county during the 54 years of our sample. Analogously, we construct binary variables for congressional politicians' party affiliations (*Aligned Representative*) and for the two incumbent senators (*Aligned Senators*) of the state being co-partisans of the president.[81]

Additionally, we exploit data on past election outcomes to test further political channels. For instance, we create two indicator variables for high- and low-support districts. The

[78] In addition to declarations in the incident type category 'Hurricane', we include declarations from the categories 'Coastal Storm', 'Flooding', and 'Severe Storm(s)' if they contain a clear reference to a specific tropical cyclone in their title or can be matched via the date of occurrence to storms in our data set. We exclude the exceptional evacuation for Hurricane Katrina victims where all counties in the nation that hosted evacuees received a declaration despite not being affected by the hurricane. Only 2% of the county observations received more than one declaration per year. Using the number of declarations as a dependent variable might cause problems due to double-declarations for individual disasters (see Reeves, 2011). *Declaration* is not prone to these outliers. Nonetheless, we show results using the count variable *Declarations* (total annual number of declarations per county and year) in the Appendix.

[79] According to FEMA, this data set is complete with no deletions or exemptions.

[80] The variable indicates the party affiliation at the beginning of November (i.e., at the point of a potential presidential election). In case of independent governors we code it as 0.

[81] We further construct the variable *Party Alignment*, which counts how many of the aforementioned political actors are aligned with the president's party. We use election data to generate variables for party affiliations of incumbent House members. The data were provided by James M. Snyder. Previous versions of this data set are used in Hainmueller et al. (2015) and Eggers et al. (2015). To match voting district data from the House to individual counties, we apply a population weighting procedure. To code *Aligned Senators*, we use state-level election results from the CQ Voting and Elections Collection.

variable *High Support District* takes a value of 1 if the incumbent president's party gained more than 60% of the votes in the most recent election, and 0 otherwise. If it won less than 40% in the last election, the variable *Low Support District* is coded as 1. We also analyze close-election subsamples and how the alignment bias differs with respect to the margin of victory of the respective governors in the previous gubernatorial election.

We document all variables explained above, as well as further covariates and their sources, in Appendix 3.7.5. Observations in our data cover all counties from the contiguous United States if they have a positive value for *Wind Speed*, *Rainfall*, or *Storm Surge*.[82] The final panel data set consists of 85,309 county-year observations over the 1965–2018 period. As a robustness test, we also show results using a fully balanced panel including observations not affected by a hurricane in a specific year, which inflates the data set with zeros (see Figure 3.18). Table 3.1 shows descriptive statistics for the main variables used in the analysis (see Appendix 3.7.5 Table 3.3 for the full summary statistics).

3.4 Empirical Strategy

We analyze U.S. presidents' disaster declaration decisions after hurricanes hitting the United States. As Section 3.2.1 explains, presidents have the discretion to declare an event a disaster or not. We use a setting that allows us to identify systematic political biases in the declaration decisions.

Table 3.1: Summary statistics of main variables

	Observations	Mean	St.dev.	Min	Max
Declaration	85,309	0.08	0.27	0.00	1.00
Emergency Declaration	85,309	0.03	0.18	0.00	1.00
Major Declaration	85,309	0.06	0.24	0.00	1.00
Declarations	85,309	0.11	0.41	0.00	5.00
Aligned Governor	85,309	0.46	0.50	0.00	1.00
Aligned Representative	85,309	0.47	0.50	0.00	1.00
Aligned Senators	85,309	0.30	0.46	0.00	1.00
Alignment Count	85,309	1.94	1.25	0.00	4.00
Wind Speed	85,309	24.28	37.37	0.00	352.71
Rainfall	85,309	57.77	67.63	0.00	1,538.73
Storm Surge	85,309	0.04	0.27	0.00	6.01
Hurricane Month	84,947	8.38	1.35	5.00	11.00

[82] We exclude Hawaii, Alaska, and Washington D.C., and all U.S. overseas territories from the analysis due to their locations, lack of data availability or quality in the observation period, and their different political and electoral rights.

Previous studies document political influence in distributive politics. However, analyses of government spending often deal with various sources of endogeneity and uncertainty about the channels of the effect. What is often unclear is whether the observed favoritism is due to the politicians' direct actions or engagements in different forms of log-rolling. Usually, executive politicians can also control the timing of their decisions to a certain extent as part of an endogenous process. Political alignment biases have a mechanical explanation in that an incumbent's ideology is consistent with the spending preferences of the areas from which politicians receive the most electoral support and that are more often politically aligned.

Our strategy overcomes potential endogeneity issues by exploiting the fact that, conditional on location, hurricane incidence and severity are random (e.g., Dell et al., 2014; Deryugina, 2017; Kunze, 2021; Strobl, 2012). That is, we observe a quasi-experiment in which politicians are randomly selected by a stochastic natural process to react to a shock unpredictable in timing and location. Hurricanes trigger the political decision-making process (i.e., politicians cannot opt-out or postpone their decision). A current exogenous event prompts them to make a declaration decision given a current exogenous event. At this point in time, all political factors are predetermined; for example, the governor of an area hit by a storm is either aligned or unaligned with the president. An additional property of hurricanes is that the hurricane season ranges from June to November. It therefore typically ends before general elections take place in November, which could alter the alignment status, potentially causing reverse causality problems.

Furthermore, the shock that politicians face is characterized by highly heterogeneous treatment patterns. Hurricanes have different strengths, and, for each individual storm, damage can range from devastating (for areas hit by the eye of a hurricane) to very light (for those affected by outer bands of a storm system). This heterogeneity in the degree to which areas are affected corresponds to different levels of need for a declaration in each place. As explained in the previous section, we rely on the assumption that stronger hurricanes, *ceteris paribus*, cause more damage.[83]

It is evident that our estimation strategy can only work in a fixed-effects-within estimation framework. Locations differ in their exposure to hurricanes, for example, coastal counties in the Southeastern United States have a higher baseline risk of a tropical storm affecting

[83] To also account for the possibility that different levels of wind speed region-specifically correspond to different levels of damage and need for relief between locations (e.g., due to differences in wealth, infrastructure, etc.), we show that our results are robust to allowing separate damage proxies for each state in Appendix Figure 3.22.

them. Additionally, some counties might have a more vulnerable infrastructure or population than others. We account for such unobserved heterogeneities that are constant over time by including county fixed effects. Similarly, differences between years (e.g., due to extraordinary storm seasons), government administrations, national elections, and general technical improvements, can cause heterogeneities between years. Year fixed effects capture these differences. Additionally, some structural differences between locations may have changed over the course of our 54-year-long panel. For instance, climatic changes may have altered the baseline pattern of storm occurrence, mitigation efforts may have changed over time, or the vulnerability of the population may have changed. We thus allow for individual linear time trends for each county. Accordingly, the following least-squares equation represents the starting point for our analysis:

$$Declaration_{i,t} = \alpha + \beta Aligned\ Governor_{s,t} + \gamma Wind\ Speed_{i,t} + \boldsymbol{X}'_{i,t}\mu + \sigma_i + \tau_t + \sigma_i \times T_t + \varepsilon_{i,s,t}, \quad (3.7)$$

where *Declaration* is the binary indicator for disaster declarations received by county i in year t.[84] Our main variable of interest is the indicator *Aligned Governor*. Additionally, $\boldsymbol{X}_{i,t}$ represents the vector of further explanatory variables, including other potential hurricane damage sources such as *Rainfall* and *Storm Surge*, and the alignment statuses of the House representatives and senators (*Aligned Representative* and *Aligned Senators*). The equation contains county fixed effects (σ_i), year fixed effects (τ_t), and county-specific linear time trends ($\sigma_i \times T_t$). The error term is defined as $\varepsilon_{i,s,t}$. While the inclusion of further covariates might improve efficiency, we do not include socioeconomic controls that are themselves likely outcomes of the exogenous storm shocks (see, e.g., Dell et al., 2014). Nevertheless, we show in Appendix Table 3.7 and Figure 3.24 that our results do not change significantly when we add a vector of socioeconomic controls including county-level income, population, and race.

Throughout the analysis, our identifying assumption for the estimation of political influence is that, conditional on the location, year, time trends, and hurricane strength, no

[84] We estimate least-squares fixed effects within regressions using the `reghdfe`-command (written by Correia, 2017) in STATA. For robustness, Appendix Table 3.6 also shows maximum-likelihood estimates from conditional fixed effects logit and probit models. We also run Poisson and Poisson Pseudo-Maximum Likelihood (PPML) models using the number of *Declarations* as the dependent variable and controlling for the number of hurricane events in a year. Coefficients of *Aligned Governor* are positive and significant in all alternative models. Average partial effects from the logit and probit regressions are nearly the same size as the coefficients in the linear probability model.

other explanatory factor systematically explains both the political alignment status and the probability of a county to receive a disaster declaration. A remaining concern might be that political alignment is not the result of an exogenous process. To show that our results are not flawed due to any systematic correlations with unobserved factors, we run robustness tests that draw on close election outcomes. In situations where incumbent governors win the election by a very close margin, it is quasi-random whether the state they represent is politically aligned or unaligned with the incumbent president because the alignment status changes discontinuously at the 50% threshold (e.g., Brollo & Nannicini, 2012; Eggers et al., 2015; Pettersson-Lidbom, 2008). We document the robustness of our full-sample findings in subsamples defined by different closeness bandwidths (see Figure 3.5).

The baseline equation presented above takes a structural approach in modeling storm damage by assuming a linear relationship between *Wind Speed* and disaster declarations. This strict functional form assumption might be an acceptable proxy, but abandoning it has major advantages for our study. First, we can show that our results do not depend on any potentially erroneous functional form assumption and that they hold when disaster severity is modelled flexibly. Second, and most importantly, only dropping this static linear assumption, allows us to test our main hypothesis of heterogeneous political effects.

To account for nonlinearities in a flexible way, we introduce two approaches. First, we replace the linear *Wind Speed* variable with a *Wind Speed* polynomial ($\sum_{h=1}^{4} \gamma_h \, Wind\ Speed_{i,t}^{h}$). We additionally interact the entire polynomial with our political variable of interest (*Aligned Governor*). The equation then becomes:

$$\begin{aligned} Declaration_{i,t} = \alpha + \beta Aligned\ Governor_{s,t} + \sum_{h=1}^{4} \gamma_h Wind\ Speed_{i,t}^{h} \\ + \sum_{h=1}^{4} \left(\delta_h WindSpeed_{i,t}^{h} \times AlignedGovernor_{s,t}\right) + \mathbf{X}'_{i,t}\mu + \sigma_i + \tau_t + \sigma_i \times T_t + \varepsilon_{i,s,t}. \end{aligned} \tag{3.8}$$

We aim for a parsimonious baseline model in order not to inflate the regression unnecessarily with additional parameters, which allows us to analyze subsamples or to add further interactions. Based on a sequence of F-tests, we select a quartic *Wind Speed* polynomial for our baseline model. Note that our results are robust to including higher order polynomials up to the ninth degree (see Appendix Table 3.21).[85]

[85] To select a baseline for the *Wind Speed* polynomial, we run a sequence of F-tests for all possible choices in which we compare an unrestricted model including interacted *Wind Speed* polynomials up to degree n with a more restricted nested model with degree $n-1$. Using both backward and forward selection, we end up

The second approach is inspired by Schlenker & Roberts (2009) and Deschênes & Greenstone (2011): it models hurricane strength semi-parametrically by defining bins of wind speed $\sum_{j=1}^{10} \gamma_j \, \mathit{Wind\ Class\ j}_{i,t}$. These are dummy variables that indicate whether the respective observations of *Wind Speed* fall into a certain interval. Analogously to the polynomial approach, all dummy variables are then interacted with the political variable of interest. *Wind Speed* can hence flexibly affect the probability of a disaster declaration, and we can estimate a separate marginal effect of the interacted political factor for every wind intensity interval.[86]

To make use of the fine-grid variation of our hurricane and declaration data, we run disaggregated estimations at the county level. The main variable of interest, *Aligned Governor*, varies on the state level. However, disasters are declared for specific counties within states. The underlying standard error structure cannot be assumed to be independent across counties and years since hurricanes affect neighboring counties in a similar way, and declarations are issued in bundles of counties. Furthermore, a county's history of storms and declarations or its geographic location might induce autocorrelation. To be conservative regarding inference, all our estimations allow error correlation both within and between observations, and we cluster standard errors on the state × year and county level. For a discussion on applying two-way clustered standard errors see, for example, Cameron & Miller (2015). Appendix Table 3.4 and Figure 3.14 show that our results are robust to all possible conventional choices of clustering the standard errors, which include clustering at the county, county and year, year, state, state × year, hurricane, and hurricane × state level. Additionally, the results are also robust to arbitrary spatial heteroskedasticity and autocorrelation consistent (HAC) errors (Colella et al., 2019) that allow errors to be correlated within a 1,000 km radius and 10 years.

Furthermore, we calculate a permutation p-value based on a nonparametric inference method using placebo treatment allocation in the spirit of Chetty et al. (2009). Using this simulation, we can also calculate confidence intervals for the political effect at each wind speed without a parametric clustering assumption. None of the alternative inference methods

with a polynomial of the fourth degree. Higher order polynomials do not yield a significantly better fit to explain declarations. Appendix Table 3.8 shows the respective F-statistics. Note that we cannot simply rely on conventional damage functions or simpler functional forms used in the literature as we model the political effect of disaster declarations and not only, e.g., hurricane damage. Additionally, we particularly argue in our theoretical model that the political influence is nonlinear.

[86] The *Wind Speed* bins each consist of a 25 km/h interval between 0 and 225 km/h and one additional category representing all wind observations above 225 km/h. Zero *Wind Speed* observations are the omitted category (observations only treated with positive storm-associated rainfall). The only functional form assumption of this approach is that effects are constant within bins.

suggest that we falsely reject the null hypothesis in the broad intermediate range of wind intensities that we show the relationship to be robust for.

3.5 Results

3.5.1 Average Alignment Effects

Turning to the results, we first provide estimates for the average relationship of political alignment and disaster declarations. This approach adds to results on the alignment bias from the previous empirical literature but making use of our fine-grid hurricane data. Table 3.2 shows the results of six fixed effects regressions explaining the issuance of disaster declarations. All estimations include county and year fixed effects and use the entirety of the 85,309 county-year-observations affected by a hurricane from 1965–2018. Our estimations control for storm intensity directly. In all regressions, coefficients of *Wind Speed* and our additional *Rainfall* control are highly significant, explaining a large share of the overall variation in disaster declarations.[87] Notably, when comparing Column 1, which only includes the hurricane measures, with the other specifications in Table 3.2, neither the coefficient size nor the significance of the hurricane variables is affected by the inclusion of the political variables. A one standard deviation increase (approx. 39 km/h) raises the probability of a disaster declaration by about 7.5 percentage points.

The second column adds our main variable of interest, i.e., *Aligned Governor*. The estimated coefficient of 0.032 is highly significant with a p-value of 0.006. Standard errors in Table 3.2 are two-way clustered at the state × year and county level to account for both, error correlation of counties within a state and correlation within counties over time. The coefficient signifies that, *ceteris paribus*, counties have, on average, a 3.2 percentage points higher chance of receiving a disaster declaration if the president and the governor are aligned. The coefficient of *Aligned Governor* remains remarkably stable when including other political variables of interest. *Aligned Representatives* and *Aligned Senators* are also related to a higher probability of receiving a disaster declaration (Column 3). Unlike governors, representatives and senators are not directly involved in the process of requesting declarations. However, they

[87] *Storm Surge* is significant and positive in the first four columns but shows an insignificant coefficient close to zero once we include the *Wind Speed*-polynomial. While *Wind Speed* and *Rainfall* explain the variation of *Declaration* in all counties, *Storm Surge* is only an important factor in low-elevation coastal zones (see Section 3.3.1 and Kunze & Strobl, 2020). In addition, *Storm Surge* is highly correlated with higher orders of *Wind Speed*. We still include *Storm Surge* in all our regressions to capture all potential damage sources of hurricanes directly.

Table 3.2: Average regression results

Dep. Var.: *Declaration*	(1)	(2)	(3)	(4)	(5)	(6)
Aligned Governor		0.032	0.027	0.027	0.027	0.026
		(0.012)	(0.011)	(0.011)	(0.011)	(0.011)
		[0.006]	[0.020]	[0.011]	[0.013]	[0.014]
Aligned Representative			0.012	0.010	0.010	0.010
			(0.005)	(0.005)	(0.005)	(0.005)
			[0.017]	[0.054]	[0.054]	[0.048]
Aligned Senators			0.026	0.024	0.027	0.026
			(0.013)	(0.014)	(0.014)	(0.014)
			[0.045]	[0.091]	[0.060]	[0.066]
Wind Speed (St. Dev.)	0.075	0.075	0.075	0.074		
	(0.007)	(0.007)	(0.007)	(0.007)		
	[0.000]	[0.000]	[0.000]	[0.000]		
Rainfall (St. Dev.)	0.072	0.072	0.072	0.069	0.069	0.069
	(0.005)	(0.005)	(0.005)	(0.005)	(0.005)	(0.005)
	[0.000]	[0.000]	[0.000]	[0.000]	[0.000]	[0.000]
Storm Surge (St. Dev.)	0.032	0.031	0.031	0.030	-0.002	-0.002
	(0.010)	(0.010)	(0.010)	(0.010)	(0.009)	(0.009)
	[0.001]	[0.001]	[0.001]	[0.002]	[0.806]	[0.789]
Time Trends				X	X	X
Wind Speed Polynomials					X	
Wind Speed Bins						X
Observations	85,309	85,309	85,309	85,309	85,309	85,309

The table displays regression coefficients with two-way clustered standard errors on the state × year and county level in parentheses (Appendix Table 3.4 documents robustness toward alternative clustering choices). P-values are shown in brackets. All estimations use the linear fixed effect-within estimator and include county and year fixed effects (Appendix Table 3.6 shows the robustness of the results to using alternative estimations such as conditional logit and probit). *Wind Speed*, *Rainfall*, and *Storm Surge* are shown in standard deviation increases (above zero). Standard deviations for *Wind Speed*, *Rainfall*, and *Storm Surge* are 38.78 km/h, 68.17 mm, and 0.8 m, respectively. Models 4-6 include county-specific linear time trends. 'Wind Speed Bins' signifies the usage of the semi-parametric approach to model wind speed and. 'Wind Speed Polynomials' indicates the usage of quartic polynomials. The sample runs from 1965-2018 in all regressions.

also lobby the president, for example, by writing supporting letters for governors' requests.[88] Significance for the senators is lower than for the representatives. The latter represent smaller areas, making it more likely that their entire electoral district is affected.

In the fourth column of Table 3.2, we allow for the existence of county-specific time trends, which account for any structural changes affecting the baseline probability of a county receiving federal disaster relief. While the coefficient of our main variable of interest, *Aligned Governor*, stays at the same level and even increases its p-value (0.011), the estimates for the representatives and senators are somewhat weaker.

Although these first results support the evidence for an alignment bias 'on average' that other studies have documented, we rate these average estimates as insufficient to uncover the true pattern of political influence. The previous approach treats all situations as equal in terms of potential exertion of political influence. However, as our theory section (3.2.2)

[88]As Sylves (2008, 91) explains, "researchers have discovered in presidential library documents evidence that presidents considering a disaster declaration [...] receive, as a matter of routine, a list of the names of the lawmakers whose districts are affected by a disaster event."

outlines, we hypothesize that the strength of political effects is very heterogeneous and highly dependent on the situation facing politicians. Attempts to capture the alignment effect with a single parameter thus involve overly stark assumptions and simplifications. To solve this issue, we introduce two flexible approaches that do not impose a strict functional form assumption. This then allows us to determine individual alignment effects for each storm intensity.

Columns 5 and 6 form the basis for our flexible estimations. By including a quartic *Wind Speed* polynomial and 10 separate 25 km/h wind speed bins, respectively, the marginal effect of hurricane strength now varies for different levels of *Wind Speed*. While the average political effects remain unchanged in these estimations, we allow our political variable of interest to interact with the flexible hurricane measures to obtain separate estimates of political influence for the different storm intensities in the following section.[89]

3.5.2 Main Results: Heterogeneous Alignment Bias

Our fine-grid storm data allow us to drop the static assumption of a homogeneous political alignment bias. By interacting *Aligned Governor* with all factors of the *Wind Speed* polynomial (in the polynomial regression) and all individual *Wind Speed* bins (for the semi-parametric approach), we examine the alignment bias in a nuanced way and find a much more differentiated pattern of political influence.

Figure 3.3 demonstrates marginal effects of *Aligned Governor* for different levels of *Wind Speed*.[90] The marginal effects, both in the polynomial (solid green line) and the semi-parametric bin approach (dashed dark green line), take the hypothesized hump-shaped form. As expected, coefficients in the semi-parametric step-function vary more wildly, but the estimates are quantitatively similar. While point estimates are close to zero and insignificant for weak wind speeds, the marginal effects increase with storm intensity, becoming significant at the 95% confidence level at around 52 km/h (32 mph) in the polynomial estimation. These are typically non-catastrophic situations in which the president issues emergency declarations to ensure the functioning and quick repair of damaged crucial infrastructure or organize local evacuations. The highest alignment effects arise for 144 km/h (89 mph) in the polynomial

[89] To show the robustness of the average effects, we run several specifications. Appendix Table 3.5 includes a variable for past *Declaration* and past *Wind Speed*. Table 3.6 demonstrates that our results are robust to different regression model choices (logit, probit, Poisson, Poisson pseudo-maximum likelihood). Finally, our findings still hold when we include a set of lagged socioeconomic control variables covering logs of *Population*, *Black Population*, *Real Income*, and *Per Capita Real Income* (see Table 3.7).

[90] We calculate marginal effects and standard errors using the `predictnl`-command in Stata. Marginal effects for *Aligned Governor* are derived from the main effect and the *Wind Speed*-interactions ($\beta + \delta_1\,Wind\ Speed + \delta_2\,Wind\ Speed^2 + \delta_3\,Wind\ Speed^3 + \delta_4\,Wind\ Speed^4$).

and the 125 km/h (78 mph) to 150 km/h (90 mph) interval in the semi-parametric approach. At its maximum, the estimated marginal effect is 0.21. This is about eight times higher than the average relationship from Table 3.2, which underlines the scope of heterogeneity present in political effects. Marginal effects decrease again for stronger wind speeds, turning insignificant for observations higher than 192 km/h (119 mph).

The importance of accounting for the distinct heterogeneity of the relationship becomes evident when making a rough calculation of the associated relief payments. Using the predicted amount of disaster relief in a county for a certain storm strength, its probability distribution and the previously calculated nonlinear political alignment effect, we calculate that the political component of hurricane relief amounts to roughly USD 500 million per year. This corresponds to about 13% of the total hurricane relief paid out by FEMA. Note that this figure only contains FEMA's public assistance and individual assistance but no other spending categories such as, e.g., hazard mitigation. Our calculation is therefore a lower-bound estimate. A holistic approach to quantify the total political bias would need to also include, for instance, the difference in long-term costs due to the presence or absence of initial relief and potential indirect costs (cf. Davlasheridze et al., 2017; Deryugina, 2017).

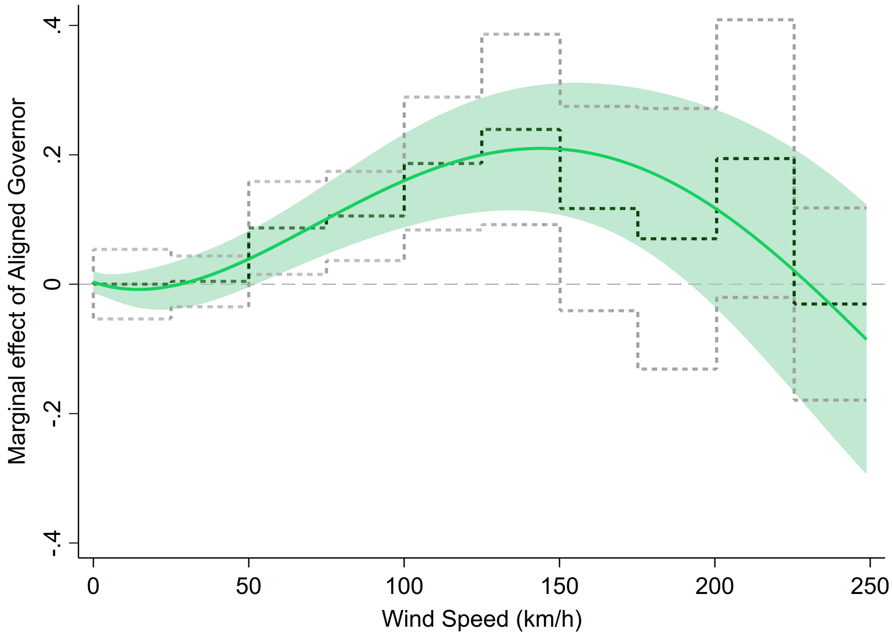

Figure 3.3: Alignment bias for different levels of *Wind Speed*

Notes: The figure displays marginal effects of *Aligned Governor* for different levels of *Wind Speed*, derived from the polynomial estimation (solid green line) and the semi-parametric approach (dashed dark green line). The light green shaded area and the dashed gray lines represent 95% confidence intervals applying two-way clustered standard errors on the state × year and county level. The sample covers 85,309 county-year observations from 1965–2018.

Notably, if we used the constant alignment effect for all disasters from Table 3.2, the resulting political relief would only add up to USD 100 million, about one-fifth of the result we obtain with our nonlinear model.

To better understand the economic significance of our heterogeneous political alignment effect, we draw a comparison to the political economy literature on the allocation of U.S. federal spending. Analyzing a wider range of federal funds, Larcinese et al. (2006) report a 2.7% increase due to gubernatorial alignment with the president. Albouy (2013), Berry et al. (2010), and Kriner & Reeves (2015) all find increases in the order of 4% for aligned federal politicians in high-variation government spending programs. Although accurate comparisons of studies are impossible due to the different spending categories, our average estimate indicates a similar magnitude (see Table 3.2). However, if we account for the nonlinear nature of the relationship, we find a substantially higher political and economic relevance.

The results demonstrate that the alignment bias is in fact negligible when locations experience very weak or extremely strong wind speeds. It seems hardly possible for a politician to declare an event a disaster if the impact was not destructive, even if party politics yield incentives to do so. Similarly, it seems politically impossible to deny a county a declaration in the case of a catastrophic hurricane impact. However, the middle of the wind speed spectrum shows where presidents use their discretionary power to declare disasters. Counties experiencing such wind speeds typically are counties not hit by the eye of the respective hurricane but are still affected by its wind field, rainfall, and potential flooding, thus resulting in damage to property. These situations leave political actors with the most leeway: if the president is undecided about whether to declare a disaster because a county experienced intermediate damage and either decision would be politically justifiable, the importance of party affiliation increases and more likely becomes the factor to tip the scales.[91]

Despite the length of our 54-year sample period, the number of hurricane events is limited. We conduct a resampling-based randomization inference to show the robustness of our findings

[91] The focus of our contribution is on the alignment bias in declaration decisions. It is also relevant but beyond the scope of our paper to evaluate to what degree politicians actually benefit from issuing declarations (see previous studies by Gasper & Reeves, 2011; Healy & Malhotra, 2009; Reeves, 2011). In Appendix Figure 3.30, we provide correlational evidence in line with their findings. This is naturally a noisy and inconclusive estimation because we only cover one disaster type, and many other relevant influences enter the vote decision within the four years of a presidential term. However, the figure shows that there exists a correlation between issuing a declaration and the change in the president's county vote share in the next election. Being negative and insignificant for weak wind intensities, the relationship is positive and significant for strong hurricanes. If presidents do not issue a declaration for intense disasters, they lose votes. Qualitatively, this result also fits our assumptions about voter behavior in the theory section, with declarations for higher wind intensities being associated with a higher electoral reward.

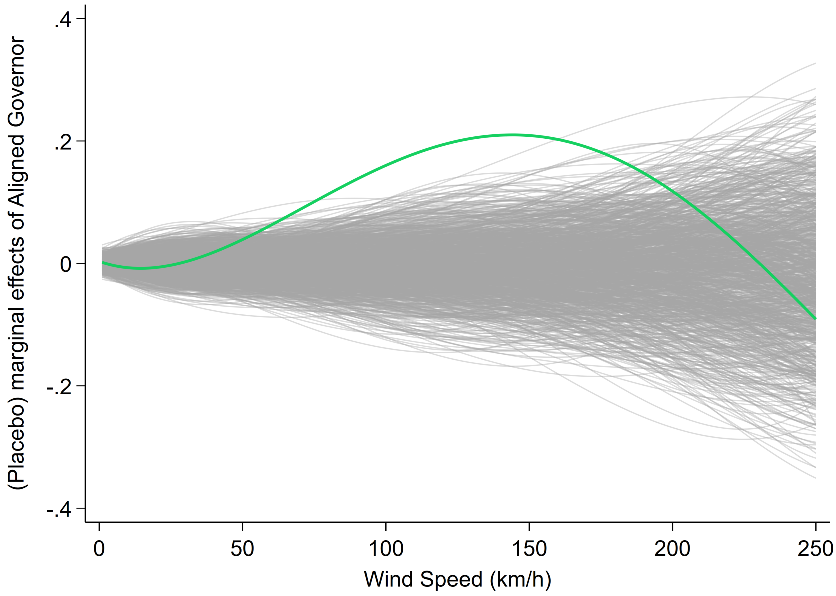

Figure 3.4: Randomization inference

Notes: The figure displays the estimated marginal effects using the true data in green. The gray lines represent marginal effects from each of the 1,000 regressions with the placebo treatments. Placebo-simulations were computed with our polynomial baseline regression. For each simulation run, we randomly reshuffle governor alignment status but kept the structure of the panel; i.e., we assign the same placebo treatment to all observations from a state within a year and we keep the total number of treatments per state as in the original data. Appendix Figure 3.15 shows a graphical representation of the permutation p-value ($p_{perm.} = N^{-1} \sum_{i=i}^{N} 1[|\beta| < |\beta_{i,placebo}|]$).

beyond alternative conventional one- and two-way-clustering choices. Appendix Figure 3.14 documents this randomization. We run a simulation in which we randomly reshuffle the alignment status between years within each state (i.e., keeping constant the number of aligned years within a state and ensuring that all counties of a state still share the same alignment status in the same year). This randomization approach provides a way to validate that our distinct hump-shaped pattern does not arise from placebo allocations of political alignment. Figure 3.4 displays the estimated marginal effects from 1,000 regressions with the random placebo treatments in gray and the true alignment status in green for comparison. For intermediate wind speeds, all effects of the placebo-simulations fall short of exceeding the estimated marginal effects using the actual alignment status. For most simulated runs, the effect is close to zero for low and intermediate wind speeds. Extremely high values of *Wind Speed* are rare, and, therefore, the simulations fan out on the right. This larger spread represents the higher uncertainty of our estimate due to the lower frequency of high-intensity hurricanes (cf. Figure 3.2 and Appendix Figure 3.11).

Similar to the procedure for the synthetic control method that Abadie et al. (2015) propose, we can use the simulated coefficients for randomization inference and calculate a permutation p-value for our estimate at different levels of *Wind Speed*. To this end, we divide the number of runs for which the absolute value of the placebo alignment effect $\beta_{i,placebo}$ exceeds the estimates β using the true data at each *Wind Speed* by the total number of simulations N:

$$p_{perm.} = \frac{1}{N} \sum_{i=i}^{N} 1[|\beta| < |\beta_{i,placebo}|].$$

We hence obtain a permutation p-value for every *Wind Speed* level and can derive the 95% confidence interval therefrom (see Appendix Figure 3.15). Based on this randomization inference approach, *Aligned Governor* has a positive and significant effect in the *Wind Speed* interval [55, 190] km/h, which is very close to the interval [52, 192] km/h, that we received from applying conventional two-way clustering to the standard errors (see Figure 3.3).

3.5.3 Sensitivity and Robustness

Before analyzing further heterogeneities of the political mechanism, we study the robustness of our main result. The results of the polynomial approach are qualitatively similar when we use different polynomials. Appendix Figure 3.21 shows marginal effects for polynomials of the third degree to ninth degree. As derived in Section 3.4, we use the fourth-degree polynomial as a baseline. To ensure clarity of the graphical representation, the following multi-panel figures display marginal effects only for the fourth-degree polynomial approach given that all flexible estimations, including the semi-parametric approach, yield qualitatively similar results.

Despite the chaotic trajectories of hurricanes, which randomly select politicians to make a decision on disaster relief, a remaining concern for our identification is the endogeneity of the political-economic process that results in the alignment patterns we observe. It is therefore important to rule out any unobserved factors that systematically explain both alignment and declarations and are not yet captured by fixed effects, time trends, and controls, are eliminated from the equation. To deal with this concern, we study whether our results hold in situations where political alignment is quasi-randomly determined, i.e., in subsamples characterized by close electoral outcomes. A vast amount of literature has studied discontinuities due to electoral thresholds (e.g., Brollo & Nannicini, 2012; Curto-Grau et al., 2018; Eggers et al.,

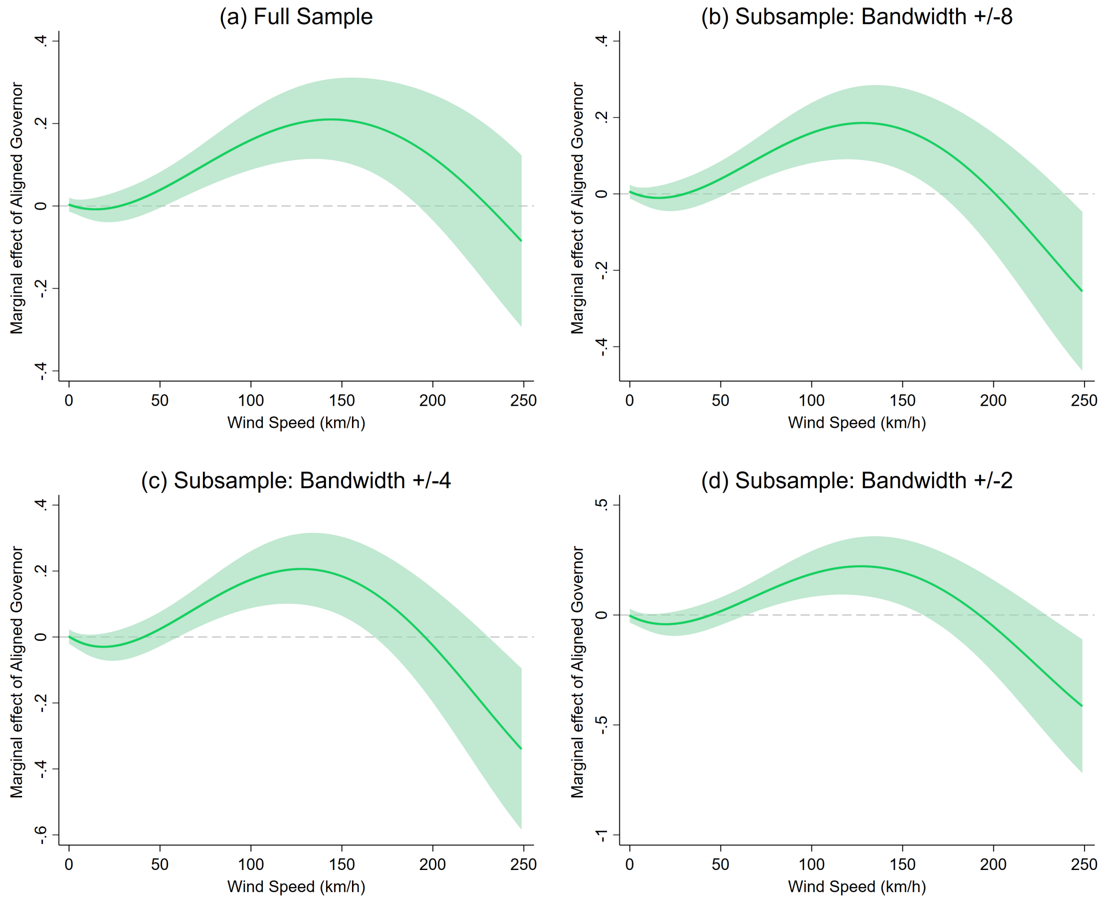

Figure 3.5: Robustness – Close election subsamples

Notes: This figure shows the sensitivity of our result in subsamples with different election-winning bandwidths. The light green shaded area represents the 95% confidence interval applying two-way clustered standard errors on the state × year and county level.

2015; Pettersson-Lidbom, 2008). In our case, political alignment changes if a politician from the opposite party wins one of the two offices. For instance, *Aligned Governor* discontinuously switches from 0 to 1 as soon as the candidate from the opposition party receives more votes in the election than the aligned incumbent governor. We can therefore use state-level electoral outcomes to define situations in which governors are just aligned or just unaligned with the president by a small margin.[92] Figure 3.5 shows the results for different bandwidths of close election outcomes. The results turn negative and insignificant for high wind speeds, but otherwise the results are not qualitatively different from what we obtain in the full sample.

[92]In addition to tight outcomes in gubernatorial elections, the U.S. winner-takes-all system in combination with the electoral college produces situations in which the electoral votes from one or few close states are pivotal for the outcome of the election; take, for instance, the 2000 Bush vs. Gore election outcome in Florida. We account for these quasi-random alignment outcomes when defining our respective close election subsamples. We assign observations either the margin of victory of the most recent gubernatorial election or the respective margin of victory from the closest state that would have tipped the respective presidential election if this margin was closer. The broader the bandwidth (defined as half the margin of victory) chosen to define the closeness samples, the more observations the sample includes.

Similarly, we test how the alignment bias differs with regard to how close a governor won the previous election. Presidents might behave more generously in providing declarations to medium-affected counties if they think their co-partisan governor needs an additional boost to secure reelection. Analogously, governors might also request more relief in these situations. Based on past statewide election outcomes, we split the alignment variable into four dummies defined by different gubernatorial margins of victory. Figure 3.6 shows that the relationship tends to be stronger for governors with narrower margins of victory. While the alignment effect arises in all instances, it is significantly positive in a broader *Wind Speed* range for governors who faced more competitive elections.[93]

The main estimation approach assumes that a certain level of wind speed corresponds to equal need for a disaster declaration at each location. However, it is possible that regions with a higher hurricane frequency might be more resilient to higher wind intensities. To demonstrate that our results do not depend on the assumption of a nationwide uniform resilience level, we allow separate *Wind Speed* effects for each state. Panel a of Appendix Figure 3.22 shows that the marginal effect estimates of our main specification remain essentially unchanged.

As different regions may have developed in divergent ways over the course of our 54-year panel, we want to control for the possibility that this factor influenced our findings. We employ county × decade fixed effects to account for within-county changes over time in a more flexible way than using linear time trends. This specification results in a slightly wider confidence interval (see Panel b of Appendix Figure 3.22).

The chaotic nature of hurricanes can result in wildly erratic treatment patterns, and one might be concerned that particular states or time periods drive our results. To alleviate these reservations, we run 48 regressions, each excluding all observations from one individual state at a time. Panel a of Figure 3.16 exhibits that dropping individual states in no case results in a major difference from the baseline. We apply the same approach to individually omit each of the six decades that our data cover. Likewise, the result is robust to excluding individual decades. However, the most recent decades seem to affect the results more. This outcome is not surprising since the introduction of the Stafford Act in 1989 and the integration of

[93]In Appendix Figure 3.20, we restrict the analysis to a subsample of states where there was a switch of the party receiving the majority of the statewide votes in one of the last three presidential (Panel a) or gubernatorial elections (Panel b). In Panel a, the peak of the alignment effect shifts to a somewhat higher *Wind Speed*, but otherwise the relationship in swing states is not significantly different from what we find for the full sample.

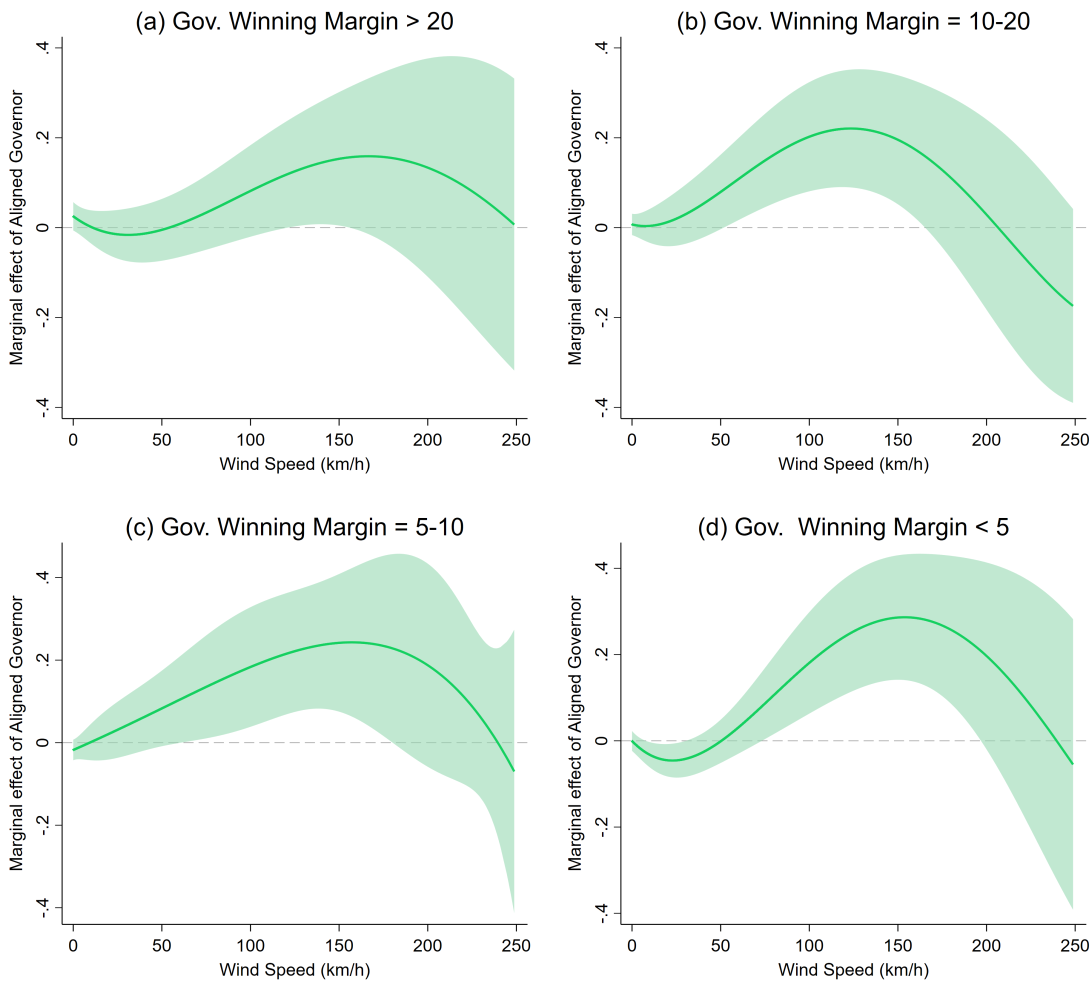

Figure 3.6: Alignment effects for Governors with different margins of victory

Notes: This figure illustrates how the alignment effect depends on the margin of victory (MOV) of the requesting governors. The solid green lines in the four panels display marginal effects of separate *Aligned Governor* indicators (depending on the margin of victory) from one joint regression. Panel a shows the marginal effect of *Aligned Governor* if the governor's statewide MOV in the previous election was larger than 20 percentage points; Panel b shows if the MOV was between 10 and 20 percentage points; Panel c indicates if the MOV was between 5 and 10 percentage points; and Panel d shows if the MOV was smaller than 5 percentage points. The light green shaded area represents the 95% confidence interval applying two-way clustered standard errors on the state × year and county level.

FEMA into the Department of Homeland Security (in 2003) were reforms that gave more power and discretion to the president.

Coastal counties are generally more strongly affected by hurricanes and face the additional hazard of storm surges. To test whether the relationship is driven by counties that face a higher baseline risk of hurricane strikes, we split the sample into coastal and non-coastal states. We use the definition of coastal watershed counties from NOAA, excluding non-Atlantic and non-Gulf counties in accordance with Strobl (2011). Appendix Figure 3.18 shows that the political bias is significantly positive in both samples but is in fact stronger in non-coastal counties. For almost all hurricanes, non-coastal counties experience less damage than coastal counties. The coast thus receives the most public attention regarding the event, and politically driven relief allocation is less feasible there. However, the president can include more inland counties in the disaster declaration and base this decision partly on partisan considerations.

We run a series of further robustness tests. If we restrict the sample to cover only emergency declarations or the more comprehensive major disaster declarations (see Appendix Figure 3.17), the maximum marginal effect for major declarations corresponds to stronger hurricane intensities than for emergency declarations. Estimates for extreme wind speeds for emergency declarations are noisier as the president issues this declaration type to ensure a quick response in non-catastrophic situations. However, both disaster types are subject to the alignment bias for intermediate hurricane intensities. Adding an additional variable that controls for the yearly frequency of hurricanes in each county (see Panel a of Appendix Figure 3.24) does not change the results. In Panel b, we replace the *Wind Speed* variable with the damage index proposed by Emanuel (2011). Given the assumptions of the damage index (see Appendix 3.7.4) the results are qualitatively and quantitatively similar. Expressed in km/h, we find a significant political alignment bias for wind speeds between 93 km/h and 165 km/h (damage index = 0.22).

We further increase the flexibility of our specification by allowing polynomial interactions of alignment with the other hurricane damage measures (*Rainfall* and *Storm Surge*) in Panel a of Appendix Figure 3.26. In Panel b, we include interactions of *Aligned Senators* and *Aligned Representatives* with the *Wind Speed* polynomial. Panel c allows for all interactions together. Neither specification alters the results substantially. In Panel d of Appendix Figure 3.26, we additionally control for non-hurricane-related disaster declarations in the respective counties as one potentially omitted factor, but the estimate of *Aligned Governor* does not change. This result is not surprising as the occurrence of hurricanes is orthogonal to other disasters and the existing political or economic conditions in a county.

Likewise, the results are not sensitive to adding a vector of socioeconomic controls (Panel c of Figure 3.24), using satellite-based rain and temperature controls on the county level (Panels d and e of Figure 3.24), and excluding the hurricane-related *Rainfall* data (Panel f). It is also imaginable that long, persistent past hurricane shocks or declaration decisions influence today's alignment status or probability of receiving a declaration. In Appendix Figure 3.25, we explicitly control for this by adding 10 lags of *Wind Speed* (Panel a) and 10 lags of the dependent variable *Declaration* (Panel b). Both estimations yield the same result as our main model. Furthermore, Panel c of Figure 3.18 shows that our results are robust to a different sample definition wherein we include only observations with a positive *Wind Speed*. Panel d of Figure 3.18 demonstrates that using a fully balanced panel of all contiguous U.S. counties (which inflates the number of zero-observations) yields a similar result. The results also prove robust to excluding outliers with high leverage, i.e., above Cook's distance cut-off, and without low- or high-intensity hurricanes (see Appendix Figure 3.19).

3.5.4 Additional Political Influences and Relief Cycles

As we found an alignment bias in the allocation of disaster declarations for medium hurricane intensities, we analyze further sources of political influence in this section. The president might take political factors other than alignment with the governors into account. We previously estimated the heterogeneous impacts of *Aligned Representative* and *Aligned Senators* – political actors who are not directly involved in the declaration process – analogously to *Aligned Governor*. The results are statistically weaker, but, qualitatively, the same pattern emerges: the relationship is positive and significant only for intermediate *Wind Speed* observations and is insignificant for both, low and high storm intensities (Figure 3.7, Panels a and b).[94]

From an electoral strategy perspective, the geographical distribution of different groups in the electorate is pivotal. To win an election and secure majorities in the United States' first-past-the-post system, politicians need their core supporters to turn out and try to win in contested areas. Two hypotheses from the distributive politics literature, the so-called core and swing voter hypotheses, suggest that politicians therefore have incentives to target these areas when they try to exert tactical redistribution (e.g., Cox & McCubbins, 1986; Lindbeck & Weibull, 1987). Neither hypothesis predicts that strongholds of the opposition party are favored.

[94]In Appendix Figure 3.23, we use *Alignment Count* as an alternative to the three individual variables. It represents the number of key politicians (i.e., governors, representatives, or senators) aligned with the president. For this count variable, we receive a significant result that is qualitatively similar to that for the politicians individually.

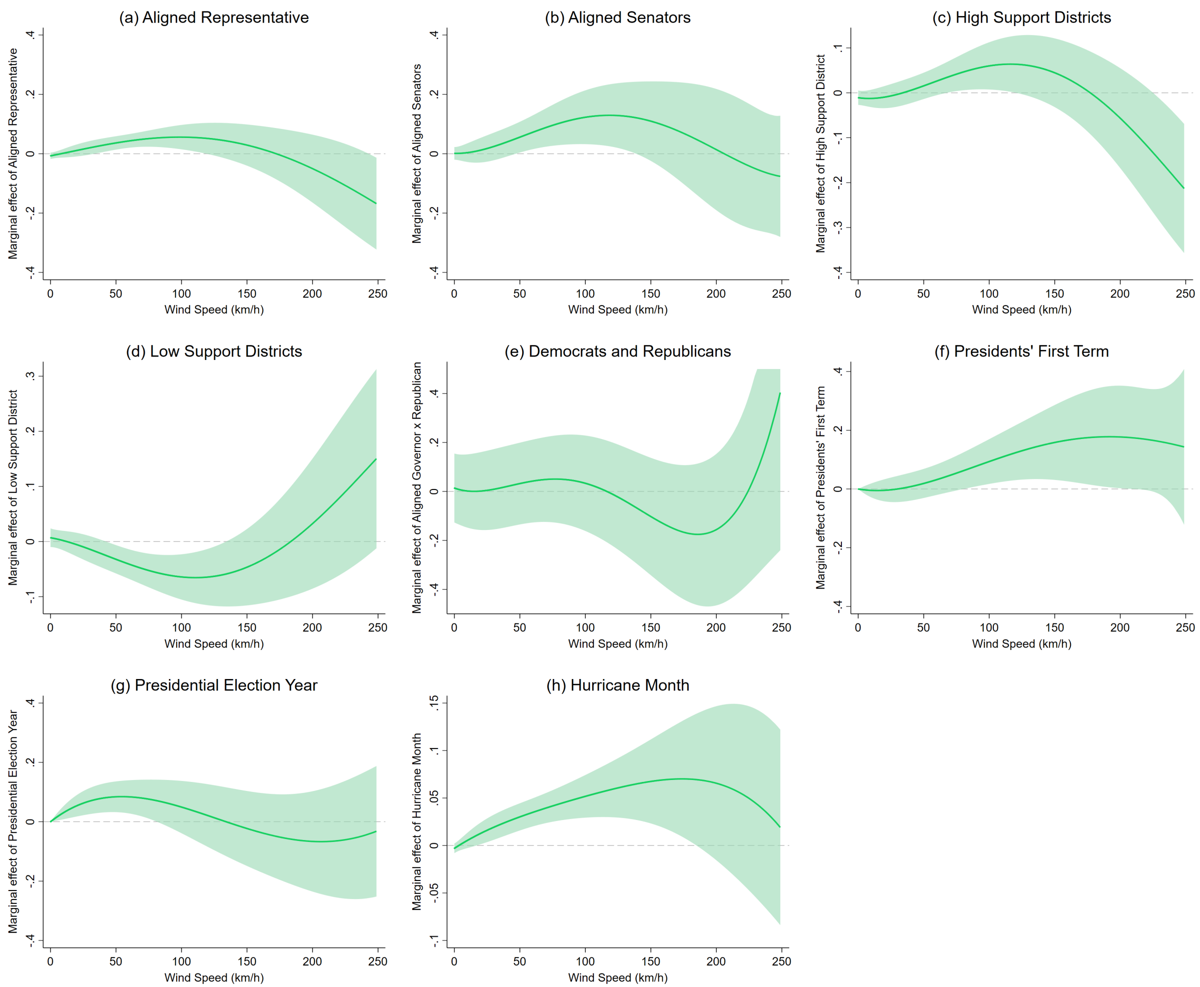

Figure 3.7: Heterogeneous political effects

Notes: The figure displays marginal effects for the variables of interest depicted on the vertical axes from eight polynomial regressions. The green shaded areas represent 95% confidence intervals applying two-way clustered standard errors on the state × year and county level. In each specification, we add the respective variable of interest as well as its interactions with the *Wind Speed* polynomial to our baseline for the estimation of heterogeneous effects. In Panel c *High Support District* is and indicator that takes the value 1 if the candidate from the party of the incumbent president received more than 60 percent of the two-party vote share in the previous congressional election; *Low Support Districts* in Panel d are those where the president's party received less than 40 percent. Panel e plots the difference of the alignment effect between Republicans and Democrats based on a triple interaction. In Panels f and g *Presidents' First Term* and *Presidential Election Year* are indicators for a president's first term and presidential election years, respectively. In Panel h *Hurricane Month* depicts the month in which the hurricane causing the strongest *Wind Speed*-observation in a specific year made landfall in the United States.

To test these propositions, we interact dummy variables for counties in *High Support Districts* and *Low Support Districts* of the incumbent president's party from recent congressional elections with the wind speed polynomial.[95] Panel c of Figure 3.7 indicates that for high-support districts, the marginal interaction effects are positive and slightly significant only for a narrow *Wind Speed* range but again show the characteristic hump-shaped pattern. In contrast, counties in *Low Support Districts* (Panel d), *ceteris paribus*, have a significantly lower probability of receiving a disaster declaration for intermediate storm intensities. For low-support counties, the marginal effects curve shows exactly the opposite shape. The estimations yield a significant negative effect for medium disasters. This suggests that presidents do not perceive investing political capital in counties whose citizens are unlikely to help them to win an election as a winning strategy, which is in line with both the core and the battleground hypotheses.

Another obvious characteristic to distinguish is the effect of aligned governors for the two major parties, Republicans and Democrats. To test this effect, we further interact *Aligned Governor* with an indicator for being in the *Republican* party. Panel e of Figure 3.7 displays the differences of the alignment effect for Republicans and Democrats from this triple interaction. The differences are insignificant. As our swing state subsample already suggested (Appendix Figure 3.20), the alignment bias does not appear to be attributable to a single party.

If the reason for the observed political bias is electorally motivated, one would expect the relationship to become potentially stronger in election years. In Panels f and g of Figure 3.7, we interact the *Wind Speed* polynomial with a dummy variable taking a value of 1 in a president's first term (f) and presidential election years (g), respectively. Both regressions show that presidents are, *ceteris paribus*, more likely to issue a disaster declaration for medium wind speeds in their first term and for low wind speeds in election years as compared to other years.

The hurricane season ranges from June to November, with most of the strongest storms occurring from August to October. Major elections in the United States usually take place in

[95] We code *High Support District* as those districts where the incumbent president's party candidate received more than 60% of the two-party vote share in the previous congressional election. *Low Support Districts* represent those where they won less than 40%. We use results from the congressional elections for this analysis because redistricting creates additional orthogonal variation. While much of the variation on the county and state levels for the other elections is captured by county fixed effects, counties occasionally belong to different congressional districts with different levels of electoral competition over the course of our 54-year sample period.

early November. To exploit this fact, we additionally collected data on the month in which the strongest hurricane-related *Wind Speed* occurred in each county and year. By interacting a linear variable for *Hurricane Month* with the *Wind Speed* polynomial, we see that – for the same levels of *Wind Speed* – storms that occur later in the year are related to a higher probability of a disaster declaration. One possible explanation for the seasonal variation of more declarations in the fall could thus be a within-year political alignment cycle, where presidents tend to declare more disasters closer to elections. However, one can, of course, still find alternative explanations for both between- and within-year political budget cycles (Eichenauer, 2020) and the previous tests alone are not more than indicative.

To show more convincing evidence for the existence of political budget cycles in U.S. disaster relief, we pursue two strategies: a placebo test for the within-year cycle, because *Hurricane Month* should only play a role in election years, and a comparison of the alignment bias between election and non-election years, as our theory predicts stronger alignment effects in election years. For both tests, we need to run regressions including triple interactions. That is, we interact the quartic *Wind Speed* polynomial with two political variables of interest at once. For the regressions shown in Panels a and b of Figure 3.8, we add the expression $\sum_{h=1}^{4}\left(Wind\ Speed_{i,t}^{h} \times Aligned\ Governor_{s,t} \times Election\ Year_t\right)$ to the estimation equation. For Panel c of Figure 3.8, we add the term $\sum_{h=1}^{4}\left(Wind\ Speed_{i,t}^{h} \times Hurricane\ Month_{i,t} \times Election\ Year_t\right)$ to our model.

Panel a of Figure 3.8 shows the results of the triple interaction regression by plotting the marginal effect of *Aligned Governor* on the vertical axis. The graphic distinguishes alignment effects by *Presidential Election Year* equaling 1 in election years (dashed blue line) or 0 in no election years (solid green line). Panel b does the same for *Any Election Year*, an indicator additionally accounting for congressional and gubernatorial election years. In both panels, the relationship emerges in all years, but the estimate of the alignment effect is larger and more significant for election years than for non-election years. However, Appendix Figure 3.27 shows in Panels a and b that the difference between both curves is not significant.

Considering within-year political alignment cycles, Panel c of Figure 3.8 tests how the month effect differs for election years (dashed blue line) and non-election years (solid green line). In non-election years, the estimated effect of *Hurricane Month* is close to zero and insignificant. In election years, however, it is positive and significant for intermediate storm intensities. Panel c of Appendix Figure 3.27 shows that this triple interaction yields a

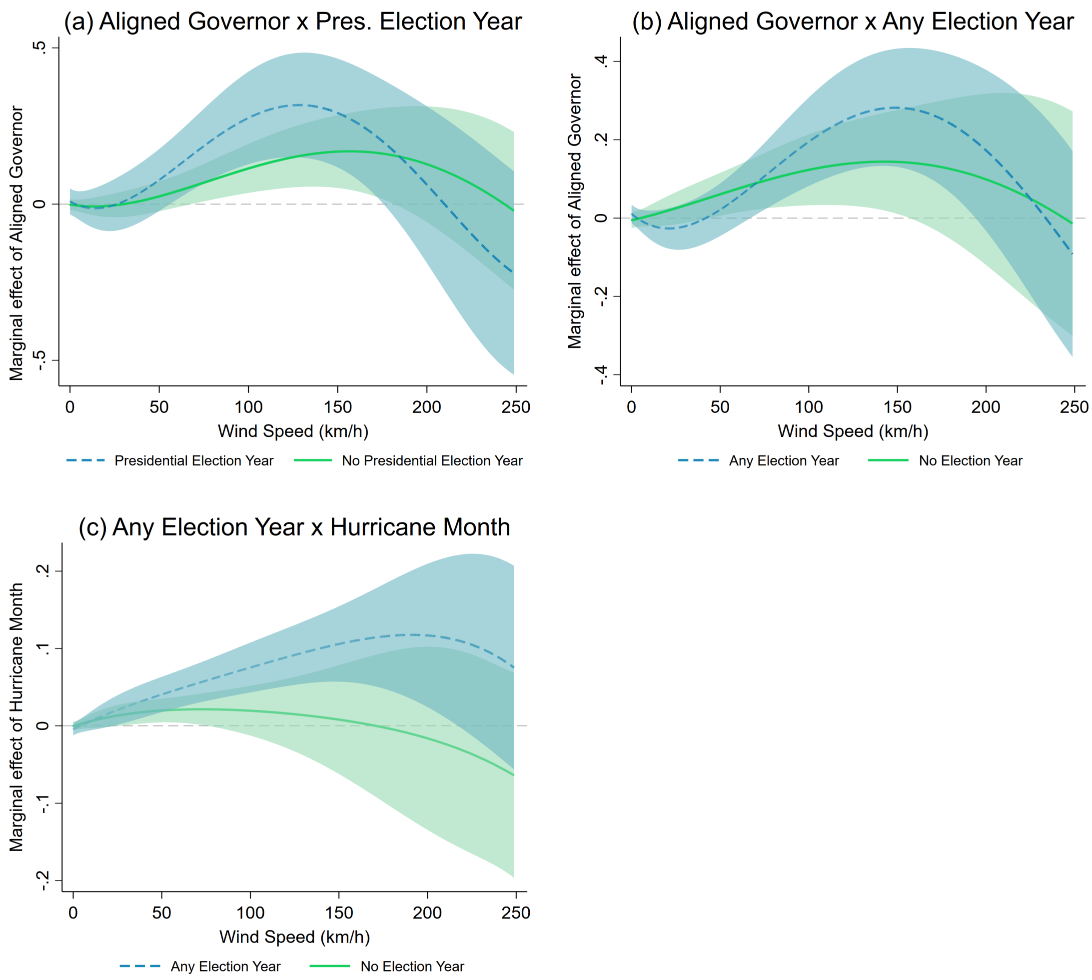

Figure 3.8: Political relief cycles – Marginal effects from triple interactions

Notes: The figure displays marginal effects for the variable specified on the respective vertical axis from three polynomial estimations including triple interactions. In each specification, we add the depicted variables of interest as well as all possible cross-interactions with the *Wind Speed* polynomial to our baseline for the estimation of heterogeneous effects. Shaded areas represent 95% confidence intervals applying two-way clustered standard errors on the state × year and county level. In Panel a, the dashed blue line displays marginal effects of *Aligned Governor* in presidential election years. The green solid line shows the estimated effect of *Aligned Governor* if *Presidential Election Year* equals 0. In Panel b, the dashed blue line displays marginal effects of *Aligned Governor* in years of major elections (i.e., presidential, gubernatorial, or congressional elections). The green solid line shows the estimated effect of *Aligned Governor* if *Any Election Year* equals 0. In Panel c, the dashed blue line shows the effect of *Aligned Governor* in election years. The green solid line displays the estimated effect of *Hurricane Month* if *Any Election Year* equals 0.

significant difference for the within-year declaration cycle between election years and non-election years. That is, hurricanes of equal intensity have a higher probability of being declared a disaster if they occur in a later month, but only in election years. The rationale here is that promising generous relief potentially has a higher leverage effect if the disaster is a salient topic just before an election.

All results contribute to the notion that there exists a political (alignment) bias in U.S. disaster relief. As our analysis demonstrates, one must look beyond average effects to understand the specifics of political influence in this domain. In our concluding remarks, we discuss how these findings add to our understanding of executive politicians' behavior and how they matter in terms of policy implications.

3.6 Conclusion

We have analyzed the political economy of disaster relief, employing a novel hurricane damage data set and focusing on hurricane-related disaster declarations in the United States from 1965–2018. Based on a simple theoretical framework, we have demonstrated that the issuance of disaster declarations involves a political bias: counties with a governor who is a co-partisan of the incumbent U.S. president, on average, have a significantly higher probability of receiving a federal disaster declaration. The main contribution of our study stems from the empirical analysis of nonlinearities in political alignment effects from applying flexible interaction models. We find a persistent nonlinear alignment bias where presidents only use their discretion strategically for hurricanes of medium intensity. While political influence only plays a minor role on average, strategic political considerations are about eight times more relevant for medium-intensity storms. Furthermore, self-interest and party political motivations seem to drive the results since we find stronger effects in election years and for hurricanes closer to elections in November. Therefore, the alignment bias is most pronounced, and the potential political returns are higher. Our results prove robust to including county-specific time trends; lagged dependent variables; including other covariates and their lags; and omitting individual decades, states, or hurricane outliers.

The results from our analysis show the necessity of accounting for possible effect heterogeneities in analyses of political-economic relationships. Disregarding the complexity of political-economic relationships in statistical estimations means that the actual nexuses remain potentially concealed and the economic consequences underestimated: while our hump-shaped continuum for the marginal effects of political alignment corresponds to annual political hurricane-relief spending of about USD 500 million, conventional average estimates for the same calculation would only suggest about one-fifth of this amount. Generally speaking, political influence may depend more on the specific constellations and opportunities that politicians face than previously revealed. Regarding disaster relief, we have shown that politicians do not require the occurrence of random third events that distract public attention from their strategic actions. They can exploit specific ambiguous decision-making situations that arise within the impact range of a single disaster event in a biased manner. The results from our analysis by no mean imply that politicians are not responsive to the needs of the electorate. In situations that clearly require a certain decision, we do not find evidence for political biases. However, we observe that democratic control of political actors does not prevent favoritism in ambiguous decision situations, particularly if they expect a high electoral return. Politicians behave strategically if the situation allows. As we have demonstrated, the degree of opportunity for strategic behavior can be very heterogeneous.

The resulting question is whether the functional form assumptions in political-economic analyses in general tend to oversimplify the underlying processes by neglecting potentially nonlinear relationships. As the nonlinear effects are substantial and persistent with regard to disaster assistance, future research should evaluate whether our findings are generalizable to other political-economic research areas. Potential relationships include various distributive policies where spending allocation involves a certain conditionality or eligibility criteria, e.g., in the EU, in international organizations, or in international aid. Whenever it is not clear that, for instance, certain domains in an underdeveloped region should receive supportive funding, political considerations have a higher potential to become the factor to tip the scales. It is important to acknowledge that our findings are not necessarily externally valid for other spending areas; but they should change the a-priori assumptions when observing comparable processes and when a lack of transparency or data availability prevents credible empirical testing.

As our findings point at an inefficiency in the disaster relief system, there are certain direct policy implications. The current mechanism makes ex-post spending more attractive for politicians than investing in preparedness, which creates a moral hazard problem. Ex-post relief is directly visible and better suited as a political tool than preparedness spending because the benefits of preparedness only emerge in the long-run and are not directly attributed to the politicians.[96] A loan-based system, higher state cost shares, more local responsibility

[96] Research shows that the government could reduce the need for ex-post spending by showing appropriate preparedness action. Davlasheridze et al. (2017) calculate that a 1% increase in ex-ante spending would reduce future damage by 2%. Healy & Malhotra (2009) estimate that USD 1 spent on preparedness mitigates future damage by USD 15. A second moral hazard problem emerges among local governments and individuals in highly exposed regions. If they have hope that the government will bail them out (particularly in a favorable political constellation), they have an incentive to underinvest in preparedness and insurance, which increases disaster vulnerability.

or payments conditional on states' preparedness efforts would make relief a less politically attractive instrument (Platt, 1999, 290; Lindsay & McCarthy, 2015).

In addition to these commonly suggested improvements, we propose institutional changes to address political influence in the disaster declaration process. First, technical improvements such as better satellite imagery would allow effective data-based issuance of declarations for disasters. In general, more rule-based criteria for disaster declarations or formulas derived from measures of affectedness and need would constitute an improvement, promoting fairness, predictability, and transparency. Second, as we do not find politicized spending patterns in the case of extreme events, the president could remain in charge of these events to ensure a quick disaster response. For intermediate cases or situations that might require a declaration not meeting predefined thresholds, the president should be required to request a mandate from an independent expert commission. Third, a sensible approach might be to depoliticize disaster declarations (cf. evidence by Bostashvili & Ujhelyi, 2019, on civil service reforms) and assign declaration authority to a suitable and skilled bureaucrat, comparable to a central banker, who does not have to run for reelection.

Admittedly, the probability for substantive changes to the process in the currently polarized political situation in the United States is low. The Senate and president have blocked past reform attempts by FEMA (Sylves, 2008, 100–101). While the U.S. relief system might not be easy to reform, countries that aim to establish or improve a system of disaster relief should draw the necessary conclusions from the existing empirical findings. This recommendation is most relevant for the many developing countries that are highly exposed and prone to various natural hazards. The urgent need to design an efficient disaster preparedness and relief system is reflected in the fact that the urban coastal population – and therefore the vulnerability to hurricanes – will likely continue to grow.

Improving resilience to natural disasters, which are expected to increase in severity in the course of climate change, will certainly constitute a major challenge of the 21st century. As Strömberg (2007, 212) notes, "it is essential that relief be given where it can do most good." A key component to ensuring this is a well-functioning system of disaster relief. Disasters would then not constitute an opportunity for political gain, but rather an opportunity to observe the advantages of a modern welfare state in disaster recovery.

3.7 Appendices

3.7.1 Disaster Relief in the United States of America

3.7.1.1 Brief Historical Review

For the first 160 years of U.S. nationhood, the role of the federal government with respect to disaster assistance was minor. Congress had to pass ad-hoc legislation when the federal state decided to provide aid on occasions of catastrophic events (Barnett, 1999). This changed in 1950 when Congress decided to make disaster relief provision an executive responsibility of the president, establishing the system of presidential disaster declarations with the Federal Disaster and Relief Act (Platt, 1999; Sylves, 2008). It "put in place a standard process by which Governors of states could ask the President to approve federal disaster assistance for their respective states and localities" (Sylves, 2008, 49). Since then, a federal disaster assistance system has existed, to deliver relief to regions in case state or local capacities are overwhelmed in the wake of natural events such as floods, earthquakes, droughts, fires, hurricanes, or other severe storms (Platt, 1999). The federal role in disaster response and recovery gradually expanded and became the primary source for disaster funding (FEMA, 2017b; Lindsay & McCarthy, 2015). FEMA's budget for relief payments over the last 10 years (2010–2019) has averaged USD 13.63 billion (Painter, 2019).

To bundle the previously scattered responsibilities for federal disaster management, including disaster preparation, mitigation, response, and recovery, under one roof, the FEMA was established in 1979 (FEMA, 2017a). The Robert T. Stafford Disaster Relief and Emergency Assistance Act from 1988 constitutes the current legislation for federal disaster relief. Among others, it augmented the discretion of presidents in judging what qualifies for disaster assistance, permits declarations for further classes of natural and certain non-natural catastrophes, and established a hazard mitigation program (Downton & Pielke Jr., 2001; Sylves, 2008). Despite the gradual expansion of the scope of federal disaster assistance and the large number of major and minor amendments to this legislation, the process of presidential disaster declarations has "changed very little over time" (Lindsay & McCarthy, 2015, 20).

3.7.1.2 The Disaster Declaration Process

Federal disaster relief in the United States is contingent upon a presidential disaster declaration. The president must declare an event a federal disaster before FEMA can start determining the amount of financial assistance and the individuals or entities eligible for relief. If a severe disaster strikes, an affected state has to activate its own emergency plan first since the United States follows a "bottom-up" approach in disaster management (McCarthy, 2014). If the governor then detects that the state and local resources are insufficient to provide an effective response, they can initiate a preliminary damage assessment (PDA), thereby collecting damage records and unmet needs at the local level (FEMA – EMI, 2017). Thereafter, the governor can formally request federal aid from the president (see FEMA, 2011, 2017b). The official request includes information from the PDA and a description of the disaster impact as well as the state's efforts to cope with it and an attestation that disaster response is beyond the state's capabilities. In the letter, the governor also states which counties they believe qualify for federal assistance (FEMA – EMI, 2017; Sylves, 2008, 83–84).

In the next step, the White House receives a recommendation from federal FEMA bureaucrats regarding the declaration decision, but it is solely at the president's discretion whether to declare the event a disaster (Downton & Pielke Jr., 2001; FEMA, 2017b). Presidents have wide discretionary power over which circumstances and areas they declare a disaster and when they deny a request (Sylves, 2008, 79).[97] Each presidential declaration is for a specific state and explicitly lists the counties eligible for federal help under the declaration. Declarations may be statewide, but only a limited number of counties are typically included

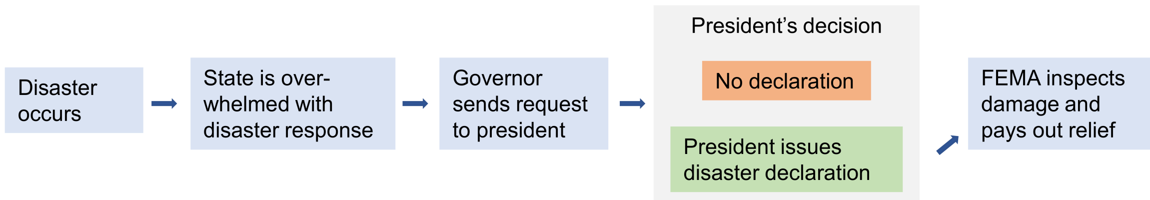

Figure 3.9: The disaster declaration process

Notes: Sketch of the main steps in the process of federal disaster declarations in the United States.

[97]Presidents are obliged not to use a fixed set of rules for their decisions because "[n]o geographic area shall be precluded from receiving assistance [...] solely by virtue of an arithmetic formula or sliding scale based on income or population" (Stafford Act, 1988). FEMA applies certain per capita damage formulas (using data from the PDA) for its recommendation (McCarthy, 2014).

in the disaster area (Downton & Pielke Jr., 2001; Sylves, 2008).[98] In exceptional cases, the president can declare an emergency without a gubernatorial request when "he determines that an emergency exists for which the primary responsibility for response rests with the United States [...]" (McCarthy, 2014, 9).

Two types of disaster declarations can be issued by the president: emergency declarations and major disaster declarations (McCarthy, 2014). The Stafford Act (1988) defines emergencies as

> "any occasion or instance for which, in the determination of the President, federal assistance is needed to supplement state and local efforts and capabilities to save lives and to protect property and public health and safety, or to lessen or avert the threat of a catastrophe [...]."

As a supplement to local and state efforts, emergency declarations should ensure a quick response and functioning of essential services (McCarthy, 2014). Emergency declarations have existed since 1974, and they are limited in scope, being restricted to USD 5 million for a single declaration. The vague language of the Stafford Act gives the president significant discretion and often creates ambiguity for governors regarding which situations qualify for emergency assistance (Sylves, 2008, 60).

The second category of declarations is the "major disaster declaration", which makes a wide range of assistance available both for short-term and permanent work in response to large scale disasters (FEMA, 2011; McCarthy, 2014). While major disaster declarations are only issued post-disaster, emergencies are sometimes even declared in anticipation of a severe event, such as the imminent landfall of a strong hurricane, to prepare the post-disaster response and to evacuate particularly vulnerable regions (Lindsay & McCarthy, 2015). A state can thus, in principle, receive a pre-hurricane emergency and a post-hurricane major disaster declaration for the same event: "While federal expenditures may be little different, the number of declarations in these instances is doubled" (Lindsay & McCarthy, 2015). This circumstance influences the choice of the dependent variable. While emergency declarations are financially capped, major disaster declarations can essentially release an unlimited amount of money, once they are issued. As long as eligibility requirements are fulfilled, FEMA is entitled to provide support (Platt, 1999, 21).

[98] Sylves (2008, 83–84) explains that "the president [...] may choose to include some but not all of the counties recommended by the governor." If necessary, counties can be added to a declaration within 30 days after the declaration (Sylves, 2008, 83–88; FEMA, 2017b).

Notably, although "FEMA – not the president – decides how much money to allocate" (Sylves, 2008, 101) once a declaration is issued,

> "the ultimate decision to approve or reject a governor's request for a declaration is made by the president, not by FEMA officials. In effect, FEMA officials have little leeway in matters of presidential declaration decision-making." (Sylves, 2008, 94)

The sequential procedure of governors requesting and the president granting or denying declarations existed throughout and was stipulated in "[b]oth the 1950 law and the Stafford Act of 1988" (Sylves, 2008, 79).

3.7.1.3 FEMA Programs and Disaster Relief Funding

Federal assistance can be divided into public assistance (PA), individual assistance (IA), and the hazard mitigation grant program (HM). PA is FEMA's largest and most frequently activated program (Lindsay, 2014). Under this program, local government and non-profit organizations receive monetary, personnel, technical, or advisory assistance for removing debris and repairing or replacing various types of damaged public infrastructure (Lindsay, 2014; Sylves, 2008). While federal help was mainly restricted to the initial repair of crucial infrastructure and the distribution of essentials in the 1950s and 1960s, further programs, such as IA (established in 1974), have since emerged. These include temporary housing, grants to rebuild, and legal and mental health services, as well as a larger range of possible payments to communities (Lindsay & McCarthy, 2015; Platt, 1999, 15–17).

IA comprises a selection of programs to meet individual and household needs. This may include, for instance, temporary housing, grants to repair and replace uninsured property destroyed by the event, food coupons, crisis counseling, disaster-related unemployment compensation, and help to guarantee the physical or mental health of those affected (DHS, 2018; Lindsay, 2014). When individual residents apply for monetary help, FEMA inspectors determine eligibility and the exact amount of grants. Currently, the maximum amount that an individual can receive is USD 33,000 (FEMA, 2017c).

HM usually aggregates 15% of the overall amount of federal assistance under a declaration (FEMA, 2018). It funds projects intended to "prevent or reduce long term risk to life and property from natural hazards" (FEMA, 2011) in accordance with existing FEMA-approved HM plans.

Federal disaster management receives funding through the Disaster Relief Fund (DRF), which is composed of regular annual appropriations by Congress and unspent authority carried over from previous years. FEMA manages the DRF and usually uses it to finance disaster relief for disasters up to a damage level of USD 500 million. In the case of extreme disasters, the president must ask Congress to release supplemental appropriations if the DRF is otherwise depleted. Granting supplemental appropriations and regular replenishments of the DRF is the only way that the legislative branch is directly involved in the declaration process (Sylves, 2008, 54). Over the years, the largest number of supplemental spending bills have been passed in the event of hurricanes (Schroeder, 2018). For a comprehensive overview, see Schroeder (2018).

3.7.2 Hurricanes

Hurricanes constitute the most severe and destructive class of storms.[99] A hurricane is a cyclonically rotating, atmospheric low-pressure system with a typical diameter of the order of 600 km, though storms vary considerably regarding their size (Aguado & Burt, 2015, 384; Korty, 2013a, 481–485). By definition, "hurricanes have sustained wind speeds of 119 km/h or greater" (Aguado & Burt, 2015, 383); the most intense hurricanes can contain peak winds of more than 350 km/h (Aguado & Burt, 2015, 384).

Hurricanes' origins are usually cloud clusters forming over the western African coast.[100] A small fraction of these tropical disturbances encounter conditions that foster the development of an organized rotating low-pressure system (i.e., a tropical depression) that drifts westward over the Atlantic. Essential condition for hurricane formation are humid conditions and a high water temperature (>27°C/81°F) to supply the storm with energy, no air-inversions or strong vertical winds, and a minimum distance from the equator, thus implying a sufficiently strong Coriolis force (Kraus & Ebel, 2003, 156–158; Aguado & Burt, 2015, 389). These criteria restrict the development of hurricanes to the marine area 5-20°N. If all preconditions are met, a self-intensifying rotating system can emerge, potentially becoming strong enough to be called a tropical storm (wind speeds above 63 km/h) or a hurricane (Kraus & Ebel, 2003, 158; Korty, 2013a, 481–482). The self-reinforcement stems from the release of latent heat from condensation in the absorbed air, which unleashes even more energy within the clouds, leading to further storm growth as long as conditions remain favorable (Aguado & Burt, 2015, 389–391).

In an established tropical storm, air flows inward to an extreme low-pressure core (the eye). While moving inward, the tropical cyclone absorbs latent energy from the warm ocean surface. Closer to the core, condensation and the release of warmth let air rise, which then spirals anticyclonically outbound. Some air also slowly sinks within the eye, which is characterized by very low wind speeds. The storm's highest intensity is within the eye-wall, the towering band of clouds 10–20 km from the storm's center. Moving away from the center, wind speed decreases quickly and steadily (Aguado & Burt, 2015, 385–386; Deryugina, 2017). The

[99] As our study deals with tropical cyclones in an American context, we use the term 'hurricane', the conventional expression for storms in the North-Atlantic and East-Pacific basin. It is a synonym for 'tropical cyclone' (Indian Ocean and Australia) and 'typhoon' (West Pacific).

[100] This is true for the majority of storms hitting the U.S. East Coast or the Gulf of Mexico area. Hurricanes also exist in the West Pacific, but most of them move away from land and thus, do not affect the contiguous United States; nevertheless, some make landfall in Mexico and affect the Southwestern United States (Aguado & Burt, 2015, 382).

strength of a hurricane is generally measured by its maximum sustained surface wind speed (Kraus & Ebel, 2003, 143–145).

Alongside extreme winds, hurricanes produce heavy precipitation. Rainfall within the hurricane is also most intense around the center. However, precipitation does not diminish as steadily as in the case for wind speeds when moving outward. The separated bands of clouds spiraling outward can cause heavy rainfall off the center (Aguado & Burt, 2015, 384–385; Deryugina, 2017; Strobl, 2011). Despite a strong overall correlation of storm strength and total rainfall, Lonfat et al. (2004) report a high asymmetry of hurricane precipitation. Additionally, Konrad et al. (2002) find that local precipitation rates can vary greatly within a single storm. Presumed causes for the vast heterogeneities in rainfall are differences in the speed of movement, the storm's diameter, and the shape of the crossed area (Knight & Davis, 2009; Konrad et al., 2002). The high degree of heterogeneity in precipitation patterns highlights the importance of using not only wind data but also rain data.

Forecasts on the approximate locations of hurricane landfall are only reliable a few days in advance – today, 48 hours before landfall, the average accuracy is 150 km because of the wildly-erratic nature of hurricane paths (Aguado & Burt, 2015, 404–405). A typical hurricane season spans from June 1 to November 30, with most storms occurring between July and October.

3.7.3 Shortcomings of Reported Damage Data

The majority of the distributive politics literature evaluates political influence by studying damage outcomes that emerge from endogenous processes. Existing studies on the political economy of disaster relief predominantly use reported damage measures from insurance data or databases such as EM-DAT or SHELDUS. A general criticism is that the measures are not comparable between different types of hazards (Gall et al., 2009). In addition, the construction of the estimates in data sets such as EM-DAT is mostly "based on insurance claims or news stories" (Felbermayr & Gröschl, 2014, 92). This can create measurement errors and selection issues. In data sets covering a long time span or many regions, temporal or spatial heterogeneities in the quality of reporting and sources can cause biased estimates (Strobl, 2012).

Analyses of U.S. disaster declarations frequently use loss estimates from the SHELDUS database (e.g., Gasper, 2015; Healy & Malhotra, 2009); this method also has its shortcomings. First, only disasters above a threshold of USD 50,000 are included prior to 1995 (Davlasheridze et al., 2017), making the data truncated. Second, SHELDUS covers self-reported data by individual weather stations, which results in a large number of missing observations (see Gallagher, 2019). As Gallagher (2019) explains in his reanalysis of Gasper & Reeves (2011), the usage of SHELDUS in the context of disaster declarations is problematic as one observes many declarations for situations with seemingly no damage according to these data. Third, to obtain county-level estimates, SHELDUS divides state-level losses equally among counties (Davlasheridze et al., 2017; Gasper & Reeves, 2011). Gasper & Reeves (2011) and Healy & Malhotra (2009) attempt to account for this by adopting population weights so that smaller counties are not over-represented. Finally, Gall et al. (2009) detect an inconsistency: estimated total losses from SHELDUS are lower than insured losses reported in other databases.

As explained in the paper, we attempt to overcome these issues by modelling damage directly from meteorological hurricane intensity measures. Our data are complete for our observation period (1965–2018), not truncated or exogenous, and do not suffer from any of the biases listed above.

3.7.4 Hurricane Data

Wind Speed

To generate a measure for hurricane damage, we adopt the tropical cyclone data that Kunze (2021) assembled with a higher resolution of 1×1 km for the United States. We use data from the International Best Track Archive for Climate Stewardship (IBTrACS), version v03r10, for the years 1965–2018 (Knapp et al., 2010). This meteorological data set contains all best track tropical cyclone data collected from weather agencies worldwide. Tropical cyclones are tracked via aviation, buoys, ships, satellites, and weather stations. The resulting data include the wind speed, minimal sea pressure, and location of the center of all tropical cyclones recorded every six hours. To generate spatially varying wind speeds out of the IBTrACS raw data, we run a meteorological wind field model. We consider all wind speed observations above a cutoff of 54 km/h. The code of this model is based on the CLIMADA model from Aznar-Siguan & Bresch (2019) but is adopted to the special needs of the IBTrACS data. It contains the well-established wind field model by Holland (1980), which calculates for each raw data track point

$$S = \begin{cases} \max\left(0, \left((M - abs(T)) * \frac{R}{D}^{\frac{3}{2}} * e^{1-\frac{R}{D}^{\frac{3}{2}}}\right) + T\right), & \text{if } D < 10 * R \text{ from center to outer core} \\ 0, & \text{if } D > 10 * R \text{ out of radius,} \end{cases} \tag{3.9}$$

where S corresponds to the resulting wind speed. It depends on the forward speed T, the distance D from the tropical cyclone center, and the maximum wind radius R. The model is restricted to tropical cyclones above a raw data wind speed of 54 km/h and a maximum coastal distance of 500 km. It computes one-hourly asymmetric wind fields at a resolution of 0.01° (approximately 1 km) for every tropical cyclone in our sample. From these calculated wind fields, we take the maximum wind speed per year and per county to construct our *Wind Speed* variable. Figure 3.10 shows the calculated wind fields for Hurricane Matthew hitting the U.S. East Coast in 2016.

One can see that the wind speed diminishes with increasing distance from the center (red dotted line) and after landfall. Figure 3.11 shows the distribution of the *Wind Speed* variable for all hurricanes over the entire sample period. While lower wind speeds are very frequent, catastrophic events are rather rare.

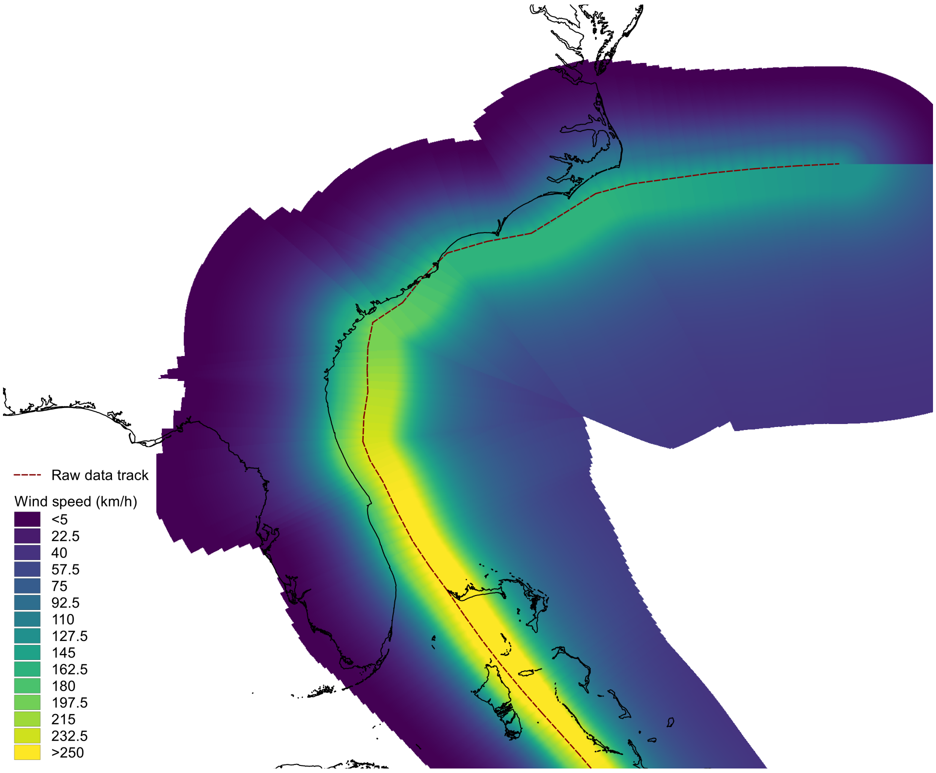

Figure 3.10: Wind field model and raw data track of Hurricane Matthew, 2016

Notes: The figure displays modeled asymmetric wind fields from our damage model for Hurricane Matthew. The colors indicate wind speed intensities. The red dotted line corresponds to the IBTrACS raw data track.

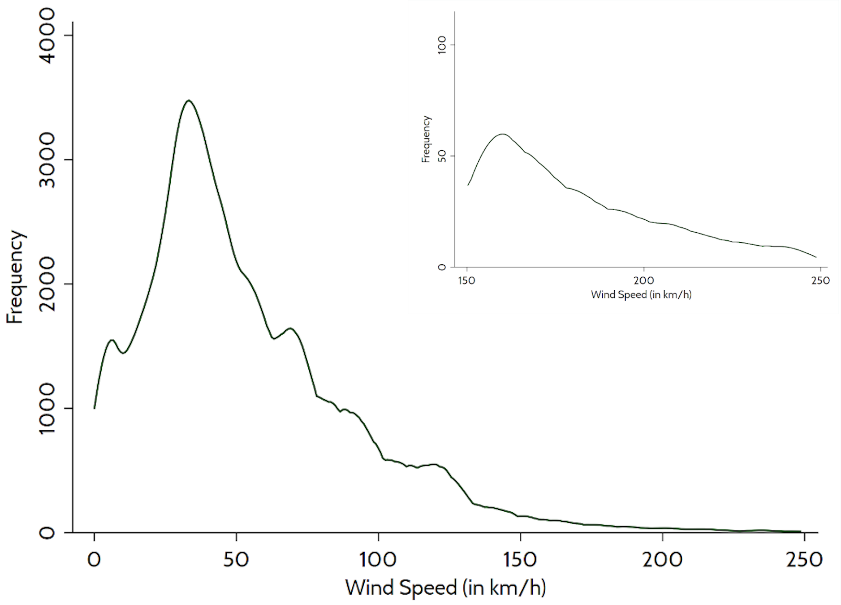

Figure 3.11: Distribution of hurricane *Wind Speeds* > 0, 1965–2018

In Panel b of Figure 3.24, we replace our *Wind Speed* damage variable with the damage function that Emanuel (2011) proposes. He suggests specific wind speed thresholds above which a certain percentage of physical damage occurs or above which 50% of the physical infrastructure is destroyed. Consequently, for each hurricane s in county i we calculate the following damage index:

$$Damage_{is} = \frac{v_{is}^3}{1 + v_{is}^3}, \tag{3.10}$$

where

$$v_{is} = \frac{max[(S_{is} - S_{thresh}), 0]}{S_{half} - S_{thresh}}. \tag{3.11}$$

S_{is} is the maximum wind speed of storm s in county i as calculated in Equation 3.9. As proposed by Emanuel (2011), we take 93 km/h as the threshold (S_{thresh}) where physical damage starts and 203 km/h as the cutoff where half of the property is destroyed (S_{half}). The resulting damage index ranges from 0 (no damage) to 1 (all buildings destroyed).

Rainfall and Storm Surge

Data on hurricane-related precipitation were provided by Roth (2018) in raw spreadsheet format. These tables report rainfall measures for hurricanes, tropical storms, and tropical depressions from weather stations at geographic locations in North America. We use data from all storms in his data set, if they caused rainfall in the contiguous United States.

As a first step, we calculate total rainfall (in mm) for every storm and every location from the daily records in the data over the entire period of rainfall from the hurricane.[101] On a spatial $0.01° \times 0.01°$ grid, we match the data to individual counties. Since flood damage increases with rainfall (Downton & Pielke Jr., 2001), we assume that the strongest rainfall events in a county had the highest likelihood of causing a declaration. We thus keep the strongest precipitation value from each county in each year.

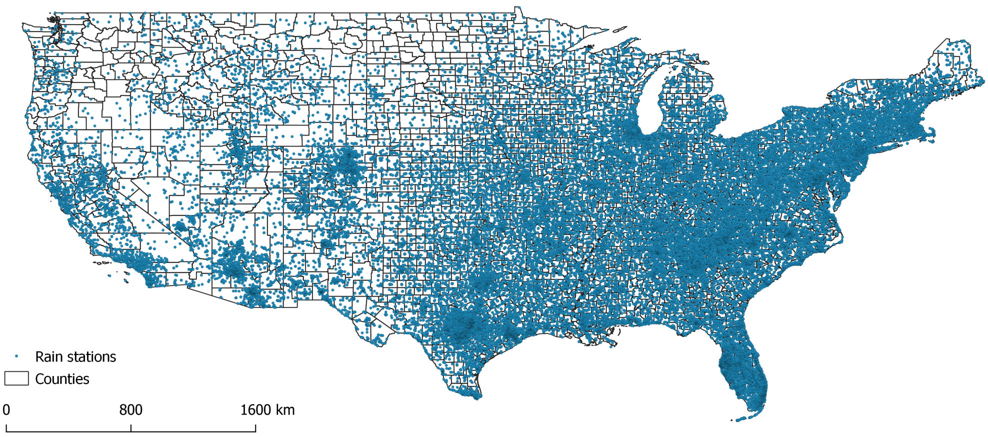

Figure 3.12: Distribution of weather stations for hurricane *Rainfall* data

We do not modify the data by interpolating or extrapolating between individual grid points. The degree of spatial interpolation would be an arbitrary choice, and it may lead to biased estimates because local extremes that cause a declaration would potentially be smoothed out from the distribution. As the above map (Figure 3.12) illustrates, our raw data contain rain stations in the majority of counties.

To generate our *Storm Surge* variable for coastal storm surge damage from hurricanes, we rely on the hydrodynamic model developed by Kunze & Strobl (2020). Within this model, the authors calculate the coastal inundation depth for each tropical cyclone in the IBTrACS Knapp et al. (2010) data set. The model runs at a spatial resolution of 0.1° and combines

[101] The data include precipitation that arises from the potential influence of weather fronts interacting with the tropical storm (Czajkowski et al., 2011; Knight & Davis, 2009).

inputs from tides, bathymetry, and tropical cyclone wind speed, and pressure drop fields in a hydrodynamic simulation using the DELFT3D software. Based on this model, we calculate the maximum inundation depth per county and year.

3.7.5 Variable Description and Summary Statistics

Declaration	Indicator taking the value 1 if a county is assigned at least one federal Emergency Declaration or Major Disaster Declaration in connection to a hurricane in a respective year, and 0 otherwise. All declarations from the categories 'Hurricane', 'Coastal Storm', 'Flooding', and 'Severe Storm(s)' in the data provided by FEMA are included if they contain a clear reference to a specific hurricane or tropical storm in their title or could be matched via the date of occurrence to storms in our wind and rain data set. The data exist on the county level since 1965, which restricts our analysis to the time period 1965–2018. Source: OpenFEMA Data set: Disaster Declarations Summaries – V1 (https://www.fema.gov/openfema, downloaded on October 16, 2017 for declarations until 2015 and on May 20, 2019 for 2016–2018).
Emergency Declaration	Analog to *Declaration* but restricted to Emergency Declarations.
Major Declaration	Analog to *Declaration* but restricted to Major Disaster Declarations.
Declarations	Sum of hurricane-related federal Emergency Declarations and Major Disaster Declarations in a county in a given year.
Aligned Governor	Indicator variable that takes the value 1 if governor and president are fellow party members and 0 otherwise. Independent governors are coded as unaligned. The variable captures alignment status as of November, before gubernatorial/presidential elections. (Source: Klarner (2013) (until 2010); for 2011–2018 coded from the National Governors Association; https://www.nga.org).
Aligned Representative	Indicator variable that takes the value 1 if the majority of a county is affiliated with a district that is represented by a politician from the incumbent president's party in the House of Representatives, and 0 otherwise. District vote results were provided by James M. Snyder. For missing data and corrections, data from the CQ Voting and Elections Collection (https://library.cqpress.com/elections/ and https://ballotpedia.org/) were used.

Aligned Senators	Indicator variable that takes the value 1 if a state is represented by two politicians from the incumbent president's party in the Senate, and 0 otherwise. The variable is coded from Senate election results, obtained from the CQ Voting and Elections Collection.
Alignment Count	A count variable, which represents the number of key politicians (Governor, Senators, and House Representative) that are co-partisans of the president in a respective county. It can thus take the values 0, 1, 2, 3, and 4.
Wind Speed	Maximum wind speed per county and year in km/h. (Source: see Appendix 3.7.4).
Rainfall	Maximum tropical cyclone related rainfall in mm per county and year. Source: Roth (2018). For further details see Appendix 3.7.4.
Storm Surge	Maximum storm surge water level in meters per county and year. Source: Kunze & Strobl (2020).
Wind Speed Count	Variable that counts the number of tropical cyclones with a positive wind speed per county and year.
Rainfall Count	Variable that counts the number of hurricanes that produced positive rainfall in a county in a given year in the data derived from Roth (2018).
Hurricane Month	The month of the strongest tropical cyclone per county and year. (Source: see Appendix 3.7.4).
Mean Annual Rainfall	Mean precipitation per county and year in millimeter calculated from https://prism.oregonstate.edu/.
Mean Annual Temperature	Mean temperature per county and year in degree Celsius calculated from https://prism.oregonstate.edu/.
High Support District	Indicator variable taking the value 1 if the candidate of the incumbent president's party obtained more than 60 percent of the vote share in a district in the most recent election and 0 otherwise.
Low Support District	Indicator variable taking the value 1 if the candidate of the incumbent president's party obtained less than 40 percent of the vote share in a district in the most recent election and 0 otherwise.

Presidential Election Year	Indicator variable taking the value 1 in a presidential election year and 0 otherwise.
Any Election Year	Indicator variable taking the value 1 if at least one major election (presidential, congressional, gubernatorial) takes place and 0 otherwise. Data for gubernatorial election years are provided by Klarner (2013). Presidential elections are held all 4 years and congressional elections in even years. Missing data for gubernatorial elections were retrieved from ballotpedia.org (last accessed April 1, 2020).
Presidents' First Term	Indicator for presidents' first electoral terms.
Years Pres. Runs for Reelection	Indicator for years in which a president runs for second term.
Electoral Votes	Number of electoral votes of a state in the Electoral College. Source: The American Presidency Project.
County Vote Change (Pres.)	Difference between the vote share of the incumbent president's party in the upcoming and the most recent presidential election. Derived from the data by James M. Snyder and complemented with information from the County Presidential Election Returns 2000–2016 MIT Election Data Sciene Lab (https://dataverse.harvard.edu/dataset.xhtml?persistentId=doi:10.7910/DVN/VOQCHQ, downloaded March 15, 2019).
Last Term Governor	Indicator for governors that are in their last term due to a constitutional restriction. Source: Klarner (2013).
Population (log)	Natural logarithm of population per county and year. Source: NBER.
Black Population (log)	Natural logarithm of black population per county and year. Source: ttps://seer.cancer.gov/popdata/yr1969_2018.19ages/us.1969_2018.19ages.adjusted.exe.
Income (log)	Natural logarithm of income in current USD 1,000 per county and year. Source: U.S. Bureau of Economic Analysis (BEA).
Income per Capita (log)	Per capita income in current USD per county and year. Source: U.S. Bureau of Economic Analysis (BEA).

Table 3.3: Summary statistics

	Observations	Mean	St.dev.	Min	Max
Declaration	85,309	0.08	0.27	0.00	1.00
Emergency Declaration	85,309	0.03	0.18	0.00	1.00
Major Declaration	85,309	0.06	0.24	0.00	1.00
Declarations	85,309	0.11	0.41	0.00	5.00
Aligned Governor	85,309	0.46	0.50	0.00	1.00
Aligned Representative	85,309	0.47	0.50	0.00	1.00
Aligned Senators	85,309	0.30	0.46	0.00	1.00
Alignment Count	85,309	1.94	1.25	0.00	4.00
Wind Speed	85,309	24.28	37.37	0.00	352.71
Rainfall	85,309	57.77	67.63	0.00	1,538.73
Storm Surge	85,309	0.04	0.27	0.00	6.01
Wind Speed Count	85,309	0.68	0.96	0.00	7.00
Rainfall Count	85,309	1.86	1.32	0.00	8.00
Hurricane Month	84,947	8.38	1.35	5.00	11.00
Mean Annual Rainfall	85,258	1,132.29	340.87	18.04	3,976.14
Mean Annual Temperature	85,258	14.18	4.16	-0.36	25.83
High Support District	85,309	0.32	0.47	0.00	1.00
Low Support District	85,309	0.38	0.49	0.00	1.00
Presidential Election Year	85,309	0.26	0.44	0.00	1.00
Any Election Year	85,309	0.55	0.50	0.00	1.00
Presidents' First Temperature	85,309	0.66	0.47	0.00	1.00
Years President Runs for Reelection	85,309	0.17	0.38	0.00	1.00
Electoral Votes	85,309	15.01	9.23	3.00	55.00
County Vote Change (Pres.)	81,412	-3.08	12.63	-71.98	88.32
Last Term Governor	71,297	0.41	0.49	0.00	1.00
Population (log)	85,240	10.43	1.31	3.69	16.13
Black population (log)	79,741	7.24	2.66	0.00	14.17
Income (log)	78,013	17.27	1.98	9.17	24.84
Income per Capita (log)	78,013	13.72	1.25	10.10	16.83

3.7.6 Robustness – Average Alignment Effects

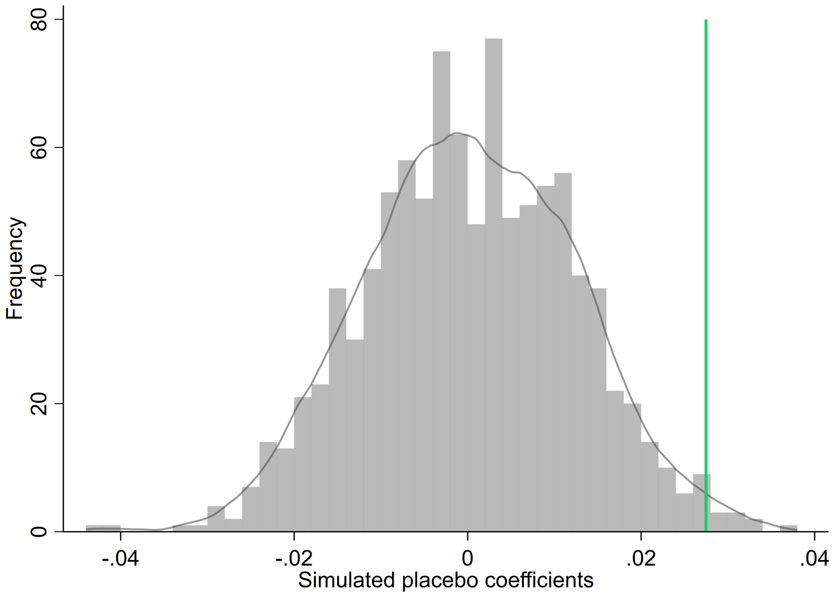

Figure 3.13: Randomization inference (average effect)

Notes: The figure displays the distribution of simulated coefficients of *Aligned Governor* for 1,000 simulation runs with placebo treatments for the regression in Table 1, column 4. The green bar represents the coefficient using the true data.

Table 3.4: Robustness – Alternative clustering

Dep. Var.: *Declaration*	(1)	(2)	(3)	(4)	(5)	(6)	(7)	(8)
Aligned Governor	0.027	0.027	0.027	0.027	0.027	0.027	0.027	0.027
	(0.002)	(0.002)	(0.010)	(0.014)	(0.011)	(0.014)	(0.009)	(0.011)
	[0.000]	[0.000]	[0.008]	[0.055]	[0.013]	[0.061]	[0.004]	[0.013]
Aligned Representative	0.010	0.010	0.010	0.010	0.010	0.012	0.011	0.011
	(0.002)	(0.002)	(0.006)	(0.005)	(0.005)	(0.006)	(0.005)	(0.005)
	[0.000]	[0.000]	[0.080]	[0.068]	[0.058]	[0.030]	[0.036]	[0.042]
Aligned Senators	0.024	0.024	0.024	0.024	0.024	0.026	0.023	0.023
	(0.002)	(0.002)	(0.014)	(0.015)	(0.014)	(0.015)	(0.012)	(0.013)
	[0.000]	[0.000]	[0.087]	[0.128]	[0.097]	[0.070]	[0.057]	[0.072]
Wind Speed (St. Dev.)	0.074	0.074	0.074	0.074	0.074	0.075	0.074	0.074
	(0.002)	(0.002)	(0.006)	(0.010)	(0.008)	(0.010)	(0.007)	(0.009)
	[0.000]	[0.000]	[0.000]	[0.000]	[0.000]	[0.000]	[0.000]	[0.000]
Rainfall (St. Dev.)	0.069	0.069	0.069	0.069	0.069	0.072	0.070	0.070
	(0.002)	(0.001)	(0.008)	(0.007)	(0.005)	(0.006)	(0.005)	(0.006)
	[0.000]	[0.000]	[0.000]	[0.000]	[0.000]	[0.000]	[0.000]	[0.000]
Storm Surge (St. Dev.)	0.030	0.030	0.030	0.030	0.030	0.031	0.028	0.028
	(0.006)	(0.005)	(0.010)	(0.011)	(0.009)	(0.011)	(0.009)	(0.010)
	[0.000]	[0.000]	[0.004]	[0.007]	[0.001]	[0.003]	[0.001]	[0.003]
Cluster	County	County & Year	State	Year	State x Year	Spatial	Hurricane x State	Hurricane
Observations	85,309	85,309	85,309	85,309	85,309	85,309	83,071	83,071

Notes: The table displays regression coefficients with different clustered standard errors in parentheses for the estimation in column 4 in the main results table. P-values are shown in brackets. All estimations use the linear fixed effect-within estimator and include county and year fixed effects. *Wind Speed*, *Rainfall*, and *Storm Surge* are shown in standard deviation increases (above zero). Standard deviations for *Wind Speed*, *Rainfall*, and *Storm Surge* are 38.78 km/h, 68.17 mm, and 0.8 m, respectively. Model 1-5 include county-specific linear time trends. Model 6 includes a HAC arbitrary spatial-temporal clustering with a radius of 1000 km up to 10 years. The sample runs from 1965-2018 in all regressions.

Table 3.5: Robustness – Lags of *Declaration* and *Wind Speed*

Dep. Var.: *Declaration*	(1)	(2)
Aligned Governor	0.029	0.027
	(0.011)	(0.011)
	[0.006]	[0.012]
Aligned Representative	0.010	0.011
	(0.005)	(0.005)
	[0.055]	[0.040]
Aligned Senators	0.022	0.025
	(0.013)	(0.014)
	[0.104]	[0.075]
Wind Speed (St. Dev.)	0.073	0.074
	(0.007)	(0.008)
	[0.000]	[0.000]
Rainfall (St. Dev.)	0.067	0.069
	(0.005)	(0.005)
	[0.000]	[0.000]
Storm Surge (St. Dev.)	0.031	0.030
	(0.009)	(0.009)
	[0.001]	[0.002]
Lags	*Declaration*	*Wind Speed*
Observations	85,309	85,309

Notes: The table displays regression coefficients with two-way clustered standard errors on the state × year and county level in parentheses. P-values are shown in brackets. All estimations use the linear fixed effect-within estimator and include county and year fixed effects as well as county-specific linear time trends. The regression model in column (1) includes 10 lags of the *Declaration* variable, and the model in column (2) includes 10 lags of the *Wind Speed* variable. *Wind Speed*, *Rainfall*, and *Storm Surge* are shown in standard deviation increases (above zero). Standard deviations for *Wind Speed*, *Rainfall*, and *Storm Surge* are 38.78 km/h, 68.17 mm, and 0.8 m, respectively. The sample runs from 1965-2018 in all regressions.

Table 3.6: Robustness – Alternative models

Dep. Var.: *Declaration(s)*	(1)	(2)	(3)	(4)
Aligned Governor	0.607	0.301	0.385	0.385
	(0.043)	(0.023)	(0.023)	(0.135)
	[0.000]	[0.000]	[0.000]	[0.004]
Aligned Representative	0.159	0.083	0.109	0.109
	(0.040)	(0.021)	(0.026)	(0.060)
	[0.000]	[0.000]	[0.000]	[0.072]
Aligned Senators	0.498	0.246	0.339	0.339
	(0.044)	(0.024)	(0.029)	(0.171)
	[0.000]	[0.000]	[0.000]	[0.048]
Wind Speed (St. Dev.)	0.926	0.489	0.452	0.452
	(0.021)	(0.011)	(0.015)	(0.043)
	[0.000]	[0.000]	[0.000]	[0.000]
Rainfall (St. Dev.)	0.765	0.413	0.204	0.204
	(0.018)	(0.009)	(0.013)	(0.031)
	[0.000]	[0.000]	[0.000]	[0.000]
Storm Surge (St. Dev.)	0.092	0.034	-0.089	-0.089
	(0.083)	(0.043)	(0.043)	(0.046)
	[0.264]	[0.429]	[0.037]	[0.056]
Model	logit	probit	Poisson	PPML
Observations	64,579	64,579	68,616	64,579

Notes: The table displays regression coefficients for different estimation models with SE in parentheses. P-values are shown in brackets. Conditional FE logit and probit estimations are computed using the Stata package written by Fernández-Val & Weidner (2016). For the Poisson pseudo-maximum likelihood (PPML) estimation, we use the package developed by Correia et al. (2020). In the logit and probit model, the dependent variable is *Declaration*, whereas for the remaining models it is *Declarations*. All models include county and year fixed effects. *Wind Speed*, *Rainfall*, and *Storm Surge* are shown in standard deviation increases (above zero). Standard deviations for *Wind Speed*, *Rainfall*, and *Storm Surge* are 38.78 km/h, 68.17 mm, and 0.8 m, respectively. The sample runs from 1965-2018 in all regressions.

Table 3.7: Robustness – Socioeconomic control variables

Dep. Var.: *Declaration*	(1)	(2)	(3)	(4)	(5)	(6)
Aligned Governor		0.032	0.027	0.027	0.026	0.026
		(0.012)	(0.011)	(0.011)	(0.011)	(0.011)
		[0.006]	[0.020]	[0.013]	[0.014]	[0.015]
Aligned Representative			0.011	0.009	0.009	0.009
			(0.005)	(0.005)	(0.005)	(0.005)
			[0.024]	[0.078]	[0.078]	[0.070]
Aligned Senators			0.026	0.023	0.026	0.025
			(0.013)	(0.014)	(0.014)	(0.014)
			[0.049]	[0.104]	[0.070]	[0.076]
Population (log)$_{t-1}$	0.010	0.011	0.012	-0.003	-0.003	-0.004
	(0.004)	(0.005)	(0.005)	(0.004)	(0.003)	(0.003)
	[0.019]	[0.017]	[0.011]	[0.348]	[0.291]	[0.204]
Black Population (log)$_{t-1}$	-0.007	-0.007	-0.005	-0.007	-0.007	-0.007
	(0.002)	(0.002)	(0.002)	(0.003)	(0.003)	(0.003)
	[0.004]	[0.008]	[0.028]	[0.009]	[0.009]	[0.009]
Real Income (log)$_{t-1}$	0.014	0.012	0.010	0.008	0.008	0.009
	(0.006)	(0.006)	(0.006)	(0.007)	(0.007)	(0.007)
	[0.014]	[0.041]	[0.108]	[0.281]	[0.252]	[0.209]
Per Capita Real Income (log)$_{t-1}$	-0.019	-0.017	-0.014	-0.009	-0.010	-0.011
	(0.009)	(0.009)	(0.009)	(0.009)	(0.009)	(0.009)
	[0.037]	[0.064]	[0.135]	[0.336]	[0.267]	[0.222]
Wind Speed (St. Dev.)	0.075	0.075	0.075	0.074		
	(0.008)	(0.007)	(0.007)	(0.007)		
	[0.000]	[0.000]	[0.000]	[0.000]		
Rainfall (St. Dev.)	0.072	0.072	0.071	0.069	0.069	0.069
	(0.005)	(0.005)	(0.005)	(0.005)	(0.005)	(0.005)
	[0.000]	[0.000]	[0.000]	[0.000]	[0.000]	[0.000]
Storm Surge (St. Dev.)	0.032	0.031	0.031	0.030	-0.002	-0.002
	(0.010)	(0.010)	(0.010)	(0.010)	(0.009)	(0.009)
	[0.001]	[0.001]	[0.001]	[0.002]	[0.813]	[0.797]
Time Trends				X	X	X
Wind Speed Polynomials					X	
Wind Speed Bins						X
Observations	85,309	85,309	85,309	85,309	85,309	85,309

Notes: The table displays regression coefficients with two-way clustered standard errors on the state × year and county level in parentheses. P-values are shown in brackets. All estimations use the linear fixed effect-within estimator and include county and year fixed effects. *Wind Speed*, *Rainfall*, and *Storm Surge* are shown in standard deviation increases (above zero). Standard deviations for *Wind Speed*, *Rainfall*, and *Storm Surge* are 38.78 km/h, 68.17 mm, and 0.8 m, respectively. Model 4-6 include county-specific linear time trends. 'Wind Speed Bins' signifies the usage of the semi-parametric approach to model wind speed. 'Wind Speed Polynomials' indicates the usage of quartic polynomials. The sample runs from 1965-2018 in all regressions.

3.7.7 Robustness and Further Results – Heterogeneous Alignment Bias

3.7.7.1 Standard Errors and Randomization Inference

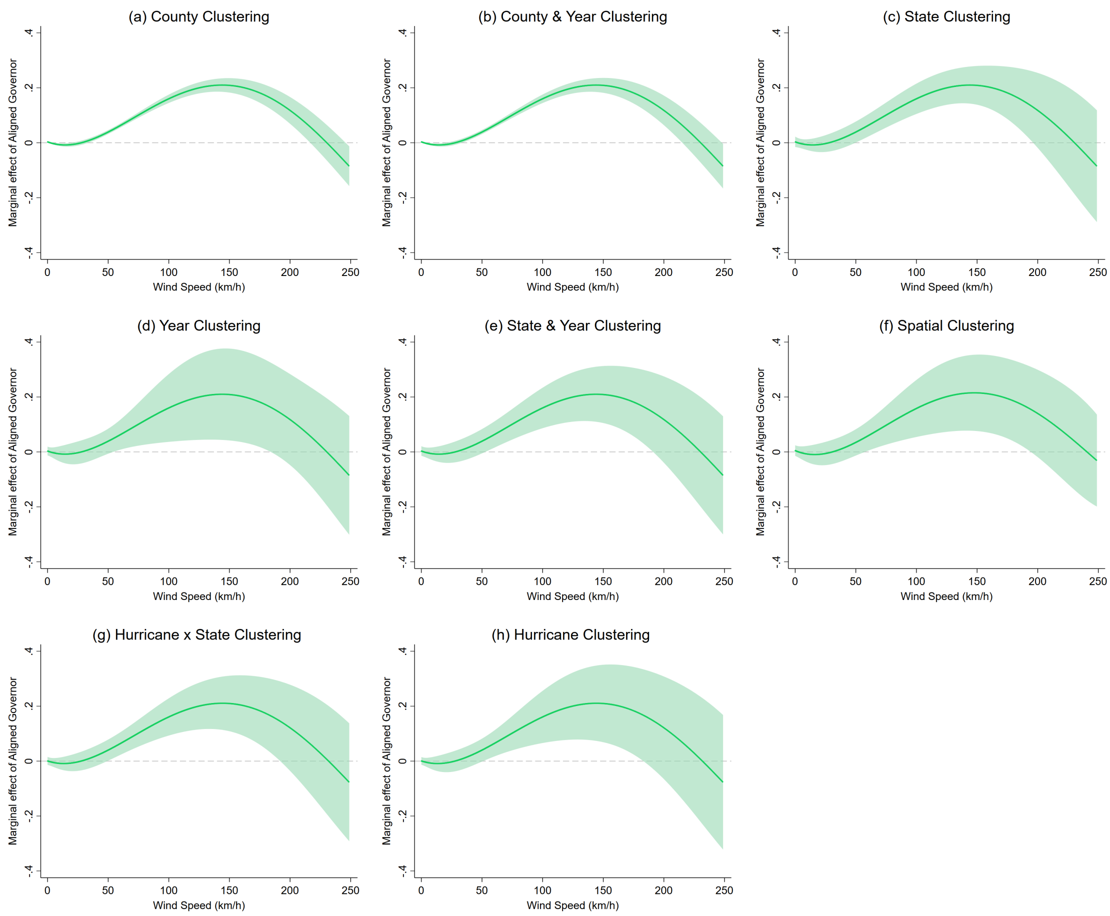

Figure 3.14: Robustness – Alternative clustering choices

Notes: The figure displays marginal effects of *Aligned Governor* for different levels of *Wind Speed*, derived from our polynomial estimation (solid green line). The light green shaded area represents the 95 percent confidence interval applying the alternative clustering levels as indicated in the panel titles. Panel f applies a HAC arbitrary spatial-temporal clustering with a radius of 1,000 km up to 10 years. The sample covers county-year observations from 1965–2018.

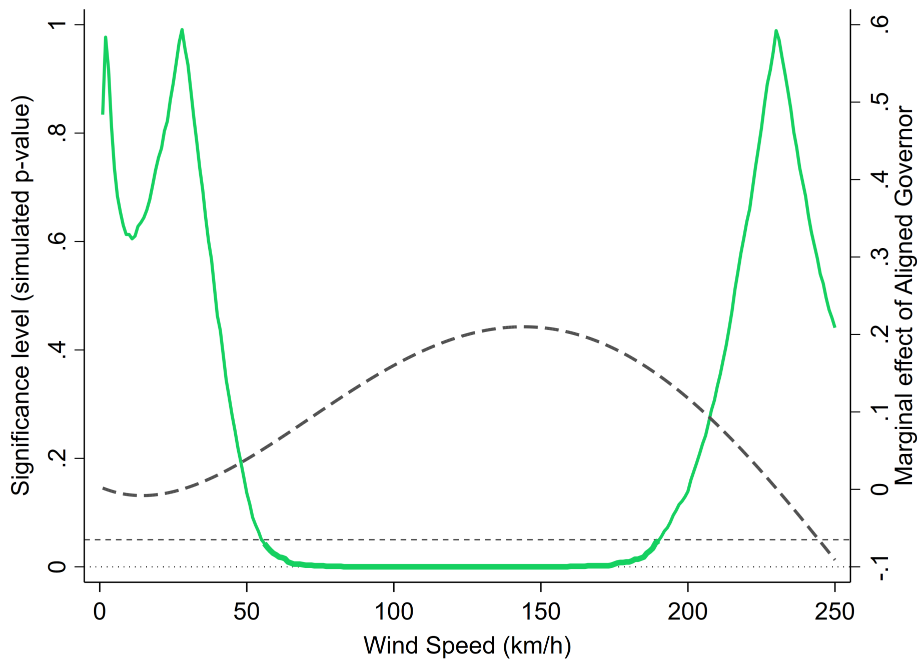

Figure 3.15: Randomization inference – Simulated p-value

Notes: The figure displays the permutation p-value ($p_{perm.} = N^{-1} \sum_{i=i}^{N} 1[|\beta| < |\beta_{i,placebo}|]$) of the marginal effect of *Aligned Governor* for every *Wind Speed* in green, in bold print for the interval significant at the 95% confidence level derived from the simulation displayed in the paper. The gray dashed line represents the coefficient size using the true data.

3.7.7.2 Subsamples

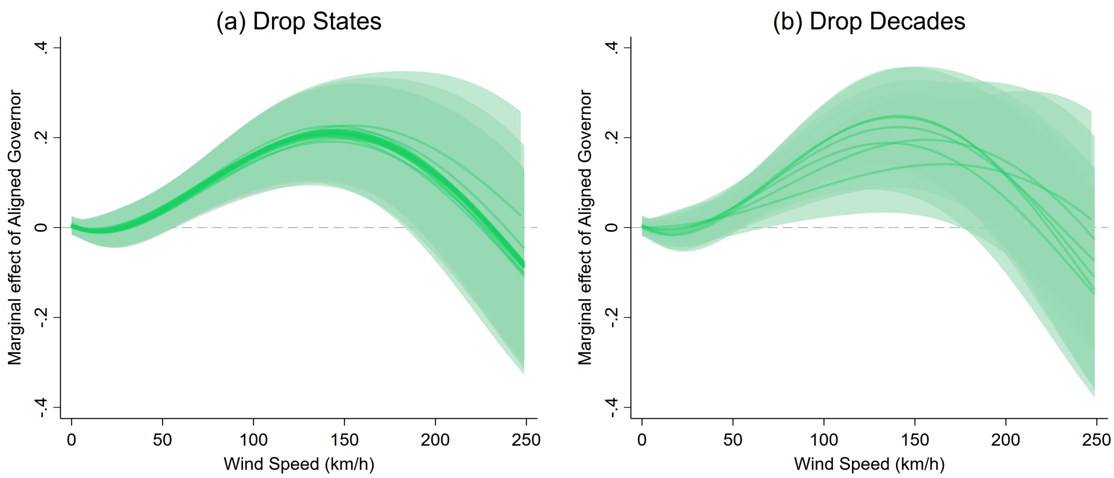

Figure 3.16: Robustness – Omitting states and decades

Notes: This figure shows the sensitivity of our result to the omission of groups of observations. It displays marginal effects of *Aligned Governor* from individual regressions, where each regression omits all observations from one state (a) or decade (b). The panels show separate lines for the predicted marginal effects from each regression. The transparent shaded areas indicate the respective 95% confidence intervals applying two-way clustered standard errors on the state × year and county level.

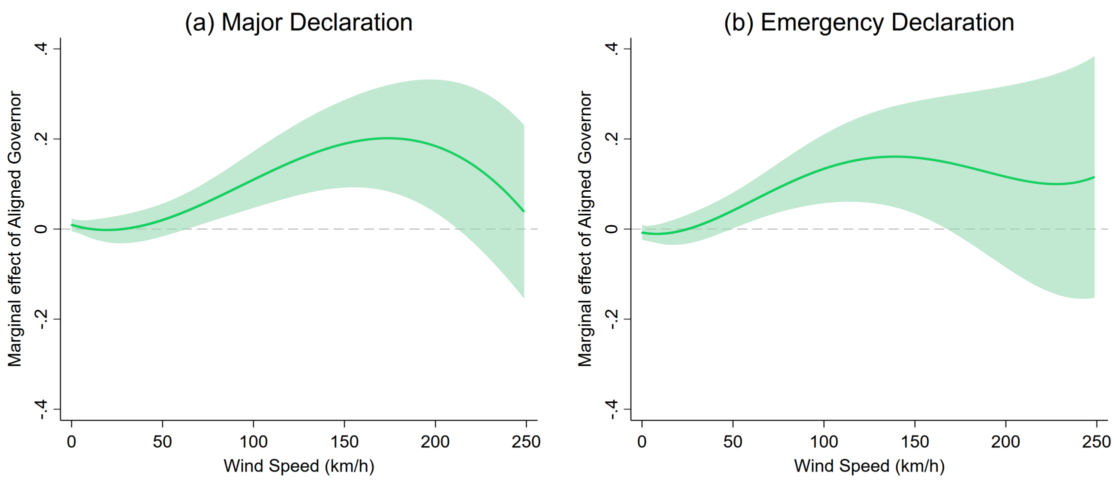

Figure 3.17: Major disaster declarations and emergency declarations

Notes: The figure displays marginal effects of *Aligned Governor* for different levels of *Wind Speed*, derived from our polynomial estimation (solid green line). The light green shaded area represents the 95 percent confidence interval applying two-way clustered standard errors on the state × year and county level. The sample covers county-year observations from 1965–2018. In Panel a, the dependent variable is *Major Declaration* and in Panel b *Emergency Declaration*.

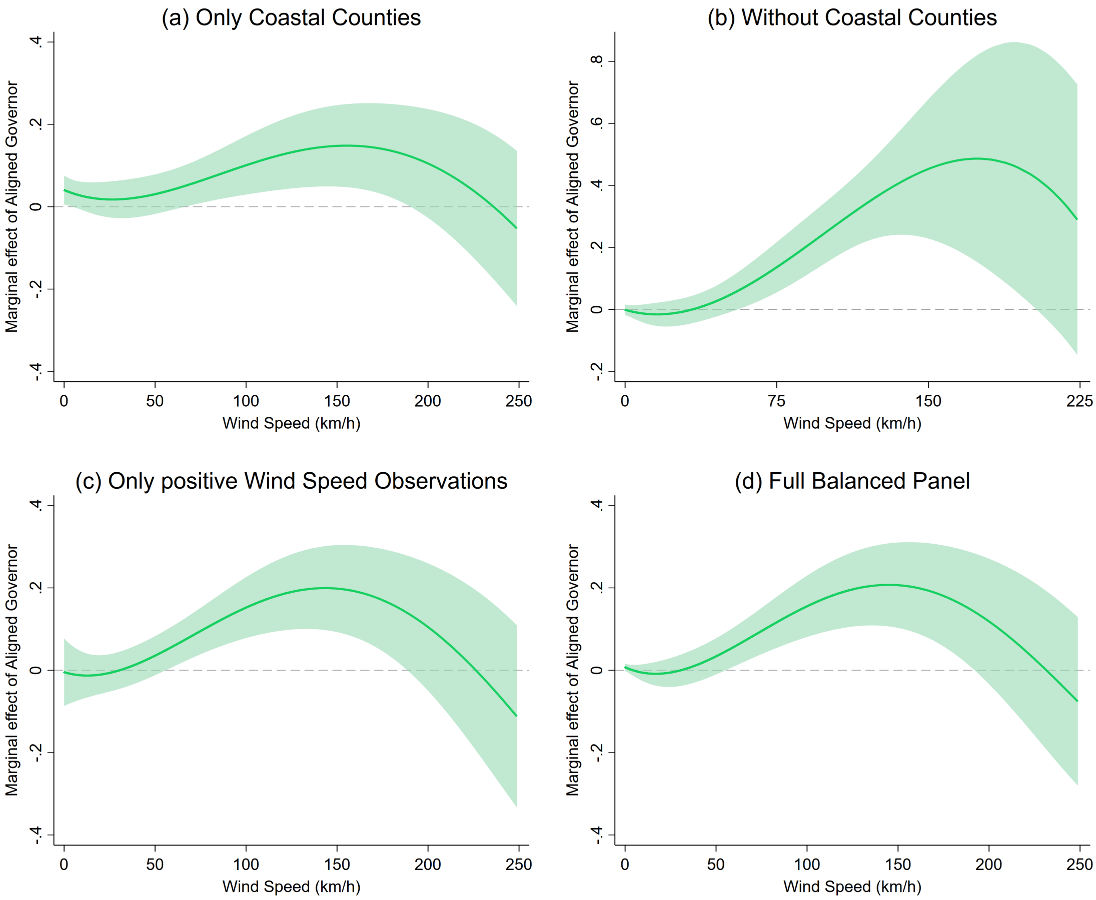

Figure 3.18: Robustness – Subsamples

Notes: The figure displays marginal effects of *Aligned Governor* for different levels of *Wind Speed*, derived from our polynomial estimation (solid green line). The light green shaded area represents the 95 percent confidence interval applying two-way clustered standard errors on the state × year and county level. Panel a uses a subsample of coastal counties and Panel b non-coastal counties. Panel c includes only observations with a positive *Wind Speed* observation. Panel d uses a full balanced panel, including observations with both zero *Wind Speed* and *Rainfall*.

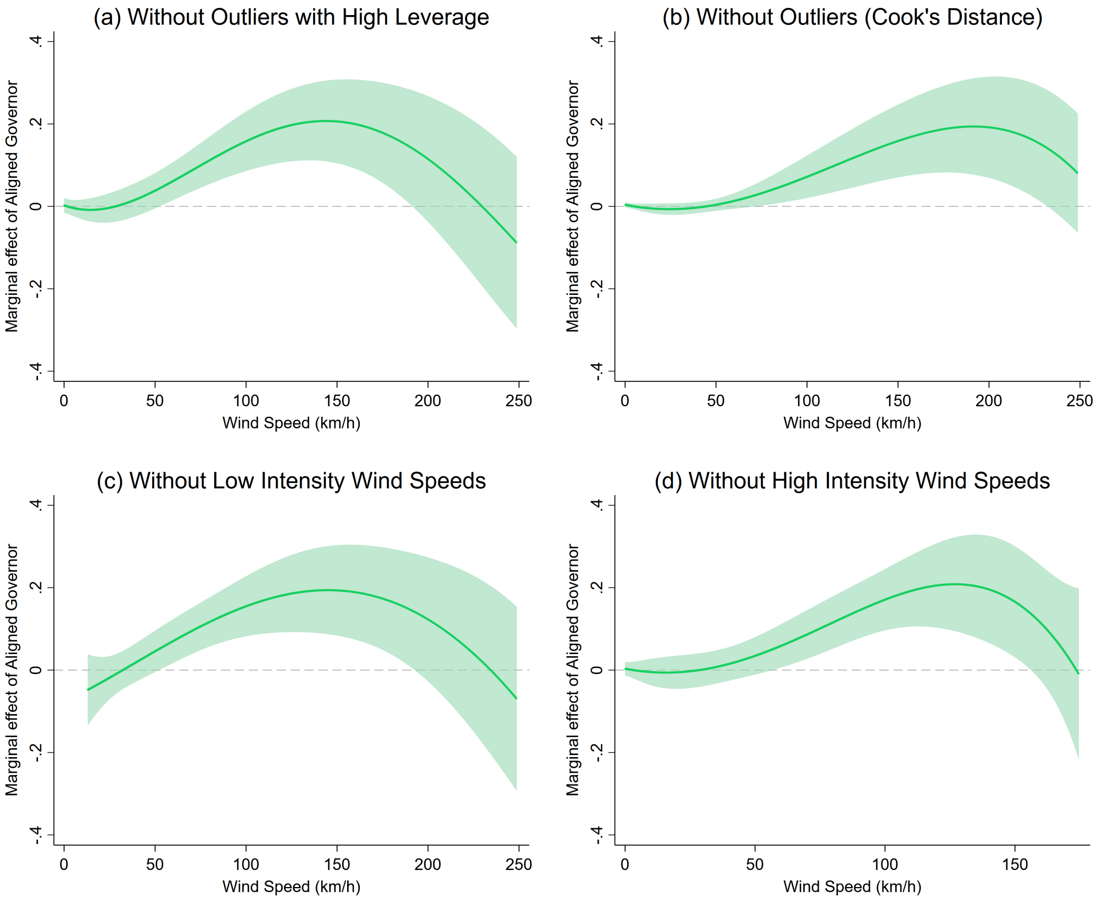

Figure 3.19: Robustness – Excluding outliers

Notes: The figure displays marginal effects of *Aligned Governor* for different levels of *Wind Speed*, derived from our polynomial estimation (solid green line). The light green shaded area represents the 95 percent confidence interval applying two-way clustered standard errors on the state × year and county level. The sample covers county-year observations from 1965–2018. Panel a excludes all observations with wind speeds below the 10% percentile (13 km/h). Panel b excludes all observations with wind speeds above the 99% percentile (183 km/h). Panel c excludes all observations above a leverage of $(2k+2)/n$. Panel d excludes all observations with a higher Cook's distance measure of $4/n$.

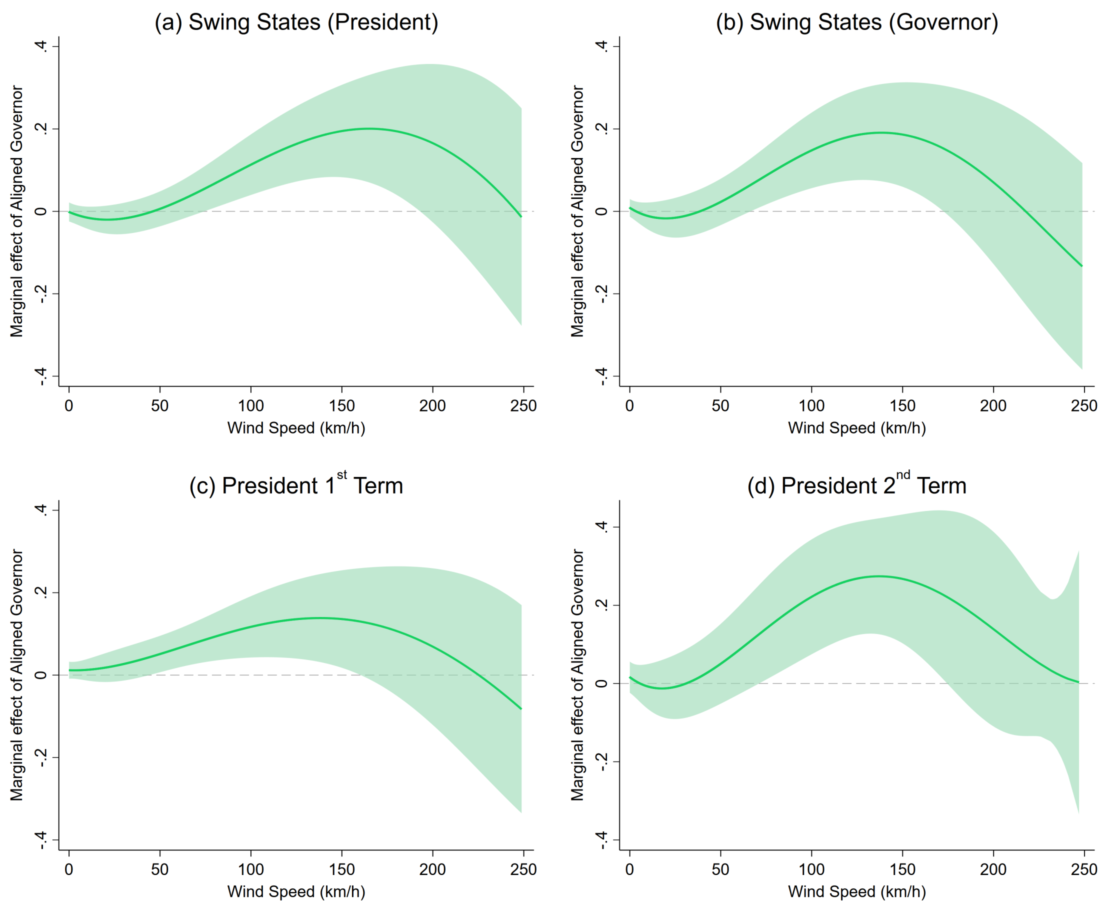

Figure 3.20: Swing states and different terms of the presidents

Notes: The figure displays marginal effects of *Aligned Governor* for different levels of *Wind Speed*, derived from our polynomial estimation (solid green line). The light green shaded area represents the 95 percent confidence interval applying two-way clustered standard errors on the state × year and county level. The sample covers county-year observations from 1965–2018. Panel a restricts the sample to swing states in terms of the presidential election (all observations in which the statewide majority shifted at least once in the last three elections). Panel b restricts the sample to swing states in terms of the gubernatorial election (all observations in which the statewide majority shifted at least once in the last three elections).
Panel c shows the results for presidents in their first term and Panel d for their second term.

3.7.7.3 Alternative Specifications and Triple Interactions

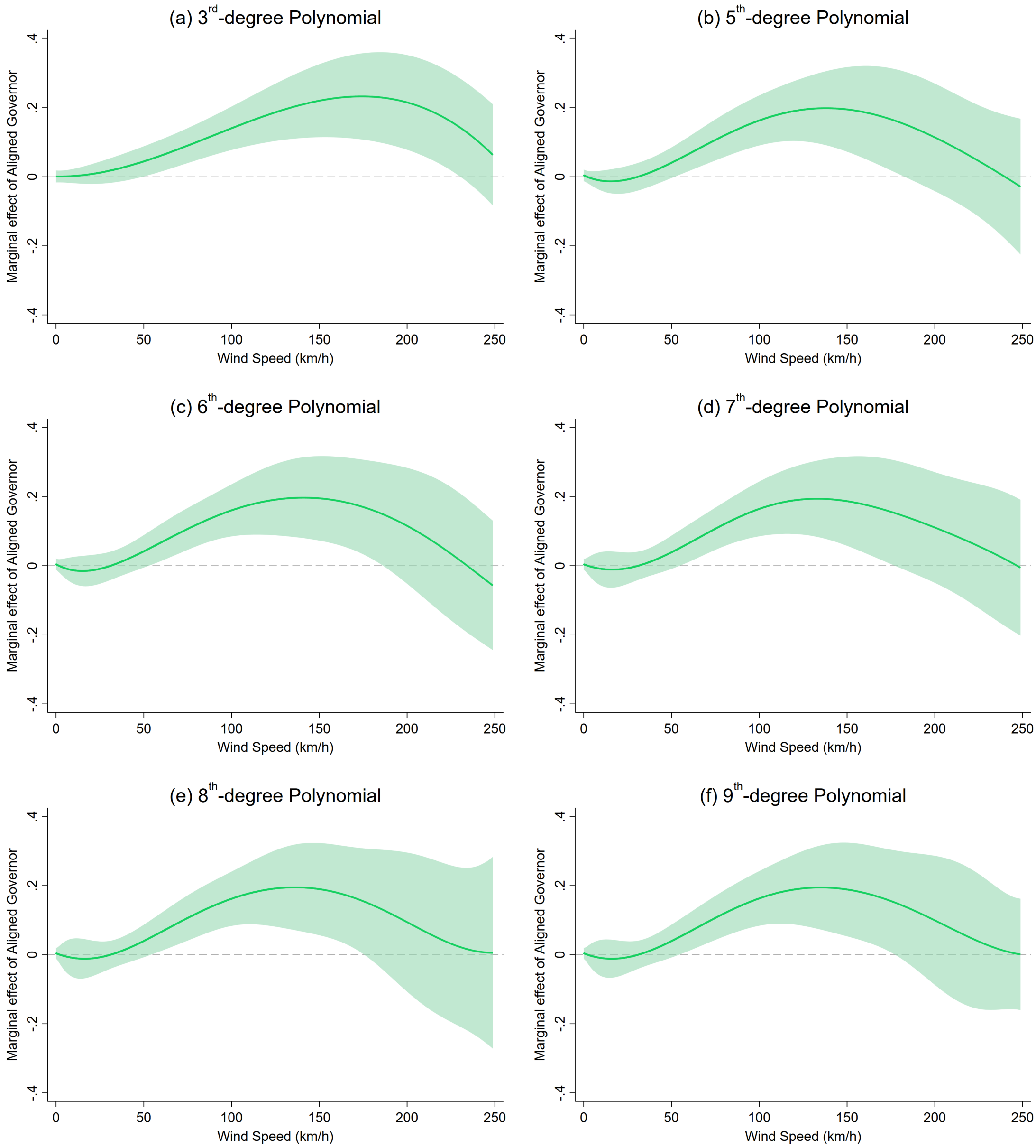

Figure 3.21: Robustness – Higher *Wind Speed* polynomials

Notes: The figure displays marginal effects of *Aligned Governor* for different levels of *Wind Speed*, derived from our polynomial estimation (solid green line). The light green shaded area represents the 95 percent confidence interval applying two-way clustered standard errors on the state × year and county level. The sample covers county-year observations from 1965–2018. Panel a-f apply a *Wind Speed* polynomial with different polynomial degrees.

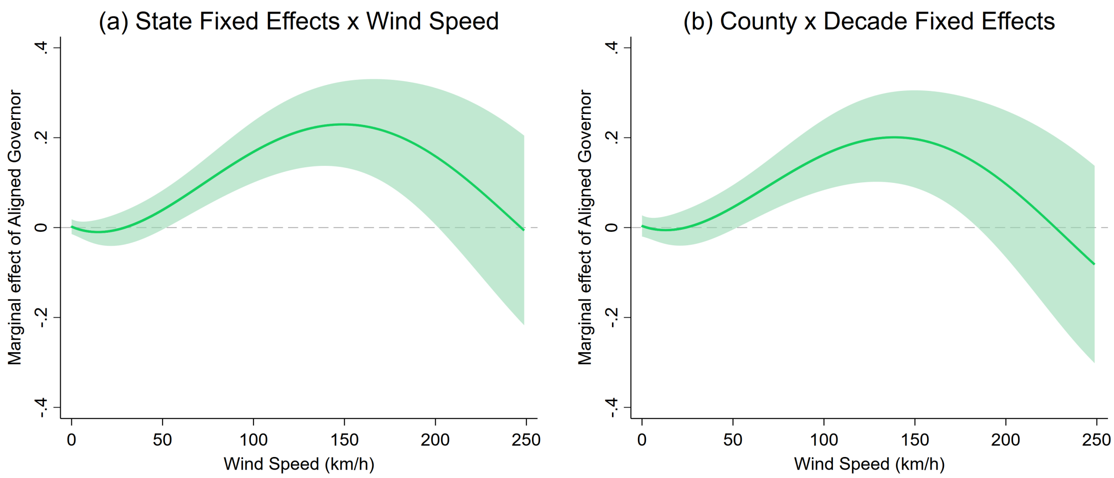

Figure 3.22: Robustness – County × decade fixed effects & state-specific *Wind Speed* controls

Notes: This figure shows the sensitivity of our main result with more flexible estimation models. The figure displays marginal effects of *Aligned Governor* for different levels of *Wind Speed* (solid green line). The light green shaded area represents 95% confidence intervals applying two-way clustered standard errors on the state × year and county level. The sample covers county-year observations from 1965–2018. Panel a adds separate linear *Wind Speed* effects for each state added to our polynomial estimation. Panel b includes county × decade fixed effects in our polynomial estimation.

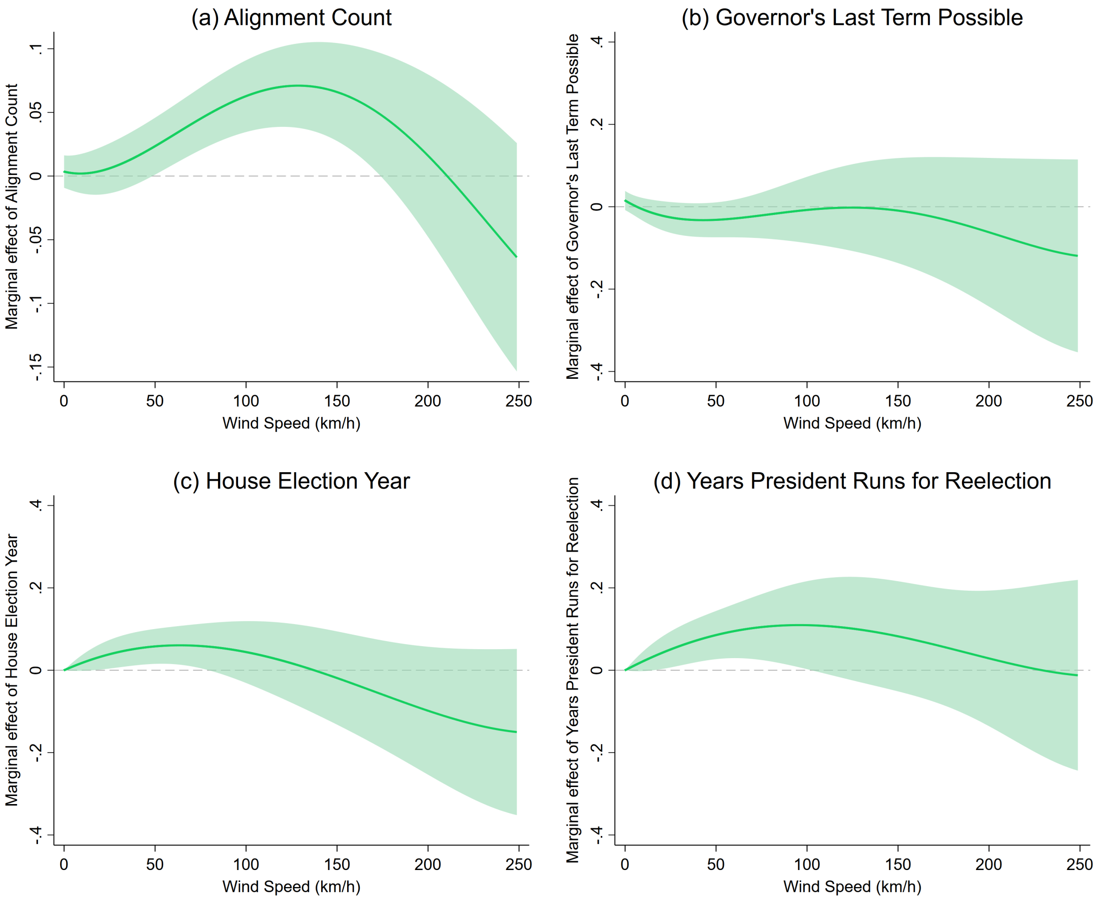

Figure 3.23: Additional specifications and further political factors

Notes: The figure displays marginal effects for the variables of interest depicted on the vertical axes from four polynomial regressions. The shaded areas represent 95 percent confidence intervals applying two-way clustered standard errors on the state × year and county level. The sample covers county-year observations from 1965–2018. In Panel a *Alignment Count* is a variable that indicates how many of the major politicians (governor, senators, representative) are aligned with the president. In Panel b *Governor's Last Term Possible* is an indicator taking the value 1 if governors are in their last term due to a constitutional restriction that prohibits them to run for the office again. Panel c includes an indicator for congressional election years. Panel d interacts an indicator for years in which an incumbent president runs for reelection with the *Wind Speed* polynomial.

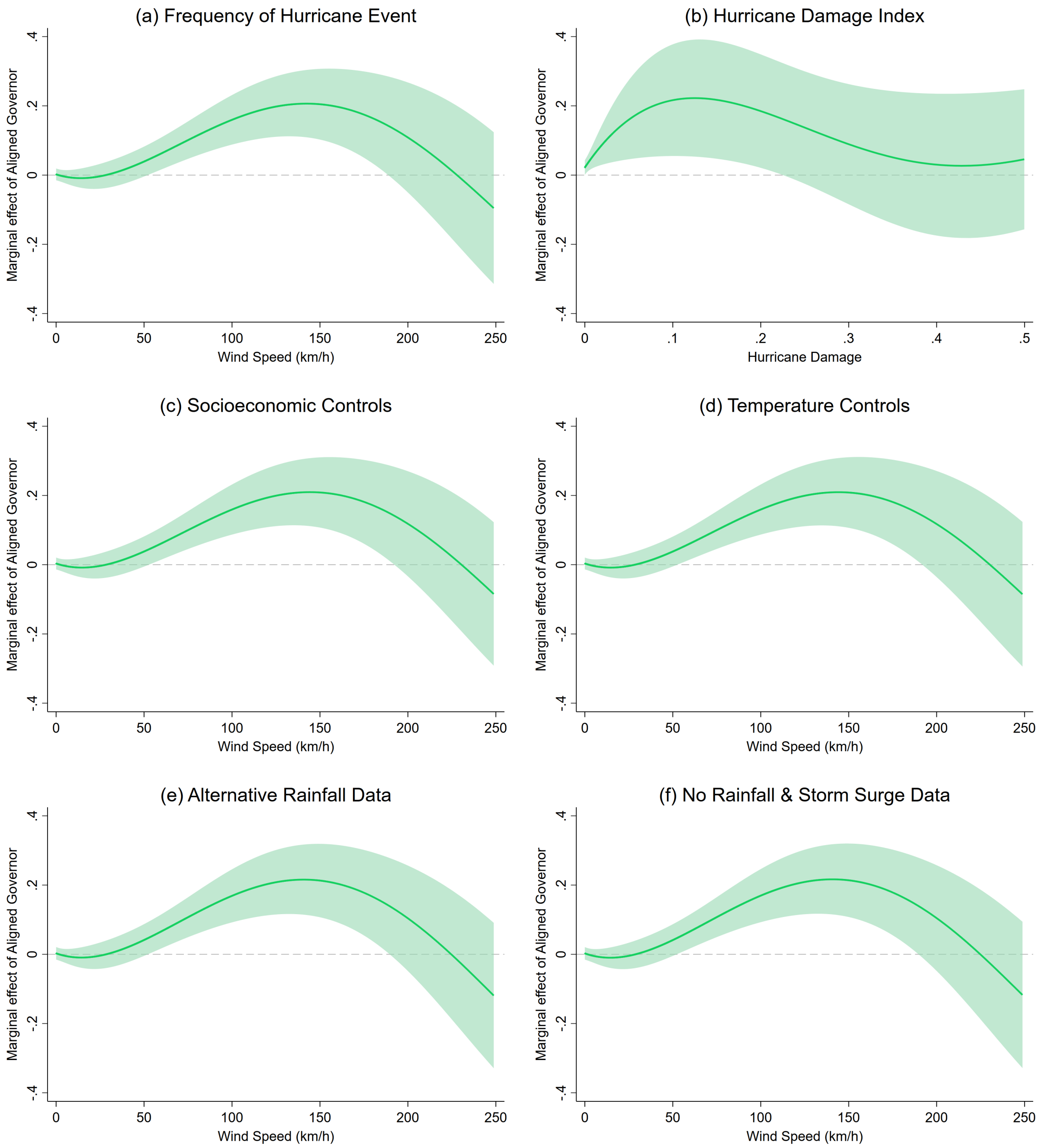

Figure 3.24: Robustness – Alternative specifications

Notes: This figure shows the robustness of our main result to alternative specifications. The panels display marginal effects of *Aligned Governor* for different levels of *Wind Speed*, derived from our polynomial estimation (solid green line). The light green shaded area represents the 95 percent confidence interval applying two-way clustered standard errors on the state × year and county level. The sample covers county-year observations from 1965–2018. Panel a includes two variables that account for the frequency of *Wind Speed* and *Rainfall* incidences respectively. Panel b includes the wind speed damage index as proposed by Emanuel (2011) instead of our *Wind Speed* measure. In Panel c the estimation includes *Population (log)*, *Black Population (log)*, *Income (log)*, *Income Per Capita (log)*, all lagged by one year. Panel d includes additional temperature controls (*Mean Annual Temperature*) from the Prism data base. Panel e uses alternative rainfall data (*Mean Annual Rainfall*) from the Prism data base. Panel f omits the *Rainfall* and *Storm Surge* control variable.

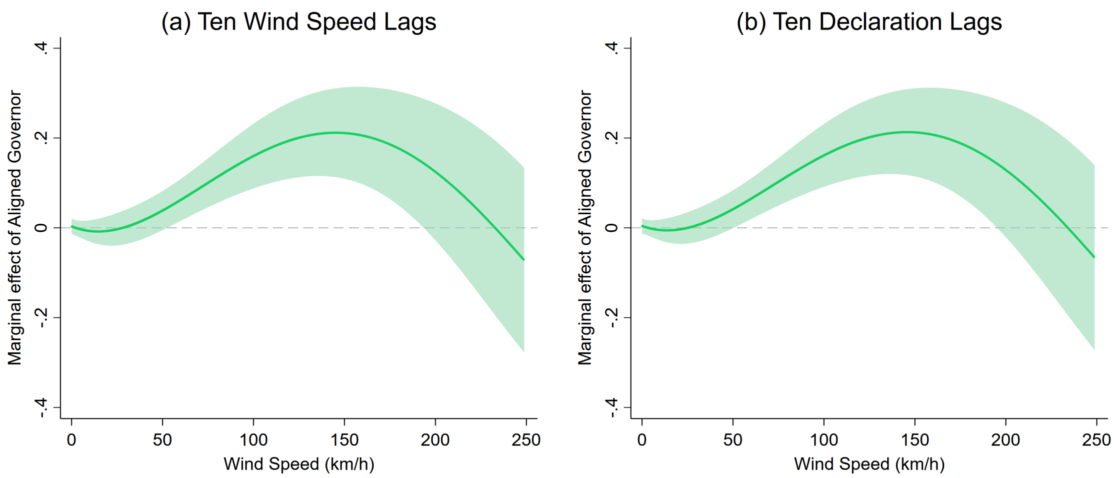

Figure 3.25: Robustness – Lags

Notes: The figure displays marginal effects of *Aligned Governor* for different levels of *Wind Speed*, derived from our polynomial estimation (solid green line). The light green shaded area represents the 95 percent confidence interval applying two-way clustered standard errors on the state × year and county level. The sample covers county-year observations from 1965–2018. Panel a adds the first ten lags of *Wind Speed* and Panel b the first ten lags of *Declaration*.

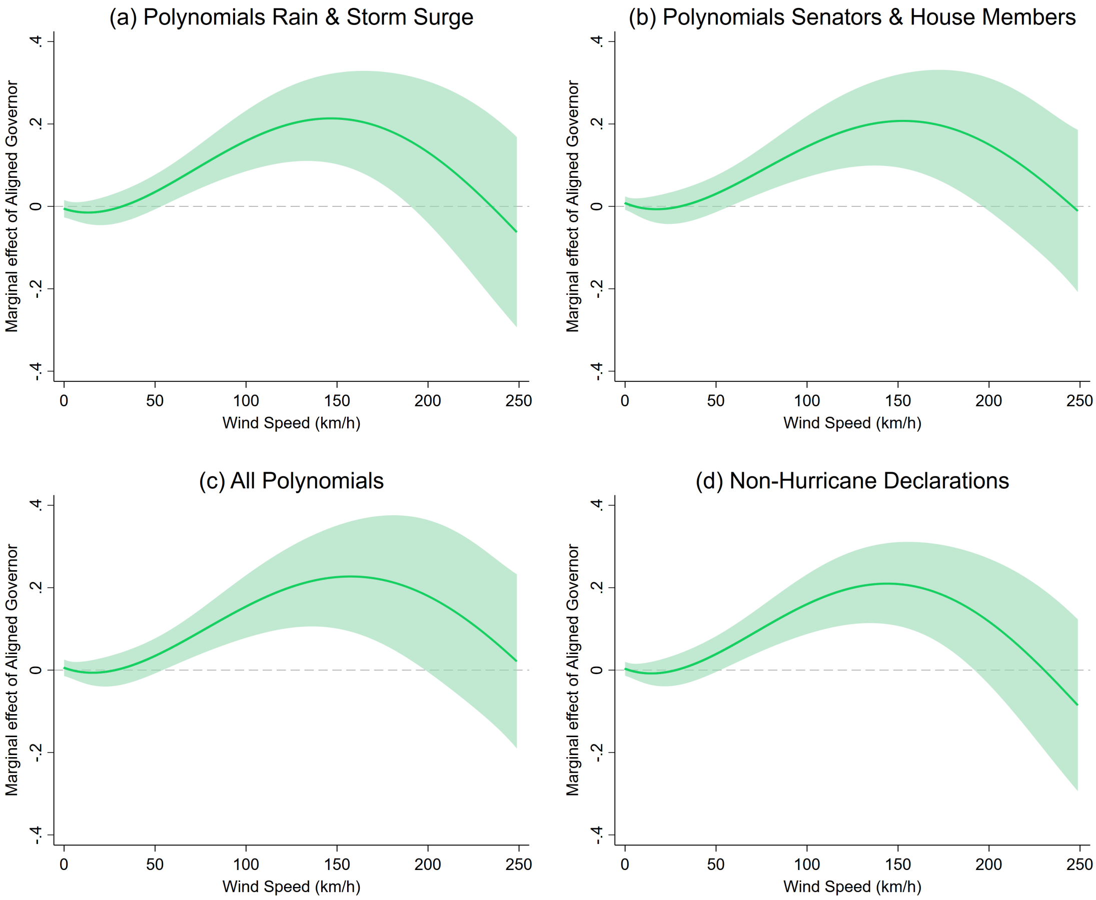

Figure 3.26: Robustness – Polynomial controls and other declarations

Notes: The figure displays marginal effects of *Aligned Governor* for different levels of *Wind Speed*, derived from our polynomial estimation (solid green line). The light green shaded area represents the 95 percent confidence interval applying two-way clustered standard errors on the state $\times$ year and county level. The sample covers county-year observations from 1965–2018. Panel a includes additional polynomial interactions of *Aligned Governor* with *Rainfall* and *Storm Surge* and Panel b adds polynomial interactions of *Wind Speed* with *Aligned Representatives* and *Aligned Senators*. Panel c allows for all interactions as described in Panel a and b. In Panel d we additionally control for the number of other disaster declarations per county and year.

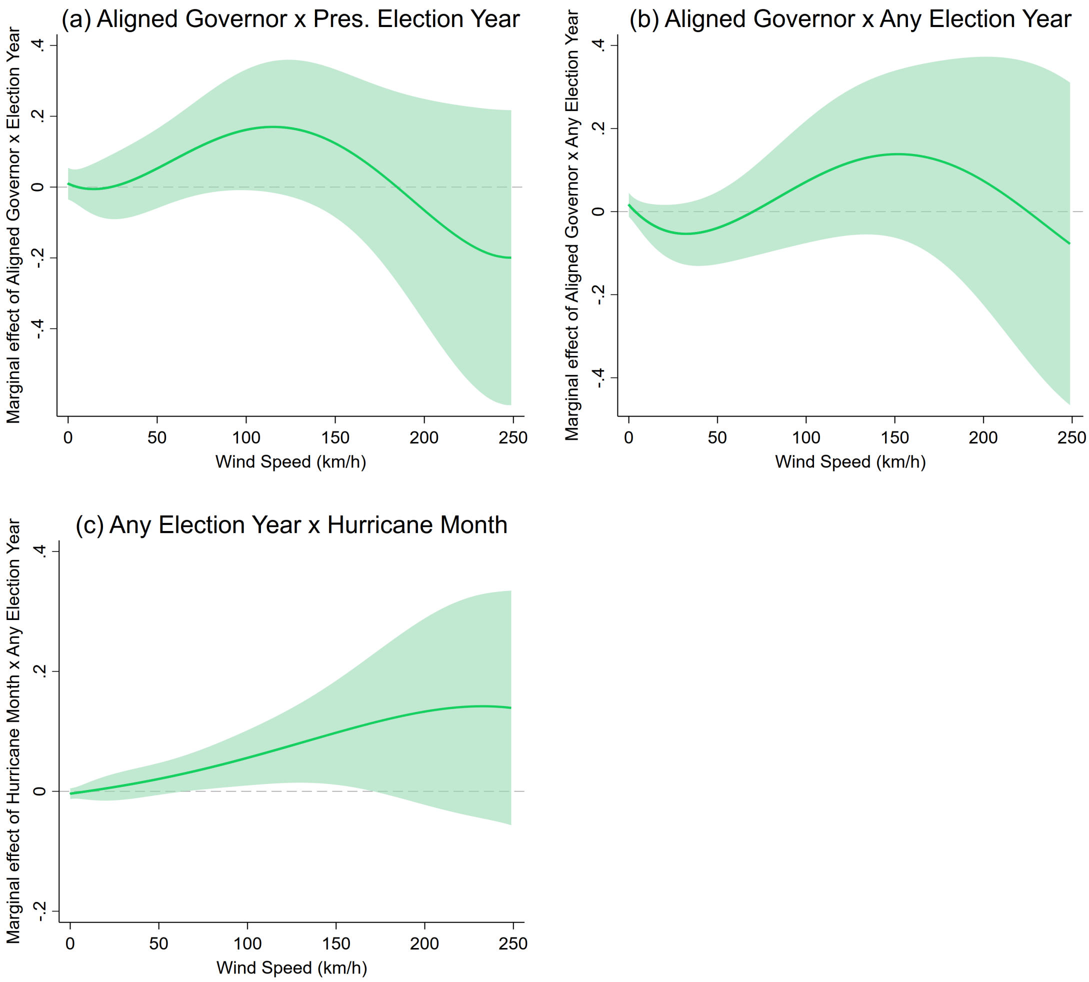

Figure 3.27: Political relief cycles – Marginal effects from triple interactions

Notes: The figure displays marginal effects for the variable specified on the respective vertical axis from three polynomial estimations including triple interactions. In each specification, we add the depicted variables of interest as well as all possible cross-interactions with the *Wind Speed* polynomial to our baseline for the estimation of heterogeneous effects. Shaded areas represent 95% confidence intervals applying two-way clustered standard errors on the state × year and county level. In comparison to the triple interaction figure shown in the paper, this figure shows only the marginal effects of the respective triple-interacted coefficients, i.e. displaying the differences in marginal effects between election years and non-election years directly.

3.7.8 Main Results – Detailed Tables and Additional Figures

Table 3.8: Sequential F-tests for *Wind Speed* polynomials x *Aligned Governor*

	F-statistic	p-value
9 vs 8	.4112046	.6629178
8 vs 7	1.177131	.3084152
7 vs 6	1.09806	.3337564
6 vs 5	.9970591	.3691808
5 vs 4	.5066077	.602628
4 vs 3	3.843388	.0216092
3 vs 2	15.35145	2.47e-07

Notes: The table displays the results of seven F-tests based on our polynomial regression model presented in the paper. We test the unrestricted model of polynomial degree n against its restricted alternative with degree $n-1$ as depicted in the leftmost column. Each restriction consists of two coefficients, the excluded *Wind Speed*-polynomial and its interaction with *Aligned Governor*. The p-values document which restrictions are associated with a significantly better fit to explain the variation in the dependent variable *Declaration*.

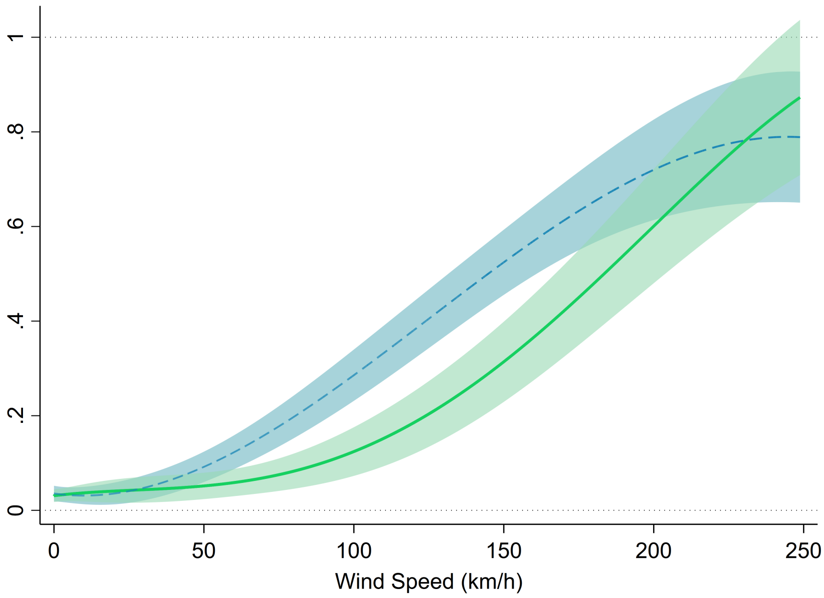

Figure 3.28: Predicted average probabilities for *Declaration* = 1

Notes: The figure shows the predicted probability for a disaster declaration in an average county depending on alignment status derived from our baseline regression. The dashed blue line represents the estimated average declaration probability if a county is aligned, the green solid line plots the probability for unaligned counties respectively. *Rainfall* and *Storm Surge* enter the prediction with regards to their average levels. All estimations include county- and year fixed effects as well as linear county-specific time trends. The shaded areas show 95% confidence intervals based two-way clustered standard errors on the state × year and county level.

Table 3.9: Polynomial regression results of main specification

Dep. Var.: *Declaration*	(1)
Wind Speed	0.0008
	(0.0009)
	[0.3902]
Wind Speed^2	-0.0000
	(0.0000)
	[0.3445]
Wind Speed^3	0.0000
	(0.0000)
	[0.0280]
Wind Speed^4	-0.0000
	(0.0000)
	[0.0056]
Rainfall	0.0010
	(0.0001)
	[0.0000]
Storm Surge	-0.0030
	(0.0105)
	[0.7777]
Aligned Governor	0.0033
	(0.0087)
	[0.7067]
Aligned Governor × *Wind Speed*	-0.0016
	(0.0012)
	[0.1730]
Aligned Governor × *Wind Speed*^{2}	0.0001
	(0.0000)
	[0.0161]
Aligned Governor × *Wind Speed*^{3}	-0.0000
	(0.0000)
	[0.0263]
Aligned Governor × *Wind Speed*^{4}	0.0000
	(0.0000)
	[0.0701]
Aligned Representative	0.0093
	(0.0052)
	[0.0741]
Aligned Senators	0.0258
	(0.0138)
	[0.0628]
Time Trends	X
Observations	85,309

Notes: The table displays regression coefficients of the main polynomial specification with two-way clustered standard errors on the state × year and county level in parentheses. P-values are shown in brackets. All estimations use the linear fixed effect-within estimator and include county and year fixed effects. The sample runs from 1965-2018 in all regressions.

Table 3.10: Bins regression results of main specification

Dep. Var.: *Declaration*	(1)
Wind Speed Bin 1	0.0052
	(0.0191)
	[0.7848]
Wind Speed Bin 2	0.0179
	(0.0140)
	[0.1999]
Wind Speed Bin 3	0.0292
	(0.0210)
	[0.1642]
Wind Speed Bin 4	0.0757
	(0.0233)
	[0.0012]
Wind Speed Bin 5	0.1088
	(0.0432)
	[0.0119]
Wind Speed Bin 6	0.1732
	(0.0639)
	[0.0068]
Wind Speed Bin 7	0.4687
	(0.0628)
	[0.0000]
Wind Speed Bin 8	0.5879
	(0.0742)
	[0.0000]
Wind Speed Bin 9	0.5219
	(0.1026)
	[0.0000]
Wind Speed Bin 10	0.7337
	(0.0584)
	[0.0000]
Rainfall	0.0010
	(0.0001)
	[0.0000]
Storm Surge	-0.0032
	(0.0104)
	[0.7583]
Aligned Governor	0.0032
	(0.0083)
	[0.6973]
Aligned Governor × *Wind Speed Bin 1*	-0.0031
	(0.0268)
	[0.9069]
Aligned Governor × *Wind Speed Bin 2*	0.0012
	(0.0197)
	[0.9517]
Aligned Governor × *Wind Speed Bin 3*	0.0838
	(0.0379)
	[0.0271]
Aligned Governor × *Wind Speed Bin 4*	0.1023
	(0.0353)
	[0.0038]
Aligned Governor × *Wind Speed Bin 5*	0.1833
	(0.0523)
	[0.0005]
Aligned Governor × *Wind Speed Bin 6*	0.2360
	(0.0760)
	[0.0019]
Aligned Governor × *Wind Speed Bin 7*	0.1137
	(0.0813)
	[0.1620]
Aligned Governor × *Wind Speed Bin 8*	0.0670
	(0.1038)
	[0.5186]
Aligned Governor × *Wind Speed Bin 9*	0.1910
	(0.1103)
	[0.0835]
Aligned Governor × *Wind Speed Bin 10*	-0.0338
	(0.0764)
	[0.6578]
Aligned Senators	0.0252
	(0.0137)
	[0.0661]
Aligned Representative	0.0096
	(0.0051)
	[0.0622]
Time Trends	X
Observations	85,309

Notes: The table displays regression coefficients of the main bin specification with two-way clustered standard errors on the state × year and county level in parentheses. P-values are shown in brackets. All estimations use the linear fixed effect-within estimator and include county and year fixed effects . The sample runs from 1965-2018 in all regressions.

3.7.9 Additional Correlations and Results

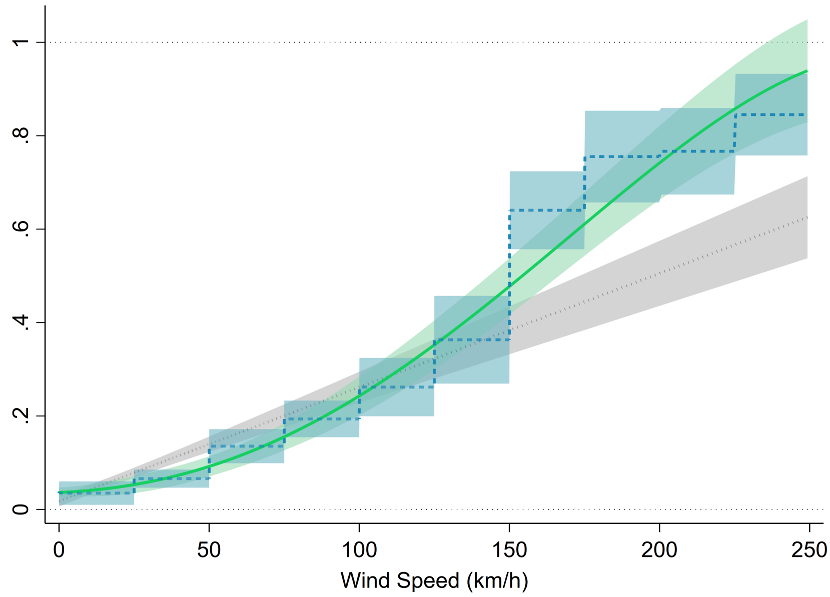

Figure 3.29: Relationship of *Wind Speeds* and disaster *Declarations*

Notes: The figure shows the predicted probability for a disaster declaration from three different estimations with *Wind Speed* as the explanatory variable. The specification represented by the black dotted line uses only a linear *Wind Speed* variable, the green solid line applies a quartic *Wind Speed* polynomial, and the blue dashed line applies ten *Wind Speed* 25 km/h bins. All estimations include county- and year fixed effects as well as linear county-specific time trends. The shaded areas show 95% confidence intervals based two-way clustered standard errors on the state × year and county level.

Table 3.11: Declaration turndowns and relief amounts

	Declaration	Public Assistance Projects	Total Public Assistance (log)
	(1)	(2)	(3)
Aligned Governor	0.014	1.734	0.806
	(0.015)	(27.522)	(0.469)
	[0.347]	[0.950]	[0.089]
Aligned Representative	0.006	-27.292	0.258
	(0.006)	(21.503)	(0.345)
	[0.306]	[0.207]	[0.457]
Aligned Senators	0.000	-2.921	-0.880
	(0.012)	(23.884)	(0.566)
	[0.970]	[0.903]	[0.124]
Time Trends	X	X	X
Wind Speed Polynomials	X	X	X
Observations	3,677	1,249	1,239

Notes: The table displays regression coefficients with two-way clustered standard errors on the state × year and county level in parentheses. P-values are shown in brackets. All estimations use the linear fixed effect-within estimator and include county and year fixed effects as well as county-specific linear time trends and *Rainfall* controls. indicates the usage of quartic polynomials. The sample in column 1 includes all county-year observations for which FEMA indicated (via FOIA and openFEMA data) that federal relief has been requested between 1992-2015. In panels 2 and 3 the sample covers all county-year observations for which a federal disaster declaration has been issued and a positive amount of public assistance has been provided (1998-2015).

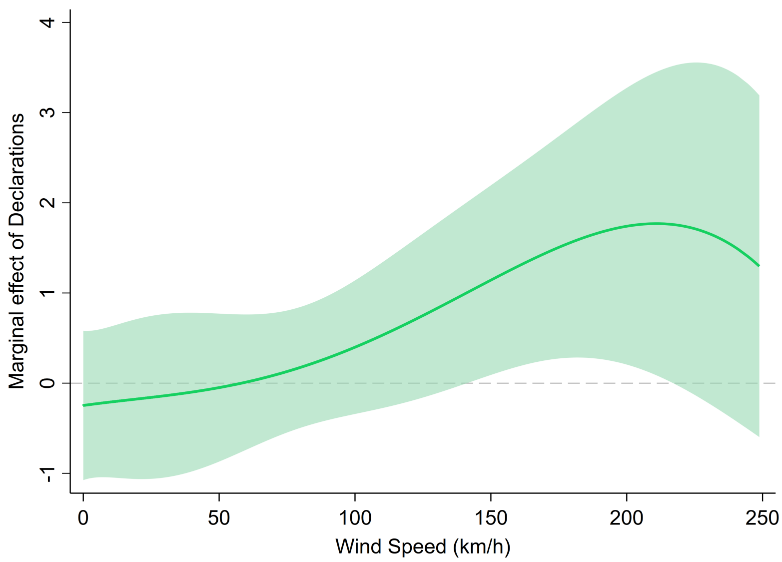

Figure 3.30: Declarations and election outcomes

Notes: This figure shows the relationship between issuing a disaster declaration and the change in the incumbent president's party county-level vote share in the upcoming presidential election, which is the dependent variable in this regression. It displays marginal effects of *Declarations* for different levels of *Wind Speed*, derived from our polynomial estimation (solid green line). The light green shaded area represents the 95 percent confidence interval applying clustered standard errors on the state level. The sample covers county-year observations from 1965–2018.

4 Distortions in Aid Allocation of United Nations Flash Appeals: Evidence from the 2015 Nepal Earthquake

This chapter is joint work with Vera Z. Eichenauer, Andreas Fuchs, and Eric Strobl.

It has been published as:

Eichenauer, Vera Z., Andreas Fuchs, Sven Kunze, & Eric Strobl (2020). Distortions in aid allocation of United Nations flash appeals: Evidence from the 2015 Nepal earthquake. *World Development 136*, 105023.

Abstract: We examine the design and implementation of the United Nations Flash Appeal triggered in response to the highly destructive 2015 Nepal earthquake. We consider how local need and various distortions affect the proposed project number, the proposed financial amount, and the subsequent funding decision by aid donors. Specifically, we investigate the extent to which the allocation of this humanitarian assistance follows municipalities' affectedness and their physical and socioeconomic vulnerabilities. We then analyze potential ethnic, religious, and political distortions. Our results show that aid allocation is associated with geophysical estimates of the earthquake damage. Controlled for disaster impact, however, aid allocation shows little regard for the specific socioeconomic and physical vulnerabilities. It is also worrisome that the allocation of the flash appeal commitments favors municipalities dominated by higher castes and disadvantages those with a greater distance to the Nepali capital Kathmandu.

4.1 Introduction

On April 25, 2015, a 7.8-magnitude earthquake struck central Nepal.[102] More than 100 subsequent aftershocks followed, of which the largest reached an intensity of 7.3 on May 12. It was one of the most destructive natural disasters in the history of Nepal. The disaster triggered substantial international attention. It is estimated to have killed 8,800 people and affected more than 5.6 million (Guha-Sapir et al., 2016), which constituted almost a fifth of Nepal's population.

Four days after the earthquake, the United Nations (UN) Office for the Coordination of Humanitarian Affairs (UNOCHA, 2016), in collaboration with the Office of the Humanitarian Coordinator (OHC), the Nepalese government, and humanitarian partners, issued a strategic response plan for Nepal, a so-called flash appeal.[103] Flash appeals have become important components of humanitarian relief in emergency situations, as demonstrated by the 76 flash appeals the UN has issued over the 2005–2016 period. During this time, the international donor community spent USD 190 billion alone on flash appeals to satisfy humanitarian needs and stimulate economic reconstruction. As can be seen from the list of the 20 largest events in Table 4.1, the 2015 Nepal earthquake triggered the seventh largest flash appeal in terms of its financial size. A common hope and expectation is that the criteria for choosing the location of aid projects after a disaster are based on disaster affectedness and the specific vulnerabilities of municipalities. Meaningful aid allocation is particularly salient since nine out of ten flash appeals are underfunded (UNOCHA, 2018).

The 2015 UN Nepal Earthquake Flash Appeal identified 184 projects and requested USD 422 million in order to provide life-saving assistance and protection for the Nepalese people in the five months after the earthquake (AidData, 2016a).[104] Although 77 donor organizations responded to the Flash Appeal, a third of the requested amount remained unmet as of May

[102] Nepal, a landlocked country situated between China and India, has 29 million inhabitants, of which 15% live below the poverty line of USD 1.90 (PPP) a day (World Bank, 2018). It is home to 125 ethnic (caste) groups. After a civil war (1996–2006), the country became a secular republic in 2008. It now is a multi-party democracy with the Communist Party of Nepal and the Nepali Congress being the dominant parties. The new political constitution has been in force since September 2015. According to the "Polity Score" of the Polity IV data set, Nepal is coded as a democracy with a value of 6 on a 21-point scale from 10 (full autocracy) to 10 (full democracy) (Marshall et al., 2018).

[103] While a flash appeal responds to new disasters, annually consolidated appeals cover protracted crises. This study only covers the former. The decision to issue an appeal is primarily left to field staff but the affected government should be consulted (UNGA, 1991).

[104] The revised flash appeal of May 4, 2015 is available at https://www.humanitarianresponse.info/sites/www.humanitarianresponse.info/files/documents/files/nepal_earthquake_2015_revised_flash_appeal_final_0.pdf, accessed January 27, 2017.

Table 4.1: List of 20 largest UN flash appeals (2005–2016)

	Flash appeal	Revised requirements (in mUSD)	Total resources available (in mUSD)	Covered
1	PAKISTAN Floods July 2010	1,963	1,371	69.9%
2	YEMEN 2015	1,601	915	57.1%
3	HAITI Earthquakes January 2010	1,502	1,101	73.3%
4	INDIAN OCEAN Earthquake/Tsunami December 2004	1,409	1,248	88.5%
5	SOUTH ASIA Earthquake October 2005	561	368	65.5%
6	MYANMAR Tropical Cyclone Nargis May 2008	477	349	73.1%
7	NEPAL Earthquake April 2015	422	282	66.8%
8	PAKISTAN Floods August 2011	357	157	44.0%
9	LIBYA Unrest and Neighbouring Countries Feb. 2011	336	279	83.1%
10	IRAQ 2016	284	276	97.4%
11	KENYA Post-Election Emergency January 2008	208	137	66.0%
12	AFGHANISTAN 2016	152	60	39.6%
13	PHILIPPINES Typhoon Ketsana September 2009	144	63	43.7%
14	HAITI Hurricane Matthew October 2016	139	86	62.2%
15	HAITI Hurricane Gustav and Tropical Storm Hanna Sept. 2008	121	73	60.5%
16	GEORGIA Crisis August 2008	114	73	63.9%
17	LEBANON Crisis July 2006	97	119	123.2%
18	KYRGYZSTAN Civil unrest June 2010	94	69	72.8%
19	NIGER Drought/Locust Invasion Food Security Crisis 2005	81	59	72.7%
20	INDONESIA Java Earthquake May 2006	80	43	53.4%

Notes: Own calculations with data from UNOCHA (2018).

2018 (UNOCHA, 2018).[105] However, the spatial heterogeneity across municipalities is large. This holds with respect to the number of aid projects, the proposed financial amount, and the degree to which proposed projects obtained funding commitments by international donors. This raises the question: What factors explain the selection of project locations and the provision of the requested funds?

By studying the allocation of UN flash appeal aid, we contribute to the broader literature on the allocation of humanitarian aid. A first strand investigates aid allocation across countries and emergencies, where emergency aid has been shown to increase with disaster severity, but is also driven by media coverage and is prone to political bias (Bommer et al., 2019; Drury et al., 2005; Eisensee & Strömberg, 2007; Fink & Redaelli, 2011; Fuchs & Klann, 2013; Raschky & Schwindt, 2012). A much smaller second strand analyzes the allocation of disaster relief within disaster-affected areas. For example, Benini et al. (2009) and Wiesenfarth & Kneib (2010) study relief supply to earthquake-affected communities in Pakistan after the 2005 earthquake and find that needs and logistical convenience of locations affect aid delivery. Francken et al. (2012) investigate politico-economic factors underlying aid allocation across communities in Madagascar in the aftermath of Cyclone Gafilo in 2004. They uncover that domestic aid is provided to regions where governments have stronger incentives to respond,

[105] The five largest official donors are the United States of America, the Central Emergency Response Fund, Norway, Canada, and the United Kingdom (see https://fts.unocha.org/appeals/486/summary, accessed December 13, 2018).

specifically those with higher radio coverage and with stronger political support from the ruling administration. At the same time, their results suggest that foreign aid is distributed to poorer areas and to those that are more easily accessible.

Our study adds to this smaller and less developed second strand of the literature by examining the role of UN flash appeals. To the best of our knowledge, no existing study analyzes the geographic pattern of proposed and funded projects following UN flash appeals—despite their importance in the immediate aftermath of a disaster.[106]

Studying the allocation of emergency aid is important as these flows are intended to improve the humanitarian situation of the population living in disaster-affected areas. Beyond the mere humanitarian aspect, empirical findings suggest that post-disaster aid can boost economic growth (Bjørnskov, 2019), speed up the recovery process of microenterprises (de Mel et al., 2012), and play a role in reducing the likelihood of escalating government repression in democracies (Wood & Wright, 2016).[107] Even critics of 'general' development aid support the continued provision of emergency relief following devastating disasters (Moyo, 2009). Since humanitarian aid flows are surprisingly small in comparison to the damage caused (Becerra et al., 2014, 2015), a need-oriented aid allocation is particularly salient.

By analyzing the humanitarian response triggered by the 2015 Nepal earthquake, this study addresses two (sequentially) related aspects of flash appeals. We study the municipal characteristics that influence the number of emergency aid projects and the financial amount committed to a particular municipality. First, we analyze the determinants of project-locations in the design stage of the 2015 UN Nepal Earthquake Flash Appeal across municipalities. Second, we investigate which proposed project locations obtain funding from international donors.

Our study makes use of a new, and so far unexploited, georeferenced aid data set from AidData that contains information on proposed and ultimately funded aid projects that have been a part of the 2015 UN Nepal Earthquake Flash Appeal (AidData, 2016a). These data cover 156 out of 184 projects in more than 850 locations. We combine these aid data with

[106]This article also adds to a burgeoning literature on the subnational allocation of development aid (Dreher et al., 2019; Dreher & Lohmann, 2015; Strandow et al., 2016). However, emergency aid is distinct from other development aid given its goal and time horizon. Emergency aid is relatively "high-speed" assistance, especially after fast-onset disasters. Donors react in days, if not hours, rather than the years that it takes to design and implement more long-term development strategies.

[107]Donor countries can also benefit from humanitarian aid if it boosts the donors' image in the recipient country. In this regard, Andrabi & Das (2017) show that for the 2005 Pakistan earthquake, trust in Americans and Europeans increased in earthquake-affected areas, i.e., areas that also benefited from aid inflows.

data on nighttime light and rainfall intensity, survey data, and electoral statistics at the local level, to evaluate whether the allocation and subsequent financing of humanitarian aid projects in Nepalese municipalities are based on actual disaster impact and the population's specific vulnerabilities or rather biased by particular interests. To assess the disaster impact, we use peak ground acceleration maps provided by USGS (2017a) and combine them with damage functions. We argue that this provides a suitable indicator for potential destruction from earthquakes to short buildings up to seven stories (USGS, 2017c). We evaluate whether aid allocation decisions also reflect socioeconomic and physical vulnerabilities of the affected population using measures of municipalities' level of development, their exposure to rainfall, and their distance to the Nepalese capital Kathmandu, amongst others. Finally, we test for ethnic, religious, and political distortions in aid giving by analyzing the role of a municipality's share of Hindus and privileged caste population, as well as the vote share of Nepal's two dominant parties in the 2013 Constituent Assembly elections.

Our empirical results show that aid allocation in the framework of the 2015 Nepal Earthquake Flash Appeal lacks need orientation and shows ethnic and political biases. At the design stage, the location choice is not guided by municipalities' level of development, as proxied by nighttime light. Moreover, it shows little regard for other socioeconomic and physical vulnerabilities – the exception being that municipalities with less solid house foundations receive more aid projects. Municipalities populated by upper castes receive more projects. The strongholds of the two major Nepali parties also benefit from larger aid amounts in the design stage. On the positive side, the initial appeal project proposals correlate positively with the extent of earthquake damage. However, the funding decisions of the international donor community show little regard of socioeconomic and physical vulnerabilities.

We conclude that the geographic selection of aid projects is distorted at all levels of decision-making. Therefore, the need orientation of geographic project selection and funding should be strengthened. This would involve different actors, namely UNOCHA, the OHC, and the national government during the design of flash appeals, as well as donor countries, multilateral donors, and non-state donors during the funding and coordination phase.

The remainder of the paper proceeds as follows. In Section 2, we outline the decision-making process that underlies the 2015 UN Nepal Earthquake Flash Appeal. We also discuss the factors that should (not) guide the selection and funding of project locations according to the flash appeal document and from a humanitarian perspective. Section 3 presents our research design and the data. We use various proxies for the needs and vulnerabilities of Nepalese municipalities to analyze whether these factors guide aid distribution. We then explore alternative allocation rules which could explain the lack of need orientation. Specifically, we test for ethnic, religious, and political distortions. In Section 4, we present and discuss our empirical results. Finally, Section 5 summarizes our findings and outlines potential avenues for future research.

4.2 The 2015 Nepal Earthquake Flash Appeal

A flash appeal is a planning tool to respond to major disasters. The UN initiates flash appeals in the direct aftermath of largescale sudden-onset disasters that require a fast and coordinated response that exceeds the capacity of the affected government, plus any single UN agency (UNOCHA, 2013). Flash appeals are presented within five to seven days of the occurrence of the emergency and include contextual information with a roadmap for all humanitarian organizations involved in disaster relief. The appeal document outlines a strategy on relief and rehabilitation plans for the months following the disaster, lists specific emergency aid projects, and determines the required resources (UNOCHA, 2015b,c). The assessment of required resources serves to fundraise with international donors.

The UN Resident Coordinator and/or Humanitarian Coordinator (HC) initiates the appeal process in consultation with the affected government and a so-called Humanitarian Country Team, which is a strategic, operational decision-making and oversight forum led by the HC. The decision to start an appeal process is, on the one hand, based on a rapid assessment of the scale and severity of the disaster and, on the other hand, a function of the respective national government's capacity to cope with the consequences. The implementation of flash appeals does not require permission from the government, but there is rarely any opposition. In practice, the government typically plays a key role in designing the appeal. Flash appeals are usually revised about a month later. Revised flash appeals typically include more complete information, improved and in-depth assessments, and describe more clearly the required early-recovery aid projects.[108]

[108] The websites https://fts.unocha.org/content/guide-funding-response-plans-andappeals and https://www.unocha.org/sites/dms/CAP/FAs_What_you_need_to_know.pdf (accessed March 21, 2020) provide more information on humanitarian response plans and appeals.

One of the financially largest emergency appeals was the Flash Appeal for the Response to the Nepal Earthquake, which was issued on April 29, 2015, i.e., four days after the first earthquake hit central Nepal.[109] At that point in time, government sources estimated a death toll of 5,006 people and the number of injured people amounted to 10,194. The appeal document called the donor community to collect USD 415 million "to reach over 8 million people with life-saving assistance and protection in the next three months" (UNOCHA, 2015c). This estimate of the required resources was based on initial results of damage assessments, earthquake intensity mapping, and secondary data analysis.

One month later, on May 29, 2015, the UNOCHA issued a revision of the Flash Appeal (UNOCHA, 2015b). The update intended to strengthen linkages between the recovery and rehabilitation program of the Nepali government and extended the appeal duration from three to five months. This also allowed the Flash Appeal to account for the damage caused by the severe aftershock on May 12, 2015. The goal was then to collect USD 422 million for 2.8 million affected and vulnerable people. The appeal document emphasizes that "[r]elief efforts will need to continue to identify and respond to distinct structural and situational factors that increase vulnerabilities at both local and community levels, including for women, children, the elderly, minorities and people with disabilities" (UNOCHA, 2015b, 6). UNOCHA based its assessment of the severity of needs on a severity index that "combines indicators that measure earthquake impact (damaged buildings, injured persons, migration), physical vulnerability (landslide and flood risk, road accessibility), and socioeconomic vulnerability (caste/ethnicity, gender inequality, Human Development Index)" (UNOCHA, 2015b, 9).

The context just described suggests a number of different aspects, which were important to the allocation of aid after the earthquake. First, it highlights that the degree to which certain areas were affected by the earthquake was intended to be an important criterion for aid allocation. The physical intensity of the earthquake showed considerable spatial variation across and within the five Nepali development regions. More specifically, the earthquake triggered the worst consequences in the Central and Western Region, including the Kathmandu Valley. Importantly, housing conditions played a crucial role in how the severity of the earthquake translated into damage. Many Nepalese homes are characterized by fragile outer walls and unstable foundations. As the revised appeal emphasizes, "the condition of houses is considered to be the most relevant proxy indicator for people in need"

[109] Appendix Table 4.5 provides a timeline of the events surrounding the 2015 Nepal earthquake flash appeal.

(UNOCHA, 2015b, 53).[110] We will test below whether municipalities that had been more severely affected by the earthquake received more proposed and subsequently funded projects.

Beyond the degree to which certain areas are affected by the catastrophe, the Flash Appeal attributes an important role to the protection of the most vulnerable populations (UNOCHA, 2015c). As the updated appeal document emphasizes, "[m]any people affected by the disaster are highly vulnerable on the basis of socioeconomic, language, religious, caste, ethnic and geographic factors" (UNOCHA, 2015b, 6). Starting with socioeconomic vulnerabilities, the document explicitly demands that "the diversity of affected communities is addressed when engaging the community" (UNOCHA, 2015b, 3). Relief activities should explicitly cover "all vulnerable groups, including internally displaced persons (IDPs), host communities, ethnic and indigenous groups and other affected people" (UNOCHA, 2015c, 4).[111] Biases in favor of privileged groups in the Flash Appeal proposal and subsequent allocation of aid would thus thwart this principle.

In spite of the appeal's stated goal to prioritize the most vulnerable population groups, Amnesty International (2015, 10) expressed its concern that "the Government of Nepal and humanitarian agencies had still not adequately factored social and economic disparities into their relief operations." Dissatisfaction with the distribution of relief aid within Nepal also sparked protests (Bhagat, 2015). Indeed, the Asia Foundation (2017) warns that Dalits, of which 90% live below the poverty line, and other lower ranked castes suffer particularly from obstacles that prevent their economic recovery. While the report also presents evidence that lower-caste people are not less likely to access aid, they do appear to struggle to receive relief aid according to their needs.[112] Lam & Kuipers (2019, 326) come to similar conclusions based on their policy analysis and field research in the aftermath of the earthquake. They argue that the Dalits "are often excluded from the community" and have trouble "accessing adequate information from local officials."

We provide a systematic test below of whether the design and financing of flash appeal projects are indeed targeted at poor municipalities and (dis)favors municipalities populated

[110] See also, for instance, Rota et al. (2008) and de Ruiter et al. (2017) in the context of other earthquakes.

[111] A report by the (Asia Foundation, 2017, vi-vii) concludes that "[h]igher demand for food is found among disadvantaged groups: people in more remote areas, of low income, low education, low caste and Janajatis [Nepal's indigenous peoples] and those with a disability."

[112] A case study carried out at Dartmouth College discusses this issue: "Already exposed to lower standards of healthcare, these [low-caste] people were often offered help last although their need was generally greatest – more low-caste people lived in poorly constructed houses, which collapsed. The majority of Nepali doctors and volunteers were high-caste, so sometimes prone to prioritize high-caste victims over Dalits." See details at https://journeys.dartmouth.edu/NepalQuake-CaseStudies/castebased-inequality/ (accessed May 11, 2018).

by Hindus, the dominant religion, and high-caste people. To analyze whether aid giving in the framework of the Flash Appeal is considering socioeconomic vulnerabilities, we will investigate whether the level of development and the religious and caste composition of a municipality are associated with the number of proposed and funded projects. Given Nepal's track record of socioeconomic exclusion (e.g., Murshed & Gates, 2005; Sharma, 2006), one is likely to expect at least some biases in favor of privileged groups in the allocation of flash appeal aid.[113]

Turning from socioeconomic to physical vulnerabilities of municipalities, the appeal documents express concerns that rural and remote areas are disadvantaged when it comes to receiving aid. The Kathmandu International Airport, for example, played the dominant role in delivering aid to Nepal. Since it is the only Nepalese airport that could handle medium to large aircrafts, nearly all international aid arrived in Kathmandu. This may have made it less likely that projects were carried out in remote areas populated by poor people. In this regard, the updated appeal document highlighted that "864,000 people in remote villages are in immediate need as they have lost their homes and live below the poverty line" (UNOCHA, 2015b, 5). However, according to observers, civil servants were "notorious for being unaccountable, corrupt and prejudiced towards the lowest castes" (The Economist, 2015). Additionally, evidence from a study carried out by Barber (2016) suggests that lower-caste members were not proactively engaged in the earthquake response provided by international donors and that those from remote communities had difficulty in obtaining relief.[114]

Moreover, the impending monsoon season had implications for needs across all sectors: "Reaching these most vulnerable communities is a priority to ensure that they are provided with adequate shelter and basic needs to strengthen their resilience ahead of the heavy monsoon rains which begin in June and can last until September" (UNOCHA, 2015b, 5). Importantly, this monsoon further impeded earthquake relief operations (UNOCHA, 2015a). In the empirical analysis below, we explore whether particular attention was given to municipalities that are geographically remote and vulnerable to heavy monsoon rain.

[113] Paudel & Ryu (2018) find that ethnic differences were already prevalent in how Nepalese ethnic groups were affected by the 1988 Nepal earthquake. Using a difference-in-differences setting, they show that human capital of low-caste groups deteriorated more permanently than when compared to high-caste groups.

[114] A case study carried out at Dartmouth College finds that the "internalization of the caste-system served in some instances to marginalize the needs of low-caste people in the face of disaster." See details at https://journeys.dartmouth.edu/NepalQuake-CaseStudies/caste-based-inequality/ (accessed May 20, 2020).

The official procedures for flash appeals recommend a strong coordination between UN agencies, NGOs, and the local government. This involvement of Nepalese parliamentarians and government officials opens the door for a potential impact of local politicians on the design and implementation of the appeal. Anecdotal evidence suggests that domestic political favoritism and patronage biased aid allocation in Nepal. Amnesty International (2015, 12) documents such claims according to which "the official distribution of tarpaulins favored those with familial, political or other institutional connections and loyalties" and reports that parliamentarians misappropriated tents originally intended for disaster victims. The human rights organization is particularly worried about political favoritism and patronage in municipalities that are dominated by a single party and that are demographically heterogeneous with respect to their religious, caste, and ethnic composition. For example, Amnesty International (2015, 10) notes that "[t]he District Committee Secretary of Nepal Congress (NC) in Nuwakot reportedly provided relief materials to one ward (where the majority of the population were NC supporters) in his VDC [village development committee] in Nuwakot" and that the Communist Party of Nepal "was also said to have manipulated relief distribution" in the Kavre district. In addition to the analysis of ethnic and religious biases mentioned above, we will thus test how municipalities governed by one of Nepal's leading parties fare in terms of proposed projects and aid funds.

We now turn to our empirical framework to test whether disaster affectedness, socioeconomic and physical vulnerabilities, as well as political favoritism are reflected in the 2015 Nepal Earthquake Flash Appeal.

4.3 Data and Method

4.3.1 Empirical Design

Our study combines data on the location of emergency aid projects proposed and funded in the framework of the 2015 UN Nepal Earthquake Flash Appeal with measures of earthquake impact collected through remote sensing and census data. Our unit of analysis are municipalities, so-called village development committees (VDCs). The VDCs correspond to the fourth subnational administrative (ADM4) level in Nepal and are grouped into 75 districts (ADM3) in 14 zones (ADM2) located in five regions (ADM1).

We proceed in two steps. In the first step, we analyze the spatial distribution of aid projects in the design stage of the Flash Appeal. Specifically, we analyze the spatial distribution of proposed appeal locations by constructing the *no. of proposed projects*. In a variant of this first step, we also analyze the spatial distribution of financial amounts as requested by the OHC using *proposed financial amount (ln)*. This variable is the logged financial value in US dollars of all appeal projects proposed for a municipality.

In the second step, we analyze the funding decision. The humanitarian aid obtained by a municipality is the outcome of individual funding decisions by international donors. As first dependent variable, we use *no. of funded projects*, which is the number of funded project locations in a given municipality. In addition to this count variable, we also analyze the financial amount of donor support provided. The variable funded *financial amount (ln)* is the logged financial value in US dollars of all funded appeal projects committed to a municipality. To isolate the factors shaping the decision-making at the funding stage, we include the number of proposed projects or, respectively, the requested project amount as a covariate to explain deviations from the proposal. Finally, we use the *share of funding obtained*, which is the ratio of the funded aid amount to the proposed aid amount. In this final specification, we are restricted to the sample of those 1,290 municipalities that were proposed by the UNOCHA and the OHC as a location for at least one appeal project.[115]

For each stage in the appeal process, we run Negative Binomial (NB) regressions whenever the project number is the dependent variable and Ordinary Least Squares (OLS) regressions in all other cases. NB regression is appropriate for count outcome variables that are non-negative and over-dispersed.[116] NB regression is a generalization of the Poisson estimation and is based on a gammaPoisson mixture distribution. This allows the variance to be larger than the mean, as is the case in our data. We estimate the following cross-sectional NB regression at the municipal level i:

$$E(ProjectNumber_i|\mathbf{D_i}, \mathbf{X_i}, PP_i) = \alpha_i * exp(\mathbf{D_i'}\beta + \mathbf{X_i'}\gamma + \delta PP_i), \tag{4.1}$$

[115]We use this restricted sample because the ratio is undefined whenever the denominator, the proposed aid amount, is zero.

[116]We do not use the zero-inflated negative binomial regression to model the excessive zeros because this would require the assumptions that, first, excess zeros are generated by a process separate from that of the count values and that, second, these excess zeros can be modeled independently. We do not believe that these two assumptions hold for our data.

where α_i, the latent exposure of a municipality i, is estimated from the data. The matrix **D** includes both the physical intensities of the first earthquake and the main aftershock, while the matrix **X** includes the remaining covariates described below. As mentioned earlier, the proposed number of projects PP is included in models analyzing the funding stage. Our unit of analysis i consists of 2,796 Nepalese municipalities.[117] Standard errors are calculated to be robust to heteroscedasticity and clustered at the level of Nepalese districts (ADM3), within which errors are thus allowed to correlate.[118]

For the continuous dependent variables, we deploy the following cross-sectional OLS equation:

$$y_i = \alpha + \mathbf{D_i'}\beta + \mathbf{X_i'}\gamma + \delta PA_i + \epsilon_i, \tag{4.2}$$

where y alternatively refers to any of the three continuous dependent variables, the *proposed financial amount (ln)*, the *funded financial amount (ln)*, or *the ratio of funding obtained*. As mentioned above, the proposed project amount PA is included in models analyzing the funding stage.

The cross-sectional nature of our data and the lack of a clean identification strategy do not always allow for a causal interpretation. However, our disaster impact measures are constructed from physical measures and from damage functions. The latter are based on pre-event distributions of building types and engineering-based relationships between peak ground acceleration and damage ratios of buildings by type. They are thus exogenous to emergency aid. Most other variables – such as religion and geographical features – cannot be affected by post-earthquake disaster aid as they were collected prior to the earthquake. Reverse causality is thus unlikely to be a concern in our setting.[119] In spite of the exogeneity of the earthquake, omitted-variables might still affect our results. We attempt to mitigate this concern by including a rich set of covariates in our baseline model and by running regressions with fixed effects at the zone (ADM2) level in robustness checks.

[117] We drop all VDCs in zones (i.e., ADM2 regions) that were entirely unaffected by the immediate earthquake according to the destruction index defined below.

[118] We cluster at the ADM3 level since we distribute those projects that are only localized at the ADM3 level to all VDCs (i.e., ADM4 regions) in that ADM3 region (using an equal split as we describe in footnote 21 below). Funding amounts per VDC are thus correlated within ADM3 areas. However, as a robustness check, we also show results where we cluster by zone (i.e., ADM2 regions). The results are similar (see Appendix Tables 4.15 and 4.16).

[119] It is however possible that measurement error in the disaster impact measure is systematically related to the dependent variable in a spatial sense. We cannot estimate the size of such a potential bias but do not believe that the measurement error is large and systematically related to the dependent variable.

4.3.2 Data on the 2015 UN Nepal Earthquake Flash Appeal

The primary data source for the dependent variables is UNOCHA's Financial Tracking Service (FTS) (UNOCHA, 2018).[120] The database collects international humanitarian funding flows since 1992 and has frequently been used in empirical analyses of humanitarian aid (e.g., Fink & Redaelli, 2011; Fuchs & Klann, 2013; Fuchs & Öhler, 2019; Raschky & Schwindt, 2012). A major innovation over previous work using FTS data is that we analyze subnational rather than cross-country variation in the allocation of humanitarian aid. Specifically, we use a new, and so far unexploited, geospatial data set by AidData (2016a). It contains the geographic location of 156 of the total 184 Nepal Earthquake Flash Appeal projects registered in FTS, of which funding was requested for 142 in the revised Flash Appeal of May 29, 2015.[121] These 142 projects were assigned to 821 project locations.[122] We use these data to build the five dependent variables described above.

While the upper panel of Figure 4.1 shows the spatial distribution of the proposed appeal projects, the lower panel displays the number of funded projects by municipality. Only 64 (56) out of the 184 (142) proposed appeal projects (with geocoded locations) obtained any funding from donors. In total, the 156 geocoded appeal projects received USD 280 million. Appendix Table 4.6 lists the 20 largest flash appeal projects funded by the international donor community.

4.3.3 Disaster Impact

The need for emergency aid increases with the severity of the catastrophe. To capture the disaster impact, we employ physical measures of disaster severity.[123] The literature in this regard makes increasing use of geo-referenced physical variables to measure the intensity

[120] The started goal of FTS "is to give credit and visibility to donors for their generosity and to show the total amount funding and resource gaps in humanitarian appeals" (UNOCHA, 2015c). Humanitarian funding is usually reported to FTS by the recipient organization and not the donor because the former is best informed about the final usage of funds.

[121] 184 – 156 = 24 of the proposed appeal projects could not be geocoded because of the nature of the project or a lack of information on the location of implementation.

[122] For projects geocoded at the district (ADM3) level, i.e., one layer above our spatial unit of analysis, we attribute a project to all VDCs in this ADM3 unit and evenly split the requested and proposed project amount across these VDCs. This implies that 3,023 of 3,957 ADM4 locations are recipients of a proposed project. If a project is coded both at the ADM3 level and at the ADM4 level, we only keep the ADM4 location.

[123] Most of the cross-country literature uses the number of fatalities or the total number of affected people from the International Disasters Database (EM-DAT) as a measure of disaster impact (Guha-Sapir & CRED, 2020; Lazzaroni & van Bergeijk, 2014). The EM-DAT data has been criticized for various reasons (e.g., Felbermayr & Gröschl, 2014). For our study, we need subnational variation of disaster severity and EM-DAT has to date only been geo-referenced for the Philippines by AidData.

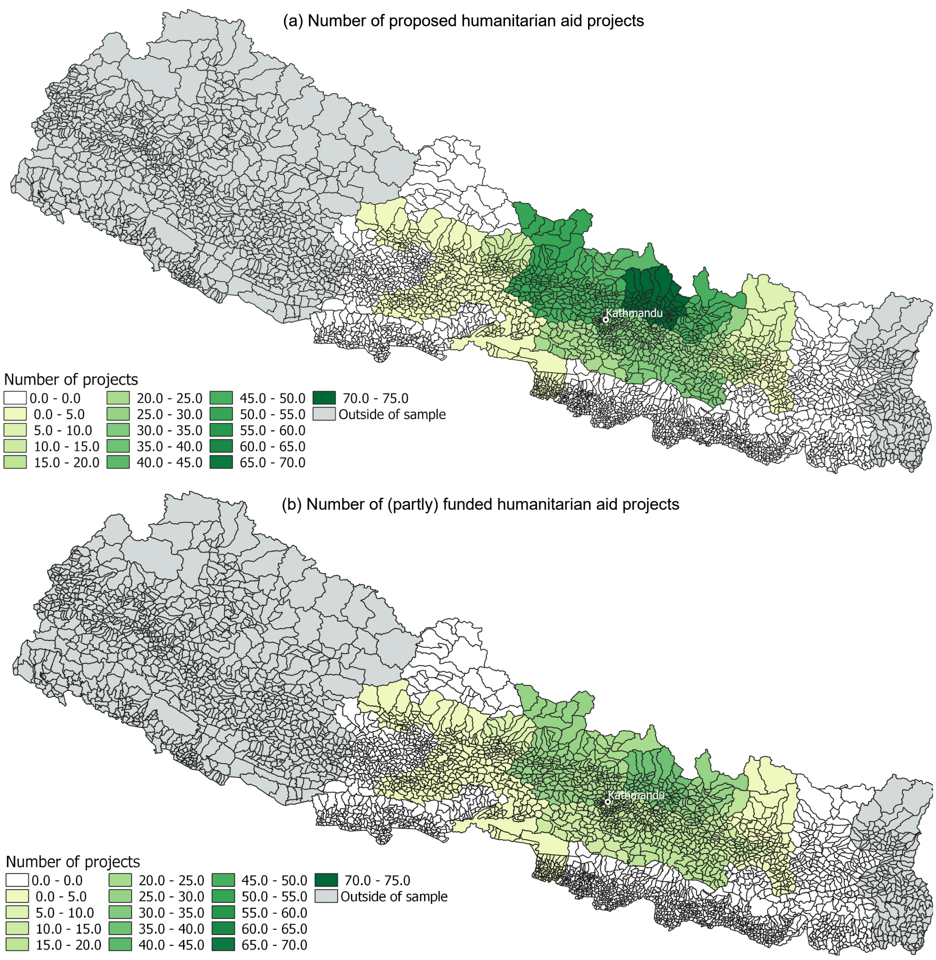

Figure 4.1: Spatial distribution of proposed and funded aid projects of the 2015 UN Nepal earthquake flash appeal across municipalities

of natural disasters (Berlemann, 2016; Bertinelli & Strobl, 2013; Felbermayr & Gröschl, 2014; Fisker, 2014; Hsiang, 2010; Kunze, 2021; Strobl, 2011, 2012). These measures have the advantage that they are exogenous to economic outcomes of interest such as economic development, thus allowing for causal inference. To measure the physical intensity of the earthquake in Nepal, we use peak ground acceleration (PGA) maps provided by USGS (2017a,b), which is arguably a suitable indicator for potential destruction from earthquakes to buildings up to seven stories tall (USGS, 2017c).

Importantly, the damage suffered from earthquakes will not only be determined by the physical features of the event, but also depends on the type of building affected.[124] To take account of this, we use information on the housing building types provided by the 2011 Census (Central Bureau of Statistics, 2011) in conjunction with fragility curves by building types developed by the Global Earthquake Safety Initiative project (GESI) (Geohazards

[124]For example, Bilham (2010) demands the construction of earthquake-resistant buildings to prevent further increases in the death toll of earthquakes.

International & United Nations Centre for Regional Development, 2001). More specifically, building types are classified into nine different categories.[125] Each building type itself is then rated according to the quality of the design, the quality of construction, and the quality of materials. Total quality is measured on a scale of zero to seven, depending on the total accumulated points from all three categories. According to the type of building and the total points acquired through the quality classification, each building is then assigned one of nine vulnerability curves, providing estimates of the percentage of building damage for a set of 28 peak ground acceleration intervals. In order to use these vulnerability curves for Nepal, we first allocate each of the five building types given in the 2011 Census to one of the less aggregated categories of the GESI building classification.[126] Given that we have no information as to the quality of buildings in Nepal in terms of design, construction, and materials, we instead assume that building quality is homogenous across building types.

In order to derive a municipality i-specific earthquake destruction index, ED, we compute the following:

$$ED_i = \sum_{s=1}^{5} w_{si} DR_s(PGA_i), \tag{4.3}$$

where w is the share of building type s in municipality i, and DR is the damage ratio of the building type s given the observed local peak ground acceleration PGA in municipality i as defined for high-quality buildings. For our analysis, we construct two variables, *immediate damage*, which captures the destruction of the main earthquake on April 25, and *aftershock damage*, which reflects the destruction of the major aftershock on May 12. The resulting measure is a damage ratio, which ranges from 0 (no building is destroyed) to 1 (all buildings are destroyed).

Figure 4.2 shows the spatial variation of our measures of disaster impact, immediate damage (Panel a) and aftershock damage (Panel b), across municipalities. The stars mark the respective epicenter of the two shakes. The different colors stand for different damage experiences according to our earthquake destruction index, ranging from light orange ("weak") to dark orange ("extreme"). Around 2.75% of our sample villages experience extreme damage with 87.5% to 100% of all buildings predicted by the index as being destroyed by the immediate earthquake. Both panels demonstrate that the majority of destruction occurs in municipalities

[125] Wood, steel, reinforced concrete, reinforced concrete or steel with unreinforced masonry infill walls, reinforced masonry, unreinforced masonry, adobe and adobe brick, stone rubble, and lightweight shack or lightweight traditional.

[126] For those buildings in the other or unassigned category, we assumed they were of the most vulnerable type, namely, lightweight shack (e.g., corrugated iron sheet) or lightweight traditional (e.g., bamboo).

(a) Damages of the immediate earthquake (April 25, 2015)

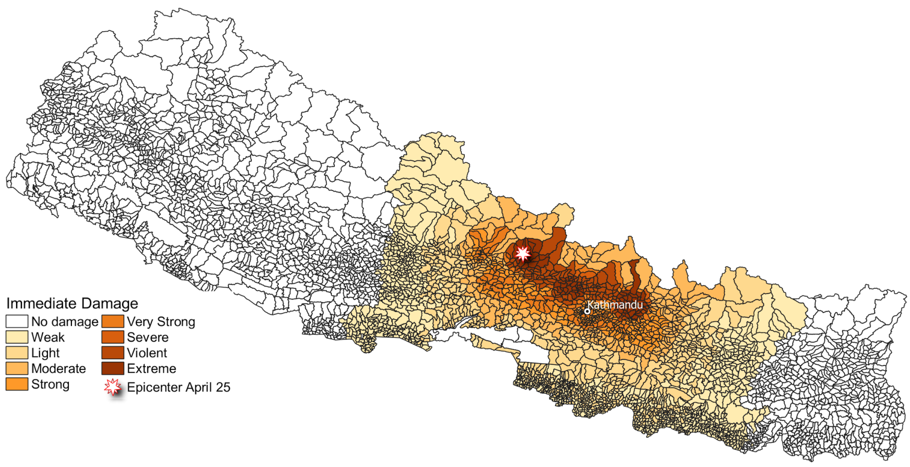

(b) Damages of the major aftershock (May 12, 2015)

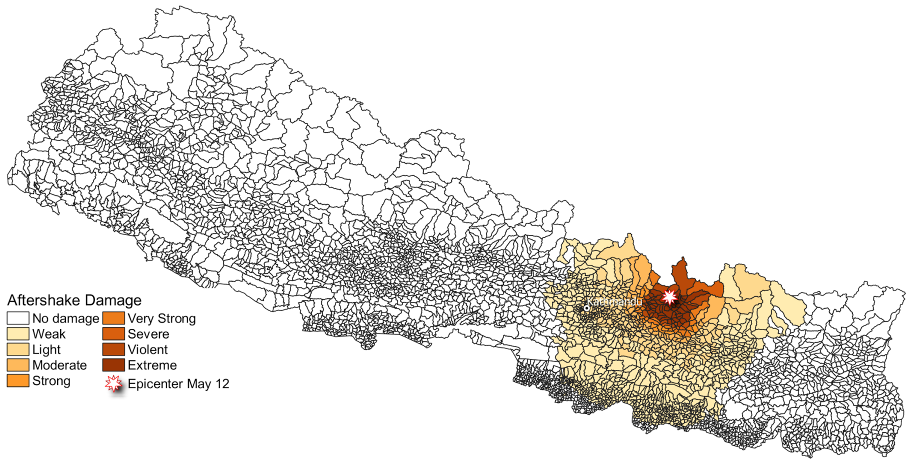

Figure 4.2: Spatial distribution of damage from the 2015 Nepal earthquake across municipalities

Notes: The red stars mark the epicenter of the respective shake. Scale: Percentage of buildings destroyed per municipality: 0%-12.5% (weak), 12.5%-25% (light), 25%-37.5% (moderate) 37.5%-50% (strong), 50%-62.5% (very strong), 62.5%-75% (severe), 75%-87.5% (violent), 87.5%-100% (extreme).

northwest and northeast of Kathmandu, whereas the relatively highly populated southern regions experience only weak or light damage.

Given that our index is not based on actual damage, it will inevitably involve some measurement error. In the classical sense, this could produce some attenuation bias and implies that our estimates would need to be interpreted as lower bounds. Hypothetically, there could also be systematic measurement error in that the error is correlated with the amount of aid given. We believe that this is unlikely since two of the underlying drivers of our damage index are based on the physical relationships (the shake maps and fragility curves). The only remaining potential culprit is our necessary assumption of building-type homogeneity within districts, which could be correlated with other ex-ante event local characteristics, such as inequality, which we do not control for but also determine aid giving. Given our list of covariates, it seems reasonable to assume that the remaining, i.e., uncontrolled, correlation between aid and potential measurement error is very small.

4.3.4 Socioeconomic and Physical Vulnerabilities

On the one hand, poorer municipalities are more vulnerable to the consequences of the earthquake and have a higher self-aid capacity. On the other hand, economically more important municipalities might have a higher ability to make their needs heard. First, to account for the level of development of municipalities, we use the average monthly nighttime light intensity (*average nightlight pre-earthquake*) from January 2012 to March 2015. In doing so, we are following a growing literature that proxies local economic output with nighttime light intensity (Alesina et al., 2016; Chen & Nordhaus, 2011; Hodler & Raschky, 2014; Michalopoulos & Papaioannou, 2014). In the absence of accurate GDP data, nighttime light offers a viable alternative since it correlates highly with survey-based measures of wealth (Weidmann & Schutte, 2016). Furthermore, Bertinelli & Strobl (2013) have provided evidence that nighttime light intensity is able to capture reported destruction from hurricanes in Caribbean countries.

Previous studies have mostly used the nighttime light series for stable light from the Defense Meteorological Satellites Program (DMSP), which offers stable and filtered yearly average data. However, it has several drawbacks, including overglow effects around cities (Small et al., 2005) and top-coding problems of city centers (Bluhm & Krause, 2018; Doll, 2008). We thus instead use data from the recently launched Visible Infrared Imaging Radiometer Suite (VIIRS) satellite, which since April 2012 has on a monthly basis offered stable, filtered, and uncensored data. For our analysis, we downloaded the Version 1 Nighttime VIIRS Day/ Night Band Composites available from the Earth Observations Group at NOAA/NDGC for January 2012 until August 2016 (NOAA, 2017). Importantly, the VIIRS images overcome most of the stated criticism of the DMSP images (Levin & Zhang, 2017). As a matter of fact, Li et al. (2013) provide evidence that the VIIRS nighttime light images have a substantially higher correlation with regional economic activity in China than the DMSP images. Moreover, with a ground footprint of 742 m * 742 m, VIIRS data provides a resolution 45 times higher than the DMSP images (Elvidge et al., 2013). This allows us to identify nighttime light luminosity even in a low electrified country such as Nepal, as can be seen in Appendix Figure 4.6.[127] The figure furthermore shows that most of the nighttime light intensity is concentrated in the Kathmandu Valley and the southern part of Nepal, whereas the northern regions only have a little luminosity. These spatial differences in nighttime light intensity correspond to the actual distribution of economic activities and population in the country. Second, as another measure of self-aid capacity, we calculate the percentage of households within each municipality with a *solid house foundation* using the 2011 Census (Central Bureau of Statistics, 2011). Features of housing quality such as housing foundation are used in many asset-based wealth indices of household surveys in developing countries (e.g., Demographic and Health Surveys and UNICEF Multiple Indicator Cluster Surveys). We define solid house foundations as houses built on a cement foundation. The map in Appendix Figure 4.7 shows how the share of solid houses is distributed across the municipalities in the regression sample.

Third, larger and more populated municipalities are more likely to host more affected people and suffer from larger damage. This follows from pure logic of scale. Thus, they are not only more likely to receive emergency aid in general but also more of it. Therefore, we control for the area, *admin 4 area*, and the (logged) population size of the municipalities, *population*, using data from the 2011 Census (Central Bureau of Statistics, 2011). The map in Appendix Figure 4.8 shows the population density of municipalities in Nepal in 2011. Accordingly, most of Nepal's population lives in the Kathmandu Valley or in southern Nepal, which corresponds to our observation concerning nighttime light intensity (see Appendix Figure 4.6).

Fourth, transport infrastructure plays a crucial role for aid delivery and we thus account for each municipality's distance to the nearest airport and to Nepal's capital, Kathmandu, with its particularly important Kathmandu International Airport. Specifically, we include the distance from each municipality to the nearest airport in (logged) kilometers (*distance to closest airport*), as measured from its centroid. The Tribhuvan airport in Kathmandu is the only international airport that can handle medium- to large-sized planes, but there are various smaller airports in Nepal. These are crucial for getting supplies to the respective areas since roads are non-existent or in a bad condition, especially after the earthquake(s) in 2015. The closest airport from the epicenter of the earthquake in Ghalychok municipality is 34 km away. Moreover, the distance to Kathmandu is an indicator for accessibility of affected

[127] VIIRS lights are measured in albedo radiance ($W\ cm^2 sr^{-1}$).

municipalities to international relief teams, as much of the international help was stranded at the international airport in Kathmandu. The distance to Kathmandu from the Ghalychok municipality is around 60 km. To take into consideration the remoteness of the individual municipality, we add the logged *distance to Kathmandu* as an additional explanatory variable for our regression. Our distance variables can thus be interpreted as proxies for delivery costs. Remote municipalities might receive less aid projects since it is more efficient to allocate more aid to easy-to-reach locations.

Fifth, municipalities with a higher mean rainfall will have a greater need for humanitarian aid if the earthquake destroyed their houses and roads. This is due to the monsoon season, which typically starts in June and lasts until September every year. Thus, we add *mean rainfall* over the period 1998–2014, measured in millimeter for each municipality, and, to account for simple nonlinear effects, the *mean rainfall squared.* To derive this measure, we use the monthly precipitation raster maps of the Tropical Rainfall Measuring Mission (TRMM), which are available from 1998 with a spatial resolution of 0.25° (Huffmann et al., 2014).

Finally, areas already affected by the 1988 earthquake might be more vulnerable to the adverse consequences of the 2015 earthquake. While being less consequential than the 2015 earthquake, the 1988 earthquake, which was of magnitude 6.7 on the Richter scale, was fatal as well with 721 causalities. More 2015 disaster aid might be directed to the areas affected by the 1988 earthquake, for example, to compensate for a worse health and educational infrastructure.[128] Indeed, Paudel & Ryu (2018) demonstrate that there are adverse long-term consequences of the 1988 earthquake on educational outcomes today. To disentangle the effects of the 2015 earthquake from the one in 1988, we add a binary variable, *1988 earthquake*, that takes a value of one if a municipality had been affected by the 1988 earthquake (i.e., had a PGA larger than zero). To create the *1988 earthquake* dummy, we use the peak PGA maps prepared by USGS (2016).[129]

4.3.5 Ethnic, Religious, and Political Distortions

Although Nepal is a secular democracy today and has made significant progress in terms of women empowerment (Paudel & de Araujo, 2017), the social and religious caste system still

[128] We thank an anonymous referee for raising this point. In the case of "building back better" (Chhibber & Laajaj, 2008), it could also be that areas affected by the 1988 earthquake have a better rather than worse infrastructure than unaffected areas.

[129] We use a dummy rather than an earthquake destruction index since we do not have any information on the housing building types for 1988 available.

plays a role in the life of many people (e.g., Nagoda & Nightingale, 2017; Williams et al., 2020). In the Nepalese society, the upper castes include the Brahmins and Chhetris.[130] Although the caste system was officially abolished in 1963, caste-based discrimination remains an issue. The upper castes still have an overproportioned influence on many decisions in Nepal and are disproportionally represented in governance institutions (Dalit Civil Society Organizations' Coalition for UPR & International Dalit Solidarity Network (IDSN), 2015; DFID & World Bank, 2006). It is therefore likely that the upper castes are well represented in the offices guiding the allocation of humanitarian aid. They might thus favor those municipalities where a high percentage of their fellow caste members live. To measure possible ethnic and religious favoritism, we calculate the percentage of privileged castes within each municipality of our sample using the 2011 Census (Central Bureau of Statistics, 2011). Panel a of Figure 4.3 displays the spatial distribution of *privileged castes*, which varies considerably within our sample. Furthermore, we include the percentage of Hindu households at the district level (*Hindu*), also constructed from the 2011 Census data. Panel b of Figure 4.3 demonstrates that Hindus are mostly concentrated in the middle and lower districts of Nepal and, therefore, are less likely to live in the Himalaya regions. To measure possible political favoritism and patronage in the allocation and funding of humanitarian aid, we use district-level data from the 2013 Constituent Assembly elections, the last national elections before the earthquake in 2015 to compute the respective percentage of the two largest parties in Nepal, the *Nepali Congress Party* and the *Communist Party of Nepal* (Election Commission Nepal, 2013). Figure 4.4 shows the spatial distribution of both variables.

4.3.6 Existing Aid Networks

It is possible that the OHC plans to make use of the existing aid infrastructure to implement emergency projects quickly and effectively and thus chooses project locations accordingly. In addition, better information on post-disaster needs might be available to the OHC from places where (local) aid staff work or have worked. To test whether municipalities where international donors have a track record of aid activities are more or less likely to be selected as destinations of emergency aid, we use information on the locations of these general development aid projects from AidData (2016b). The data have been geo-referenced by using

[130] Following Paudel & de Araujo (2017), we consider Brahmins and Chhetris as higher castes. In contrast to Murshed & Gates (2005), we thus exclude the Newar cultural group from our definition of privileged castes. The Newar people are a civilization that has their own caste system that is similar to the Hindu caste system. It would thus be inaccurate to consider the entire Newar cultural group as a privileged caste.

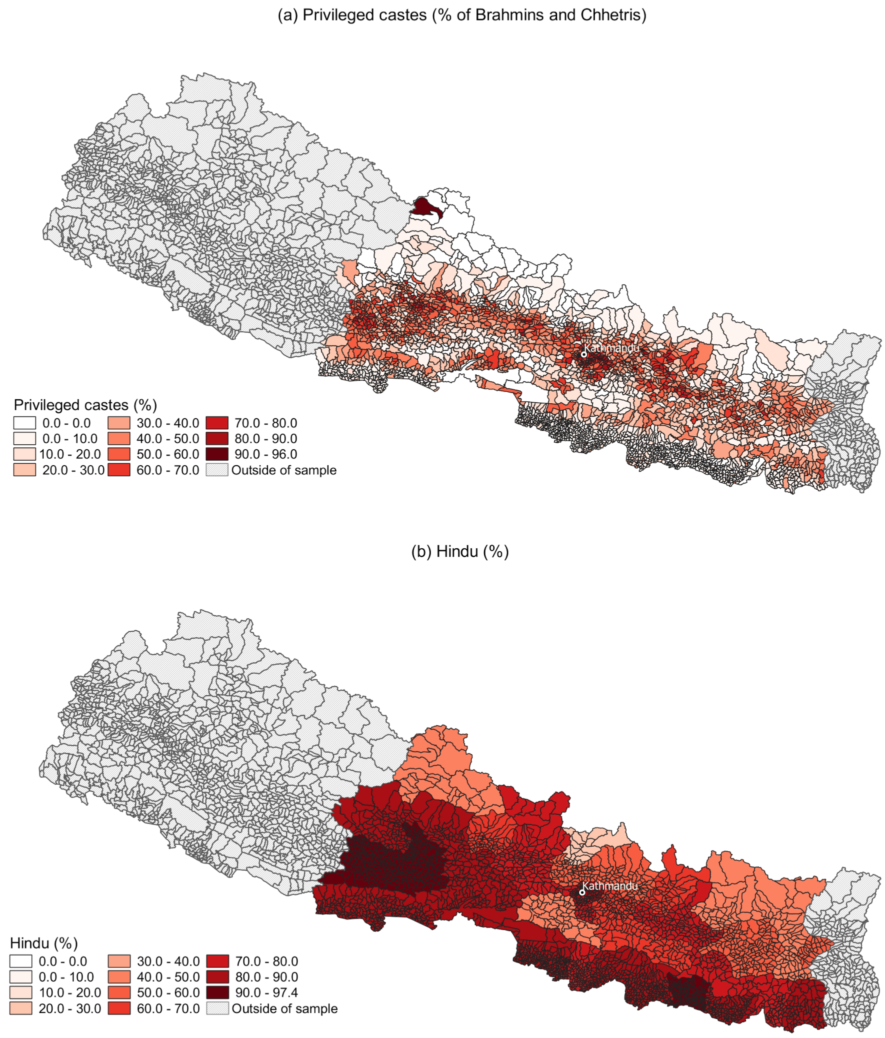

Figure 4.3: Spatial distribution of privileged castes and Hindu households across municipalities

the project information contained in the Aid Management Platform (AMP) within the Aid Information Management System (AIMS) of Nepal's Ministry of Finance. This includes 148 projects, which were implemented in more than 15,088 locations. Their aggregate value amounts to more than USD 1.32 billion. For our analysis, we calculate the probability of receiving aid in a given year over the 2002–2014 period, *general aid probability*, for each municipality in our sample.

Table 4.2 provides descriptive statistics of all variables employed in our paper. As can be seen, around 11.6 projects are proposed for each municipality on average, which corresponds to USD 2.4 million. Of these 11.6 projects, 6.5 get funded on average, which amounts to almost USD 1.0 million. According to our damage index, the immediate earthquake damage resulted on average in 19% of all houses being destroyed, whereas an average of 6% were

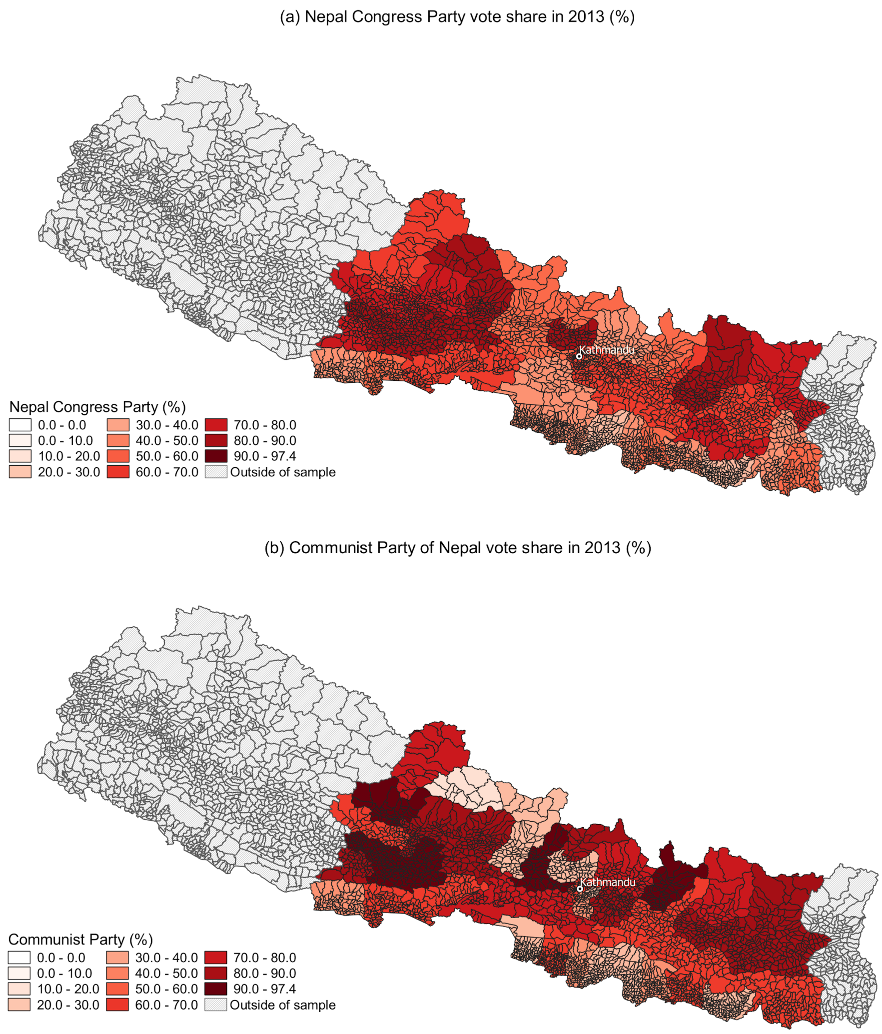

Figure 4.4: Spatial distribution of voting shares of dominant parties across municipalities

destroyed by the aftershock earthquake. The average municipality has 7,200 inhabitants, 11% of the population live in houses with a solid foundation, emits with 0.28 Wcm^2sr^{-1} only very little light at night, has an area of 27 square kilometers, a yearly rainfall of 153 mm, and is 128 km away from Kathmandu and 24 km from the next airport. On average, 77% of the population are Hindu and 21% belong to privileged castes. The Communist Party of Nepal had a vote share of 24% and the Nepali Congress Party 25% on average in the 2011 election. Appendix Table 4.7 lists all definitions with data sources, and Appendix Table 4.8 provides a correlation matrix for all variables employed in this paper.

Table 4.2: Descriptive statistics

		Count	Mean	Std. dev.	Min	Max
Dependent variables						
No. of proposed projects	Count	2,816	11.56	19.78	0.00	75.00
No. of funded projects	Count	2,816	6.49	10.76	0.00	40.00
Proposed financial amount	1,000 USD	2,816	2,429.42	2,905.68	0.00	9,834.33
Funded financial amount	1,000 USD	2,816	960.77	1,282.14	0.00	5,232.67
Share of funding obtained	Ratio	2,816	0.18	0.22	0.00	0.60
Disaster impact variables						
Immediate damage	Ratio	2,816	0.19	0.23	0.00	0.98
Aftershock damage	Ratio	2,816	0.06	0.16	0.00	1.00
Socioeconomic and physical vulnerabilities						
Population	Count	2,816	7,193.51	12,822.10	0.00	255,465.00
Solid house foundation	%	2,816	10.55	13.53	0.00	77.86
Pre-earthquake nightlight	W cm^{-2} sr^{-1}	2,816	0.28	0.33	0.10	6.39
Urban location	Dummy	2,816	0.03	0.17	0.00	1.00
Admin 4 area	km^2	2,816	27.43	53.31	1.17	888.55
Mean rainfall	mm	2,816	152.54	15.98	36.20	182.99
Distance to Kathmandu	km	2,816	128.30	64.45	0.00	271.28
Distance to airport	km	2,816	24.42	13.16	0.19	67.48
1988 earthquake	Dummy	2,816	0.76	0.43	0.00	1.00
Ethnic, religious, and political distortions						
Hindu	%	2,816	76.88	14.45	26.08	97.39
Privileged castes	%	2,804	21.28	20.92	0.00	96.02
Communist Party of Nepal	%	2,816	24.29	8.93	6.95	39.82
Nepali Congress Party	%	2,816	25.39	8.13	10.83	40.84
Existing aid networks						
General aid probability	Ratio	2,797	0.12	0.07	0.08	0.62

4.4 Results

4.4.1 Design Stage: Proposed Projects

We start by examining the factors associated with the number of proposed Flash Appeal projects per municipality. Column 1 of Table 4.3 presents the marginal effects at the mean of the covariates, where we exclude the variables proxying ethnic, religious, and political distortions in the design of the Flash Appeal. Apart from our measures of earthquake severity, Column 1 also includes measures of socioeconomic vulnerabilities (logged population, solid house foundation, and average nighttime light before the earthquake), and of physical vulnerabilities (the municipality's logged area in square kilometers, mean rainfall and its square in the years before the earthquake (1998–2014), logged distance to Kathmandu and to the nearest airport, and the 1988 earthquake dummy), and existing aid networks (the probability of receiving general development aid projects in the decade before the earthquake). As expected, a municipality's likelihood to obtain a proposed appeal project increases with the earthquake destruction index of the major shake (April 25, 2015) and the major aftershock (May 12, 2015). This is indicated by the statistically significant marginal effects of *immediate damage* and *aftershock damage*. Quantitatively, a one-standard deviation increase in immediate damage corresponds to an increase in the number of proposed projects by 0.9.[131] Put differently, a municipality that is completely damaged (index value of one) receives 3.8 more projects than a municipality that is unaffected by the major shake. The impact of the aftershock still receives economically and statistically significant attention albeit it is considerably less. A completely damaged municipality obtains only 2.6 more projects than one completely unaffected by the aftershock. These results for the exogenous proxies of earthquake damage show that the location choice of the Flash Appeal follows actual needs on the ground—but only to a certain extent as we will show when we analyze potential distortions below.

Table 4.3: Design stage – Proposed flash appeal projects after the 2015 Nepal earthquake

	(1) *No. of proposed projects*	(2) *No. of proposed projects*	(3) *Proposed financial amount (ln)*	(4) *Proposed financial amount (ln)*
Immediate damage	3.842**	3.245**	7.312**	7.229**
	[1.682]	[1.266]	[3.140]	[3.081]
Aftershock damage	2.589***	2.494***	4.700***	3.079
	[0.637]	[0.598]	[1.626]	[2.099]
Population (ln)	-0.124	0.030	-0.833***	-0.445*
	[0.126]	[0.081]	[0.284]	[0.238]
Solid house foundation (%)	-0.072***	-0.045**	-0.075**	-0.018
	[0.026]	[0.019]	[0.037]	[0.030]
Pre-earthquake nightlight (ln)	-1.094*	-0.556	-1.417	-0.561
	[0.580]	[0.386]	[1.013]	[0.796]
Admin 4 area (ln)	0.783***	0.651***	0.972**	0.604
	[0.247]	[0.216]	[0.476]	[0.449]
Mean rainfall	0.134	0.078	0.270	0.264*
	[0.128]	[0.083]	[0.164]	[0.156]
Mean rainfall squared	0.000	0.000	-0.001	-0.001
	[0.000]	[0.000]	[0.001]	[0.001]
Distance to Kathmandu (ln)	-3.185***	-2.432***	-4.247***	-4.282***
	[0.742]	[0.522]	[0.819]	[0.811]
Distance to airport (ln)	-0.525	0.077	-1.572*	-0.926
	[0.372]	[0.276]	[0.931]	[0.815]
1988 earthquake	1.185	1.644*	-1.631	0.926
	[0.927]	[0.908]	[2.112]	[1.523]
General aid probability	2.850	2.008	2.958	5.810
	[1.916]	[1.232]	[4.891]	[4.066]
Privileged castes (%)		0.014**		-0.025
		[0.006]		[0.020]
Hindu (%)		-0.012		0.012
		[0.020]		[0.050]
Communist Party of Nepal (%)		-0.005		0.227**
		[0.043]		[0.109]
Nepali Congress Party (%)		0.106**		0.198**
		[0.043]		[0.091]
Adjusted R-squared			0.526	0.605
N of observations	2796	2793	2796	2793
N of clusters	47	47	47	47

Notes: Results in Columns 1 and 2 are estimated with NB regression and Columns 3 and 4 with OLS. Columns 1 and 2 show marginal effects at the mean. Robust standard errors (in brackets) are clustered at the district level (ADM3). * (**, ***) indicates statistical significance at the 10% (5%, 1%) level.

[131] 3.842*0.23.

It is also reassuring that, according to Column 1 of Table 4.3, geographically larger areas and areas with less solid house foundations still receive more aid, as indicated by the respective statistically significant marginal effects on *admin 4 area (ln)* and *solid house foundation (%)*. While it seems at first sight that poorer regions get more projects in the proposal, the significant negative effect of *pre-earthquake nightlight* disappears once we control for ethnic, religious, and political biases later on. Moreover, the marginal effects on *population (ln)* and *mean rainfall* (and its squared term) do not reach statistical significance at conventional levels. This implies that more populous municipalities, those that were more affected by an intense monsoon in the past, and those that were less developed at the time of the earthquake do not receive more aid. Turning to our distance variables, the insignificant marginal effect of *distance to airport (ln)* suggests that municipalities closer to an airport are not attracting more proposed projects. However, we find that municipalities closer to the capital receive more proposed projects in the Flash Appeal, as indicated by the highly significant negative marginal effect of *distance to Kathmandu (ln)*. If decision-makers allocate aid dollars where they see the biggest bang-for-the-buck, they naturally disadvantage more distant, hard-to-reach locations.

The marginal effect of *general aid probability* is positive but does not reach statistical significance at conventional levels. We thus do not find evidence for aid inertia in that municipalities that have benefitted from general development aid in the past are not more likely to be included in the Flash Appeal.

Summarizing our results so far, it appears that socioeconomic and physical vulnerabilities are not sufficiently taken into consideration when the locations of proposed projects are assembled in the Flash Appeal. These results qualify our earlier interpretation of a need-based allocation of aid.

In Column 2 of Table 4.3, we find some evidence suggesting that ethnic and political distortions play a role. While there is no indication that municipalities with a higher share of Hindus receive more or less proposed projects, regions with a higher share of privileged castes receive significantly more projects at the design stage. According to the marginal effect of *privileged castes (%)*, a municipality that is entirely populated by Brahmins and Chhetris receives 1.4 additional proposed projects compared to a municipality without high-caste people.

We also examine how the municipal share of privileged castes interacts with immediate and aftershock damage by enhancing the specification of Column 2 with the two interaction terms. The marginal effects are presented graphically in Panels a and b of Appendix Figure 4.9.[132] Municipalities with a higher share of privileged castes receive significantly more aid projects only when low levels of immediate damage have been registered, i.e., when less than 40% of buildings are damaged (at the 90% level of significance). Ethnic favoritism disappears at high levels of immediate damage where need considerations seem to dominate. Turning to the aftershock, we observe that significantly more projects flow to municipalities with a larger share of privileged cases at all levels of aftershock damage. Finally, there is evidence that typical strongholds of the Nepali Congress Party receive favorable treatment at the design stage.

Ultimately, there is evidence that typical strongholds of the *Nepali Congress Party* receive favorable treatment at the design stage. Municipalities with a 10% higher vote share receive 1.1 additional aid projects. We present the importance of the factors associated with the number of proposed projects in Figure 4.5. The figure displays the effect of a one-standard-deviation increase in the number of proposed projects per municipality for each of the statistically significant variables.

We repeat our analysis with logged proposed financial amounts rather than project numbers as the dependent variable. The results in Columns 3 and 4 largely support our

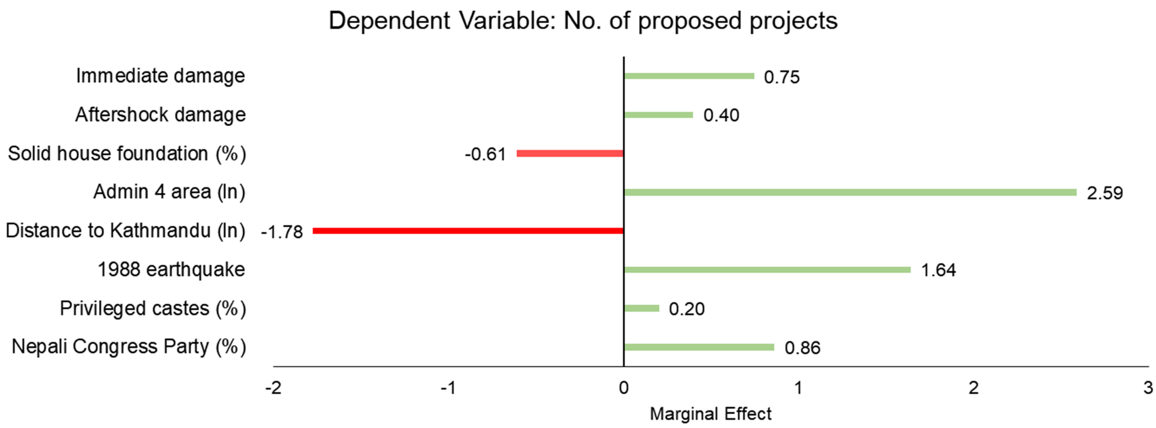

Figure 4.5: Significant regression results – Design stage

Notes: This figure shows the effect of a one standard deviation increase on the number of proposed projects per municipality. Based on results from Table 4.3, Column 2. The corresponding standard deviations can be found in Table 4.2.

[132]We estimate a linear probability model since the interpretation of interaction effects is not straightforward in nonlinear models (Ai & Norton, 2003).

earlier findings. We again discover a strong response to municipalities' damage following the major shock and – albeit less robust – the aftershock.[133]

From a humanitarian perspective, it is worrisome that we again find that municipalities closer to Kathmandu obtain more aid and that the design is also not responsive to the level of development of municipalities, as measured by nighttime light emissions. The negative coefficient on *population (ln)* even suggests that larger municipalities receive smaller financial amounts of aid rather than more support for the larger amount of (needy) people. There is however also some good news. Municipalities with less solid house foundations, arguably those with a lower self-aid capacity, and those with heavier rain receive more aid, but the significance of these effects depends on the specification.

We again find some evidence suggesting that political favoritism or patronage plays a role. More specifically, we find that larger financial amounts flow into strongholds of the Nepali Congress Party, the party that was in power at the time of the design of the Flash Appeal. The same is true for the Communist Party of Nepal.[134] While it appears counter-intuitive at first sight that the strongholds of the major opposition party were similarly favored, the Nepali government had a large interest in buying support for the upcoming referendum on the Nepali constitution (Sharma & Barry, 2015). All remaining variables show no significant marginal effects in the full specification in Column 4 of Table 4.3.[135]

To close this subsection, we test whether the distortions identified by our analysis are driven by rural and remote areas. To do this, we break our sample into (1) municipalities close to Kathmandu (<50 km) and municipalities distant to Kathmandu (>50 km), as well as (2) urban and rural municipalities and rerun our main regressions.[136] While we report the detailed regression results in Appendix Tables 4.11 and 4.13, we only highlight the most interesting results here. First, our finding that municipalities with larger population shares of privileged castes receive more proposed projects is only visible in remote and rural municipalities. The

[133] Note that the coefficient on *aftershock damage* loses its statistical significance when we control for potential ethnic, religious, and political distortions in Column 4, but it regains statistical significance when we run regressions with binary indicators for each zone (ADM2 region) to account for unobserved regional characteristics zone dummies (see Appendix Table 4.9).

[134] The coefficients on *Communist Party of Nepal (%)* and *Nepali Congress Party (%)* are not statistically significantly different from one another.

[135] Our major findings are largely robust when we exclude Nepal's capital from the sample. We provide detailed regression results in Appendix Table 4.9. We also examine whether the municipal share of privileged castes interacts with immediate and aftershock damage by enhancing the specification in Column 4 of Table 4.3 with the two interaction terms (see Appendix Figure 4.9, Panels c and d). Across all damage levels, we do not find that a higher municipal share of privileged castes affects the requested amount of aid.

[136] Urban municipalities are defined following the Central Bureau of Statistics (2014) definition. Note that the urban designation could not be made with our source for some VDCs due to the Nepali municipality district reform in 2014.

same holds for municipalities with a larger vote share for the Nepali Congress Party. Second, there is some evidence that areas closer to Kathmandu are advantaged in all four subsamples, i.e., central, remote, urban and rural parts of the country.

4.4.2 Funding Stage: Committed Projects

Table 4.4 analyzes the funding stage. Columns 1 and 3 display the results with the number of funded projects, and Columns 2 and 4 show those with the funded financial amount as the dependent variable, respectively. Qualitatively, the results in the first two columns largely mimic those for the design stage in Table 4.3.[137] Quantitatively, the marginal effects tend to be smaller, which partly reflects the fact that the 2015 Nepal Earthquake Flash Appeal has been underfunded.

To understand the mechanisms at the funding stage, we need to disentangle it from the design stage. Therefore, Columns 3 and 4 include the number of proposed projects and the proposed financial amount, respectively, as additional covariates. By conditioning on proposed aid, we can analyze the factors that are associated with deviations from the initial proposal.

It appears that the funding decisions of donors aggravate some of the distortions in aid allocation. First, donors are more likely to support and provide more funding to projects closer to Kathmandu, which likely reflects accessibility for aid delivery. In other words, logistical convenience matters, which is in line with the findings for Pakistan in Benini et al. (2009). Second, we find that areas that already suffered from the 1988 earthquake are more likely to get their projects funded. Finally, since there is no evidence that the share of the privileged castes plays a role for the number of funded projects once we control for proposed aid, the bias from the design stage seems to persist. The bias based on a municipality's electoral record even seems to aggravate as suggested by the positive and highly significant marginal effect of *Nepali Congress Party (%)* and the weaker but still significant marginal effect of *Communist Party of Nepal (%)*.

There are a few positive aspects to highlight. First, donors put more emphasis on the aftershock damage, which was undervalued at the design stage (Column 4). Second, donors

[137] The only noteworthy exception is the positive and now weakly significant marginal effect of *general aid probability* in Column 1. Projects appear to be more likely to be carried out in municipalities that have benefited from general development aid in the past. The marginal effect suggests that a municipality that received an aid project on an annual basis obtains funding for 1.8 additional Flash Appeal projects compared to a municipality that never received general development aid over the 2002–2014 period.

Table 4.4: Funding stage – Funded flash appeal projects after the 2015 Nepal earthquake

	(1) *No. of funded projects*	(2) *Funded financial amount (ln)*	(3) *No. of funded projects*	(4) *Funded financial amount (ln)*	(5) *Share of funding obtained*
Immediate damage	2.153**	6.765**	-0.914*	0.177	-0.066
	[0.897]	[2.884]	[0.491]	[0.215]	[0.066]
Aftershock damage	1.825***	3.364*	-0.330	0.557***	0.145**
	[0.420]	[1.848]	[0.369]	[0.207]	[0.065]
Population (ln)	0.015	-0.389*	-0.005	0.017*	0.005
	[0.062]	[0.216]	[0.042]	[0.009]	[0.004]
Solid house foundation (%)	-0.034**	-0.018	-0.018***	-0.002	-0.001
	[0.014]	[0.027]	[0.007]	[0.001]	[0.001]
Pre-earthquake nightlight (ln)	-0.465	-0.502	-0.044	0.010	-0.024
	[0.290]	[0.729]	[0.134]	[0.047]	[0.016]
Admin 4 area (ln)	0.465***	0.579	0.197***	0.029	0.017
	[0.156]	[0.414]	[0.073]	[0.020]	[0.011]
Mean rainfall	0.054	0.242*	0.025	0.001	-0.001
	[0.064]	[0.140]	[0.034]	[0.008]	[0.005]
Mean rainfall squared	0.000	-0.001	0.000	0.000	0.000
	[0.000]	[0.001]	[0.000]	[0.000]	[0.000]
Distance to Kathmandu (ln)	-1.780***	-4.123***	-0.664***	-0.221***	-0.134***
	[0.363]	[0.752]	[0.219]	[0.046]	[0.022]
Distance to airport (ln)	0.008	-0.814	-0.081	0.030	0.035*
	[0.212]	[0.735]	[0.108]	[0.044]	[0.020]
1988 earthquake	1.287*	0.819	1.392**	-0.026	0.038
	[0.683]	[1.399]	[0.588]	[0.077]	[0.058]
General aid probability	1.778*	5.447	1.450	0.152	0.223**
	[0.934]	[3.837]	[1.042]	[0.305]	[0.098]
Privileged castes (%)	0.010**	-0.022	0.002	0.001	0.001**
	[0.005]	[0.018]	[0.002]	[0.001]	[0.000]
Hindu (%)	-0.001	0.008	0.004	-0.003	-0.001
	[0.015]	[0.046]	[0.009]	[0.003]	[0.002]
Communist Party of Nepal (%)	0.005	0.201**	0.031*	-0.006	-0.003
	[0.033]	[0.099]	[0.017]	[0.005]	[0.003]
Nepali Congress Party (%)	0.070**	0.189**	0.071***	0.008	0.005
	[0.032]	[0.085]	[0.019]	[0.007]	[0.003]
No. of proposed projects			0.070***		
			[0.016]		
Proposed financial amount (ln)				0.911***	
				[0.008]	
Adjusted R-squared		0.623		0.999	0.668
N of observations	2793	2793	2793	2793	1290
N of clusters	47	47	47	47	24

Notes: Results in Columns 1 and 3 are estimated with negative binomial regressions and Columns 2, 4, and 5 with OLS. Columns 1 and 3 show marginal effects at the mean. Robust standard errors (in brackets) are clustered at the district level (ADM3). * (**, ***) indicates statistical significance at the 10% (5%, 1%) level.

fund more projects in municipalities with less solid house foundations and channel higher amounts to larger municipalities as suggested by the significant marginal effects on *solid house foundation (%)* and *population (ln)* in Columns 3 and 4, respectively. It is, however, worrisome that most of the weaknesses of the design stage are not corrected at the funding stage. For example, we find no robust evidence that municipalities with heavy monsoon rain or those with a large share of low-caste people obtain more funding since the corresponding coefficients on *mean rainfall* and *privileged castes (%)* are not statistically significant at conventional levels in Columns 3 and 4.

In Column 5 of Table 4.4 the dependent variable is the ratio of the received funding from international donors to the requested aid amount. We confirm that donors are more likely to fund municipalities suffering from the aftershock than originally planned according to the Flash Appeal. In line with our earlier findings, there is no evidence that funding decisions respond to the specific socioeconomic and physical vulnerabilities. Rather the results suggest that projects in municipalities closer to Kathmandu obtain a larger share of funding. We find that donors support their aid darlings by channeling more funds to previous aid beneficiaries. Instead of sticking to the plans outlined in the Flash Appeal, donors appear to cuddle their aid darlings. If a municipality's propensity of past aid receipt increases from 0 (never received general development aid) to 1 (received aid each year), then the ratio of the received funding increases by 22%. Finally, we observe that donors favor municipalities populated by higher castes also in the funding stage, which strengthens the ethnic bias from the design stage. A municipality that is entirely inhabited by privileged castes obtains an additional funding share of ten percentage points compared to a municipality without high-caste people.[138]

Taken together, our results suggest that the need orientation of the spatial project selection and funding should be strengthened at all levels of decision-making: during the design of flash appeals by UNOCHA and the OHC, as well as in the coordination and funding phase of donor countries and non-state donors.

4.5 Concluding Remarks

Four days after the 2015 Nepal earthquake, when the UN issued its Flash Appeal, the death toll already stood at 5,006 and the number of injured people was at five-figure levels (UNOCHA, 2015c). At that point in time, national and international relief efforts were already underway, but were far from meeting the needs on the ground. To scale up such efforts, the Flash Appeal called upon the international community to provide an additional USD 422 million in response to the most urgent humanitarian needs over a period of three months. From the inception of UN flash appeals in 2003 until 2015, a total of 78 such appeals have been launched to quickly respond to the severe fast-onset humanitarian disasters worldwide. However, their design and implementation have been largely ignored by scholarly research.

[138] We also checked for the impact of an exclusion of Kathmandu from our sample and ran regressions with binary indicators for each zone (ADM2 region). We provide detailed regression results in Appendix Table 4.10. While some variables lose statistical significance in some specifications, our major conclusions are unaffected. Finally, remote and rural municipalities dominated by privileged castes obtain funding for a larger share of their proposed aid funds (Columns 8 and 9 of Appendix Tables 4.12 and 4.13).

This paper attempts to fill this gap. More specifically, we analyzed the factors that drive the selection of proposed and funded project locations, as well as the size of the funds in the framework of the 2015 Nepal Earthquake Flash Appeal. By doing so, we have not only provided the first quantitative analysis of the design and implementation of UN flash appeals, but also contributed to the emerging literature on the subnational analysis of aid allocation (Briggs, 2014, 2017, 2018; Dreher et al., 2019; Findley et al., 2011; Nunnenkamp et al., 2017; Öhler et al., 2019).

Our results suggest that the allocation of proposed project locations is related to earthquake damage. However, other local need indicators, such as the population size and the level of development of municipalities (as proxied by nighttime light emissions), appear to not influence the design of flash appeals in the expected direction. There is also evidence that municipalities close to the Nepalese capital are more likely to attract projects. Even if this were the outcome of cost-benefit analyses, this finding highlights that individuals living in more distant, hard-to-reach locations are disadvantaged. Given that remote locations are also likely to be disadvantaged by national decision-makers, it is worrisome that international donors do not fill the void. Moreover, in some specifications, we find evidence that the spatial distribution of privileged castes and the vote shares of Nepal's major political parties drive aid decisions. This is worrisome given the mandate of the UN. What is more, funding decisions counteract the need orientation of project proposals and show little regard for the specific socioeconomic and physical vulnerabilities of the affected population. Although these results should be treated with caution because of the above discussed concerns about causality and measurement error, one may carefully conclude that the need orientation of geographic project selection should be strengthened and that further measures are warranted to reduce the influence of ethnic and political distortions in the design and implementation of flash appeals. More precisely, UNOCHA and the OHC need to choose more carefully the proposed project locations in the design phase of the Flash Appeal, while international donors should improve the need orientation of their funding decisions.

Our study has some weaknesses that future research hopefully will be able to address. First, since the present paper focuses only on decisions made after a single disaster, it is an open question as to whether our findings can be generalized to other UN flash appeals. Future research should thus investigate other major catastrophes as more geo-referenced aid data become available to increase the external validity of our findings. Second, although previous research shows for other parts of the world that measures of disaster impact based on physical features of the event and damage functions like ours were valid proxies (Anttila-Hughes & Hsiang, 2013), it remains only an estimate of actual destructions. Future research could endeavor to use daytime remote-sensing data on the state of physical infrastructure to obtain a more comprehensive picture of changes in local wealth in the aftermath of disasters. Third, we were not able to analyze gender as a form of exclusion since we focus on the geospatial allocation of aid. Future studies could look at this with individual-level data that allows one to detect discrimination between the two sexes. Fourth, while data availability restricted the focus of the present paper on the design and funding of flash appeal projects, research in the future could analyze whether such projects are indeed (successfully) carried out on the ground.

Finally, it would be interesting to analyze differences in aid allocation decisions between different types of funding organizations and different types of implementing organizations. Donors can be grouped into members of the OECD's Development Assistance Committee (DAC) and non-DAC bilateral donors, international organizations, non-governmental organizations (NGOs), and companies. More precisely, some donors might allocate aid to better use than others, as they select where and by whom aid projects are carried out. For example, regarding the decision to provide emergency aid, Fuchs & Klann (2013) find that nonDAC donor countries attach relatively more importance to political motives and that authoritarian donor countries favor countries rich in natural resources and disfavor democracies. Investigating differences in the extent to which different donors are more or less need-oriented than others would be a valuable addition to the literature on 'non-traditional' donors (Acht et al., 2015; Dreher et al., 2011; Fuchs & Vadlamannati, 2013; Nunnenkamp & Öhler, 2011; Semrau & Thiele, 2017).

These and other endeavors that carry out evidence-based research on UN flash appeals are highly warranted. Moreover, climate change is likely to make extreme weather events more frequent and lead to an increase in the incidence of climate-related catastrophes (Easterling, 2000). At the same time, the number of conflicts has been on the rise over the past years (Dupuy & Rustad, 2018). These developments will increase the frequency of UN flash appeals and will fuel demands to increase the transparency on the allocation of emergency aid, including the design, implementation, and effects of flash appeals.

4.6 Appendix

Table 4.5: Timeline of the 2015 Nepal earthquake flash appeal

Date	**Event**
2015-04-25	Earthquake (7.8 Magnitude) (major shake)
2015-04-25	Aftershock (6.6 Magnitude)
2015-04-25	Aftershock (6.7 Magnitude)
2015-04-26	Aftershock (6.7 Magnitude)
2015-04-29	Launch of initial Flash Appeal (April-July, USD 415 million)
2015-04-29	First aid reaches Nepal
2015-05-04	Update of initial Flash Appeal document
2015-05-12	Earthquake (7.3 Magnitude) (major aftershock)
2015-05-29	Launch of revised Flash Appeal (April-September, USD 422 million)
2015-06-13	Arrival of Monsoon season
2015-09-20	Constitution of Nepal came into effect
2015-09-30	End of revised relief phase (due to monsoon season)
2015-10-11	Change of government

Notes: The sources for this table are: Bhattacharjee (2016); UNOCHA (2015b,c), and internet research.

Table 4.6: List of the 20 largest funded 2015 Nepal earthquake flash appeal projects

Emergency Food Assistance to Earthquake Affected Populations	23.1 mUSD
Logistics Augmentation and Coordination in Response to the Earthquake in Nepal	14.8 mUSD
Provide live saving emergency Water, Sanitation and Hygiene services for earthquake affected population, especially women and children in Nepal	14.0 mUSD
Provision of Emergency Shelter, Non Food Items (NFI) and shelter support to self-recovery to Earthquake Affected Population in Nepal for 25,000 Vulnerable Households	12.8 mUSD
Provision of Humanitarian Air Services in Nepal	11.2 mUSD
Provision of Education in Emergencies to Earthquake-Affected Children in Nepal	10.4 mUSD
Equitable emergency and lifesaving primary health care services for mothers, newborns and children	10.1 mUSD
Shelter support through NFIs and training	8.7 mUSD
Emergency Shelter	7.0 mUSD
Addressing health needs in the earthquake affected population	6.6 mUSD
Comprehensive Emergency Nutrition Response for Children and Mothers	5.6 mUSD
Prevention and response to protect children in affected areas.	5.3 mUSD
Emergency assistance to re-establish agricultural-based livelihoods of vulnerable earthquake-affected smallholder farmers in the six most affected districts in Nepal	5.2 mUSD
Emergency and transitional shelter assistance to earthquake-affected populations	4.4 mUSD
Protection monitoring, legal and psychosocial support to people affected by earthquake	4.0 mUSD
Oxfam WASH Earthquake Response	3.6 mUSD
Rehabilitation of community based infrastructure and emergency employment for immediate livelihoods support	3.5 mUSD
Shelter assistance for 20,000 most vulnerable earthquake-affected families	3.4 mUSD
Coordination response	3.3 mUSD
To deliver a shelter response that supports appropriate, flexible, progressive solutions to affected, vulnerable populations that contributes to their own self recovery to provide a safer, more resilient and durable shelter	3.2 mUSD

Notes: The source for this table is (UNOCHA, 2016).

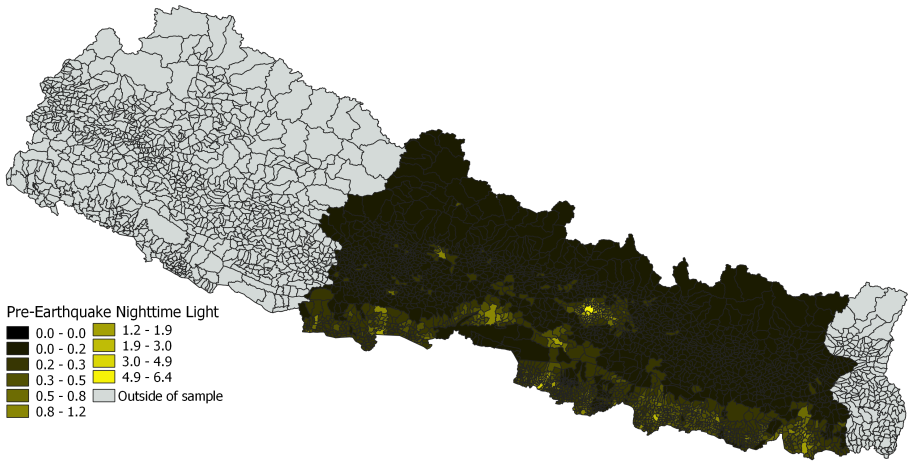

Figure 4.6: Spatial distribution of nighttime light prior to the 2015 Nepal earthquake across municipalities

Notes: The figure displays nighttime light intensity (measured in $W * cm^{-2} * sr^{-1})$ assembled from the VIIRS satellite.

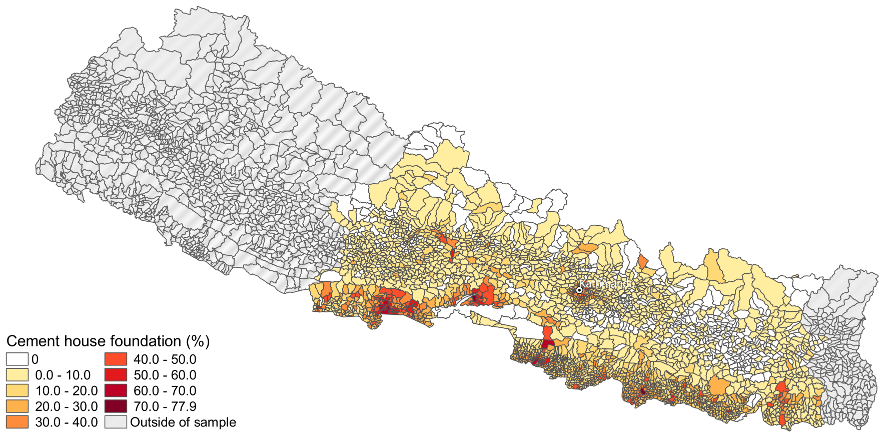

Figure 4.7: Spatial distribution of households with solid house foundation (cement) across municipalities, 2011

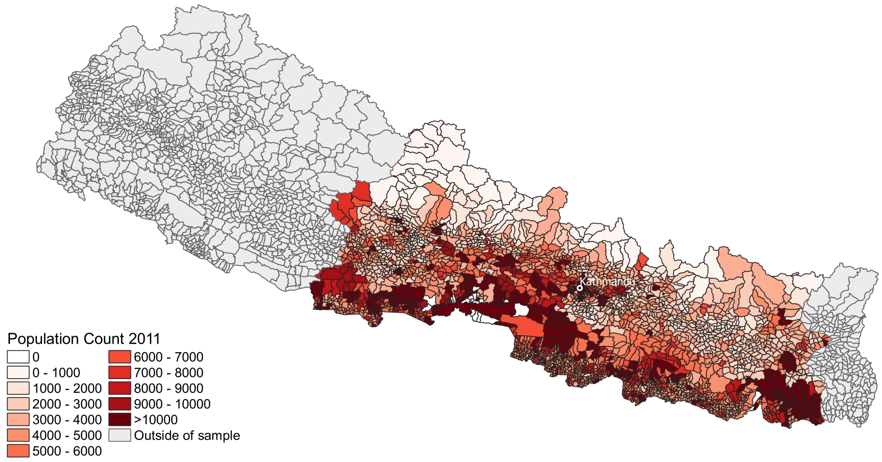

Figure 4.8: Spatial distribution of Nepal's population (population count) across municipalities, 2011

Table 4.7: Variable list with definitions and sources

	Definition	Data Source
Dependent variables		
No. of proposed projects	Number of proposed disaster aid projects in the municipality	AidData (2016a)
No. of funded projects	Number of funded disaster aid projects in the municipality	AidData (2016a)
Proposed financial amount (USD) (ln)	Financial value of all proposed disaster aid projects in the municipality (in 1000 US$)	AidData (2016a)
Funded financial amount (USD) (ln)	Financial value of all funded disaster aid projects in the municipality (in 1000 US$)	AidData (2016a)
Share of funding obtained	Ratio of funded to requested financial value of disaster aid projects in the municipality	AidData (2016a)
Disaster impact variables		
Immediate damage	Earthquake destruction index of the first earthquake (April 25, 2015) for the highest quality building type scenario, ranging from 0 (no destruction) to 1 (all building are destroyed)	USGS (2017b)
Aftershock damage	Earthquake destruction index of the major aftershock earthquake (Mai 12, 2015) for the highest quality building type scenario, ranging from 0 (no destruction) to 1 (all building are destroyed)	USGS (2017c)
Socioeconomic vulnerabilities		
Population (ln)	Logarithm of the population size of the municipality	Central Bureau of Statistics (2011)
Solid house foundation (%)	Percentage of households with solid house foundation (cement) in the municipality in 2011	Central Bureau of Statistics (2011)
Pre-earthquake nightlight (ln)	Average nighttime light intensity in the municipality between January 2012 to March 2015	NOAA (2017)
Urban location	Binary variable equal to 1 if a VDC was declared as an urban municipality	Central Bureau of Statistics (2014)
Physical vulnerabilities		
Admin 4 area (ln)	Logarithm of the area (km^2) of the municipality	Central Bureau of Statistics (2011)
Mean rainfall	Mean rainfall over the period 1998-2014 per municipality in mm	Own calculations based on Huffmann et al. (2014)
Distance to Kathmandu (ln)	Logged distance from the municipality centroid to Kathmandu in kilometer	Own calculations
Distance to airport (ln)	Logged distance from the municipality centroid to the closest airport in kilometer	Own calculations
1988 earthquake	Binary variable equal to 1 if the municipality was affected by the 1988 earthquake (i.e., had a PGA larger than zero)	USGS (2016)
Ethnic, religious and political distortions		
Hindu (%)	Percentage of Hindus within the respective district (administrative level 3)	Central Bureau of Statistics (2011)
Privileged castes (%)	Percentage of people belonging to the Brahmin ("brahmanhill" and "brahmantarai") and Chhetri ("chhetree") castes in the municipality	Central Bureau of Statistics (2011)
Communist Party of Nepal (%)	Percentage of votes won by the Communist Party of Nepal (unified Marxist-Leninist) at the 2013 election within the respective district (administrative level 3)	Election Commission Nepal (2013)
Nepali Congress Party (%)	Percentage of votes won by the Nepali Congress Party at the 2013 election within the respective district (administrative level 3)	Election Commission Nepal (2013)
Existing aid networks		
General aid probability	Probability to receive general aid over the period 2002-2014	AidData (2016b)

Table 4.8: Correlation matrix

		(1)	(2)	(3)	(4)	(5)	(6)	(7)	(8)	(9)	(10)	(11)	(12)	(13)	(14)	(15)
(1)	Immediate damage	100%														
(2)	Aftershock damage	35%	100%													
(3)	Population (ln)	-1%	-6%	100%												
(4)	Admin 4 area (ln)	5%	3%	-16%	100%											
(5)	Mean rainfall	23%	-2%	10%	7%	100%										
(6)	Pre-earthquake nightlight (ln)	-5%	-9%	31%	-48%	-7%	100%									
(7)	Solid house foundation (%)	-14%	-14%	22%	-36%	-8%	75%	100%								
(8)	Distance to Kathmandu (ln)	-74%	-34%	-7%	14%	-29%	-25%	-6%	100%							
(9)	Distance to airport (ln)	0%	-4%	4%	13%	-7%	-15%	-15%	9%	100%						
(10)	1988 earthquake	32%	23%	2%	-6%	-4%	16%	1%	-42%	-12%	100%					
(11)	General aid probability	4%	14%	2%	10%	-4%	4%	6%	-7%	4%	11%	100%				
(12)	Privileged castes (%)	17%	15%	-6%	3%	36%	-19%	-20%	-14%	-17%	-24%	0%	100%			
(13)	Hindu (%)	-32%	-23%	17%	-37%	-9%	34%	36%	23%	11%	-44%	-4%	-2%	100%		
(14)	Communist Party of Nepal (%)	-2%	17%	-22%	29%	27%	-48%	-44%	14%	1%	-31%	-9%	41%	-21%	100%	
(15)	Nepali Congress Party (%)	14%	-3%	-23%	29%	27%	-45%	-42%	1%	-16%	-35%	-11%	46%	-11%	61%	100%

Table 4.9: Robustness – Design stage (based on Table 4.3)

	(1)	(2)	(3)	(4)	(5)	(6)
		Table 4.3, col. 2			*Table 4.3, col. 4*	
	Baseline	Exclude Kathmandu	ADM2 FE	Baseline	Exclude Kathmandu	ADM2 FE
Immediate damage	3.245**	2.859**	0.173	7.229**	6.556*	4.710**
	[1.266]	[1.131]	[0.112]	[3.081]	[3.297]	[1.966]
Aftershock damage	2.494***	2.216***	0.287**	3.079	2.945	3.848*
	[0.598]	[0.558]	[0.136]	[2.099]	[2.137]	[2.152]
Population (ln)	0.030	0.030	0.000	-0.445*	-0.431*	-0.203
	[0.081]	[0.077]	[0.012]	[0.238]	[0.234]	[0.167]
Solid house foundation (%)	-0.045**	-0.042**	-0.006**	-0.018	-0.018	-0.043
	[0.019]	[0.018]	[0.003]	[0.030]	[0.031]	[0.026]
Pre-earthquake nightlight (ln)	-0.556	-0.558	-0.070	-0.561	-0.446	0.622
	[0.386]	[0.397]	[0.061]	[0.796]	[0.874]	[0.775]
Admin 4 area (ln)	0.651***	0.610***	0.071***	0.604	0.630	0.539
	[0.216]	[0.202]	[0.026]	[0.449]	[0.451]	[0.352]
Mean rainfall	0.078	0.076	0.013	0.264*	0.270*	0.149
	[0.083]	[0.077]	[0.010]	[0.156]	[0.158]	[0.163]
Mean rainfall squared	0.000	0.000	0.000	-0.001	-0.001	0.000
	[0.000]	[0.000]	[0.000]	[0.001]	[0.001]	[0.001]
Distance to Kathmandu (ln)	-2.432***	-2.270***	-0.420***	-4.282***	-4.760***	-2.230*
	[0.522]	[0.524]	[0.105]	[0.811]	[1.008]	[1.292]
Distance to airport (ln)	0.077	0.056	0.007	-0.926	-0.994	-0.771
	[0.276]	[0.249]	[0.035]	[0.815]	[0.821]	[0.584]
1988 earthquake	1.644*	1.477*	0.462*	0.926	0.832	-2.377*
	[0.908]	[0.834]	[0.269]	[1.523]	[1.531]	[1.321]
General aid probability	2.008	1.797	0.348*	5.810	5.315	1.672
	[1.232]	[1.107]	[0.194]	[4.066]	[4.205]	[4.055]
Privileged castes (%)	0.014**	0.013**	0.002**	-0.025	-0.024	-0.017
	[0.006]	[0.006]	[0.001]	[0.020]	[0.019]	[0.016]
Hindu (%)	-0.012	-0.009	-0.006**	0.012	0.013	-0.072
	[0.020]	[0.018]	[0.003]	[0.050]	[0.051]	[0.045]
Communist Party of Nepal (%)	-0.005	-0.004	0.010*	0.227**	0.232**	0.254**
	[0.043]	[0.038]	[0.006]	[0.109]	[0.109]	[0.103]
Nepali Congress Party (%)	0.106**	0.094**	0.009	0.198**	0.198**	0.101
	[0.043]	[0.039]	[0.007]	[0.091]	[0.092]	[0.082]
Adjusted R-squared				0.605	0.598	0.716
N of observations	2793	2735	2793	2793	2735	2793
N of clusters	47	46	47	47	46	47

Notes: The dependent variable is *no. of proposed projects* in Columns 1–3 and *proposed financial amount (ln)* in Columns 4–6. Results in Columns 1–3 are estimated with NB regression and Columns 4–6 with OLS. Columns 1–3 show marginal effects at the mean. Robust standard errors (in brackets) are clustered at the district level (ADM3). * (**, ***) indicates statistical significance at the 10% (5%, 1%) level.

Table 4.10: Robustness – Funding stage (based on Table 4.4)

	(1) Baseline (Table 4.4, col. 3)	(2) Exclude Kath-mandu	(3) ADM2 FE	(4) Baseline (Table 4.4, col. 4)	(5) Exclude Kath-mandu	(6) ADM2 FE	(7) Baseline (Table 4.4, col. 5)	(8) Exclude Kath-mandu	(9) ADM2 FE
Immediate damage	-0.914*	-0.949**	-0.082***	0.177	0.196	0.224	-0.066	-0.056	-0.026
	[0.491]	[0.475]	[0.029]	[0.215]	[0.215]	[0.175]	[0.066]	[0.064]	[0.047]
Aftershock damage	-0.330	-0.381	-0.074**	0.557***	0.563***	0.468**	0.145**	0.151**	0.073
	[0.369]	[0.366]	[0.033]	[0.207]	[0.208]	[0.218]	[0.065]	[0.066]	[0.059]
Population (ln)	-0.005	-0.003	-0.002	0.017*	0.017*	0.010	0.005	0.005	0.002
	[0.042]	[0.040]	[0.004]	[0.009]	[0.009]	[0.007]	[0.004]	[0.004]	[0.004]
Solid house foundation (%)	-0.018***	-0.015**	-0.001**	-0.002	-0.002	-0.001	-0.001	-0.001	0.000
	[0.007]	[0.007]	[0.001]	[0.001]	[0.001]	[0.001]	[0.001]	[0.001]	[0.001]
Pre-earthquake nightlight (ln)	-0.044	-0.055	0.006	0.010	0.011	-0.003	-0.024	-0.022	-0.016
	[0.134]	[0.142]	[0.012]	[0.047]	[0.050]	[0.044]	[0.016]	[0.019]	[0.016]
Admin 4 area (ln)	0.197***	0.188***	0.008	0.029	0.029	0.023	0.017	0.018	0.010
	[0.073]	[0.068]	[0.005]	[0.020]	[0.020]	[0.019]	[0.011]	[0.011]	[0.009]
Mean rainfall	0.025	0.031	-0.001	0.001	0.001	0.000	-0.001	-0.002	-0.004
	[0.034]	[0.033]	[0.002]	[0.008]	[0.008]	[0.006]	[0.005]	[0.005]	[0.005]
Mean rainfall squared	0.000	0.000	0.000	0.000	0.000	0.000	0.000	0.000	0.000
	[0.000]	[0.000]	[0.000]	[0.000]	[0.000]	[0.000]	[0.000]	[0.000]	[0.000]
Distance to Kathmandu (ln)	-0.664***	-0.700***	-0.072***	-0.221***	-0.205***	-0.273***	-0.134***	-0.121***	-0.139***
	[0.219]	[0.222]	[0.017]	[0.046]	[0.055]	[0.076]	[0.022]	[0.030]	[0.030]
Distance to airport (ln)	-0.081	-0.090	-0.001	0.030	0.031	0.036	0.035*	0.036*	0.044***
	[0.108]	[0.096]	[0.009]	[0.044]	[0.043]	[0.040]	[0.020]	[0.020]	[0.010]
1988 earthquake	1.392**	1.255**	0.115**	-0.026	-0.024	0.017	0.038	0.037	0.033
	[0.588]	[0.538]	[0.052]	[0.077]	[0.077]	[0.101]	[0.058]	[0.059]	[0.046]
General aid probability	1.450	1.250	0.067	0.152	0.172	0.173	0.223**	0.233**	0.157*
	[1.042]	[0.948]	[0.061]	[0.305]	[0.305]	[0.267]	[0.098]	[0.096]	[0.088]
Privileged castes (%)	0.002	0.002	0.000*	0.001	0.001	0.001	0.001**	0.001**	0.000**
	[0.002]	[0.002]	[0.000]	[0.001]	[0.001]	[0.001]	[0.000]	[0.000]	[0.000]
Hindu (%)	0.004	0.005	-0.001	-0.003	-0.003	-0.002	-0.001	-0.001	-0.002
	[0.009]	[0.008]	[0.001]	[0.003]	[0.003]	[0.004]	[0.002]	[0.002]	[0.002]
Communist Party of Nepal (%)	0.031*	0.031*	0.004***	-0.006	-0.006	-0.007	-0.003	-0.003	-0.003
	[0.017]	[0.017]	[0.001]	[0.005]	[0.005]	[0.005]	[0.003]	[0.003]	[0.003]
Nepali Congress Party (%)	0.071***	0.065***	0.007***	0.008	0.008	0.008	0.005	0.005	0.004
	[0.019]	[0.017]	[0.002]	[0.007]	[0.007]	[0.008]	[0.003]	[0.003]	[0.005]
No. of proposed projects	0.070***	0.065***	0.007***						
	[0.016]	[0.015]	[0.001]						
Proposed financial amount (ln)				0.911***	0.911***	0.918***			
				[0.008]	[0.008]	[0.007]			
Adjusted R-squared				0.999	0.999	0.999	0.668	0.649	0.708
N of observations	2793	2735	2793	2793	2735	2793	1290	1232	1290
N of clusters	47	46	47	47	46	47	24	23	24

Notes: The dependent variable is *no. of funded projects* in Columns 1–3, *funded financial amount (ln)* in Columns 4–6, and *share of funding obtained* in Columns 7–9. Results in Columns 1–3 are estimated with NB regression and Columns 4–9 with OLS. Columns 1–3 show marginal effects at the mean. Robust standard errors (in brackets) are clustered at the district level (ADM3). * (**, ***) indicates statistical significance at the 10% (5%, 1%) level.

Table 4.11: Robustness – Design stage (sample split with distance to Kathmandu, based on Table 4.3)

	(1)	(2)	(3)	(4)	(5)	(6)
		Table 4.3, col. 2			*Table 4.3, col. 4*	
	Baseline	<50km from Kath-mandu	>50km from Kath-mandu	Baseline	<50km from Kath-mandu	>50km from Kath-mandu
Immediate damage	3.245**	33.076***	0.795**	7.229**	0.828	11.748**
	[1.266]	[3.586]	[0.318]	[3.081]	[0.760]	[5.461]
Aftershock damage	2.494***	23.837***	0.057	3.079	1.234	0.392
	[0.598]	[5.461]	[0.309]	[2.099]	[0.984]	[3.695]
Population (ln)	0.030	-2.093**	-0.008	-0.445*	-0.108	-0.329
	[0.081]	[0.997]	[0.028]	[0.238]	[0.201]	[0.243]
Solid house foundation (%)	-0.045**	0.096	-0.013**	-0.018	-0.028	-0.045
	[0.019]	[0.112]	[0.006]	[0.030]	[0.023]	[0.033]
Pre-earthquake nightlight (ln)	-0.556	-6.847**	-0.053	-0.561	0.069	0.733
	[0.386]	[3.375]	[0.151]	[0.796]	[0.477]	[1.292]
Admin 4 area (ln)	0.651***	-1.662	0.136***	0.604	-0.461	0.562
	[0.216]	[1.210]	[0.052]	[0.449]	[0.289]	[0.452]
Mean rainfall	0.078	-0.929	0.045*	0.264*	-0.415	0.346*
	[0.083]	[1.728]	[0.027]	[0.156]	[0.245]	[0.173]
Mean rainfall squared	0.000	0.002	-0.000*	-0.001	0.001	-0.001*
	[0.000]	[0.006]	[0.000]	[0.001]	[0.001]	[0.001]
Distance to Kathmandu (ln)	-2.432***	-16.168**	-1.673***	-4.282***	-2.212	-7.407*
	[0.522]	[6.735]	[0.548]	[0.811]	[1.357]	[3.853]
Distance to airport (ln)	0.077	6.438*	-0.017	-0.926	0.926	-1.230
	[0.276]	[3.753]	[0.081]	[0.815]	[0.795]	[0.940]
1988 earthquake	1.644*		-0.174	0.926		-1.125
	[0.908]		[0.229]	[1.523]		[1.748]
General aid probability	2.008	19.358*	-0.084	5.810	2.329	2.922
	[1.232]	[10.533]	[0.384]	[4.066]	[1.799]	[6.251]
Privileged castes (%)	0.014**	-0.035	0.004**	-0.025	-0.005	-0.017
	[0.006]	[0.043]	[0.002]	[0.020]	[0.004]	[0.019]
Hindu (%)	-0.012	0.133	-0.012	0.012	-0.036	-0.035
	[0.020]	[0.113]	[0.009]	[0.050]	[0.026]	[0.061]
Communist Party of Nepal (%)	-0.005	0.272	0.004	0.227**	0.127	0.242
	[0.043]	[0.405]	[0.013]	[0.109]	[0.074]	[0.146]
Nepali Congress Party (%)	0.106**	-0.103	0.034**	0.198**	0.118	0.184
	[0.043]	[0.436]	[0.016]	[0.091]	[0.073]	[0.135]
Adjusted R-squared				0.605	0.346	0.550
N of observations	2793	457	2336	2793	457	2336
N of clusters	47	14	41	47	14	41

Notes: The dependent variable is *no. of proposed projects* in Columns 1–3 and *proposed financial amount (ln)* in Columns 4–6. Results in Columns 1–3 are estimated with NB regression and Columns 4–6 with OLS. Columns 1–3 show marginal effects at the mean. Robust standard errors (in brackets) are clustered at the district level (ADM3). * (**, ***) indicates statistical significance at the 10% (5%, 1%) level.

Table 4.12: Robustness – Funding stage (sample split with distance to Kathmandu, based on Table 4.4)

	(1) Baseline (Table 4.4, col. 3)	(2) <50km from Kathmandu	(3) >50km from Kathmandu	(4) Baseline (Table 4, col. 4)	(5) <50km from Kathmandu	(6) >50km from Kathmandu	(7) Baseline (Table 4.4, col. 5)	(8) <50km from Kathmandu	(9) >50km from Kathmandu
Immediate damage	-0.914*	-1.806*	-0.291	0.177	-0.150***	0.497*	-0.066	-0.066***	-0.046
	[0.491]	[0.946]	[0.227]	[0.215]	[0.032]	[0.255]	[0.066]	[0.015]	[0.077]
Aftershock damage	-0.330	-1.417	-0.364	0.557***	-0.001	0.800***	0.145**	0.002	0.135*
	[0.369]	[1.482]	[0.230]	[0.207]	[0.031]	[0.248]	[0.065]	[0.013]	[0.074]
Population (ln)	-0.005	-0.071	-0.018	0.017*	-0.002	0.016	0.005	-0.002	-0.004
	[0.042]	[0.158]	[0.015]	[0.009]	[0.004]	[0.011]	[0.004]	[0.002]	[0.004]
Solid house foundation (%)	-0.018***	0.017	-0.008	-0.002	0.001*	-0.001	-0.001	0.001**	0.000
	[0.007]	[0.025]	[0.005]	[0.001]	[0.001]	[0.001]	[0.001]	[0.000]	[0.001]
Pre-earthquake nightlight (ln)	-0.044	-0.163	0.022	0.010	-0.003	0.001	-0.024	-0.005	-0.033
	[0.134]	[0.439]	[0.099]	[0.047]	[0.017]	[0.061]	[0.016]	[0.008]	[0.020]
Admin 4 area (ln)	0.197***	-0.476*	0.048**	0.029	-0.012*	0.006	0.017	-0.007*	0.013
	[0.073]	[0.271]	[0.024]	[0.020]	[0.006]	[0.018]	[0.011]	[0.003]	[0.008]
Mean rainfall	0.025	-0.257	0.029	0.001	0.000	0.006	-0.001	-0.002	0.013**
	[0.034]	[0.215]	[0.019]	[0.008]	[0.008]	[0.007]	[0.005]	[0.003]	[0.005]
Mean rainfall squared	0.000	0.001	0.000	0.000	0.000	0.000	0.000	0.000	-0.000**
	[0.000]	[0.001]	[0.000]	[0.000]	[0.000]	[0.000]	[0.000]	[0.000]	[0.000]
Distance to Kathmandu (ln)	-0.664***	-1.322	-0.758***	-0.221***	-0.062	-0.018	-0.134***	-0.033	-0.310***
	[0.219]	[1.022]	[0.277]	[0.046]	[0.041]	[0.077]	[0.022]	[0.021]	[0.091]
Distance to airport (ln)	-0.081	0.183	-0.050	0.030	0.035	0.027	0.035*	0.016	0.012
	[0.108]	[0.546]	[0.048]	[0.044]	[0.025]	[0.040]	[0.020]	[0.012]	[0.019]
1988 earthquake	1.392**		0.186	-0.026		0.013	0.038		-0.094**
	[0.588]		[0.170]	[0.077]		[0.081]	[0.058]		[0.044]
General aid probability	1.450	-0.093	0.362	0.152	-0.110	0.171	0.223**	-0.042	0.167**
	[1.042]	[1.722]	[0.272]	[0.305]	[0.092]	[0.342]	[0.098]	[0.036]	[0.078]
Privileged castes (%)	0.002	-0.002	0.000	0.001	0.000	0.001	0.001**	0.000	0.001*
	[0.002]	[0.004]	[0.001]	[0.001]	[0.000]	[0.001]	[0.000]	[0.000]	[0.000]
Hindu (%)	0.004	0.044	-0.001	-0.003	0.000	-0.003	-0.001	0.000	-0.002
	[0.009]	[0.034]	[0.003]	[0.003]	[0.001]	[0.003]	[0.002]	[0.001]	[0.002]
Communist Party of Nepal (%)	0.031*	0.212**	0.011	-0.006	0.001	-0.013**	-0.003	0.001	-0.007***
	[0.017]	[0.084]	[0.007]	[0.005]	[0.003]	[0.006]	[0.003]	[0.001]	[0.002]
Nepali Congress Party (%)	0.071***	0.237**	0.037***	0.008	0.001	0.015	0.005	0.000	0.011**
	[0.019]	[0.094]	[0.010]	[0.007]	[0.003]	[0.009]	[0.003]	[0.001]	[0.004]
No. of proposed projects	0.070***	0.514***	0.027***						
	[0.016]	[0.035]	[0.007]						
Proposed financial amount (ln)				0.911***	0.953***	0.910***			
				[0.008]	[0.005]	[0.008]			
Adjusted R-squared				0.999	0.999	0.999	0.668	0.593	0.749
N of observations	2793	457	2336	2793	457	2336	1290	451	839
N of clusters	47	14	41	47	14	41	24	12	18

Notes: The dependent variable is *no. of funded projects* in Columns 1–3, *funded financial amount (ln)* in Columns 4–6, and *share of funding obtained* in Columns 7–9. Results in Columns 1–3 are estimated with NB regression and Columns 4–9 with OLS. Columns 1–3 show marginal effects at the mean. Robust standard errors (in brackets) are clustered at the district level (ADM3). * (**, ***) indicates statistical significance at the 10% (5%, 1%) level.

Table 4.13: Robustness – Design stage (urban vs. non-urban, based on Table 4.3)

	(1)	(2)	(3)	(4)	(5)	(6)
	Table 4.3, col. 2			*Table 4.3, col. 4*		
	Baseline	Urban	Non-urban	Baseline	Urban	Non-urban
Immediate damage	3.245**	1.030**	3.206**	7.229**	13.599***	7.064**
	[1.266]	[0.418]	[1.252]	[3.081]	[3.720]	[3.058]
Aftershock damage	2.494***	-0.042	2.552***	3.079	-4.297	3.146
	[0.598]	[0.212]	[0.606]	[2.099]	[3.750]	[2.083]
Population (ln)	0.030	0.105	0.034	-0.445*	-0.454	-0.436*
	[0.081]	[0.078]	[0.084]	[0.238]	[0.725]	[0.248]
Solid house foundation (%)	-0.045**	0.002	-0.045**	-0.018	-0.065	-0.016
	[0.019]	[0.007]	[0.019]	[0.030]	[0.061]	[0.030]
Pre-earthquake nightlight (ln)	-0.556	-0.235	-0.629	-0.561	1.992	-0.650
	[0.386]	[0.212]	[0.431]	[0.796]	[1.507]	[0.858]
Admin 4 area (ln)	0.651***	-0.069	0.679***	0.604	-0.337	0.659
	[0.216]	[0.083]	[0.219]	[0.449]	[0.664]	[0.464]
Mean rainfall	0.078	0.160	0.081	0.264*	0.467	0.266*
	[0.083]	[0.139]	[0.085]	[0.156]	[0.838]	[0.155]
Mean rainfall squared	0.000	0.000	0.000	-0.001	-0.001	-0.001
	[0.000]	[0.000]	[0.000]	[0.001]	[0.003]	[0.001]
Distance to Kathmandu (ln)	-2.432***	-0.523**	-2.511***	-4.282***	-1.635	-4.337***
	[0.522]	[0.221]	[0.546]	[0.811]	[1.116]	[0.828]
Distance to airport (ln)	0.077	-0.067	0.062	-0.926	-0.215	-0.949
	[0.276]	[0.096]	[0.284]	[0.815]	[0.909]	[0.824]
1988 earthquake	1.644*	-0.344	1.752*	0.926	0.808	1.009
	[0.908]	[0.242]	[0.930]	[1.523]	[1.370]	[1.559]
General aid probability	2.008	2.682***	1.864	5.810	14.387***	5.427
	[1.232]	[0.882]	[1.352]	[4.066]	[4.697]	[4.700]
Privileged castes (%)	0.014**	0.001	0.014**	-0.025	-0.012	-0.024
	[0.006]	[0.005]	[0.006]	[0.020]	[0.044]	[0.020]
Hindu (%)	-0.012	-0.014*	-0.010	0.012	0.110**	0.013
	[0.020]	[0.008]	[0.020]	[0.050]	[0.049]	[0.050]
Communist Party of Nepal (%)	-0.005	0.015	-0.005	0.227**	0.446***	0.223**
	[0.043]	[0.012]	[0.044]	[0.109]	[0.093]	[0.109]
Nepali Congress Party (%)	0.106**	0.003	0.107**	0.198**	0.129	0.197**
	[0.043]	[0.014]	[0.043]	[0.091]	[0.109]	[0.091]
Adjusted R-squared				0.605	0.598	0.716
N of observations	2793	2735	2793	2793	2735	2793
N of clusters	47	46	47	47	46	47

Notes: The dependent variable is *no. of proposed projects* in Columns 1–3 and *proposed financial amount (ln)* in Columns 4–6. Results in Columns 1–3 are estimated with NB regression and Columns 4–6 with OLS. Columns 1–3 show marginal effects at the mean. Robust standard errors (in brackets) are clustered at the district level (ADM3). * (**, ***) indicates statistical significance at the 10% (5%, 1%) level.

Table 4.14: Robustness – Funding stage (urban vs. non-urban, based on Table 4.4)

	(1) Baseline (Table 4.4, col. 3)	(2) Urban	(3) Non-urban	(4) Baseline (Table 4.4, col. 4)	(5) Urban	(6) Non-urban	(7) Baseline (Table 4.4, col. 5)	(8) Urban	(9) Non-urban
Immediate damage	-0.914*	0.108	-0.915*	0.177	0.349	0.179	-0.066	-0.021	-0.063
	[0.491]	[0.224]	[0.497]	[0.215]	[0.236]	[0.213]	[0.066]	[0.053]	[0.065]
Aftershock damage	-0.330	-0.035	-0.321	0.557***	0.514**	0.556***	0.145**	0.195***	0.147**
	[0.369]	[0.205]	[0.376]	[0.207]	[0.223]	[0.206]	[0.065]	[0.059]	[0.065]
Population (ln)	-0.005	-0.022	-0.002	0.017*	0.029	0.017*	0.005	0.011	0.005
	[0.042]	[0.040]	[0.042]	[0.009]	[0.029]	[0.009]	[0.004]	[0.017]	[0.004]
Solid house foundation (%)	-0.018***	-0.011**	-0.017**	-0.002	0.000	-0.002	-0.001	0.001	-0.001
	[0.007]	[0.005]	[0.007]	[0.001]	[0.001]	[0.001]	[0.001]	[0.001]	[0.001]
Pre-earthquake nightlight (ln)	-0.044	0.119	-0.053	0.010	0.035	0.015	-0.024	-0.037	-0.018
	[0.134]	[0.133]	[0.146]	[0.047]	[0.058]	[0.047]	[0.016]	[0.022]	[0.017]
Admin 4 area (ln)	0.197***	-0.011	0.214***	0.029	0.011	0.033	0.017	0.010	0.019
	[0.073]	[0.079]	[0.075]	[0.020]	[0.034]	[0.020]	[0.011]	[0.021]	[0.011]
Mean rainfall	0.025	0.199	0.026	0.001	0.004	0.001	-0.001	0.170***	-0.001
	[0.034]	[0.153]	[0.035]	[0.008]	[0.034]	[0.008]	[0.005]	[0.050]	[0.005]
Mean rainfall squared	0.000	-0.001	0.000	0.000	0.000	0.000	0.000	-0.001***	0.000
	[0.000]	[0.000]	[0.000]	[0.000]	[0.000]	[0.000]	[0.000]	[0.000]	[0.000]
Distance to Kathmandu (ln)	-0.664***	-0.053	-0.671***	-0.221***	-0.151**	-0.222***	-0.134***	-0.098***	-0.132***
	[0.219]	[0.109]	[0.230]	[0.046]	[0.060]	[0.046]	[0.022]	[0.023]	[0.022]
Distance to airport (ln)	-0.081	-0.029	-0.084	0.030	0.033	0.029	0.035*	0.024*	0.035*
	[0.108]	[0.090]	[0.111]	[0.044]	[0.039]	[0.045]	[0.020]	[0.013]	[0.020]
1988 earthquake	1.392**	0.085	1.445**	-0.026	-0.110	-0.022	0.038	-0.090*	0.040
	[0.588]	[0.253]	[0.604]	[0.077]	[0.066]	[0.077]	[0.058]	[0.043]	[0.058]
General aid probability	1.450	1.193**	1.576	0.152	0.067	0.212	0.223**	0.187**	0.264**
	[1.042]	[0.506]	[1.180]	[0.305]	[0.217]	[0.337]	[0.098]	[0.078]	[0.103]
Privileged castes (%)	0.002	0.007*	0.002	0.001	-0.001	0.001	0.001**	0.000	0.001**
	[0.002]	[0.003]	[0.002]	[0.001]	[0.002]	[0.001]	[0.000]	[0.001]	[0.000]
Hindu (%)	0.004	0.001	0.004	-0.003	-0.006**	-0.003	-0.001	-0.004***	-0.001
	[0.009]	[0.005]	[0.009]	[0.003]	[0.003]	[0.003]	[0.002]	[0.001]	[0.002]
Communist Party of Nepal (%)	0.031*	0.012***	0.032*	-0.006	-0.003	-0.006	-0.003	0.000	-0.003
	[0.017]	[0.005]	[0.017]	[0.005]	[0.007]	[0.005]	[0.003]	[0.002]	[0.003]
Nepali Congress Party (%)	0.071***	0.009	0.072***	0.008	0.001	0.008	0.005	-0.004***	0.005
	[0.019]	[0.008]	[0.019]	[0.007]	[0.005]	[0.007]	[0.003]	[0.001]	[0.003]
No. of proposed projects	0.070***	0.024***	0.071***						
	[0.016]	[0.007]	[0.016]						
Proposed financial amount (ln)				0.911***	0.908***	0.911***			
				[0.008]	[0.009]	[0.008]			
Adjusted R-squared				0.999	0.999	0.999	0.668	0.918	0.669
N of observations	2793	82	2711	2793	82	2711	1290	30	1260
N of clusters				47	38	47	24	19	24

Notes: The dependent variable is *no. of funded projects* in Columns 1–3, *funded financial amount (ln)* in Columns 4–6, and *share of funding obtained* in Columns 7–9. Results in Columns 1–3 are estimated with NB regression and Columns 4–9 with OLS. Columns 1–3 show marginal effects at the mean. Robust standard errors (in brackets) are clustered at the district level (ADM3). * (**, ***) indicates statistical significance at the 10% (5%, 1%) level.

Table 4.15: Robustness – Design stage (ADM2 cluster, based on Table 4.3)

	(1)	(2)	(3)	(4)
	Table 4.3, col. 2		*Table 4.3, col. 4*	
	Baseline	ADM2 cluster	Baseline	ADM2 cluster
Immediate damage	3.245**	3.245**	7.229**	7.229*
	[1.266]	[1.501]	[3.081]	[3.650]
Aftershock damage	2.494***	2.494***	3.079	3.079
	[0.598]	[0.688]	[2.099]	[2.118]
Population (ln)	0.030	0.030	-0.445*	-0.445
	[0.081]	[0.077]	[0.238]	[0.284]
Solid house foundation (%)	-0.045**	-0.045***	-0.018	-0.018
	[0.019]	[0.014]	[0.030]	[0.018]
Pre-earthquake nightlight (ln)	-0.556	-0.556	-0.561	-0.561
	[0.386]	[0.440]	[0.796]	[1.015]
Admin 4 area (ln)	0.651***	0.651***	0.604	0.604
	[0.216]	[0.183]	[0.449]	[0.325]
Mean rainfall	0.078	0.078	0.264*	0.264*
	[0.083]	[0.089]	[0.156]	[0.132]
Mean rainfall squared	0.000	0.000	-0.001	-0.001
	[0.000]	[0.000]	[0.001]	[0.001]
Distance to Kathmandu (ln)	-2.432***	-2.432***	-4.282***	-4.282***
	[0.522]	[0.353]	[0.811]	[0.881]
Distance to airport (ln)	0.077	0.077	-0.926	-0.926
	[0.276]	[0.155]	[0.815]	[0.906]
1988 earthquake	1.644*	1.644	0.926	0.926
	[0.908]	[1.011]	[1.523]	[1.201]
General aid probability	2.008	2.008	5.810	5.810*
	[1.232]	[1.356]	[4.066]	[3.046]
Privileged castes (%)	0.014**	0.014*	-0.025	-0.025
	[0.006]	[0.008]	[0.020]	[0.021]
Hindu (%)	-0.012	-0.012	0.012	0.012
	[0.020]	[0.026]	[0.050]	[0.077]
Communist Party of Nepal (%)	-0.005	-0.005	0.227**	0.227**
	[0.043]	[0.042]	[0.109]	[0.083]
Nepali Congress Party (%)	0.106**	0.106***	0.198**	0.198**
	[0.043]	[0.033]	[0.091]	[0.058]
Adjusted R-squared			0.605	0.716
N of observations	2793	2793	2793	2793
N of clusters	47	8	47	8

Notes: The dependent variable is *no. of proposed projects* in Columns 1–2 and *proposed financial amount (ln)* in Columns 3–4. Results in Columns 1–2 are estimated with NB regression and Columns 3–4 with OLS. Columns 1–2 show marginal effects at the mean. Robust standard errors (in brackets) are clustered at the district level (ADM3) in Columns 1 and 3 and at the zone level (ADM2) in Columns 2 and 4. * (**, ***) indicates statistical significance at the 10% (5%, 1%) level.

Table 4.16: Robustness – Funding stage (ADM2 cluster, based on Table 4.4)

	(1) Baseline	(2) ADM2 cluster	(3) Baseline	(4) ADM2 cluster	(5) Baseline	(6) ADM2 cluster
Immediate damage	-0.914*	-0.914**	0.177	0.177	-0.066	-0.066
	[0.491]	[0.451]	[0.215]	[0.102]	[0.066]	[0.043]
Aftershock damage	-0.330	-0.330	0.557***	0.557**	0.145**	0.145*
	[0.369]	[0.270]	[0.207]	[0.221]	[0.065]	[0.072]
Population (ln)	-0.005	-0.005	0.017*	0.017**	0.005	0.005
	[0.042]	[0.026]	[0.009]	[0.006]	[0.004]	[0.003]
Solid house foundation (%)	-0.018***	-0.018**	-0.002	-0.002	-0.001	-0.001
	[0.007]	[0.007]	[0.001]	[0.001]	[0.001]	[0.001]
Pre-earthquake nightlight (ln)	-0.044	-0.044	0.010	0.010	-0.024	-0.024**
	[0.134]	[0.152]	[0.047]	[0.033]	[0.016]	[0.010]
Admin 4 area (ln)	0.197***	0.197***	0.029	0.029***	0.017	0.017*
	[0.073]	[0.048]	[0.020]	[0.007]	[0.011]	[0.008]
Mean rainfall	0.025	0.025	0.001	0.001	-0.001	-0.001
	[0.034]	[0.040]	[0.008]	[0.006]	[0.005]	[0.005]
Mean rainfall squared	0.000	0.000	0.000	0.000	0.000	0.000
	[0.000]	[0.000]	[0.000]	[0.000]	[0.000]	[0.000]
Distance to Kathmandu (ln)	-0.664***	-0.664***	-0.221***	-0.221***	-0.134***	-0.134***
	[0.219]	[0.183]	[0.046]	[0.043]	[0.022]	[0.020]
Distance to airport (ln)	-0.081	-0.081	0.030	0.030	0.035*	0.035*
	[0.108]	[0.085]	[0.044]	[0.017]	[0.020]	[0.015]
1988 earthquake	1.392**	1.392*	-0.026	-0.026	0.038	0.038
	[0.588]	[0.758]	[0.077]	[0.066]	[0.058]	[0.066]
General aid probability	1.450	1.450**	0.152	0.152	0.223**	0.223**
	[1.042]	[0.739]	[0.305]	[0.110]	[0.098]	[0.079]
Privileged castes (%)	0.002	0.002	0.001	0.001	0.001**	0.001*
	[0.002]	[0.002]	[0.001]	[0.001]	[0.000]	[0.000]
Hindu (%)	0.004	0.004	-0.003	-0.003	-0.001	-0.001
	[0.009]	[0.007]	[0.003]	[0.002]	[0.002]	[0.001]
Communist Party of Nepal (%)	0.031*	0.031***	-0.006	-0.006	-0.003	-0.003
	[0.017]	[0.008]	[0.005]	[0.005]	[0.003]	[0.004]
Nepali Congress Party (%)	0.071***	0.071***	0.008	0.008	0.005	0.005
	[0.019]	[0.012]	[0.007]	[0.009]	[0.003]	[0.005]
No. of proposed projects	0.070***	0.070***				
	[0.016]	[0.017]				
Proposed financial amount (ln)			0.911***	0.911***		
			[0.008]	[0.006]		
Adjusted R-squared			0.999	0.605	0.598	0.716
N of observations	2793	2735	2793	2793	2735	2793
N of clusters	47	46	47	47	46	47

Notes: The dependent variable is *no. of funded projects* in Columns 1–2, *funded financial amount (ln)* in Columns 3–4, and *share of funding obtained* in Columns 5–6. Results in Columns 1–2 are estimated with NB regression and Columns 3–6 with OLS. Columns 1–2 show marginal effects at the mean. Robust standard errors (in brackets) are clustered at the district level (ADM3). * (**, ***) indicates statistical significance at the 10% (5%, 1%) level.

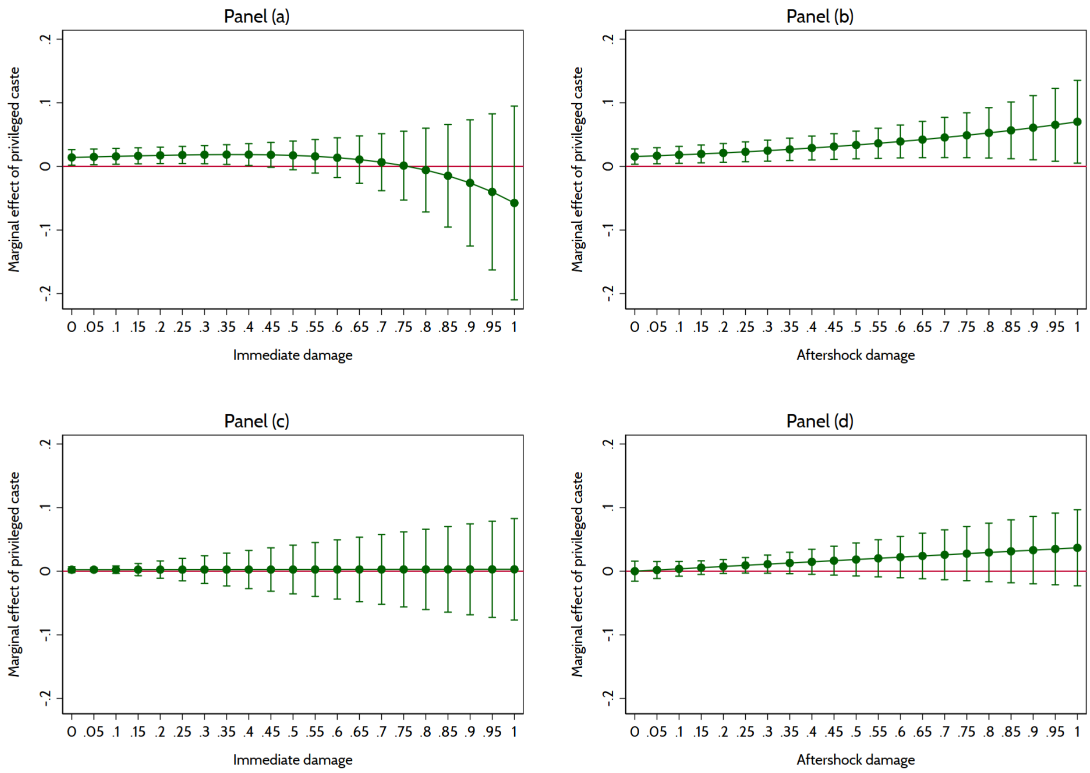

Figure 4.9: Interaction of disaster impact with privileged castes

Notes: Panels a and b show marginal effects with 90% confidence intervals for extensions of the baseline specification in Column 2 of Table 4.4 and Panels c and d for the baseline specification in Column 4 of Table 4.4. Specifically, we add two interaction terms to the respective baseline specification: (i) between privileged castes and immediate damage in Panels a and c and (ii) between privileged castes and aftershock damage in Panels b and d.

References

Abadie, A., Diamond, A., & Hainmueller, J. (2015). Comparative politics and the synthetic control method. *American Journal of Political Science*, *59*(2), 495–510.

Acemoglu, D., Carvalho, V. M., Ozdaglar, A., & Tahbaz-Salehi, A. (2012). The network origins of aggregate fluctuations. *Econometrica*, *80*(5), 1977–2016.

Acht, M., Mahmoud, T. O., & Thiele, R. (2015). Corrupt governments do not receive more state-to-state aid: Governance and the delivery of foreign aid through non-state actors. *Journal of Development Economics*, *114*, 20–33.

Aguado, E., & Burt, J. E. (2015). *Understanding Weather and Climate*. Boston, Mass. [a.o.]: Pearson, 7th ed.

Ai, C., & Norton, E. C. (2003). Interaction terms in logit and probit models. *Economics Letters*, *80*(1), 123–129.

AidData (2016a). FTS Nepal earthquake, 2015 appeals, level 1, version 1.0.
URL https://www.aiddata.org/data/nepal-earthquake-geocoded-research-release-level-1-v1-0

AidData (2016b). Nepal AIMS, level 1, version 1.4.1.
URL https://www.aiddata.org/data/nepal-aims-geocoded-research-release-level-1-v1-4-1

Aidt, T., Asatryan, Z., Badalyan, L., & Heinemann, F. (2020). Vote buying or (political) business (cycles) as usual? *The Review of Economics and Statistics*, *102*(3), 1–17.

Albala-Bertrand, J.-M. (1993). Natural disaster situations and growth: A macro-economic model for sudden disaster impacts. *World Development*, *21*(9), 1417–1434.

Albouy, D. (2013). Partisan representation in congress and the geographic distribution of federal funds. *The Review of Economics and Statistics*, *95*(1), 127–141.

Alesina, A., & Angeletos, G.-M. (2005). Fairness and redistribution. *American Economic Review*, *95*(4), 960–980.

Alesina, A., Michalopoulos, S., & Papaioannou, E. (2016). Ethnic inequality. *Journal of Political Economy*, *124*(2), 428–488.

Alesina, A., & Tabellini, G. E. (2007). Bureaucrats or politicians? Part i: A single policy task. *American Economic Review*, *97*(1), 169–179.

Amnesty International (2015). Nepal earthquake recovery must safeguard human rights.
URL http://www.preventionweb.net/publications/view/44973

Andrabi, T., & Das, J. (2017). In aid we trust: Hearts and minds and the Pakistan earthquake of 2005. *The Review of Economics and Statistics*, *99*(3), 371–386.

Angrist, J. D., & Pischke, J.-S. (2009). *Mostly harmless econometrics: An empiricist's companion*. Princeton: Princeton University Press.

Ansolabehere, S., & Snyder, J. M. (2006). Party control of state government and the distribution of public expenditures. *The Scandinavian Journal of Economics*, *108*(4), 547–569.

Anttila-Hughes, J. K., & Hsiang, S. M. (2013). Destruction, disinvestment, and death: Economic and human losses following environmental disaster. Working paper.
URL http://dx.doi.org/10.2139/ssrn.2220501

Arulampalam, W., Dasgupta, S., Dhillon, A., & Dutta, B. (2009). Electoral goals and center-state transfers: A theoretical model and empirical evidence from India. *Journal of Development Economics*, *88*(1), 103–119.

Asatryan, Z., & Havlik, A. (2020). The political economy of multilateral lending to European regions. *The Review of International Organizations*, *15*(3), 707–740.

Asia Foundation (2017). Aid and recovery in post-earthquake Nepal: Independent impacts and recovery monitoring phase 4.
URL https://asiafoundation.org/publication/aid-recovery-post-earthquake-nepal-synthesis-report-phase-4/

Auffhammer, M. (2018). Quantifying economic damages from climate change. *Journal of Economic Perspectives*, *32*(4), 33–52.

Auffhammer, M., Baylis, P., & Hausman, C. H. (2017). Climate change is projected to have severe impacts on the frequency and intensity of peak electricity demand across the United States. *Proceedings of the National Academy of Sciences*, *114*(8), 1886–1891.

Auffhammer, M., Hsiang, S. M., Schlenker, W., & Sobel, A. (2013). Using weather data and climate model output in economic analyses of climate change. *Review of Environmental Economics and Policy*, *7*(2), 181–198.

Aznar-Siguan, G., & Bresch, D. N. (2019). CLIMADA v1: A global weather and climate risk assessment platform. *Geoscientific Model Development*, *12*(7), 3085–3097.

Bacheler, N. N., Shertzer, K. W., Cheshire, R. T., & MacMahan, J. H. (2019). Tropical storms influence the movement behavior of a demersal oceanic fish species. *Scientific Reports*, *9*(1), 2045–2322.

Bakkensen, L. A., & Mendelsohn, R. O. (2016). Risk and adaptation: Evidence from global hurricane damages and fatalities. *Journal of the Association of Environmental and Resource Economists*, *3*(3), 555–587.

Bakkensen, L. A., Park, D.-S. R., & Sarkar, R. S. R. (2018). Climate costs of tropical cyclone losses also depend on rain. *Environmental Research Letters*, *13*(7), 074034.

Balles, P., Matter, U., & Stutzer, A. (2020). Special interest groups versus voters and the political economics of attention. WWZ Working Paper, 2020/06.
URL https://edoc.unibas.ch/76482/1/20200424102512_5ea2a268b0bb5.pdf

Barber, R. (2016). Did the humanitarian response to the Nepal earthquake ensure no one was left behind? Save the Children in Nepal.
URL https://reliefweb.int/sites/reliefweb.int/files/resources/Nepal%20earthquake%20report%20March%202016.pdf

Barnett, B. J. (1999). US government natural disaster assistance: Historical analysis and a proposal for the future. *Disasters*, *23*(2), 139–155.

Barragán, J. M., & de Andrés, M. (2015). Analysis and trends of the world's coastal cities and agglomerations. *Ocean & Coastal Management*, *114*, 11–20.

Barrot, J.-N., & Sauvagnat, J. (2016). Input specificity and the propagation of idiosyncratic shocks in production networks. *The Quarterly Journal of Economics*, *131*(3), 1543–1592.

Becerra, O., Cavallo, E., & Noy, I. (2014). Foreign aid in the aftermath of large natural disasters: Aid after disasters. *Review of Development Economics*, *18*(3), 445–460.

Becerra, O., Cavallo, E., & Noy, I. (2015). Where is the money? Post-disaster foreign aid flows. *Environment and Development Economics*, *20*(5), 561–586.

Bechtel, M. M., & Hainmueller, J. (2011). How lasting is voter gratitude? An analysis of the short- and long-term electoral returns to beneficial policy. *American Journal of Political Science*, *55*(4), 852–868.

Bechtel, M. M., & Mannino, M. (2017). How do voters judge policy responses to natural disasters? Working Paper.
URL http://dx.doi.org/10.2139/ssrn.2943046

Benini, A., Conley, C., Dittemore, B., & Waksman, Z. (2009). Survivor needs or logistical convenience? Factors shaping decisions to deliver relief to earthquake-affected communities, Pakistan 2005-06. *Disasters*, *33*(1), 110–131.

Berlemann, M. (2016). Does hurricane risk affect individual well-being? Empirical evidence on the indirect effects of natural disasters. *Ecological Economics*, *124*, 99–113.

Berlemann, M., & Steinhardt, M. F. (2017). Climate change, natural disasters, and migration–A survey of the empirical evidence. *CESifo Economic Studies*, *63*(4), 353–385.

Berry, C. R., Burden, B. C., & Howell, W. G. (2010). The president and the distribution of federal spending. *American Political Science Review*, *104*(4), 783–799.

Bertinelli, L., & Strobl, E. (2013). Quantifying the local economic growth impact of hurricane strikes: An analysis from outer space for the Caribbean. *Journal of Applied Meteorology and Climatology*, *52*(8), 1688–1697.

Besley, T., & Burgess, R. (2002). The political economy of government responsiveness: Theory and evidence from India. *The Quarterly Journal of Economics*, *117*(4), 1415–1451.

Besley, T., & Case, A. (1995). Does electoral accountability affect economic policy choices? Evidence from gubernatorial term limits. *The Quarterly Journal of Economics*, *110*(3), 769–798.

Bhagat, P. (2015). An earthquake exposes Nepal's political rot: The disaster could spur urgently needed democratization. But don't hold your breath. *Foreign Policy*.

Bhatia, K. T., Vecchi, G. A., Knutson, T. R., Murakami, H., Kossin, J., Dixon, K. W., & Whitlock, C. E. (2019). Recent increases in tropical cyclone intensification rates. *Nature Communications*, *10*(1), 635.

Bhattacharjee, A. (2016). After-action review of Nepal earthquake response: Final report. UNDP.
URL http://flagship2.nrrc.org.np/sites/default/files/knowledge/AAR%20Nepal%20Earthquake%20Response%20%20-%20UNDP%20Nov2016.pdf

Bilham, R. (2010). Lessons from the Haiti earthquake. *Nature*, *463*(7283), 878–879.

Bjørnskov, C. (2019). Types of foreign aid. In N. Dutta, & C. R. Williamson (Eds.) *Lessons on foreign aid and economic development*, (pp. 33–62). Palgrave Macmillan.

Bjørnskov, C., & Voigt, S. (2020). When does terror induce a state of emergency? And what are the effects? *Journal of Conflict Resolution*, *64*(4), 579–613.

Black, R., Arnell, N. W., Adger, W. N., Thomas, D., & Geddes, A. (2013). Migration, immobility and displacement outcomes following extreme events. *Environmental Science & Policy*, *27*, S32–S43.

Blanc, E., & Strobl, E. (2016). Assessing the impact of typhoons on rice production in the Philippines. *Journal of Applied Meteorology and Climatology*, *55*(4), 993–1007.

Bloemendaal, N., Muis, S., Haarsma, R. J., Verlaan, M., Irazoqui Apecechea, M., de Moel, H., Ward, P. J., & Aerts, Jeroen C. J. H. (2019). Global modeling of tropical cyclone storm surges using high-resolution forecasts. *Climate Dynamics*, *52*(7), 5031–5044.

Bluhm, R., & Krause, M. (2018). Top lights: Bright cities and their contribution to economic development. MERIT Working Papers 2018-041.
URL https://ideas.repec.org/p/unm/unumer/2018041.html

Boehm, C. E., Flaaen, A., & Pandalai-Nayar, N. (2019). Input linkages and the transmission of shocks: Firm-level evidence from the 2011 Tohoku earthquake. *The Review of Economics and Statistics*, *101*.

Bohn, F., & Sturm, J.-E. (2020). Do expected downturns kill political budget cycles? *The Review of International Organizations*.

Bohra-Mishra, P., Oppenheimer, M., & Hsiang, S. M. (2014). Nonlinear permanent migration response to climatic variations but minimal response to disasters. *Proceedings of the National Academy of Sciences of the United States of America*, *111*(27), 9780–9785.

Bommer, C., Dreher, A., & Pérez-Alvarez, M. (2019). Regional and ethnic favoritism in the allocation of humanitarian aid. CRC-PEG Discussion Paper 266.
URL https://cepr.org/sites/default/files/news/FreeDP_Sep05.pdf

Bostashvili, D., & Ujhelyi, G. (2019). Political budget cycles and the civil service: Evidence from highway spending in US states. *Journal of Public Economics*, *175*, 17–28.

Botzen, W. J. W., Deschenes, O., & Sanders, M. (2019). The economic impacts of natural disasters: A review of models and empirical studies. *Review of Environmental Economics and Policy*, *13*(2), 167–188.

Botzen, W. J. W., Kunreuther, H., & Michel-Kerjan, E. (2015). Divergence between individual perceptions and objective indicators of tail risks: Evidence from floodplain residents in New York City. *Judgment and Decision Making*, *10*(4), 365–385.

Boustan, L. P., Kahn, M. E., & Rhode, P. W. (2012). Coping with economic and environmental shocks: Institutions and outcomes: Moving to higher ground: Migration response to natural disasters in the early twentieth century. *American Economic Review*, *102*(3), 238–244.

Boustan, L. P., Kahn, M. E., Rhode, P. W., & Yanguas, M. L. (2020). The effect of natural disasters on economic activity in US counties: A century of data. *Journal of Urban Economics*, *118*, 103257.

Bouwer, L. M. (2018). Next-generation coastal risk models. *Nature Climate Change*, *8*, 765–766.

Bouwer, L. M., & Jonkman, S. N. (2018). Global mortality from storm surges is decreasing. *Environmental Research Letters*, *13*.

Bracco, E., Lockwood, B., Porcelli, F., & Redoano, M. (2015). Intergovernmental grants as signals and the alignment effect: Theory and evidence. *Journal of Public Economics*, *123*, 78–91.

Brecht, H., Dasgupta, S., Laplante, B., Murray, S., & Wheeler, D. (2007). Sea-level rise and storm surges. *Journal of Environment & Development*, *21*(1), 120–138.

Brender, A., & Drazen, A. (2008). How do budget deficits and economic growth affect reelection prospects? Evidence from a large panel of countries. *American Economic Review*, *98*(5), 2203–2220.

Briggs, R. C. (2014). Aiding and abetting: Project aid and ethnic politics in Kenya. *World Development*, *64*, 194–205.

Briggs, R. C. (2017). Does foreign aid target the poorest? *International Organization*, *71*(1), 187–206.

Briggs, R. C. (2018). Poor targeting: A gridded spatial analysis of the degree to which aid reaches the poor in Africa. *World Development*, *103*, 133–148.

British Oceanographic Data Centre (2010). GEBCO 08 Grid.
URL https://www.gebco.net/data_and_products/gridded_bathymetry_data/version_20100927/

Brollo, F., & Nannicini, T. (2012). Tying your enemy's hands in close races: The politics of federal transfers in Brazil. *American Political Science Review*, *106*(4), 742–761.

Budjan, A. J., & Fuchs, A. (forthcoming). Democracy and aid donorship. *American Economic Journal: Economic Policy*.

Bulte, E., Xu, L., & Zhang, X. (2018). Post-disaster aid and development of the manufacturing sector: Lessons from a natural experiment in China. *European Economic Review*, *101*, 441 – 458.

Burgess, R., Jedwab, R., Miguel, E., Morjaria, A., & Padró i Miquel, G. (2015). The value of democracy: Evidence from road building in Kenya. *American Economic Review*, *105*(6), 1817–1851.

Burke, M., Hsiang, S. M., & Miguel, E. (2015). Global non-linear effect of temperature on economic production. *Nature*, *527*(7577), 235–239.

Cameron, A. C., & Miller, D. L. (2015). A practitioners guide to cluster-robust inference. *Journal of Human Resources*, *50*(2), 317–372.

Cameron, L., & Shah, M. (2015). Risk-taking behavior in the wake of natural disasters. *Journal of Human Resources*, *50*(2), 484–515.

Carozzi, F., Cipullo, D., & Repetto, L. (forthcoming). Political fragmentation and government stability. Evidence from local governments in Spain. *American Economic Journal: Applied Economics*.

Carozzi, F., & Repetto, L. (2016). Sending the pork home: Birth town bias in transfers to Italian municipalities. *Journal of Public Economics*, *134*, 42–52.

Cavallo, E., & Noy, I. (2011). Natural disasters and the economy–A survey. *International Review of Environmental and Resource Economics*, *5*(1), 63–102.

Central Bureau of Statistics (2011). National population and housing census 2011: Village development committee & municipality report (household & population).
URL https://nada.cbs.gov.np/index.php/catalog/54/download/467

Central Bureau of Statistics (2014). Population monograph of Nepal (Volume III).
URL https://nepal.unfpa.org/sites/default/files/pub-pdf/Population%20Monograph%20V03.pdf

Chen, X., & Nordhaus, W. D. (2011). Using luminosity data as a proxy for economic statistics. *Proceedings of the National Academy of Sciences*, *108*(21), 8589–8594.

Chetty, R., Looney, A., & Kroft, K. (2009). Salience and taxation: Theory and evidence. *American Economic Review*, *99*(4), 1145–1177.

Chhibber, A., & Laajaj, R. (2008). Disasters, climate change and economic development in Sub-Saharan Africa: Lessons and directions. *Journal of African Economies*, *17*(Supplement 2), ii7–ii49.

Christenson, D. P., & Kriner, D. L. (2019). Does public opinion constrain presidential unilateralism? *American Political Science Review*, *113*(4), 1071–1077.

Cohen, C., & Werker, E. (2008). The political economy of "natural" disasters. *Journal of Conflict Resolution*, *52*(6), 795–819.

Cole, M. A., Elliott, R. J. R., Okubo, T., & Strobl, E. (2019). Natural disasters and spatial heterogeneity in damages: The birth, life and death of manufacturing plants. *Journal of Economic Geography*, *19*(2), 373–408.

Cole, S., Healy, A., & Werker, E. (2012). Do voters demand responsive governments? Evidence from Indian disaster relief. *Journal of Development Economics*, *97*(2), 167–181.

Colella, F., Lalive, R., Sakalli, S. O., & Thoenig, M. (2019). Inference with arbitrary clustering. IZA DP 12584.
URL http://ftp.iza.org/dp12584.pdf

Correia, S. (2017). REGHDFE: Stata module for linear and instrumental-variable/GMM regression absorbing multiple levels of fixed effects: Statistical software components, s457874.
URL https://ideas.repec.org/c/boc/bocode/s457874.html

Correia, S., Guimarães, P., & Zylkin, T. (2020). The fast poisson estimation with high-dimensional fixed effects. *The Stata Journal*, *20*(1), 95–115.

Cox, G. W., & McCubbins, M. D. (1986). Electoral politics as a redistributive game. *Journal of Politics*, *48*(2), 370–389.

Cuaresma, J. C., Hlouskova, J., & Obersteiner, M. (2008). Natural disasters as creative destruction? Evidence from developing countries. *Economic Inquiry*, *46*(2), 214–226.

Curto-Grau, M., Solé-Ollé, A., & Sorribas-Navarro, P. (2018). Does electoral competition curb party favoritism? *American Economic Journal: Applied Economics*, *10*(4), 378–407.

Czajkowski, J., Simmons, K., & Sutter, D. (2011). An analysis of coastal and inland fatalities in landfalling US hurricanes. *Natural Hazards*, *59*(3), 1513–1531.

Dalit Civil Society Organizations' Coalition for UPR, & International Dalit Solidarity Network (IDSN) (2015). Human rights situation of Dalit community in Nepal.
URL https://idsn.org/wp-content/uploads/2015/11/Nepal-UPR-2015-Dalit-Coalition-and-IDSN-report.pdf

Davlasheridze, M., Fisher-Vanden, K., & Klaiber, H. A. (2017). The effects of adaptation measures on hurricane induced property losses: Which FEMA investments have the highest returns? *Journal of Environmental Economics and Management*, *81*, 93–114.

de La O, A. L. (2013). Do conditional cash transfers affect electoral behavior? Evidence from a randomized experiment in Mexico. *American Journal of Political Science*, *57*(1), 1–14.

de Mel, S., McKenzie, D., & Woodruff, C. (2012). Enterprise recovery following natural disasters. *The Economic Journal*, *122*(559), 64–91.

de Ruiter, M. C., Ward, P. J., Daniell, J. E., & Aerts, J. C. J. H. (2017). Review article: A comparison of flood and earthquake vulnerability assessment indicators. *Natural Hazards and Earth System Sciences*, *17*(7), 1231–1251.

de Sherbinin, A., Levy, M., Adamo, S., MacManus, K., Yetman, G., Mara, V., Razafindrazay, L., Goodrich, B., Srebotnjak, T., Aichele, C., & Pistolesi, L. (2012). Migration and risk: Net migration in marginal ecosystems and hazardous areas. *Environmental Research Letters*, *7*(4), 045602.

Dell, M., Jones, B. F., & Olken, B. A. (2012). Temperature shocks and economic growth: Evidence from the last half century. *American Economic Journal: Macroeconomics*, *4*(3), 66–95.

Dell, M., Jones, B. F., & Olken, B. A. (2014). What do we learn from the weather? The new climate-economy literature. *Journal of Economic Literature*, *52*(3), 740–798.

Deryugina, T. (2017). The fiscal cost of hurricanes: Disaster aid versus social insurance. *American Economic Journal: Economic Policy*, *9*(3).

Deryugina, T., Kawano, L., & Levitt, S. (2018). The economic impact of Hurricane Katrina on its victims: Evidence from individual tax returns. *American Economic Journal: Applied Economics*, *10*(2), 202–233.

Deschênes, O., & Greenstone, M. (2011). Climate change, mortality, and adaptation: Evidence from annual fluctuations in weather in the US. *American Economic Journal: Applied Economics*, *3*(4), 152–185.

Deschenes, O., Greenstone, M., & Guryan, J. (2009). Climate change and birth weight. *American Economic Review*, *99*(2), 211–17.

DFID, & World Bank (2006). Unequal citizens: Gender, caste and ethnic exclusion in Nepal.
URL http://documents.worldbank.org/curated/en/745031468324021366/pdf/379660v20WP0Un0Box0361508B0PUBLIC0.pdf

DHS (2018). Disaster response and recovery.
URL https://www.dhs.gov/topic/disaster-response-and-recovery

Dixit, A., & Londregan, J. (1998). Fiscal federalism and redistributive politics. *Journal of Public Economics*, *68*(2), 153–180.

Djourelova, M., & Durante, R. (2019). Media attention and strategic timing in politics: Evidence from U.S. presidential executive orders. CEPR Discussion Paper Series 13961. URL https://papers.ssrn.com/sol3/papers.cfm?abstract_id=3464486

Doll, C. (2008). CIESIN thematic guide to night-time light remote sensing and its applications. Center for International Earth Science Information Network of Columbia, Palisades, NY. URL https://sedac.ciesin.columbia.edu/binaries/web/sedac/thematic-guides/ciesin_nl_tg.pdf

Downton, M. W., & Pielke Jr., R. A. (2001). Discretion without accountability: Politics, flood damage, and climate. *Natural Hazards Review*, *2*(4), 157–166.

Dreher, A., Fuchs, A., Hodler, R., Parks, B. C., Raschky, P. A., & Tierney, M. J. (2019). African leaders and the geography of China's foreign assistance. *Journal of Development Economics*, *140*, 44–71.

Dreher, A., & Lohmann, S. (2015). Aid and growth at the regional level. *Oxford Review of Economic Policy*, *31*(3-4), 420–446.

Dreher, A., Nunnenkamp, P., & Thiele, R. (2011). Are 'new' donors different? Comparing the allocation of bilateral aid between non-DAC and DAC donor countries. *World Development*, *39*(11), 1950–1968.

Dreher, A., Sturm, J.-E., & Vreeland, J. R. (2009). Development aid and international politics: Does membership on the UN security council influence World Bank decisions? *Journal of Development Economics*, *88*(1), 1–18.

Drury, A. C., Olson, R. S., & van Belle, D. A. (2005). The politics of humanitarian aid: U.S. foreign disaster assistance, 1964–1995. *Journal of Politics*, *67*(2), 454–473.

Dupor, B. (1999). Aggregation and irrelevance in multi-sector models. *Journal of Monetary Economics*, *43*(2), 391–409.

Dupuy, K., & Rustad, S. A. (2018). Trends in armed conflict, 1946–2017. *Conflict Trends, 5*.

Durante, R., Putterman, L., & van der Weele, J. (2014). Preferences for redistribution and perception of fairness: An experimental study. *Journal of the European Economic Association*, *12*(4), 1059–1086.

Durante, R., & Zhuravskaya, E. (2018). Attack when the world is not watching? US news and the Israeli-Palestinian conflict. *Journal of Political Economy*, *126*(3), 1085–1133.

Dynes, A. M., & Huber, G. A. (2015). Partisanship and the allocation of federal spending: Do same-party legislators or voters benefit from shared party affiliation with the president and house majority? *American Political Science Review*, *109*(1), 172–186.

Easterling, D. R. (2000). Climate extremes: Observations, modeling, and impacts. *Science*, *289*(5487), 2068–2074.

Egbert, G. D., & Erofeeva, S. Y. (2002). Efficient inverse modeling of barotropic ocean tides. *Journal of Atmospheric and Oceanic Technology*, *19*(2), 183–204.

Eggers, A. C., Fowler, A., Hainmueller, J., Hall, A. B., & Snyder, J. M. (2015). On the validity of the regression discontinuity design for estimating electoral effects: New evidence from over 40,000 close races. *American Journal of Political Science*, *59*(1), 259–274.

Eichenauer, V. Z. (2020). December fever in public finance. KOF Working Papers 470. URL https://doi.org/10.3929/ethz-b-000393827

Eichenauer, V. Z., Fuchs, A., Kunze, S., & Strobl, E. (2020). Distortions in aid allocation of United Nations flash appeals: Evidence from the 2015 Nepal earthquake. *World Development*, *136*.

Eilander, D., Couasnon, A., Ikeuchi, H., Muis, S., Yamazaki, D., Winsemius, H. C., & Ward, P. J. (2020). The effect of surge on riverine flood hazard and impact in deltas globally. *Environmental Research Letters*, *15*(10), 104007.

Eisensee, T., & Strömberg, D. (2007). News droughts, news floods and U.S. disaster relief. *The Quarterly Journal of Economics*, *122*(2), 693–728.

Election Commission Nepal (2013). District wise total vote count 2013. URL last accessed May 2019.
URL http://election.gov.np/CA2070/CAResults/reportBody.php?selectedMenu=5&rand=1493305367

Elinder, M., Jordahl, H., & Poutvaara, P. (2015). Promises, policies and pocketbook voting. *European Economic Review*, *75*, 177–194.

Elliott, R. J., Liu, Y., Strobl, E., & Tong, M. (2019). Estimating the direct and indirect impact of typhoons on plant performance: Evidence from Chinese manufacturers. *Journal of Environmental Economics and Management*, *98*, 102252.

Elliott, R. J., Strobl, E., & Sun, P. (2015). The local impact of typhoons on economic activity in China: A view from outer space. *Journal of Urban Economics*, *88*, 50–66.

Elsner, J. B., Kossin, J. P., & Jagger, T. H. (2008). The increasing intensity of the strongest tropical cyclones. *Nature*, *455*(7209), 92–95.

Elvidge, C., Baugh, K., Zhizhin, M., & Hsu, F.-C. (2013). Why VIIRS data are superior to DMSP for mapping nighttime lights. *Proceedings of the Asia-Pacific Advanced Network*, *35*, 62–69.

Emanuel, K. (2006). Climate and tropical cyclone activity: A new model downscaling approach. *Journal of Climate*, *19*(19), 4797–4802.

Emanuel, K. (2011). Global warming effects on U.S. hurricane damage. *Weather, Climate, and Society*, *3*(4), 261–268.

Evans, R. W., Hu, Y., & Zhao, Z. (2010). The fertility effect of catastrophe: US hurricane births. *Journal of Population Economics*, *23*(1), 1–36.

Fang, Y., & Jawitz, J. W. (2019). The evolution of human population distance to water in the USA from 1790 to 2010. *Nature Communications*, *10*(430).

Faye, M., & Niehaus, P. (2012). Political aid cycles. *American Economic Review*, *102*(7), 3516–3530.

Felbermayr, G., & Gröschl, J. (2014). Naturally negative: The growth effects of natural disasters. *Journal of Development Economics*, *111*, 92–106.

Felbermayr, G., & Gröschl, J. (2013). Natural disasters and the effect of trade on income: A new panel IV approach. *European Economic Review*, *58*, 18–30.

FEMA (2011). Fact sheet – disaster declaration process.
URL https://www.fema.gov/pdf/media/factsheets/dad_disaster_declaration.pdf

FEMA (2017a). About the agency.
URL https://www.fema.gov/about-agency

FEMA (2017b). The disaster declaration process.
URL https://www.fema.gov/disaster-declaration-process

FEMA (2017c). What is FEMA's individual assistance program? Fact sheet.
URL https://www.fema.gov/media-library-data/1565194429982-5674cd81399feaeb00cc72ab7fc4d84f/FACTSHEETIndividualAssistanceProgram.pdf

FEMA (2018). Hazard mitigation assistance.
URL https://www.fema.gov/hazard-mitigation-assistance

FEMA (2019). OpenFEMA dataset: Disaster declarations summaries – V1.
URL https://www.fema.gov/openfema-data-page/disaster-declarations-summaries

FEMA – EMI (2017). Unit three: Overview of federal disaster assistance.
URL https://training.fema.gov/emiweb/downloads/is7unit_3.pdf

Fernández-Val, I., & Weidner, M. (2016). Individual and time effects in nonlinear panel models with large N, T. *Journal of Econometrics*, *192*(1), 291–312.

Fetzer, T. (2020). Can workfare programs moderate conflict? Evidence from India. *Journal of the European Economic Association*.

Findley, M. G., Powell, J., Strandow, D., & Tanner, J. (2011). The localized geography of foreign aid: A new dataset and application to violent armed conflict. *World Development*, *39*(11), 1995–2009.

Fink, G., & Redaelli, S. (2011). Determinants of international emergency aid – Humanitarian need only? *World Development*, *39*(5), 741–757.

Fischer, P. A., & Malmberg, G. (2001). Settled people don't move: On life course and (im-)mobility in Sweden. *International Journal of Population Geography*, *7*(5), 357–371.

Fisker, P. (2014). Green lights: Quantifying the economic impacts of drought. IFRO Working Paper 2014/11.
URL https://EconPapers.repec.org/RePEc:foi:wpaper:2014_11

Fiva, J. H., & Halse, A. H. (2016). Local favoritism in at-large proportional representation systems. *Journal of Public Economics*, *143*, 15–26.

Forster, J., Schuhmann, P. W., Lake, I. R., & Gill, J. A. (2012). The influence of hurricane risk on tourist destination choice in the Caribbean. *Climatic Change*, *114*(3), 745–768.

Francken, N., Minten, B., & Swinnen, J. (2012). The political economy of relief aid allocation: Evidence from Madagascar. *World Development*, *40*(3), 486–500.

Frankenberger, E., Cecep, S., & Duncan, T. (2020). Effects of a natural disaster on mortality risks over the longer term. *Nature Sustainability*, *3*(8), 614–619.

Fuchs, A., & Klann, N.-H. (2013). Emergency aid 2.0: Annual conference 2013: Competition policy and regulation in a global economic order 79898. Verein für Socialpolitik / German Economic Association.
URL https://ideas.repec.org/p/zbw/vfsc13/79898.html

Fuchs, A., & Öhler, H. (2019). Does private aid follow the flag? An empirical analysis of humanitarian assistance. *World Economy*, *44*(3), 671–705.

Fuchs, A., & Vadlamannati, K. C. (2013). The needy donor: An empirical analysis of India's aid motives. *World Development*, *44*, 110–128.

Gall, M., Borden, K. A., & Cutter, S. L. (2009). When do losses count? Six fallacies of natural hazards loss data. *Bulletin of the American Meteorological Society*, *90*(6), 799–809.

Gallagher, J. (2019). Natural disasters that cause no damage: Retrospective voting and a reanalysis of 'make it rain'. Mimeo.
URL https://justinpgallagher.com/pdfs/disasters_electorate_011620.pdf

Garrett, T. A., & Sobel, R. S. (2003). The political economy of FEMA disaster payments. *Economic Inquiry*, *41*(3), 496–509.

Gasper, J. T. (2015). The politics of denying aid: An analysis of disaster declaration turndowns. *Journal of Public Management & Social Policy*, *22*(2).

Gasper, J. T., & Reeves, A. (2011). Make it rain? Retrospection and the attentive electorate in the context of natural disasters. *American Journal of Political Science*, *55*(2), 340–355.

Gassebner, M., & Gnutzmann-Mkrtchyan, A. (2018). Politicized trade: What drives withdrawal of trade preferences? *Economics Letters*, *167*, 10–13.

Gehring, K., & Schneider, S. A. (2018). Towards the greater good? EU commissioners' nationality and budget allocation in the European Union. *American Economic Journal: Economic Policy*, *10*(1), 214–239.

Gehring, K., & Schneider, S. A. (2020). Regional resources and democratic secessionism. *Journal of Public Economics*, *181*, 1–18.

Genovese, E., & Green, C. (2015). Assessment of storm surge damage to coastal settlements in Southeast Florida. *Journal of Risk Research*, *18*(4), 407–427.

Geohazards International, & United Nations Centre for Regional Development (2001). Global earthquake safety initiative (GESI): Pilot project.
URL https://www.preventionweb.net/files/5573_gesireport.pdf

Geys, B., & Vermeir, J. (2014). Party cues in elections under multilevel governance: Theory and evidence from US states. *Journal of the European Economic Association*, *12*(4), 1029–1058.

Ghosh, A. (1958). Input-output approach in an allocation system. *Economica*, *25*(97), 58–64.

Gonschorek, G. J., Schulze, G. G., & Sjahrir, B. S. (2018). To the ones in need or the ones you need? The political economy of central discretionary grants – Empirical evidence from Indonesia. *European Journal of Political Economy*, *54*, 240–260.

Gröger, A., & Zylberberg, Y. (2016). Internal labor migration as a shock coping strategy: Evidence from a typhoon. *American Economic Journal: Applied Economics*, *8*(2), 123–153.

Guha-Sapir, D., & CRED (2020). EM-DAT: The emergency events database. Université catholique de Louvain (UCL).
URL www.emdat.be

Guha-Sapir, D., Hoyois, P., Wallemacq, P., & Below, R. (2016). Annual disaster statistical review 2016: The numbers and trends. Université catholique de Louvain (UCL).

Haimes, Y. Y., & Jiang, P. (2001). Leontief-based model of risk in complex interconnected infrastructures. *Journal of Infrastructure Systems*, *7*(1), 1–12.

Hainmueller, J., Hall, A. B., & Snyder, J. M. (2015). Assessing the external validity of election RD estimates: An investigation of the incumbency advantage. *Journal of Politics*, *77*(3), 707–720.

Hallegatte, S., Green, C., Nicholls, R. J., & Corfee-Morlot, J. (2013). Future flood losses in major coastal cities. *Nature Climate Change*, *3*(9), 802–806.

Hallegatte, S., & Przyluski, V. (2010). The economics of natural disasters: Concepts and methods. World Bank Policy Research Working Paper 5507.
URL http://hdl.handle.net/10986/3991

Hallegatte, S., Vogt-Schilb, A., Bangalore, M., & Rozenberg, J. (2016). *Unbreakable: Building the Resilience of the Poor in the Face of Natural Disasters*. The World Bank.
URL https://elibrary.worldbank.org/doi/abs/10.1596/978-1-4648-1003-9

Hamano, M., & Vermeulen, W. N. (2019). Natural disasters and trade: The mitigating impact of port substitution. *Journal of Economic Geography*, *20*(3), 809–856.

Hanich, Q., Wabnitz, C. C., Ota, Y., Amos, M., Donato-Hunt, C., & Hunt, A. (2018). Small-scale fisheries under climate change in the Pacific Islands region. *Marine Policy*, *88*, 279–284.

Hauer, M. E. (2017). Migration induced by sea-level rise could reshape the US population landscape. *Nature Climate Change*, *7*(5), 321–325.

Hauer, M. E., Fussell, E., Mueller, V., Burkett, M., Call, M., Abel, K., McLeman, R., & Wrathall, D. (2020). Sea-level rise and human migration. *Nature Reviews Earth & Environment*, *1*(1), 28–39.

Healy, A., & Malhotra, N. (2009). Myopic voters and natural disaster policy. *American Political Science Review*, *103*(3), 387–406.

Heinen, A., Khadan, J., & Strobl, E. (2018). The price impact of extreme weather in developing countries. *The Economic Journal*, *129*(619), 1327–1342.

Heß, S. (2017). Randomization inference with Stata: A guide and software. *The Stata Journal*, *17*(3), 630–651.

Hodler, R., Loertscher, S., & Rohner, D. (2010). Inefficient policies and incumbency advantage. *Journal of Public Economics*, *94*(9), 761–767.

Hodler, R., & Raschky, P. A. (2014). Regional favoritism. *The Quarterly Journal of Economics*, *129*(2), 995–1033.

Hofmann, H., Wickham, H., & Kafadar, K. (2017). Letter-Value plots: Boxplots for large data. *Journal of Computational and Graphical Statistics*, *26*(3), 469–477.

Holland, G. J. (1980). An analytic model of the wind and pressure profiles in hurricanes. *Monthly Weather Review*, *108*(8), 1212–1218.

Horvath, M. (2000). Sectoral shocks and aggregate fluctuations. *Journal of Monetary Economics*, *45*(1), 69–106.

Hsiang, S. M. (2010). Temperatures and cyclones strongly associated with economic production in the Caribbean and Central America. *Proceedings of the National Academy of Sciences of the United States of America*, *107*(35), 15367–15372.

Hsiang, S. M. (2016). Climate econometrics. *Annual Review of Resource Economics*, *8*(1), 43–75.

Hsiang, S. M., Burke, M., & Miguel, E. (2013). Quantifying the influence of climate on human conflict. *Science*, *341*(6151).

Hsiang, S. M., & Jina, A. S. (2014). The causal effect of environmental catastrophe on long-run economic growth: Evidence from 6,700 cyclones. NBER Working Paper 20352.
URL http://www.nber.org/papers/w20352.pdf

Huffmann, G. J., Bolvin, D. T., Braithwaite, K. H., Joyce, R., & Xie, P. (2014). Integrated multi-satellite retrievals for GPM (IMERG), version 4.4. NASA's Precipitation Processing Center.
URL https://pmm.nasa.gov/data-access/downloads/trmm

Intergovernmental Panel on Climate Change (1994). Preparing to meet coastal challenges in the 21st century: Conference report, World Coast Conference 1993.
URL http://publicaties.minienm.nl/download-bijlage/27073/preparing-to-meet-the-coastal-chalanges-of-the-21st-century-wcc93conference.pdf

IPCC (2014). *Climate Change 2014: Impacts, Adaptation, and Vulnerability. Part A: Global and Sectoral Aspects. Contribution of Working Group II to the Fifth Assessment Report of the Intergovernmental Panel on Climate Change*. Cambridge, UK: Cambridge University Press.

Islam, N. (1995). Growth empirics: A panel data approach. *The Quarterly Journal of Economics*, *110*(4), 1127–1170.

Jongman, B., Ward, P. J., & Aerts, J. C. (2012). Global exposure to river and coastal flooding: Long term trends and changes. *Global Environmental Change*, *22*(4), 823–835.

Kalkuhl, M., & Wenz, L. (2020). The impact of climate conditions on economic production. Evidence from a global panel of regions. *Journal of Environmental Economics and Management*, *103*.

Kauder, B., Potrafke, N., & Reischmann, M. (2016). Do politicians reward core supporters? Evidence from a discretionary grant program. *European Journal of Political Economy*, *45*, 39–56.

Klarner, C. (2013). Governors dataset.
URL http://hdl.handle.net/1902.1/20408

Klein Goldewijk, K., Beusen, A., Doelman, J., & Stehfest, E. (2017). Anthropogenic land use estimates for the holocene – HYDE 3.2. *Earth System Science Data*, *9*(2), 927–953.

Klein Goldewijk, K., Beusen, A., van Drecht, G., & de Vos, M. (2011). The HYDE 3.1 spatially explicit database of human-induced global land-use change over the past 12,000 years. *Global Ecology and Biogeography*, *20*(1), 73–86.

Klomp, J. G. (2016). Economic development and natural disasters: A satellite data analysis. *Global Environmental Change*, *36*, 67–88.

Klomp, J. G., & Valckx, K. (2014). Natural disasters and economic growth: A meta-analysis. *Global Environmental Change*, *26*, 183–195.

Knapp, K. R. (2016). International best track archive for climate stewardship: Third workshop: Report and recommendations. World Meteorological Organization.

Knapp, K. R., Kruk, M. C., Levinson, D. H., Diamond, H. J., & Neumann, C. J. (2010). The international best track archive for climate stewardship (IBTrACS). *Bulletin of the American Meteorological Society*, *91*(3), 363–376.

Knight, D. B., & Davis, R. E. (2009). Contribution of tropical cyclones to extreme rainfall events in the Southeastern United States. *Journal of Geophysical Research*, *114*.

Knutson, T., Camargo, S. J., Chan, J. C., Emanuel, K., Ho, C.-H., Kossin, J., Mohapatra, M., Satoh, M., Sugi, M., Walsh, K., et al. (2020). Tropical cyclones and climate change assessment: Part II: Projected response to anthropogenic warming. *Bulletin of the American Meteorological Society*, *101*(3), E303–E322.

Kocornik-Mina, A., McDermott, T. K. J., Michaels, G., & Rauch, F. (2020). Flooded cities. *American Economic Journal: Applied Economics*, *12*(2), 35–66.

Konrad, C. E., Meaux, M. F., & Meaux, D. A. (2002). Relationships between tropical cyclone attributes and precipitation totals: Considerations of scale. *International Journal of Climatology*, *22*(2), 237–247.

Korty, R. (2013a). Economics of disasters. In P. T. Bobrowsky (Ed.) *Encyclopedia of Natural Hazards*. Dordrecht and New York: Springer.

Korty, R. (2013b). Hurricane (typhoon, cyclone). In P. T. Bobrowsky (Ed.) *Encyclopedia of Natural Hazards*, (pp. 481–494). Dordrecht and New York: Springer.

Kossin, J. P., Olander, T. L., & Knapp, K. R. (2013). Trend analysis with a new global record of tropical cyclone intensity. *Journal of Climate*, *26*(24), 9960–9976.

Kousky, C. (2014). Informing climate adaptation: A review of the economic costs of natural disasters. *Energy Economics*, *46*, 576–592.

Kraus, H., & Ebel, U. (2003). *Risiko Wetter: Die Entstehung von Stürmen und anderen atmosphärischen Gefahren*. Berlin and Heidelberg [a.o.]: Springer.

Kriner, D. L., & Reeves, A. (2015). Presidential particularism and divide-the-dollar politics. *American Political Science Review*, *109*(1), 155–171.

Kruk, M. C., Knapp, K. R., & Levinson, D. H. (2010). A technique for combining global tropical cyclone best track data. *Journal of Atmospheric and Oceanic Technology*, *27*(4), 680–692.

Kulp, S. A., & Strauss, B. H. (2019). New elevation data triple estimates of global vulnerability to sea-level rise and coastal flooding. *Nature Communications*, *10*(4844).

Kunze, S. (2021). Unraveling the effects of tropical cyclones on economic sectors worldwide: Direct and indirect impacts. *Environmental and Resource Economics*, *78*, 545–569.

Kunze, S., & Strobl, E. (2020). The global long-term effects of storm surge damage on human settlements in coastal areas. Mimeo.

Kuziemko, I., & Werker, E. (2006). How much is a seat on the security council worth? *Journal of Political Economy*, *114*(5), 905–930.

Lahmeyer, J. (2004). Populstat database. Growth of the population per country in a historical perspective, including their administrative divisions and principal towns. URL http://www.populstat.info/

Lam, L. M., & Kuipers, R. (2019). Resilience and disaster governance: Some insights from the 2015 Nepal earthquake. *International Journal of Disaster Risk Reduction*, *33*, 321–331.

Landscan (2006). Landscan global population database, the 2004 revision. URL https://www.osti.gov/biblio/1231332-landscan-high-resolution-global-population-data-set

Lang, V. F., & Presbitero, A. F. (2018). Room for discretion? Biased decision-making in international financial institutions. *Journal of Development Economics*, *130*, 1–16.

Larcinese, V., Rizzo, L., & Testa, C. (2006). Allocating the U.S. federal budget to the states: The impact of the president. *Journal of Politics*, *68*(2), 447–456.

Lazarev, E., Sobolev, A., Soboleva, I. V., & Sokolov, B. (2014). Trial by fire: A natural disaster's impact on support for the authorities in rural Russia. *World Politics*, *66*(4), 641–668.

Lazzaroni, S., & van Bergeijk, P. (2014). Natural disasters' impact, factors of resilience and development: A meta-analysis of the macroeconomic literature. *Ecological Economics*, *107*, 333–346.

Le Cozannet, G., Modaressi, H., Pedreros, R., Garcin, M., Krien, Y., & Desramaut, N. (2013). Storm surges. In P. T. Bobrowsky (Ed.) *Encyclopedia of Natural Hazards*, (p. 940). Dordrecht and New York: Springer.

Lenzen, M., Kanemoto, K., Moran, D., & Geschke, A. (2012). Mapping the structure of the world economy. *Environmental Science & Technology*, *46*(15), 8374–8381.

Lenzen, M., Malik, A., Kenway, S., Daniels, P., Lam, K. L., & Geschke, A. (2019). Economic damage and spillovers from a tropical cyclone. *Natural Hazards and Earth System Sciences*, *19*(1), 137–151.

Lenzen, M., Moran, D., Kanemoto, K., & Geschke, A. (2013). Building Eora: A global multi-region input-output database at high country and sector resolution. *Economic Systems Research*, *25*(1), 20–49.

Levin, N., & Zhang, Q. (2017). A global analysis of factors controlling VIIRS nighttime light levels from densely populated areas. *Remote Sensing of Environment*, *190*, 366–382.

Levitt, S. D., & Snyder, J. M. (1997). The impact of federal spending on house election outcomes. *Journal of Political Economy*, *105*(1), 30–53.

Leyk, S., Gaughan, A. E., Adamo, S. B., de Sherbinin, A., Balk, D., Freire, S., Rose, A., Stevens, F. R., Blankespoor, B., Frye, C., Comenetz, J., Sorichetta, A., MacManus, K., Pistolesi, L., Levy, M., Tatem, A., & Pesaresi, M. (2019). The spatial allocation of population: A review of large-scale gridded population data products and their fitness for use. *Earth System Science Data*, *11*(3).

Li, X., Xu, H., Chen, X., & Li, C. (2013). Potential of NPP-VIIRS nighttime light imagery for modeling the regional economy of China. *Remote Sensing*, *5*(6), 3057–3081.

Lin, C.-Y. C. (2010). Instability, investment, disasters, and demography: Natural disasters and fertility in Italy (1820–1962) and Japan (1671–1965). *Population and Environment*, *31*(4), 255–281.

Lindbeck, A., & Weibull, J. W. (1987). Balanced-budget redistribution as the outcome of political competition. *Public Choice*, *52*(3), 273–297.

Lindsay, B. R. (2014). FEMA's disaster relief fund: Overview and selected issues: CRS Report. Congressional Research Service.
URL https://fas.org/sgp/crs/homesec/R43537.pdf

Lindsay, B. R., & McCarthy, F. X. (2015). Stafford act declarations 1953-2014: Trends, analyses, and implications for congress: CRS Report. Congressional Research Service.
URL https://fas.org/sgp/crs/homesec/R42702.pdf

Livi Bacci, M. (2007). *A concise history of world population*. Oxford: Blackwell, 4. ed. ed.

Loayza, N. V., Olaberría, E., Rigolini, J., & Christiaensen, L. (2012). Natural disasters and growth: Going beyond the averages. *World Development*, *40*(7), 1317–1336.

Lonfat, M., Marks, F. D., & Chen, S. S. (2004). Precipitation distribution in tropical cyclones using the tropical rainfall measuring mission (TRMM) microwave imager: A global perspective. *Monthly Weather Review*, *132*(7), 1645–1660.

Lonfat, M., Rogers, R., Marchok, T., & Marks, F. D. (2007). A parametric model for predicting hurricane rainfall. *Monthly Weather Review*, *135*(9), 3086–3097.

Lu, X., Wrathall, D. J., Sundsøy, P. R., Nadiruzzaman, M., Wetter, E., Iqbal, A., Qureshi, T., Tatem, A., Canright, G., Engø-Monsen, K., & Bengtsson, L. (2016). Unveiling hidden migration and mobility patterns in climate stressed regions: A longitudinal study of six million anonymous mobile phone users in Bangladesh. *Global Environmental Change*, *38*, 1–7.

Maddison, A. (2001). *The world economy: A millennial perspective*. Paris, France: OECD.

Manacorda, M., Miguel, E., & Vigorito, A. (2011). Government transfers and political support. *American Economic Journal: Applied Economics*, *3*(3), 1–28.

Mansour, S. (2019). Geospatial modelling of tropical cyclone risks to the southern Oman coasts. *International Journal of Disaster Risk Reduction*, *40*, 101151.

Marshall, M. G., Gurr, T. R., & Jaggers, K. (2018). Polity IV. Center for systemic peace.
URL http://www.systemicpeace.org/inscr/p4v2017.xls

McCarthy, F. X. (2014). FEMA's disaster declaration process: A primer: CRS Report. Congressional Research Service.
URL https://fas.org/sgp/crs/homesec/R43784.pdf

McCaughey, J. W., Daly, P., Mundir, I., Mahdi, S., & Patt, A. (2018). Socio-economic consequences of post-disaster reconstruction in hazard-exposed areas. *Nature Sustainability*, *1*(1), 38–43.

McEvedy, C., & Jones, R. (1978). *Atlas of world population history*. Penguin reference books. Harmondsworth, Middlesex: Penguin.

McGranahan, G., Balk, D., & Anderson, B. (2007). The rising tide: Assessing the risks of climate change and human settlements in low elevation coastal zones. *Environment and Urbanization*, *19*(1), 17–37.

Mendelsohn, R., Emanuel, K., Chonabayashi, S., & Bakkensen, L. (2012). The impact of climate change on global tropical cyclone damage. *Nature Climate Change*, *2*(3), 205–209.

Meya, J., Poutvaara, P., & Schwager, R. (2020). Pocketbook voting, social preferences, and expressive motives in referenda. *Journal of Economic Behavior & Organization*, *175*, 185–205.

Michaelowa, K., Reinsberg, B., & Schneider, C. J. (2018). The politics of double delegation in the European Union. *International Studies Quarterly*, *62*(4), 821–833.

Michalopoulos, S., & Papaioannou, E. (2014). National institutions and subnational development in Africa. *The Quarterly Journal of Economics*, *129*(1), 151–213.

Mohan, P. (2017). Impact of hurricanes on agriculture: Evidence from the Caribbean. *Natural Hazards Review*, *18*(3), 04016012.

Mohan, P., & Strobl, E. (2017). The short-term economic impact of tropical Cyclone Pam: an analysis using VIIRS nightlight satellite imagery. *International Journal of Remote Sensing*, *38*(21), 5992–6006.

Motamed, M. J., M., F. R. J. G., & Masters, W. A. (2014). Agriculture, transportation and the timing of urbanization: Global analysis at the grid cell level. *Journal of Economic Growth*, *19*(3), 339–368.

Moyo, D. (2009). Why foreign aid is hurting Africa. *The Wall Street Journal*.

Muis, S., Verlaan, M., Winsemius, H. C., Aerts, J. C. J. H., & Ward, P. J. (2016). A global reanalysis of storm surges and extreme sea levels. *Nature Communications*, *7*(11969).

Munich Re (2018). NatCatSERVICE – Relevant natural loss events worldwide 1980–2018.
URL https://www.munichre.com/en/solutions/for-industry-clients/natcatservice.html

Murnane, R. J., & Elsner, J. B. (2012). Maximum wind speeds and US hurricane losses. *Geophysical Research Letters*, *39*(16).

Murshed, S. M., & Gates, S. (2005). Spatial-horizontal inequality and the Maoist insurgency in Nepal. *Review of Development Economics*, *9*(1), 121–134.

Nagoda, S., & Nightingale, A. J. (2017). Participation and power in climate change adaptation policies: Vulnerability in food security programs in Nepal. *World Development*, *100*, 85–93.

National Weather Service (2015). Tropical cyclone winds and energy. URL last accessed Nov. 2017.
URL http://www.prh.noaa.gov/cphc/pages/FAQ/Winds_and_Energy.php

Needham, H. F., & Keim, B. D. (2012). A storm surge database for the US Gulf Coast. *International Journal of Climatology*, *32*, 2108–2123.

Needham, H. F., Keim, B. D., & Sathiaraj, D. (2015). A review of tropical cyclone-generated storm surges: Global data sources, observations, and impacts. *Reviews of Geophysics*, *53*, 545–591.

Nel, P., & Righarts, M. (2008). Natural Disasters and the Risk of Violent Civil Conflict. *International Studies Quarterly*, *52*(1), 159–185.

Neumann, B., Vafeidis, A. T., Zimmermann, J., Nicholls, R. J., & Kumar, L. (2015). Future coastal population growth and exposure to sea-level rise and coastal flooding – A global assessment. *PLOS ONE*, *10*(3), e0118571.

Newey, W. K., & West, K. D. (1987). A simple, positive semi-definite, heteroskedasticity and autocorrelation consistent covariance matrix. *Econometrica*, *55*(3), 703–708.

Newson, R. (1998). PARMEST: Stata module to create new data set with one observation per parameter of most recent model. *Statistical Software Components S352601*.

Nguyen, C. N., & Noy, I. (2019). Measuring the impact of insurance on urban earthquake recovery using nightlights. *Journal of Economic Geography*, *20*(3).

NHC (2016). National hurricane center forecast verification.
URL http://www.nhc.noaa.gov/verification/verify5.shtml

Nickell, S. J. (1981). Biases in dynamic models with fixed effects. *Econometrica*, *49*(6), 1417–1426.

NOAA (2017). VIIRS DNB cloud free composites: Version 1 nighttime VIIRS day/night band composites.
URL https://ngdc.noaa.gov/eog/viirs/download_dnb_composites.html

Nordhaus, W. D. (2010). The economics of hurricanes and implications of global warming. *Climate Change Economics*, *1*(1), 1–20.

Noy, I. (2009). The macroeconomic consequences of disasters. *Journal of Development Economics*, *88*(2), 221–231.

Nunnenkamp, P., & Öhler, H. (2011). Aid allocation through various official and private channels: Need, merit, and self-interest as motives of German donors. *World Development*, *39*(3), 308–323.

Nunnenkamp, P., Öhler, H., & Sosa Andrés, M. (2017). Need, merit and politics in multilateral aid allocation: A district-level analysis of World Bank projects in India. *Review of Development Economics*, *21*(1), 126–156.

Öhler, H., Negre, M., Smets, L., Massari, R., Bogetić, Ž., & Paniagua, J. (2019). Putting your money where your mouth is: Geographic targeting of World Bank projects to the bottom 40 percent. *PLOS ONE*, *14*(6), e0218671.

Onuma, H., Shin, K. J., & Managi, S. (2020). Short-, medium-, and long-term growth impacts of catastrophic and non-catastrophic natural disasters. *Economics of Disasters and Climate Change*, (pp. 2511–1299).

Oosterhaven, J. (2017). On the limited usability of the inoperability IO model. *Economic Systems Research*, *29*(3), 452–461.

Ouattara, B., & Strobl, E. (2013). The fiscal implications of hurricane strikes in the Caribbean. *Ecological Economics*, *85*, 105–115.

Painter, W. L. (2019). The disaster relief fund: Overview and issues: CRS report. Congressional Research Service.
URL https://fas.org/sgp/crs/homesec/R45484.pdf

Paudel, J., & de Araujo, P. (2017). Demographic responses to a political transformation: Evidence of women's empowerment from Nepal. *Journal of Comparative Economics*, *45*(2), 325–343.

Paudel, J., & Ryu, H. (2018). Natural disasters and human capital: The case of Nepal's earthquake. *World Development*, *111*, 1–12.

Pettersson-Lidbom, P. (2008). Do parties matter for economic outcomes? A regression-discontinuity approach. *Journal of the European Economic Association*, *6*(5), 1037–1056.

Plane, D. A., Henrie, C. J., & Perry, M. J. (2005). Migration up and down the urban hierarchy and across the life course. *Proceedings of the National Academy of Sciences of the United States of America*, *102*(43), 15313–15318.

Platt, R. H. (1999). *Disasters and Democracy: The Politics of Extreme Natural Events*. Washington D.C.: Island Press.

Potrafke, N. (2020). General or central government? Empirical evidence on political cycles in budget composition using new data for OECD countries. *European Journal of Political Economy*, *63*, 101860.

Quinckhardt, M. (2019). The effect of political alignment and connectedness on intergovernmental transfers. Mimeo.

Rahmstorf, S. (2017). Rising hazard of storm-surge flooding. *Proceedings of the National Academy of Sciences of the United States of America*, *114*(45), 11806–11808.

Rappaport, E. N., Franklin, J. L., Avila, L. A., Baig, S. R., Beven II, J. L., Blake, E. S., Burr, C. A., Jiing, J.-G., Juckins, C. A., Knabb, R. D., Landsea, C. W., Mainelli, M., Mayfield, M., McAdie, C. J., Pasch, R. J., Sisko, C., Stewart, S. R., & Tribble, A. N. (2009). Advances and challenges at the national hurricane center. *Weather and Forecasting*, *24*(2), 395–419.

Rappaport, J., & Sachs, J. D. (2003). The United States as a coastal nation. *Journal of Economic Growth*, *8*(1), 5–46.

Raschky, P. A., & Schwindt, M. (2012). On the channel and type of aid: The case of international disaster assistance. *European Journal of Political Economy*, *28*(1), 119–131.

Reeves, A. (2011). Political disaster: Unilateral powers, electoral incentives, and presidential disaster declarations. *Journal of Politics*, *73*(4), 1142–1151.

Ripple, W. J., Wolf, C., Newsome, T. M., Barnard, P., & Moomaw, W. R. (2019). World Scientists' Warning of a Climate Emergency. *BioScience*, *70*(1), 8–12.

Rota, M., Penna, A., Strobbia, C., & Magenes, G. (2008). Direct derivation of fragility curves from Italian post-earthquake survey data. Paper presented at the 14th World Conference on Earthquake Engineering, Beijing, China.

Roth, D. M. (2018). Tropical cyclone rainfall data (1965–2018).
URL http://www.wpc.ncep.noaa.gov/tropical/rain/tcrainfall.html

Rozenberg, J., & Hallegatte, S. (2016). Model and methods for estimating the number of people living in extreme poverty because of the direct impacts of natural disasters (English). World Bank Policy Research Working Paper 7887.
URL http://documents.worldbank.org/curated/en/836301478979358386/Model-and-methods-for-estimating-the-number-of-people-living-in-extreme-poverty-because-of-the-direct-impacts-of-natural-disasters

Schlenker, W., & Roberts, M. J. (2009). Nonlinear temperature effects indicate severe damages to U.S. crop yields under climate change. *Proceedings of the National Academy of Sciences of the United States of America*, *106*(37), 15594–15598.

Schneider, C. J. (2010). Fighting with one hand tied behind the back: Political budget cycles in the West German states. *Public Choice*, *142*(1/2), 125–150.

Schreck, C. J., Knapp, K. R., & Kossin, J. P. (2014). The impact of best track discrepancies on global tropical cyclone climatologies using IBTrACS. *Monthly Weather Review*, *142*(10), 3881–3899.

Schroeder, S. C. (2018). Does America's new disaster relief law provide the relief America needs. *Houston Law Review*, *56*, 1177–1212.

Semrau, F. O., & Thiele, R. (2017). Brazil's development cooperation: Following in China's and India's footsteps? Brazil's development cooperation. *Journal of International Development*, *29*(3), 287–307.

Sharma, B., & Barry, E. (2015). Earthquake prods Nepal parties to make constitution deal. *The New York Times*.

Sharma, K. (2006). The political economy of civil war in Nepal. *World Development*, *34*(7), 1237–1253.

Shi, M., & Svensson, J. (2006). Political budget cycles: Do they differ across countries and why? *Journal of Public Economics*, *90*(8), 1367–1389.

Shughrue, C., Werner, B., & Seto, K. C. (2020). Global spread of local cyclone damages through urban trade networks. *Nature Sustainability*, *3*(8), 606–613.

Sieg, T., Schinko, T., Vogel, K., Mechler, R., Merz, B., & Kreibich, H. (2019). Integrated assessment of short-term direct and indirect economic flood impacts including uncertainty quantification. *PLOS ONE*, *14*(4), 1–21.

Small, C., Pozzi, F., & Elvidge, C. (2005). Spatial analysis of global urban extent from DMSP-OLS night lights. *Remote Sensing of Environment*, *96*(3-4), 277–291.

Snyder, J. M., & Strömberg, D. (2010). Press coverage and political accountability. *Journal of Political Economy*, *118*(2), 355–408.

Solé-Ollé, A., & Sorribas-Navarro, P. (2008). The effects of partisan alignment on the allocation of intergovernmental transfers. Differences-in-Differences estimates for Spain. *Journal of Public Economics*, *92*(12), 2302–2319.

Stafford Act (1988). Robert T. Stafford disaster relief and emergency assistance act. Public Law 93-288, as amended, 42 U.S.C. 5121 et seq., and Related Authorities.

Strandow, D., Findley, M. G., & Young, J. K. (2016). Foreign aid and the intensity of violent armed conflict. AidData Working Paper 24.
URL http://docs.aiddata.org/ad4/pdfs/wps24_foreign_aid_and_the_intensity_of_violent_armed_conflict.pdf

Strobl, E. (2011). The economic growth impact of hurricanes: Evidence from U.S. coastal counties. *The Review of Economics and Statistics*, *93*(2), 575–589.

Strobl, E. (2012). The economic growth impact of natural disasters in developing countries: Evidence from hurricane strikes in the Central American and Caribbean Regions. *Journal of Development Economics*, *97*(1), 130–141.

Strömberg, D. (2004). Radio's impact on public spending. *The Quarterly Journal of Economics*, *119*(1), 189–221.

Strömberg, D. (2007). Natural disasters, economic development, and humanitarian aid. *Journal of Economic Perspectives*, *21*(3), 199–222.

Sylves, R. (2008). *Disaster Policy and Politics: Emergency Management and Homeland Security*. Washington D.C.: CQ Press, 1st ed.

Terry, J. P. (2007). *Tropical cyclones: Climatology and impacts in the South Pacific*. New York and London: Springer.

The Economist (2015). To the rescue.
URL https://www.economist.com/asia/2015/04/30/to-the-rescue

Toya, H., & Skidmore, M. (2007). Economic development and the impacts of natural disasters. *Economics Letters*, *94*(1), 20–25.

UNDRR (2019). Global assessment report on disaster risk reduction.
URL https://gar.undrr.org/report-2019

UNFCCC (2015). Paris agreement.
URL https://unfccc.int/files/essential_background/convention/application/pdf/english_paris_agreement.pdf

UNGA (1991). United Nations resolution A/RES/46/182: Strengthening of the coordination of humanitarian emergency assistance of the United Nations.

UNISDR (2015). Sendai framework for disaster risk reduction 2015–2030.
URL http://www.unisdr.org/files/43291_sendaiframeworkfordrren.pdf

United Nations Statistical Division (2015a). Glossary – Definition of term: Value added – gross.
URL https://unstats.un.org/unsd/snaama/Metadata/Glossary#

United Nations Statistical Division (2015b). Methodology for the national accounts main aggregates database.
URL https://unstats.un.org/unsd/snaama/assets/pdf/methodology.pdf

United Nations Statistical Division (2015c). UN data.
URL http://data.un.org/Explorer.aspx?d=SNAAMA

University of East Anglia Climatic Research Unit, Harris, I. C., & Jones, P. D. (2017). CRU TS4.01: Climatic research unit (CRU) time-series (TS) version 4.01 of high-resolution gridded data of month-by-month variation in climate (Jan. 1901–Dec. 2016). Centre for Environmental Data Analysis (CEDA).

UNOCHA (2013). Preliminary response plan guidance. United Nations office for the coordination of humanitarian affairs – Programme support branche.
URL https://www.humanitarianresponse.info/sites/www.humanitarianresponse.info/files/documents/files/Working%20DRAFT%201_Preliminary%20Response%20Plan%20Guidance%205%20December2013.pdf

UNOCHA (2015a). Humanitarian bulletin Nepal earthquake. Issue 01.
URL https://www.humanitarianresponse.info/fr/operations/nepal/document/nepal-earthquake-humanitarian-bulletin-issue-01-june-2015

UNOCHA (2015b). Nepal – flash appeal revision – Nepal earthquake April–September 2015.
URL https://reliefweb.int/sites/reliefweb.int/files/resources/nepal_earthquake_2015_revised_flash_appeal_june.pdf

UNOCHA (2015c). Nepal flash appeal for the response to the Nepal earthquake April–July 2015.
URL https://www.humanitarianresponse.info/sites/www.humanitarianresponse.info/files/documents/files/nepal_earthquake_2015_revised_flash_appeal_final_0.pdf

UNOCHA (2016). FTS archive.
URL http://fts.unocha.org/

UNOCHA (2018). Nepal – Earthquake – April 2015.
URL https://ftsarchive.unocha.org/pageloader.aspx?page=emerg-emergencyDetails&appealID=1100

USGS (2016). M 6.9 – Nepal-India border region.
URL https://earthquake.usgs.gov/earthquakes/eventpage/usp0003k6t/shakemap/intensity

USGS (2017a). Earthquake hazards 201 – Technical Q&A.
URL https://www.usgs.gov/natural-hazards/earthquake-hazards/science/earthquake-hazards-201-technical-qa?qt-science_center_objects=0#qt-science_center_objects

USGS (2017b). M 7.3 – 19km SE of Kodari, Nepal.
URL https://earthquake.usgs.gov/earthquakes/eventpage/us20002ejl#shakemap

USGS (2017c). Shakemap us20002926.
URL https://earthquake.usgs.gov/earthquakes/eventpage/us20002926/executive

Ward, P. J., Jongman, B., Aerts, J. C. J. H., Bates, P. D., Botzen, W. J. W., Diaz Loaiza, A., Hallegatte, S., Kind, J. M., Kwadijk, J., Scussolini, P., & Winsemius, H. C. (2017). A global framework for future costs and benefits of river-flood protection in urban areas. *Nature Climate Change*, *7*(9), 642–646.

Weidmann, N. B., & Schutte, S. (2016). Using night light emissions for the prediction of local wealth. *Journal of Peace Research*, *54*(2), 125–140.

Weingast, B. R., Shepsle, K. A., & Johnsen, C. (1981). The political economy of benefits and costs: A neoclassical approach to distributive politics. *Journal of Political Economy*, *89*(4), 642–664.

Wenz, L., & Levermann, A. (2016). Enhanced economic connectivity to foster heat stress–related losses. *Science Advances*, *2*(6).

Wiesenfarth, M., & Kneib, T. (2010). Bayesian geoadditive sample selection models. *Journal of the Royal Statistical Society: Series C (Applied Statistics)*, *59*(3), 381–404.

Williams, N. E., Bhandari, P., Young-DeMarco, L., Swindle, J., Hughes, C., Chan, L., Thornton, A., & Sun, C. (2020). Ethno-caste influences on migration rates and destinations. *World Development*, *130*, 104912.

Wood, R. M., & Wright, T. M. (2016). Responding to catastrophe: Repression dynamics following rapid-onset natural disasters. *Journal of Conflict Resolution*, *60*(8), 1446–1472.

Woodruff, J. D., Irish, J. L., & Camargo, S. J. (2013). Coastal flooding by tropical cyclones and sea-level rise. *Nature*, *504*(7478), 44–52.

World Bank (2010). Natural hazards, unnatural disasters: The economics of effective prevention: Overview.
URL http://hdl.handle.net/10986/2512

World Bank (2018). World Bank development indicators.
URL https://data.worldbank.org/country/nepal

Wrathall, D. J., Mueller, V., Clark, P. U., Bell, A., Oppenheimer, M., Hauer, M., Kulp, S., Gilmore, E., Adams, H., Kopp, R., Abel, K., Call, M., Chen, J., deSherbinin, A., Fussell, E., Hay, C., Jones, B., Magliocca, N., Marino, E., Slangen, A., & Warner, K. (2019). Meeting the looming policy challenge of sea-level change and human migration. *Nature Climate Change*, *9*(12), 898–901.

Yang, D. (2008). Coping with disaster: The impact of hurricanes on international financial flows, 1970-2002. *The B.E. Journal of Economic Analysis & Policy*, *8*(1), 13.

Zabel, F., Putzenlechner, B., & Mauser, W. (2014). Global agricultural land resources – A high resolution suitability evaluation and its perspectives until 2100 under climate change conditions. *PLOS ONE*, *9*(9), 1–12.

Zudenkova, G. (2011). A political agency model of coattail voting. *Journal of Public Economics*, *95*(11), 1652–1660.

All internet sources have been last accessed on October 31, 2020 if not stated differently.

Acknowledgments

Many people have contributed to this dissertation. First of all, I am deeply thankful to Axel Dreher for all of his advice, support, and valuable feedback in the last seven years. I am very grateful to him for letting me develop my own research agenda and for providing me the financial support to attend every workshop and conference I asked for. This clearly helped me a lot to develop my personal research network. His fast and constructive feedback contributed substantially to the development of each chapter of this dissertation. Furthermore, I am especially thankful for all of his strategic advice and tips on how academic networking during and after conferences functions. Similarly, I am thankful to Eric Strobl for accepting to be my second supervisor already at an early stage of my PhD. His support, feedback, understanding, and steady availability for skype calls helped and motivated me a lot. I also thank him for giving me the opportunity for a research stay in Bern. Furthermore, I am thankful for Jale Tosun to immediately accepting to serve as third examiner of this dissertation.

In addition to my supervisors, I am thankful for many great and supportive colleagues in Heidelberg. I thank Vera for giving much advice and support in the beginning. I thank Andi for his universal support in all steps of my dissertation. I am particularly grateful to Andi and Vera for giving me the opportunity to organize and attend such a great Workshop on Disaster Aid in the first year of my PhD. I thank John for being a great office mate and organizing so many chair drink events. I thank Katha for always being very empathetic. I thank Sarah for being so positive and engaged for the team spirit. I thank Valentin for sharing his econometric knowledge enthusiastically. I thank Lenny for his endless support, his collegiality, and because he always cared for the integrity of the whole chair. I thank Angelika for her support during our research stay in Berkeley and the Mannheim courses. I thank Gerda for her positive attitude and her support during the Mannheim courses. I thank Zain for being so supportive in the final phase of my PhD. I thank Johannes and Lukas for giving me much feedback on all the figures I have created and supporting me in the final phase of my dissertation. I am also deeply thankful for the great support of all our research assistants: Stephan, Franzi, Patrick, Theresa, Dominik, and Tim. Furthermore, I am thankful to all the administrative support from Heike and Mrs. Arnold, which made my work much easier. Additionally, I thank the whole IT Team and especially Christoph Schineller for always helping me with my special requests in calculating big data sets.

Three of my chapters profited from many gifted co-authors from whom I learned a lot. I thank Stephan for being such an engaged co-author who always pushed me forward in critical thinking and illustrating research results. I thank Vera for sharing many Stata coding insights. I thank Andi for his curiosity and his research design thinking. I thank Eric for sharing many interdisciplinary approaches and his ability to directly see strengths and weaknesses of a paper. I also thank Maximilian Auffhammer for inviting me to the ARE department at UC Berkeley. These four months were incredibly motivating and productive. Finally, I also thank the Joachim Herz Stiftung for granting me the Fellowship for Interdisciplinary Economics, which allowed me to finance the research stay at the UC Berkeley, many in-situ meetings with my co-authors, and insightful summer schools.

This thesis would not have been possible without the continuous support of my family and friends. I thank my parents and my grandmother, to whom I dedicate this thesis, for always believing in me and giving me all the possible support to pursue my goals. I also thank my two brothers whose advice have always been invaluable for me. I thank all of my friends for supporting me and always helping to keep me in a good “work-life” balance. But most of all I thank Christina for her long and unwavering love and support without which I would not be where I am today.

Furthermore, I would like to acknowledge the following colleagues for their input to the individual chapters:

Chapter 1: I am grateful for comments made by Axel Dreher, Vera Eichenauer, Andreas Fuchs, Lennart Kaplan, Eric Strobl, and Christina Vonnahme. I further thank seminar participants at Heidelberg University (2016), the AERE Summer Conference in Breckenridge (6/2016), the EAERE Meeting in Zurich (06/2016), the BBQ Workshop in Salzburg (07/2016), the “Geospatial Analysis of Disasters: Measuring Welfare Impacts of Emergency Relief” Workshop in Heidelberg (07/2016), the Oeschger Climate Summer School in Grindelwald

(08/2016), the Conference on Econometric Models of Climate Change in Oxford (9/2017), the Impacts World Conference in Potsdam (10/2017), and the 8th Annual Interdisciplinary Ph.D. Workshop in Sustainable Development at Columbia University (04/2018). Excellent proofreading was provided by Jamie Parsons and Harrison Bardwell.

Chapter 2: We thank Axel Dreher, Andrew Hultgren, and Leonie Wenz for helpful comments. We also thank participants at the 6th World Congress of Environmental and Resource Economists 2018 at the University of Gothenburg, of the Global Policy Lab at UC Berkeley, the Summer Conference of the Association of Environmental and Resource Economists (AERE) 2019 in Lake Tahoe, the Econometric Models of Climate Change Conference 2019 at the University of Milano-Bicocca, the Congress "Extreme Events: Building Climate Resilient Societies" of the Volkswagen Foundation in Hanover. Moreover, we thank Tim Deisemann, Theresa Geyer, and Tobias Hellmundt for their excellent research assistance. Sven Kunze received funding for this project from the Joachim Herz Foundation.

Chapter 3: We thank Axel Dreher, Peter Egger, Vera Z. Eichenauer, Roland Hodler, Panu Poutvaara, Lynda Powell, Leo K. Simon, Eric Strobl, Jan-Egbert Sturm, and Katherine R. H. Wagner. We also thank participants at the Beyond Basic Questions Workshop 2018 in Gengenbach, the European Public Choice Society Meeting 2019 in Jerusalem, the Giannini ARE Student Conference (GARESC) 2019 at UC Davis, the SkiLLS Workshop 2020 in Engelberg, Silvaplana Workshop on Political Economy 2020, the Spring Meeting of Young Economists 2019 in Brussels, the Conference of the Verein für Socialpolitik 2019 in Leipzig, the Young Swiss Economists Meeting 2019 in Zurich, and research seminars at Freiburg University and Heidelberg University for their valuable comments. Furthermore, we are very grateful to David M. Roth, who generously provided the raw data for the precipitation measure that this study uses, as well as Carl E. Klarner and James M. Snyder for sharing their datasets, and Richard Sylves for detailed information about the disaster declaration process. Moreover, we thank Theresa Geyer, Tobias Hellmundt, and Mathias Schneider for their excellent research assistance. Sven Kunze received funding for this project from the Joachim Herz Foundation.

Chapter 4: We thank Katja Michaelowa, Rainer Thiele, seminar participants at Heidelberg University, as well as conference and workshop participants at the Young Scientists Workshop of the VfS Research Group on Environmental and Resource Economics (University of Basel, February 2017), Columbia University's Alliance Graduate Summer School "Research Methods in Sustainable Development" (Columbia Global Centers Paris, May 2017), the Annual International Conference of the VfS Research Group on Development Economics (University of Goettingen, June 2017), and the Beyond Basic Questions Workshop (Gengenbach/ Black Forest, August 2018) for very valuable comments. A special thanks to AidData for having compiled the geo-referenced data set on aid allocation after the 2015 Nepal earthquake. Eliana Chavarria, Laura Mahoney, Keonhi Son, Samuel Siewers, Franziska Volk, and Nicolas Wesseler provided excellent research assistance. This research did not receive any specific grant from funding agencies in the public, commercial, or not-for-profit sectors.

Sven Kunze

Heidelberg, June 2021